NASA Contractor Report 166011

DESIGN, ANCILLARY TESTING, ANALYSIS, AND FABRICATION DATA FOR THE ADVANCED COMPOSITE STABILIZER FOR BOEING 737 AIRCRAFT

VOLUME II–FINAL REPORT

R. B. Aniversario
S. T. Harvey
J. E. McCarty
J. T. Parsons
D. C. Peterson
L. D. Pritchett
D. R. Wilson
E. R. Wogulis

BOEING COMMERCIAL AIRPLANE COMPANY
P.O. BOX 3707, SEATTLE, WA 98124

CONTRACT NAS1-15025
December 1982

NASA
National Aeronautics and
Space Administration

Langley Research Center
Hampton, Virginia 23665

NASA Contractor Report 166011

DESIGN, ANCILLARY TESTING, ANALYSIS, AND FABRICATION DATA FOR THE ADVANCED COMPOSITE STABILIZER FOR BOEING 737 AIRCRAFT

VOLUME II–FINAL REPORT

R. B. Aniversario
S. T. Harvey
J. E. McCarty
J. T. Parsons
D. C. Peterson
L. D. Pritchett
D. R. Wilson
E. R. Wogulis

BOEING COMMERCIAL AIRPLANE COMPANY
P.O. BOX 3707, SEATTLE, WA 98124

CONTRACT NAS1-15025

NASA
National Aeronautics and
Space Administration

Langley Research Center
Hampton, Virginia 23665

FOREWORD

This final technical report (vol. II) and a technical summary (vol. I, ref. 1) were prepared by the Boeing Commerical Airplane Company, Renton, Washington, under NASA Contract NAS1-15025. They cover work performed between July 1977 and December 1981. The program was sponsored by the National Aeronautics and Space Administration, Langley Research Center (NASA-LRC). Dr. Herbert A. Leybold, Marvin B. Dow, and Andrew J. Chapman were the NASA-LRC project managers.

The following Boeing personnel were principal contributors to the program:

Program Director
S. T. Harvey

Design
G. Ohgi
R. J. Nicoli
E. R. Wogulis
W. C. Brown

Structural Analysis
D. R. Wilson
R. W. Johnson
J. E. McCarty

Weight and Balance Analysis
G. Nishimura
J. T. Parsons
R. E. Baum

Manufacturing Technology
M. C. Garvey
V. S. Thompson
E. S. Jamison

Production Manager
J. E. Gallant
W. D. Grant

Technical Operations Manager
L. D. Pritchett

Business Management
C. M. Lytle
M. R. Wiebe
D. V. Chovil

SUMMARY

This is the final report for design, ancillary testing, analysis, and fabrication detail for the NASA Aircraft Energy Efficiency (ACEE) program on the Boeing 737 commerical transport. It covers all work performed on the program from July 1977 through December 1981.

Program objectives were to design and produce an advanced composite stabilizer that would meet the same functional criteria as those for the existing metal stabilizer. Preliminary design activities were devoted to developing and analyzing alternative design concepts and selecting the final configuration. Trade studies evaluated durability, inspectability, producibility, repairability, and customer acceptance. Preliminary development efforts were devoted to evaluating and selecting material, identifying structural development test requirements, and defining full-scale ground and flight test requirements necessary to obtain Federal Aviation Administration (FAA) certification.

After selecting the best structural arrangement, detail design started and included basic configuration design improvements resulting from manufacturing verification hardware, the test program, weight analysis, and structural analysis. Nonautomated detail and assembly tools were designed and fabricated to support a full-scale production program rather than a limited run. The producibility development programs verified tooling approaches, fabrication processes, and inspection methods for the production mode. Quality parts were fabricated and assembled with a minimum rejection rate, using existing inspection methods.

Basic program goals were:

- To make extensive and effective use of advanced composite material
- To obtain a minimum weight reduction of the composite stabilizer over the metal stabilizer of 20%
- To demonstrate cost effectiveness of composite structure and collect cost data

All program technical goals were realized when the design met or exceeded all established design requirements, criteria, and objectives with an FAA certification granted in August of 1982. Actual cost experience on this program showed that composite structure was not currently competitive with metal. Composite structures can become competitive by applying automated manufacturing methods and engineering designs tailored to automation.

Manufacturing of the composite stabilizer was performed in a semiproduction environment by production employees. Hand methods were used for cutting and layup of broadgoods, ply-by-ply inspection, and trimming. The limited production quantity of five-and-one-half shipsets did not warrant automated manufacturing that would be used in quantity production; therefore, a cost-competitive status with metal could not be demonstrated by the actual program cost. Automated manufacturing methods and the expected reduction in relative material cost will aid in achieving cost parity with metal structure.

CONTENTS

FIGURES

TABLES

1.0 INTRODUCTION

The escalation of jet fuel prices has motivated assessment of new technology concepts for designing and building commercial aircraft. Advanced composite materials, if used extensively in airframe components, offer high potential for reducing structural weight and thereby direct operating costs of commercial transport aircraft. To achieve the goal of production commitments to advanced composite structures, there is a need to convincingly demonstrate that these structures save weight, possess long-term durability, and can be fabricated at costs competitive with conventional metal structures.

To meet this need, NASA has established a program for composite structures under the Aircraft Energy Efficiency (ACEE) program. As part of this program, Boeing has redesigned and fabricated the horizontal stabilizer of the 737 transport using composite materials, has submitted data to FAA, and has obtained certification. Five shipsets of composite stabilizers have been manufactured to establish a firm basis for estimating production costs and to provide sufficient units for evaluation in airline service This work has been performed under NASA Contract NAS1-15025.

The broad objective of the ACEE Composite Structures program is to accelerate the use of composite structures in new transport aircraft by developing technology and processes for early progressive introduction of composite structures into production commercial transport aircraft. Specific objectives of the 737 Composite Horizontal Stabilizer program were to:

- Provide structural weight at least 20% less than the metal stabilizer
- Fabricate at least 40% by weight of the stabilizer constituent parts, from advanced composite materials
- Demonstrate cost competitiveness with the metal stabilizer
- Obtain FAA certification for the composite stabilizer
- Evaluate the composite stabilizer on aircraft in airline service

To achieve these objectives, Boeing concentrated efforts on conceiving, developing, and analyzing alternative stabilizer design concepts. After design selection, the following were performed: materials evaluation, ancillary tests to determine material design properties, structural elements tests, and full-scale ground and flight tests to satisfy FAA certification requirements. Specific program activities to achieve objectives included:

- Program management and plan development
- Establishing design criteria
- Conceptual and preliminary design
- Manufacturing process development
- Material evaluation and selection
- Verification testing
- Detail design
- FAA certification

Work accomplished in each of these areas is described in detail in this document and summarized in Reference 1.

NOTE: Certain commercial products are identified in this document in order to specify adequately the characteristics of the material and components under investigation. In no case does such identification imply recommendation or endorsement of the product by NASA or Boeing, nor does it imply that the materials are necessarily the only ones available for the purpose.

2.0 SYMBOLS AND ABBREVIATIONS

A	area
a	zone of intense energy
ACEE	aircraft energy efficiency
ATLAS	computer program
b	element width
BMS	Boeing Material Specification
c	distance from neutral axis to point of analysis
C	end fixity
^{o}C	degree Celsius
$\mathbb{C}_L$	centerline
c_N	total airplane normal force coefficient
CSK	countersink
D	diameter
dB	decibel
DSC	differential scanning calorimetry
DUL	design ultimate load
DVR	design value correction factor
E	modulus of elasticity
EA	axial stiffness
E_1	modulus of elasticity in (1) direction
E_2	modulus of elasticity in (2) direction

EI	bending stiffness
E/D	edge margin ratio
^{o}F	degree Fahrenheit
FAA	Federal Aviation Administration
FAR	Federal Aviation Regulation
FEP	fluorinated ethylene propylene (Teflon)
F_{TU}	ultimate tension stress
GJ	torsional stiffness
I	moment of inertia
IR&D	independent research and development
kA	kiloampere
$K_{B_{\infty}}$	"B" basis factor for infinite sample
K_{IC}	material fracture toughness
K_{SB}	shear bearing stress factor
K_{T}	tension stress factor
K_{θ}	oblique tension loading factor
L	column length, half-crack length
LC	load case
LS	lower skin
MCF	material correction factor
M_{D}	flight boundary, design dive speed, Mach number
MS	margin of safety

ms	millisecond
MVF	material variability factor
n	limit load factor
NDI	nondestructive inspection
OASPL	overall sound pressure levels
P	load
P_c	compression load
P_{cr}	critical load
P_H	horizontal component of load
P_{SB}	shear-bearing load
P-static	precipitation static
PT	part thickness
P_T	tensile load
P_s	shear load
P_V	vertical component of load
q	shear flow
Q	amount of electricity in a capacitor
R&D	research and development
RH	relative humidity
RS	rear spar

s	second
S	strength
S_M	mean strength of distribution
T_G	glass transition temperature
TGA	thermo-gravimetric analysis
t_{sk}	skin thickness
TTU	Through-Transmission Ultrasonic
TWIST	standardized fatigue load sequence
US	upper skin
V_A	design maneuver speed
V_B	design gust intensity speed
V_C	design cruise speed
V_D	design dive speed, flight boundary, knots equivalent air speed (keas)
V_F	design flap speed
V-n	airplane flight envelope
VMF	variation magnification factor
V_{S_1}	stall speed with flaps retracted
W_E	effective skin width
W_{SK_i}	effective buckled skin, $0.85\ t\sqrt{\frac{E}{Fc}}$

δ	deflection
γ	shear strain
ϵ	strain
μs	microsecond
ν	variance
σ	stress
$\Sigma\epsilon$	summation of strains
τ	shear stress

3.0 DESIGN

3.1 CONCEPT DEVELOPMENT

Concept development consisted of establishing design criteria and objectives, evaluating and selecting materials, and establishing an optimum baseline configuration for the advanced composite stabilizer. Several trade studies were conducted during the concept development phase in which skin stiffening concepts, spar lug configurations, and inspar rib configurations were evaluated.

3.1.1 Design Criteria and Objectives

The design criteria and objectives were established to provide a cost- and weight-efficient stabilizer for airline operation on current model 737 commercial transports. The basic design criteria and objectives for the advanced composite horizontal stabilizer were essentially the same as those for any new design replacement stabilizer. The advanced composite stabilizer was required to comply with both Federal Aviation Regulations and Boeing structural design criteria for model 737. Additional criteria used were:

- The composite stabilizer would be interchangeable with the existing production metal stabilizer.
- The airplane flight or handling characteristics would not be significantly changed with the installation of an advanced composite horizontal stabilizer. The advanced composite stabilizer would closely match the existing metal stabilizer's bending and torsional stiffness.
- The geometry and aerodynamic shape of the advanced composite stabilizer would be the same as the existing model 737 stabilizer.
- The structure would be designed as damage-tolerant (fail-safe).
- The strength, durability, inspectability, and serviceability would be equivalent to, or better than, that of the metal stabilizer.
- Maintenance and repair procedures would be developed for airline use.

In addition to the preceding criteria, the following contract objectives were imposed:

- The component weight target would reduce the weight of the redesigned structure by a minimum of 20%.
- The production cost of the composite stabilizer would be cost competitive with the metal stabilizer at the same unit number.

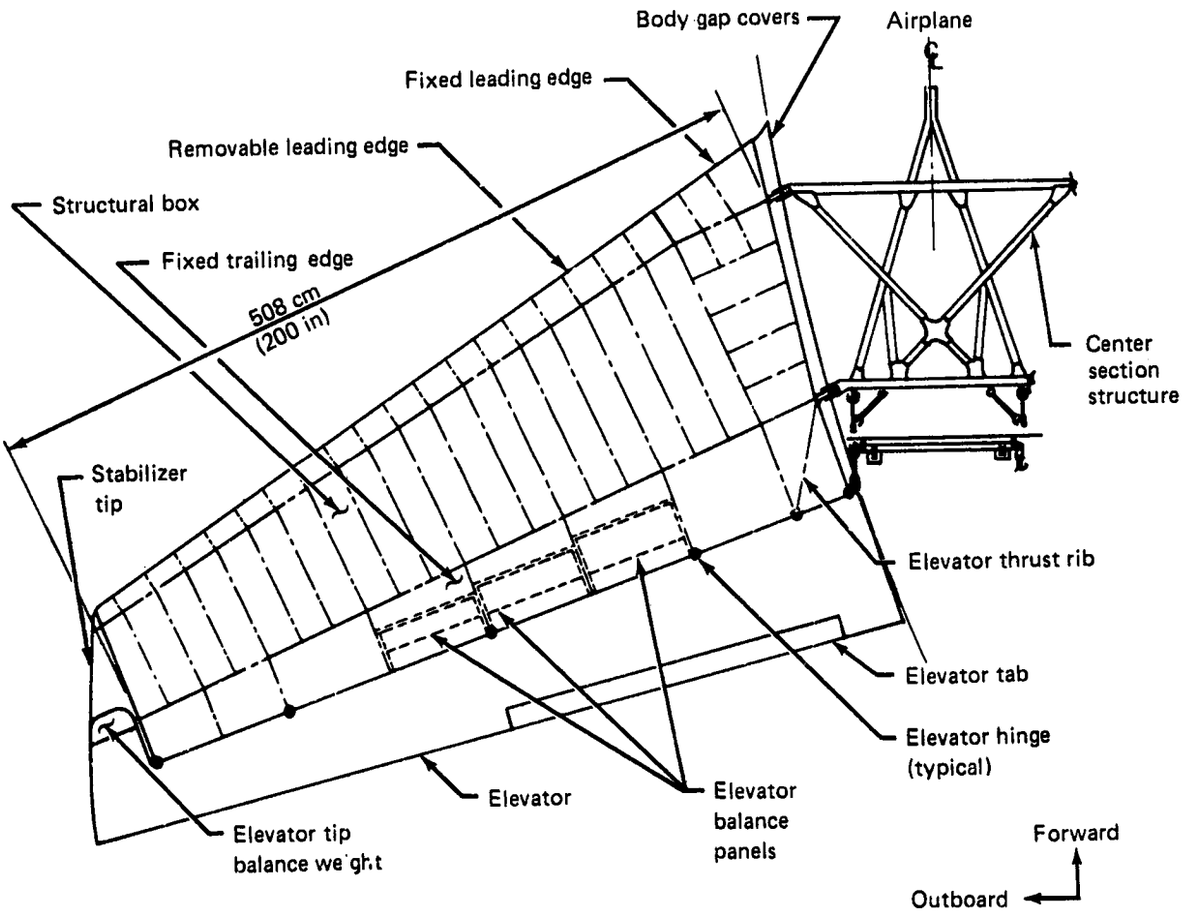

Figure 1. Horizontal Stabilizer—General Arrangement

3.1.2 Metal Stabilizer Configuration

The 737 horizontal stabilizer shown in Figure 1 consists of a structural box, leading edge, tip, fixed trailing edge, elevator, and body gap covers. Each stabilizer is attached to an aluminum center section structure with three bolts at the rear spar and two bolts at the front spar. The third joint on the rear spar is for fail-safety.

These five pin joints are the points of interchange for the entire stabilizer assembly. A sketch of the center section and its interfaces is shown in Figure 2.

The structural box has aluminum skins with bonded doublers. The ribs and spars are built-up aluminum construction. The structural box is 5.08m (200 in) long, 1.28m (50.5 in) wide at the root, and 0.635m (25 in). wide at the tip. Each box weighs 118.2 kg (260.6 lb). The leading edge is aluminum skin over aluminum ribs. The tip is fiberglass laminate, and the fixed trailing edge is fiberglass honeycomb sandwich panels with an aluminum trailing-edge beam. The trailing-edge ribs are built-up aluminum construction using bonded aluminum honeycomb webs. The lower trailing-edge panels are removable. The elevator consists of fiberglass honeycomb cover panels and built-up aluminum spars and ribs. The body gap covers and support structure are aluminum. A horizontal stabilizer section is shown in Figure 3.

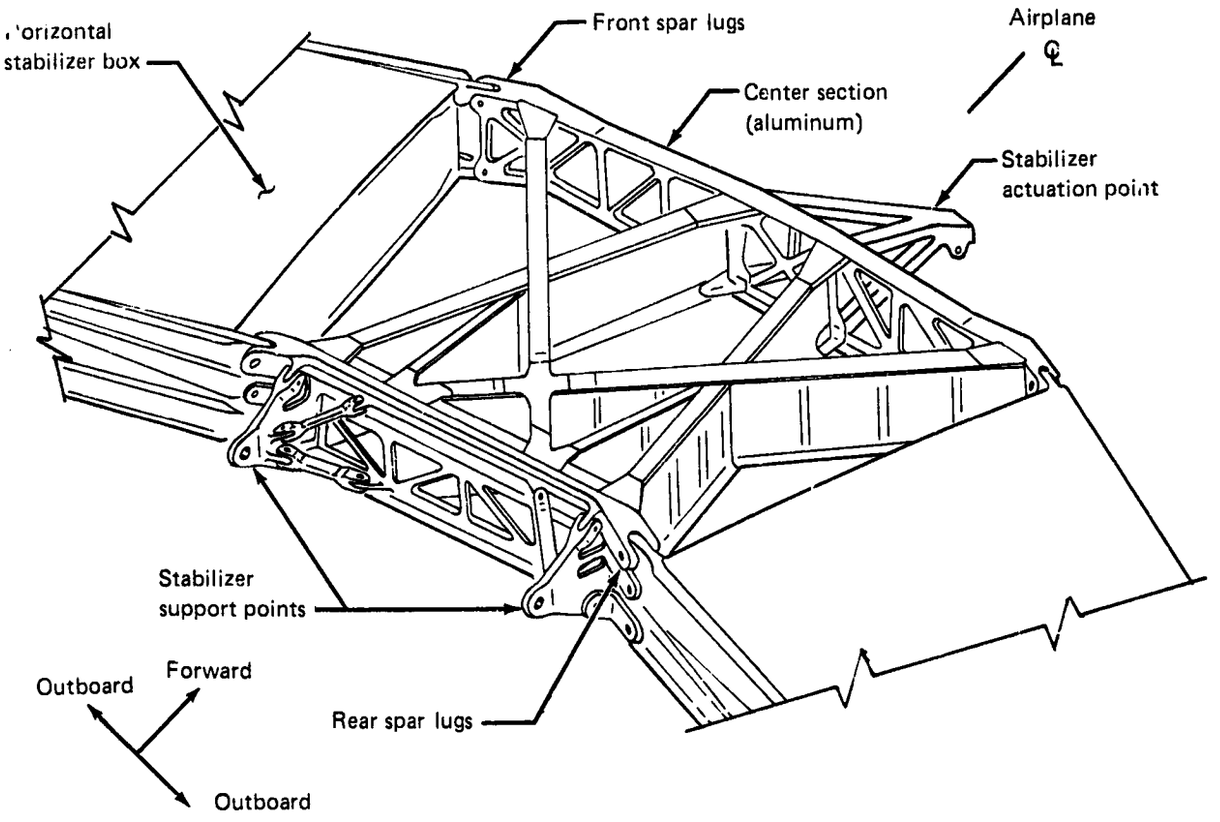

Figure 2. Center Section Interfaces

3.1.3 Design Trade Studies

3.1.3.1 Stabilizer Configuration

The primary box structure was redesigned using advanced composites. The box consists of the front spar, rear spar, inspar ribs, inboard and outboard closure ribs, and upper and lower skin panels. To satisfy requirements for interchangeability, no change was made to the interface with the center section and the elevator and to the spare parts. Included are components such as the tip, removable trailing-edge panels, and the gap covers. Other components in the trailing-edge and the fixed leading-edge structures were retained and modified as required to make them compatible with the new graphite-epoxy structural box. The skin gage of the removable leading edge was increased to satisfy the latest FAA bird-strike requirement.

3.1.3.2 Material Evaluation and Selection

A Boeing-sponsored independent research and development (IR&D) program selected and evaluated possible material systems using the tests and manufacturing considerations discussed in this section. In addition, an evaluation of material history and current industrial usage was made. The graphite fiber-epoxy resin systems investigated were:

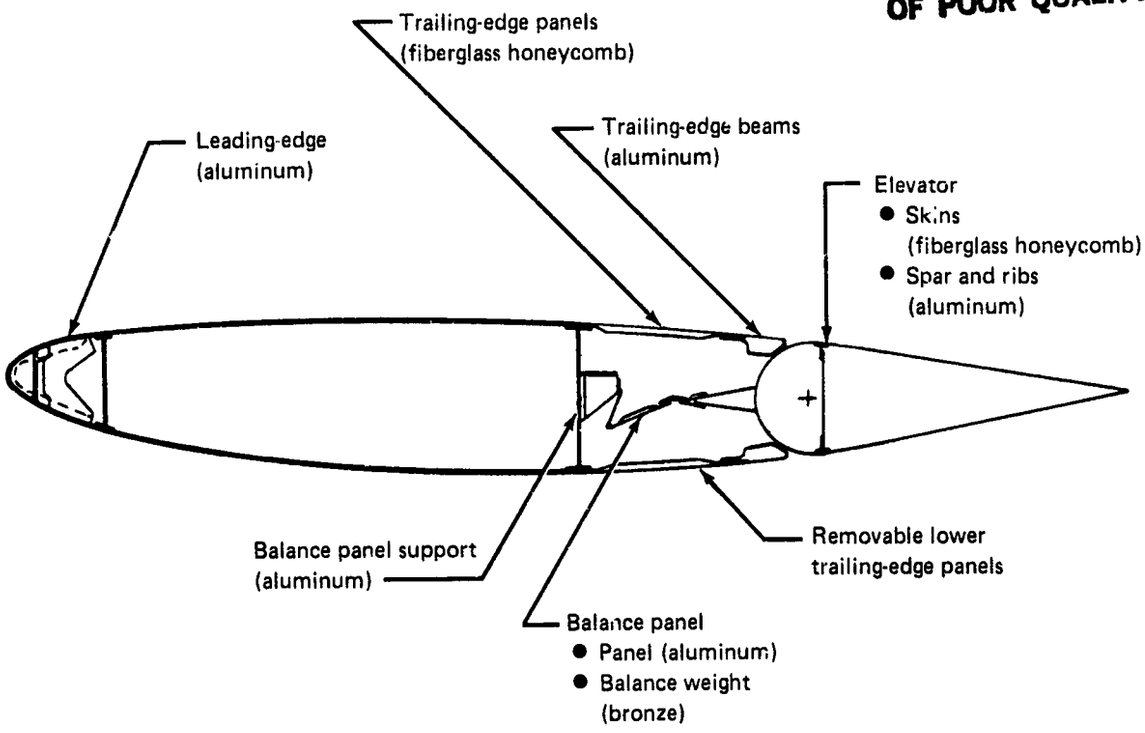

Figure 3. Horizontal Stabilizer Section

Graphite Fiber-Epoxy Resin System	Supplier
T300/5208	Narmco
T300/5235	Narmco
T300/934	Fiberite
T300/976	Fiberite
AS/3501-5A	Hercules
T300/F263	Hexcel
T300/F288	Hexcel

Each system was ordered and tested in the following forms:

- Preplied tape prepreg, 3.5-mil, 2-ply
- Unidirectional tape prepreg, 5.2-mil
- Plain-weave fabric prepreg, 7.0-mil

The materials were ordered to comply with specific tolerances on prepreg and cured laminate physical properties. Testing included:

- Resin
  - Differential scanning calorimetry (DSC)
  - Liquid chromatography (LC)
  - Thermal gravimetric analysis (TGA)
  - Glass transition temperature (TG)

- Prepreg
  - Resin content
  - Volatile content
  - Resin gel time
  - Resin flow
  - Graphite areal weight
  - T[illegible]k

- Laminate properties
  - Fiber volume
  - Density, thickness/ply, and void content
  - Weight
  - Tensile modulus
  - Elongation: tension and compression
  - Short beam shear
  - Ultimate strength: tension and compression
- Sandwich properties
  - Flatwide tension
  - Porosity
  - Peel strength
  - Weight

Manufacturing producibility was evaluated by fabricating from each candidate material a test panel representing typical layup complexity of actual structure. Drape, tack, work time, and degree of difficulty in layup were determined for each material system and form. Quality Control performed receiving inspection tests on all materials used in the evaluation and made a thorough comparison of supplier-certified test data and Boeing test results. In all instances, the supplier test data and Boeing test results compared favorably within acceptable limits. A Boeing process specification that describes autoclave cure cycles was developed before the contract go-ahead. The cure cycle developed for the process specification is shown in Figure 4.

Material selection consisted of analysis and comparison of the above tests and included additional factors such as:

- Available industrial data base
- Demonstrated resin durability in different environments
- Supplier production experience
- Supplier production capacity and control
- Supplier ability to provide all material forms
- Supplier cooperation for process audit

This Boeing-funded material evaluation resulted in selection of the Narmco 5208 resin system because it best satisfied a majority of the selection criteria.

3.1.3.3 Structural Box Arrangements

Three concepts were studied and evaluated for the stabilizer box structural design: a multiple rib, honeycomb, and stiffened skin. They are shown in Figure 5.

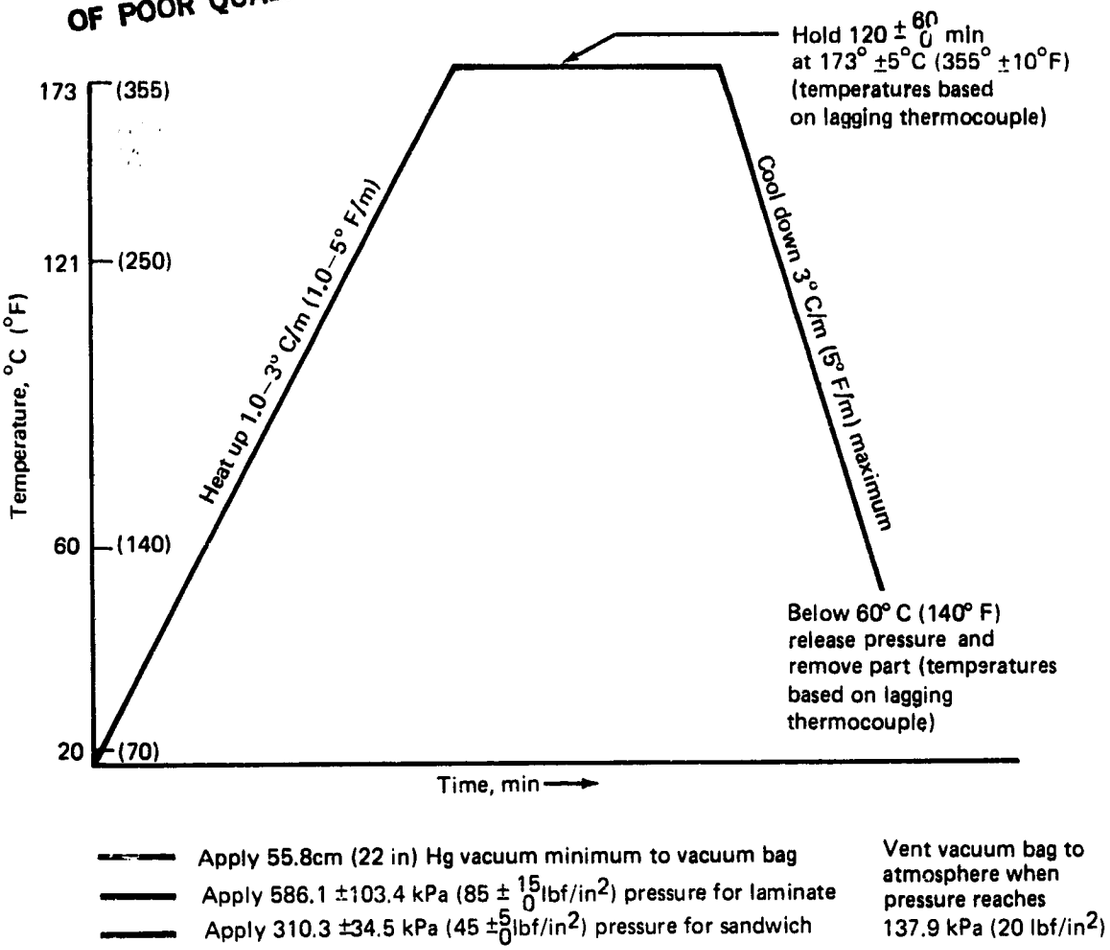

Figure 4. Cure Cycle—No-Bleed Material

Multiple Rib Concept—This design required numerous detail parts and fasteners. Although some of the details were simplified using the technology available with the use of advanced composites, this concept inherently required a large number of assembled parts. In addition, numerous layup tools were required to fabricate the ribs.

Honeycomb Concept—This design required a midspar to provide skin panel efficiency as well as several ribs to react the chordwise loads from the trailing edge and elevator. To be compatible with the current side-of-body attachment and to make the provisions for trailing-edge loads at elevator hinge support ribs, a large number of local doublers, pads, fillers, and pottings were required, making this concept increasingly more complicated.

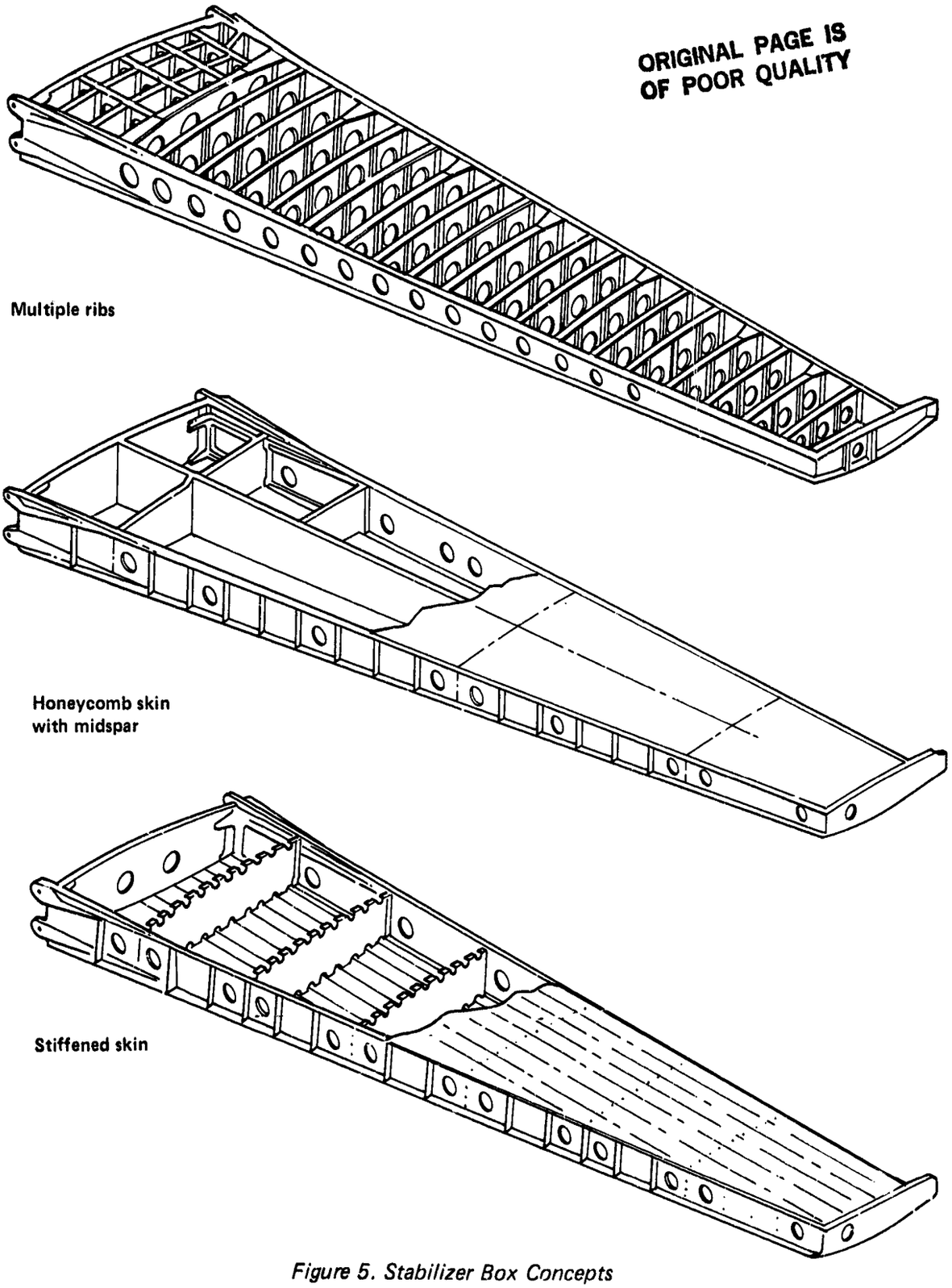

Figure 5. Stabilizer Box Concepts

Stiffened Skin Concept--This design concentrated the fabrication complexities in the skin panel and simplified the substructure by reducing the number of parts. The complexities in the skin fabrication lay in the detail tooling concepts for the stiffeners, and the basic layup tooling was the same as for the other concepts. Using the ability to cocure and bond large composite assemblies, the number of fasteners used in assembly was greatly reduced.

Because the weight of the three concepts was comparable, weight was not a deciding factor in the selection. The stiffened skin concept was selected for its high structural efficiency and minimum program cost. Another factor that reinforced the selection of this concept was the design concepts, technology, and experience that were directly applicable to a more highly loaded primary structure.

3.1.3.4 Stiffened Skin Concepts

After selecting the stiffened skin panel as the prime candidate, three types of stiffened skin concepts were evaluated: a hat section stiffener panel, blade stiffener panel, and an I-section stiffener panel. The three concepts are shown in Figure 6.

As an important design consideration, the entire skin/stiffener combination was cocured to achieve high bond reliability and to reduce fabrication costs.

Hat Stiffener Panel--This is an efficient and stable design; however, the cocuring process required internal tools considered difficult to remove from a compound contoured part, particularly in a 5.08m (200 in) long panel.

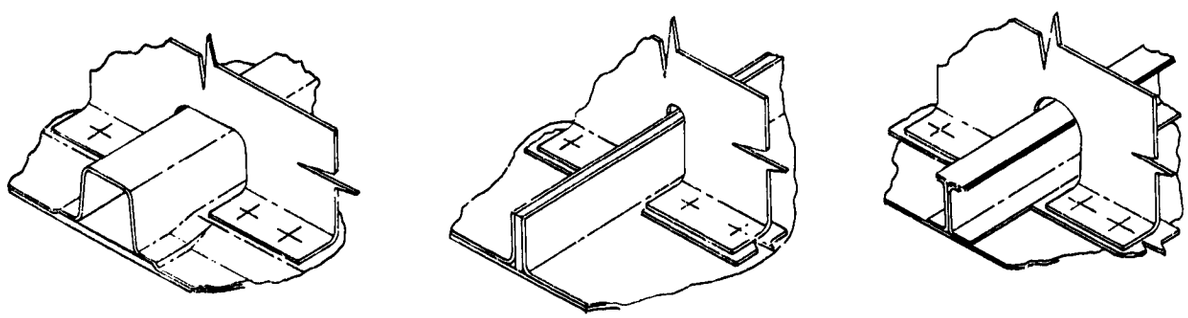

Hat stiffener panel | Blade stiffener panel | I-section stiffener panel

Figure 6. Skin Panel Concepts

Blade Stiffener Panel--This was a considerably simpler concept to design and build than was the hat stiffener. The design loses its efficiency, however, when used in conjunction with the rib spacing selected for the stabilizer. The critical design condition is the effect of air pressure on the skin surface combining with the panel end load to impose a beam-column loading on the panel.

I-Section Stiffener Panel--This design was efficient in the previously discussed beam-column loading. A low-cost, cocuring method that employed inexpensive tooling and used "as-extruded" constant aluminum sections was developed. Its manufacturing feasibility was verified by several panels that were fabricated on a Boeing-sponsored IR&D program. The I-stiffener panel was selected for this program because of its efficient and cost-effective tailoring to a wide range of design conditions.

3.1.3.5 Spar Chord/Lug Concepts

The lug joint between the composite stabilizer and the aluminum center section involved a large point-load transfer with a thickness restriction imposed by the clevis on the center section. A trade study was performed to examine various design concepts.

This trade study included a bolted titanium reinforced concept, a bonded interleaved titanium concept, and an all-graphite concept. The three designs are shown in Figure 7.

Bolted Titanium Plate Design—This concept used two machined titanium plates that were bonded using a polysulphide sealant for sealing purposes only and then bolted externally to a precured graphite-epoxy chord. It involved well-proven manufacturing methods that could be applied with a high degree of confidence.

Bonded Interleaved Titanium Design—This concept used two titanium plates that were precision step chem-milled and required the graphite-epoxy chord plies to be laid up net on the plates. The plates were bonded to the graphite-epoxy chords during the cure of the chord material.

All-Graphite Design—This concept involved transferring all the point-load through an all-graphite lug. This was the simplest configuration to design and fabricate; however, it required a larger lug for a given loading than the preceding two concepts, negating interchange at the side-of-body attachment.

The three lug concepts were fabricated and tested in an early Boeing-sponsored IR&D program. The test program was necessary because thick laminate and lug design data for these concepts were not available. The lug tests consisted of tension and compression ultimate static tests.

The bolted titanium-reinforced lug was selected for the program. Data generated during the test component fabrication showed this design to be the lowest in cost of the three concepts and the one that involved minimum risk.

3.1.3.6 Inspar Rib Concepts

Because of the large number of ribs required for the stabilizer box, Boeing sponsored an IR&D program to determine production characteristics of these components and associated projected costs of two design concepts. The two

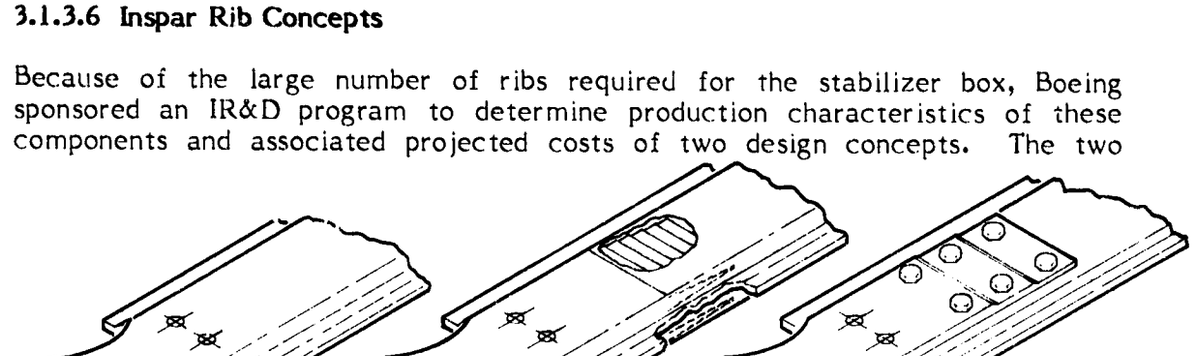

Figure 7. Spar Lug Concepts

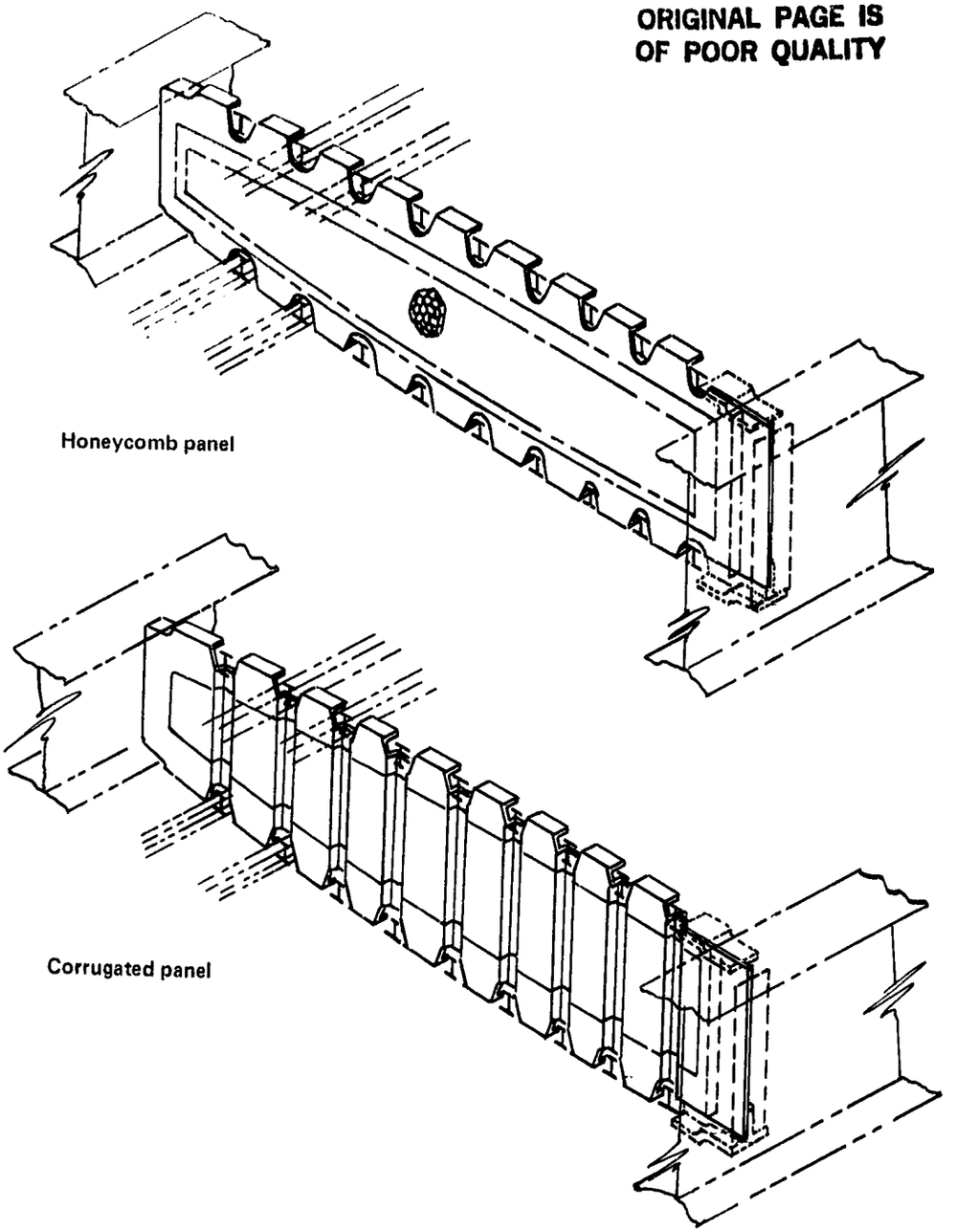

Figure 8. Rib Concepts

concepts studied were a honeycomb sandwich rib and a corrugated web rib shown in Figure 8. Compression tests were conducted on a section cut from fabricated specimens of each configuration. Figure 9 shows configuration, test results, design loads, and weights for the two rib concepts. Studies showed that the corrugated rib, using the proposed tooling and fabrication methods, was more than double the cost of the honeycomb version. The cost factors involved were:

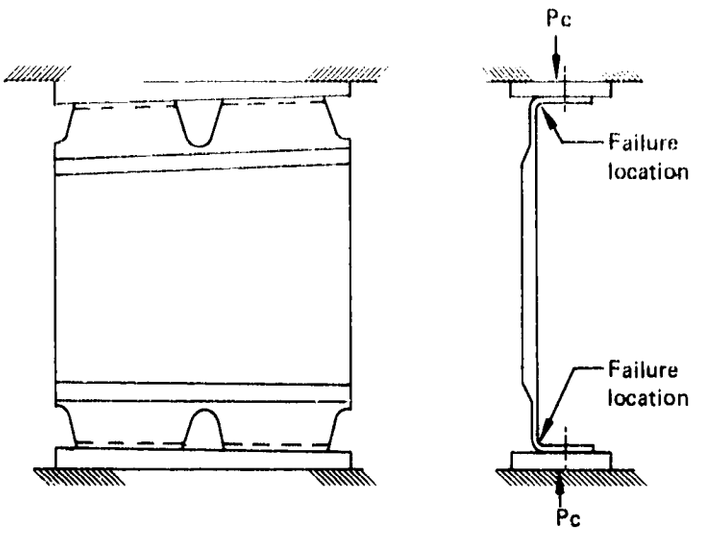

Predicted (calculated) failure load, N (lb)	4981 (1120)	Honeycomb rib and corrugated rib
Test failure load, N (lb)	6140 (1380)	Honeycomb rib
	12 450 (2800)	Corrugated rib
Honeycomb rib spring stiffness, N/m (lb/in)	8 633 751 (49 300)	
Corrugated rib spring stiffness, N/m (lb/in)	10 665 222 (60 900)	
Rib spring constant required to stabilize skin/stringer panel, N/m (lb/in)	140 101 (800)	
Honeycomb rib test load, N (lb) [1]	6140 (1 380)	
Honeycomb rib test load, N/m (lb/in) [1]	31 348 (179)	
Corrugation stiffened rib test load, N (lb) [1]	12 450 (2 800)	
Corrugation stiffened rib test load, N/m (lb/in) [1]	63 746 (364)	
Rib design crushing load, N/m (lb/in) (10% of panel end load)	17 512 (100)	
Calculated rib design crushing load, N/m (lb/in) [2]	5 604 (32)	
Actual weight of honeycomb rib, kg (lb)	1 (2.2)	
Actual weight of corrugation stiffened rib, kg (lb)	0.9 (2.0)	

[1] Specimen length, 195.6 mm (7.70 in).
[2] Reference: Niles and Newell, Aircraft Structures, vol. II, 3d ed., Wiley, 1943.

Figure 9. Rib Compression Test

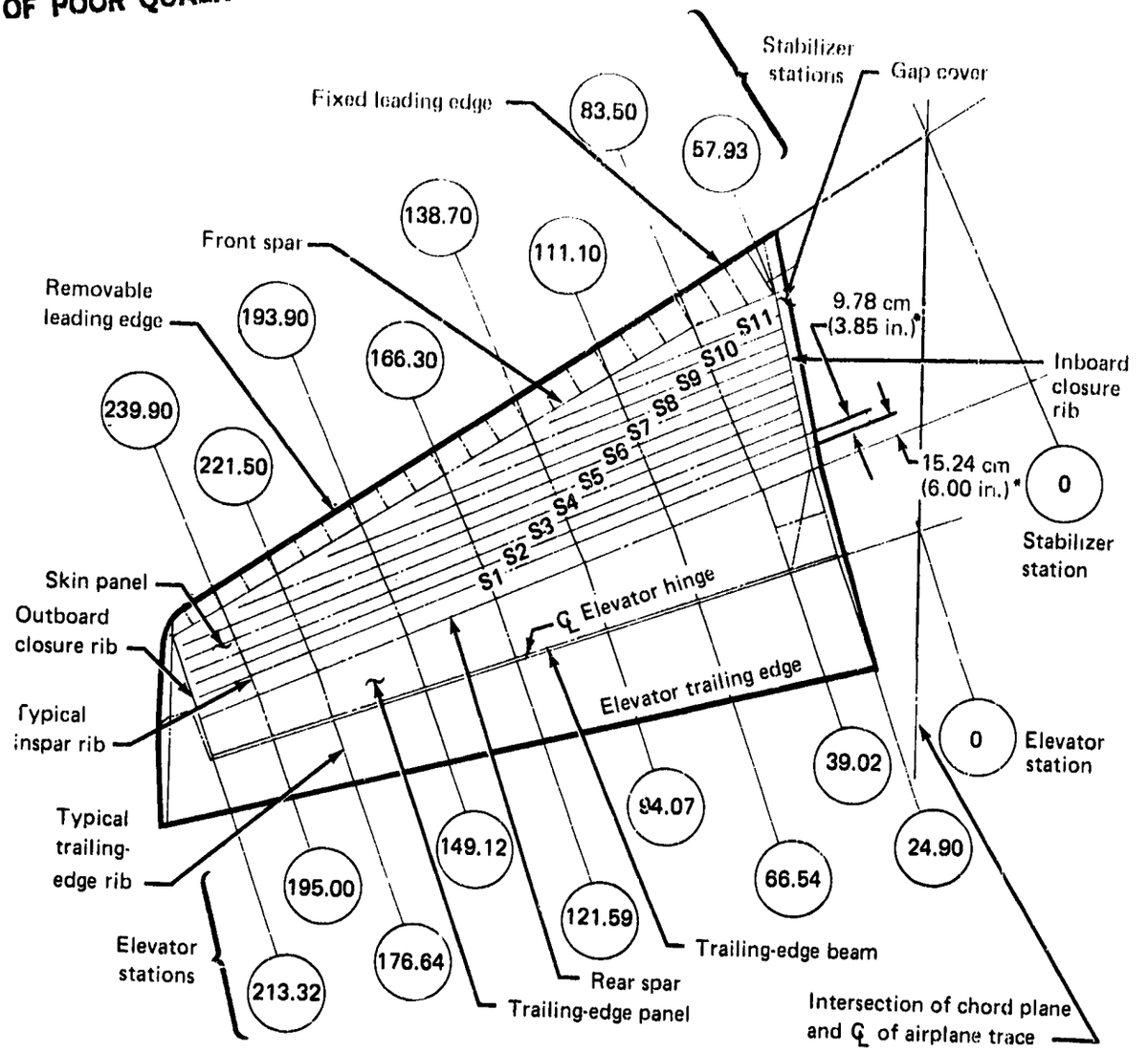

*Same for upper and lower panel.

Figure 10. Advanced Composite Horizontal Stabilizer

- The corrugated rib concept: this is a labor intensified concept with hand layup. It is susceptible to bridging problems in corner radii and requires individual tool dies because of contour changes if automated (molding process). It is expensive.

- The honeycomb concept: this concept involves simple flat surfaces and is easy to lay up by hand or automation. It lends itself to the use of a tape laminator.

The honeycomb design was chosen.

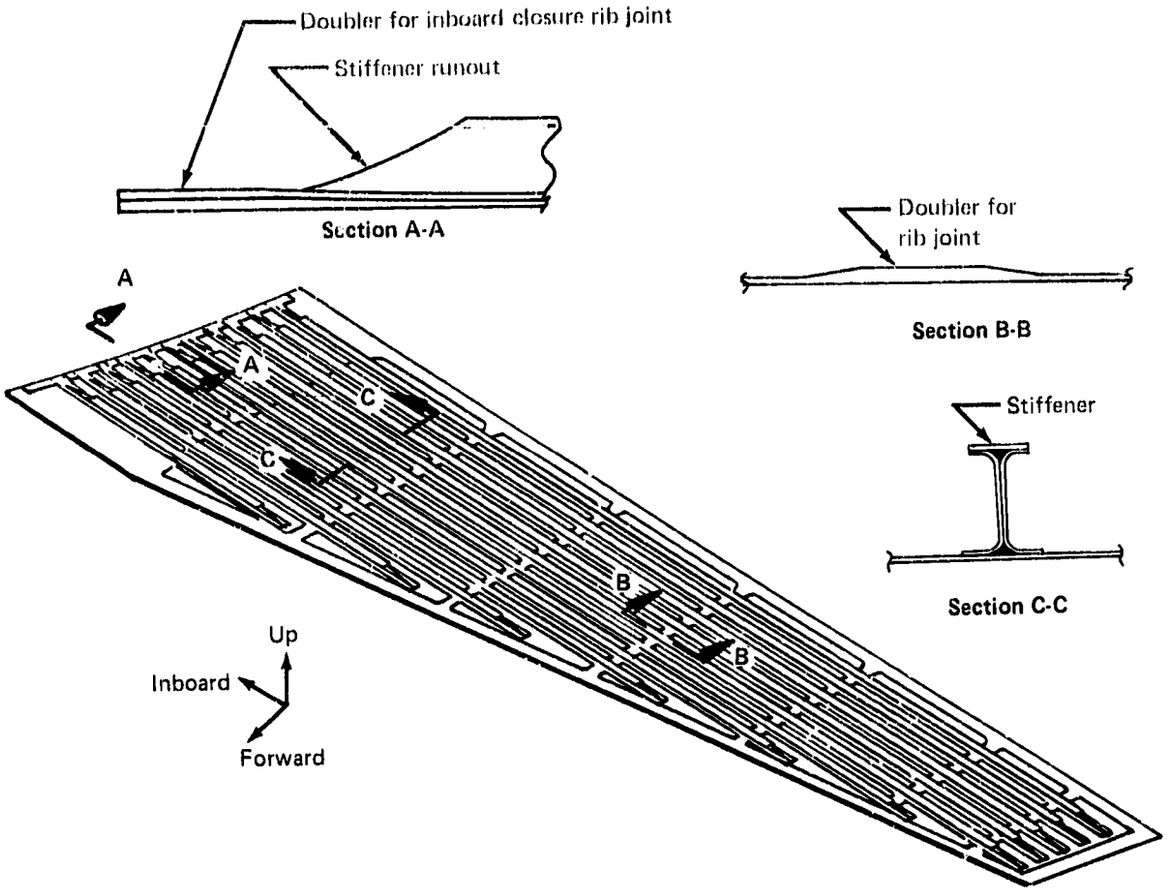

Figure 11. Skin Panel

3.2 DETAIL DESIGN–COMPONENT DEFINITION

The structural arrangement of the advanced composite stabilizer (fig. 10) was selected to achieve maximum commonality with the model 737 metal configuration. As a consequence, the front and rear spars were located on the same centerlines as the existing stabilizer to simplify the interface with the stabilizer center-section structure and to minimize changes to the existing leading- and trailing-edge structure interfacing with the spars. The inspar ribs were placed at existing trailing-edge rib locations. This produced a rib spacing of 69.8 cm (27.5 in) except at the outboard end of the stabilizer where the spacings were smaller.

3.2.1 Skin Panel Configuration

The I-section stiffener skin panel design was used in both upper and lower surfaces. Contours of the upper and lower surfaces are different, but structural configurations are basically the same for the two panels.

Each skin panel is a single piece, cocured graphite-epoxy laminate extending from the side of the body to the stabilizer tip and from the front spar to the rear spar as shown in Figure 11. The length of each skin is 485.1 cm (191.0 in), and the width is

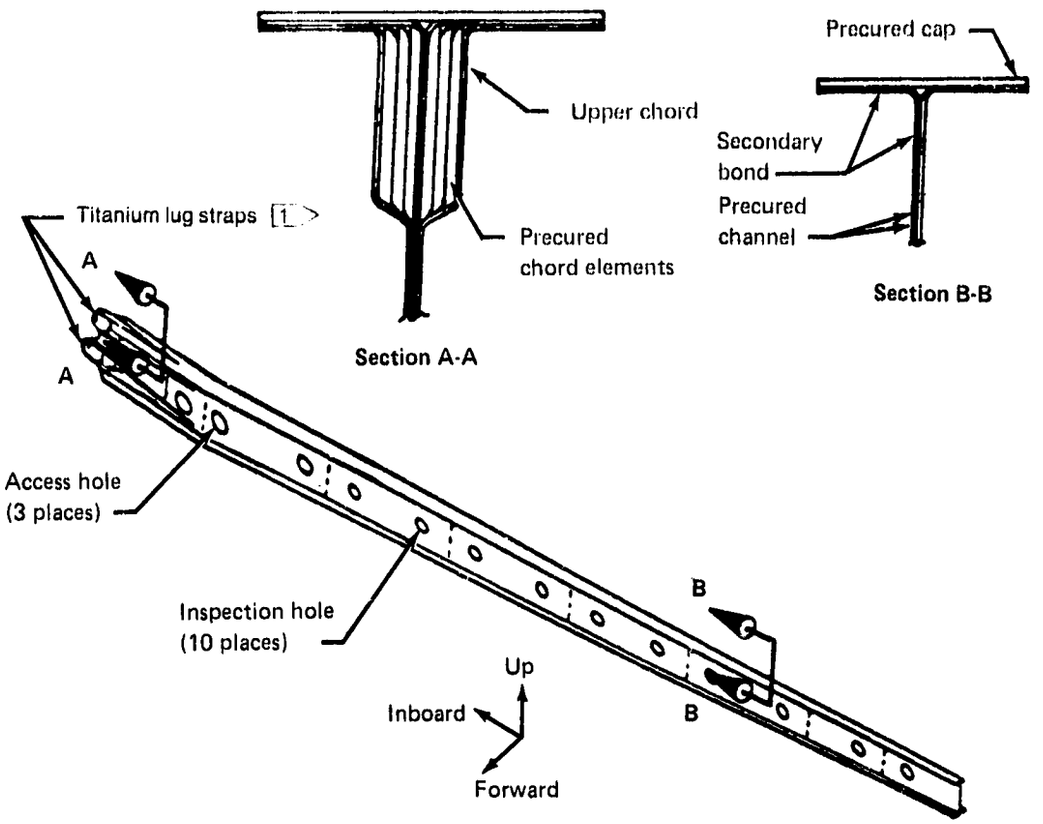

[1] (15-5 PH) stainless steel was substituted because of the unavailability of heat-treated titanium.

Figure 12. Front Spar

128.3 cm (50.5 in) at the inboard end. Stiffeners are spaced 9.8 cm (3.85 in) apart and are located parallel to the rear-spar centerline. Stiffener spacing was selected to allow adequate space for a mechanical joint between the skin and the rib flanges while providing the support required by the skin to react the compressive and shear loads. The I-section stiffener was fabricated from two fabric layup channels that were placed back to back. Unidirectional graphite-epoxy tape was placed on top of the channels to provide additional material.

The basic skin thickness and the graphite fiber orientation were selected to match the torsional stiffness of the model 737 metal horizontal stabilizer. Doublers were provided on:

- The skin at the inboard end where the inspar stiffener and skin loads were transferred to the spar chords and spar lugs.
- The skin panels along the spar attachment to improve the bearing load capability of the mechanical joints.

Skin pads also were provided at each rib interface. These reinforcements improved the pull-through strength of the countersunk heads of the mechanical fasteners under the external air pressure loading.

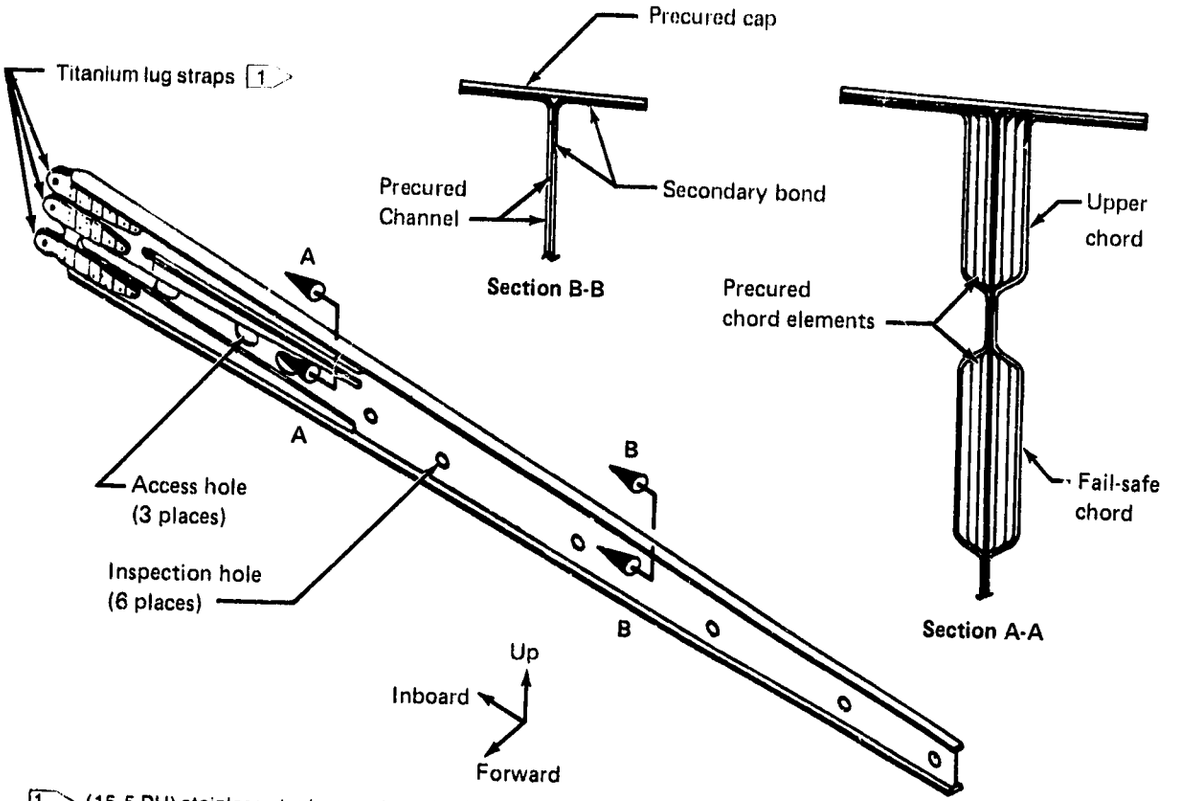

[1] (15-5 PH) stainless steel was substituted because of the unavailability of heat-treated titanium.

Figure 13. Rear Spar

3.2.2 Spar Configuration

Both front and rear spars are bonded assemblies of graphite-epoxy laminates extending the entire length of the stabilizer from the side of the body to the tip. The rear spar is 485.1 cm (191.0 in) long and 38.7 cm (15.25 in) deep at the inboard end. The front spar is 509.3 cm (200.5 in) long and 31.1 cm (12.25 in) deep at the inboard end. The design concept is the same for both spars except that the rear spar chord areas are significantly greater than those of the front spar because of higher loads carried by the rear spar.

The rear spar is a straight member along the centerline, but the front spar contains a bend 65.0 cm (25.6 in) from the inboard end, as shown in Figure 12. The rear spar is shown in Figure 13.

Both spars are reinforced with titanium straps at the lugs that join the stabilizer to the center-section structure as shown in Figure 14. Development work performed on the titanium reinforcement concept is described in Section 3.1.3.5.

The basic spar is an I-section that provides attachment flanges for the stabilizer box skins and leading and trailing edges. The I-section is constructed of two precured channels and two precured caps that are subsequently bonded together. The spar web thicknesses and the graphite fiber orientations are selected to match the shear stiffness of the model 737 metal stabilizer webs. The web is stiffened with mechanically attached angle stiffeners.

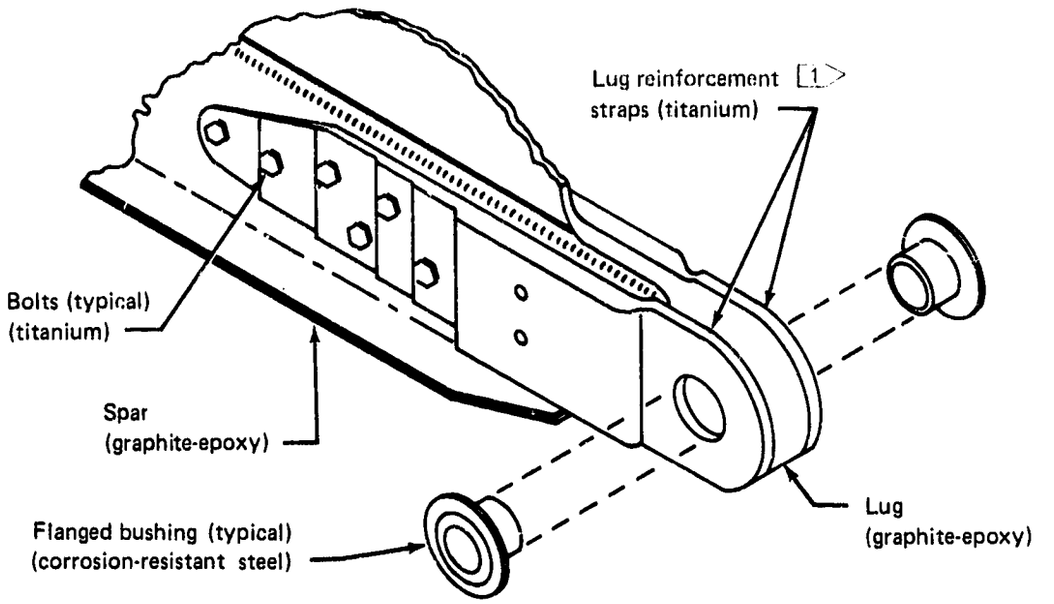

[1] (15-5 PH) stainless steel was substituted because of the unavailability of heat-treated titanium.

Figure 14. Spar Lug

Chord areas increase significantly near the inboard end where the skin panel loads are transferred into the spar and to the lugs. The spar chords in these areas, where very thick laminates are required, are made with stacked, precured laminate strips to ensure quality control during the epoxy cure cycle and to provide easier quality control inspections of these areas.

The rear spar contains a third lug to provide for fail-safety. A similar lug is not required on the front spar because load paths remain with a failure in either front spar lug.

3.2.3 Typical Inspar Rib Configuration

There are seven inspar ribs in the stabilizer box. These ribs are a cocured honeycomb sandwich design that resulted from the trade study described in Section 3.1.3.6. The ribs have channel-shaped cross sections with cutouts along the upper and lower integral attach angles to allow clear passage of the skin panel I-stiffeners shown in Figure 15. The attach angle for the front spar is integral with the rib web. At the rear spar, there is a separate attach angle to take up manufacturing tolerances. The attach angles provide mechanical joining of the skins and spars to the ribs. The honeycomb core is protected from moisture absorption through the face sheets by a Tedlar film applied on the bag side and paint on the tool side.

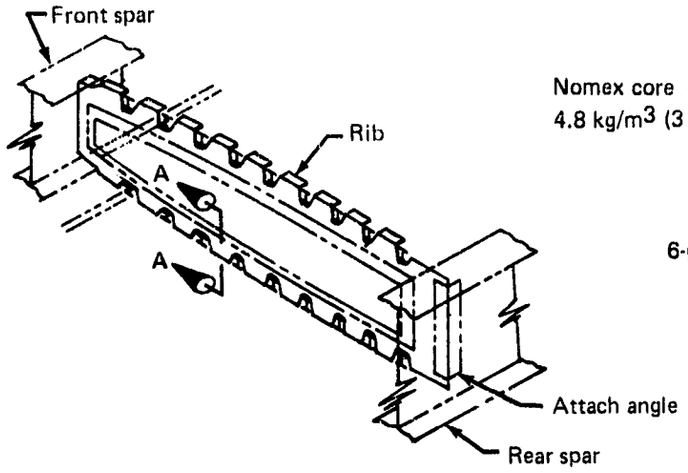

Typical inspar rib

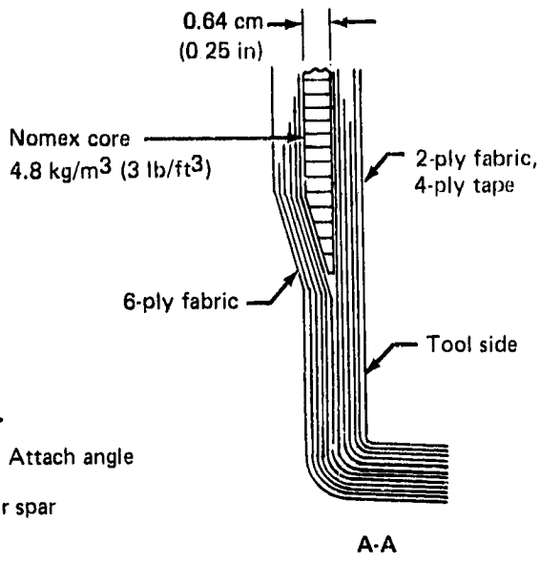

A-A

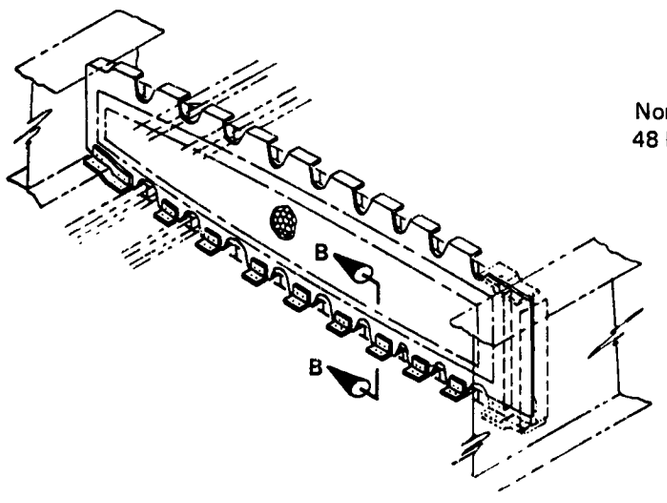

Inspar rib

Stabilizer station 83.50

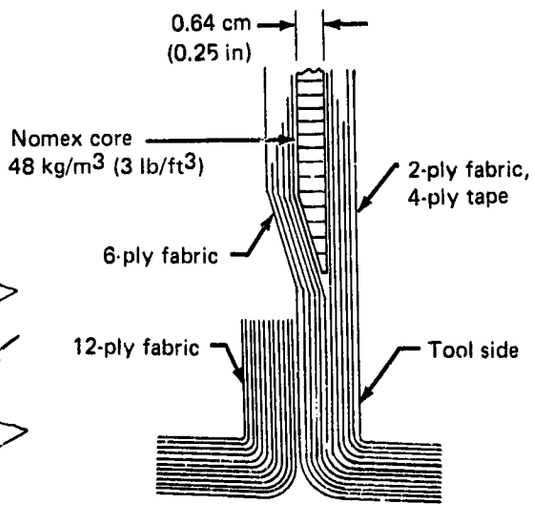

B-B

Figure 15. Inspar Rib

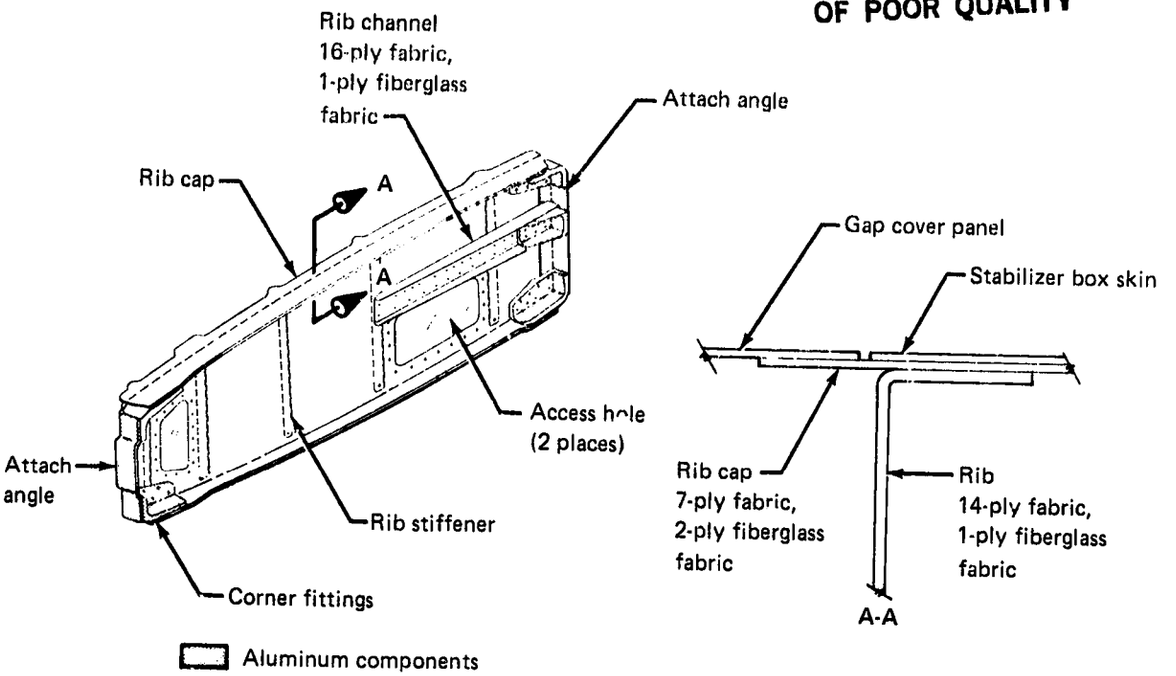

Figure 16. Inboard Closure Rib

3.2.4 Inboard Closure Rib

The rib closes the inboard end of the stabilizer box assembly. Its structural function is to react against the torsional shear load in the skin panels and distribute the load into the front and rear spars, which are reacted by the stabilizer center section. The height of the rib is 41.7 cm (16.4 in), and the width is 127 cm (50 in).

The rib is a mechanically joined assembly of a channel-shaped graphite-epoxy laminate section with graphite-epoxy cap strips along the upper and lower sides that form an I-section (fig. 16). The outer sides of the cap strips attach to the stabilizer box skins, and the inboard sides are attached to the body gap cover panels.

On the inboard side of the rib, channel-shaped intercostals are mechanically fastened to the rib web. These stabilize the web under shear and compression loads and provide support for the body gap covers.

Access holes are located in the forward and aft ends of the rib to provide generous access for assembly and inservice inspection of the front and rear spar lugs. These holes are covered with structural access covers that are mechanically attached with bolts and nutplates.

The rib is joined to the spars with aluminum "bathtub" corner fittings and machined aluminum attach angles. The corner fittings redirect the leading- and trailing-edge loads into the rib. At the rear spar, an additional aluminum bathtub fitting joins the fail-safe lug to the rib web. A channel-shaped stiffener is used to transfer the load from the fitting into the rib web.

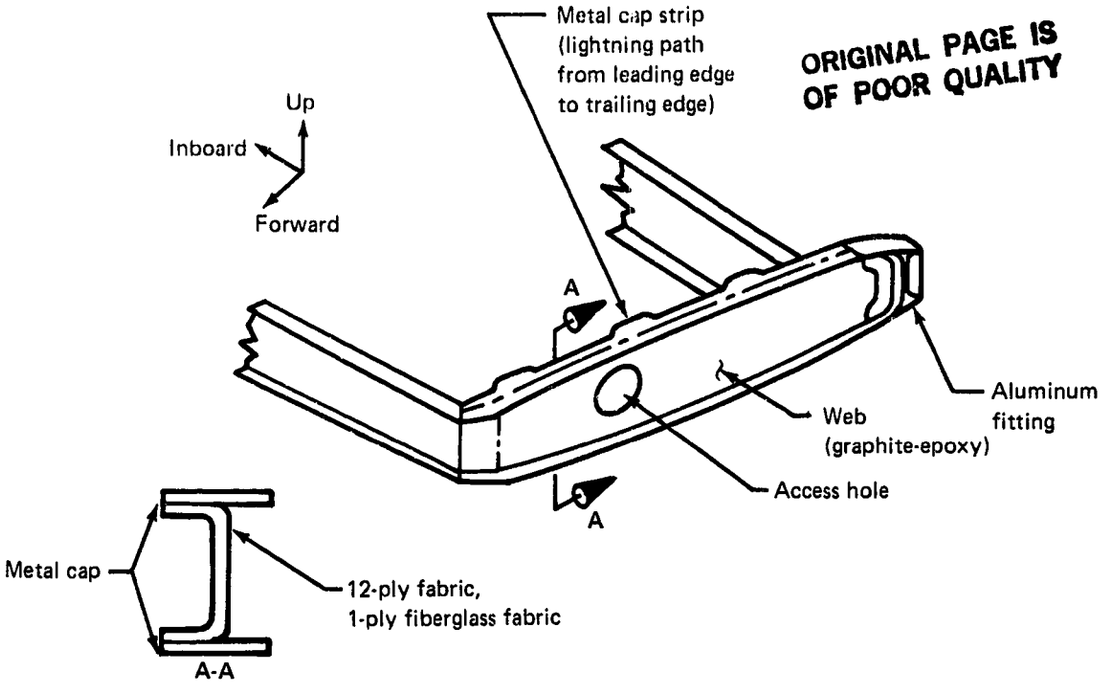

Figure 17. Outboard Closure Rib

All details making up the rib assembly are of constant thickness graphite-epoxy laminate parts. The graphite-epoxy details interfacing with aluminum fittings have 1 ply of fiberglass on their mating surface for corrosion protection of the aluminum fitting. The aluminum fittings and attach angles are made from existing forgings and extrusions used on the metal stabilizers.

3.2.5 Outboard Closure Rib

This rib closes the outer end of the stabilizer box and provides attachment for the most outboard elevator hinge. The rib, shown in Figure 17, is a channel-shaped laminate section with aluminum upper and lower cap strips that form an I-section. The outboard side of the cap strip joins to the tip fairing assembly, and the inboard side attaches to the stabilizer box skins. At the forward end of the rib, there is an integral attach angle that is mechanically fastened to the front spar web. At the aft end, the rib and the aluminum cap strips are mechanically attached to the aluminum elevator hinge-support fitting. The rear spar is mechanically attached to the rib web through a separate attach angle.

The rib channel is a constant thickness graphite-epoxy laminate with 1 ply of fiberglass on the outer surface for corrosion protection of the aluminum details. The cap strips are aluminum to provide an electrical path between the metal leading-edge assembly on the forward end and the elevator aluminum spar. The electrically conductive paint on the fiberglass tip fairing and the flame-sprayed coatings on the outer surfaces of the stabilizer skin panels are electrically tied to the aluminum cap strips through mechanical fasteners. This is detailed in Section 3.2.9.

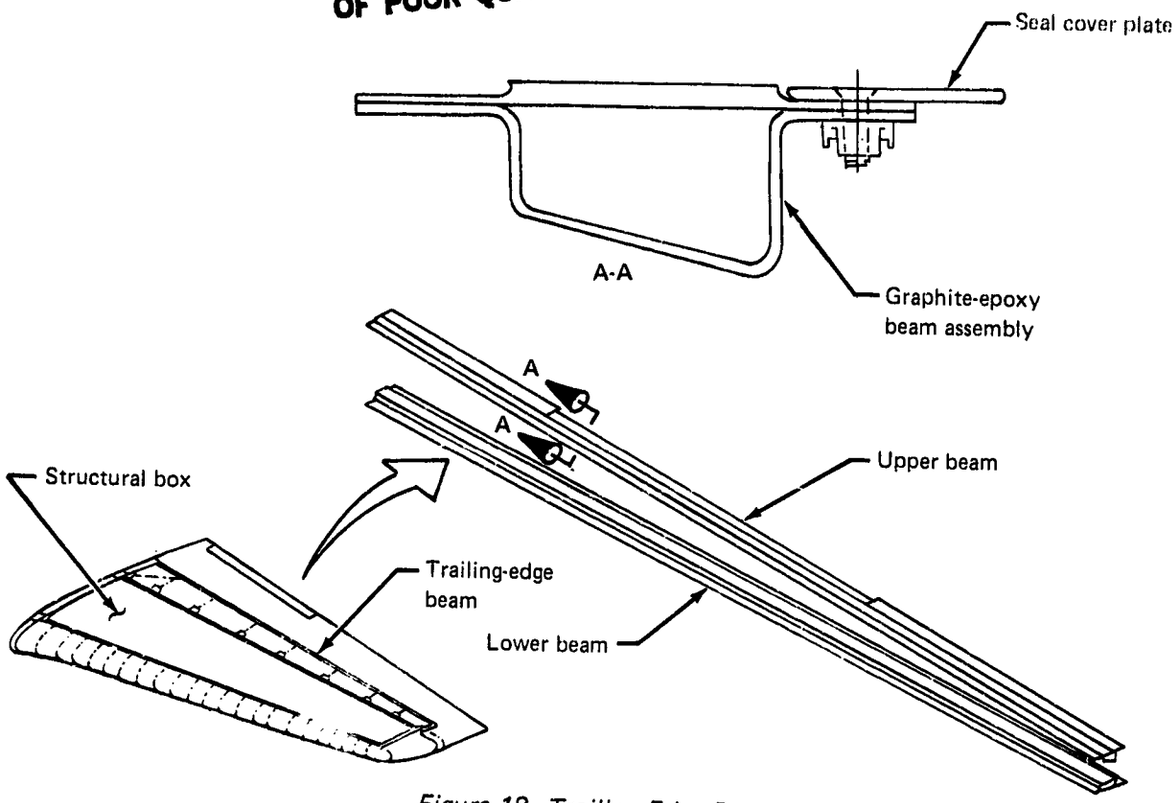

Figure 18,. Trailing-Edge Beam

3.2.6 Trailing-Edge Beam

The trailing-edge beam (fig. 18) supports the aft edge of the trailing-edge panels and longitudinally ties the trailing-edge ribs together. The beam was made from graphite-epoxy as part of the design to accommodate thermal expansion in the stabilizer trailing-edge area. To use existing assembly tools and to minimize changes to interfacing components, the external shape of the graphite-epoxy beam is identical to the current aluminum beam. To maintain the same deflections under airloads, the beam was designed with the same stiffness as was the current aluminum beam.

The beam is a bonded assembly of a hat-shaped section and a two-piece flat sheet cap. All details are constant thickness graphite-epoxy laminates. The beam is mechanically attached to the trailing-edge panels and ribs. A stabilizer-to-elevator gap seal is mechanically attached to the beam.

3.2.7 Stabilizer Assembly

The stabilizer box was assembled with mechanical fasteners. Titanium Hi-Lok fasteners with corrosion-resistant steel (CRES) collars and washers were used whenever possible. Whenever internal access was limited for Hi-Lok installation tools, CRES nuts were used with CRES washers. For closeout areas, the Monogram "Bigfoot" blind bolts were used. Removable panels, doors, and seals were assembled with CRES bolts and nutplates. All fasteners in graphite-epoxy parts were installed in 0.000 to 0.008 cm (0.000 to 0.003 in) clearance holes.

3.2.8 Corrosion Protection System

A corrosion protection system was developed for use on the advanced composite stabilizer. Basically, the corrosion protection system was designed to isolate graphite-epoxy surfaces from aluminum structure to minimize the cathodic area (graphite) available for electrochemical reactions. This minimizes the potential current flow and thus, galvanic corrosion of aluminum structure.

The corrosion protection system provides a level of corrosion resistance for the advanced composite stabilizer equivalent to that of the existing aluminum stabilizer. This was determined by comparing the amount of corrosion products on samples that were representative of the aluminum stabilizer structure and the advanced composite structure after exposure to salt spray. Several corrosion protection designs (including the use of fiberglass, Tedlar, paint, and polysulfide sealant to isolate the aluminum from the graphite) were investigated in a Boeing-funded study. Assemblies incorporating candidate corrosion protection systems were subjected to salt spray. Conventional anodized and primed aluminum parts were used as control specimens to compare the corrosion resistance of the parts under test.

The corrosion protection system selected consisted of covering graphite-epoxy surfaces that interface with aluminum structure with a ply of fiberglass cocured with the graphite-epoxy or painted with primer and epoxy enamel. All graphite-epoxy surfaces that are within 7.62 cm (3 in) of aluminum, including cut edges, were primed and enameled. An exception was on surfaces where Tedlar film could be applied to the graphite-epoxy layup during cure. Tedlar film is preferred over primer and enamel because Tedlar is lighter and the cost of application is less than that of paint. If the part was not painted, the cut edges were fillet sealed on assembly. In addition to the isolation of graphite-epoxy surfaces from aluminum structure, all aluminum details were anodized or alodine treated, primed, and enameled. On assembly, a polysulfide faying surface seal was applied between the graphite-epoxy part and the aluminum part. Fasteners through the aluminum part were installed with wet polysulfide sealant. An example of the corrosion protection system is detailed in Figure 19.

3.2.9 Lightning Protection System

A lightning protection system was developed for use on the advanced composite stabilizer. The system provided an electrical path around the entire perimeter of the graphite-epoxy structural box and supplied conductive coating over the graphite-epoxy structural box in the critical strike area, as shown in Figure 20.

The electrical path around the graphite-epoxy box was provided by the aluminum leading edge, the aluminum rib cap of the outboard closure rib, and the aluminum elevator spar. These components were electrically connected by bonding straps. The stabilizer was electrically grounded to the fuselage through the aluminum center section. The electrical path to the center section was provided through the titanium lug straps and the leading- and trailing-edge ribs.

In the critical strike area, aluminum flame-spray was applied over the outboard 48 cm (18 in) of the upper and lower skin surfaces. Over these surface areas, a layer of fiberglass was cocured with the skin panels to provide an insulation layer.

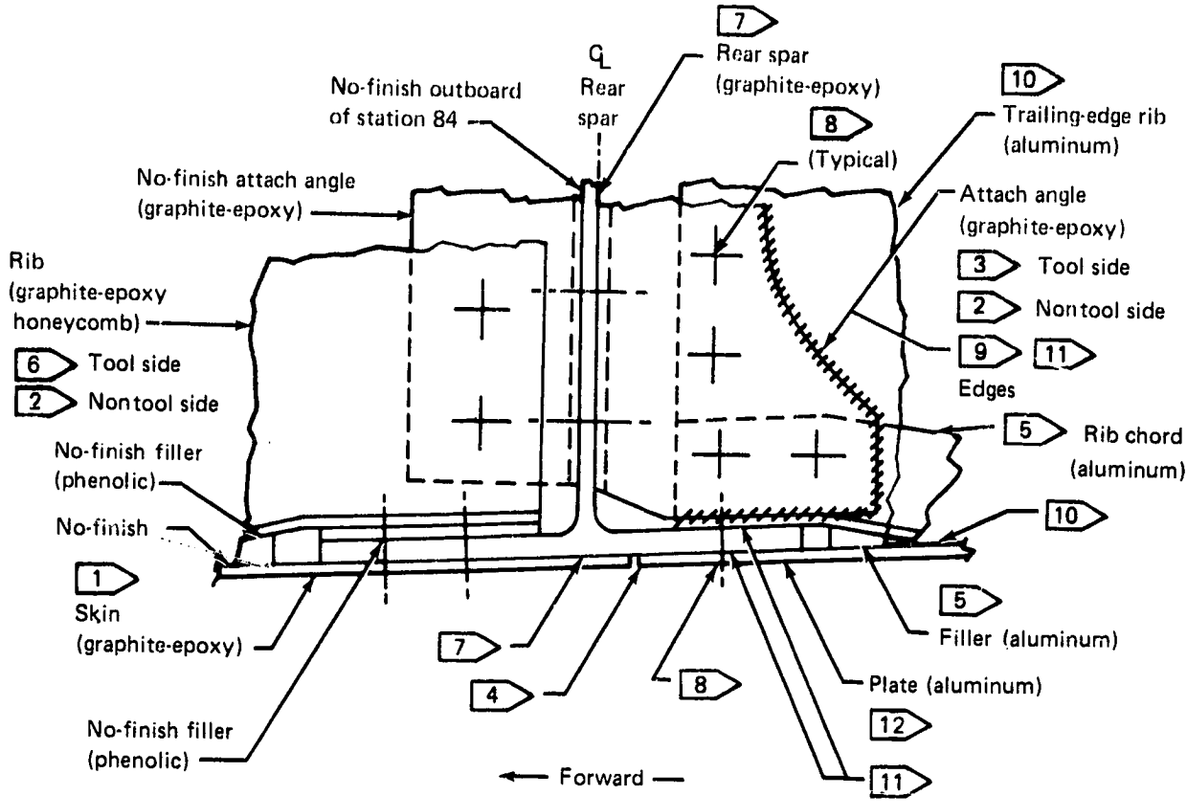

1 Pinhole filler and surfacer + primer and polyurethane gray enamel

2 1 ply Tedlar film (PVF) transparent 100 BG, 30 TR

3 Epoxy impregnated fiberglass fabric, type 120; cocure with graphite-epoxy

4 Aerodynamic smoother

5 Anodize and primer + white enamel

6 Pinhole filler and surfacer + primer and white epoxy enamel

7 Same as 6 except surfacer omitted

8 Wet install fastener with corrosion protection sealing

9 Fillet seal

10 Alodine and prim[illegible] + white enamel

11 Faying surface seal

12 Alodine and primer + polyurethane gray enamel

Figure 19. Corrosion Protection System

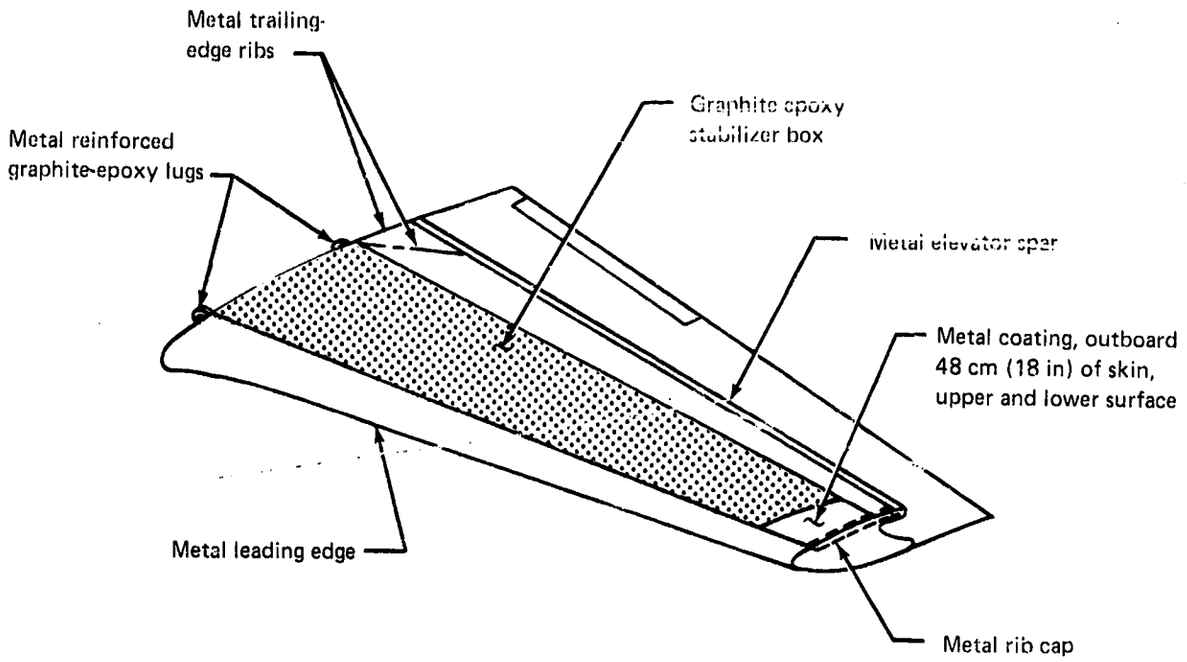

Figure 20. Stabilizer Lightning Protection

The flame-spray was applied after the skin panel fabrication. This process eliminated any induced thermal stress that would occur from the high-temperature cure cycle required for skin fabrication. On final assembly, the conductive coating was electrically connected to the aluminum rib cap of the outboard closure rib by four mechanical fasteners and dimpled washers (sec. 3.2.5). The flame-spray surface was then alodine coated, primed, and painted with the decorative finish. This is shown in Figure 21.

3.2.10 Thermal Expansion Compensating System

The greater thermal expansion of the existing aluminum/fiberglass elevator, in comparison to the graphite-epoxy stabilizer box, required modifications in the trailing-edge area to limit thermal stress levels and to allow for unrestricted movement of the elevator. The structural components that required attention were the elevator hinge support structure, the interfaces of the balance panels with the support structure, and the fixed trailing-edge structure.

The design approach was to replace the aluminum trailing-edge beam with a graphite-epoxy design (sec. 3.2.6). This eliminated any thermal-induced loads in the fixed trailing-edge structure. Next, a thermal compensating mechanism was designed to provide the primary load path for the elevator side load at elevator station 39.02, while allowing the elevator thermal-induced length change to be centered about elevator station 121.59 (fig. 22).

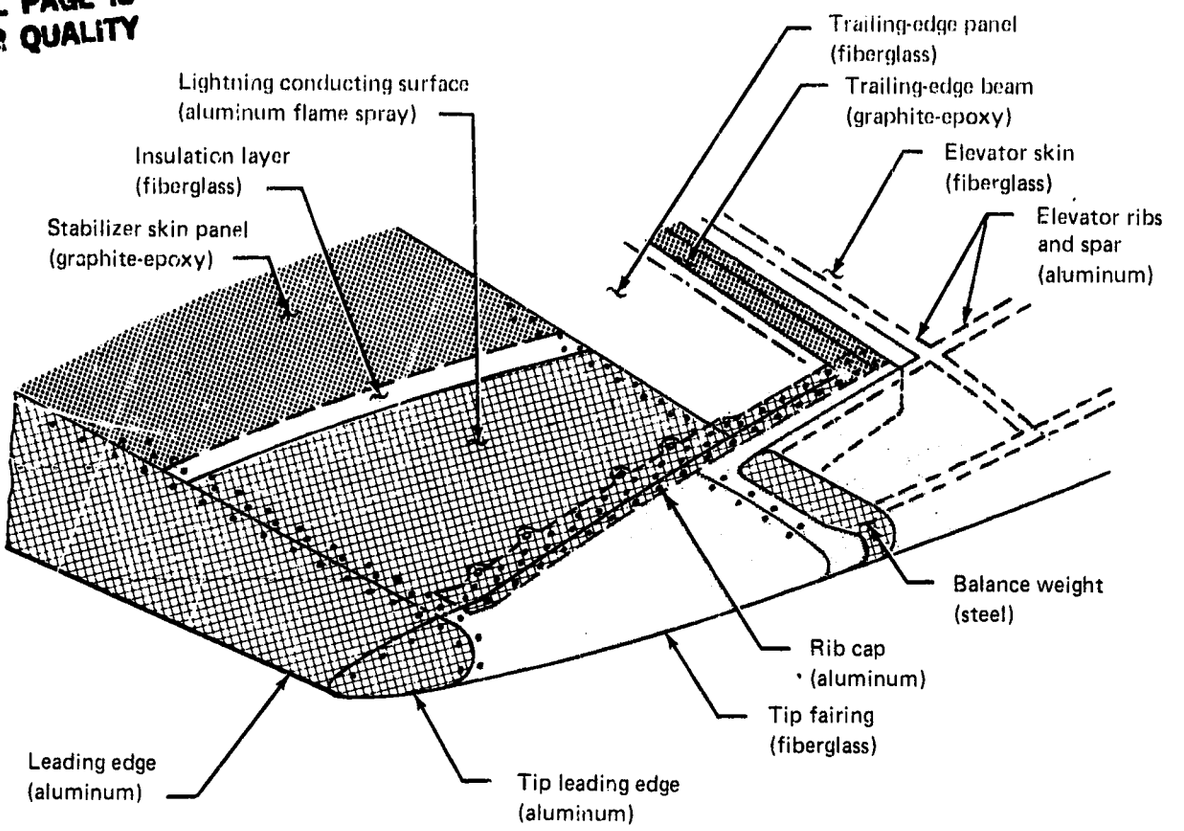

Figure 21. Lightning Protection System

This mechanism automatically adjusted for the elevator thermal expansion by amplifying the relative movement of the aluminum strut with respect to the graphite-epoxy rear spar causing the side-load hinge fitting to rotate in unison with the elevator expansion. At elevator stations 24.90, 66.54, 176.64, and 213.32, the stabilizer hinge support fittings were modified to provide a sliding bushing design. This allowed the elevator to expand without any lateral constraint. At elevator station 121.59, the existing clamped hinge design was kept to provide a fail-safe load path for the side-load condition. Because the thermal compensating mechanism keeps the elevator thermal expansions centered about this hinge location, the existing elevator has unrestricted movement regardless of the temperature changes, while existing load paths are maintained. Finally, the piano hinge attachment for the balance panels at the stabilizer interface were slotted to allow free movement of the balance panels with elevator thermal expansions.

3.2.11 Structural Repair Documentation

Structural repair requirements and techniques were developed for the advanced composite stabilizer and published in the Advanced Composite Horizontal Stabilizer for Boeing 737 Aircraft, Structural Repair Manual, D6-46035 (app. A). The repair procedures were qualified by testing discussed in Section 4.2.6.

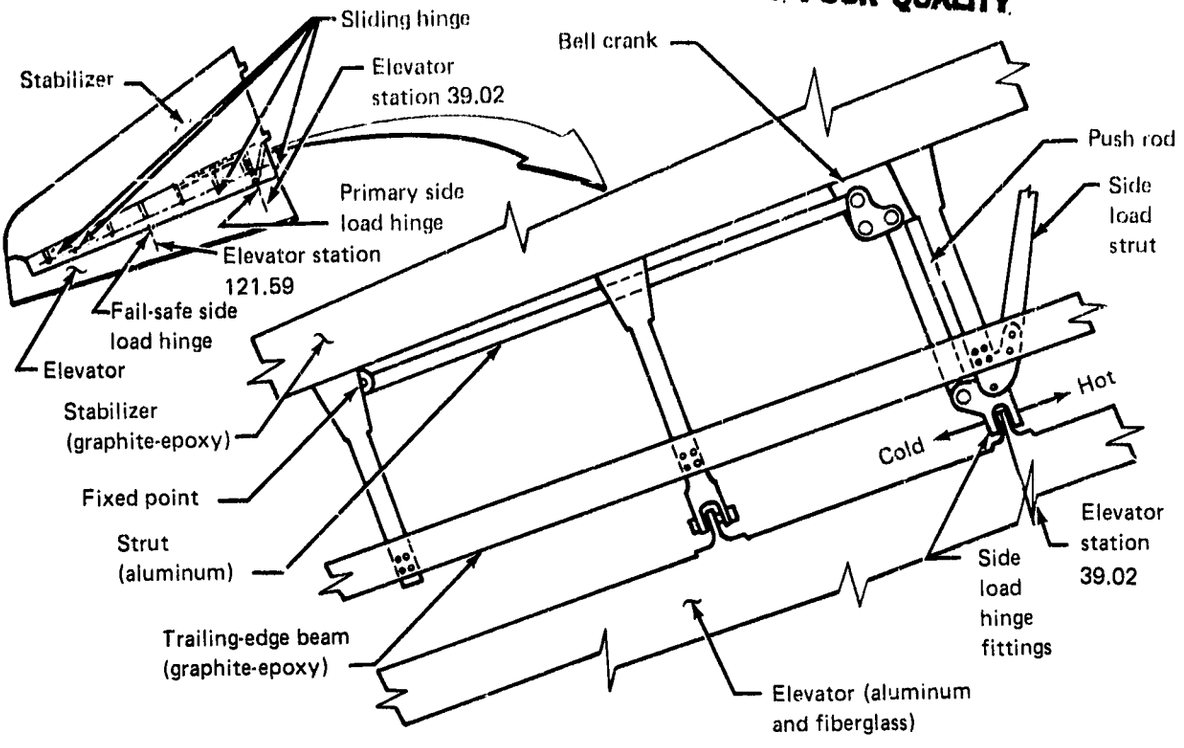

Figure 22. Thermal Expansion Compensating Mechanism

3.2.12 Maintenance and Inspection Documentation

Maintenance planning recommendations were developed as a general guide for individual airlines as they establish maintenance programs for Boeing model 737-200 aircraft with advanced composite stabilizers. These recommendations are published in the Maintenance Planning Data, Aircraft Structural Inspection, Composite Horizontal Stabilizer, D6-46036 (app. B).

4.0 ANALYSIS AND TEST

Analysis and test tasks were performed during this program to substantiate the advanced composite stabilizer for airline flight use and to provide the basis for FAA certification. Ultimate strength, flutter, and stability and control analyses were performed to provide an analytical base. Ancillary and full-scale ground structural tests, flutter, and stability and control flight tests were performed to verify the analyses.

4.1 ANALYSIS

The analysis tasks are similar to those typically performed for similar metal structures. Moisture and temperature effects for the composite material were accounted for in the final strength analysis by using design values developed from environmentally conditioned specimens and subcomponents. This procedure is discussed in detail in Section 4.1.6.

The composite stabilizer was designed in accordance with applicable Federal Aviation Regulations (FAR 25) (ref. 2) and all applicable Boeing design documents. The Composite Aircraft Structure Advisory Circular (AC20-107) (ref. 3) was used as the basic guide to show compliance with the regulations.

4.1.1 Structural Criteria

Structural criteria were defined to provide a base for the design. In most cases, the criteria were based on existing metal design practices. Other criteria that are unique to composite structure were based on knowledge obtained from prior composite programs. Sections 4.1.1.1 through 4.1.1.5 define specific criteria.

4.1.1.1 Loads

The external loads for the advanced composite stabilizer were the maximum loads expected in service on any model of the 737 aircraft. These loads were adequate in scope to meet all Boeing and FAA design requirements. The airplane flight envelope (V-n diagram) remained unchanged. All components of the stabilizer were designed to withstand ultimate loads. Ultimate and limit load definitions were identical to those of current metal structure.

4.1.1.2 Flutter and Vibration

A flutter analysis was conducted for the present 737 airplane with the advanced composite stabilizer. The flutter analysis was verified by ground vibration and flight tests.

The effects of stabilizer stiffness and mass changes on the airplane flutter characteristics were assessed.

4.1.1.3 Sonic

The advanced composite stabilizer was designed for the most critical local sonic environment encountered on the horizontal tail of any 737 airplane model.

4.1.1.4 Electrodynamics

Precipitation static (P-static) and lightning protection requirements were incorporated into the design of the graphite-epoxy composite stabilizer. An analysis determined the extent of lightning protection required, including lightning strike damage at the contact point, possible lightning current paths through the structure, and stabilizer electrical bonding and ground requirements.

For qualification testing, there are four current components, A, B, C, and D, that are used to determine direct effects. Each simulates a different characteristic of the current in a natural lightning flash and is shown in Figure 23. They are applied individually or as a composite of two or more components together in one test. The objective of each test, along with setup, measurement, and data requirements, is described in the appropriate test method description of MIL-STD-1757 (ref. 4).

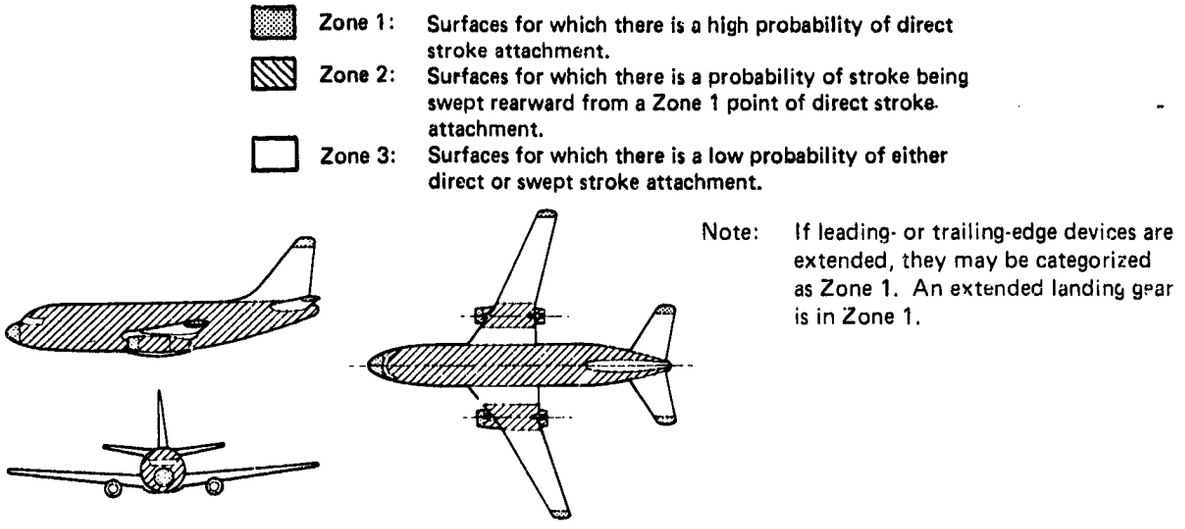

(a) 737 aircraft lightning strike zone locations

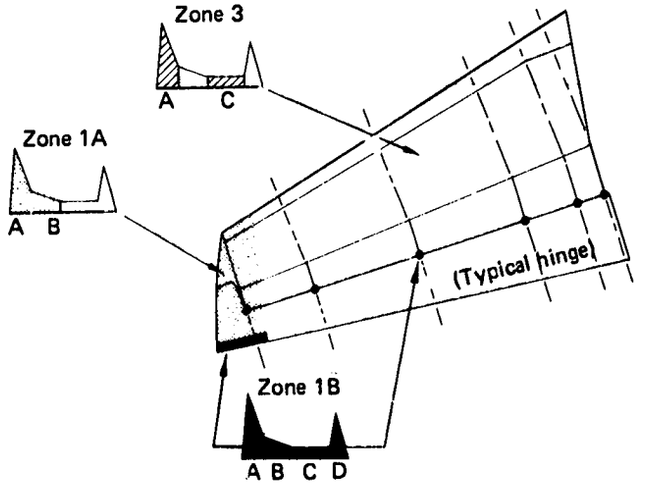

(b) 737 horizontal stabilizer lightning strike zone locations

Figure 23. Lightning Strike Threat

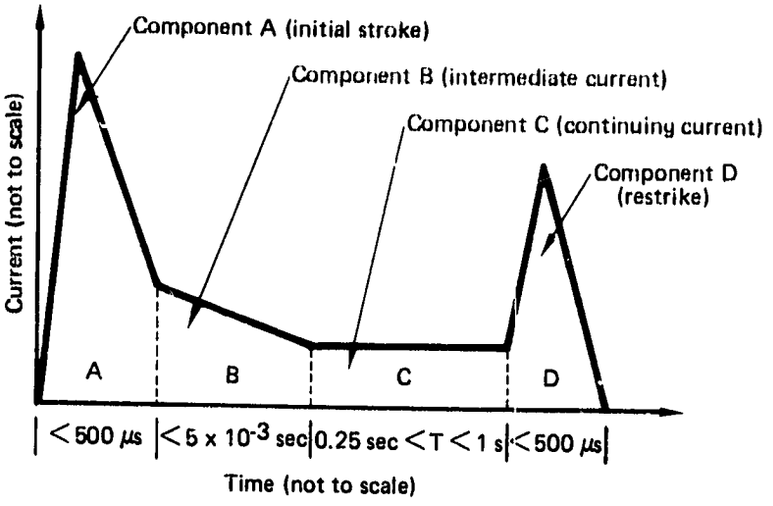

Test waveform	Parameter	Recommended test value*
Component A	I_{peak} (ampere)	200 000
	A(kiloampere^2-sec)	2 000
Component B	I_{avg} (ampere)	2 000
	Q (coulomb)	10
Component C	I_{avg} (ampere)	500
	Q (coulomb)	200
Component D	I_{peak} (ampere)	100 000
	A(kiloampere^2-sec)	250

*MIL-STD-1757

(c) Lightning discharge current waveform components

Figure 23. Lightning Strike Threat (Concluded)

- Component A: initial high peak current. Component A has a peak amplitude of 200 kA (±10%) and an action integral of 2×10^6 A^2·s (±20%) with a total time duration not exceeding 500 μs. This components may be unidirectional or oscillatory.

- Component B: intermediate current. Component B has an average amplitude of 2 kA (±10%) flowing for a maximum duration of 5 ms and a maximum charge transfer of 10 coulombs. The waveform shall be unidirectional; e.g., rectangular, exponential, or linearly decaying.

- Component C: continuing current. Component C transfers a charge of 200 coulombs (±20%) in a time of between 0.25s and 1s. The waveform shall be unidirectional; e.g., rectangular, exponential, or linearly decaying.

- Component D: restrike current. Component D has a peak amplitude of 100 kA (±10%) and an action integral of 0.25×10^6 $A^2 \cdot s$ (±20%). This component may be either unidirectional or oscillatory with a total time duration not exceeding 500 μs.

4.1.1.5 Environment

The advanced composite stabilizer was designed to be compatible with the current 737 airplane certified structural operational environment.

Inservice moisture and temperature effects on physical and mechanical properties of structural materials were accounted for in the design, analysis, and testing of the advanced composite stabilizer. Conservative moisture and temperature envelope values for airline service exposure were used to establish design, analysis, and test temperature and moisture absorption levels. (See secs. 4.1.5, Thermal Analysis, and 4.1.6, Moisture Analysis.) Moisture and temperature effects were accounted for when evaluating test results obtained from components exposed only to ambient temperature and humidity.

4.1.2 External Loads Analysis

The external loads used for the structural analysis were obtained from the most highly loaded model 737 airplane. The requirements of FAR 25 (ref. 2) and Boeing design specifications were met. The load requirements included limit and ultimate loads, durability, dynamics and vibration, and flutter. The various loading conditions for the airplane are represented on the graph of limit load factor, n, plotted against equivalent airspeed, V. The (V-n) diagram for the 737 airplane is shown in Figure 24 and defines the maximum load conditions for design of the aircraft structure. The fatigue loads were derived from the same flight-load spectrum as that used for current production airplanes.

4.1.3 Stiffness Analysis

4.1.3.1 Stiffness Calculation

The spanwise bending stiffness (EI) and torsional stiffness (GJ) comparisons of the production aluminum stabilizer and the graphite-epoxy composite stabilizer are shown in Figures 25 and 26.

The bending stiffness for the production aluminum stabilizer was calculated using the amount of compression skin effective at limit load. A similar method of analysis was used to calculate the bending stiffness of the graphite structure.

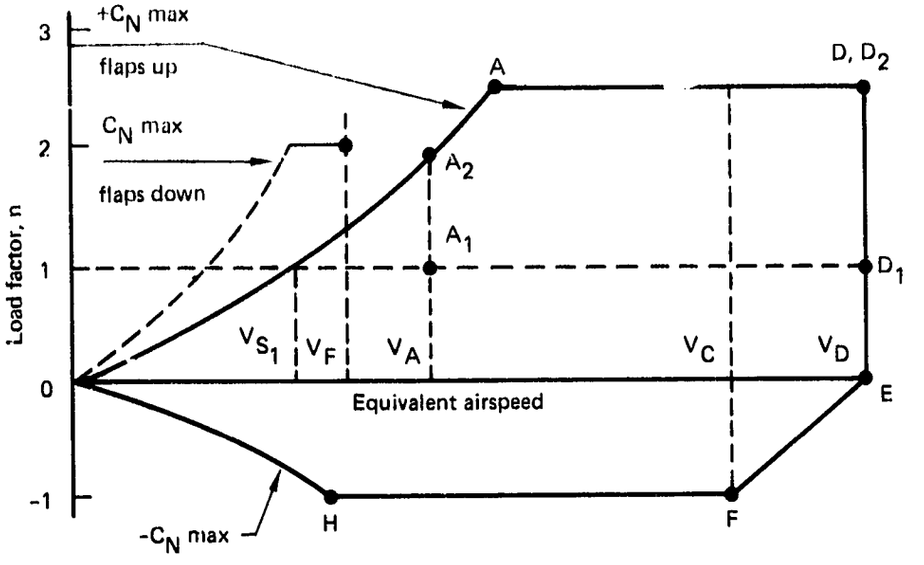

V_{S_1}	Stall speed with flaps retracted	V_C	Design cruise speed
V_F	Design flap speed	V_D	Design dive speed
V_A	Design maneuver speed	C_N	Total airplane normal force coefficient
n	Inertial forces acting at airplane center of gravity		

Figure 24. FAR 25 V-n Diagram

Properties were calculated at each stabilizer rib station. Bending stiffness values plotted are the average of the foregoing values. Stiffnesses were determined in the same manner for the existing aluminum stabilizer.

4.1.3.2 Stability and Control

The calculated bending and torsional stiffness for the composite stabilizer resulted in a control effectiveness that was within the acceptable tolerance band.

Further substantiation that the graphite-epoxy stabilizer had acceptable stability and control aeroelastic characteristics was provided with the successful completion of the flight test program reported in References 5 and 6.

4.1.3.3 Flutter

A flutter analysis was conducted for the model 737 airplane with a graphite-epoxy composite stabilizer. Symmetric and antisymmetric flutter analyses were performed that encompassed stabilizer center-of-gravity extremes with both power-on and power-off operation. The analytical results show that a 737 with a composite stabilizer does not suffer any degradation of flutter characteristics or speeds when compared with the production aluminum stabilizer.

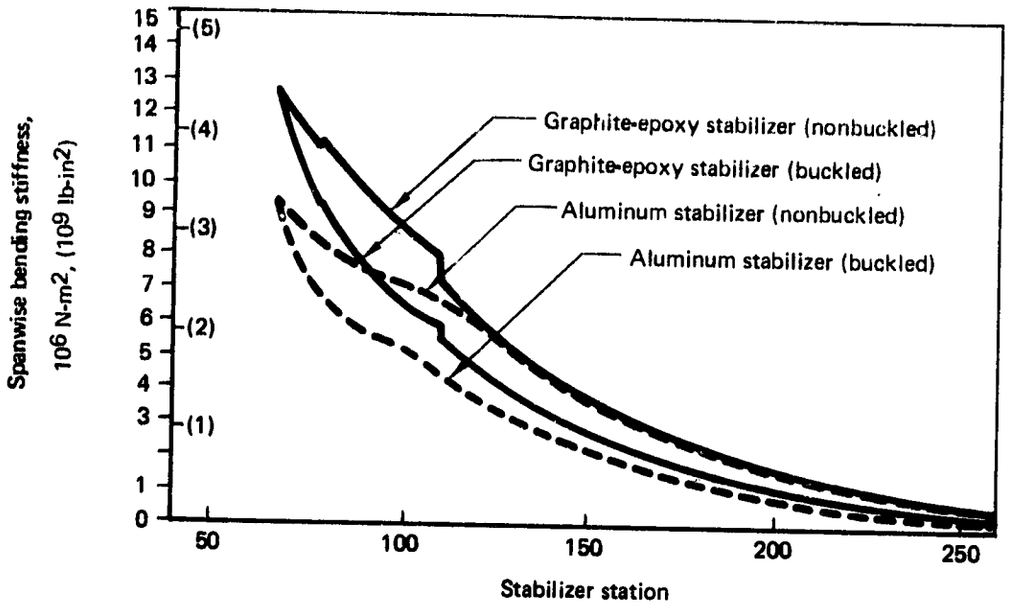

Figure 25. Stabilizer Bending Stiffness

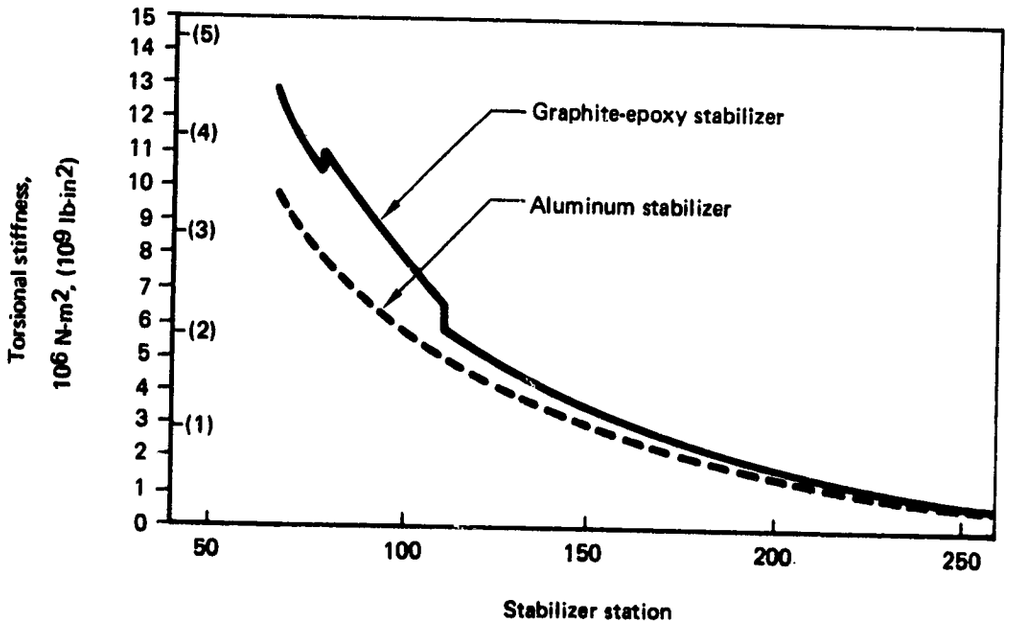

Figure 26. Stabilizer Torsional Stiffness

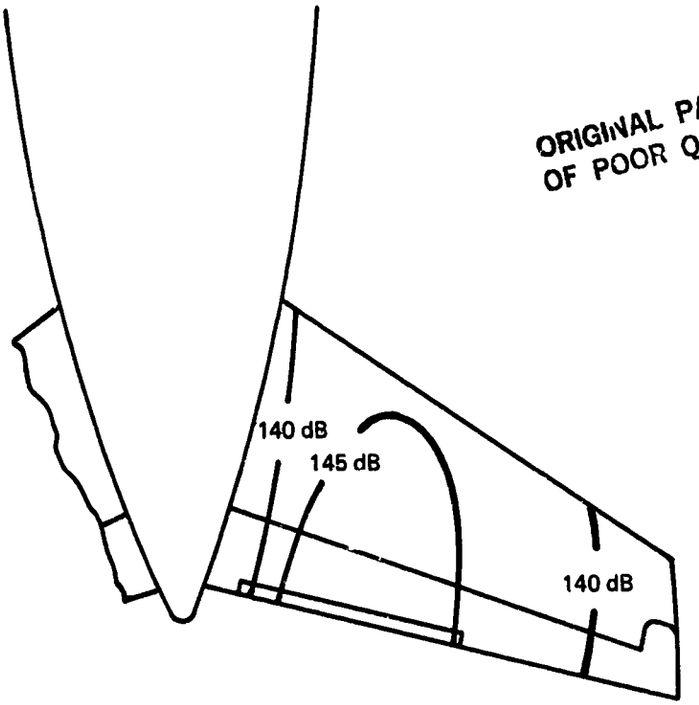

Figure 27. Maximum Overall Sound Pressure Level on 737 Horizontal Tail

Both ground vibration and inflight flutter tests are reported in Sections 3.2 and 3.3 of Reference 6.

4.1.4 Sonic Analysis

Maximum overall sound pressure levels (OASPL) for the lower surface of the 737 horizontal tail are shown in Figure 27. These values are based on measurements that have been adjusted to account for the highest possible OASPL attainable on any 737 airplane.

Based on this OASPL of 145 dB, a series of tests was established with increased noise levels to determine resistance of the graphite structure to damage in a sonic environment. This test is reported in Section 4.2.8 of this document.

4.1.5 Thermal Analysis

The temperature excursion used in the design of the graphite-epoxy stabilizer was established as 82°C to -59°C (180°F to -75°F). The maximum temperature was obtained from a thermal analysis that accounted for ambient air temperature, radiation and convection heat transfer, surface absorptivity and emissivity characteristics, and cooling effects during taxi, takeoff, and flight. The thermal model and boundary conditions established for the thermal model are shown in Figure 28.

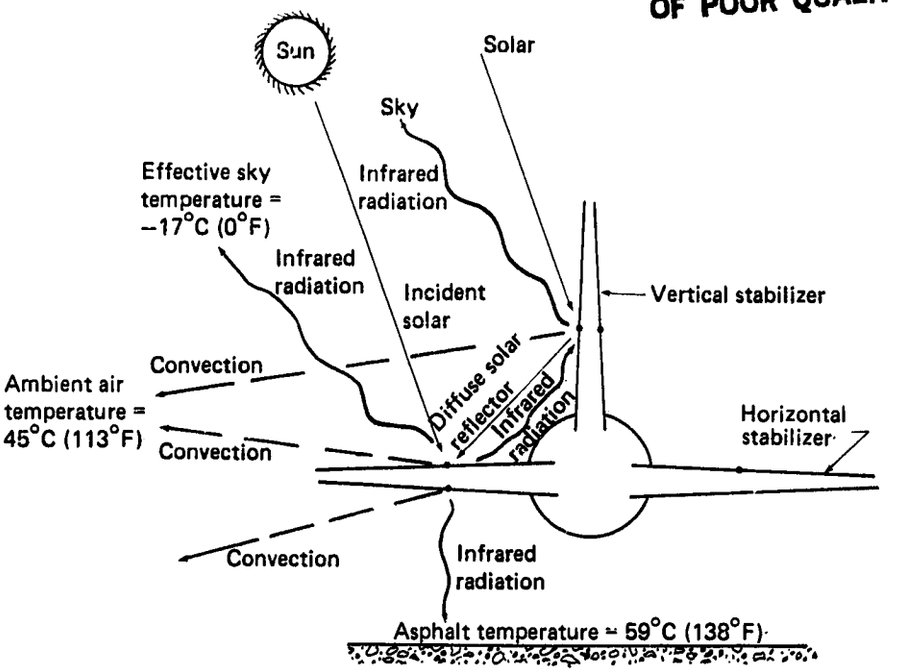

Figure 28. 737 Horizontal Stabilizer Thermal Model

A dark paint system was conservatively assumed. The steady-state temperatures achieved in the model are shown in Figure 28 at time = 0. A transient analysis then was performed, and the results are shown in Figure 29. The conditions and assumptions used for the transient analysis were defined as a 4-min taxi run with a constant relative wind velocity of 20 kn followed by constant takeoff, acceleration, and climb to 190 kn in 1.2 min. This point was selected as the earliest possible time that the aircraft could be subjected to significant maneuver or gust loads and would occur at 1.2 min after brake release (fig. 29).

The thermal analysis showed that at the end of 1.2 min of flight, the stabilizer stringer would be at 82°C (180°F). This temperature was conservatively used for all stabilizer structure. The minimum temperature of -59°C (-75°F) was based on the lowest ambient temperature experienced in flight, modified by the effect of aerodynamic heating.

4.1.6 Moisture Analysis

The conservative amount of moisture that can be expected to be absorbed by graphite-epoxy laminates in service was determined analytically. World environmental conditions were surveyed, and existing industry data were reviewed (refs. 7 and 8). An analytical diffusion model was set up using average diffusivity coefficients obtained from industry. The results of this analysis showed that a moisture content of 1.1 $\pm$0.1% of the total weight could be expected in the structure in service.

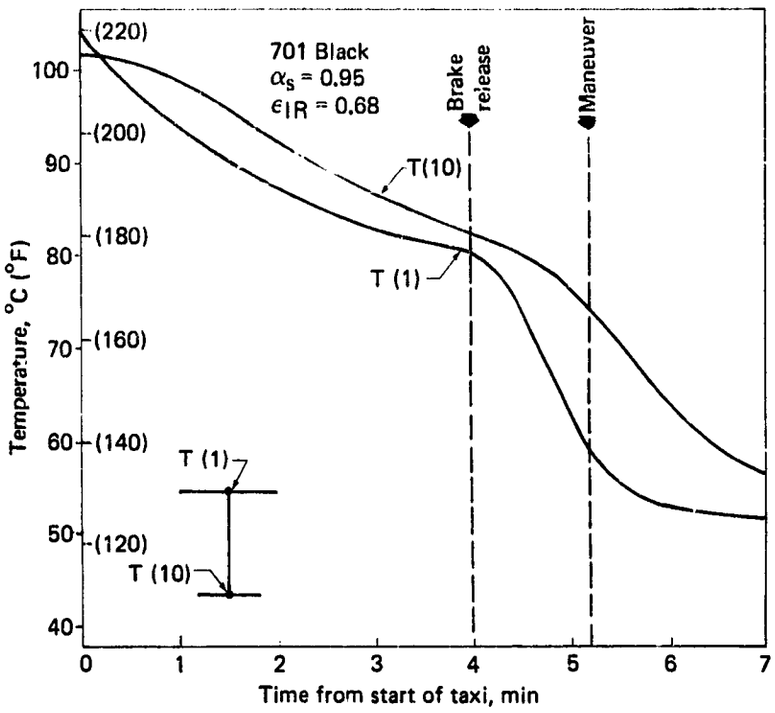

Figure 29. Transient Thermal Response

To provide a control for moisture-conditioned test parts in the ancillary test program, a moisture rider coupon was used. The laminate moisture rider was a 12-ply fabric laminate. These moisture riders were calibrated by placing them in a humidity chamber at 100% relative humidity and 60°C (140°F). A typical weight-gain curve for the 12-ply laminate is shown in Figure 30. These tests were used to establish typical moisture pickup rates.

In the ancillary test program, these standardized moisture coupons were placed in the conditioning chamber along with the test specimen. When the rider coupon had attained 1.1% moisture, the test specimen was removed from the chamber and tested.

4.1.7 Strength Analysis

4.1.7.1 Finite Element Model

General—An ATLAS finite element model (ref. 9) was developed for the horizontal stabilizer and was attached to a center support structure model to ensure that the flight and ground test configuration was duplicated. The elevator was modeled as a loaded beam with the stiffness characteristics of the production item. The elevator was held in the neutral position.

The stabilizer was modeled in five data sets (fig. 31), including the center-mount, to identify the major areas of the stabilizer.

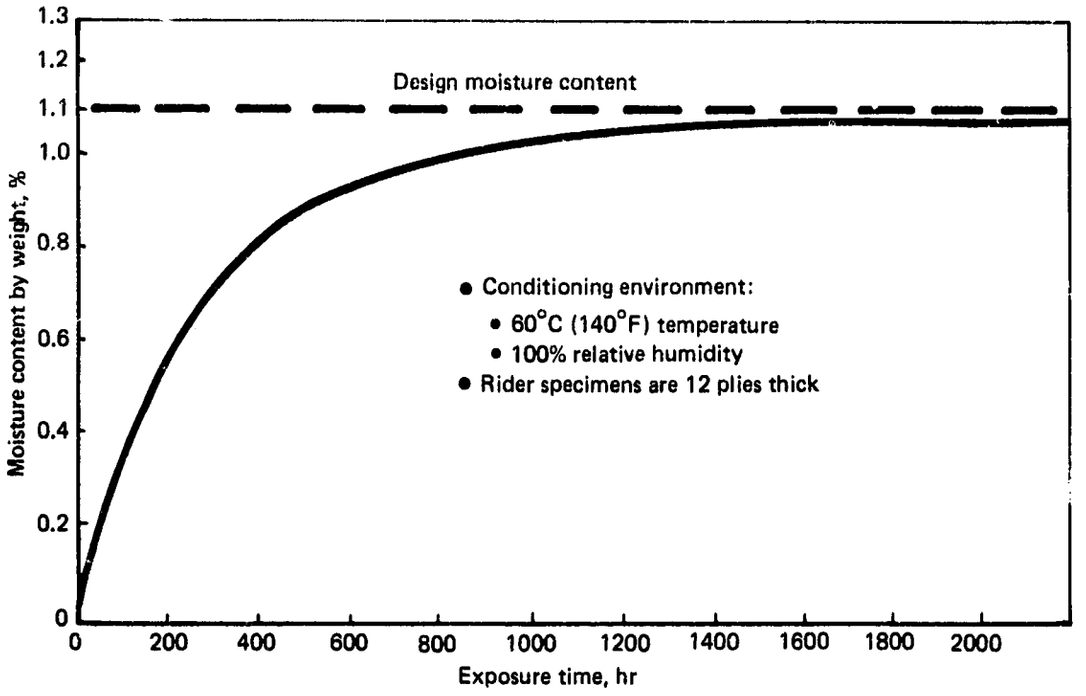

Figure 30. Exposure Time Versus Moisture Content for Laminates

Geometry and Material Input—Element definitions for the structural model components were drawn from the selection available in the ATLAS program. The material properties for the graphite-epoxy components were obtained from Boeing specifications shown in Figures 32 and 33. Examples of stabilizer structure and the use of ATLAS finite elements to simulate these sections are illustrated and tabulated in Figures 34 and 35 and Tables 1 and 2. The simulated production center-mount component material properties were Boeing standard values for metal components.

Loads—The external load cases that were used for the ultimate strength analysis are listed in Table 3. In addition to these flight load cases, two temperature thermal conditions of 82°C and -59°C (180°F and -75°F), previously defined in Section 4.1.5, and one moisture condition of 1% absorption defined in Section 4.1.6, were analyzed.

Aerodynamic loads were developed as panel pressures on the upper and lower surfaces. These panel pressures were apportioned and summed at the ground test load pad locations. For the ATLAS model, the load pad forces were distributed to the nearest skin grid points. Leading-edge loads were applied to the front spar, and the elevator loads were distributed along the length of the elevator beam.

ATLAS Output—Selected stress and strain levels for the ultimate load cases (table 3) for the upper and lower surfaces are shown in Figures 36 through 47. Ultimate loads are the maximum loads the airplane will encounter in service multiplied by a factor of safety. The output data are used to identify the location of maximum strain for each load case. The critical values for the skin surfaces are shown in

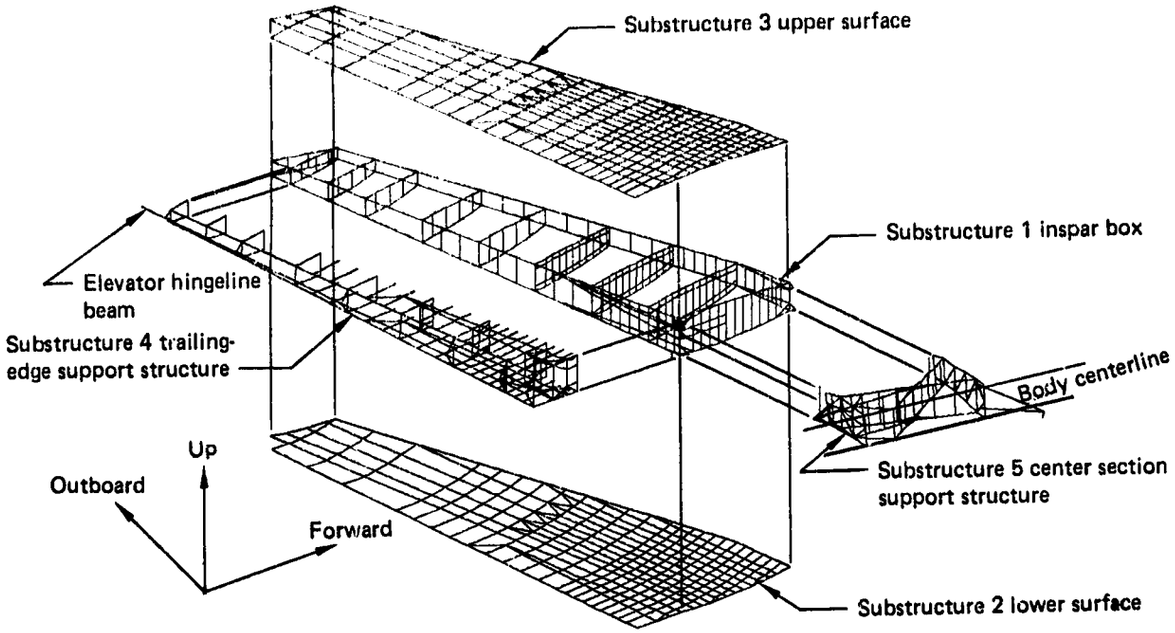

Figure 31. Finite Element Model Substructure Definition

Figures 41 and 44. Typical thermal- and moisture-induced strains for a skin surface are shown in Figure 48 and 49. The final design ultimate strain for any detail was obtained by algebraically combining the ultimate flight loads strains with 1.5 times the thermal and moisture analysis strains. The final design ultimate strain is compared to the allowable design value at corresponding environmental conditions to provide the detail margin of safety.

4.1.7.2 Ultimate Strength Analysis

Analyses were conducted on composite stabilizer structural details. Margins of safety were checked at -59°C, 21°C, and 82°C (-75°F, 70°F, and 180°F) using corresponding detail strains and design values at each temperature.

The design values used throughout the strength analysis were based on coupon or structural element test data from the ancillary test program (sec. 4.2). Average test values were reduced in a manner similar to the probability and confidence levels of MIL-HDBK-5B "B" basis; namely, that 90% of the population will be higher with a confidence of 95%. These reduction factors conservatively accounted for material strength variations, test specimen geometry variations, and test condition variations.

Material strength correction factors for each test condition were based on process control test results. Process control panel data were collected from the ancillary test program specimens and analyzed to establish the strength variations. A material correction factor (MCF) was used to correct each test point to the mean

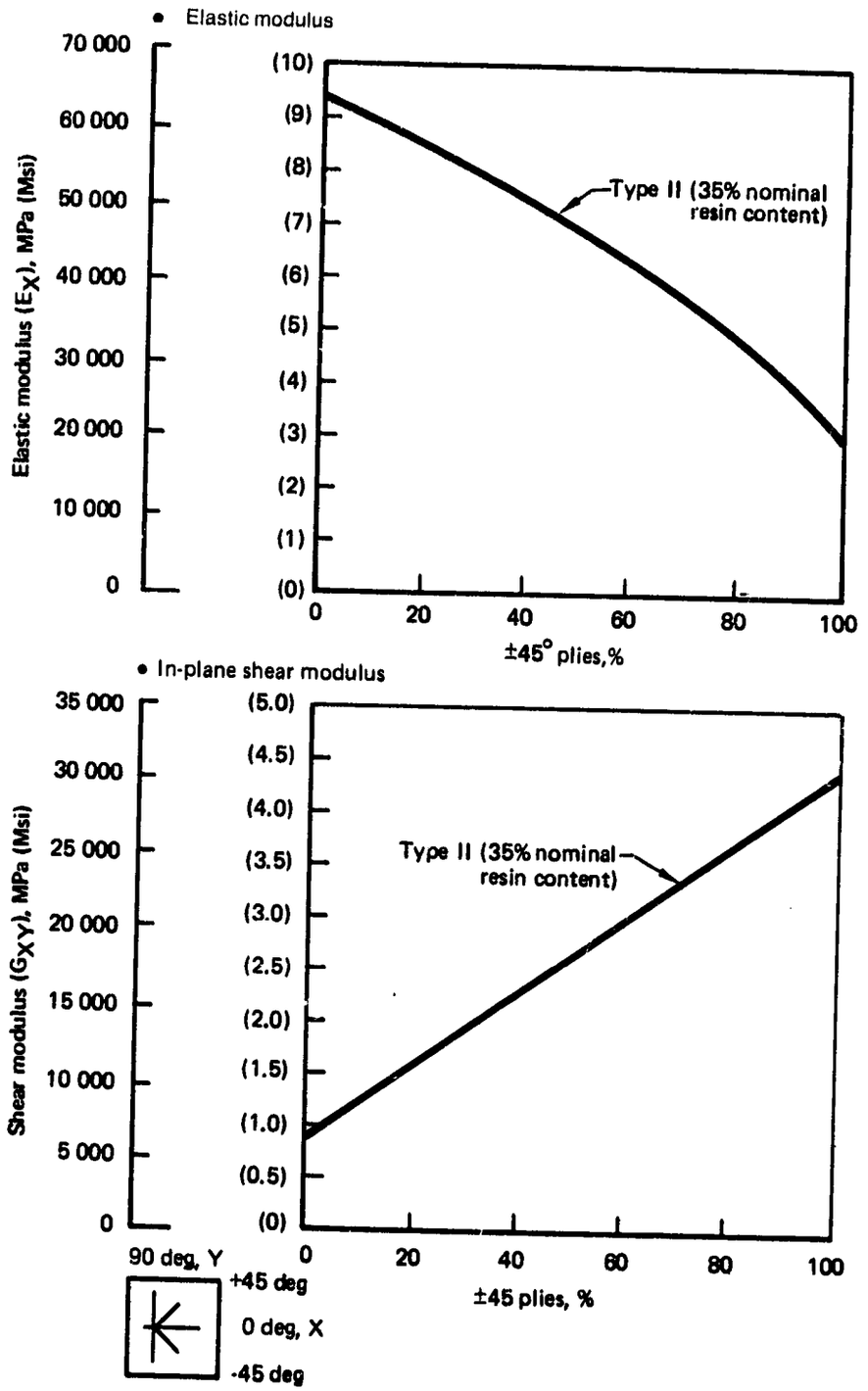

Figure 32. Material Properties--Graphite-Epoxy Fabric, T300/5208

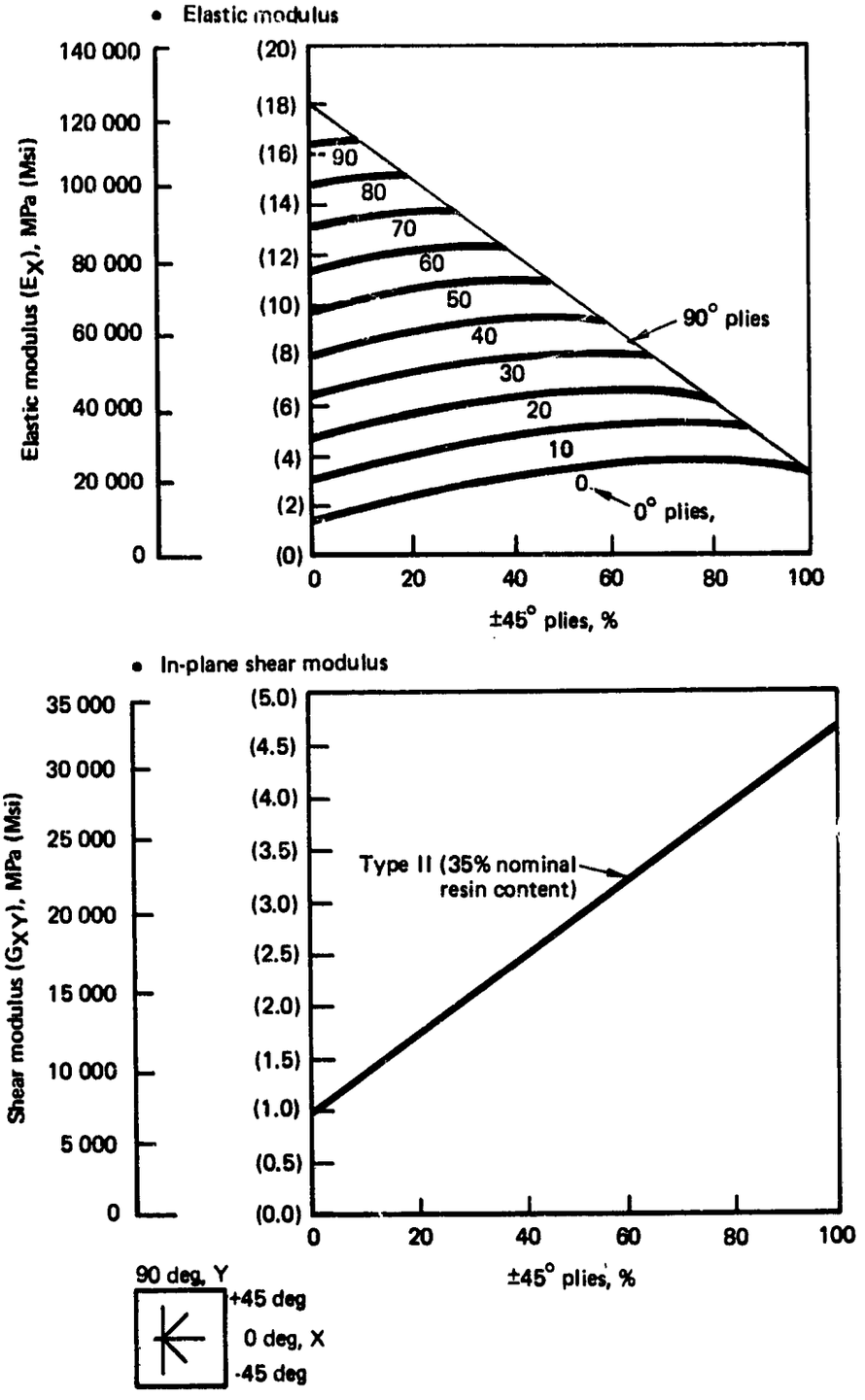

Figure 33. Material Properties–Graphite-Epoxy Tape, T300/5208

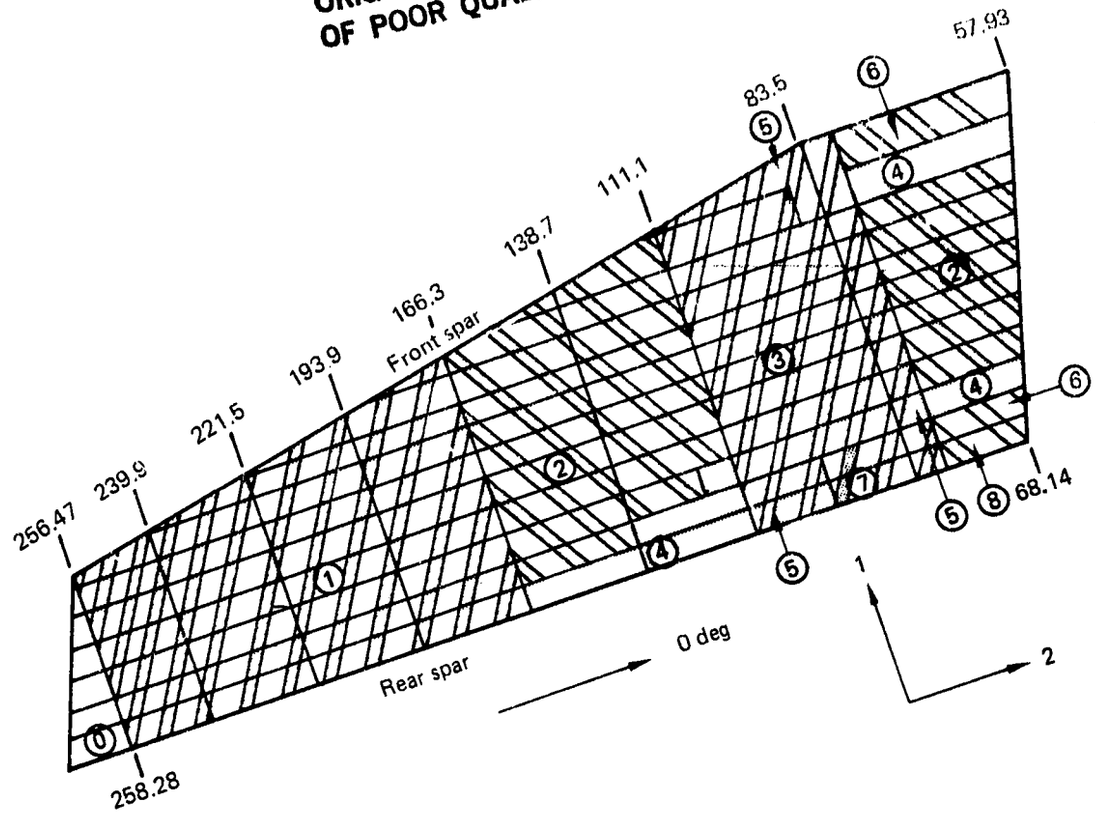

○ Zone
▷ Number of plies in each zone

Zone / Layup	0	1	2	3	4	5	6	7	8
±45 fabric 0/90 fabric 90 tape		4 2	5 2	5 2 2	7 3	7 3 2	9 3	9 3 2	10 4
Thickness mm(in)	1.27 (0.05)	1.14 (0.045)	1.35 (0.053)	1.70 (0.067)	1.91 (0.075)	2.29 (0.090)	2.03 (0.080)	2.67 (0.105)	2.67 (0.105)
E_1, MPa (lbf/in^2)	18 614 (2.7 x 10^6)	39 985 (5.8 x 10^6)	37 572 (5.45 x 10^6)	56 600 (8.21 x 10^6)	38 262 (5.55 x 10^6)	52 394 (7.6 x 10^6)	35 849 (5.2 x 10^6)	48 327 (7.01 x 10^6)	37 572 (5.45 x 10^6)
E_2, MPa (lbf/in^2)	18 614 (2.7 x 10^6)	39 985 (5.8 x 10^6)	37 572 (5.45 x 10^6)	33 229 (4.82 x 10^6)	38 262 (5.55 x 10^6)	34 884 (5.06 x 10^6)	35 849 (5.2 x 10^6)	33 298 (4.83 x 10^6)	37 572 (5.45 x 10^6)
G, MPa (lbf/in^2)	5 515 (0.8 x 10^6)	21 371 (3.1 x 10^6)	22 406 (3.25 x 10^6)	19 165 (2.78 x 10^6)	22 406 (3.25 x 10^6)	19 786 (2.87 x 10^6)	23 440 (3.4 x 10^6)	21 027 (3.05 x 10^6)	22 406 (3.25 x 10^6)
ν	0.15	0.40	0.43	0.42	0.43	0.42	0.47	0.46	0.43

Figure 34. Horizontal Stabilizer Upper Skin Layup

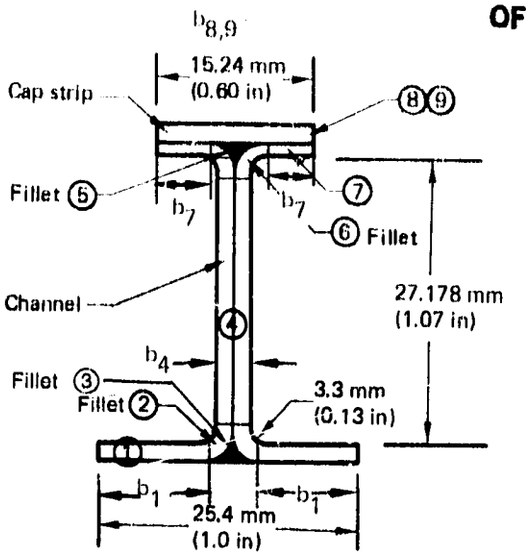

- Fabric: T300/5208, Style 3K-70-P
- Tape: T300/5208, Grade 145

b Element width

t Element thickness

▷ Unit width effective (smeared) for aerial distribution

Item	b, mm(in)	t, mm (in)	E, MPa (lbf/in^2)	Ebt, N (lbf)
1	17.653 (0.695)	0.5715 (0.0225)	39 985 (5.8 x 10^6)	404 786 (91 000)
2	25.4 (1.0) ▷	0.254 (0.0100)	39 985 (5.8 x 10^6)	257 996 (58 000)
3	25.4 (1.0) ▷	0.254 (0.0100)	82 728 (12 x 10^6)	533 784 (120 000)
4	1.143 (0.045)	20.574 (0.8100)	39 985 (5.8 x 10^6)	938 570 (211 000)
5	(25.4 (1.0) ▷	0.254 0.0100)	82 728) (12 x 10^6)	533 784 (120 000)
6	25.4 (1.0) ▷	0.254 (0.0100)	39 985 (5.8 x 10^6)	257 996 (58 000)
7	7.493 (0.295)	0.5715 (0.0225)	39 985 (5.8 x 10^6)	169 032 (38 000)
8	15.24 (0.600)	0.2845 (0.0112)	124 092 (18 x 10^6)	538 232 (121 000)
9	15.24 (0.600)	0.1905 (0.0075)	20 682 (3.0 x 10^6)	62 275 (14 000)
			Σ	3 696 454 (831 000)

Figure 35. Horizontal Stabilizer Graphite-Epoxy Stringer

Table 1. Skin and Stringer Segment—ATLAS Input for Upper Skin

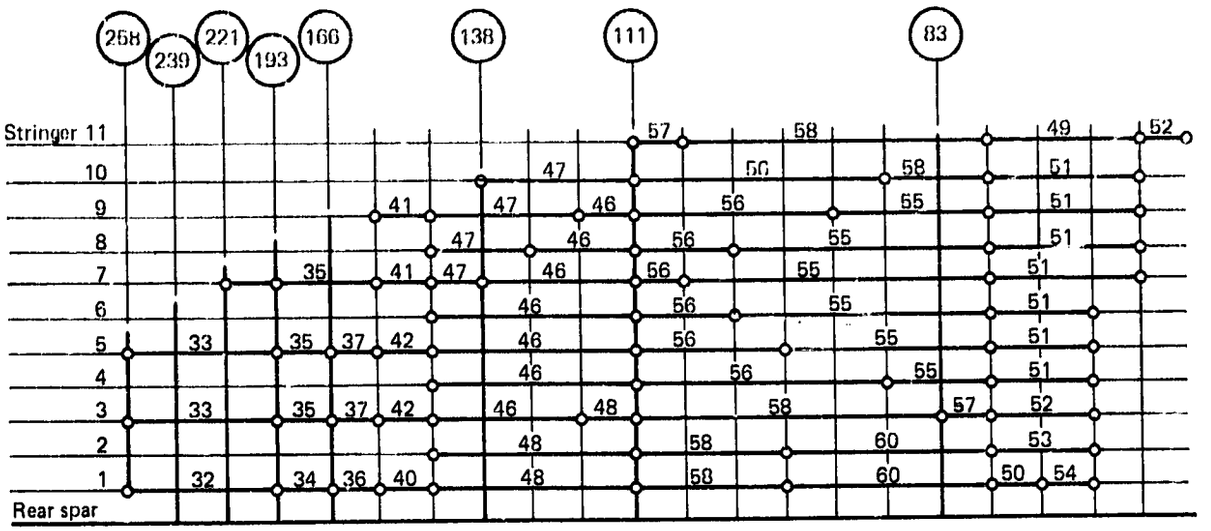

Stringer	E, MPa (lbf/in^2)	Area, mm^2 (in^2)	I, mm^4 (in^4)	Stringer	E, MPa (lbf/in^2)	Area, mm^2 (in^2)	I, mm^4 (in^4)
32	38 606 (5.6×10^6)	140.84 (0.2183)	5.7856×10^4 (0.1390)	48	45 500 (6.6×10^6)	128 (0.1984)	6.1894×10^4 (0.1487)
33	38 606 (5.6×10^6)	187.74 (0.2910)	7.7128×10^4 (0.1853)	49	45 500 (6.6×10^6)	128 (0.1984)	6.2809×10^4 (0.1509)
34	38 606 (5.6×10^6)	178.64 (0.2769)	9.6940×10^4 (0.2329)	50	45 500 (6.6×10^6)	128 (0.1984)	6.3725×10^4 (0.1531)
35	38 606 (5.6×10^6)	238.19 (0.3692)	12.9240×10^4 (0.3105)	51	38 606 (5.6×10^6)	119.10 (0.1846)	6.1477×10^4 (0.1477)
36	45 500 (6.6×10^6)	192 (0.2976)	9.9896×10^4 (0.2400)	52	38 606 (5.6×10^6)	119.10 (0.1846)	6.2809×10^4 (0.1509)
37	45 500 (6.6×10^6)	256 (0.3968)	12.7617×10^4 (0.3066)	53	38 606 (5.6×10^6)	119.10 (0.1846)	6.3725×10^4 (0.1531)
38	38 606 (5.6×10^6)	187.74 (0.2910)	7.7128×10^4 (0.1853)	54	38 606 (5.6×10^6)	119.10 (0.1846)	6.4641×10^4 (0.1553)
40	45 500 (6.6×10^6)	192 (0.2976)	9.9896×10^4 (0.2400)	55	38 606 (5.6×10^6)	119.10 (0.1846)	6.2351×10^4 (0.1498)
41	38 606 (5.6×10^6)	238.19 (0.3692)	12.9240×10^4 (0.3105)	56	45 500 (6.6×10^6)	128 (0.1984)	6.1436×10^4 (0.1476)
42	45 500 (6.6×10^6)	256 (0.3968)	12.7617×10^4 (0.3066)	57	38 606 (5.6×10^6)	119.10 (0.1846)	6.3725×10^4 (0.1531)
46	45 500 (6.6×10^6)	128 (0.1984)	6.0520×10^4 (0.1454)	58	45 500 (6.6×10^6)	128 (0.1984)	6.2809×10^4 (0.1509)
47	38 606 (5.6×10^6)	119.10 (0.1846)	6.1477×10^4 (0.1477)	60	45 500 (6.6×10^6)	128 (0.1984)	6.3725×10^4 (0.1531)

Table 2. Descriptions and Typical Applications of ATLAS Finite Elements

ATLAS element	Description	Typical application
Rod	Straight element with a linear area variation and a constant axial load	Rib and spar stiffeners, upper and lower skin panel edge pad-up
Beam	Straight element with linearly varying properties based on Navier's theory of bending and St. Venant's theory of torsion	Front and rear spar chords, upper and lower surface skin/ stringer segments
SPlate	Constant thickness, four- or eight-node quadrilateral shear panel	Front and rear spar shear panels, rib shear panels
Plate	Triangular or quadrilateral membrane element with orthotropic material capability and smeared uniaxial stiffening	Upper and lower skin panels
GPlate	Triangular or quadrilateral plate element with uncoupled membrane and out-of-plane bending stiffnesses and orthotropic material capability	Front and rear spar inboard chords

Table 3. 737 Design Ultimate Loads

Airplane load case	ATLAS load case	Description
3710	11	Positive maneuver at V_D (maximum positive torsion)
4010	12	Flaps-down maneuver (maximum negative moment)
4761	13	Negative gust at V_D (maximum surface pressures)
4430	14	Positive gust at V_B (maximum positive shear and moment, FAR requirement)

- Upper shear, lbf/in^2

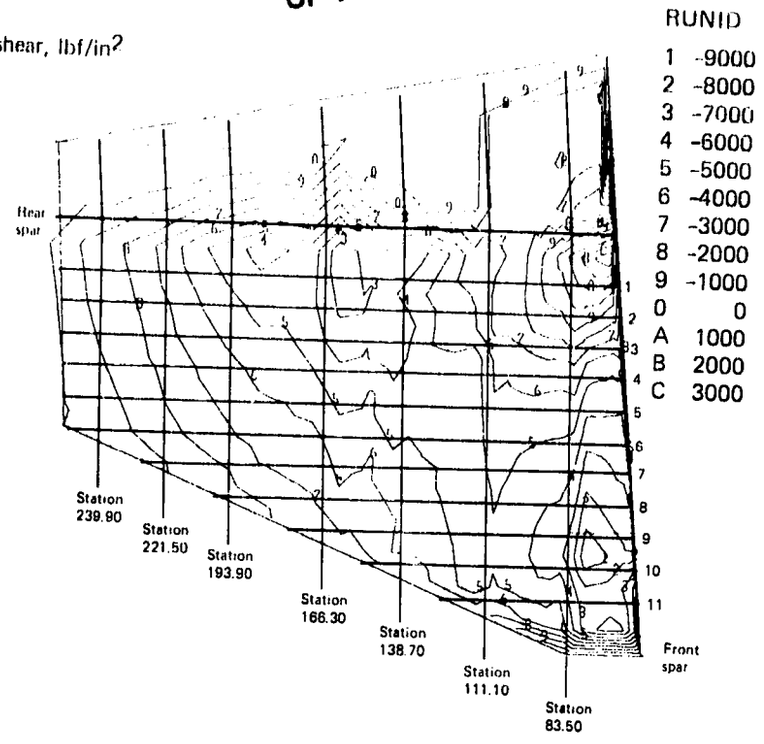

- Lower shear, lbf/in^2

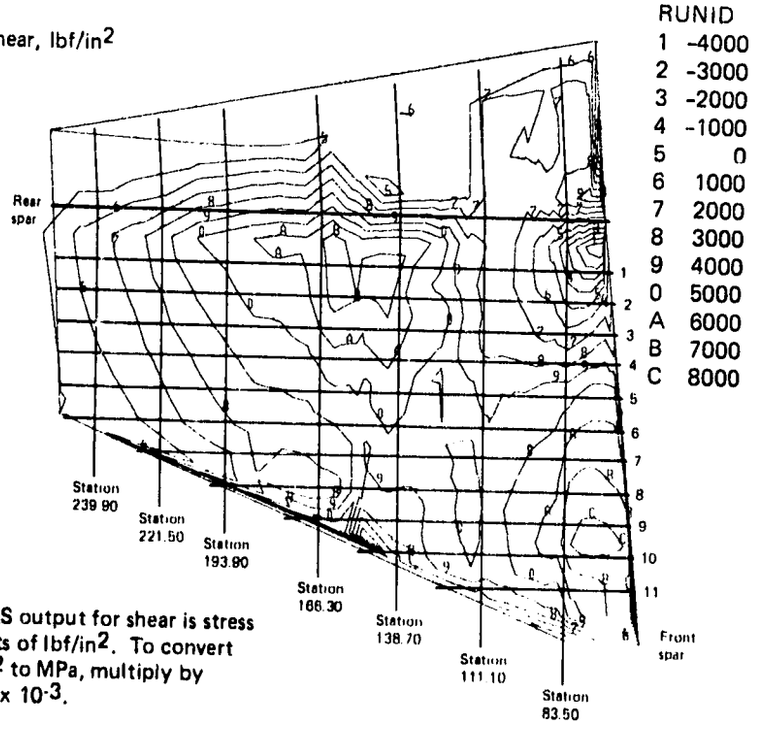

Note: ATLAS output for shear is stress in units of lbf/in^2. To convert lbf/in^2 to MPa, multiply by 6.895×10^{-3}.

Figure 36. Ultimate Loads–Shear Stress (Load Case 3710)

- Upper streamwise strain

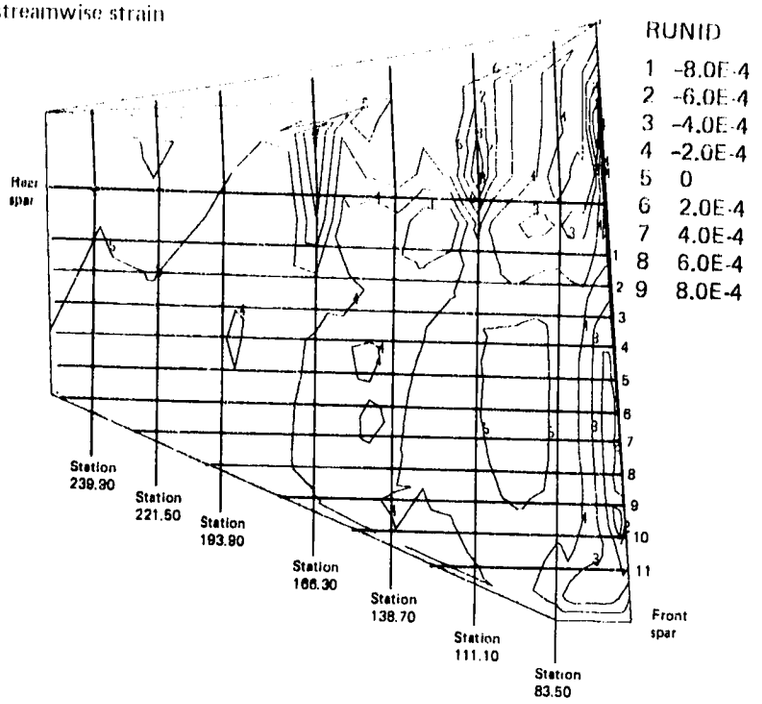

- Lower streamwise strain

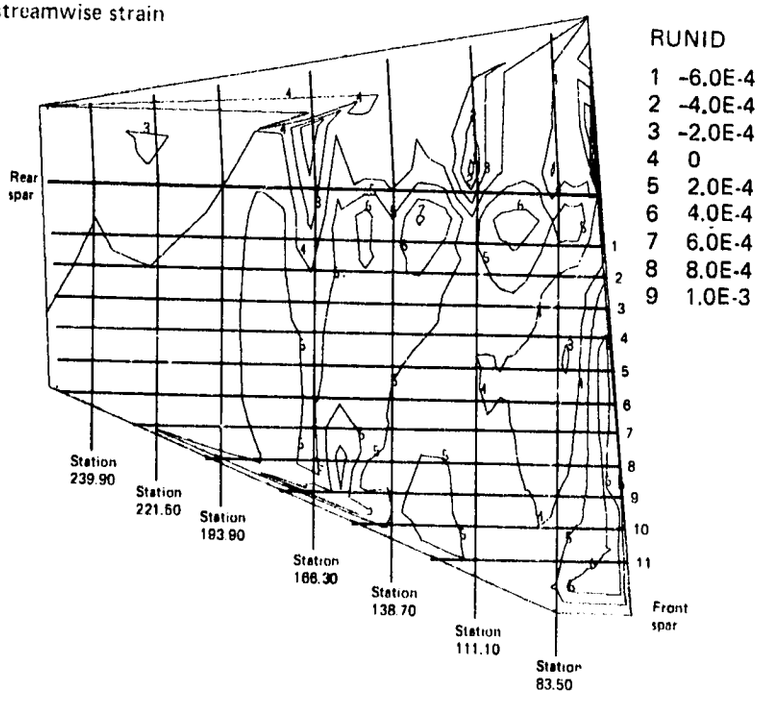

Figure 37. Ultimate Loads--Streamwise Strain (Load Case 3710)

- Upper spanwise strain

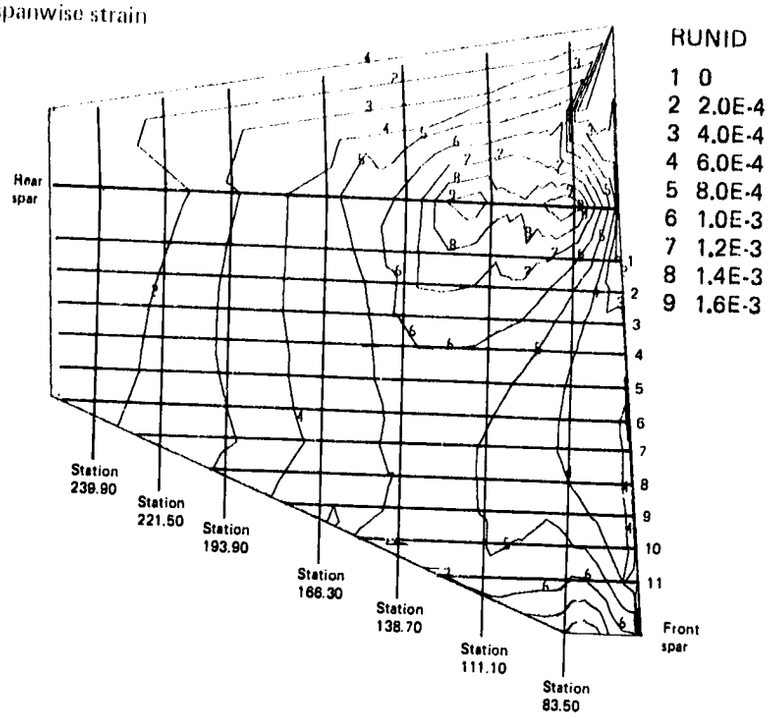

- Lower spanwise strain

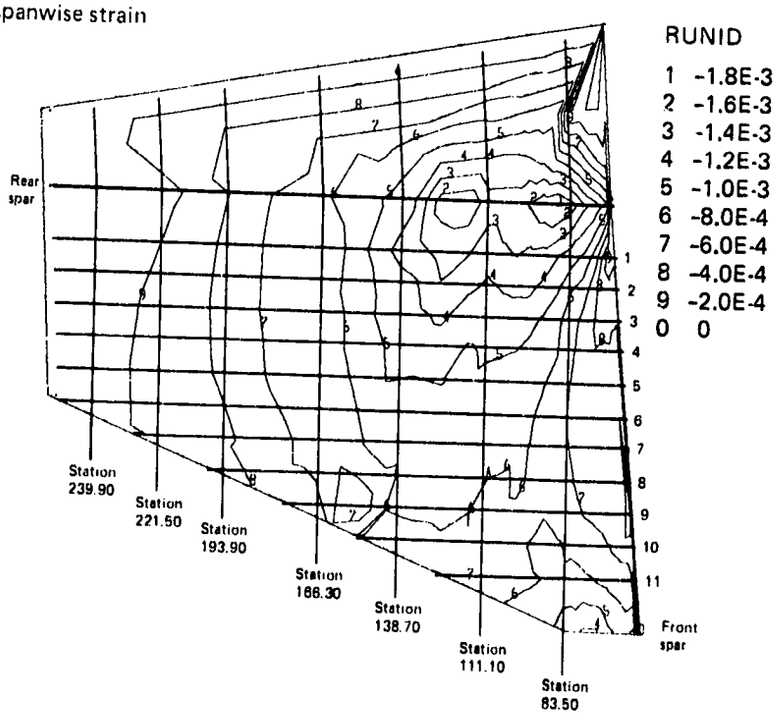

Figure 38. Ultimate Loads–Spanwise Strain (Load Case 3710)

- Upper shear, lbf/in^2

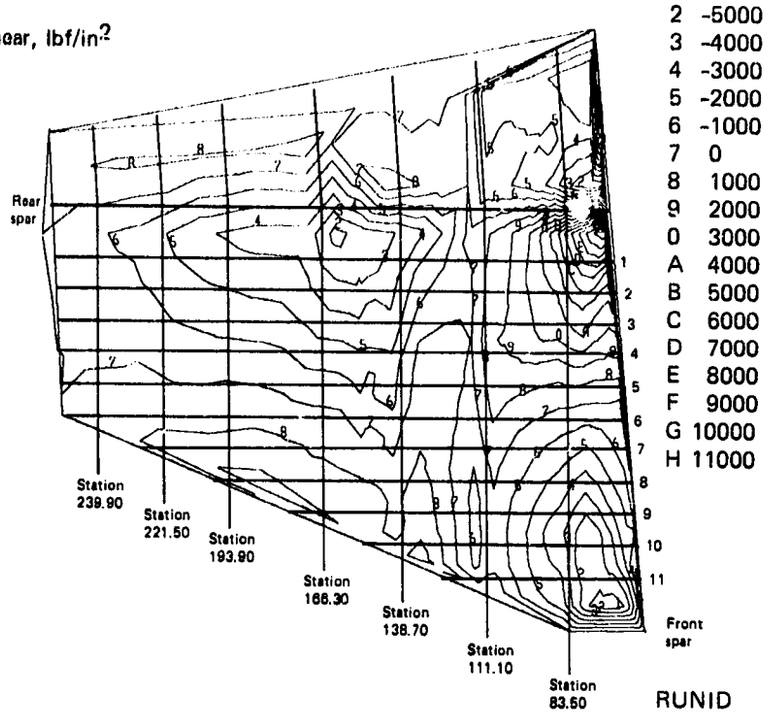

- Lower shear, lbf/in^2

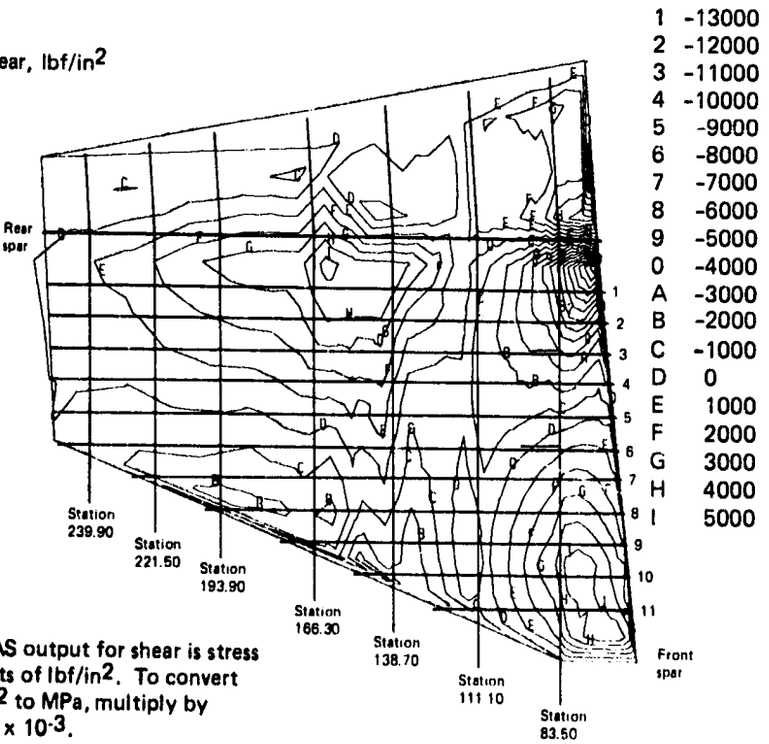

Note: ATLAS output for shear is stress in units of lbf/in^2. To convert lbf/in^2 to MPa, multiply by 6.895×10^{-3}.

Figure 39. Ultimate Loads–Shear Stress (Load Case 4010)

- Upper streamwise strain

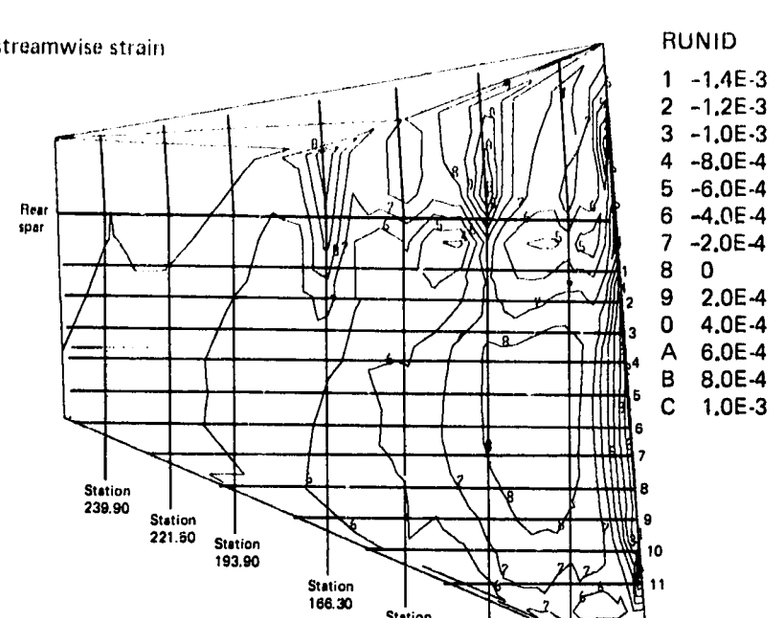

- Lower streamwise strain

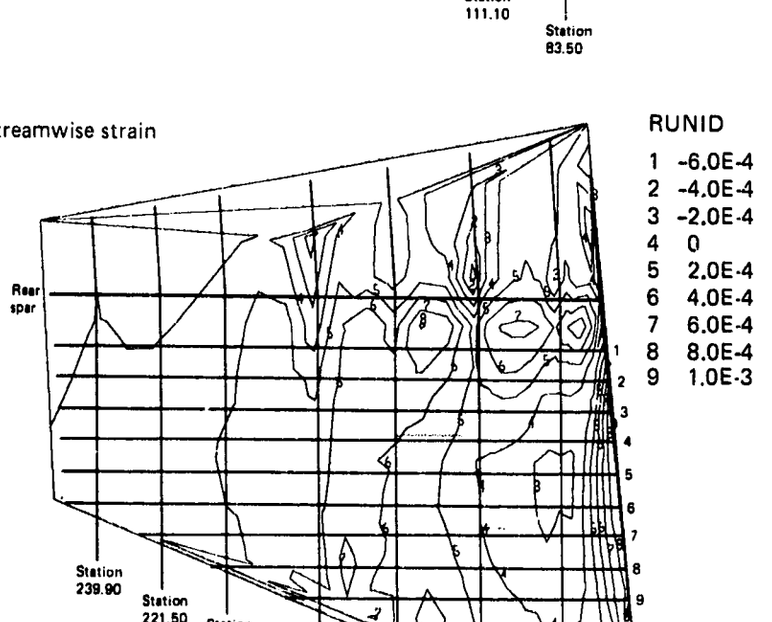

Figure 40. Ultimate Loads–Streamwise Strain (Load Case 4010)

• Upper spanwise strain

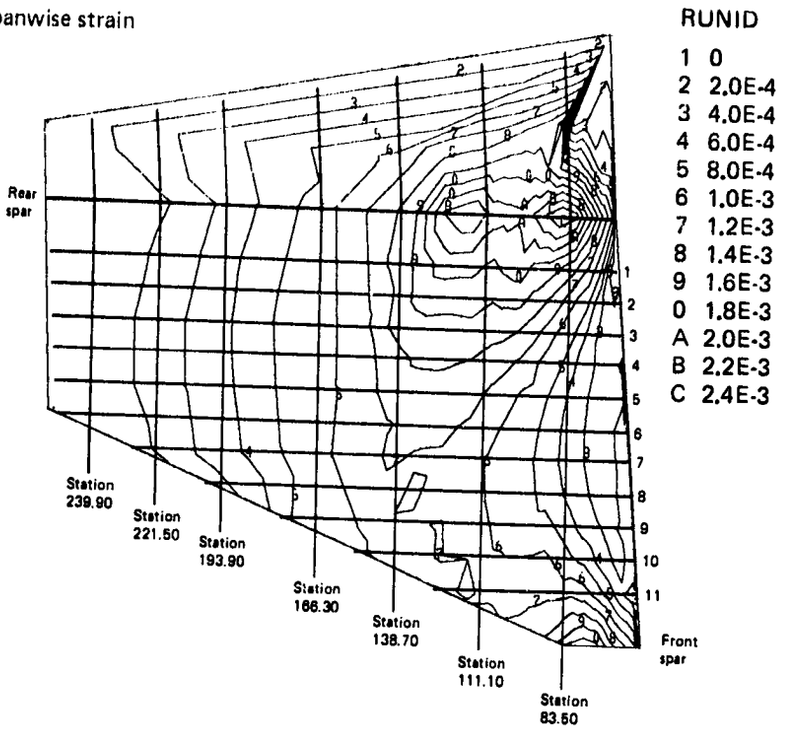

• Lower spanwise strain

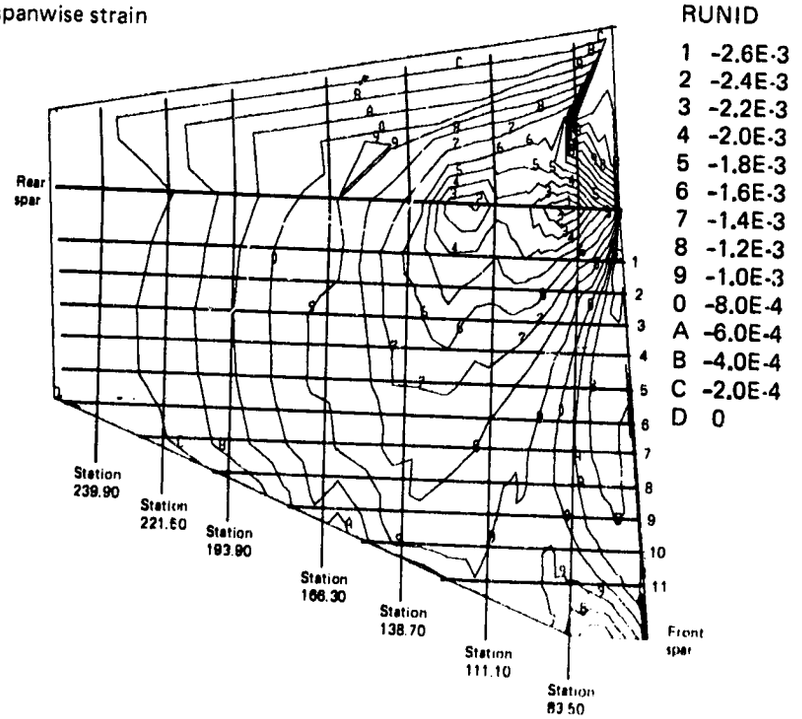

Figure 41. Ultimate Loads–Spanwise Strain (Load Case 4010)

- Upper shear, lbf/in^2

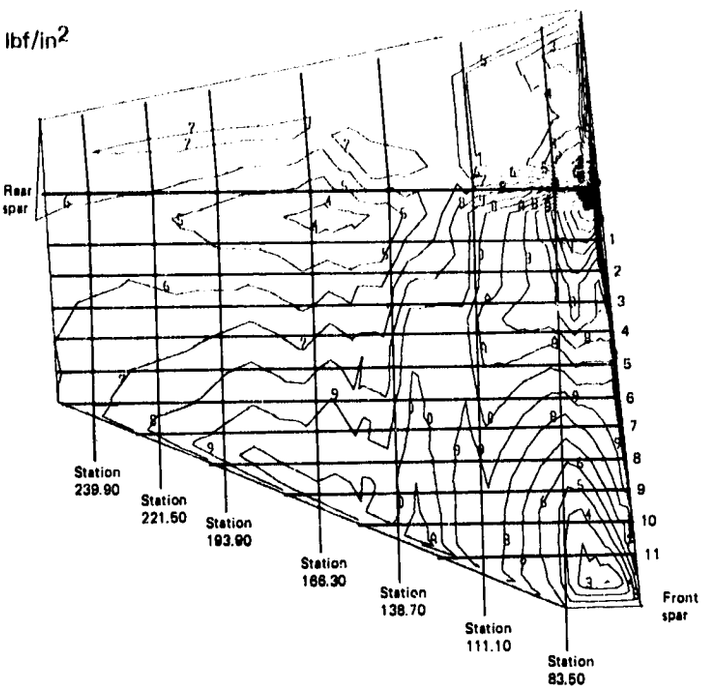

RUNID	
1	-5000
2	-4000
3	-3000
4	-2000
5	-1000
6	0
7	1000
8	2000
9	3000
0	4000
A	5000
B	6000
C	7000
D	8000
E	9000
F	10000
G	11000
H	12000
I	13000

- Lower shear, lbf/in^2

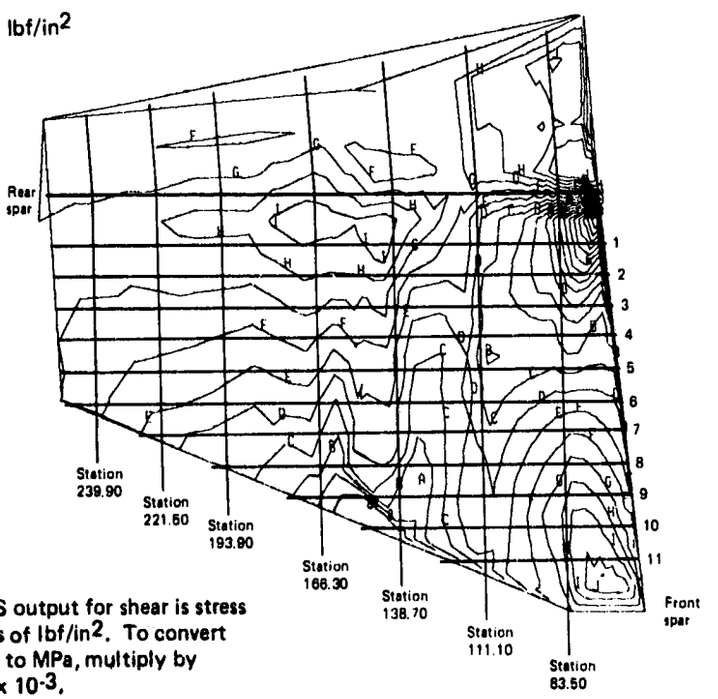

RUNID	
1	-16000
2	-15000
3	-14000
4	-13000
5	-12000
6	-11000
7	-10000
8	-9000
9	-8000
0	-7000
A	-6000
B	-5000
C	-4000
D	-3000
E	-2000
F	-1000
G	0
H	1000
I	2000
J	3000

Note: ATLAS output for shear is stress in units of lbf/in^2. To convert lbf/in^2 to MPa, multiply by 6.895×10^{-3}.

Figure 42. Ultimate Loads—Shear Stress (Load Case 4761)

- Upper streamwise strain

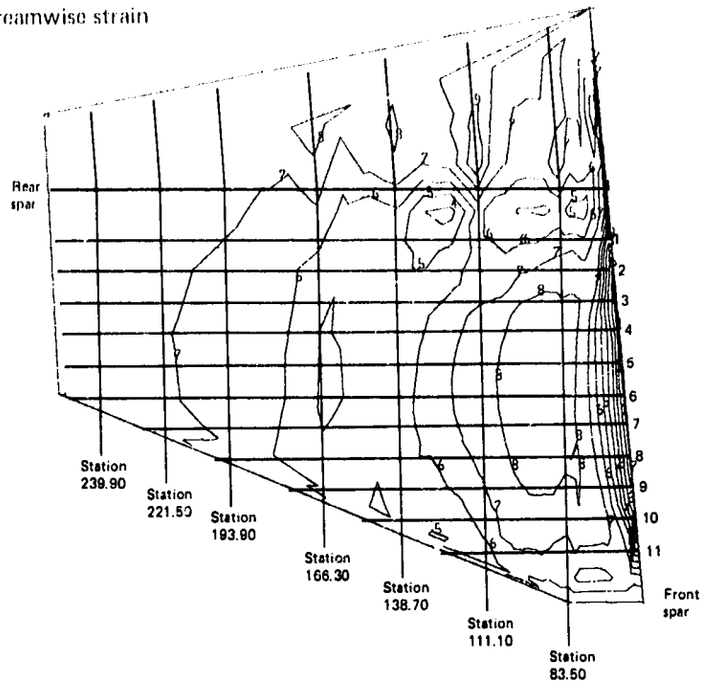

RUNID
1 -1.4E-3
2 -1.2E-3
3 -1.0E-3
4 -8.0E-4
5 -6.0E-4
6 -4.0E-4
7 -2.0E-4
8 0
9 2.0E-4
0 4.0E-4

- Lower streamwise strain

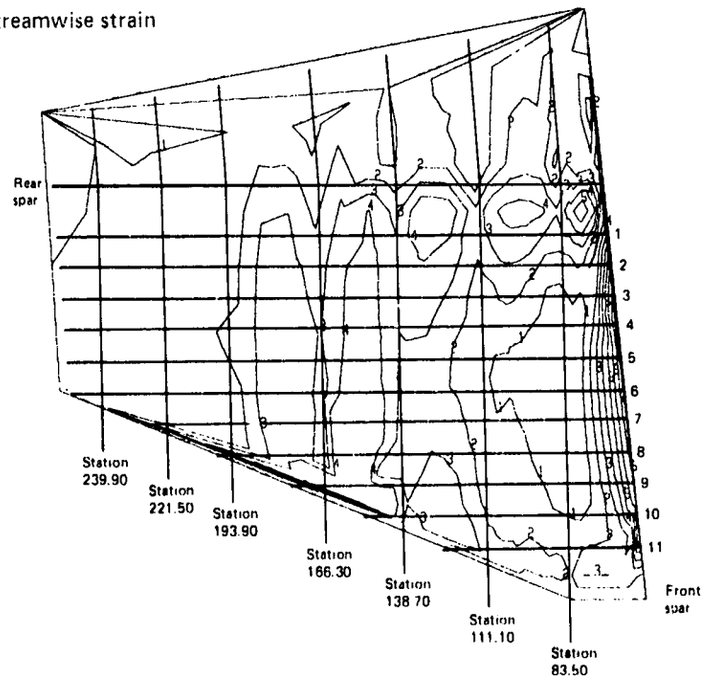

RUNID
1 0
2 2.0E-4
3 4.0E-4
4 6.0E-4
5 8.0E-4
6 1.0E-3
7 1.2E-3

Figure 43. Ultimate Loads--Streamwise Strain (Load Case 4761)

- Upper spanwise strain

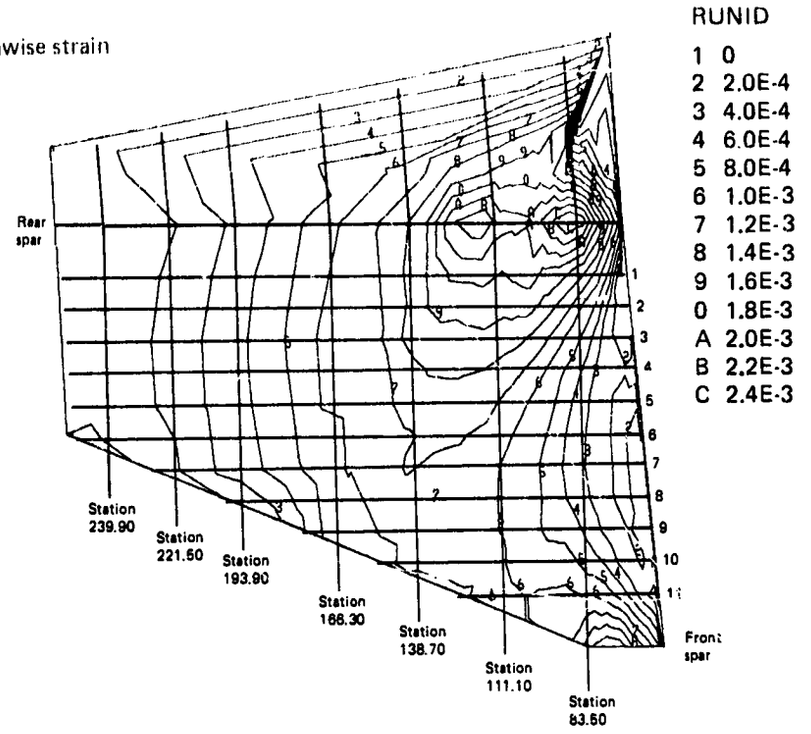

- Lower spanwise strain

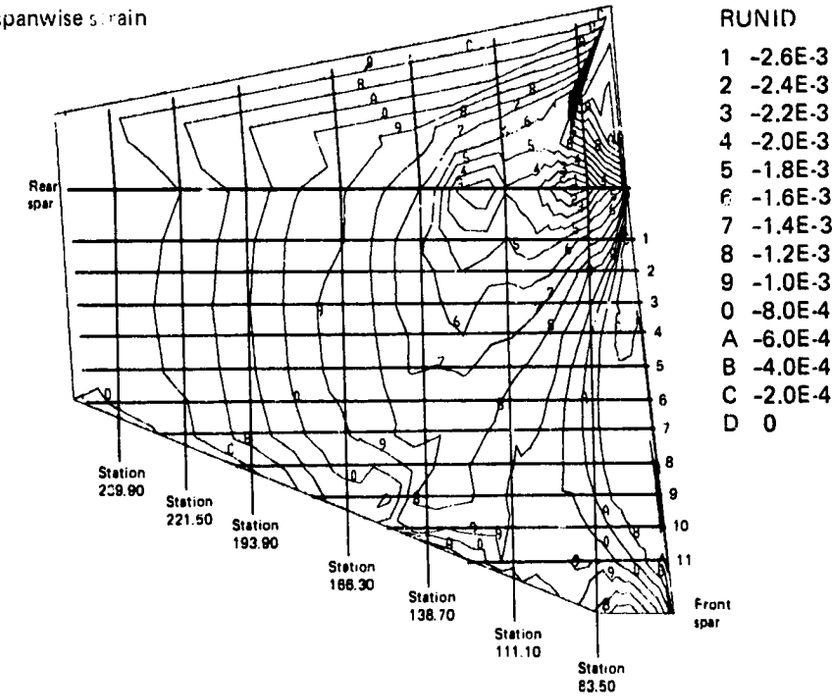

Figure 44. Ultimate Loads–Spanwise Strain (Load Condition 4761)

• Upper shear, lbf/in^2

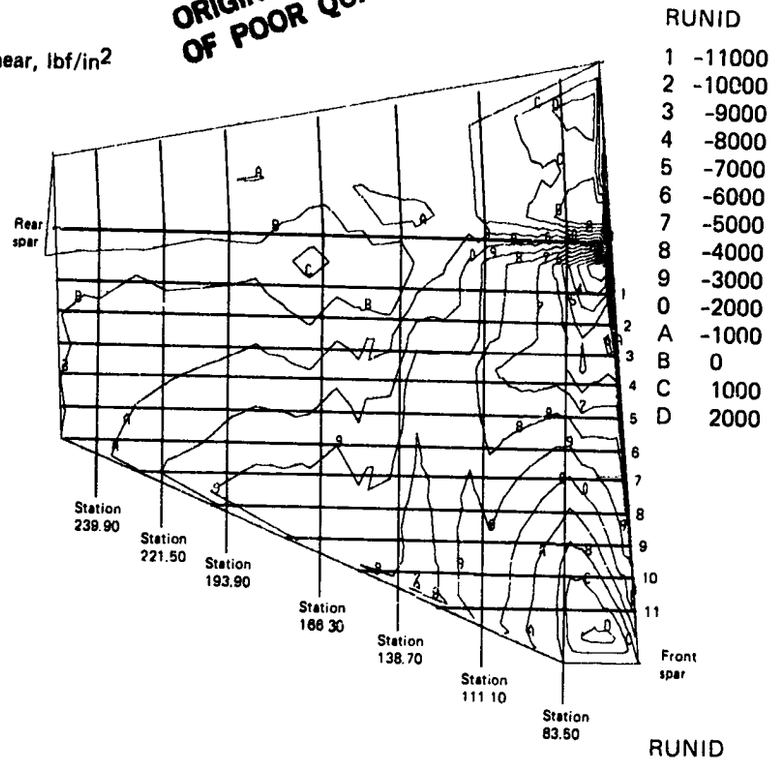

• Lower shear, lbf/in^2

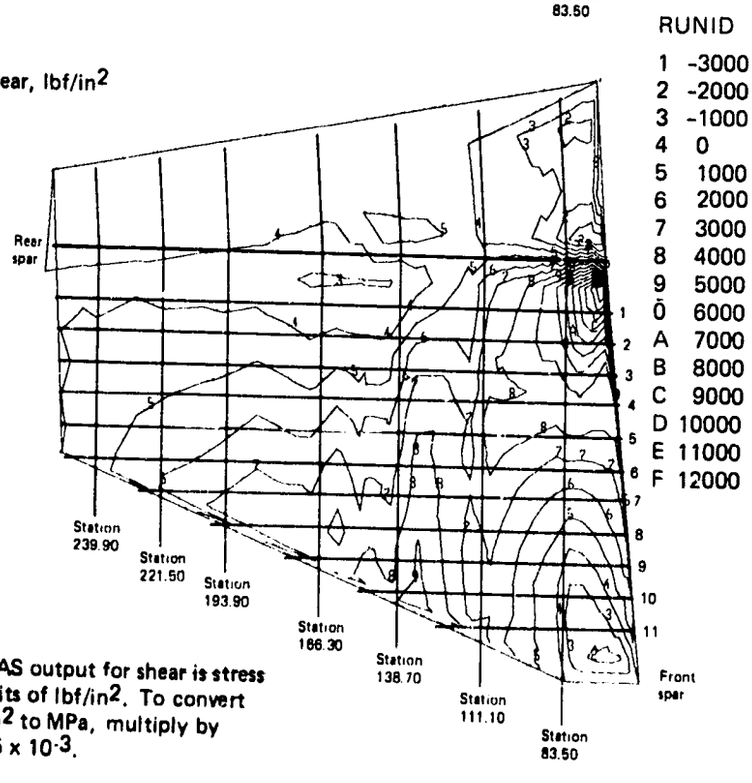

Note: ATLAS output for shear is stress in units of lbf/in^2. To convert lbf/in^2 to MPa, multiply by 6.895×10^{-3}.

Figure 45. Ultimate Loads–Shear Stress (Load Case 4430)

- Upper streamwise strain

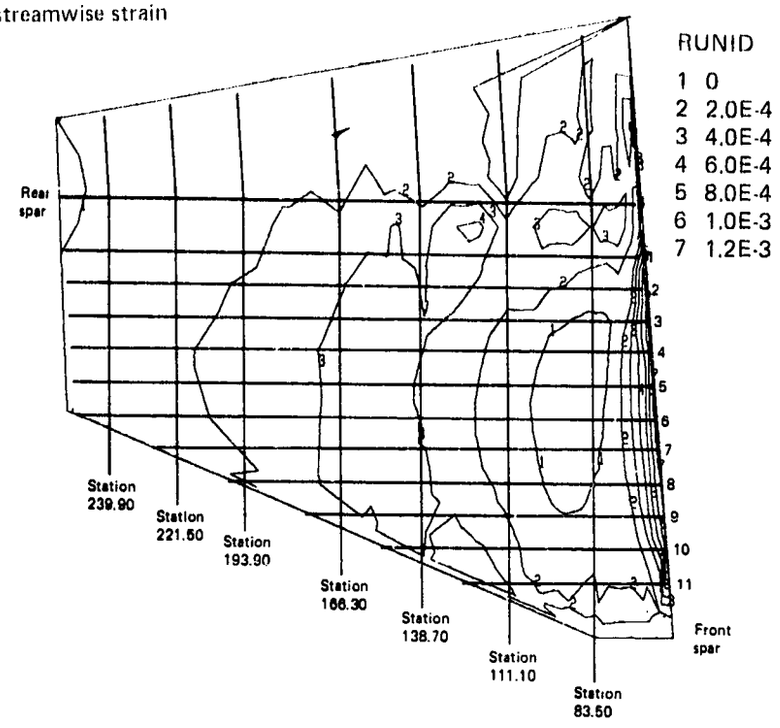

- Lower streamwise strain

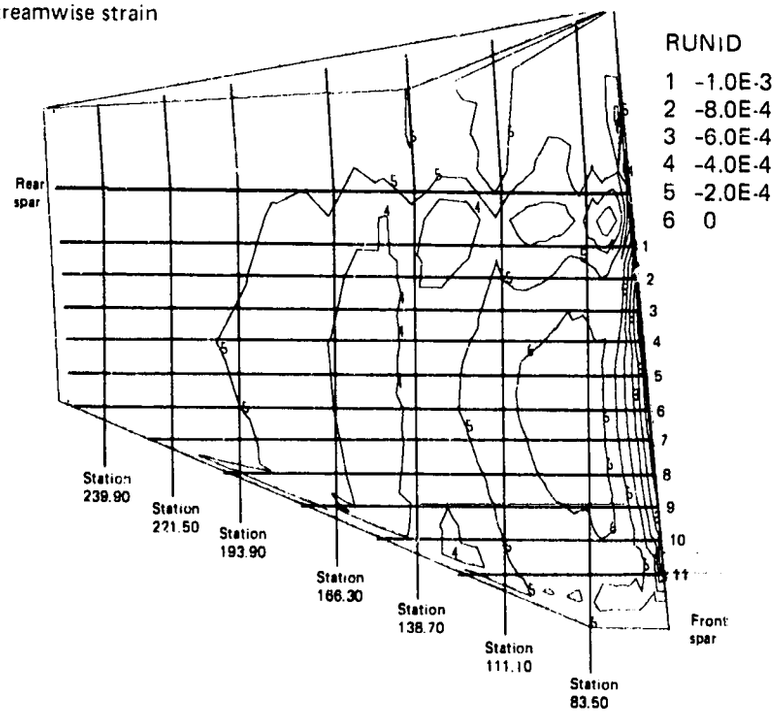

Figure 46. Ultimate Loads–Streamwise Strain (Load Case 4430)

- Upper spanwise strain

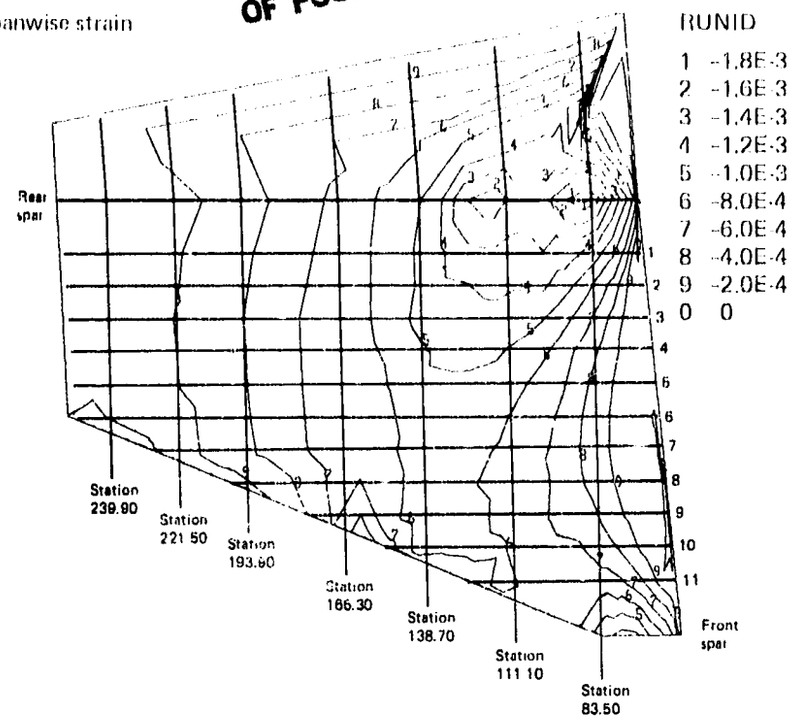

- Lower spanwise strain

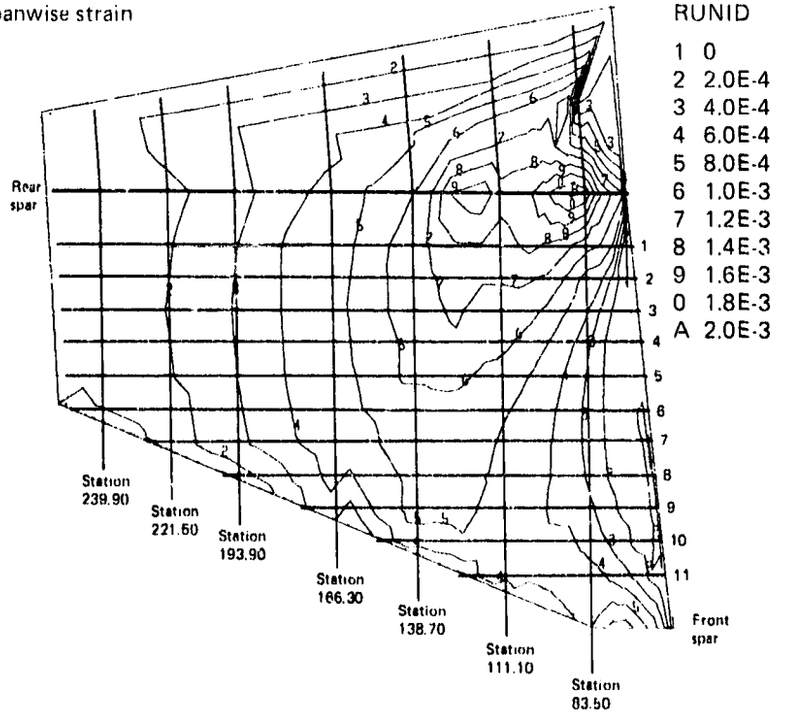

Figure 47. Ultimate Loads—Spanwise Strain (Load Case 4430)

- Upper spanwise strains

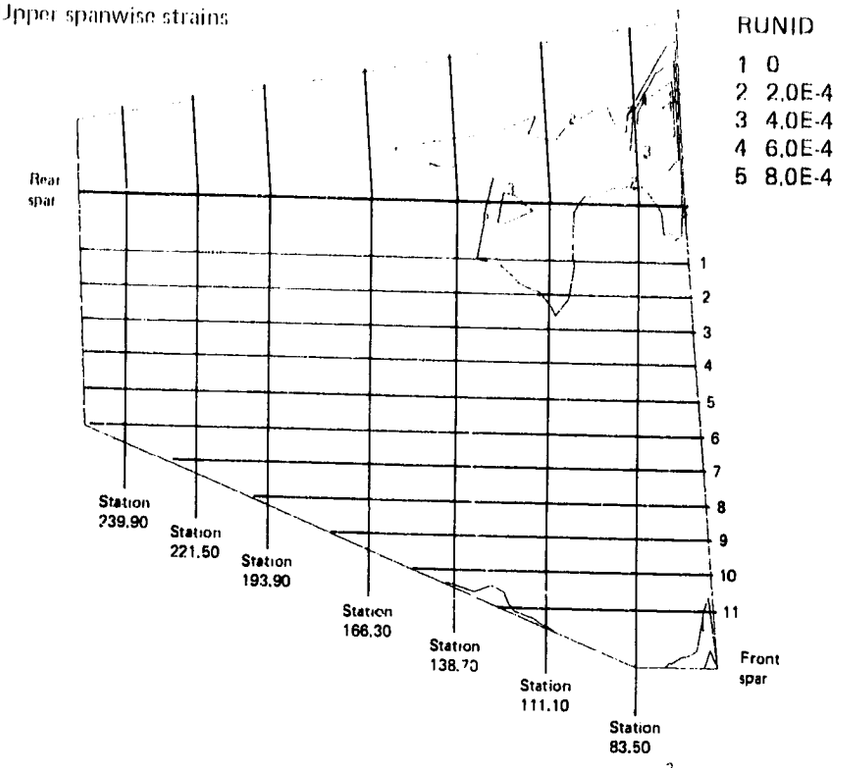

- Upper streamwise strains

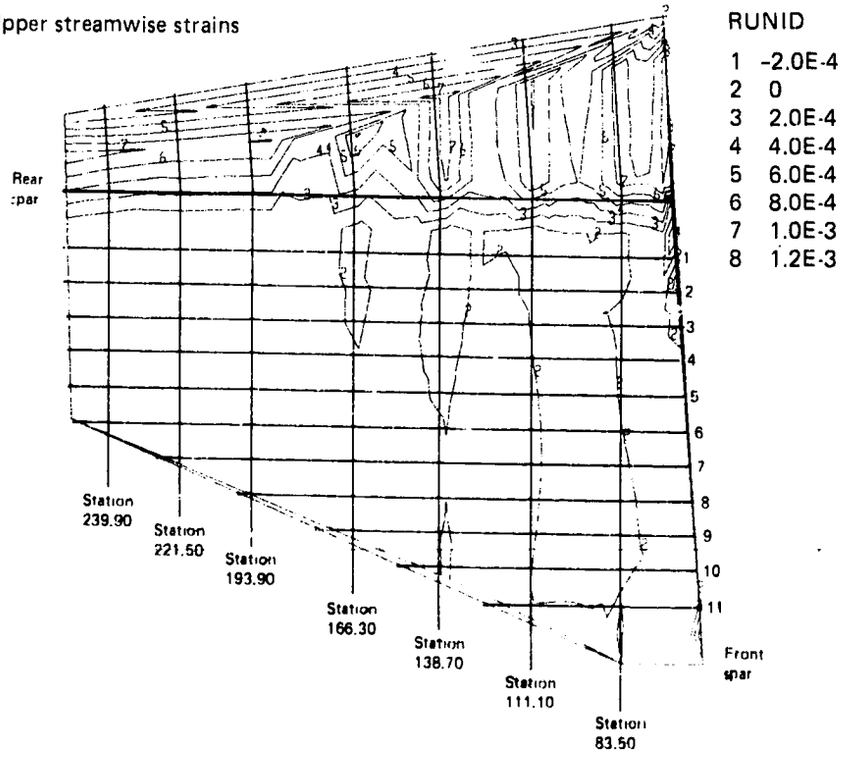

Figure 48. Typical Thermal-Induced Strains, Temperature = 180°

- Upper spanwise strain

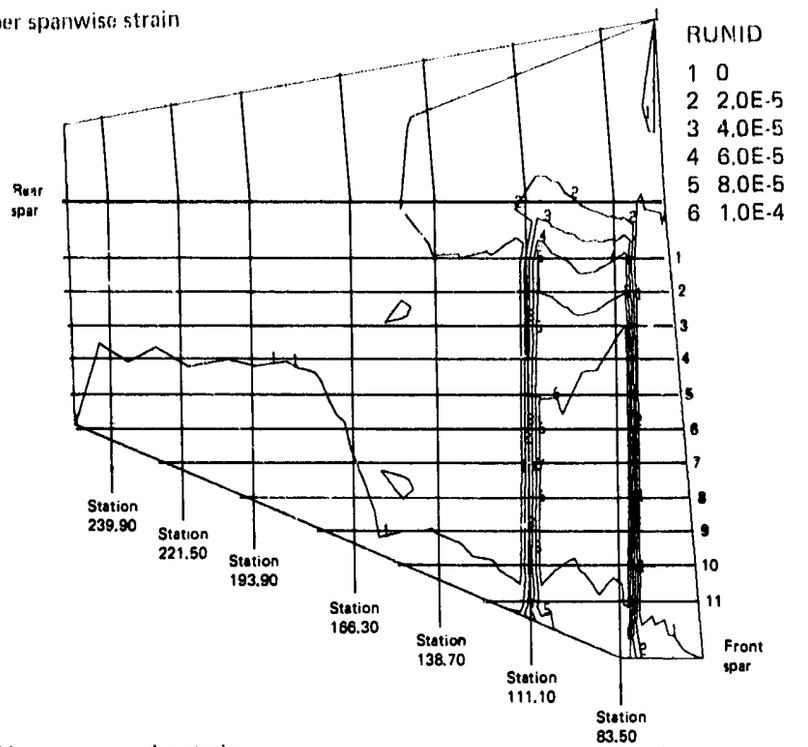

- Upper streamwise strain

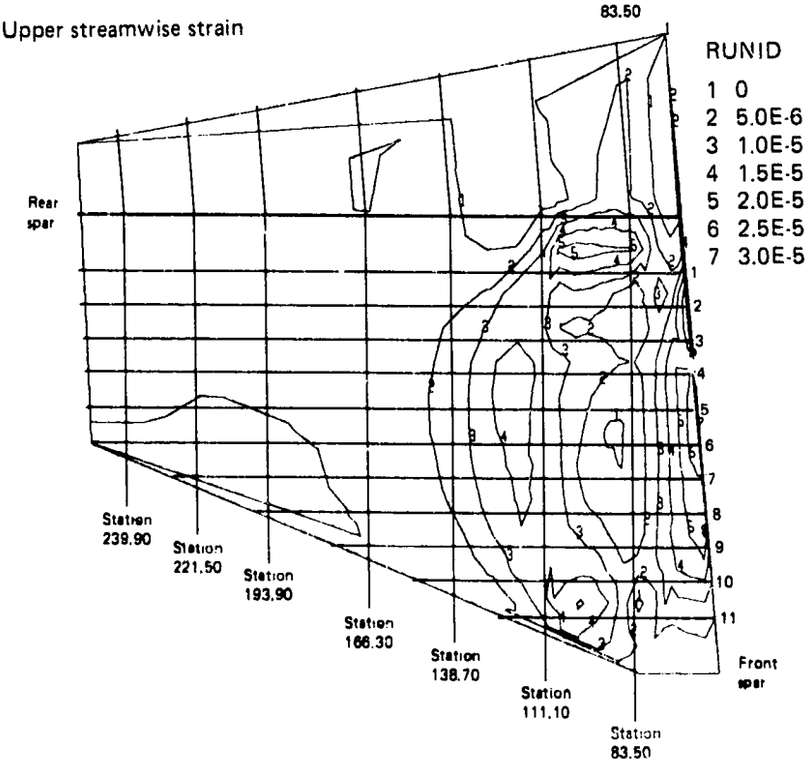

Figure 49. Typical Moisture-Induced Strains, 1.0% Moisture

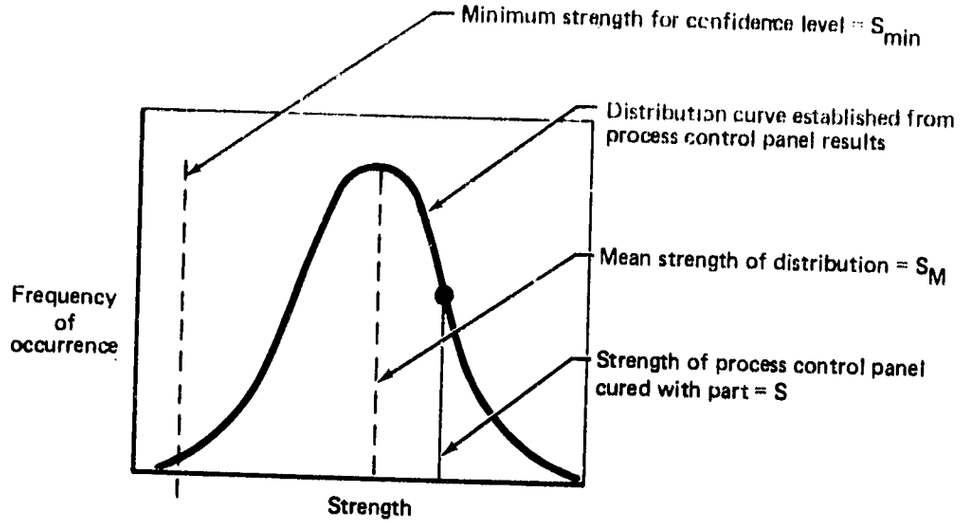

- Material correction factor, MCF = $\frac{S_M}{S}$
- Material variability factor, MVF = $\frac{S_{min}}{S_M}$

Figure 50. Material Strength Correction Factors

of the process panel population, and a material variability factor (MVF) was used to correct the mean value to the required confidence level. These factors are illustrated in Figure 50.

A variation magnification factor (VMF) was determined that accounted for variations in test specimen geometry, procedures, and conditions. Coefficients of variation for every unique test condition and specimen geometry were calculated. A distribution analysis of these coefficients of variations was performed. From this distribution, the maximum variance with less than a 5% probability of exceedance was determined to be 8.1%. The variation magnification factor then was computed as:

$$VMF = 1 - K_{B_\infty} \nu_{MAX}$$

where K_{B_∞} is the equivalent to "B" basis factor for an infinite sample. The ν_{MAX} is the maximum variance.

The final design values were obtained by multiplying the average test values by the three correction factors. An example of the correction factors is:

- MCF: material correction factor, values vary from 0.8 to 1.2
- MVF: material variability factor, 0.89 for fiber-controlled failure, 0.87 for resin-controlled failure

- VMF: variation magnification factor, 0.9
- DVR = (MCF) (MVF) (VMF)
- Design value = (DVR) (average test value)

Analyses of several examples of stabilizer structural details are contained in Figures 51 through 53.

4.1.7.3 Fail-Safe and Damage-Tolerance Analysis

An analysis was made on the stabilizer structure to show compliance with the fail-safe strength requirements of FAR Part 25 (ref. 2). The conditions are shown in Table 4. Fail-safe features in the stabilizer structure include bending capacity in both front and rear spars and a redundant fail-safe chord with terminal lug in the rear spar.

Validated damage-growth models that included spectrum-loading effects were not available to support the stabilizer program; therefore, a no-damage-growth approach was adopted. This approach simply states that damage, which is visible and is not critical, does not propagate during spectrum loading. Based on this approach, any visibly undetected damage is not critical. To verify this approach, the design and analysis of the structure included this consideration along with the test progam that contained structural element and subcomponent tests where visible damage was introduced and spectrum-type repeated loading was applied. The damage sites were inspected for growth, and residual strengths were obtained. These tests were performed at the extremes of the environmental conditions.

The full-scale ground test reported in Section 3.1 of Reference 6 demonstrated that graphite-epoxy composite material exhibits immunity to fatigue crack formation and to detrimental growth of visible accidental damage at the strain levels experienced in service.

Compliance with fail-safe requirements associated with bird-strike conditions was shown by comparative analysis. The composite horizontal stabilizer was required to meet the FAR 25.632 bird-strike requirements of a 3.6-kg (8-lb) bird for empennage structure. This is a new requirement since certification of the original 737 aircraft and was met by increasing the current 0.1-cm- (0.04-in-) thick aluminum leading edge to 0.2-cm- (0.08-in-) thick aluminum. This increase in gage was established by showing design similarity to the structures tested in References 10 and 11. The gage was selected to completely stop the bird at the leading edge. In addition, a large section of the supporting graphite-epoxy structure was assumed to be damaged, and the remaining structure was analyzed and shown to be adequate for the required critical loads.

Damage Conditions—Four cases of damage related to the terminal fittings and five cases of damage between the inboard closure rib and station 111.1 were selected.

Damage conditions FS5 through FS8 were consistent with the assumptions used for the existing horizontal stabilizer, assuming loss of tensile capability but retention of compression capability for any one of the four front- or rear-spar upper or lower chord terminal lugs.

- Lug is graphite plus two 15-5 PH CRES plates.
- At ultimate loads assume steel plates carry 100%.
- Maximum ultimate lug loads—condition 4740.

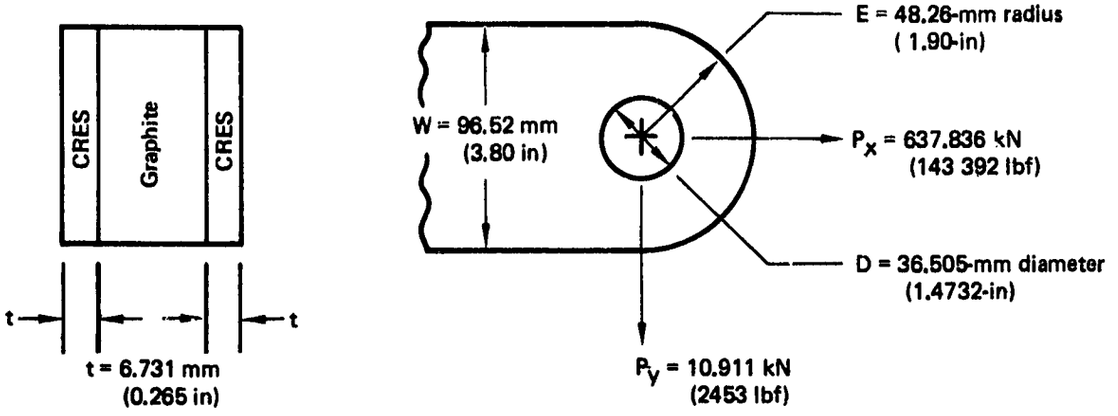

Material: 15-5 PH CRES, ref. MIL-HDBK-5B

F_{TU}	F_{TY}	F_{CY}	F_{SU}	F_{BRU}	E	G	μ
1.24×10^3 (180×10^3)	1.137×10^3 (165×10^3)	1.137×10^3 (165×10^3)	7.99×10^2 (116×10^3)	1.894×10^3 (275×10^3)	1.963×10^5 (28.5×10^6)	7.716×10^4 (11.2×10^6)	0.272 0.272

Note: All measurements in MPa (lbf/in^2).

Resultant load $P = \left[(637.836)^2 + (10.911)^2\right]^{1/2} = 637\,930\text{N}\ (143\,413\ \text{lbf})$

$$\frac{W}{D} = \frac{96.52}{36.505} = 2.644, \qquad \frac{E}{D} = \frac{48.26}{36.505} = 1.322$$

$K_T = 1.47, \quad K_{SB} = 1.22, \quad K_\theta = 0.98$

$$P_T = K_T K_\theta F_{TU} Dt = (1.47)(0.98)(1.24 \times 10^3)(0.0365)(0.006731)(10^6)(2) = 8.778 \times 10^5\text{N}\ (197\,347\ \text{lbf})$$

$$MS = \frac{P_T}{P} \cdot 1 = \frac{8.778 \times 10^5}{6.37930 \times 10^5} \cdot 1 = 0.38$$

$$P_{SB} = K_{SB} K_\theta F_{TU} Dt = (1.22)(0.98)(1.24 \times 10^3)(0.0365)(0.006731)(10^6)(2) = 7.2857 \times 10^5\text{N}\ (163\,797\ \text{lbf})$$

$$MS = \frac{P_{SB}}{P} \cdot 1 = \frac{7.2857 \times 10^5}{6.3793 \times 10^5} \cdot 1 = 0.14$$

Figure 51. Front- or Rear-Spar Lug Analysis

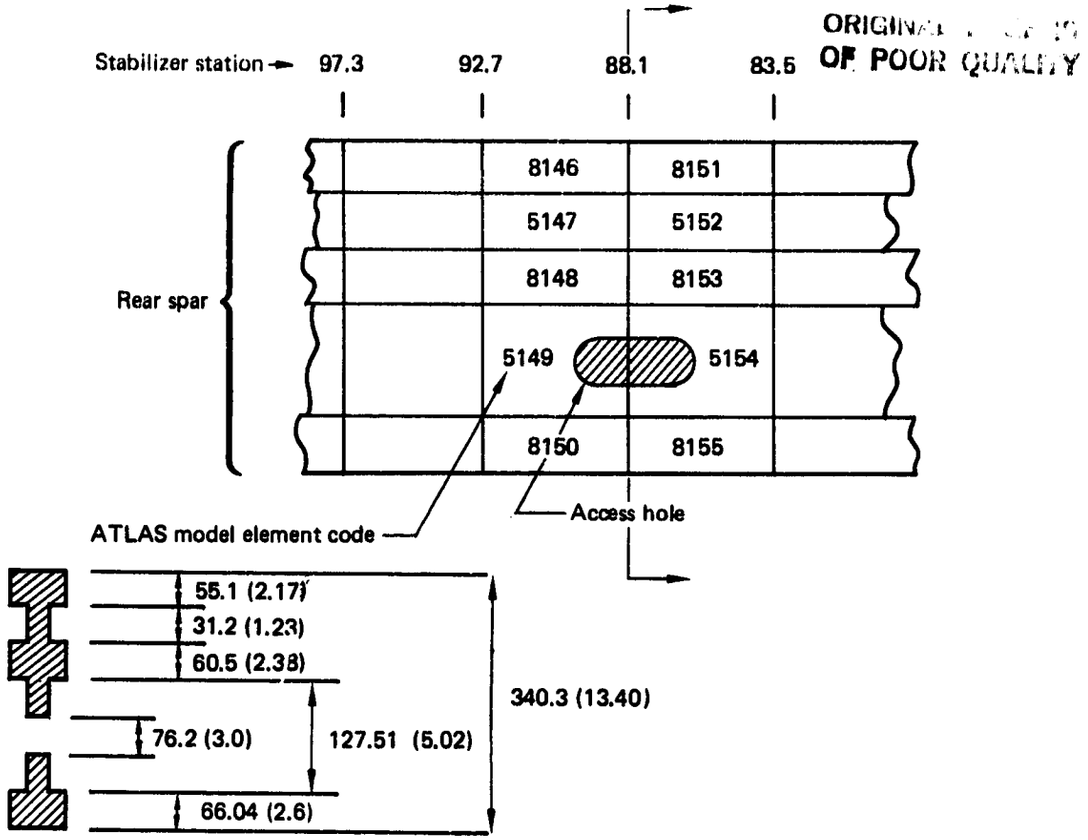

Note: All measurements in mm(in).

		ATLAS model element shear, N/m (lbf/in)			
Panel	Thickness	LC 4010 21.1°C (70°F)	1% moisture absorption	82.2°C (180°F)	Σq hot, wet
5149	4.57 mm (0.18 in)	233 793 (1 335)	Negligible	11 909 (68)	245 702 (1 403)

$G = 22\,061$ MPa $(3.2 \times 10^6$ lbf/in$^2)$

$\gamma_{test} = 0.003870$ m/m (ref.sec. 4.2.2.3)

$\gamma_{design} = \gamma_{test} \times DVR = 0.003870(0.72) = 0.002784$ m/m

$q_{all} = (\gamma_{design})(t)(G) = (0.002784)(4.57 \times 10^{-3})(22\,061 \times 10^6) = 280\,677$N/m (1603 lbf/in)

$$MS = \frac{q_{all}}{\Sigma q_{hot,\,wet}} \cdot 1 = \frac{280\,677}{245\,702} \cdot 1 = 0.14$$

Figure 52. Spar Web Shear Analysis

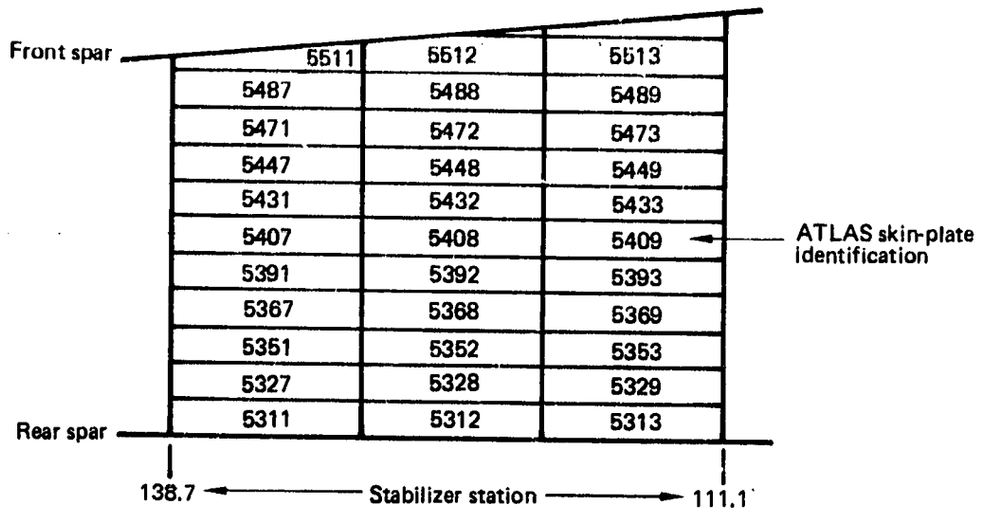

		ATLAS model element shear, N/m (lbf/in)					
Panel	Thickness	LC 3710	1% moisture	-59.4°C (-75.0°F)	82.2°C (180.0°F)	Σ cold, wet	Σ hot, wet
5448	1.35 mm (0.0532 in)	-48 510 (-277)	-701 (-4)	-2627 (-15)	2102 (12)	-51 837 (-296)	-47 109 (-269)
		ATLAS model element stresses, MPa (lbf/in^2)					
	σ_1	12.147 (1762)	Negligible	1.999 (290)	1.489 (216)	14.146 (2052)	13.636 (1978)
	σ_2	36.000 (5222)	Negligible	-2.268 (-329)	-1.661 (-241)	33.732 (4893)	34.305 (4976)

$$\sigma_{principal} = \frac{\sigma_2 + \sigma_1}{2} + \left[\frac{(\sigma_2 - \sigma_1)^2}{4} + \tau^2\right]^{1/2}$$

$$\tau_{5448} = q/t = \frac{51837}{0.00135} = 38.398 \text{ MPa } (5564 \text{ lbf/in}^2)$$

$$\sigma_{principal} = \frac{33.732 + 14.146}{2} + \left[\frac{(33.732 - 14.146)^2}{4} + (38.398)^2\right]^{1/2} = 63.528 \text{ MPa } (9215 \text{ lbf/in}^2)$$

Impacted coupon testing shows (ref. sec. 4.2.1):

$$\sigma_{design} = \sigma_{test} \text{ (DVR)} = (228.1)(0.86) = 196.2 \text{ MPa } (28\,400 \text{ lbf/in}^2)$$

$$MS = \frac{\sigma_{design}}{\sigma_{principal}} \cdot 1 = \frac{196.2}{63.528} \cdot 1 = 2.08$$

Figure 53. Combined Stresses for Upper Surface With Maximum Shear Plus Axial Tensile Stress

Table 4. Fail-Safe and Damage-Tolerance Load Conditions

Model condition	Limit load case	Description
FS5	4010	Down bending, rear-spar, upper lug bolt removed
FS6	4430	Up bending, rear-spar lower lug bolt removed
FS7	4010	Down bending, front-spar upper lug bolt removed
FS8	4430	Up bending, front-spar lower lug bolt removed
DT1	3710 4010 4761 4430	Failure in rear-spar lower inboard shear web
DT2	3710 4010 4761 4430	Failure of stringer 2 and skin between stringers 1 and 3 adjacent to stringer 1 maximum stress
DT3	3710 4010 4761 4430	Failure of stringer 1 and skin between the rear spar and stringer 2
DT4	3710 4010 4761 4430	Partial fracture of the rear-spar inboard upper chord
DT5	3710 4010 4761 4430	Failure of aft inboard corner of the lower skin

Selection of the other five damage conditions, DT1 through DT5, was based on the premise that damage occurs in or adjacent to the most critically loaded member.

DT1 represented failure in a far inboard rear-spar lower shear web adjacent to a steel reinforcing plate. Foreign object impact was the presumed cause of damage in the lower inboard skin structure for conditions DT2, DT3, and DT5. DT4 represented partial fracture of the inboard upper chord of the rear spar.

Methods of Analysis--For all damage conditions and the undamaged base condition, all internal load distributions were determined by linear finite element analysis. Detail stresses and strains, including the influences of structural nonlinearities, were obtained by hand calculations using conventional engineering practices.

Examples of analysis of the damaged structure are illustrated in Figures 54 through 56.

- Critical condition: FS6, temperature at 82°C (180°F).
  This represents the worst tension load on the rear-spar fail-safe lug for a fail-safe load condition.
- Assume half of the load is applied to each side plate and none to the graphite-epoxy portion of the lug.

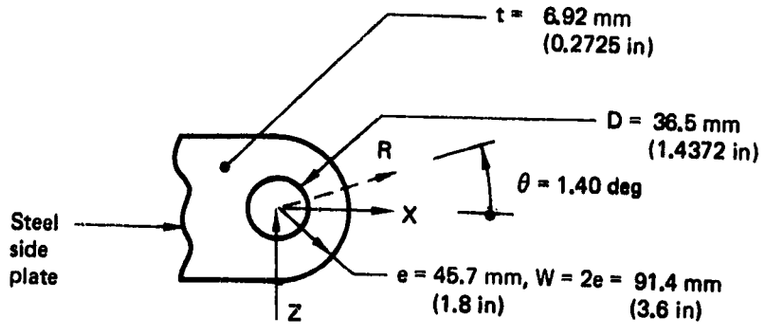

		ATLAS fail-safe loads			
Load case	Temperature	X	Z	R	θ
4430 FS6	82.2°C (180°F)	3.151×10^5N (70 841 lbf)	7989N (1796 lbf)	3.152×10^6 N (70 864 lbf)	1.4 deg

$K_\theta \cong 1.0$

$\frac{e}{D} = \frac{45.7}{36.5} = 1.25, \frac{W}{D} = \frac{91.40}{36.5} = 2.50$

$K_T = 1.36, K_{SB} = 1.14$

$P_T = K_T F_{TU} Dt = (1.36)(36.5)(6.92) F_{TU} = 343.51 F_{TU}$

$P_{SB} = K_{SB} F_{TU_{min}} Dt = (1.14)(36.5)(6.92) F_{TU_{min}} = 288.04 F_{TU_{min}}$

$F_{TU_{min}}$ (82°C) = (1240.92)(0.965) [2] = 1197.49 MPa (173 700 lbf/in^2) [1]

$P_{allow} = (288.04)(1197.49) = 3.4499 \times 10^5$N (77 557 lbf)

$MS = \frac{3.4499 \times 10^5}{3.152 \times 10^5} - 1 = 0.09$

[1] Material properties reference Figure 51. [2] Temperature factor.

Figure 54. Rear-Spar Steel Reinforcement Fitting Analysis

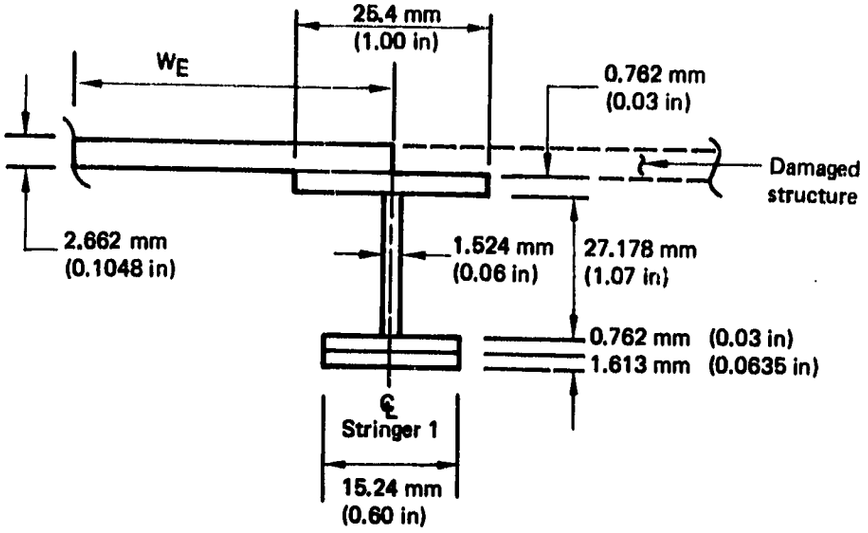

Section of skin/stringer 1 at lower surface stabilizer station 101.9

Figure 55. Skin/Stringer Section for Damaged Structure Load Condition, (DT2, Load Case 4010)

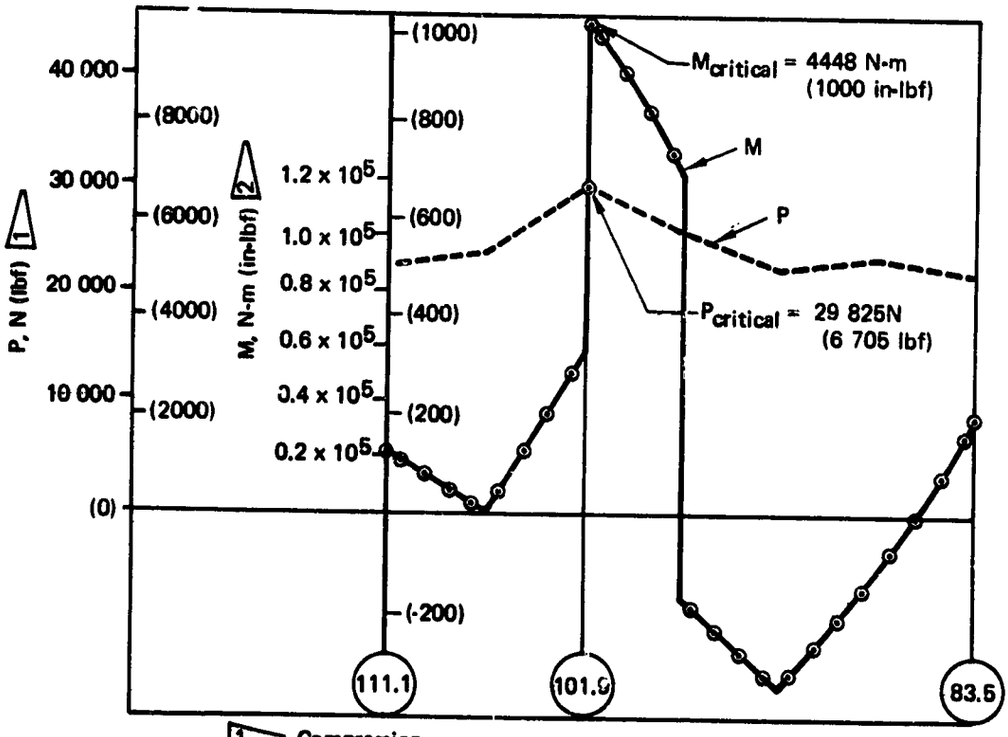

Design loads for stringer 1 between stabilizer stations 111.1 and 83.5 on lower surface

Figure 56. Loads for Lowest Margin of Safety

The following combination of loads and environment produces the lowest margin of safety:

- Load: axial compression and bending
- Temperature: 21.1°C (70°F)
- Moisture condition: wet

$$W_E = 6.35 + W_{SK_i}$$

$$= 6.35 + 0.85\,(2.662)(\epsilon_{design})^{-0.5}$$

$$\epsilon_{design} = -0.003920 \text{ m/m}\ ,\ 21.1^{\circ}\text{C}\ (70^{\circ}\text{F})\ \boxed{1}\text{, wet}$$

$$W_E = 6.35 + 0.85(2.662)(-0.00392)^{-0.5} = 42.48 \text{ mm } (1.673 \text{ in})$$

$$EA = 9.8029 \times 10^6 \text{N}$$

$$\left(\frac{EI}{c}\right)_{skin} = 5.4642 \times 10^6 \text{ N·m}$$

$$\epsilon_{\substack{skin \\ basic}} = -\frac{P_{cr}}{EA} - \frac{M_{cr}c}{EI}\ ,\ 21.1^{\circ}\text{C}\ (70^{\circ}\text{F}),\ \text{dry}$$

$$= -\frac{29\,825}{9.8029 \times 10^6} - \frac{4448}{5.4642 \times 10^6} = -0.003856$$

$$\epsilon_{1\%\ moisture} = 0.000058 \text{m/m (ref. fig. 49)}$$

$$\Sigma\epsilon = \epsilon_{basic} + \epsilon_{moisture}$$

$$= -0.003856 - 0.000058 = -0.003796$$

$$MS = \frac{\epsilon_{design}}{\Sigma\epsilon} - 1 = \frac{-0.003920}{-0.003796} - 1 = 0.03$$

$\boxed{1}$ σ_{test} = 196 MPa(28.4 lbf/in^2 x 10^3)Layup A impact = 2.82 Nm (25 lb-in) (ref. sec. 4.2, fig. 57)

E = 4 x 10^4 MPa (5.8 x 10^6 lbf/in^2) (ref. fig. 32)

DVR = MCF x MVF x VMF = 1.00(0.89)(0.90) = 0.80 (ref. sec. 4.1.7.2)

$$\epsilon_{design} = \left(\frac{\sigma_{test}}{E}\right) DVR = \left(\frac{196 \text{ MPa}}{4 \times 10^4 \text{ MPa}}\right)(0.80) = 0.00392 \text{ m/m}$$

Figure 56. Loads for Lowest Margin of Safety (Concluded)

4.2 ANCILLARY TESTING

The ancillary test plan encompassed all testing except ground and flight tests of the full-scale model and included coupon, structural element, and subcomponent tests. The test plan provided:

- Material design values, including environmental effects for FAA certification
- Strength and fatigue performance
- Verification of final design details
- Strength and fatigue performance of repairs

Moisture conditioning of test specimens was accomplished by placing the parts in an environmental chamber at 60°C (140°F) and 100% relative humidity (RH) until the required moisture level was obtained as defined in Section 4.1.6. The detailed ancillary test plan is presented in Tables 5 through 8. Flag notes, ▷, are used to denote specific test conditions in a series. For example, in Table 6, Test 9, 1+3 ▷2 indicates that one specimen was subjected to one life spectrum cyclic test followed by static test to failure, and three specimens were subjected to two life spectra cyclic tests followed by static test to failure.

The data from the tests are shown in the following sections with specimen descriptions. Test data are presented in Appendix C and summary tables and graphs are shown in this section.

4.2.1 Coupon Tests

The material coupon test, Test 1, included impacted static tension and compression coupons and static tension fastener bearing specimens. Impact levels were imposed to establish the effect of both visible and nonvisible damage. Data from these tests were used to establish design values for certification. The failure stresses for the impacted coupons were calculated from the failure load, nominal thickness, and actual width. The fastener bearing stresses were calculated using nominal fastener diameter and nominal thickness.

Figure 57 shows the effects of moisture, temperature, and several levels of impact on various ply layups. Figures 58 and 59 show the effects of moisture and temperature on the bearing stress of the fastener bearing specimens.

4.2.2 Structural Element Tests

Design development structural element tests were performed to obtain design values for structural elements. Included are Tests 5, 9, 11, 7, 10 (crippling panel), and 35.

4.2.2.1 Mechanical Joints

Figure 60 shows the effect of moisture and fastener spacing on fastener bearing specimens from Test 5 with 4.76-mm- (0.1875-in-) diameter Hi-Lok fasteners. Figure 61 shows the effects of the same variables on 6.35-mm- (0.25-in-) diameter Hi-Lok fasteners. The test data are presented in Appendix C.

Table 5. Material Design Values—Mechanical Properties

Test	Specimen 65C17758	Cloth laminate, deg	Size, mm (in)	Environmental condition	Temperature and number of tests: 21°C (70°F)	-54°C (-65°F)	82°C (180°F)	Data	Instrumentation	Purpose	Remarks
Test 1	Impact defect compression test 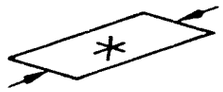 Type 1	$0/\pm45_2/90$	406 x 76 (16 x 3)	Wet	6	3	9	Load/strain	Extensometer	Effect of stress concentration	•Two thicknesses •Two impact levels
				Dry	25	19	6				
		0/±45/90		Wet	12		6				
				Dry	12	6	6				
Test 1	Impact defect tension test 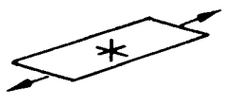 Type 2	0/±45/90	406 x 76 (16 x 3)	Wet	8	3	7	Load/strain	Extensometer	Effect of stress concentration	•Two thicknesses •Two impact levels
				Dry	15	12	6				
		0/±45/90		Wet	11	6	10				
				Dry	12	12	6				
Test 1	Fastener bearing 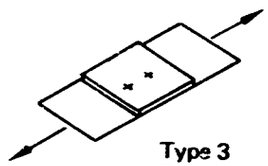 Type 3 Double shear	0/±45/90	381 x 14.2 (15 x 0.56) to 381 x 31.75 (15 x 1.25)	Wet	12	3	12	Failure load and mode of failure		Bearing strength	• Two sizes of fastener • Two W/Ds
				Dry	15	12	3				
Test 1	Fastener bearing 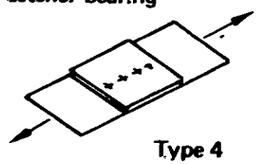 Type 4 Double shear	0/±45/90	381 x 23.9 (15 x 0.94) to 381 x 44.45 (15 x 1.75)	Wet	12		12	Failure load and mode of failure		Bearing strength	• Two sizes of fastener • Two W/Ds
				Dry	12	12					

Note: Wet condition denotes 1.1% moisture content achieved by conditioning in a 100% relative humidity chamber at 60°C (140°F).

Table 6. Design Development Structural Element Test Plan

Test number	Specimen	Size, mm (in)	Configuration (4)	Environmental condition	Temperature and number of tests: 21°C (70°F)	Temperature and number of tests: -54°C (-65°F)	Temperature and number of tests: 82°C (180°F)	Data	Remarks
Test 5	Mechanical joint box fastener pattern 65C17769 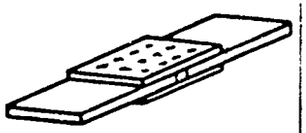 Laminate [0/±45/90]	533 x 71 (21 x 2.8) to 813 x 34 (32 x 5.25)	-1 to -4	Dry	12	–	–	Static tension failure load and mode	• Two fastener sizes • Two W/D ratios
				Wet	12	–	–		
			-9, -10	Dry	6	–	–	Static compression failure load and mode	
			-1, -2	Dry	6	–	–	Cyclic life (1)	
Test 5	Mechanical joint staggered fastener pattern 65C17769 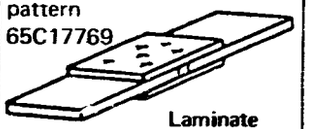 Laminate [0/±45$_2$/90]	432 x 43 (17 x 1.7) to 660 x 95 (26 x 3.75)	-5 to -8	Wet	12	–	–	Static tension failure load and mode	• Two fastener sizes • Two W/D ratios
				Dry	12	–	–		
			-5, -6	Dry	6	–	–	Cyclic life (1)	
Test 9	Skin panel to rib attachment 65C17786 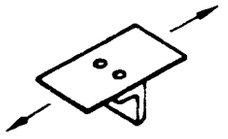	508 x 76 (20 x 3)	-1	Dry	3	3	–	Failure load and mode of failure	Static strength
				Wet	3	–	3		
			-2	Dry	2	–	–		
			-1	Dry	1+3 (2)	1 (3)	–	Cyclic life	One life spectrum cyclic test followed by static test to failure
					1 (3)			Load and cycles to failure (1)	
				Wet	1 (3)	–	1 (3)		

Note: Wet condition denotes 1.1% moisture content achieved by conditioning in a 100% relative humidity chamber at 60°C (140°F).

(1) Damage growth rates measured. (2) Two life spectra cyclic tests followed by static test to failure for three of four total specimens. (3) Initial impact damage. (4) Reference Appendix C.

Table 6. Design Development Structural Element Test Plan (Continued)

Test number	Specimen	Size, mm (in)	Config-uration	Environ-mental condition	Temperature and number of tests			Data	Remarks
					21°C (70°F)	-54°C (-65°F)	82°C (180°F)		
Test 11	Spar shear web 65C17789 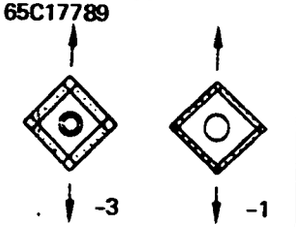	330 x 330 (13 x 13)	-1	Dry	3	3	–	Failure load and mode of failure stiffness measure-ments	Static strength
				Wet	3	–	3		
			-3	Dry	3	3	–		
				Wet	3	–	3		
Test 7	Spar chord crippling 65C17791 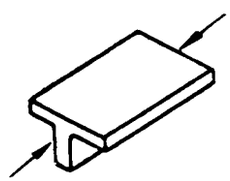	254 (10)	-1 Front spar chord	Dry	3	3	–	Failure load and mode of failure	Static strength
				Wet	3	–	3		
			-2 Rear spar chord	Dry	3	–	–		
				Wet	3	–	3		
Test 10	Skin panel/stiffener crippling 65C17773 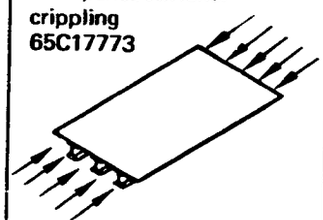 3 stiffeners 3 load levels	381 x 254 (15 x 10)	-60	Dry	1	–	–	Failure load and mode of failure	Static strength
			-61	Dry	1	–	–		
			-62	Dry	3	–	–		

Note: Wet condition denotes 1.1% moisture content achieved by conditioning in a 100% relative humidity chamber at 60°C (140°F).

Table 6. Design Development Structural Element Test Plan (Concluded)

Test number	Specimen NHS1-VNS	Size, mm (in)	Configuration	Environmental condition	Temperature and number of tests			Data	Remarks
					21°C (70°F)	-54°C (-65°F)	82°C (180°F)		
Test 35	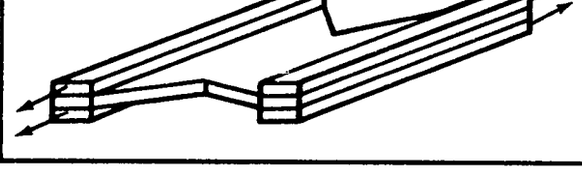	152 x 76	-1	Wet	5	5	5	Laminate shear strength	Static strength
		(6 x 3)		Dry	5	5	5		

Table 7. Stabilizer Subcomponent Test Plan

Test number	Specimen 65C17773	Size, mm (in)	Configuration	Environmental condition	Temperature and number of tests: 21°C (70°F)	-54°C (-65°F)	82°C (180°F)	Data	Load condition
Test 10	Stiffened skin panel Compression 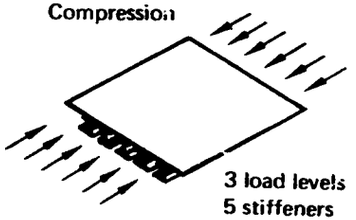 3 load levels 5 stiffeners	1400 x 442 (55 x 17.4)	-1	Dry	3^{+1}_{+2} [1] [2]	1+1 [2]	–	Failure load and mode of failure	Static strength [1] Panels used for lightning strike protection testing [2] Defect or damaged part
				Wet	2+1 [2]	–	1+1 [2]		
			-2	Dry	1	–	–		
Test 10	Stiffened skin panel Shear loading 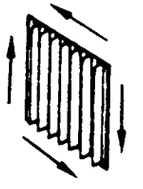 3 load levels 7 stiffeners	864 x 940 (34 x 37)	-6	Dry	3^{+1}_{+2} [1] [2]	1+1 [2]	–		
				Wet	2+1 [2]	–	1+1 [2]		
			-7	Dry	1	–	–		
			-5		1	–	–		
Test 10	Stiffened skin panel Compression and shear  2 load levels 7 stiffeners	1067 x 1067 (42 x 42)	-43	Dry	3+2 [2]	–	–		
				Wet	–	–	1		
			-42	Dry	1	–	–		

Note: Wet condition denotes 1.1% moisture content achieved by conditioning in a 100% relative humidity chamber at 60°C (140°F).

Table 7. Stabilizer Subcomponent Test Plan (Continued)

Test number	Specimen	Size, mm (in)	Config-uration	Environ-mental condition	Temperature and number of tests			Data	Load condition
					21°C (70°F)	-54°C (-65°F)	82°C (180°F)		
Test 10	Stiffened skin panel—fatigue 65C17773 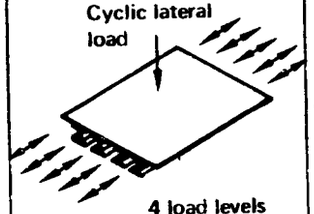	1321 x 345 (52 x 13.6)	-9 [3]	Dry	1 [1] 1 [2]	1 [2]	—	Cyclic life—load and cycles to failure Damage growth rate	Spectrum cyclic loads
				Wet	1 [1]	—	1 [4]		
			-10 [5]	Dry	1 [1]	—	—		
			-81 [3]	Dry	1 [1] 1 [2]	1 [4]	—		
				Wet	1 [1]	—	1 [4]		
Test 12	Root lug tests 65C17774 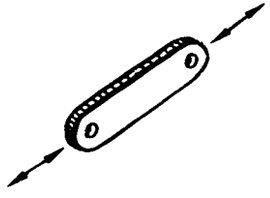	508 x 76 x 38 (20 x 3 x 1.5)	Tension	Dry Wet	2 2	2 —	— 2	Failure load and mode of failure	Static strength tension and compression
			Compres-sion	Dry Wet	2 —	2 —	2 2		
			Fatigue	Dry Wet	3T, 3C —	3T,3C —	— 1T, 1C	Failure mode and cyclic life Damage growth rates	Spectrum cyclic loads [6] T—tension spectrum C—compression spectrum

Note: Wet condition denotes 1.1% moisture content achieved by conditioning in a 100% relative humidity chamber at 60°C (140°F).

[1] Test plan type A.
[2] Test plan type B.
[4] Test plan type C.
} See Table 14.

[3] Upper surface.
[5] Lower surface.

[6] Two of each set will be subjected to two life spectra fatigue tests followed by static test to failure, and the remaining specimen of each set will be subjected to four life spectra fatigue tests.

Table 7. Stabilizer Subcomponent Test Plan (Continued)

Test number	Test	Skin laminate	Load condition	Specimen 65C17989 [1]	Environmental condition	Number of specimens versus crack width and temperature, °C (°F)						Data	Remarks
						a mm (in)	21 (70)	a mm (in)	-59 (-75)	a mm (in)	82 (180)		
Test 31	Fracture panels	12 plies (7-mil fabric) (9 at 45, 3 at 0/90)	Tension 2a Center crack	-1	Dry	6.40 (0.25)	2	6.40 (0.25)	2			Failure load	Static strength
				-2	Dry			25.4 (1.00)	2				
			Compression 0 2a Center crack	-13	Dry	6.40 (0.25)	2						
				-13	Wet					6.40 (0.25)	2		
				-14	Wet					25.4 (1.00)	2		
			Tension a Edge crack	-3	Dry	6.40 (0.25)	2	6.40 (0.25)	2				
				-4	Dry			25.4 (1.00)	2				
			Compression a Edge crack	-15	Dry	6.40 (0.25)	2						
				-15	Wet					6.40 (0.25)	2		
				-16	Wet					25.4 (1.00)	2		
		7 plies (7-mil fabric) (5 at 45, 2 at 0) 2 plies (7-mil tape) (0)	Tension 2a Center crack	-5	Dry	6.40 (0.25)	2	6.40 (0.25)	2				
				-6	Dry			25.4 (1.00)	2				
			Compression 0 2a Center crack	-17	Dry	6.40 (0.25)	2						
				-17	Wet					6.40 (0.25)	2		
				-18	Wet					25.4 (1.00)	2		
			Tension a Edge crack	-7	Dry	6.40 (0.25)	2	6.40 (0.25)	2				
				-8	Dry			25.4 (1.00)	2				
			Compression a Edge crack	-19	Dry	6.40 (0.25)	2						
				-19	Wet					6.40 (0.25)	2		
				20	Wet					25.4 (1.00)	2		
		7 plies (7-mil fabric) (5 at 45, 2 at 0/90) 2 plies (7-mil tape) (90)	Tension 2a Center crack	-9	Dry	6.40 (0.25)	2	6.40 (0.25)	2				
				-10	Dry			25.4 (1.00)	2				
			Compression 0 2a Center crack	-21	Dry	6.40 (0.25)	2						
				-21	Wet					6.40 (0.25)	2		
				-22	Wet					25.4 (1.00)	2		
			Tension Edge crack	-11	Dry	6.40 (0.25)	2	6.40 (0.25)	2				
				-12	Dry			25.4 (1.00)	2				
			Compression a Edge crack	-23	Dry	6.40 (0.25)	2						
				23	Wet					6.40 (0.25)	2		
				-24	Wet					25.4 (1.00)	2		

[1] See Figure 125 for dimensions.

Table 7. Stabilizer Subcomponent Test Plan (Continued)

Test number	Specimen	Size, mm (in)	Config-uration	Environ-mental condition	Temperature and number of tests			Data	Load condition
					21°C (70°F)	-54°C (-65°F)	82°C (180°F)		
Test 12B	Root lug tests 65C17986 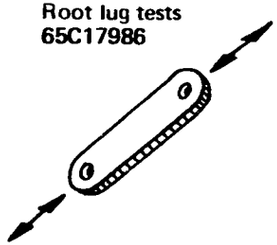	914 x 102 x 38 (36 x 4 x 1.5)	-20	Dry	–	3	–	Failure load and mode of failure	Static tension strength
			-21	Dry Wet	– –	2T –	– 4C	Failure mode and cyclic life Damage growth rates	T – Tension spectrum C – Compression spectrum [1]
			-22 flawed	Dry Wet	– –	2T –	– 2C		
			-23 flawed	Dry Wet	– –	2T –	– 2C		
Test 27	Skin/rib joint 69-69824 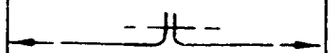	305 x 76 (12 x 3)	-1	Dry Wet	5 –	3 3	3 3	Joint strength	Static tension
			-3	Dry Wet	5 –	3 3	3 3		
	69-69823 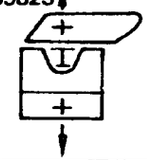	305 x 102 (12 x 4)	-1	Dry	5	–	–		
			-3	Dry	5	–	–		
	69-69818 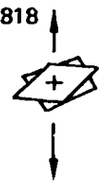	38 x 38 (1.5 x 1.5)	-5	Dry Wet	5 –	3 3	3 3		

[1] Spectrum cyclic load followed by static tension (for dry specimens) and static compression (for wet specimens) to failure.

Table 7. Stabilizer Subcomponent Test Plan (Continued)

Test number	Specimen 65C17984	Size, mm (in)	Configuration	Environmental condition	Temperature and number of tests			Data	Load conditions
					21°C (70°F)	-54°C (-65°F)	82°C (180°F)		
Test 28	Tip section 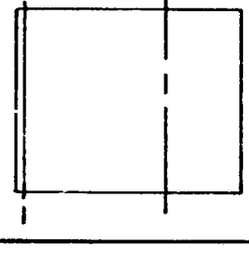	940 x 838 (37 x 33)	-1	Dry	1			Damage assessment	Lightning strike
	Spar/rib intersection 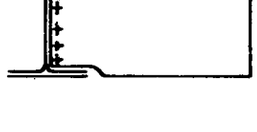	762 x 457 (30 x 18)	-2	Dry	1				
	Spar/trailing-edge panel 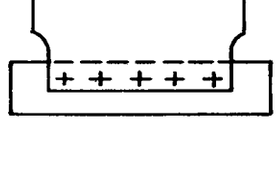	686 x 406 (27 x 16)	-3	Dry	1				

Table 7. Stabilizer Subcomponent Test Plan (Continued)

Test number	Specimen	Size, mm (in)	Configuration	Environmental condition	Temperature and number of tests			Data	Load condition
					21°C (70°F)	-54°C (-65°F)	82°C (180°F)		
Test 20	Sonic test box **65C17792** 2 skin panels 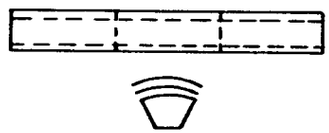	762 x 762 (30 x 30)	-1	Dry	1	–	–	Time to failure	Sonic fatigue
			-2	Dry	1	–	–		
Test 22	Discontinuous laminate **65C17980** 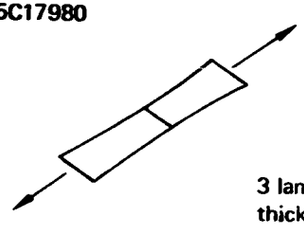 3 laminate thickness ratios	305 x 51 (12 x 2)	-1	Dry	3	3	–	Delamination strain levels	Static tension
			-2	Dry	3	3	–		
			-3	Dry	3	3	–		
Test 24	Pressure/shear skin joint **65C17981** 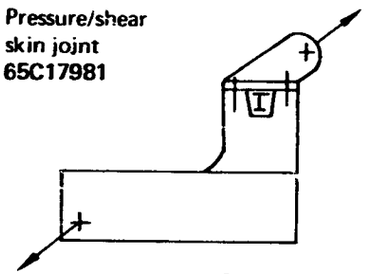 2 configurations	305 x 305 (12 x 12)	-1	Dry	3	3	–	Joint strength	Static tension
			-2	Dry	5	1	–		

Table 7. Stabilizer Subcomponent Test Plan (Concluded)

Test number	Test	Specimen 65C17980	Laminated skin buildup	Load	Environmental condition	Temperature and number of tests: 21°C (70°F)	-59°C (-75°F)	82°C (180°F)	Data	Remarks
Test 31	Basic laminate	-10 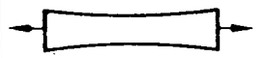	6 plies (7-mil fabric) (4 at 45, 2 at 0/90) 2 plies (4-mil tape)(45) 2 plies (6-mil tape)(0) 2 plies (7-mil tape) (0)	Tension	Dry	3	3	3	Failure load	Static strength
					Wet	3	3	3		
		-11 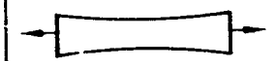	9 plies (7-mil fabric) (6 at 45, 3 at 0/90) 2 plies (4-mil tape)(45) 2 plies (7-mil tape)(0)	Tension	Dry	3	3			
					Wet			3		
		-12 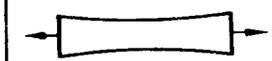	13 plies (7-mil fabric) (9 at 45, 4 at 0/90) 2 plies (4-mil tape)(45) 2 plies (7-mil tape)(0)	Tension	Dry	3	3			
					Wet			3		
	Fracture coupon control specimens	-13 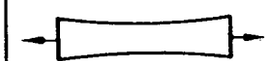	12 plies (7-mil fabric) (9 at 45, 3 at 0)	Tension	Dry	2	2			
				Compression	Dry Wet	2		2		
		-14 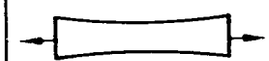	7 plies (7-mil fabric) (5 at 45, 2 at 0/90) 2 plies (7-mil tape)(0)	Tension	Dry	2	2			
				Compression	Dry Wet	2		2		
		-15 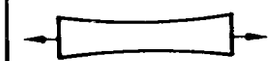	7 plies (7-mil fabric) (5 at 45, 2 at 0/90) 2 plies (7-mil tape)(90)	Tension	Dry	2	2			
				Compression	Dry Wet	2		2		

Table 8. Maintenance and Repair Test Plan

Test number	Specimen 65C17787	Size mm (in)	Configuration	Environmental condition	Temperature and number of tests [1] 21°C (70°F)	-54°C (-65°F)	82°C (180°F)	Data	Load condition
Test 15	Skin panel repair compression 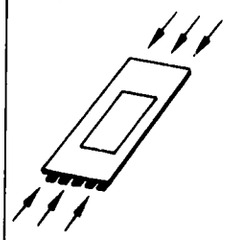 Two load levels Five stiffeners	1,397 x 432 (55 x 17)	-1	Dry	1	–	–	Failure load and mode of failure	Static strength
				Wet	–	–	1		
			-2	Dry	2	–	–		
				Wet	2	2	2		
Test 15	Skin panel repair cyclic load 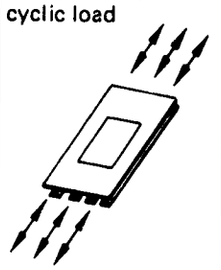 Two load levels Four stiffeners	1,321 x 345 (52 x 13.6)	-3	Dry	1	1	–	Failure load and mode of failure	Spectrum cyclic load [4]
				Wet	2 [2]	2	2 [3]		
			-4	Dry	1	–	–		
				Wet	–	1	–		

Note: Wet condition denotes 1.1% moisture content achieved by conditioning in a 100% relative humidity chamber at 60°C (140°F).

[1] All cyclic load panels except those noted will be cycled and statically tested at the same conditions.

[2] One panel will be cycled at -59°C (-75°F) and one at room temperature.

[3] Both panels will be cycled at -59°C (-75°F).

[4] Each panel will be subjected to two life spectra cyclic load tests followed by static test to failure.

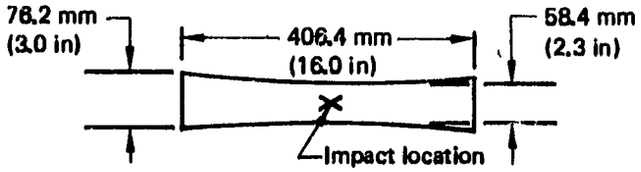

- Data from Test 1, Appendix C

Ply code	Ply layup	t mm (in)	E GPa (Msi)
A	Fabric: 5(0, 90), 10(±45)	2.86 (0.1125)	4.0 (5.8)
B	Fabric: 8(0, 90), 16(±45)	4.57 (0.18)	4.0 (5.8)
C	Fabric: 8(0, 90), 8(±45)	3.05 (0.12)	4.76 (6.9)
D	Fabric: 12(0, 90), 12(±45)	4.57 (0.18)	4.76 (6.9)

Legend:

- ⊙ No impact
- □ 2.82 N-m (25 lb-in) impact
- ○ 5.65 N-m (50 lb-in) impact
- △ 8.36 N-m (74 lb-in) impact

Environmental condition

- ——— Dry
- – – – – Wet

- Tension loading
- Layup A
- t = 2.86 mm (0.1125 in)

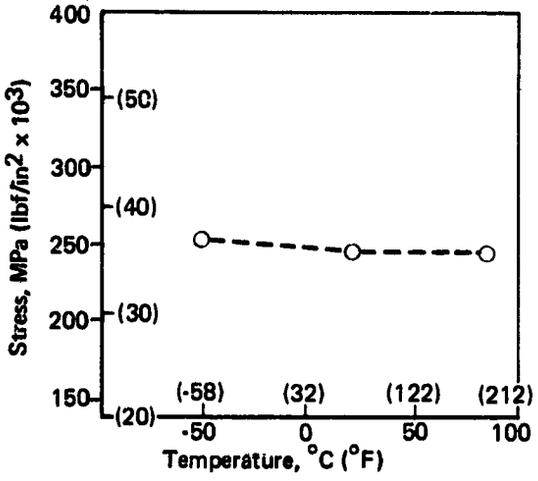

- Tension loading
- Layup C
- t = 3.05 mm (0.12 in)

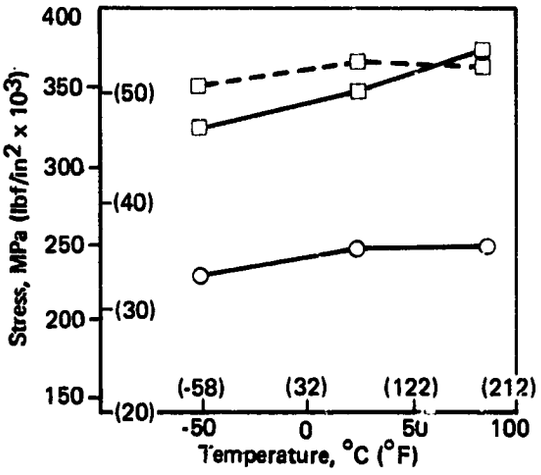

- Tension loading
- Layup D
- t = 4.57 mm (0.18 in)

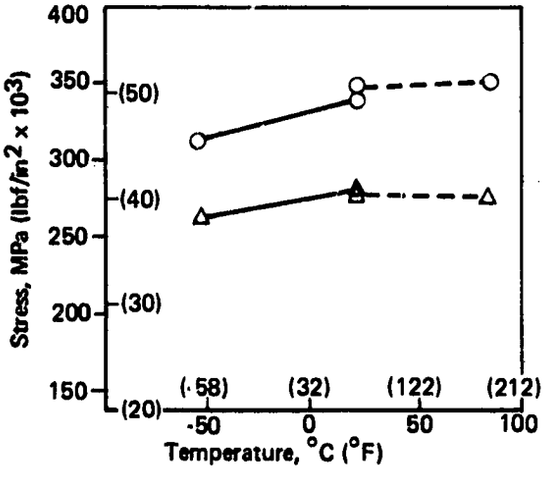

- Compression loading
- Layup A
- t = 2.86 mm (0.1125 in)

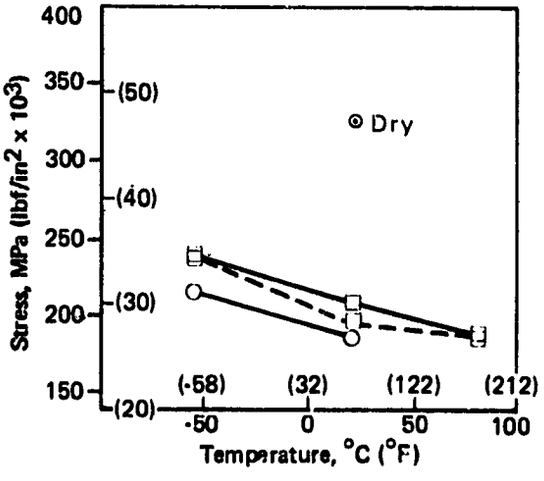

Figure 57. Effect of Moisture, Temperature, Impact, and Laminate Orientation on Coupon Failure Stresses

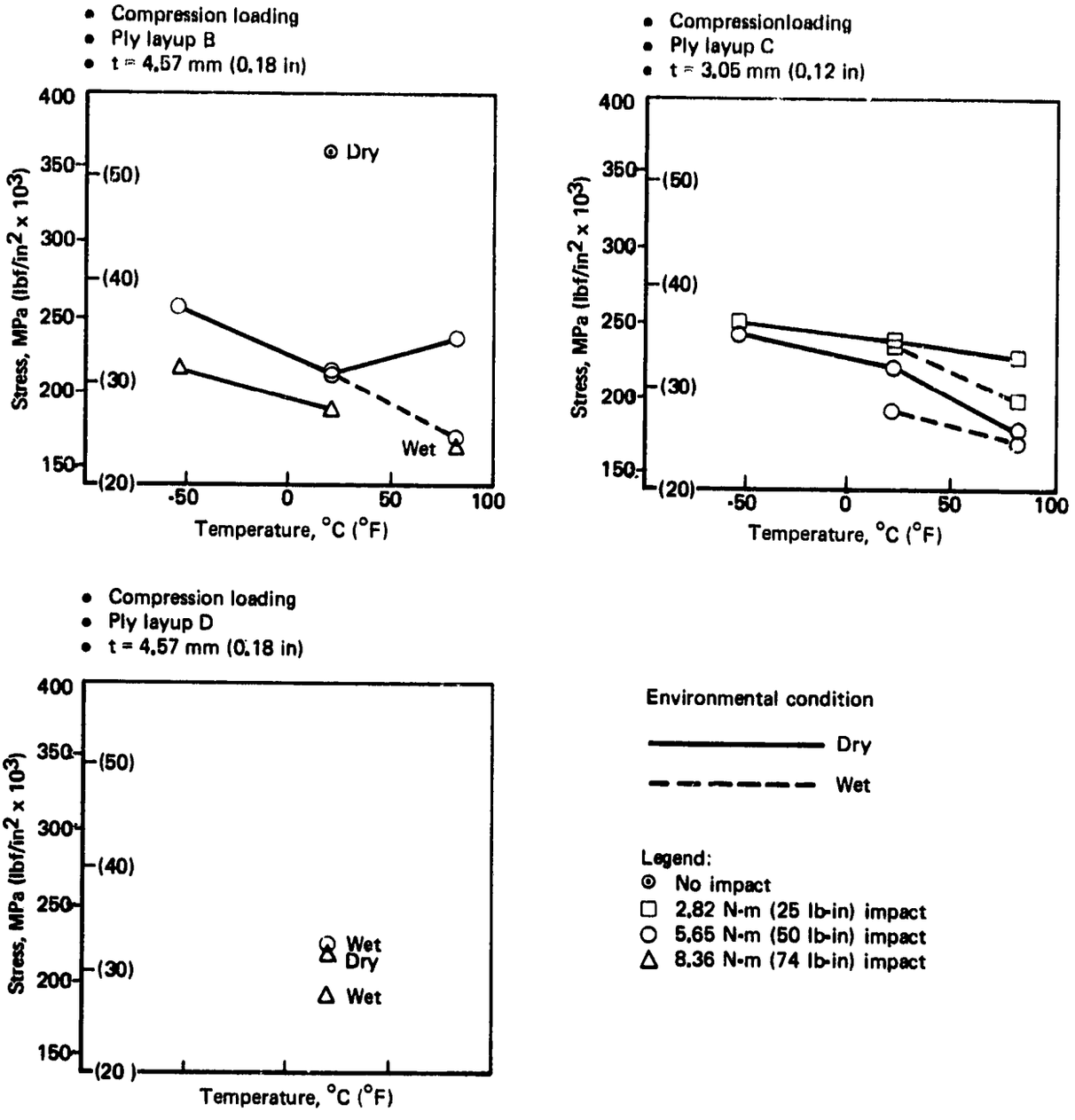

Figure 57. Effect of Moisture, Temperature, Impact, and Laminate Orientation on Coupon Failure Stresses (Concluded)

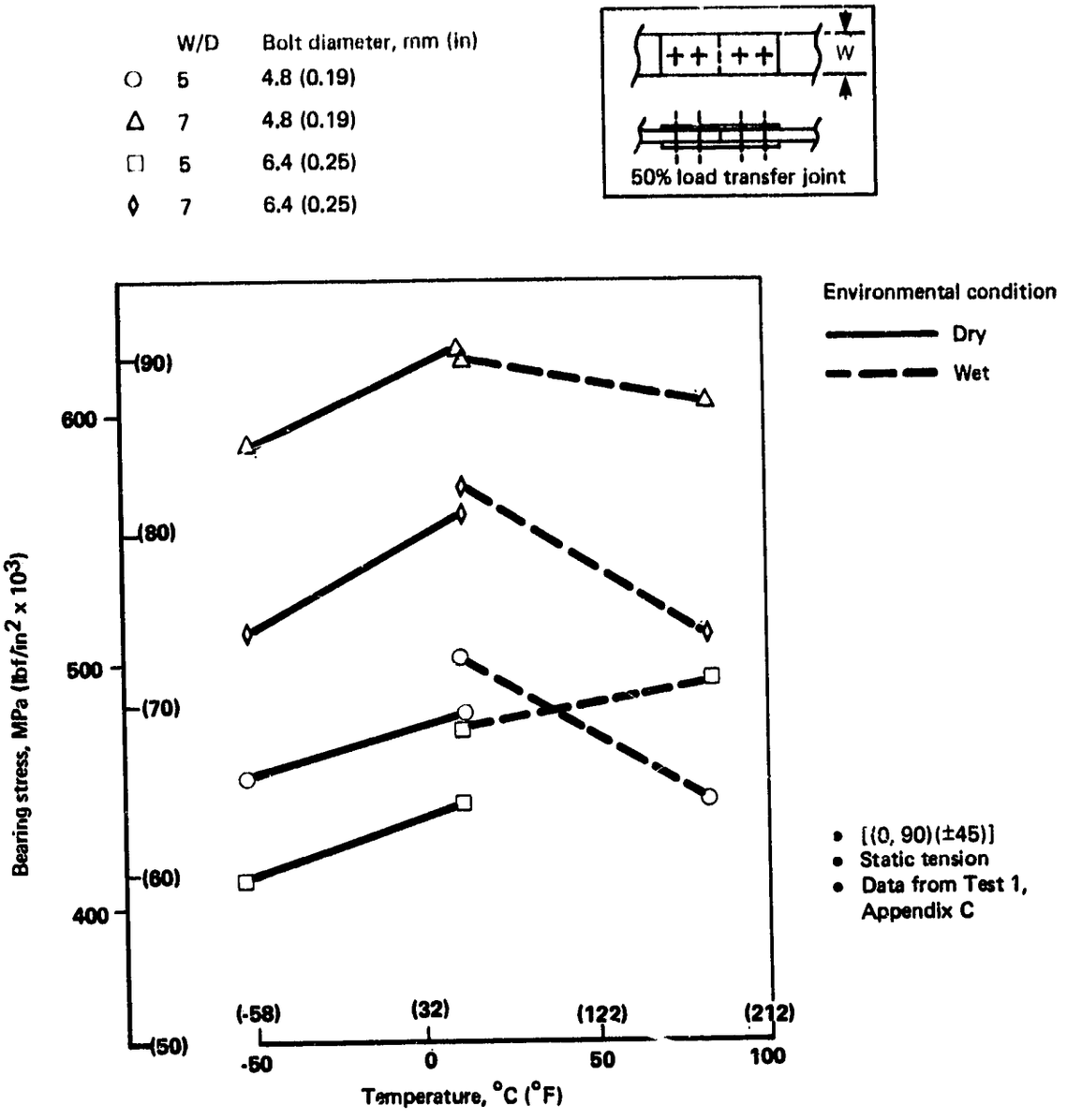

Note: Wet specimen conditioned at 60°C (140°F), 100% relative humidity until 0.23-cm (0.09-in) rider specimen reached 1.1% moisture content.

Figure 58. Effect of Environment on 50% Load Transfer Joint

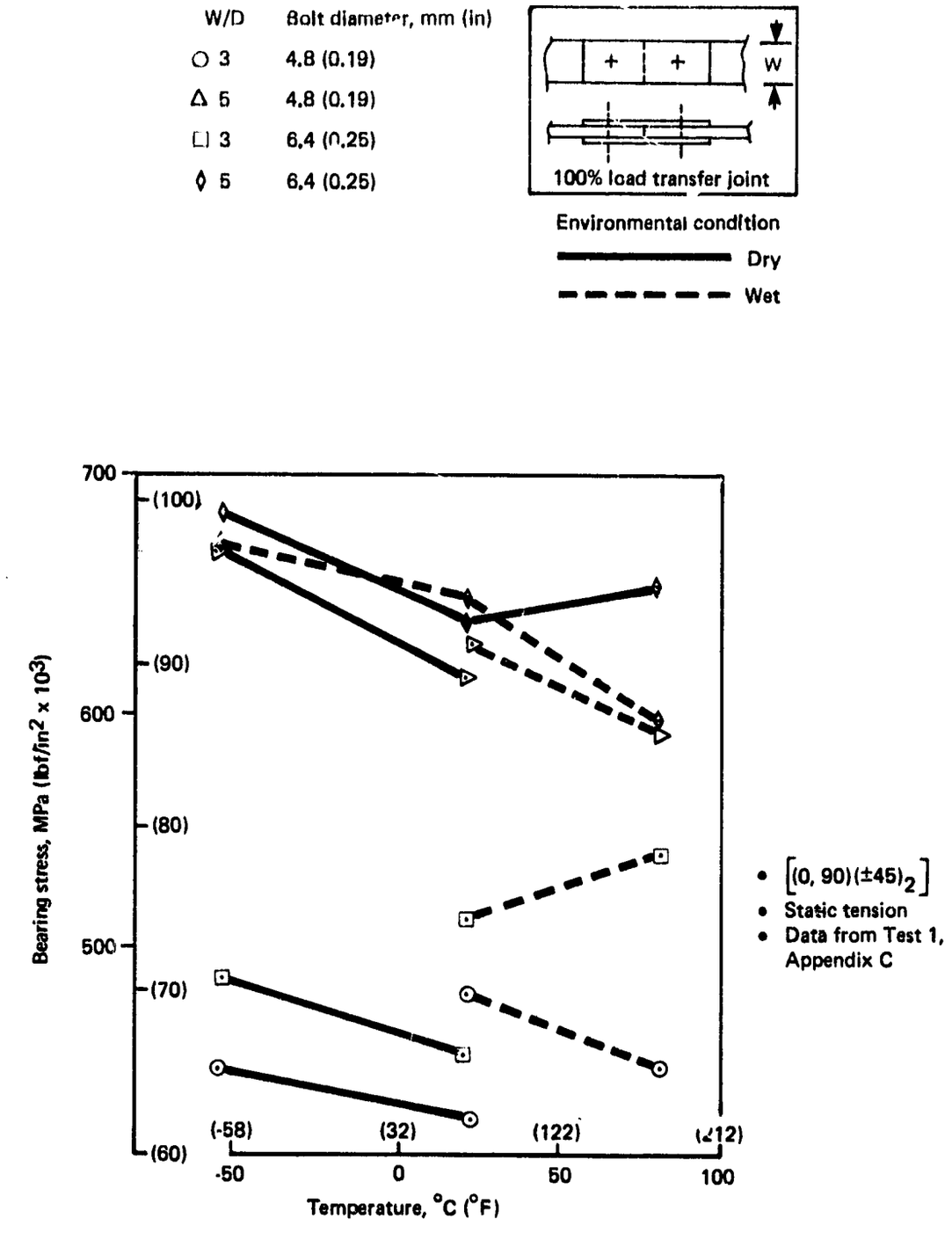

Note: Wet specimen conditioned at 60°C (140°F), 100% relative humidity until 0.23-cm (0.09-in) rider specimen reached 1.1% moisture content.

Figure 59. Effect of Environment on 100% Load Transfer Joint

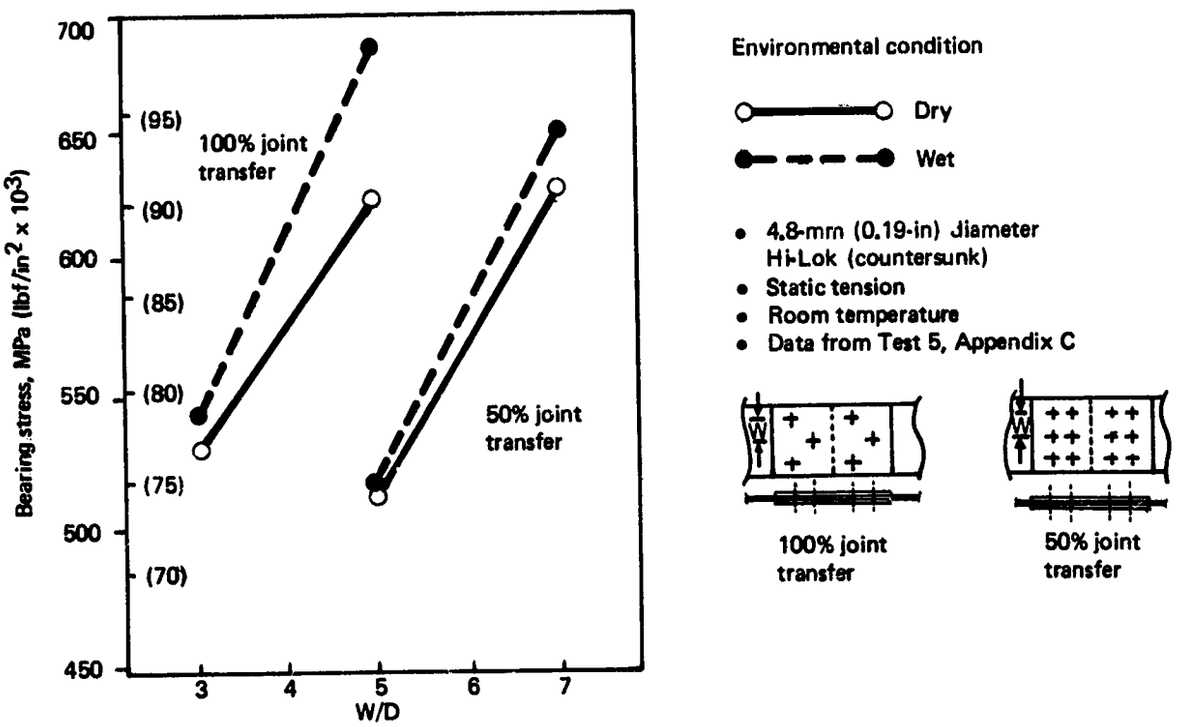

Figure 60. Effect of Moisture and Fastener Spacing (W/D) on Bearing Stress for 4.8-mm (0.19-in) Diameter Hi-Loks

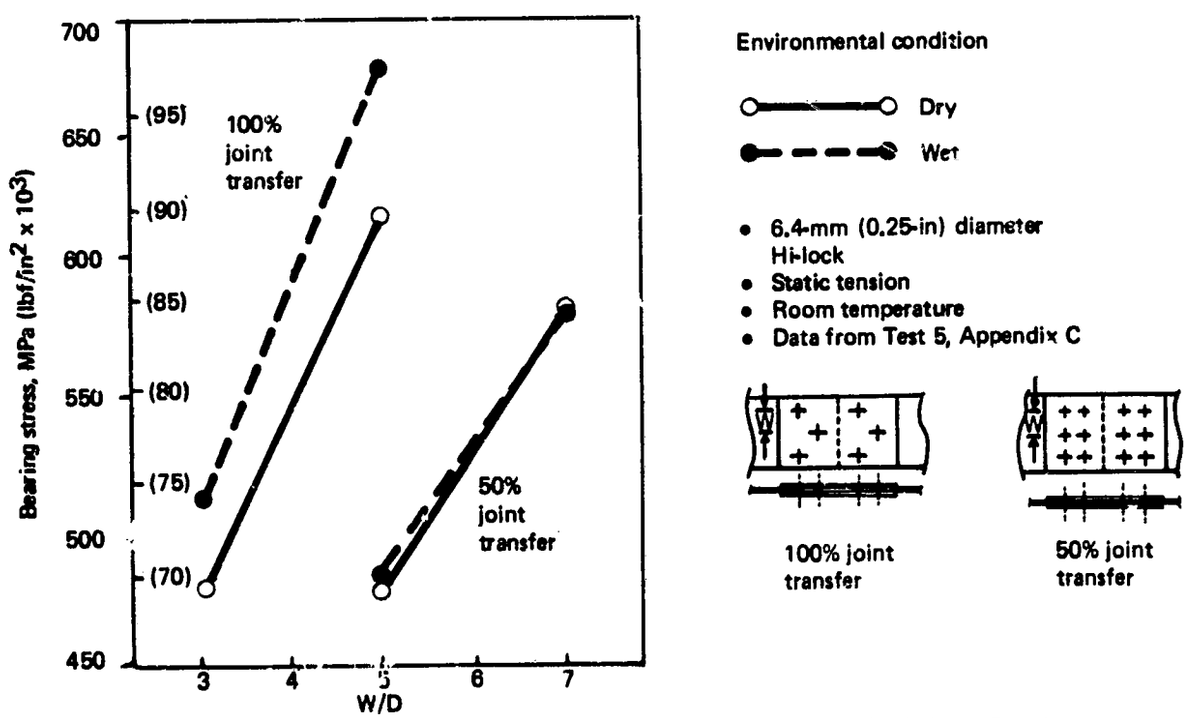

Figure 61. Effect of Moisture and Fastener Spacing (W/D) on Bearing Stress for 6.35-mm (0.25-in) Diameter Hi-Loks

Figures 62 and 63 show the comparison between Test 1, single fastener, and Test 5, multifasteners.

4.2.2.2 Skin Panel-to-Rib Attachment

Figure 64 shows the effect of pad-up on skin-to-rib attachments and the effects of damage and cyclic loadings. The results show an increase in strength after fatigue cycling.

4.2.2.3 Spar Shear Web

The spar shear web test (fig. 65) determined the effect of the cutout on thick webs (Configuration 1) and thin webs with doublers (Configuration 2).

These shear panels had a built-up fiberglass frame (edgeband) around the edges where the panel attaches to the loading frame. Because the edge buildup is

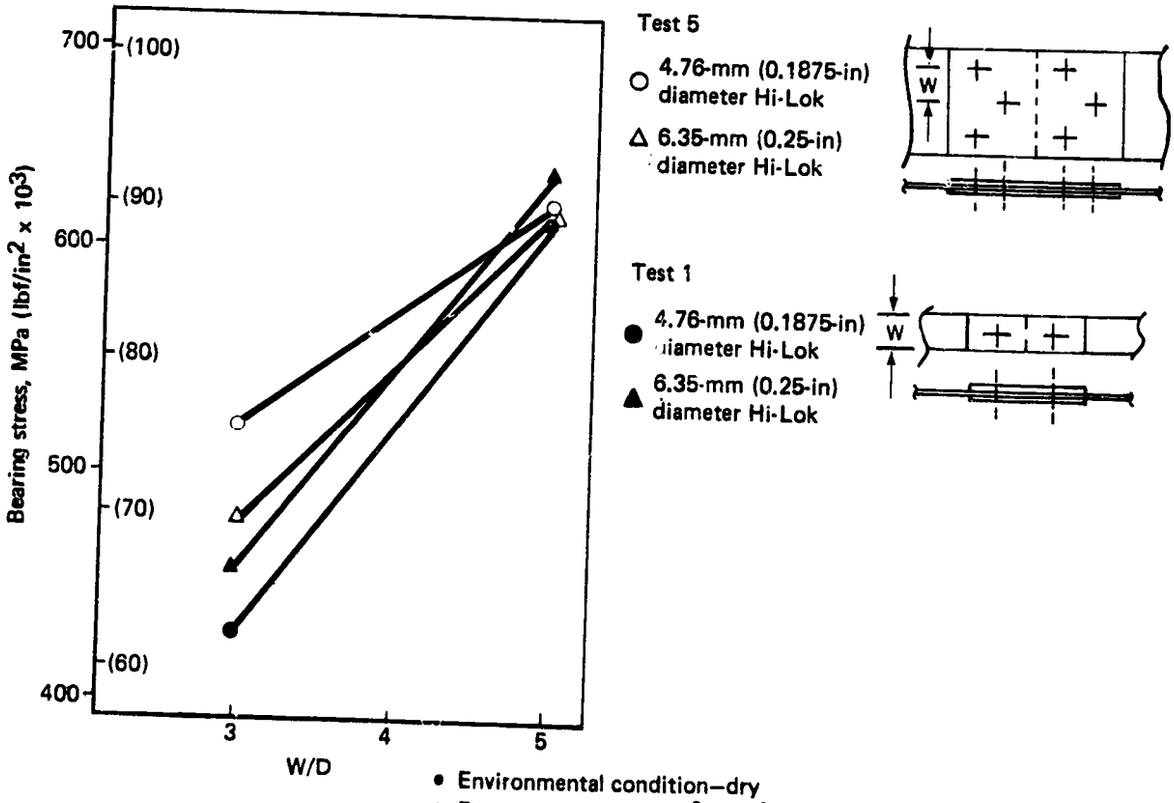

Figure 62. 100% Load Transfer Joint

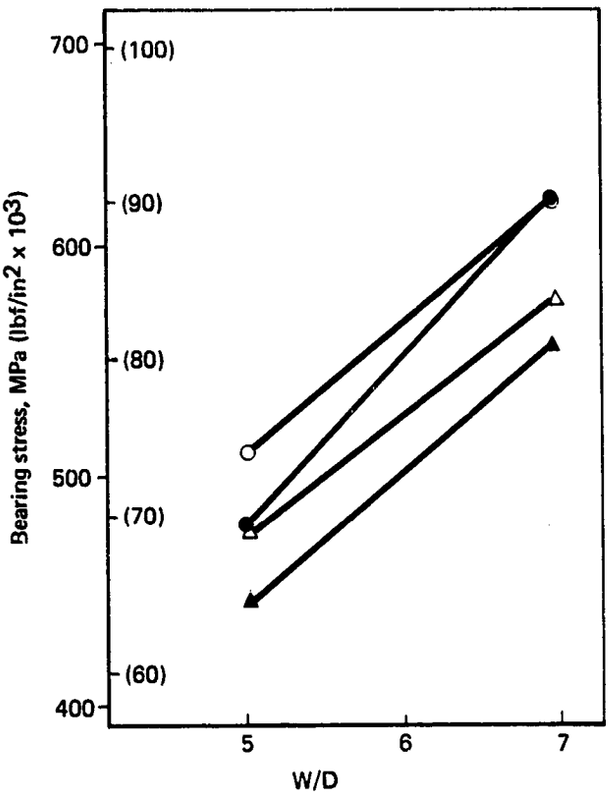

- Environmental condition—dry
- Room temperature—21°C (70°F)
- [(0/90)(±45)] { center plate—24 plies, t = 4.57 mm (0.18 in) / splice plate—12 plies, t = 2.29 mm (0.09 in)
- Static tension
- Each point—average of three tests
- Data from Test 1 and Test 5, Appendix C

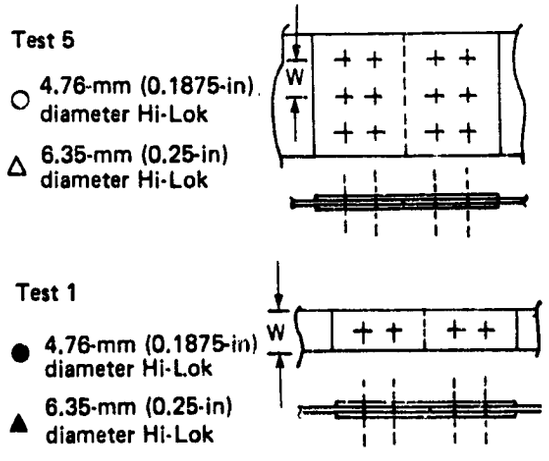

Figure 63. 50% Load Transfer Joint

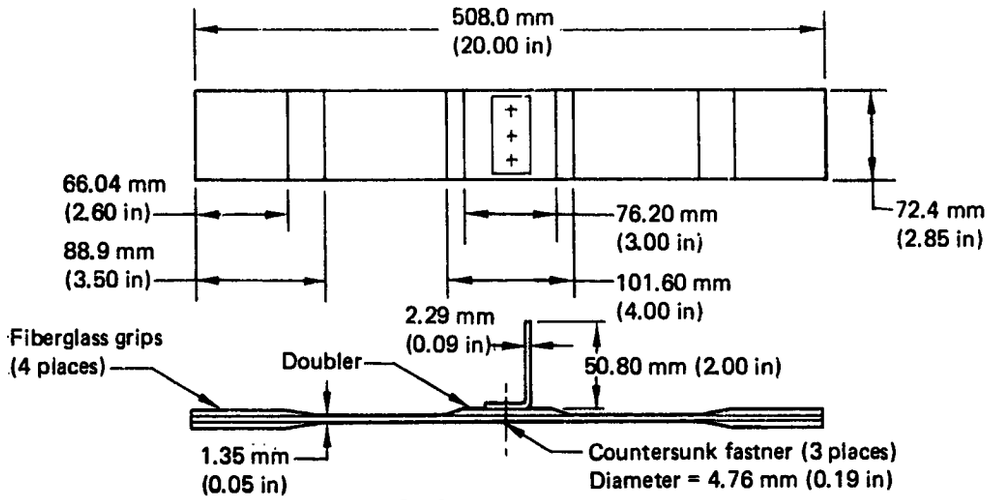

Configurations 1 and 2

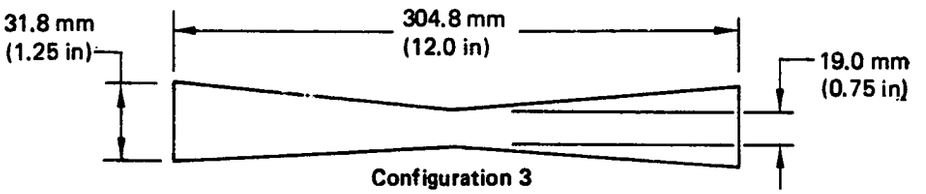

Configuration 3

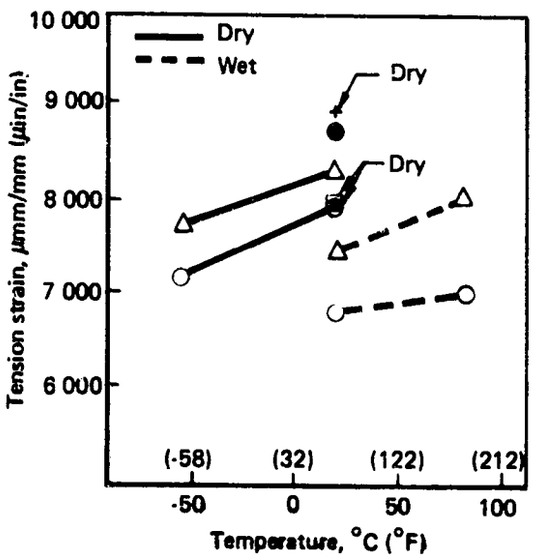

Symbol	Configuration	Cycled	Impacted
○	1	No	No
●	2	No	No
□	1	1 life	No
△	1	1 life	25 lb-in
▲	1	2 lives	No
+	3	No	No

- All material used is fabric
- Basic skin: (configurations 1, 2, 3) 7-ply: 5 at 0, 90; 2 at ±45
- Doubler: (configuration 1) 3-ply at ±45
  (configuration 2) 5-ply: 1 at 0, 90; 4 at ±45
  (configuration 3) no doubler
- Static tension and residual tension strength
- Data from Test 9, Appendix C

Figure 64. Effect of Moisture and Temperature on Skin Panel-to-Rib Attachments

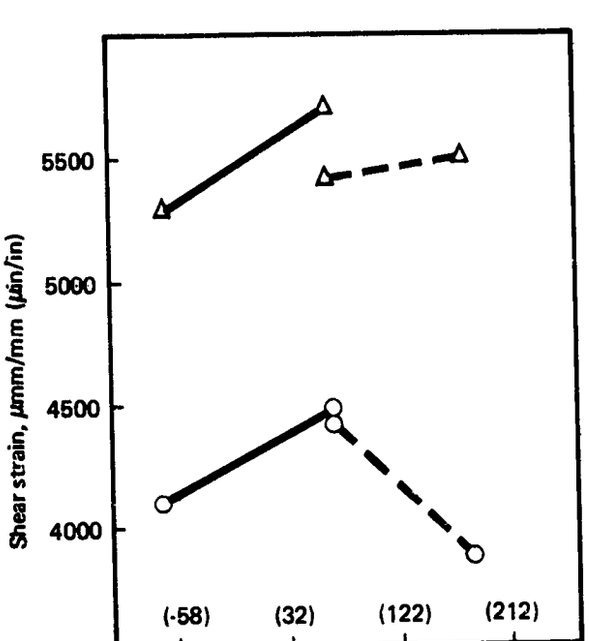

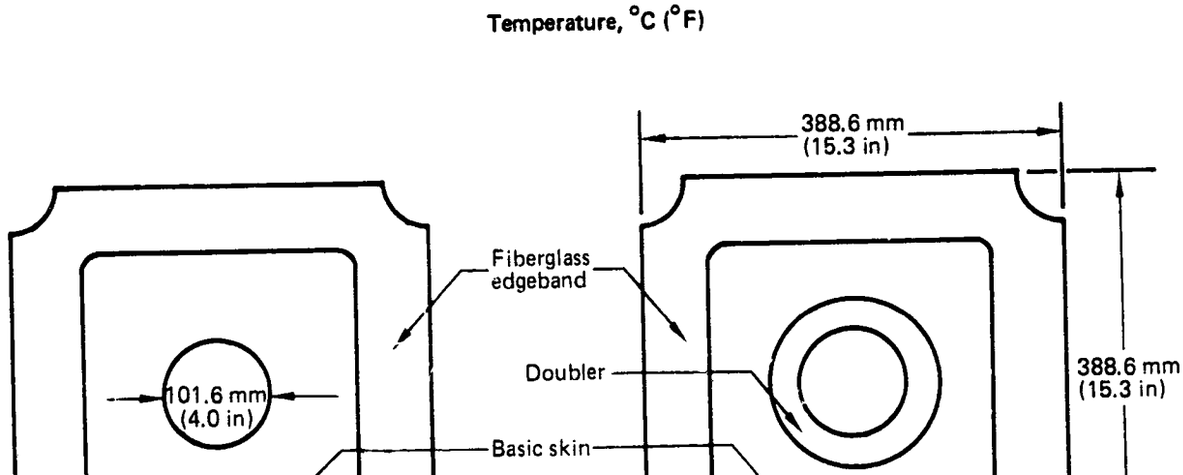

Configuration 1

Basic skin: 24 plies (7-mil fabric)—
16 at ±45, 8 at 0/90
t = 4.57 mm (0.18 in)

Configuration 2

Basic skin: 6 plies (7-mil fabric)—
4 at ±45, 2 at 0/90
t = 1.14 mm (0.045 in)

Doubler: 14 plies (7-mil fabric)—
all at ±45
t = 2.67 mm (0.105 in)

- ○ Configuration 1
- △ Configuration 2
- Data from Test 11, Appendix C

Figure 65. Effect of Moisture and Temperature on Spar Shear Webs With and Without Doublers

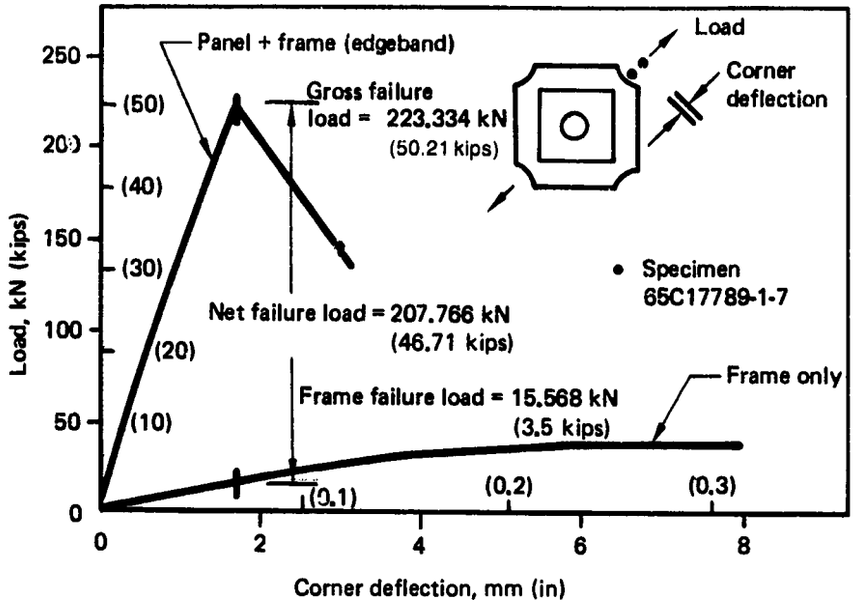

Figure 66. Load Deflection for Typical Configuration 1 Shear Panel (Test 11)

continuous, some of the shear load is taken in the edgeband. To determine the magnitude of this load, an individual edgeband was tested to failure. Cross-corner deflection measurements of all panels were obtained, and the net test panel load was determined as the difference between failure loads of the complete test panel and those of the edgeband itself at the failure deflection level. This procedure is displayed for a typical panel geometry in Figure 66. As demonstrated in Appendix C, all the test panels have been corrected for the edgeband load.

A plot of shear strains for both configurations is shown in Figure 65 as a function of test temperature and moisture conditioning.

The Configuration 1 panels were shear resistant, and panels failed by compression failure of the fibers at the edge of the hole. All Configuration 2 panels were slightly dished and, as a result, experienced out-of-plane deflections. All the panels failed by tension and compression failure of the fibers at the edge of the hole.

4.2.2.4 Spar Chord Crippling

The failure loads and test conditions for Test 7 (spar chord crippling) are presented in Table 9. Specimen dimensions and laminate definitions are shown in Figure 67. The strain data obtained from specimen 65C17791-1-1D are plotted in Figure 68. The strain difference that gives a measure of the buckling deformation also is shown. As noted in the figure, the plot of strain difference would go to infinity at approximately 33 360N (7500 lb), if there were no postbuckling constraints. This load level is defined as the elastic buckling load for the total

Table 9. Spar Chord Crippling Test Data

Specimen 65C17791		Temperature, C°	Temperature, (°F)	Environmental condition	(P_{cr}) ultimate, N	(P_{cr}) ultimate, (lb)	(P_{cr}) elastic, N	(P_{cr}) elastic, (lb)	(ϵ_{cr}) elastic, με
-1	-1A	21	(70)	Dry	54 933	(12 350)	31 136	(7 000)	1850
	-1B				53 376	(12 000)	31 803	(7 150)	1920
	-1C				52 486	(11 800)	30 469	(6 850)	1820
	-1D	53	(65)		51 152	(11 500)	33 360	(7 500)	1930
	-1E				48 038	(10 800)	29 802	(6 700)	1870
	-1F				46 704	(10 500)	31 136	(7 000)	1900
	-1G	21	(70)	Wet	39 587	(8 900)	28 022	(6 300)	1730
	-1H				47 594	(10 700)	26 688	(6 000)	1780
	-1I				44 035	(9 900)	30 246	(6 800)	1970
	-1J	82	(180)		39 142	(8 800)	28 467	(6 400)	1880
	-1K				29 802	(6 700)	29 802	(6 700)	1860
	-1L				35 584	(8 000)	28 022	(6 300)	1790
-2	-1	21	(70)	Dry	169 914	(38 200)	145 005	(32 600)	5800
	-2				169 914	(38 200)	142 336	(32 000)	5007
	-3				152 566	(34 300)	136 109	(30 600)	4858
	-4	21	(70)	Wet	142 781	(32 100)	130 326	(29 300)	5100
	-5				149 008	(33 500)	137 888	(31 000)	5275
	-6				170 358	(38 300)	137 888	(31 000)	5080
	-7	82	(180)		153 901	(34 600)	126 768	(28 500)	4940
	-8				123 654	(27 800)	117 427	(26 400)	4520
	-9				128 547	(28 900)	125 434	(28 200)	4790

Cap strip { [(0/90)(±45)(0/90)(±45)(0/90)]$_s$ (-1)
[(0/90)(±45)(0/90)$_2$(±45)(0/90)]$_s$ (-2) ▷

Angle { [(±45)(0/90)(±45)] (-1)
[(±45)(0/90)(±45)$_2$(0/90)(±45)]$_s$ (-2) ▷

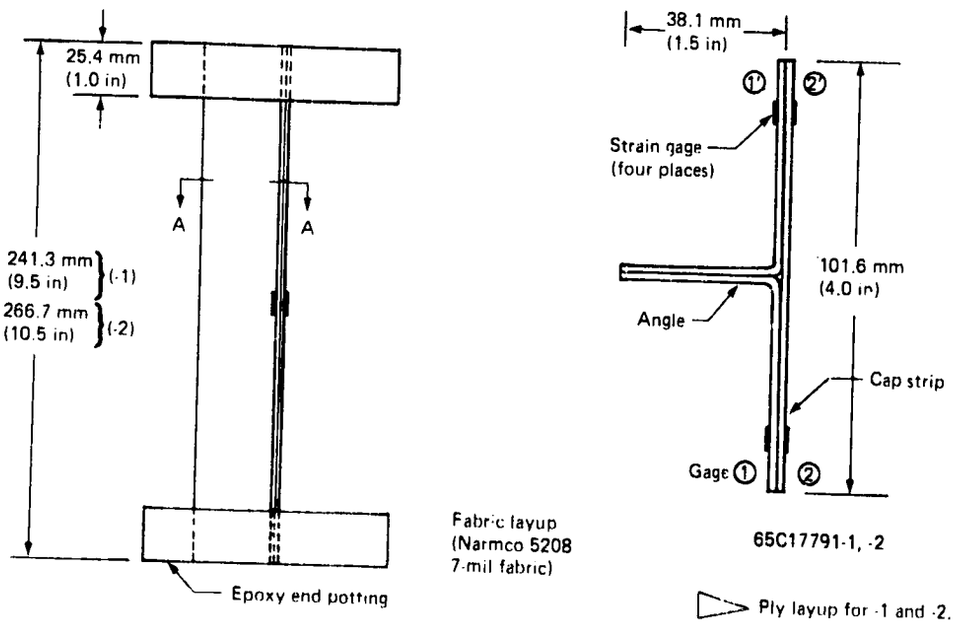

Figure 67. Spar Chord Crippling Specimen

section. The two sets of strain gage readings were averaged, and a strain level at buckling was determined as shown in Figure 68. All test specimens were evaluated in a similar manner, and the data are included in Table 9. Gross area strains for the specimens are presented in Appendix C.

Critical ultimate and elastic loads are plotted as a function of test temperature and environment in Figure 69. These results indicate that cold-dry and hot-wet environment reduced the crippling strength of all specimens compared with room temperature dry conditions.

4.2.2.5 Skin Stringer Panels: Crippling

The skin panel/stiffener crippling test (Test 10) results are presented in Table 10. The panel geometry is defined in Figure 70, and a typical test setup is shown in Figure 71. Strain gage plots for the panels are presented in Figures 72 through 77.

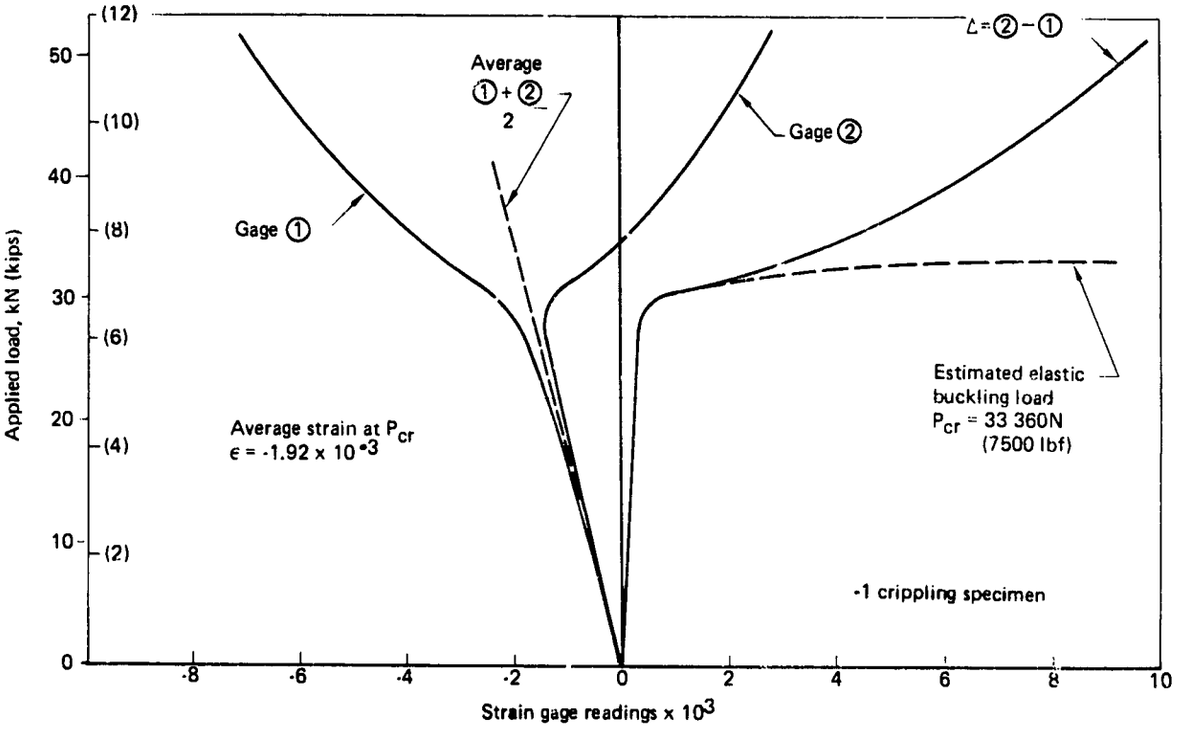

Figure 68. Spar Chord Crippling Strain Gage Data Versus Applied Load

For each of the crippling panel geometries, an estimated skin panel buckling strain was calculated, based on an assumed, simply supported skin panel width of 85.1 mm (3.35 in) and nominal values of modulus and thickness, using the PANBUCK analysis from Reference 12. The estimated buckling strain is shown for each panel geometry, and results compare favorably with the back-to-back skin panel strain gage data for each panel.

The stringer strain gage plots for each of the crippling panels correlate well with the estimated value up to the point where the skin buckles. Beyond this point, the stringer strain readings deviate somewhat from the estimated linear strain/load plot because, with the skin buckled, the stringers accept more of the load.

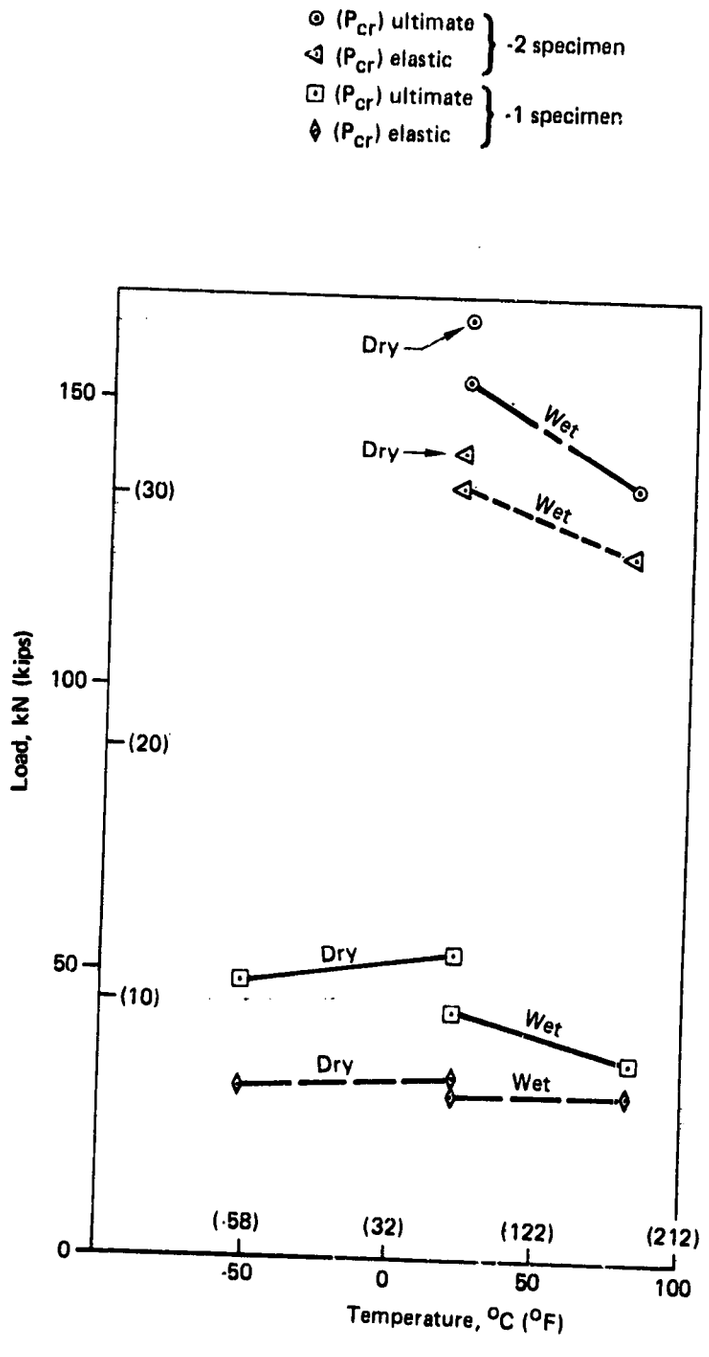

Figure 69. Effect of Temperature and Environmental Conditioning on Spar Chord Crippling Specimens

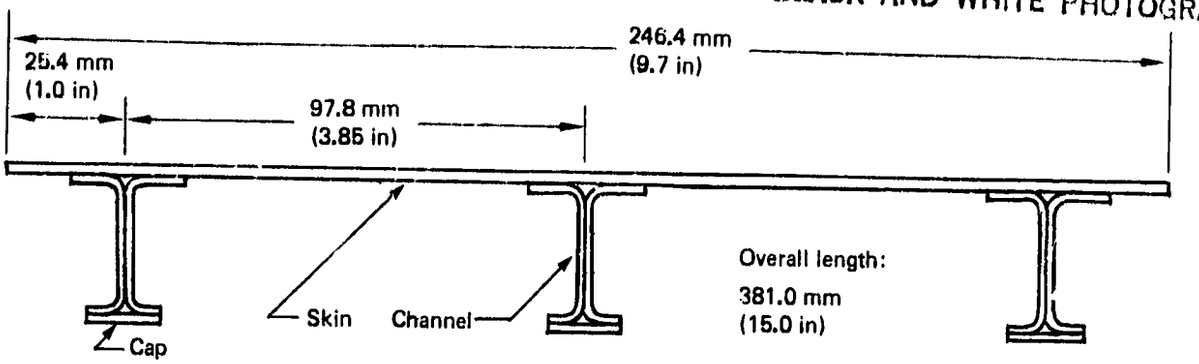

Specimen	Panel description		
	Skin	Channel	Cap
65C17773-60	7-ply fabric (5 at ±45, 2 at 0/90)	3-ply fabric (2 at ±45, 1 at 0/90)	1-ply fabric at 0/90
65C17773-61	7-ply fabric (5 at ±45, 2 at 0/90)	4-ply fabric (2 at ±45, 2 at 0/90)	9-ply fabric at 0/90
65C17773-62	10-ply fabric (7 at ±45 3 at 0/90) 2-ply grade 190 tape at 90	4-ply fabric (2 at ±45, 2 at 0/90)	9-ply fabric at 0/90

Figure 70. Crippling Panel Definition (Test 10)

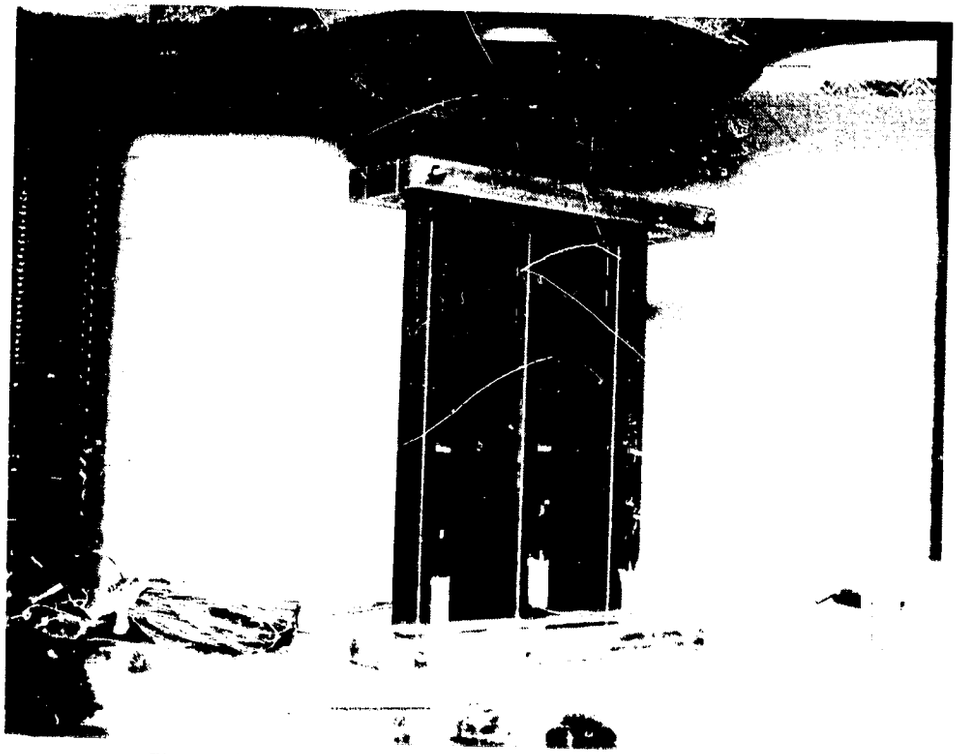

Figure 71. Typical Crippling Panel Test Setup (Test 10)

Table 10. Crippling Panel Test Results (Test 10)

Specimen	Temperature, °C	(°F)	Failure load, N	(lb)	Strain at failure [1]
65C17773-60-001	21	(70)	78 952	(17 750)	0.0033
65C17773-61-001	21	(70	142 336	(32 000)	0.0044
65C17773-62-001	21	(70)	191 718	(43 100)	0.0049
65C17773-62-002	21	(70)	186 816	(42 000)	0.0048
65C17773-62-003	21	(70)	212 837	(47 850)	0.0055

[1] Strain based on nominal values of modulus and area.

4.2.2.6 Rail Shear

Rail shear tests were performed on a laminate with varying temperatures in a dry environment. The specimen configuration and results are shown in Figure 78. The test data are presented in Appendix C.

4.2.3 Subcomponent Tests

The test results from this phase of the program were used to verify the design and durability of specific subcomponents prior to fabrication of the first stabilizer unit.

4.2.3.1 Skin/Stringer Panels: Compression

Five-stringer compression test panels from Test 10 were tested to verify Euler column buckling characteristics of the stabilizer skin/stringer system. The results are presented in Table 11, and the panel definition is shown in Figure 79. The potted ends of the specimen are shown in Figure 80. Figure 81 defines the strain gage and deflection indicator locations. Figures 82 and 83 present deflection data for Configurations 1 and 2, respectively. Strain plots for the center stringer and skin panel at the panel midlength position are shown in Figure 84 for the Configuration 1 panel, and Figure 85 presents a typical result for Configuration 2 at the same location.

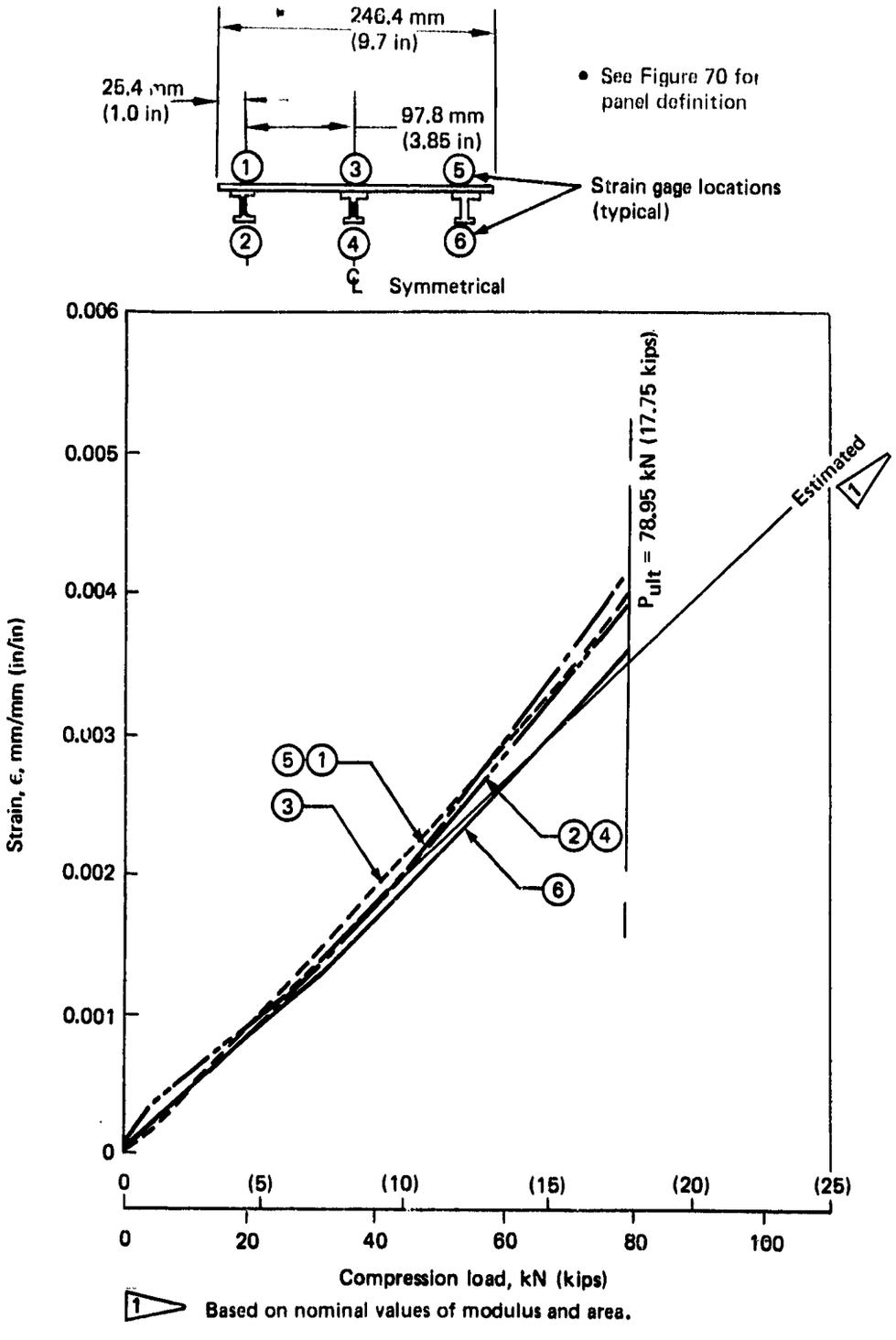

Figure 72. Stringer (Specimen 65C17773-60-001) Strain Gage Readings Versus Compression Load (Test 10)

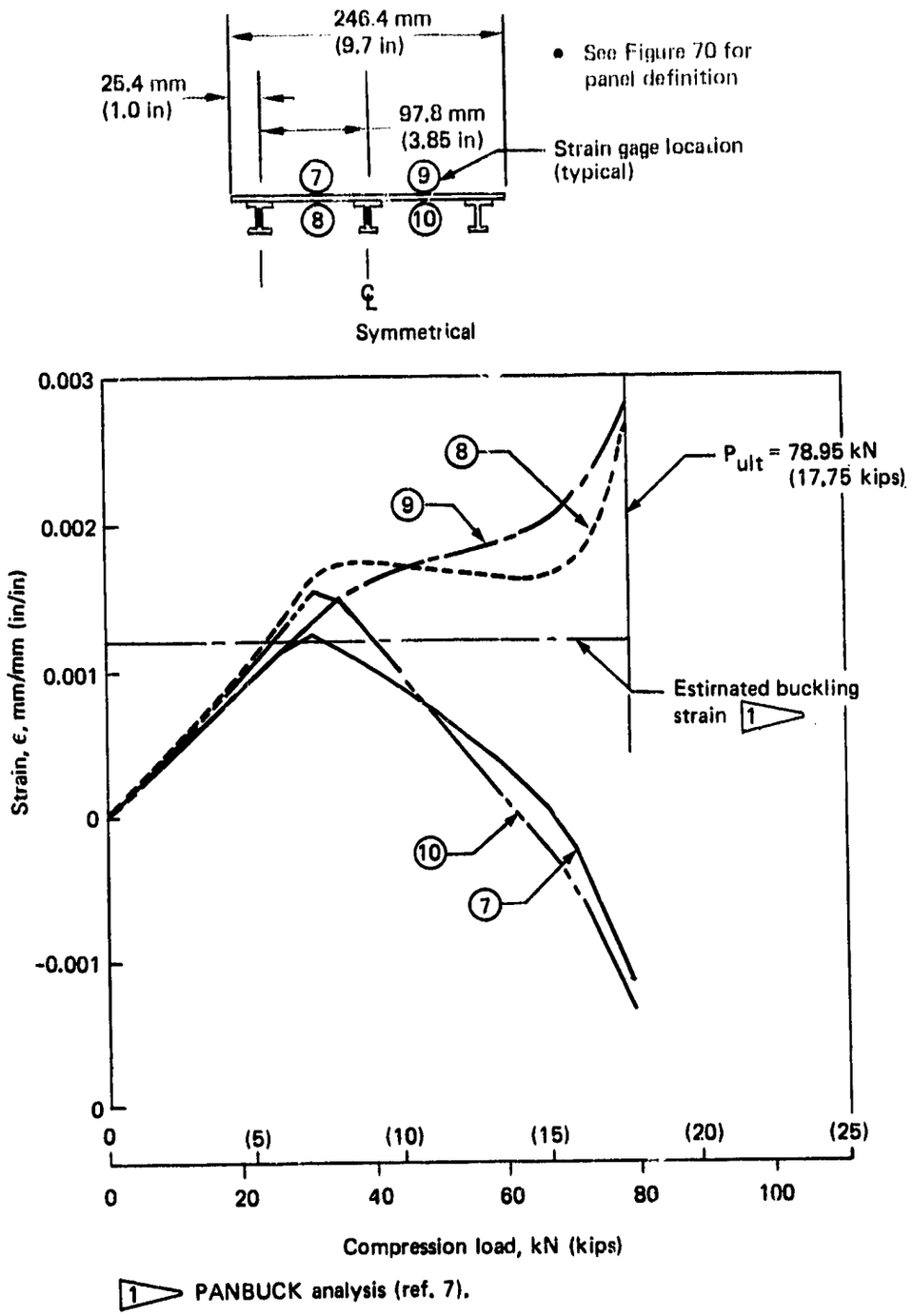

Figure 73. Skin Panel (Specimen 65C17773-60-001) Strain Gage Readings Versus Compression Load (Test 10)

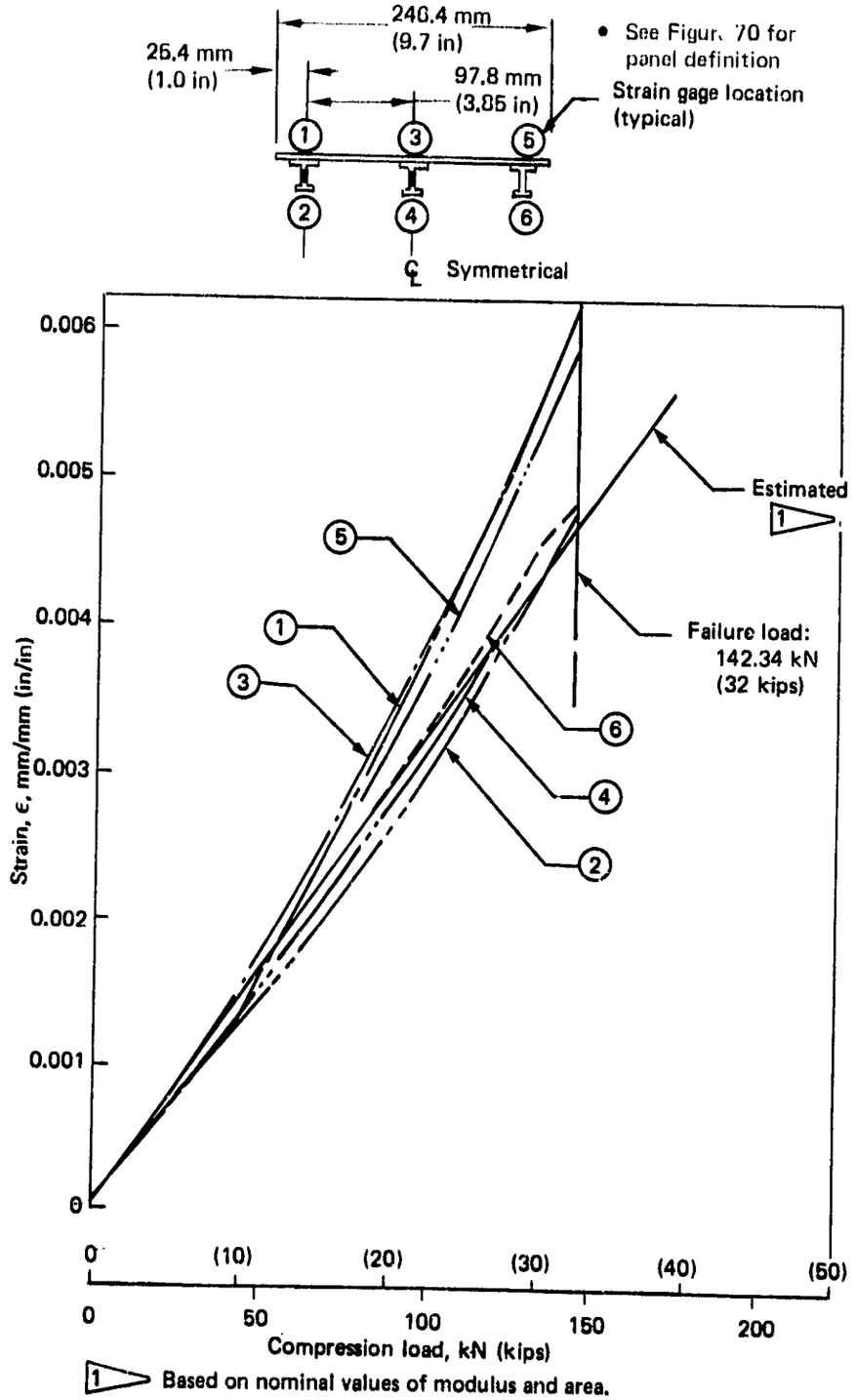

Figure 74. Stringer (Specimen 65C17773-61-001) Strain Gage Readings Versus Compression Load (Test 10)

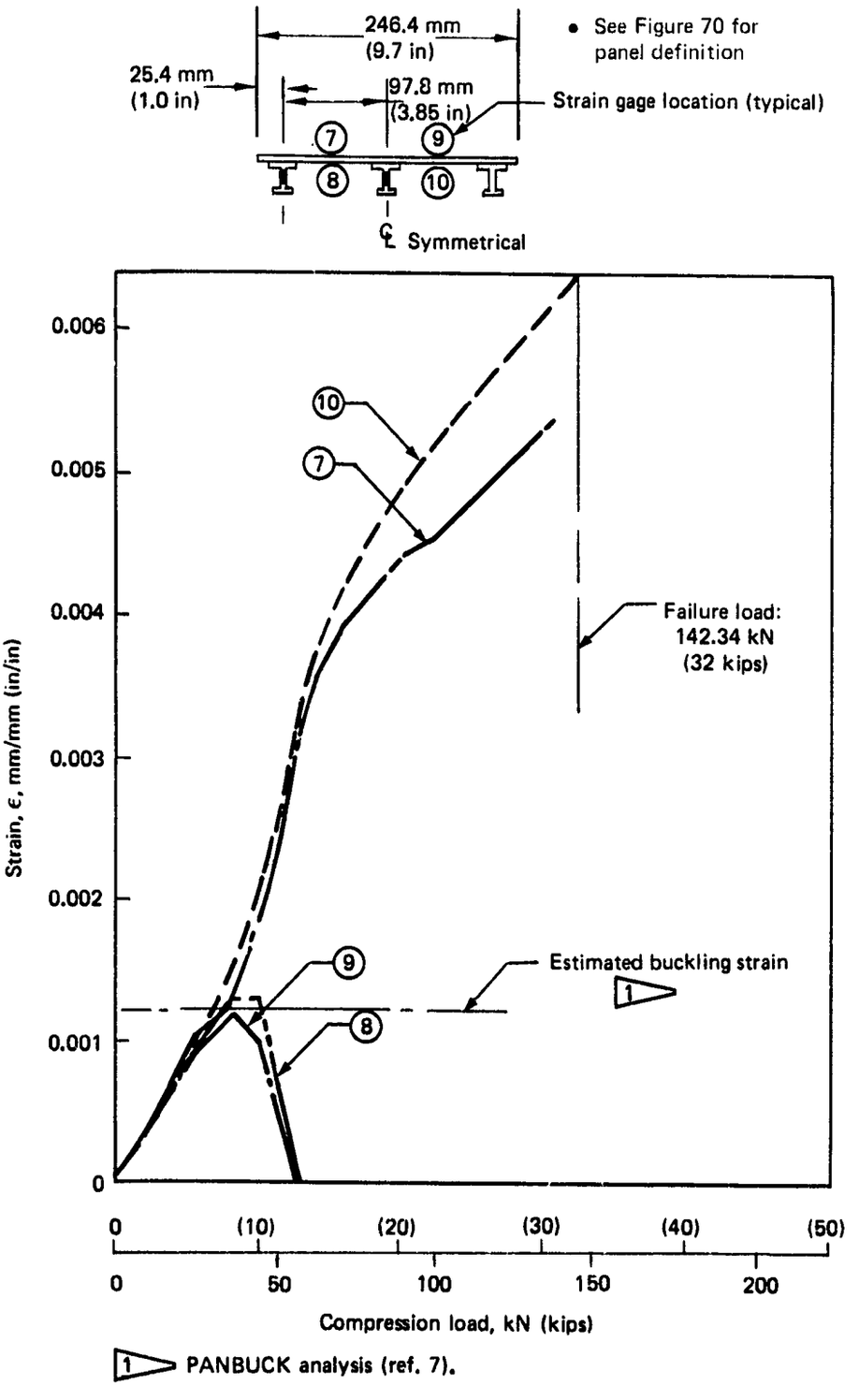

Figure 75. Skin Panel (Specimen 65C17773-61-001) Strain Gage Readings Versus Compression Load (Test 10)

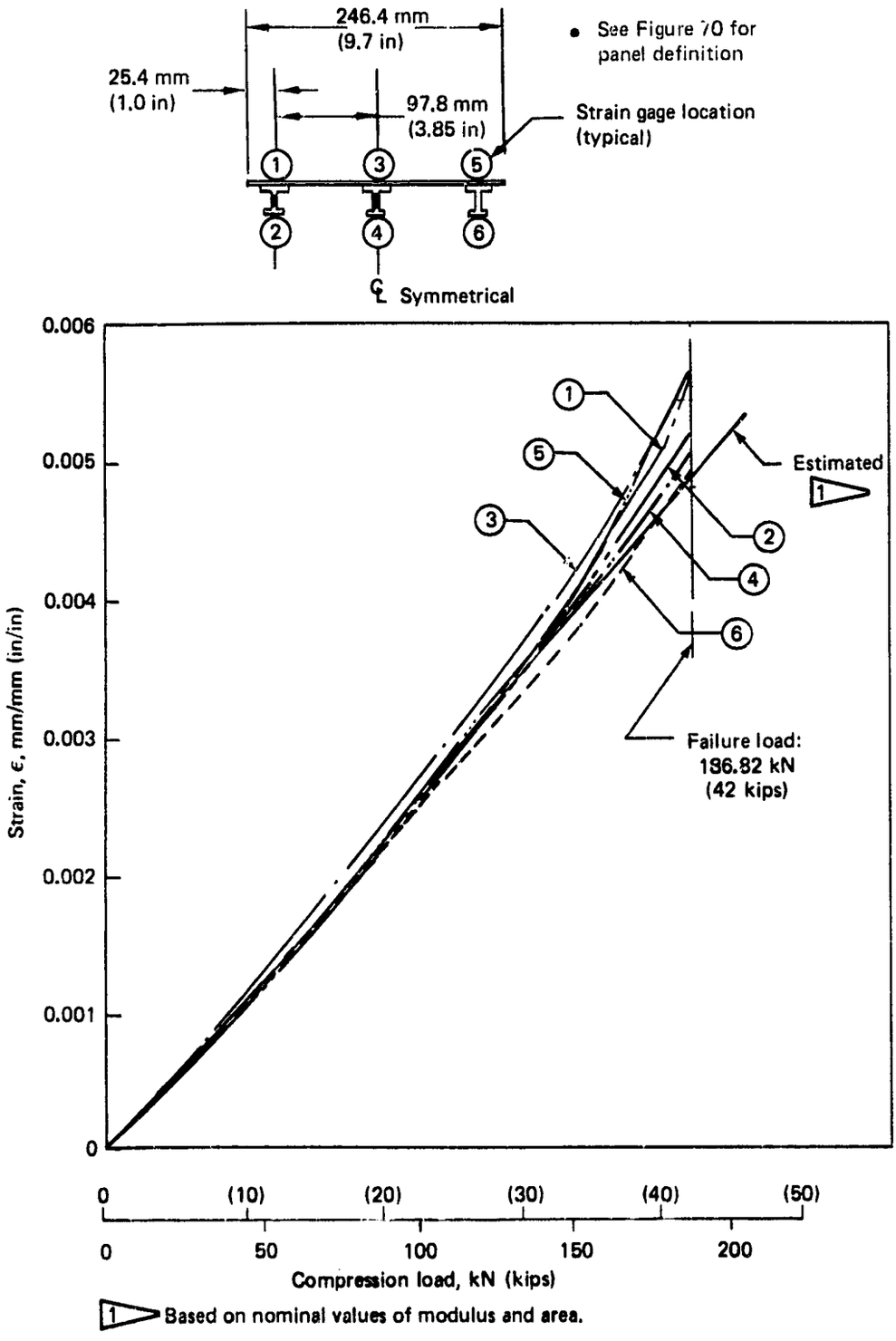

Figure 76. Stringer (Specimen 65C17773-62-002) Strain Gage Readings Versus Compression Load (Test 10)

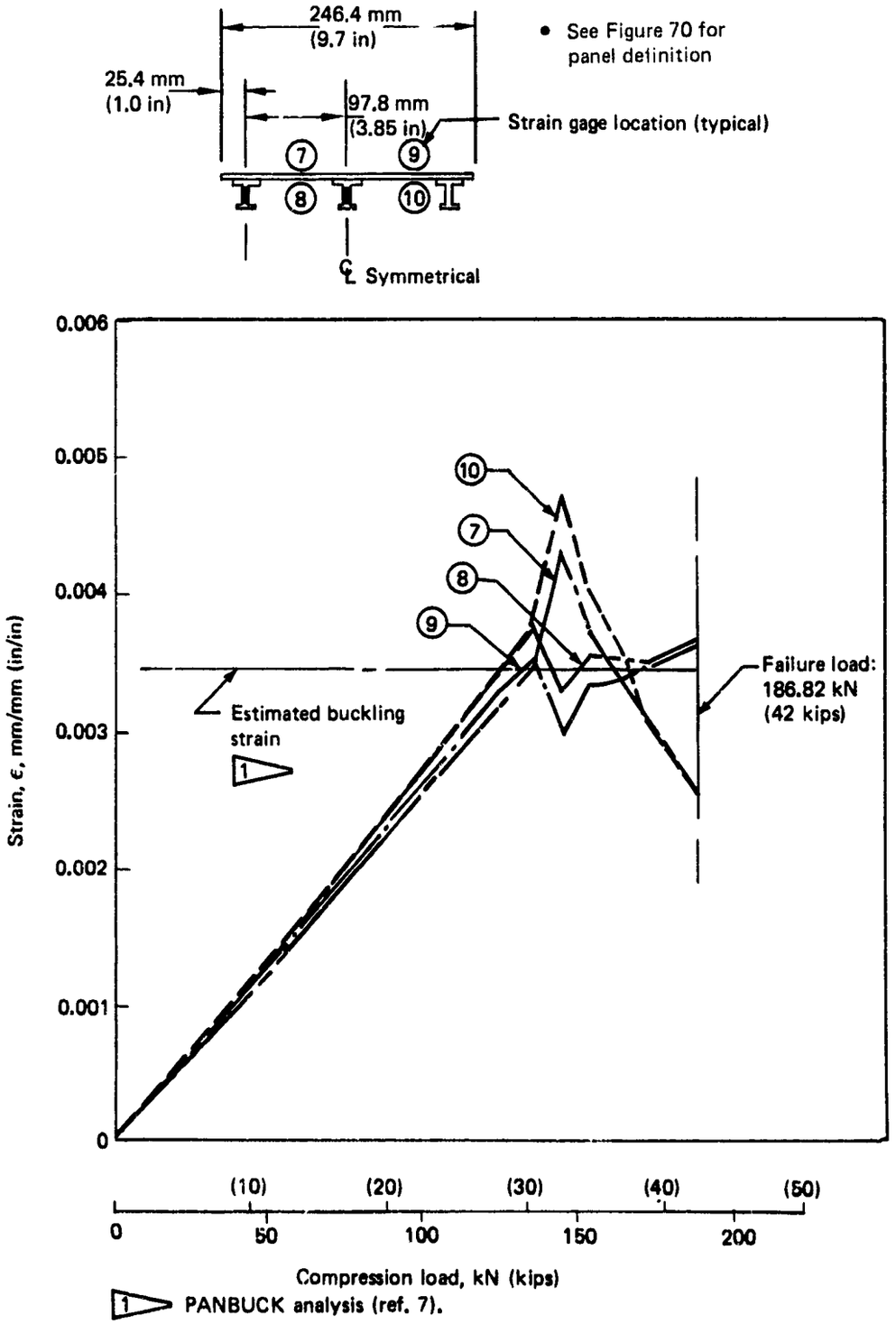

Figure 77. Skin Panel (Specimen 65C17773-62-002) Strain Gage Readings Versus Compression Load (Test 10)

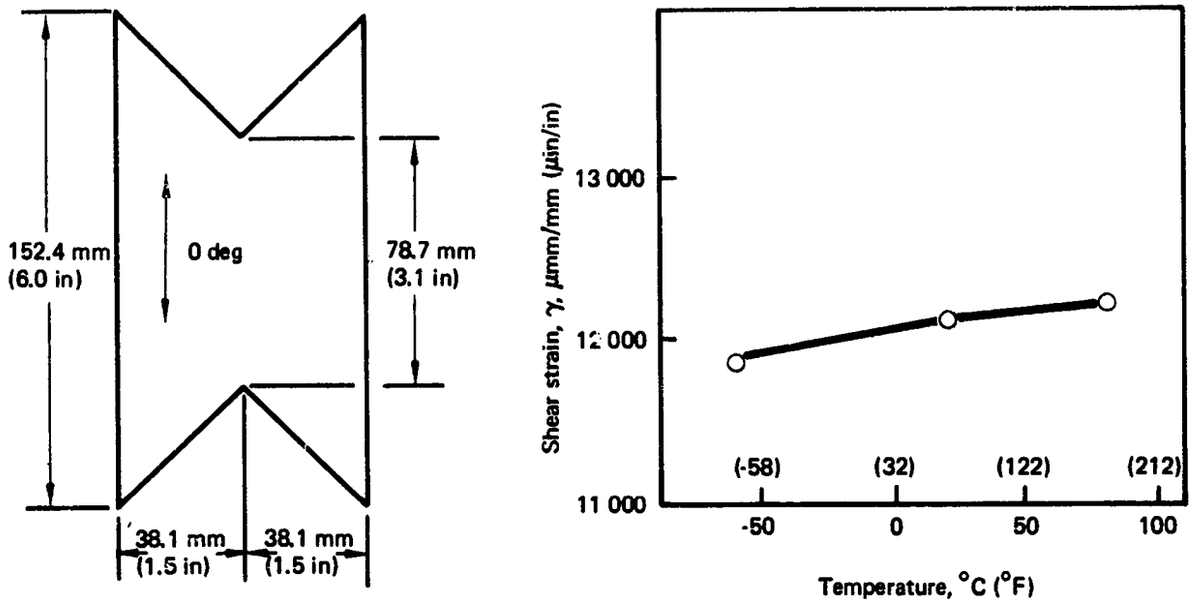

- Ply layup—5(0, 90), 7(±45)
- Environment—dry test,
- Data from rail shear test, Appendix C

Figure 78. Effect of Temperature on Rail Shear Specimens

Table 11. Compression Panel Test Results (Test 10)

Specimen	Temperature, °C (°F)	Environmental condition	Test load, kN (kip)
65C17773-1	21 (70)	Dry	147 (33.0)
65C17773-2	21 (70)	Dry	174 (39.0)
		Dry	182 (40.8)
		Dry	165 (37.1)
		Wet	188 (42.3)
			180 (40.4)
	21 (70)		202 (45.5)
	82 (180)		177 (39.7)
	82 (180)	Wet	193 (43.0)
	-54 (-65)	Dry	180 (40.4)
	-54 (-65)		181 (40.6)
[1]	21 (70)		183 (41.1)
[1]			173 (39.0)
6C17773-66 [2]	21 (70)	Dry	195 (43.9)

[1] Impact damage test panel.

[2] Lightning strike test panel (same configuration as 65C17773-2).

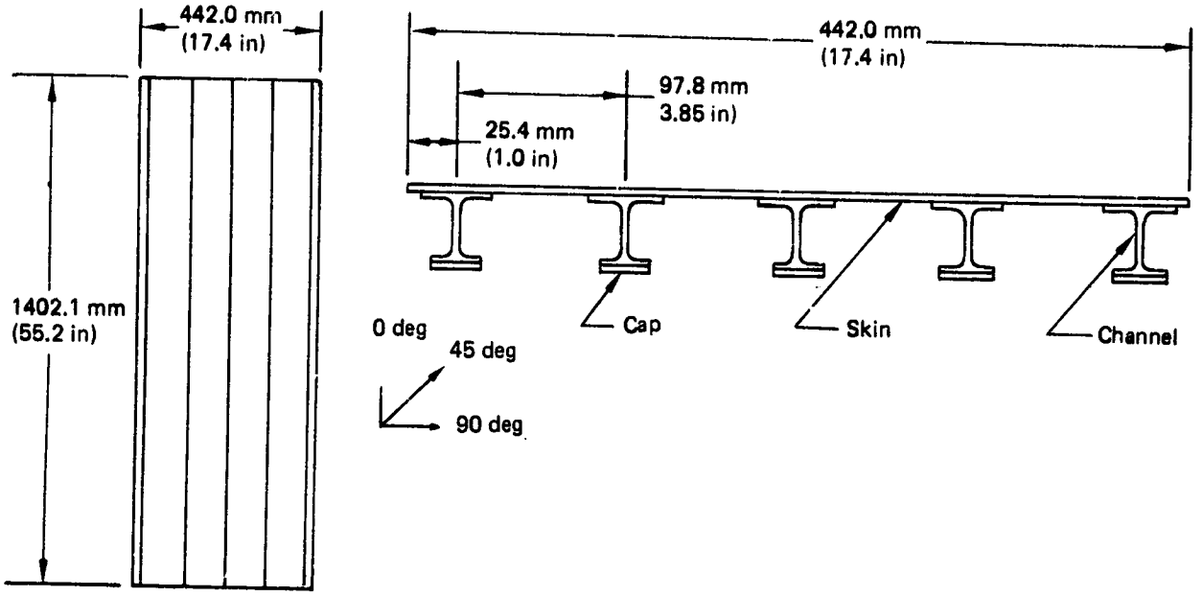

Specimen	Panel description		
	Skin	Channel	Cap
65C17773-1	7-ply fabric (5 at ±45, 2 at 0/90)	4-ply fabric (2 at ±45, 2 at 0/90)	9-ply fabric at 0/90
65C17773-2	10-ply fabric (7 at ±45, 3 at 0/90) 2-ply grade 190 tape (at 90)	4-ply fabric (2 at ±45, 2 at 0/90)	9-ply fabric at 0/90

Figure 79. Compression Panel Definition

The strain plot for the Configuration 1 panel (fig. 84) indicates that the skin panel between stiffeners buckled at an average strain of approximately -0.0017 mm/mm (in/in). This result agrees closely with the data for the 65C17773-61 crippling panel (fig. 75). The Moire fringe photo of the Configuration 1 panel (fig. 86) shows the well-developed buckle pattern at 133.4-kN (30-kips) load. The Moire fringe photo also shows the reduction of buckle deformation in the skin pad-up areas at the rib locations.

The strain plot for the Configuration 2 panel (fig. 85) indicates that the skin panel did not buckle prior to column failure. This result agrees with the 65C17773-62 crippling panel test (fig. 77). The Moire fringe photo of the Configuration 2 panel at 169 kN (38 kips) (fig. 87) confirms the absence of a well-defined buckle pattern.

The bending strain versus end-load plots for both Configuration 1 and 2 panels were used to construct Southwell plots and are shown in Figures 88 and 89. The Southwell plots for both panels yielded failure load predictions very close to the actual buckling loads. This close agreement indicates that the panels failed as proper Euler columns. The procedure of using bending strains to construct Southwell plots has been previously demonstrated in Reference 13.

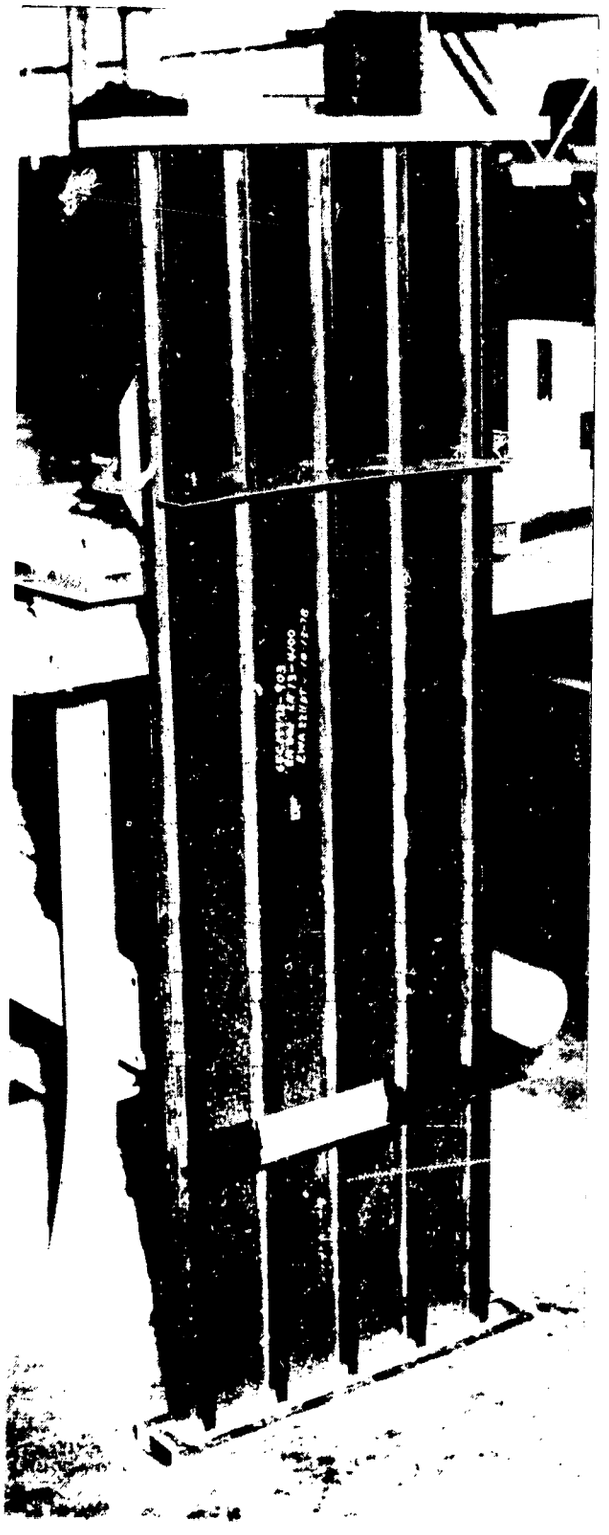

Figure 80. Compression Test Panel (Test 10)

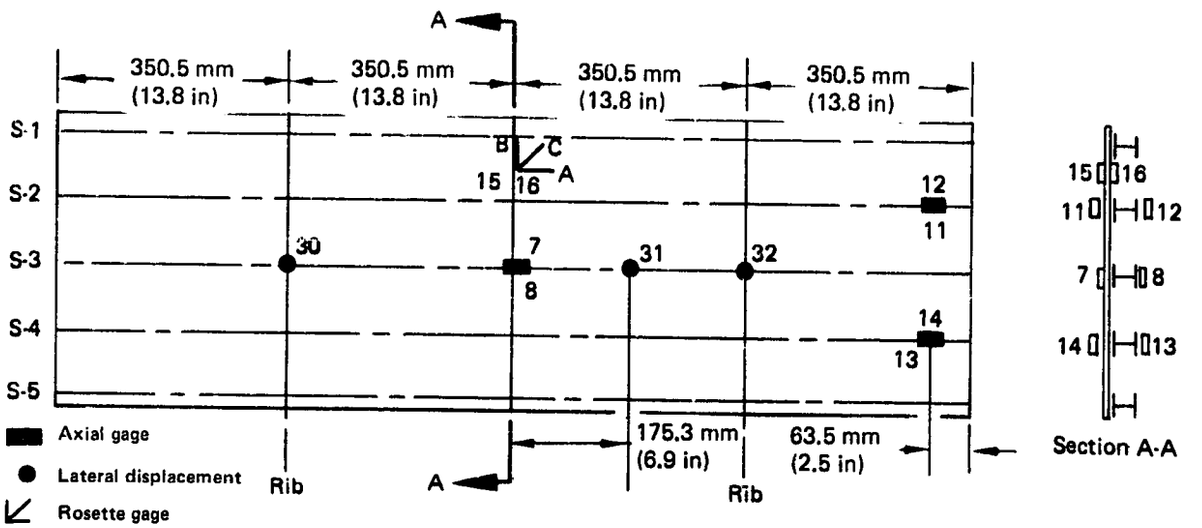

Figure 81. Strain Gage and Displacement Transducer Location for Compression Panels (Test 10)

The Euler column calculation for Configuration 1 or 2 panels is shown in Figure 90. Modulus values for each segment have been obtained from existing Boeing data. The 2W effective width calculation is the standard form used for metal stringer stiffened panels. The close agreement between the calculated and test values indicates that similar procedures can be used for calculating column buckling loads for both metal-stiffened and advanced-composites-stiffened panels.

4.2.3.2 Skin/Stringer Panels: Shear

Fifteen shear panels were tested to verify shear strength. The specimen configuration is shown in Figure 91, and test setup is depicted in Figure 92. The test results are tabulated in Table 12 and depicted in Figure 93.

4.2.3.3 Skin/Stringer Panels: Shear/Compression

Shear/compression panel test (Test 10) results are shown in Table 13. The test fixture consists of a compression and shear loading frame. The shear loads are introduced into the test panel through corrugated shear webs. The compression and shear frames are pinned together, and because the corrugated shear webs have a very low transverse stiffness, all the compression load is taken by the test panel. The panel is loaded in compression with four load cylinders, and the shear load is supplied by a cylinder (fig. 94). The test assembly is shown in Figure 95, and the test panel configuration is illustrated in Figure 96. The Configuration 43 test panel was tested at ratios of compression to shear of 4/1, 3/1, and 2/1.

4.2.3.4 Skin/Stringer Panels: Fatigue

Table 14 summarizes the test sequence, test conditions, and failure loads for the fatigue panels. Figure 97 shows the specimen geometry and ply layups. No failures

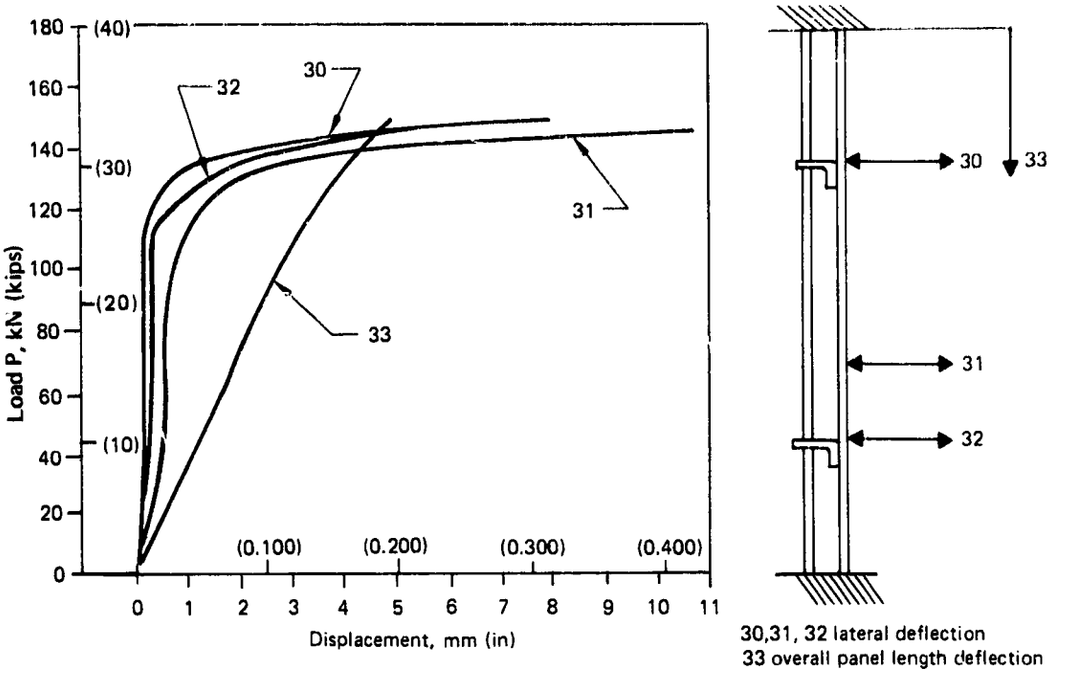

Figure 82. Displacement Transducer Readings Versus Load for Compression Specimen 65C17773-1-1 (Test 10)

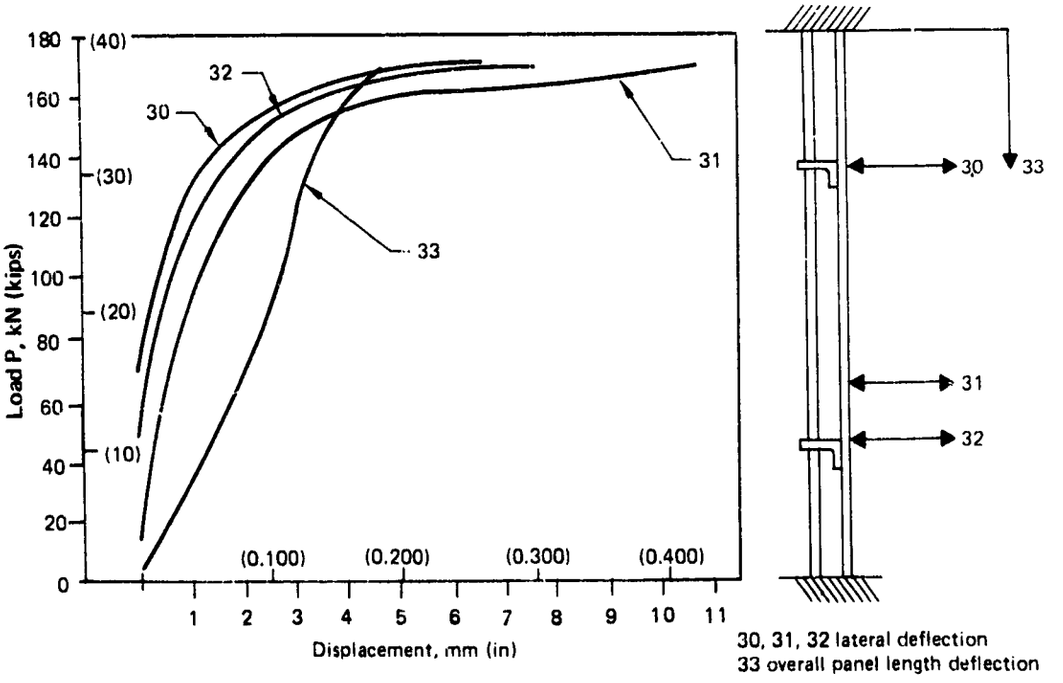

Figure 83. Displacement Transducer Readings Versus Load for Compression Specimen 65C17773-2-6 (Test 10)

See Figure 81 { 7, 8 stringer axial gages
15A, 16A skin panel rosette longitudinal gage

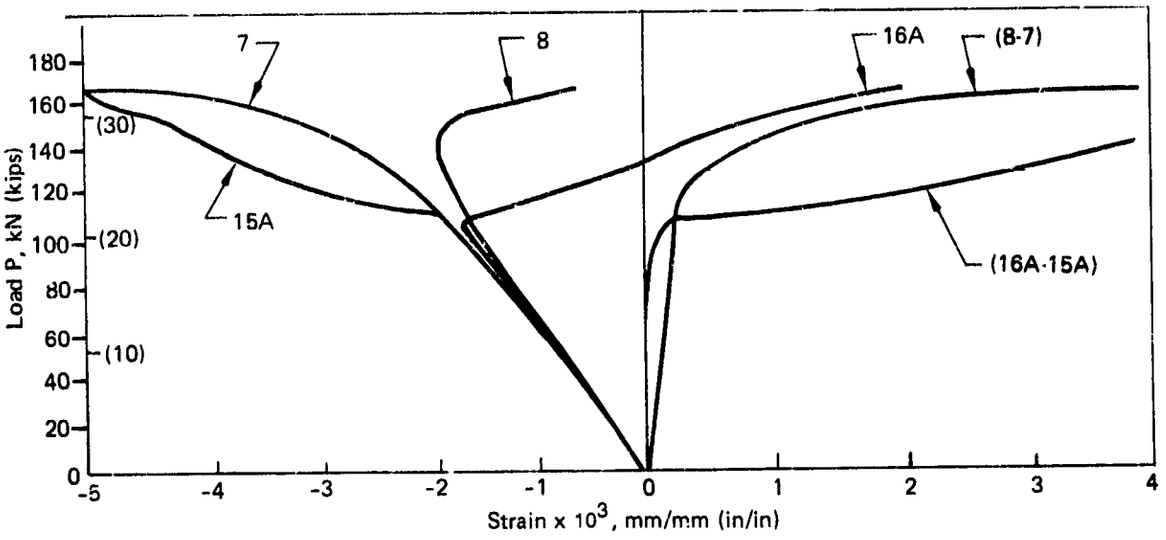

Figure 84. Strain Gage Readings Versus Load for Specimen 65C17773-1-1

See Figure 81 { 7, 8 stringer axial gage
15A, 16A skin panel rosette longitudinal gage

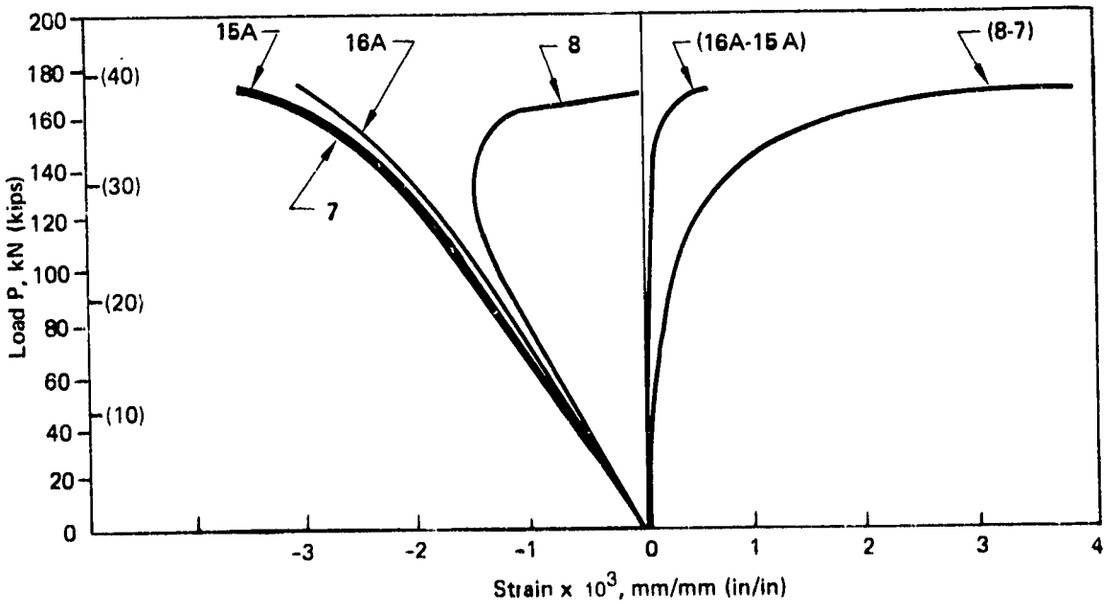

Figure 85. Strain Gage Readings Versus Load for Specimen 65C17773-2-6

Figure 86. Moire Fringe Photo of Compression Specimen 65C17773-1 at 133.4-kN (30-kips) Load (Test 10)

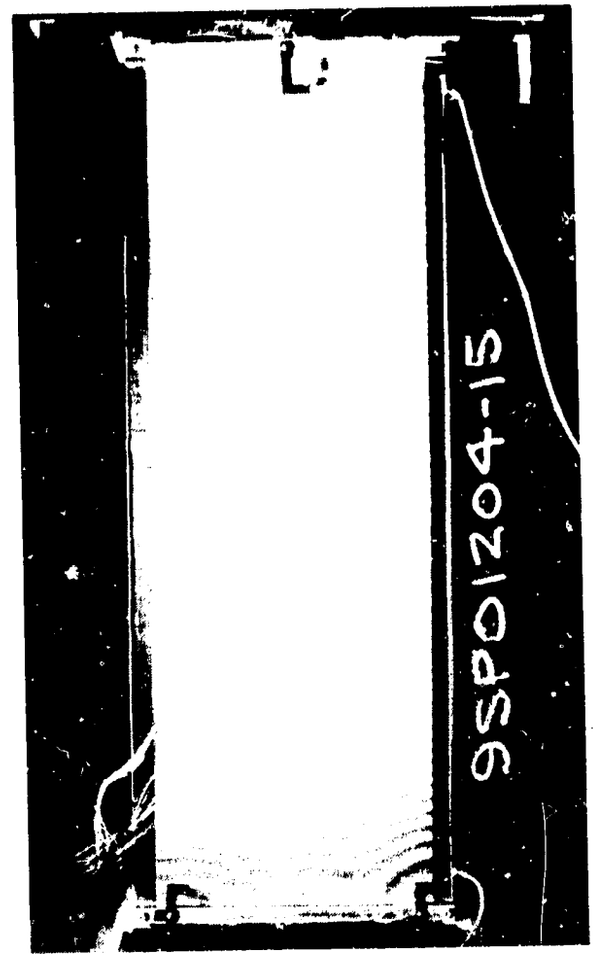

Figure 87. Moire Fringe Photo of Compression Specimen 65C17773-2 at 169-kN (38-kips) Load (Test 10)

occurred during the initial fatigue testing. In test condition A, the panels were able to sustain the limit compression strain after fatigue cycling and then were failed in tension.

In test condition B, the panels were damaged after one lifetime of fatigue testing. Figure 98 shows the damage locations and the energy levels used to damage the panels. Figures 99 through 103 show the initial damage discussed in test condition B. The damage was monitored during the one-half-lifetime fatigue test, using both X-ray and ultrasonic inspection. No growth was detected. The panel was subjected to the limit compression strain. The damage level was then increased at location 2 (figs. 104 and 105), limit compression strain was reapplied, and the panel then failed in tension.

4.2.3.5 Spar Root Lug

Spar root lug static test (Test 12) results are summarized in Table 15. The tension specimen geometry is shown in Figure 106. The compression specimen was

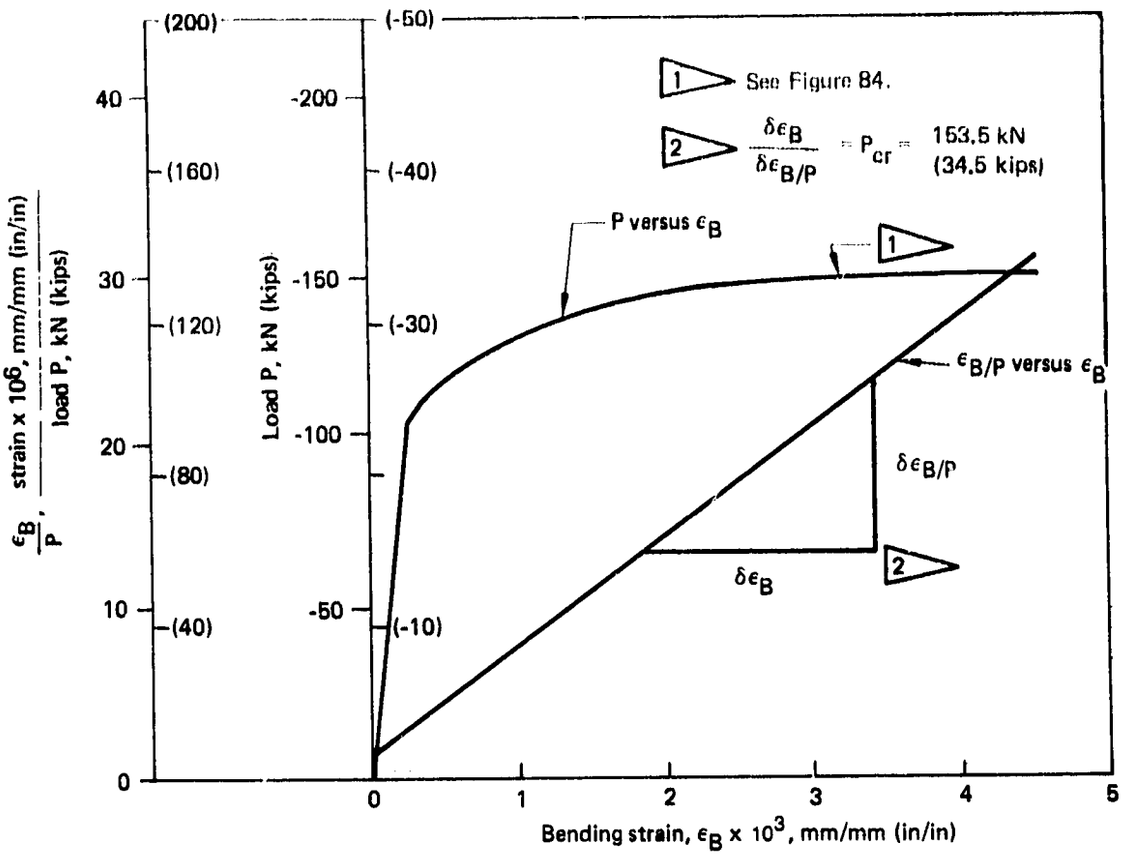

Figure 88. Southwell Plot for Compression Specimen 65C17773-1-1 (Test 10)

obtained by cutting the tension specimen in half, and casting an epoxy ring around the end to stabilize the compression loaded surface. Figure 107 shows a typical tension test setup, and Figure 108 shows a typical compression test setup.

All the tension specimens failed in net area tension in the region of the last fastener. Figure 109 shows a typical tension failure. The compression specimen failed by ultimate material compression failure at the epoxy ring surface. This typical failure is seen in Figure 108.

Strain gage readings from the 65C17774-1-1 tension specimen are plotted in Figure 110 (see fig. 106 for location). Strain gages 17 and 18 show that no significant bending was present during test. These two gages indicated that the graphite-epoxy failed at an average gross section strain of 3387 microstrain ($\mu\epsilon$). Geometry calculations of the specimen cross section show that the section had an EA value of 170.04N (38.23×10^6 lb) using nominal modulus values. At the failure load of 572.4×10^3N (130.9 kips), the strain would be 3425 $\mu\epsilon$, which is within 1.1% of the measured value.

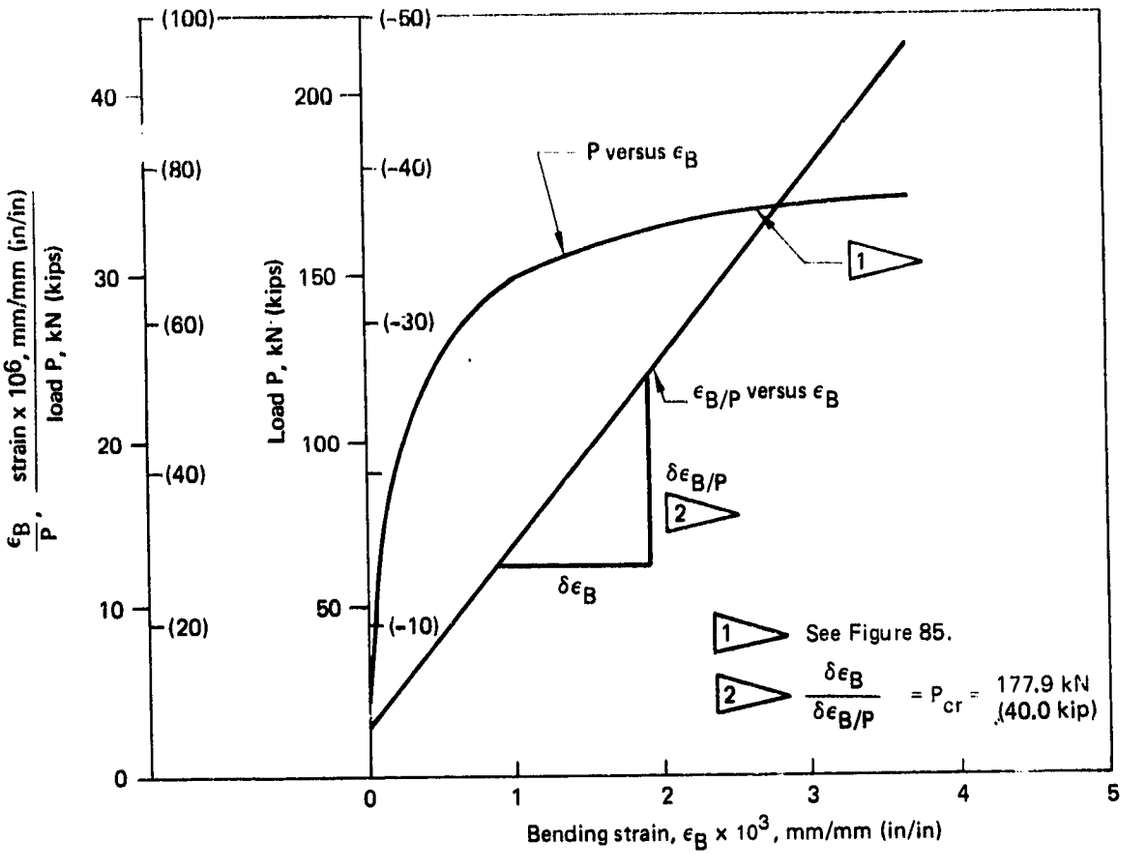

Figure 89. Southwell Plot for Compression Specimen 65C17773-2-6 (Test 10)

Strain gages 15 and 16, plotted in Figure 110, indicated significant changes in load distribution near the ultimate load. Load redistribution was caused by local fracture of the graphite-epoxy laminate in the lug area, resulting in a change in the fastener load pattern. A typical graphite-epoxy laminate failure in the area of the lug is shown in Figure 111.

The stub box strain survey results (Test 21) and the spar lug test results were reviewed and compared. The comparison showed that the spar lug tension design had a margin of safety (MS) of 11%. Based on this MS and the unknowns of extrapolating the stub box data to ultimate conditions, it was decided to improve the spar lug joint strength. Therefore, a program was initiated with Boeing funds to design and evaluate a new configuration.

To select the redesign approach, an analysis was made of the failed specimens. The tension specimen failure area (fig. 109) was inspected, and there appeared to be an interaction between the last two fasteners in the titanium plates. The first improvement was to change the fastener pattern to reduce the stress concentration factor. The end fastener also was reduced in size to increase the net area.

Euler Column Buckling Load

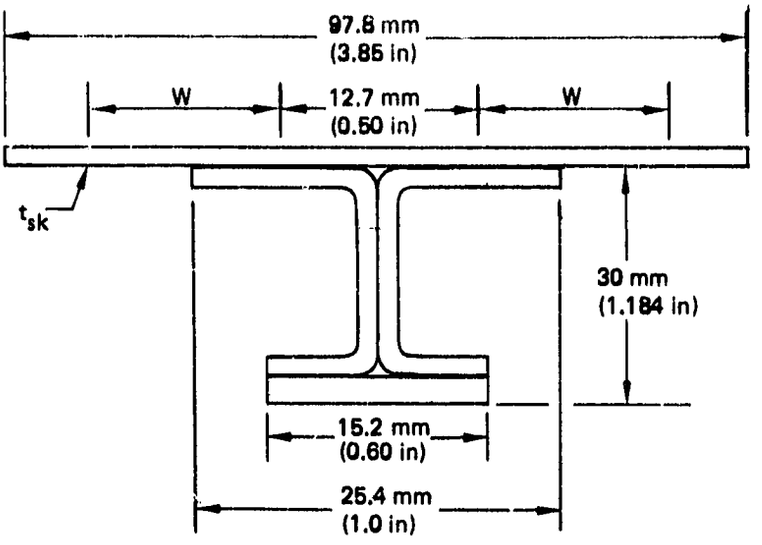

- Test specimen 65C17773-1-1

$$P_{cr} = \frac{\pi^2 EI}{(L/\sqrt{C})^2}$$

E = Elastic modulus

I = Moment of inertia

L = Column length

C = End fixity

- See Figure 79 for laminate definition

Moment of inertia (I) includes effective skin width

$W_e = 0.5 + 2W$ — 0.5 = Basic effective skin width

$2W = 1.7\ t_{sk} \sqrt{\frac{1}{\epsilon_B}}$ — t_{sk} = Skin thickness

2W = 45.0 mm (1.77 in) — ϵ_B = Axial strain at maximum load

W_e = 57.7 mm (2.27 in) = 0.0030 mm/mm (in/in)

Column section { E = 5.23×10^4 MPa (7.59×10^6 lbf/in)
I = 153.6×10^3 mm^4 (0.369 in^4)

Column length L = 1402.1 mm (55.2 in)

Column end fixity C = 3.5

$$P_{cr} = \frac{\pi^2 EI}{(L/\sqrt{C})^2} = 141\,373\text{N (31 782 lb)}$$

- Comparison with test

$$\frac{P_{cr}\ \text{test}}{P_{cr}\ \text{theoretical}} = \frac{146\,784}{141\,373} = 1.04$$

Figure 90. Euler Column Calculations for Compression Specimen 65C17773-1 (Test 10)

ORIGINAL PAGE
BLACK AND WHITE PHOTOGRAPH

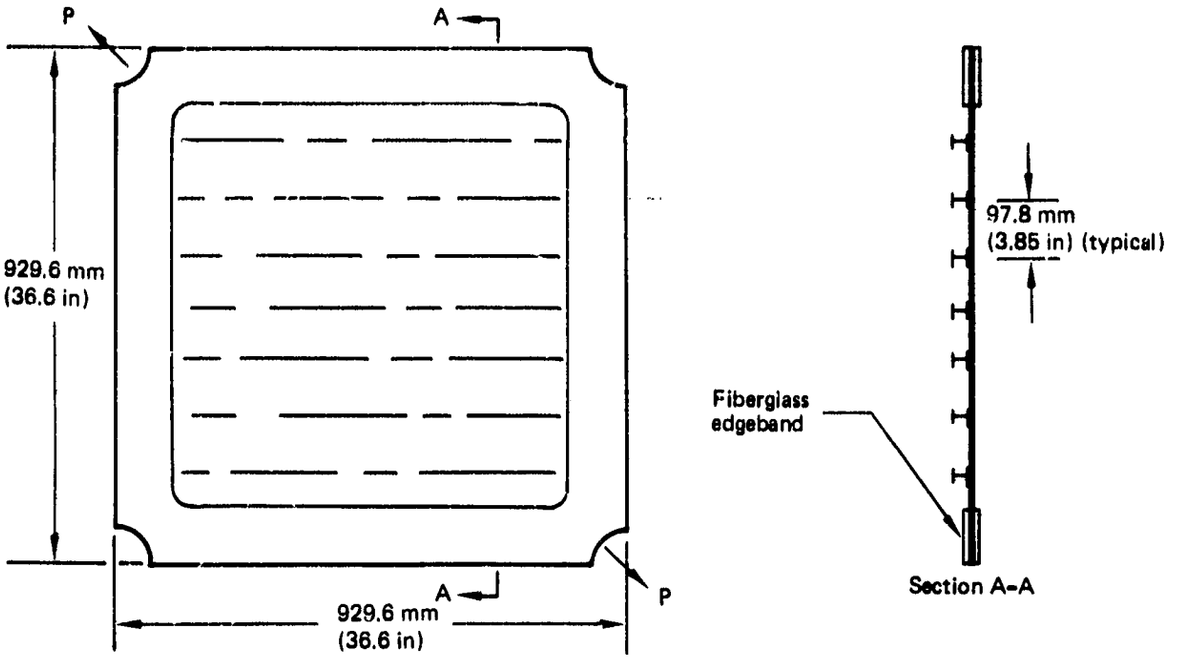

Figure 91. Shear Panel Geometry (Specimens 65C17773-5, -6, -7)

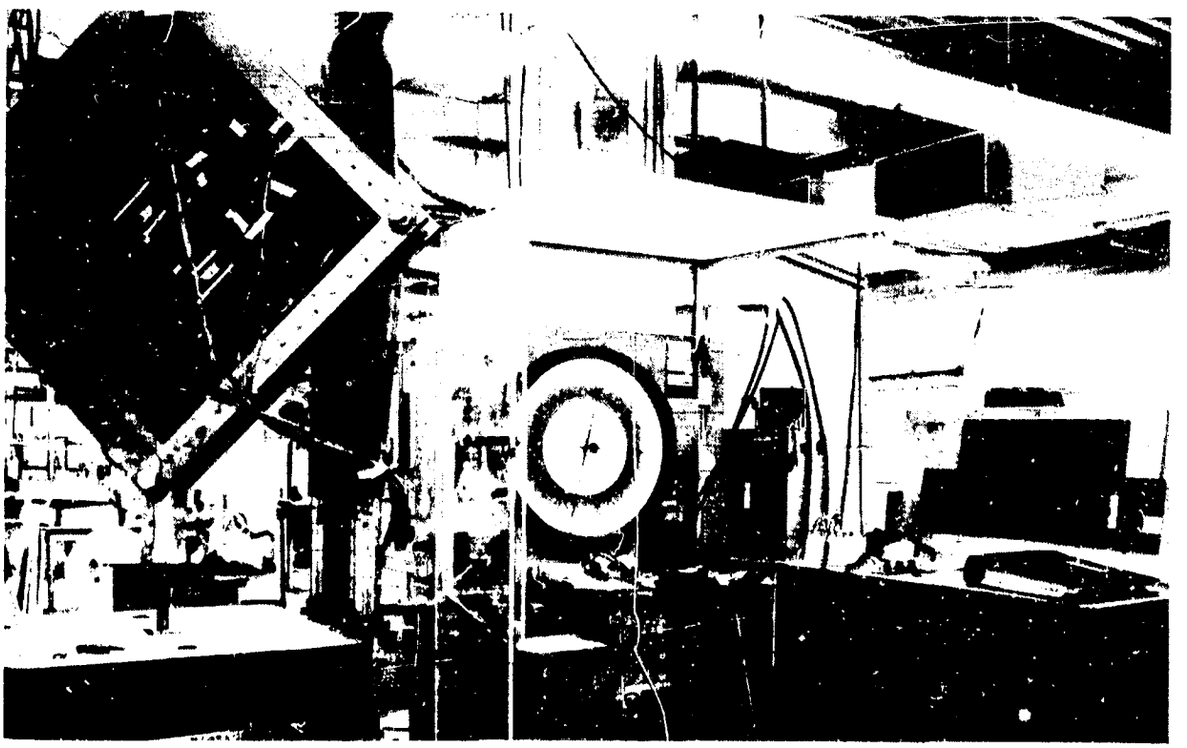

Figure 92. Shear Panel Test Setup

Table 12. Shear Panel Test Results

Specimen 65C17773-	Panel definition	Environmental condition		Failure load		Shear flow	
		Humidity	Temperature, °C (°F)	kN	(kips)	N/mm	(lb/in)
-5	Skin: 7-ply fabric (5 at ±45, 2 at 0/90) Channel: 3-ply fabric (2 at ±45, 1 at 0/90) Cap: 9-ply fabric at 0/90	Dry	21 (70)	108	(24.2)	88	(502)
-6	Skin: 10-ply fabric (7 at ±45, 3 at 0/90) Channel: 4-ply Grade 190 tape at 90 Cap: 9-ply fabric at 0/90			186	(41.6)	151	(861)
				185	(41.3)	150	(856)
			21 (70)	193	(43.0)	156	(892)
		Dry	-54 (-65)	154	(34.7)	126	(719)
		Wet	21 (70)	218	(49.1)	179	(1019)
			21 (70)	173	(39.0)	142	(809)
		Wet	82 (180)	162	(36.4)	132	(755)
		Dry	21 (70)	160 [1]	(36.0)	131	(747)
			21 (70)	170 [1]	(38.3)	139	(794)
		Dry	-54 (-65)	201 [1]	(44.8)	163	(929)
		Wet	21 (70)	162 [1]	(36.5)	133	(757)
		Wet	82 (180)	165 [1]	(37.0)	134	(767)
-7	Skin: 7-ply fabric (5 at ±45, 2 at 0/90) Channel: 3-ply fabric (2 at ±45, 1 at 0/90) Cap: 1-ply fabric at 0/90	Dry	21 (70)	131 [2]	(29.5)	106	(612)
-67	Same as 65C17773-6	Dry	21 (70)	192 [3]	(42.7)	155	(886)

[1] Impact damage test panel.

[2] Apparent premature failure by stringer delamination.

[3] Lightning-strike test panel (same configuration as 65C17773-6).

The second improvement was to increase the graphite-epoxy laminate axial modulus which, in turn, would increase the load capability. This improvement assumed that the failure strain would not be reduced by the higher stiffness material. The average modulus of the lug cross section was increased from 64.12 GPa (9.3 x 10^6 lbf/in^2) to 69.64 GPa (10.1 x 10^6 lbf/in^2).

Two specimens of this new configuration were fabricated and tested. With this new configuration, the gross section failure strain in the graphite-epoxy increased from an average of 3500 με to 3928 με, and the MS for the tension lug in the graphite-epoxy area was increased from 11% to 24%. A tested specimen of this new configuration is shown in Figure 112.

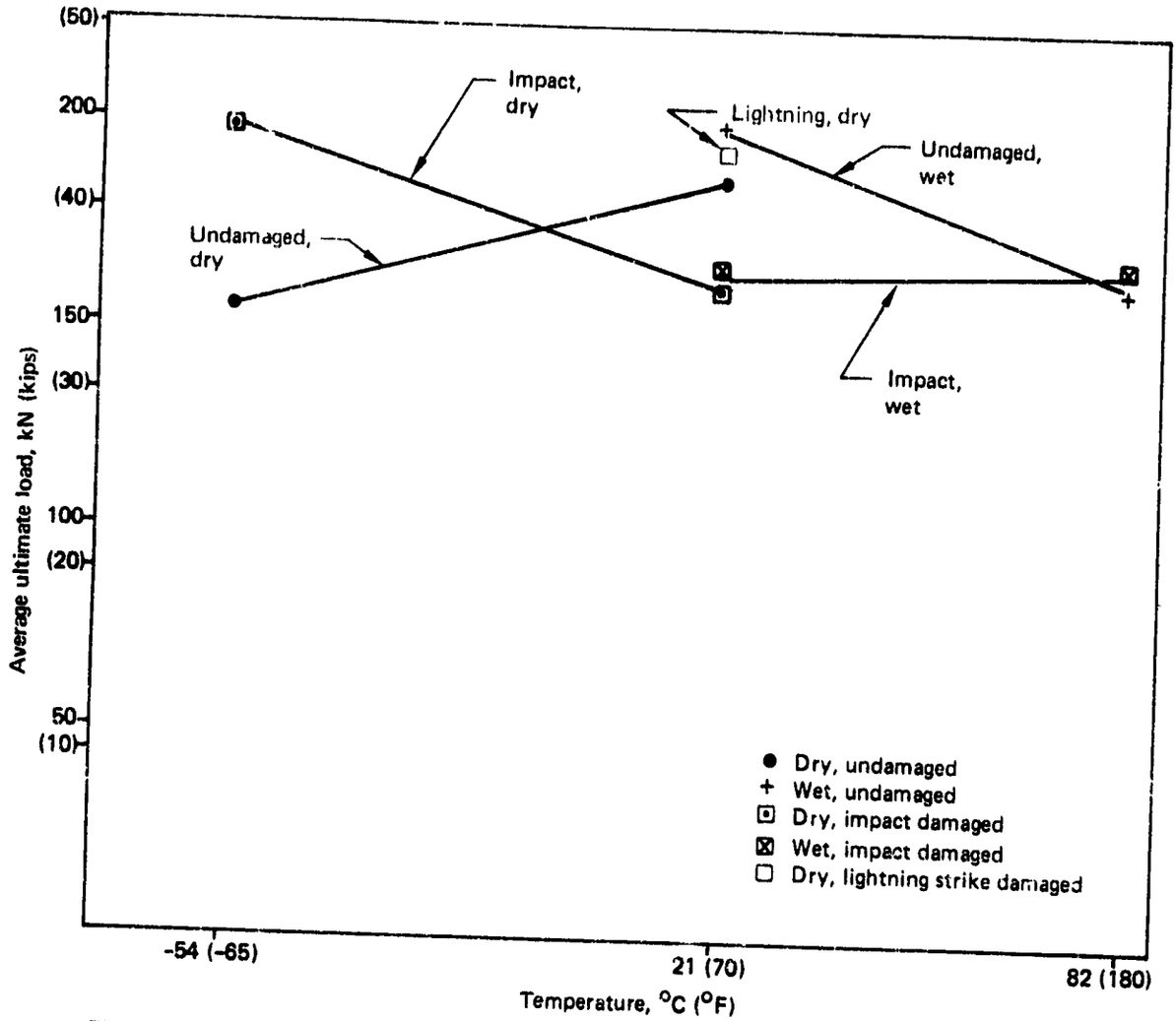

Figure 93. Shear Panels, Average Ultimate Load Versus Temperature and Humidity (Test 10)

These new configuration specimens were initially tested by loading them through the lug pins. Both specimens failed in tension in the titanium lug area. The specimens then were clamped in the test machine grips and loaded again until failure. Both specimens failed in the graphite-epoxy net section. Both types of failure are seen in Figure 112, and the test results are summarized in Table 16.

All of the heat-treated titanium lug straps fabricated for the stabilizer production and test program were partially annealed and had sustained surface contamination. This was caused by a manufacturing heat soak process to straighten the lug straps after machining. Following a review of this condition, a decision was made to scrap all the titanium straps except those installed on the ground test article. The partially annealed straps will provide acceptable test results for the ground test article based on results from the stub box ultimate and fatigue tests. Replacement titanium plate material was impossible to obtain to support the production schedule. Therefore, 15-5 PH stainless steel plate, heat treated from 1240 to 1380 MPa (180 to 200 $lbf/in^2 \times 10^3$), was substituted.

Table 13. Shear/Compression Panel Test Results

Specimen 65C17773-	Panel definition	Environmental condition		Ratio, compression to shear	Test load, kN (kips)	
		Humidity	Temperature, °C (°F)		Compression	Shear
-42	Skin: 10-ply fabric (7 at ±45, 3 at 0/90), 2-ply Grade 190 tape at 90 Channel: 4-ply fabric (2 at ±45, 2 at 0/90) Cap: 9-ply fabric at 0/90	Dry	21 (70)	4/1	721 (162)	180 (40.5)
-43	Skin: 7-ply fabric (5 at ±45, 2 at 0/90), 2-ply Grade 190 tape at 90 Channel: 3-ply fabric (2 at ±45, 1 at 0/90) Cap: 9-ply fabric at 0/90	Dry	21 (70)	4/1	498 (112)	125 (28.0)
				3/1	463 (104)	154 (34.6)
		Dry	21 (70)	2/1	391 (88)	196 (44.0)
		Wet	82 (180)	4/1	409 (92)	102 (23.0)
		Dry [1]	21 (70)	4/1	400 (90)	100 (22.5)
		Dry [1]	21 (70)	3/1	467 (105)	151 (34.0)

[1] Impact damaged panel.

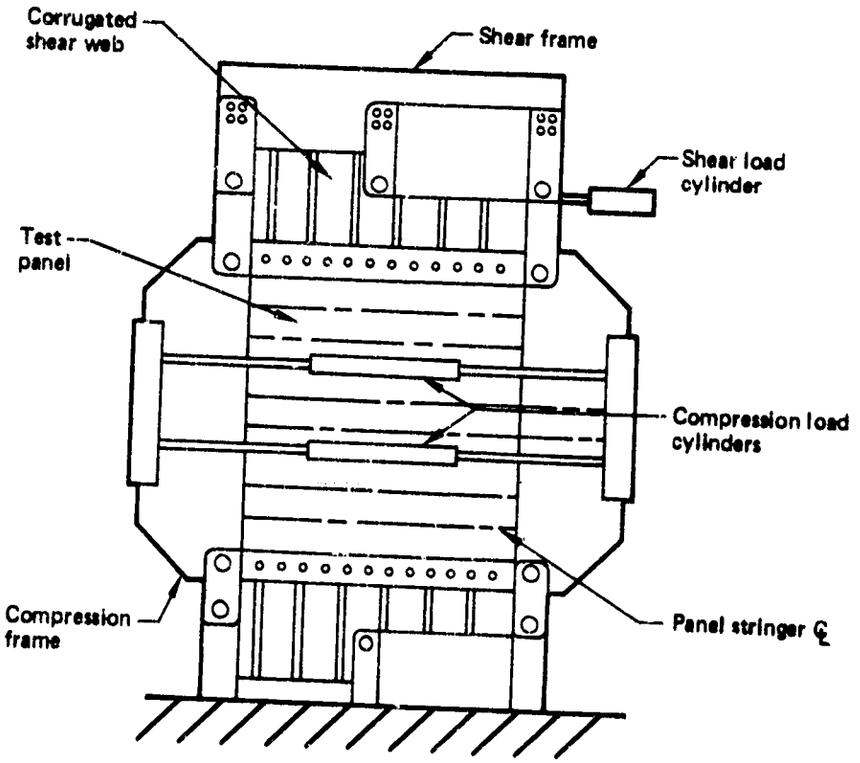

Figure 94. Shear/Compression Panel Test Fixture Assembly

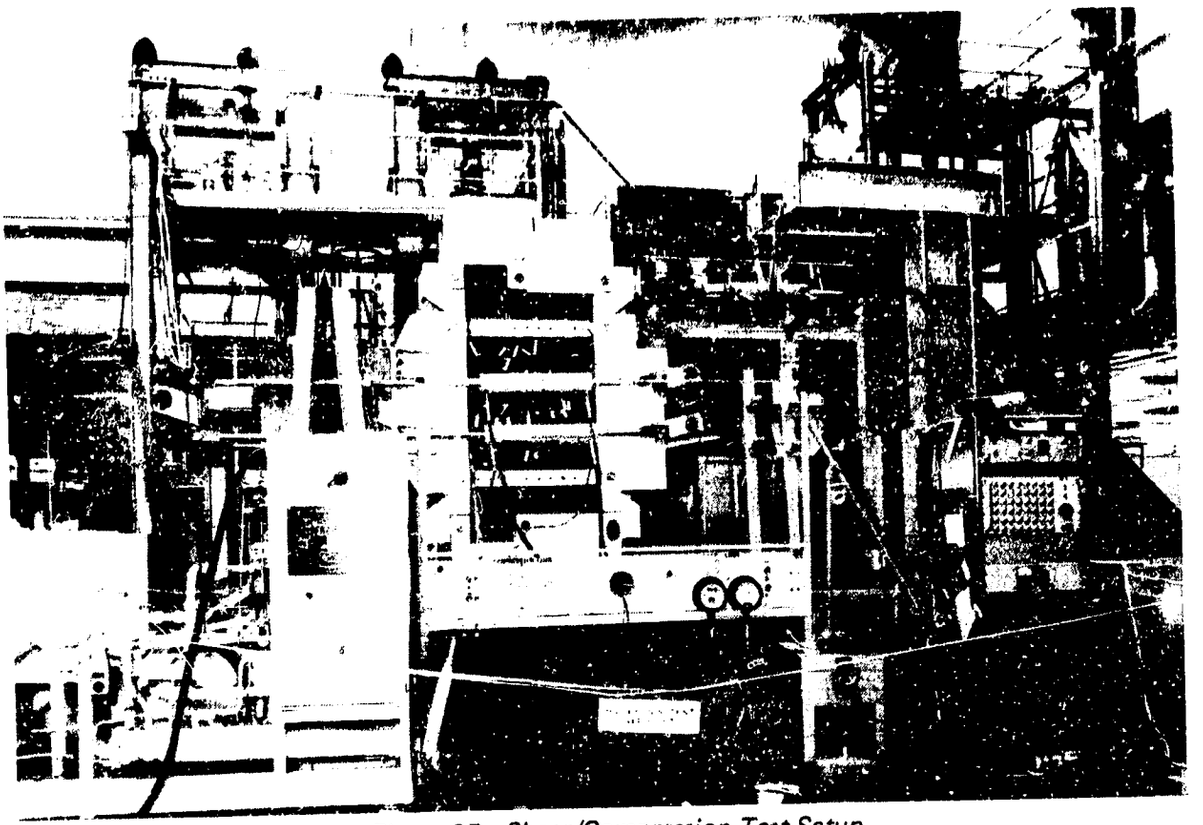

Figure 95. Shear/Compression Test Setup

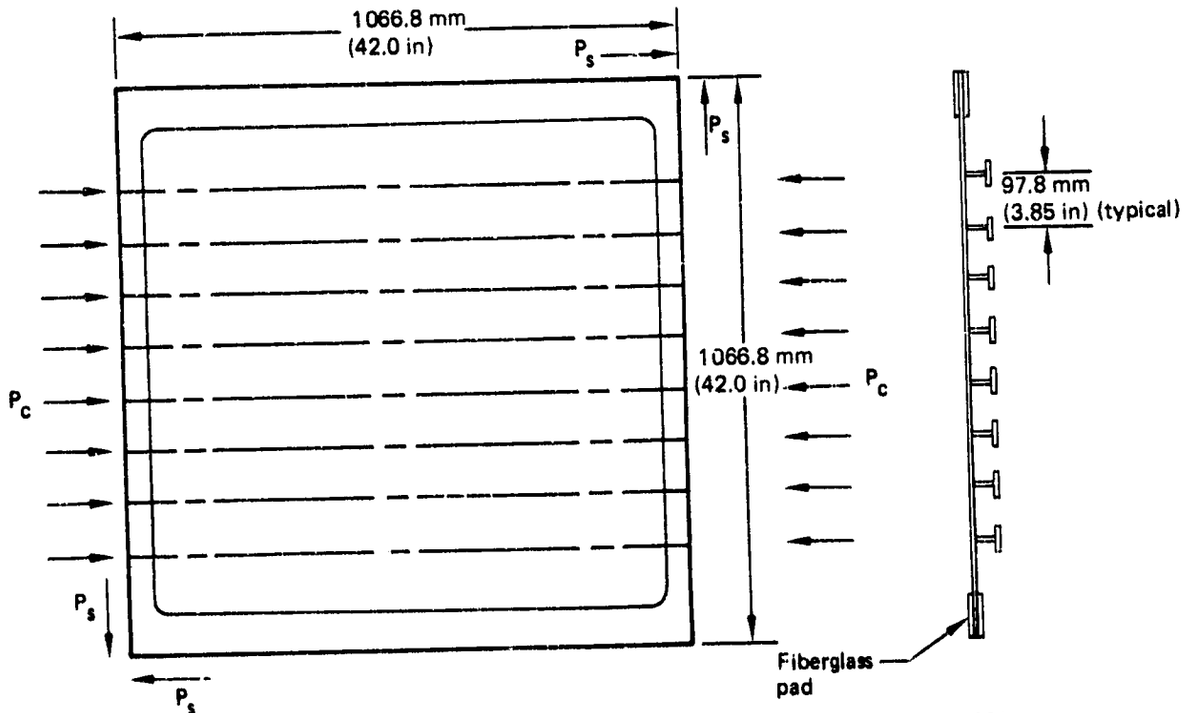

Figure 96. Shear/Compression Panel, (Specimens 65C17773-42, -43)

Table 14. Fatigue Test Results—Skin Panel Tests (Test 10)

Condition	Assembly number —identification number	Temperature, °C (°F)	Environmental condition	Load, P_T kN (kips)
A	-9 -001	21 (70)[1]	Dry	222.2 (49 950)
	-9 -004	↓	Wet	231.7 (52 100)
	-10 -002		Dry	276.2 (62 100)
	-81 -003		Dry	222.9 (50 100)
	-81 -004		Wet	255.1 (57 350)
B	-9 -001R	21 (70)	Dry	78.7 (17 700)
	-9 -003	-54 (-65)	↓	70.0 (15 750)
	-81 -002	21 (70)		90.5 (20 340)
C	-81 -004R	-54 (-65)	Dry	67.3 (15 140)
	-81 -005	82 (180)	Wet	99.8 (22 440)
	-9 -005	82 (180)	Wet	94.1 (21 150)

- Test condition A
  - One life spectrum fatigue test
  - Limit strain in compression
  - Tension loading to failure
- Test condition B
  - One life spectrum fatigue test
  - Damage inflicted at three locations (see ref. 1)
  - One-half life spectrum fatigue test (periodic inspection)
  - Limit strain in compression
  - Increase damage level by cutting stiffener (area cut = 18%)
  - Limit strain in compression
  - Tension loading to failure
- Test condition C
  - One-half life spectrum fatigue test
  - Damage inflicted at three locations (see ref. 1)
  - One life spectrum fatigue test (periodic inspection)
  - Limit strain in compression
  - Increase damage level by cutting stiffener (area cut = 18%)
  - Limit strain in compression
  - Tension loading to failure

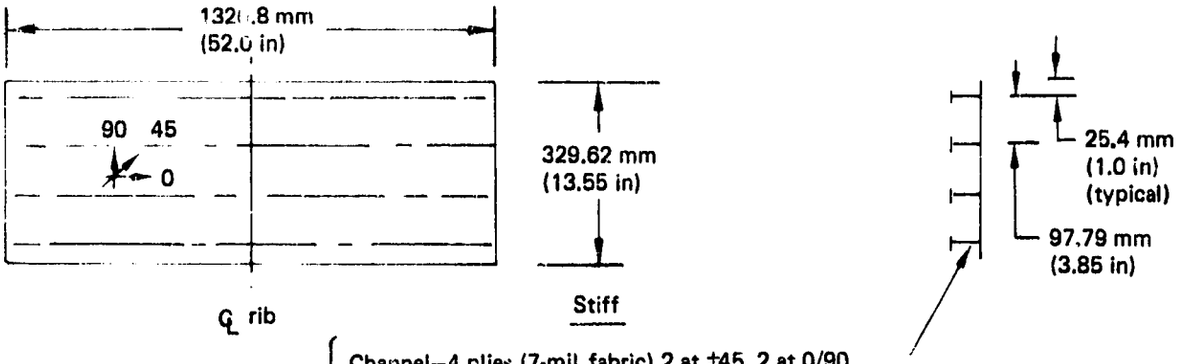

Specimen 65C17773 { Channel—4 plies (7-mil fabric) 2 at ±45, 2 at 0/90
Cap—9 plies (7-mil fabric) at 0/90

Assembly number	Basic skin layup	Rib pad layup
-9	7-ply fabric (5 at ±45, 2 at 0/90)	+2-ply tape, Grade 190, at 90 +2-ply tape, Grade 145, at 90
-10	10-ply fabric (7 at ±45, 3 at 0/90) +2-ply tape, grade 190, at 90	Same as -9
-81	Same as -9	Basic skin + 2-ply tape, Grade 190, at 90

Figure 97. Fatigue Panel Geometry—Skin Panel Tests (Test 10)

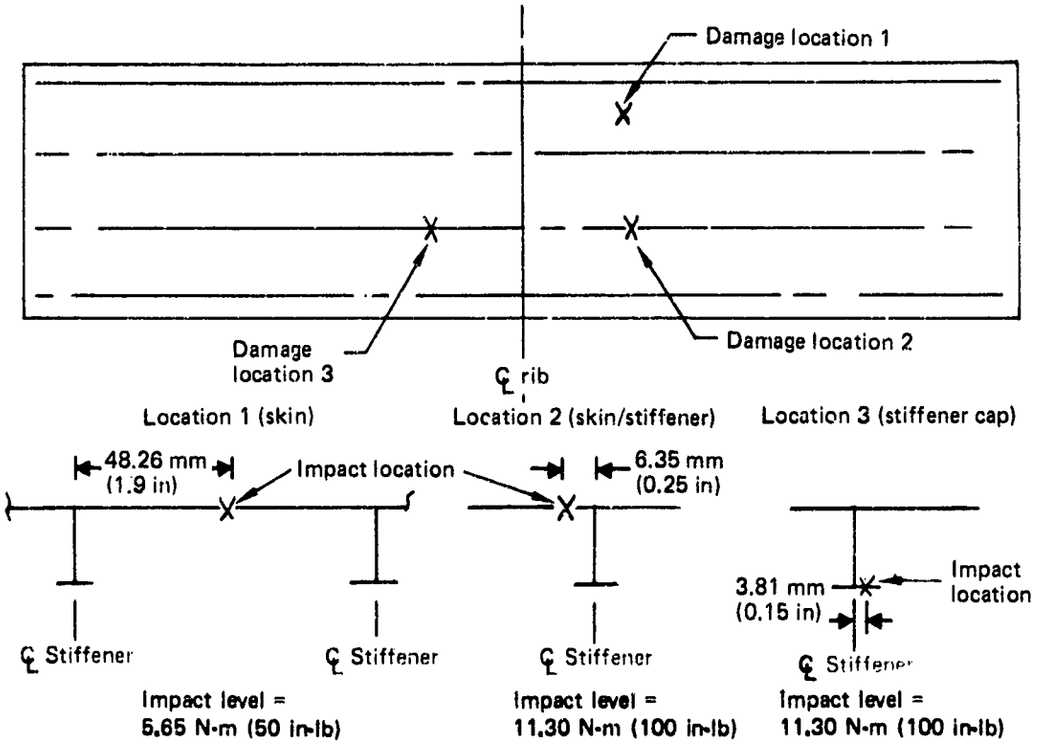

Figure 98. Fatigue Panel Damage Levels and Location—Skin Panel Tests (Test 10)

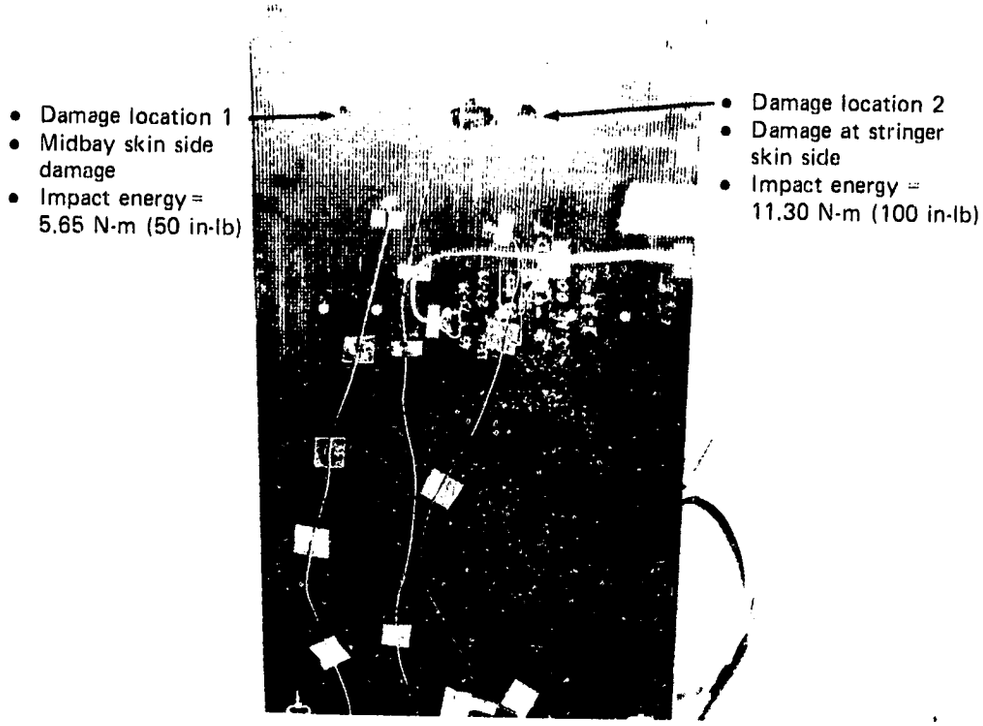

Figure 99. Test Panel Damage Locations 1 and 2—Skin Panel Tests (Test 10)

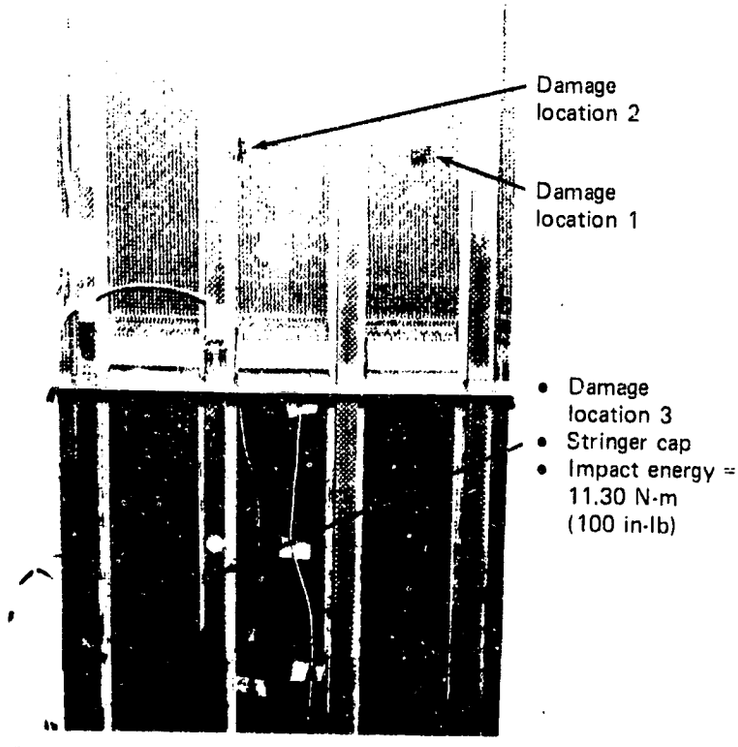

Figure 100. Test Panel Locations 1, 2, and 3—Skin Panel Tests (Test 10)

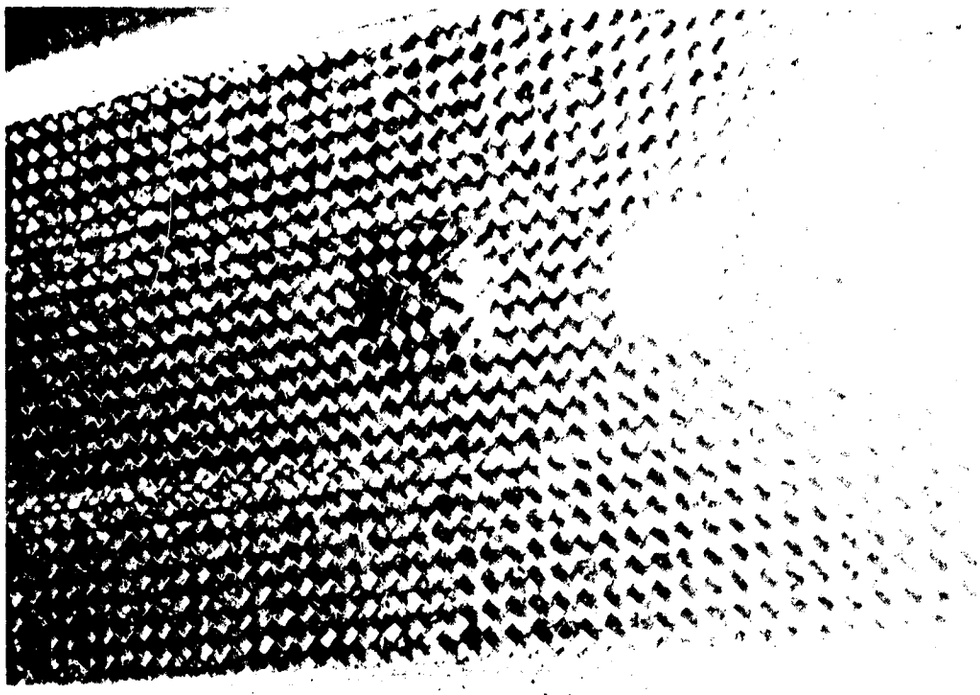

Figure 101. Damage Location 1, Stiffener Side—Skin Panel Tests (Test 10)

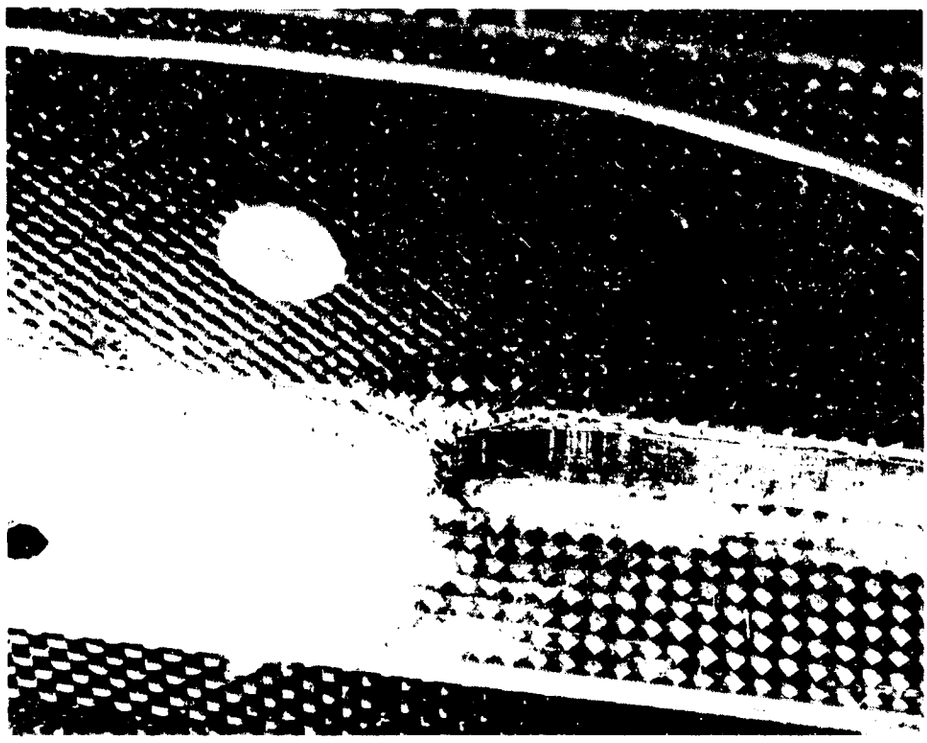

Figure 102. Damage Location 2, Stiffener Side—Skin Panel Tests (Test 10)

Figure 103. Damage Location 3—Skin Panel Tests (Test 10)

Figure 104. Additional Damage Location 2, Skin Side—Skin Panel Tests (Test 10)

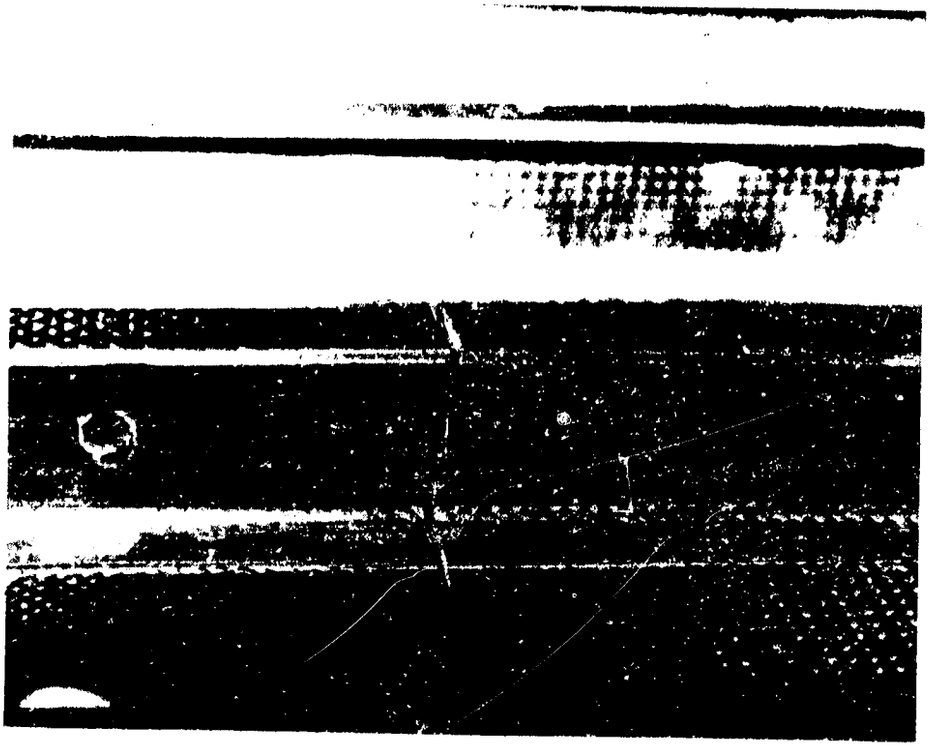

Figure 105. Additional Damage Location 2, Stiffener Side–Skin Panel Tests

Table 15. Spar Root Lug Static Test Results (Test 12)

Specimen number		Temperature, °C	Temperature, (°F)	Environmental condition [1]	Condition	Failure load, N	Failure load, (lb)	Gross section strain, με [2]
65C17774-1	1	21	(70)	Dry	Tension	582 377	(130 930)	3425
	2	21	(70)			602 704	(135 500)	3544
	3	-54	(-65)			633 840	(142 500)	3727
	4	-54	(-65)			556 000	(125 000)	3270
	5	21	(70)	Wet		582 688	(131 000)	3427
	9	21	(70)			582 688	(131 000)	3427
	7	82	(180)			597 144	(134 250)	3512
	8	82	(180)			601 592	(135 250)	3538
65C17774-2	1	21	(70)	Dry	Compression	1 209 856	(272 000)	7115
-2	2	21	(70)			934 080	(210 000)	5193
-2	3	-54	(-65)			980 780	(220 500)	5768
-16 [3]	1	-54	(-65)			986 340	(221 750)	5800
-16	2	82	(180)			936 304	(210 500)	5506
-16	3	82	(180)			885 152	(199 000)	5205
-2	4	82	(180)	Wet		927 408	(208 500)	5454
-16	4	82	(180)	Wet		786 184	(176 750)	4623

[1] Specimen conditioned at 60°C (140°F), 100% relative humidity until 2.29-mm (0.09-in) rider specimen reaches 1.1% moisture content.

[2] Based on a gross section EA of 170.04N (38.23 x 10^6 lb).

[3] -2 and -16 are the two halves cut from the -1.

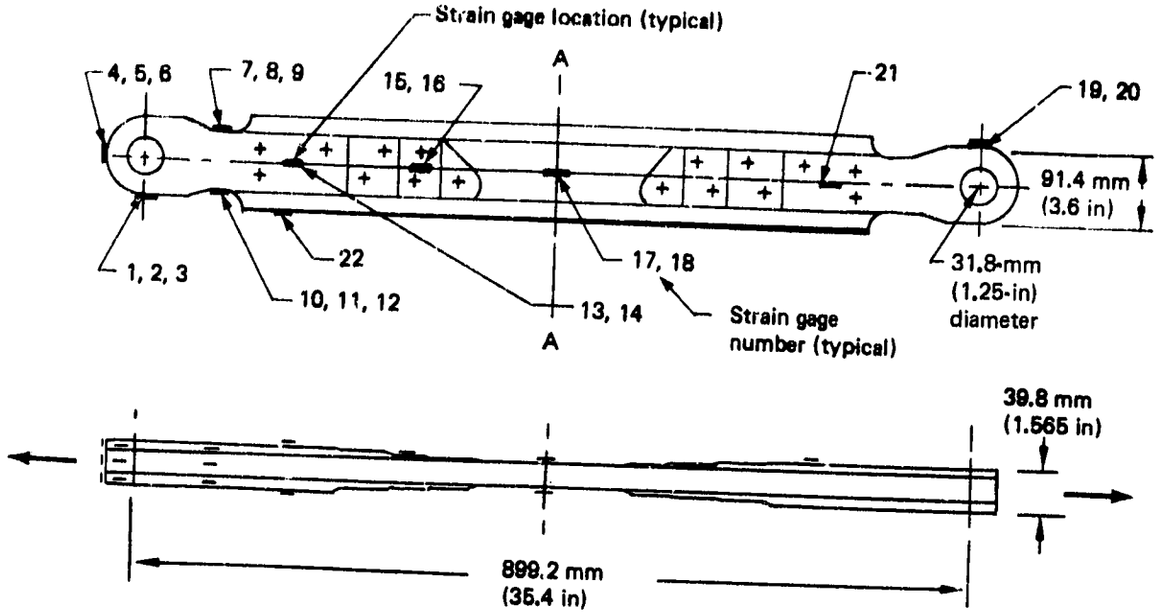

Figure 106. Spar Root Lug Test Specimen (Test 12)

Figure 107. Spar Lug Tension Test Setup (Test 12)

ORIGINAL PAGE
BLACK AND WHITE PHOTOGRAPH

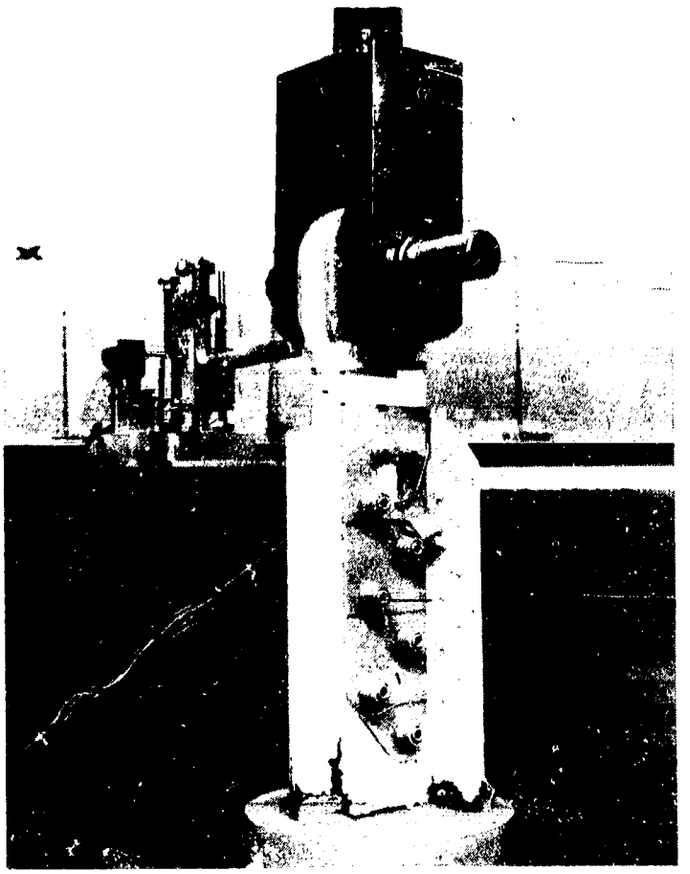

Figure 108. Spar Lug Compression Test Setup (Test 12)

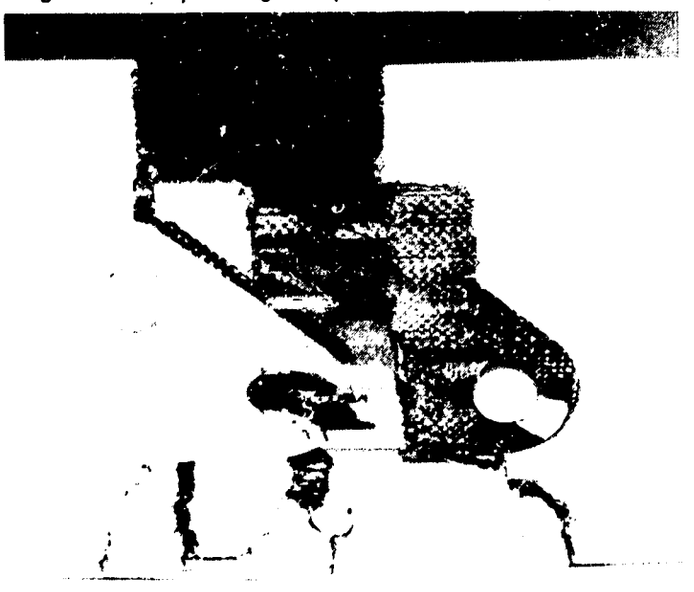

Figure 109. Spar Lug Typical Tension Failure (Test 12)

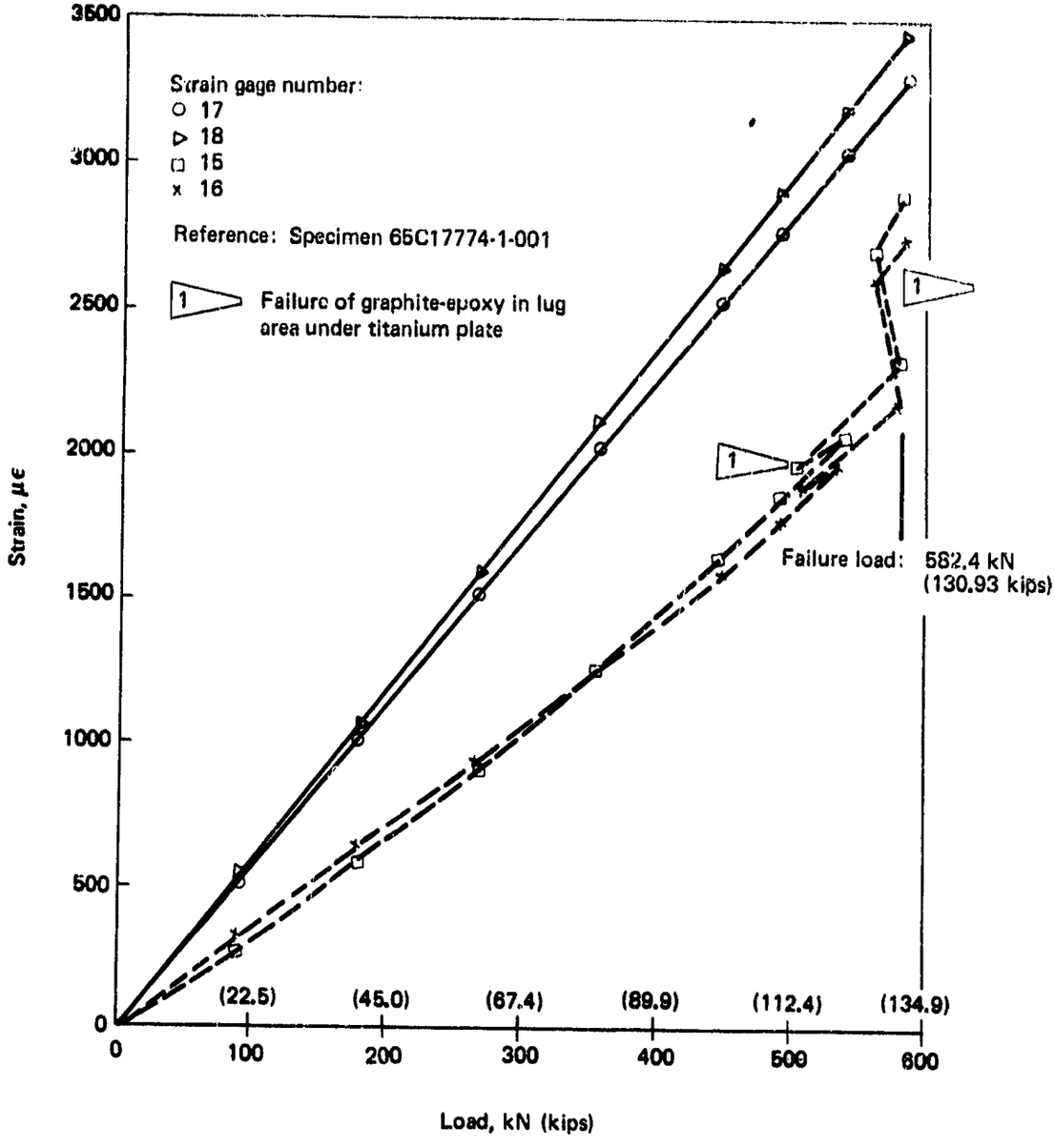

Figure 110. Spar Lug Specimen–Strain Gage Readings (Test 12)

The test results are presented in Table 17, and the specimen configuration is shown in Figure 113. This set of test specimens demonstrated sufficient load-carrying capability.

4.2.3.6 Discontinuous Laminate

Discontinuous laminate (Test 22) was conducted to determine stress concentration factors for discontinuous cocured laminates. Three laminate geometries that represent areas on the stabilizer skin panel were tested at 21°C (70°F) (room

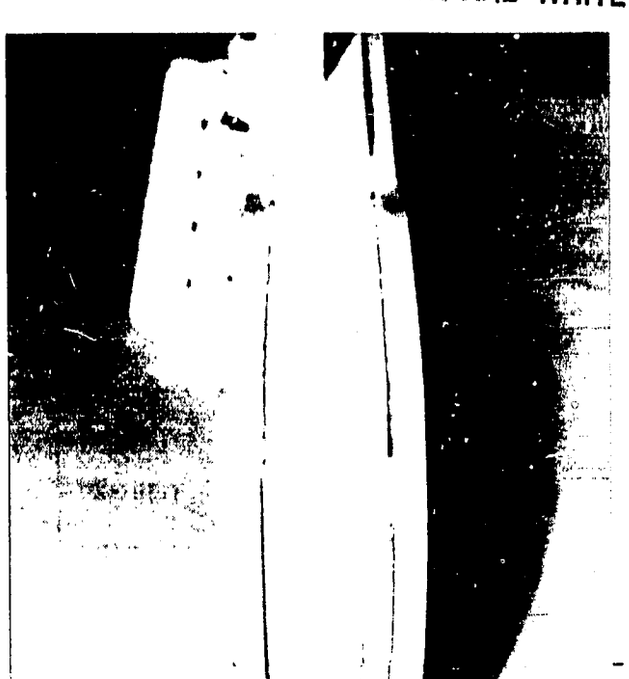

Figure 111. Graphite-Epoxy Laminate Failure in Lug Area (Test 12)

Figure 112. Modified Spar Lug Tension Specimen (Test 12)

Table 16. Modified Spar Lug Specimen Test Results (Test 12)

Specimen 65C17983	Temperature, °C (°F)	Environmental condition	Failure load, N (lbf)	Gross section strain, με [1]	Failure location
-902 -1	21 (70)	Dry	638 288 (143 500)	3682	Lug
-1	↓ ↓	↓	656 080 (147 500)	3956	Graphite-epoxy net section
-2	↓ ↓	↓	653 856 (147 000)	3780	Lug
-2	21 (70)	Dry	665 865 (149 700)	3900	Graphite-epoxy net section
-901 -1	21 (70)	Dry	613 855 (138 000)	3700	Graphite-epoxy net section
-2	21 (70)	Dry	613 855 (138 000)	3780	Graphite-epoxy net section

[1] Strain-gage measured values.

Table 17. Spar Lug Test Results (Test 12B)

Specimen	Temperature, °C (°F)	Environmental condition	Condition	Failure load, kN (kip)	Gross section strain, με [1]	
-20-001	-53 (-65)	Dry	Tension	828.7 (186.3)	2966	
-20-002	↓ ↓	↓	↓	770.9 (173.3)	2689	[2] [3]
-21-002	↓ ↓	↓	↓	781.5 (176.5)	2713	[3]
-21-003	↓ ↓	↓	↓	496.0 (111.5)	3052	[4]
-21-004	↓ ↓	↓	↓	536.0 (120.5)	3328	[4]
-22-001	↓ ↓	↓	↓	479.5 (107.8)	2965	[5]
-22-002	↓ ↓	↓	↓	472.8 (106.3)	2868	[4] [5]
-23-001	↓ ↓	↓	↓	504.0 (113.3)	2960	[6]
-23-002	-53 (-65)	Dry	Tension	521.8 (117.3)	3269	[4] [6]
-21-005A	82 (180)	Wet	Compression	899.9 (202.3)	–	[7]
-21-005B	↓ ↓	↓	↓	1066.7 (239.8)	–	↓
-21-006A	↓ ↓	↓	↓	1046.7 (235.3)	–	
-21-006B	↓ ↓	↓	↓	1142.3 (256.8)	–	
22-003A	↓ ↓	↓	↓	1104.5 (248.3)	–	[5]
22-003B	↓ ↓	↓	↓	1217.9 (273.8)	–	[5]
23-003A	↓ ↓	↓	↓	1073.4 (241.3)	–	[6]
-23-003B	82 (180)	Wet	Compression	1040.9 (234.0)	–	[7] [6]

[1] Strains from strain gage readings taken at midpoint of tension specimens. No measurements are available for the compression specimens.

[2] Specimen 21-002 was tested in the -20 configuration.

[3] Specimen failed in lug.

[4] Specimen subjected to two tension spectra.

[5] Flawed specimen—impact defect.

[6] Flawed specimen—sealant omitted.

[7] Specimen subjected to two compression spectra.

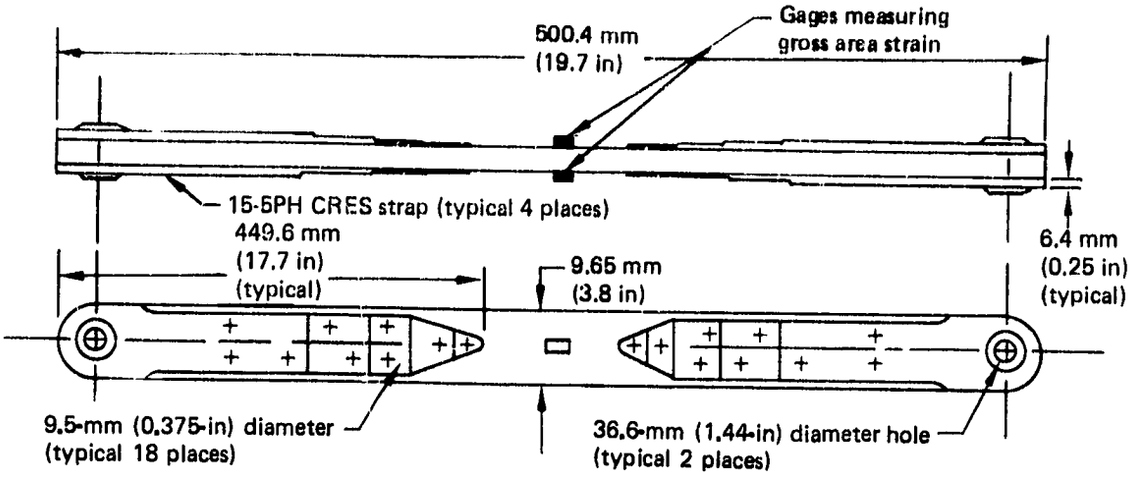

Fatigue Specimen 65C17986-21

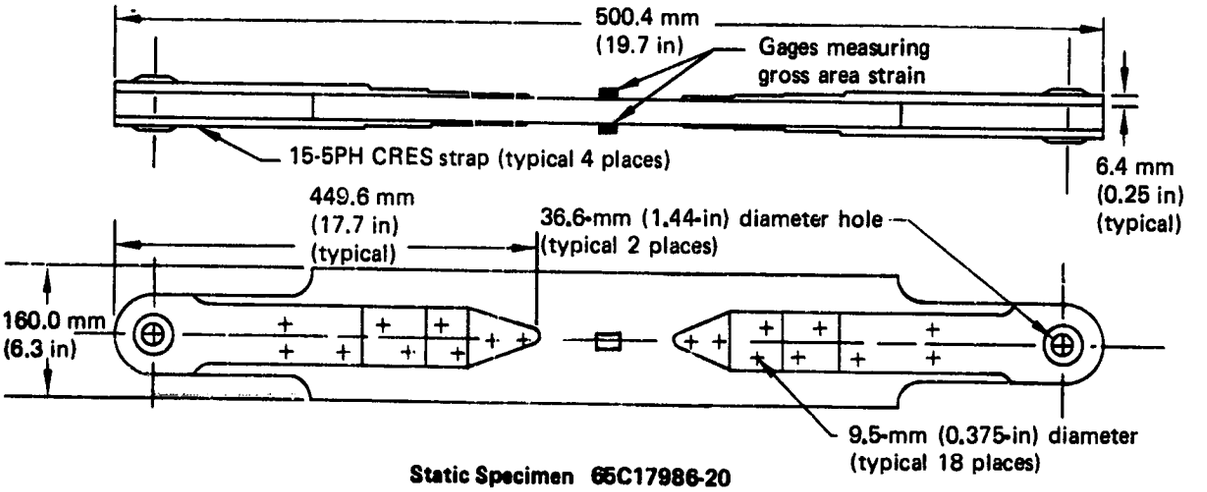

Static Specimen 65C17986-20

Figure 113. Spar Lug Configuration (Test 12B)

temperature) and -54°C (-65°F). Coupons with and without discontinuous doublers were tested. The specimen geometry and laminate definition are presented in Figure 114, and the test setup is shown in Figure 115.

4.2.3.7 Pressure/Shear Skin Joint

The pressure/shear skin joint test (Test 24) is shown in Figure 116. Test specimens were fabricated to simulate the anticipated cover panel and rib for the lower and upper surfaces. Specimens were loaded at one of two angles to determine the effect of horizontal load component on fastener tension strength. The results (table 18) indicate that upper surface specimens (ribs attached with 4.8-mm [0.19-in] shear-head bolts) failed by the bolt pulling through the skin, whereas the lower surface specimens (using 4.0-mm [0.16-in] tension-head bolts) failed in the rib clip radius.

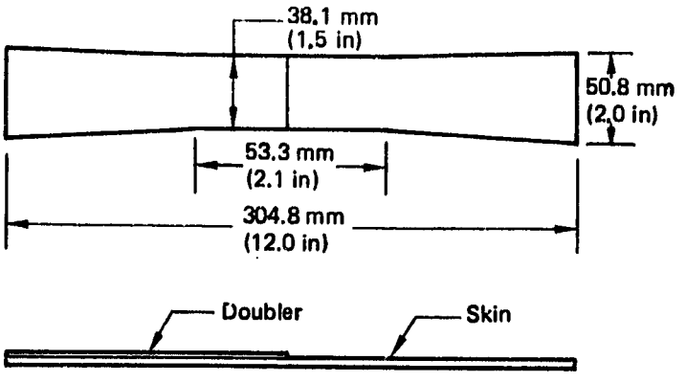

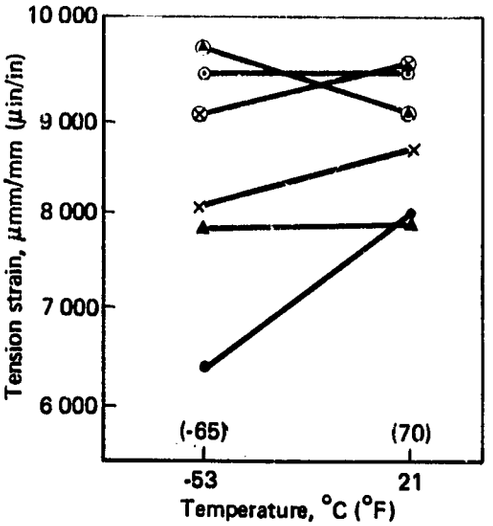

Specimen	Skin layup	Doubler layup
1	7-ply fabric	3-ply fabric
2	7-ply fabric, 4 -ply tape	4-ply fabric
3	15-ply fabric	3-ply fabric
5	Same as 1	No doubler
7	Same as 2	No doubler
9	Same as 3	No doubler

- Environmental condition—dry
- Data from Test 22, Appendix C

Symbol	Specimen
×	1
⊗	5
●	2
⊙	7
▲	3
◕	9

Figure 114. Effect of Moisture and Temperature on Discontinuous Laminates

4.2.3.8 Skin/Rib Joint

The skin/rib joint test (Test 27) provided additional data for the rib flange-to-skin attachment and assessed the effect of environmental conditions on fastener pull-through and rib flange strength. It consisted of three specimen types (figs. 117 through 119): a rib-to-skin specimen similar to the Test 24 specimens, a rib clip specimen, and a lap tension specimen. The rib-to-skin specimens were tested with only vertical loads on the 4.8-mm (0.19-in) shear-head fasteners, and the test results (table 19) for this configuration are not significantly different from the Test 24 specimen results. The rib clip specimens were tested using a 4.0-mm (0.16-in) protruding head bolt. All tests of the rib clip specimen (table 20) show that failure occurred by delaminations in the rib clip radius. The tests at the 82°C (180°F) wet conditions produced the greatest reduction in load capability. The lap tension test results (table 21), using a 4.8-mm (0.19-in) shear-head bolt, indicate a maximum reduction of 6% in strength for both the high- and low-temperature test conditions.

Additional rib clip tests were conducted following the decision to use unidirectional tape on the stabilizer ribs to improve the surface quality. Consequently, test

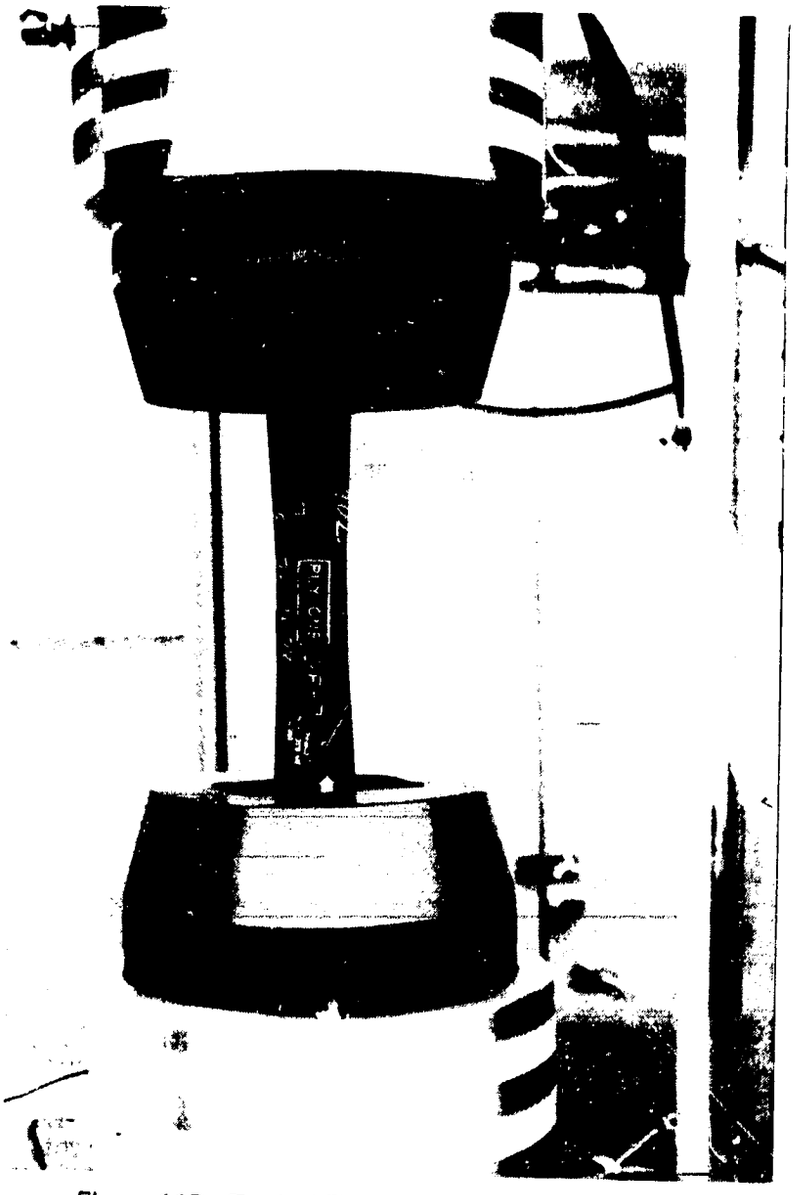

Figure 115. Typical Test Setup (Test 22)

specimens were produced that resembled the Test 27 rib clip specimen (fig. 118) except that four layers of 0.188-mm- (0.0074-in-) thick tape (two at 45, one at 0, and one at 90) and a layer of fiberglass replaced four layers of fabric. As with the other specimens, environmental conditions weakened the specimens by as much as 8% (hot, wet condition). The nontape specimens were about 6% stronger than the tape specimens.

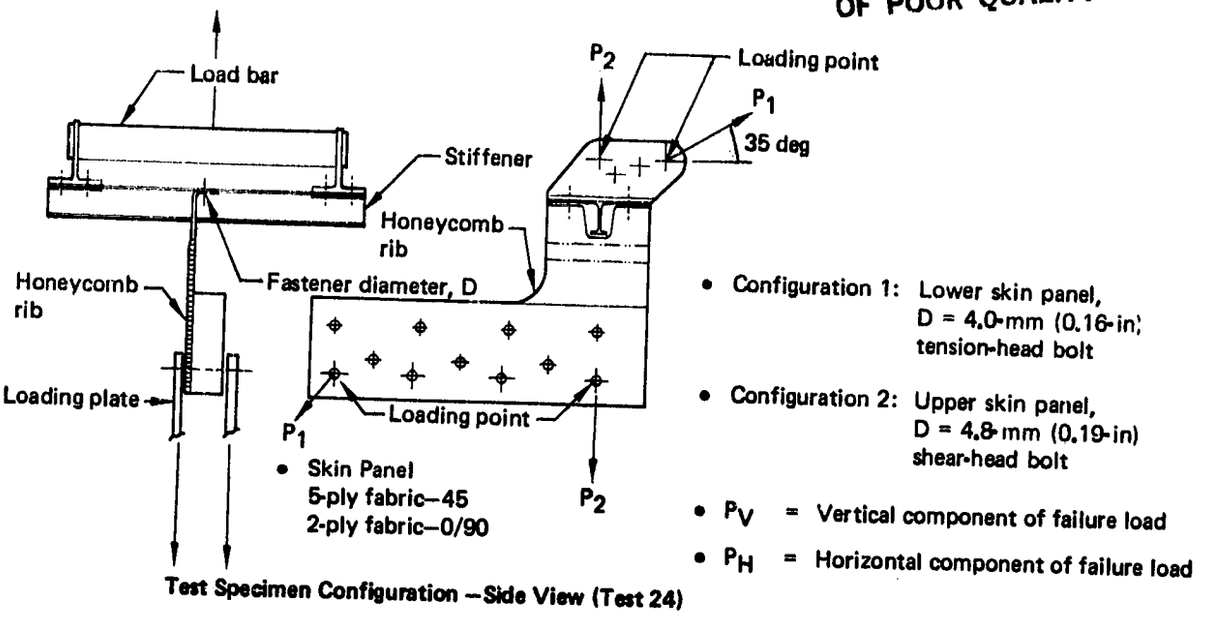

Figure 116. Pressure/Shear Skin Joint Test Specimen

Table 18. Pressure/Shear Skin Joint Test Specimens and Results

Configuration	Temperature, °C	(°F)	Environmental condition	Direction of applied load	Failure load, N	(lbf)	P_V, N	(lbf)	P_H, N	(lbf)
1	21	(70)	Dry	P_1	3781	(850)	2171	(488)	3096	(696)
	21	(70)		P_1	4141	(931)	2375	(534)	3394	(763)
	21	(70)		P_2	2865	(644)	2865	(644)	–	–
	-53	(-65)		P_1	4186	(941)	2402	(540)	3430	(771)
	-53	(-65)		P_2	2629	(591)	2629	(591)	–	–
1	-53	(-65)		P_2	2402	(540)	2402	(540)	–	–
2	21	(70)		P_1	2740	(616)	1570	(353)	2246	(505)
	21	(70)		P_1	3696	(831)	2122	(477)	3029	(681)
	21	(70)		P_2	2055	(462)	2055	(462)	–	–
	21	(70)		P_2	2037	(458)	2037	(458)	–	–
	21	(70)		P_2	2220	(499)	2220	(499)	–	–
2	-53	(-65)	Dry	P_2	2153	(484)	2153	(484)	–	–

During production of the five shipsets of graphite-epoxy stabilizers, some lower surface panel holes were misdrilled for 4.8-mm (0.19-in) shear-head fasteners. To rectify the problem, use of 4.8-mm (0.19-in) tension-head bolts was suggested. To verify using these fasteners, five specimens were fabricated with 4.8-mm (0.19-in) tension-head bolts, which were the same configuration as shown in Figure 117. Specimen testing verified that production ribs could meet required strength by using the larger tension-head fastener (table 19). Specimens failed by delamination in the rib clip radius.

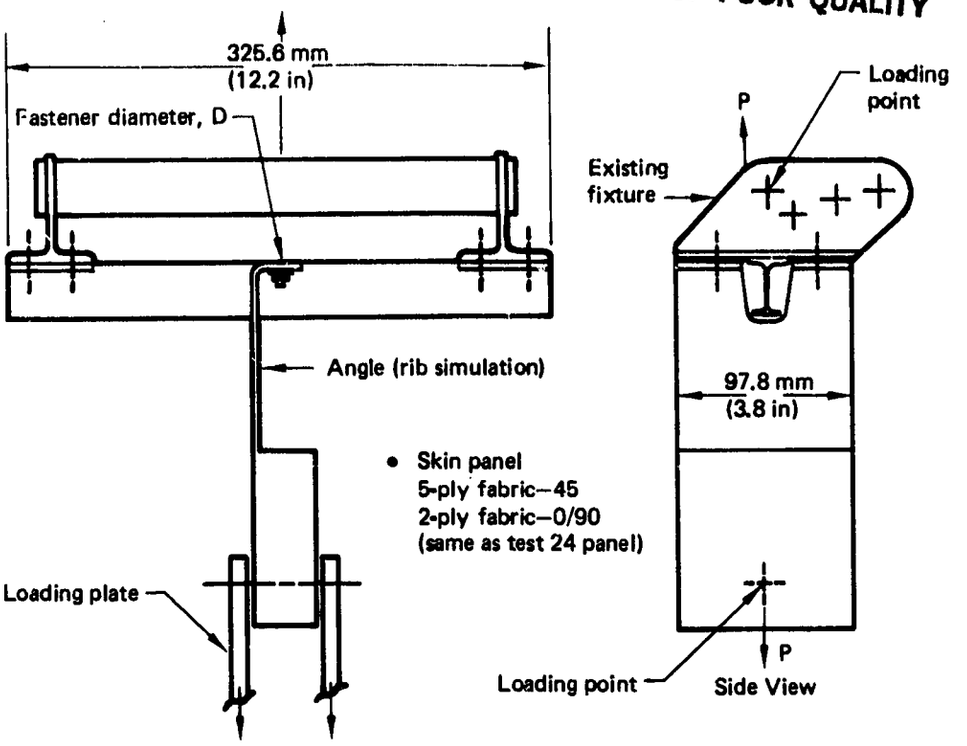

Figure 117. Skin/Rib Joint Specimen (Configurations 3 and 4)

4.2.3.9 Basic Laminate and Fracture Coupons

The decision to incorporate tape on the stabilizer panels to improve surface quality generated a test requirement to provide additional data for the basic laminates used in the horizontal stabilizer. Static tension tests were performed on three laminate configurations to determine design values for the skin material. Basic laminate test results are shown in Appendix C.

A model proposed by Waddoups et al. in Reference 14 was modified for use in analyzing the data obtained in the fracture program. Waddoups model is stated as

$$\sigma_c = \frac{K_{IC}}{\sqrt{\pi (L + a)}}$$

where σ_c is the gross area stress at failure

K_{IC} is the material's fracture toughness

L is the half crack length

"a" is a zone of intense energy at the tip of the crack.

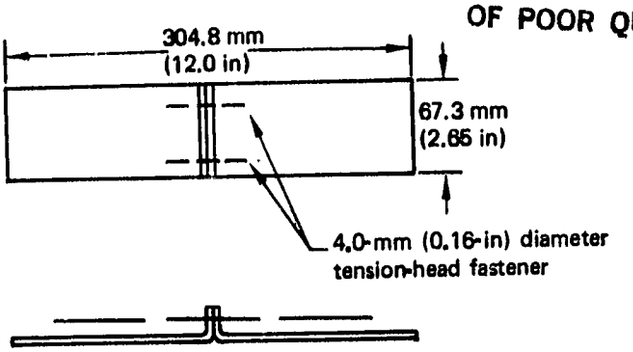

- Configuration 5: 12-ply fabric–6 at (0, 90), 6 at (±45)
- Configuration 6: 8-ply fabric–4 at (0, 90), 4 at (±45);4-ply Grade 190 tape–1 at (90), 1 at (+45), 1 at (-45), 1 at (0)

Figure 118. Rib Clip Test Specimen (Configurations 5 and 6)

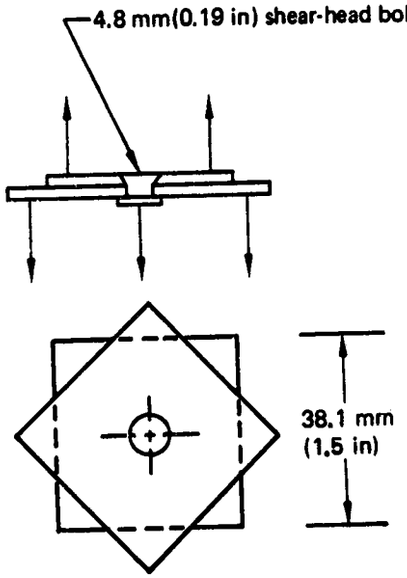

- Each plate fabricated with 10-plies of fabric–7 at (0, 90), 3 at(±45); and 2-plies of Grade 190 tape at (±45).

Figure 119. Lap Tension Specimen

Table 19. Skin/Rib Joint Test Results (Configurations 3 and 4)

- Configuration 3: D = 4.8-mm (0.19-in) shear-head fastener
- Configuration 4: D = 4.8-mm (0.19-in) tension-head fastener

Configuration	Temperature, °C	(°F)	Environmental condition	Failure load, N	(lbf)
3	21	(70)	Dry	2302	(517.5)
↓	↓	↓	↓	2115	(475.5)
3				2453	(551.5)
4				2380	(535.0)
↓				2295	(516.0)
4				2500	(562.0)
				2927	(658.0)
				2834	(637.0)
				3087	(694.0)
4	21	(70)	Dry	3078	(692.0)

ORIGINAL PAGE IS OF POOR QUALITY

Table 20. Rib Clip Results (Configurations 5 and 6)

Configuration	Temperature, °C	(°F)	Environmental condition	Failure load, N	(lbf)
5	21	(70)	Dry	3714	(835)
↓	↓	↓	↓	3541	(796)
				3599	(809)
				3585	(806)
	21	(70)		3710	(834)
	-53	-65		3581	(805)
	↓	↓	↓	3608	(811)
			Dry	3358	(755)
			Wet	3608	(811)
			Wet	3452	(776)
	-53	-65	Wet	3616	(813)
	80	180	Dry	3523	(792)
	↓	↓	Dry	3594	(808)
			Dry	3403	(765)
			Wet	3123	(702)
↓			Wet	3385	(761)
5	82	180	Wet	3069	(690)
6	21	(70)	Dry	3274	(736)
↓	21	(70)	↓	3234	(727)
	21	(70)		3465	(779)
	-53	-65		3265	(734)
	-53	-65		3309	(774)
	-53	-56	Dry	3674	(826)
	82	180	Wet	3541	(796)
	82	180	Wet	3145	(707)
6	82	180	Wet	2727	(613)

Table 21. Lap Tension Test Results

Configuration	Temperature, °C	(°F)	Environmental condition	Failure load, N	(lbf)
Lap tension	21	(70)	Dry	2100	(472)
	21	(70)		2073	(466)
	-53	(-65)		2002	(450)
	-53	(-65)		2157	(485)
	-53	(-65)		1971	(443)
	82	(180)		1962	(441)
	82	(180)		1957	(440)
	82	(180)		1868	(420)
	-53	(-65)	Dry	1984	(446)
	-53	(-65)	Wet	1882	(423)
	-53	(-65)		1962	(441)
	82	(180)		2233	(502)
	82	(180)		2024	(455)
Lap tension	82	(180)	Wet	2055	(462)
				2015	(453)
				2002	(450)
				1855	(417)

The factors K_{IC} and "a" are found by testing specimens with and without cracks and equating the following expressions:

$$K_{IC} = \sigma_o \sqrt{\pi a} \qquad \text{(no crack)}$$

$$K_{IC} = \sigma_c \sqrt{\pi (L + a)} \qquad \text{(crack)}$$

Then

$$a = \frac{L}{\left(\sigma_o/\sigma_c\right)^2 - 1}$$

For the purposes of this program the gross area stresses were replaced by their equivalent strains so that

$$a_o = \frac{a}{\left(\epsilon_o/\epsilon_c\right)^2 - 1}$$

$$K_\epsilon = \epsilon_o \sqrt{\pi a_o}$$

Table 22. Tension Fracture Coupon Test Data

Specimen layup	Crack size and location [1]	Temperature, °C (°F)	Environmental	Failure load, kN (lbf)	Gross area, mm² (in²)	Modulus, E, MPa x 10⁴ (lbf/in² x 10⁶)	Strain, μm/m (μin/in)	Comparative strain [2]
A	6.35C (0.25C)	21 (70)	Dry	109.0 (24 500)	580.6 (0.90)	3.6 (5.2)	5240	9170
	↓	21 (70)	↓	121.4 (27 300)	↓ ↓	↓ ↓	5830	9170
	6.35C (0.25C)	-59 (-75)		102.0 (22 940)			4900	8480
		-59 (-75)		93.2 (20 960)			4480	8480
	25.4C (1.00C)	-59 (-75)					—	—
	25.4C (1.00C)	-59 (-75)		58.3 (13 100)			2800	8480
	6.35E (0.25E)	21 (70)		106.3 (23 900)			5110	9170
	↓	21 (70)		113.9 (25 600)			5470	9170
	6.35E (0.25E)	-59 (-75)		90.6 (20 360)			4350	8480
		-59 (-75)		96.4 (21 680)			4630	8480
	25.4E (1.00E)	-59 (-75)	↓	45.0 (10 110)	↓ ↓	↓ ↓	2160	8480
	25.4E (1.00E)	-59 (-75)	Dry	51.2 (11 510)	580.6 (0.90)	3.6 (5.2)	2460	8480
B	6.35C (0.25C)	21 (70)	Dry	91.6 (20 600)	434.2 (0.673)	5.7 (8.2)	3730	9530
	↓	21 (70)	↓	92.5 (20 800)	↓ ↓	↓ ↓	3770	9530
	6.35C (0.25C)	-59 (-75)		83.3 (18 720)			3390	8590
		-59 (-75)		84.8 (19 060)			3450	8590
	25.4C (1.00C)	-59 (-75)		45.4 (10 200)			1850	8590
	25.4C (1.00C)	-59 (-75)		43.5 (9 770)			1770	8590
	6.35E (0.25E)	21 (70)		96.4 (21 680)			3930	9530
	↓	21 (70)		91.9 (20 650)			3740	9530
	6.35E (0.25E)	-59 (-75)		83.7 (18 820)			3410	8590
		-59 (-75)		78.7 (17 690)			3210	↓
	25.4E (1.00E)	-59 (-75)	↓	42.5 (9 560)	↓ ↓	↓ ↓	1730	
	25.4E (1.00E)	-59 (-75)	Dry	42.6 (9 580)	434.2 (0.673)	5.7 (8.2)	1740	8590
C	6.35C (0.25C)	21 (70)	Dry	75.2 (16 900)	434.2 (0.673)	3.1 (4.5)	5580	9410
	↓	21 (70)	↓	71.1 (15 990)	↓ ↓	↓ ↓	5280	9410
	6.35C (0.25C)	-59 (-75)		59.7 (13 420)			4430	8460
		-59 (-75)		57.6 (12 960)			4280	8460
	25.4C (1.00C)	-59 (-75)		34.3 (7 700)			2540	8460
	25.4C (1.00C)	-59 (-75)		33.5 (7 520)			2480	8460
	6.35E (0.25E)	21 (70)		63.1 (14 190)			4690	9410
	↓	21 (70)		57.9 (13 020)			4300	9410
	6.35E (0.25E)	-59 (-75)		58.9 (13 240)			4370	8460
		-59 (-75)		49.8 (11 200)			3700	↓
	25.4E (1.00E)	-59 (-75)	↓	31.1 (7 000)	↓ ↓	↓ ↓	2310	
	25.4E (1.00E)	-59 (-75)	Dry	28.5 (6 410)	434.2 (0.673)	3.1 (4.5)	2120	8460

[1] C Center notch.
E Edge notch.

[2] Failure strain of coupon without notches, see Appendix C, Fracture Coupon Control Specimens.

where "a" has been substituted for L and a_o for "a." Thus,

$$\epsilon_{cr} = \frac{K_\epsilon}{\sqrt{\pi (a + a_o)}}$$

Fracture panel test results are shown in Tables 22 and 23, tension and compression, respectively. The ply layups are shown in Table 24. Fracture coupon control specimens (detailed in app. C) were used in conjunction with the data from the 6.4-mm (0.25-in) half-crack-length test panels to calculate the K_ϵ and a_o values for the fracture equation. The circular symbols on the curves (figs. 120 through 125) at a = 6.4 mm (0.25 in) indicate the fracture panel test results. The fracture panels with a = 25.4 mm (1.0 in) are shown to verify the curve. Verification for the tension specimens was good. The test results show that the edge notch is more severe than the center notch. The -59°C (-75°F) critical fracture strain is lower than the 21°C (70°F) value that is consistent with the unnotched data. The compression curves are shown in Figures 123, 124, and 125. Because of the increased scatter for the compression specimens, accurate correlation cannot be made at this time.

Table 23. Compression Fracture Coupon Test Data

Specimen layup	Crack size and location [1]	Temperature, °C (°F)	Environmental condition	Failure load, kN (lb)	Gross area, mm² (in²)	Modulus, E_y, MPa x 10^4 (lbf/in² x 10^6)	Strain, μm/m (μin/in)	Comparative strain [2]
A	6.35C (0.25C)	21 (70)	Dry	104.5 (23 500)	580.6 (0.90)	3.6 (5.2)	5020	8300
	↓	21 (70)	Dry	105.6 (23 740)	↓ ↓	↓ ↓	5070	9300
		82 (180)	Wet	98.4 (22 120)			4730	8380
	6.35C (0.25C)	82 (180)	Wet	102.5 (23 044)			4920	↓
	25.4C (1.00C)	82 (180)	Wet	60.1 (13 500)			2880	
	25.4C (1.00C)	82 (180)	Wet	65.7 (14 770)			3160	8380
	6.35E (0.25E)	21 (70)	Dry	94.3 (21 210)			4530	9300
	↓	21 (70)	Dry	100.8 (22 660)			4840	9300
		82 (180)	Wet	101.7 (22 870)			4890	8380
	6.35E (0.25E)	82 (180)	Wet	96.2 (21 632)			4620	↓
	25.4E (1.00E)	82 (180)	Wet	66.5 (14 960)	↓ ↓	↓ ↓	3200	
	25.4E (1.00E)	82 (180)	Wet	55.4 (12 463)	580.6 (0.90)	3.6 (5.2)	2660	8380
B	6.35C (0.25C)	21 (70)	Dry	83.6 (18 800)	434.2 (0.673)	5.7 (8.2)	3410	6750
	↓	21 (70)	Dry	76.8 (17 260)	↓ ↓	↓ ↓	3130	6750
		82 (180)	Wet	81.4 (18 293)			3310	6700
	6.35C (0.25C)	82 (180)	Wet	82.6 (18 573)			3370	↓
	25.4C (1.00C)	82 (180)	Wet	– –	↓ ↓	↓ ↓	–	
	25.4C (1.00C)	82 (180)	Wet	56.3 (12 660)	434.2 (0.673)	5.7 (8.2)	2290	6700
	6.35E (0.25E)	21 (70)	Dry	79.3 (17 820)	43.4 (0.673)	5.7 (8.2)	3230	6750
	↓	21 (70)	Dry	80.0 (17 990)	↓ ↓	↓ ↓	3260	6750
		82 (180)	Wet	75.2 (18 906)			3060	6700
	6.35E (0.25E)	82 (180)	Wet	65.5 (14 730)			2670	↓
	25.4E (1.00E)	82 (180)	Wet	46.5 (10 460)			1900	
	25.4E (1.00E)	82 (180)	Wet	51.8 (11 650)		↓ ↓	2110	6700
C	6.35C (0.25C)	21 (70)	Dry	68.3 (15 350)		3.1 (4.5)	5070	9070
	↓	21 (70)	Dry	59.1 (13 275)		↓ ↓	4380	9070
		82 (180)	Wet	55.8 (12 547)			4140	7430
	6.35C (0.25C)	82 (180)	Wet	57.4 (12 897)			4260	↓
	25.4C (1.00C)	82 (180)	Wet	40.0 (9 000)			2970	
	25.4C (1.00C)	82 (180)	Wet	42.0 (9 440)			3120	7430
	6.35E (0.25E)	21 (70)	Dry	54.0 (12 140)			4010	9070
	↓	21 (70)	Dry	53.7 (12 070)			3990	9070
		82 (180)	Wet	53.1 (11 940)			3940	7430
	6.35E (0.25E)	82 (180)	Wet	51.9 (11 660)			3850	↓
	25.4E (1.00E)	82 (180)	Wet	45.4 (10 210)	↓ ↓	↓ ↓	3370	
	25.4E (1.00E)	82 (180)	Wet	38.7 (8 700)	43.4 (0.673)	3.1 (4.5)	2870	7430

[1] C Center notch.
E Edge notch.

[2] Failure strain of coupon without notches, see Appendix C, Fracture Coupon Control Specimens.

4.2.4 Production Verification Tests

Production verification (Test 25) was conducted to determine baseline material properties of critical sections of the stabilizer that had been fabricated on production tools (fig. 126). Specimens were cut from production tool tryout sections of skin panels, ribs, and spars in the areas defined in Figures 127 through 130. The test results are presented in Tables 25 through 27, and the detail specimen dimensions are shown in Figure 131.

4.2.5 Rear-Spar Manufacturing Feasibility

A rear-spar manufacturing feasibility study was initiated early in the program to verify tooling and manufacturing concepts. The drawings for the rear spar were modified to include defects varying in size from 0.64 cm^2 (0.25 in^2) to 5.72 by 15.24 cm (2.25 by 6 in). These defects were placed at various depths in the details (fig. 132). The defects were created by introducing two layers of Teflon 0.005-cm (0.002-in) thick between the fabric plies and in the bondline of the precured details.

Table 24. Fracture Panel Laminate Definition

Layup designation	Ply layup	Thickness mm (in)
A	Fabric: 3(0, 90) 9(±45)	2.29 (0.09)
B	Fabric: 2(0, 90) 5(±45) Tape: 2(90) Grade 190	1.71 (0.0673)
C	Fabric: 2(0, 90) 5(±45) Tape: 2(90) Grade 190	1.71 (0.0673)

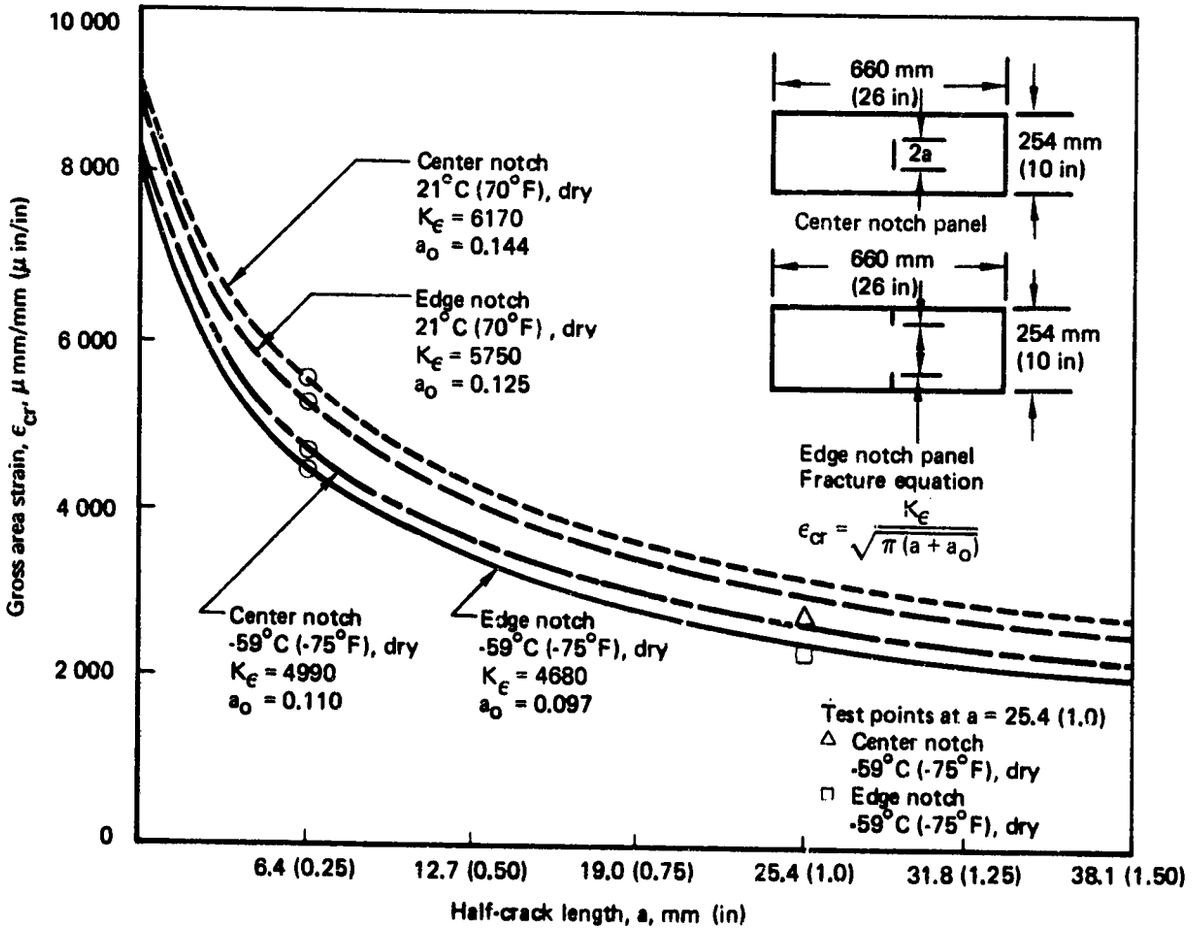

Figure 120. Tension Fracture Coupons (Layup A)

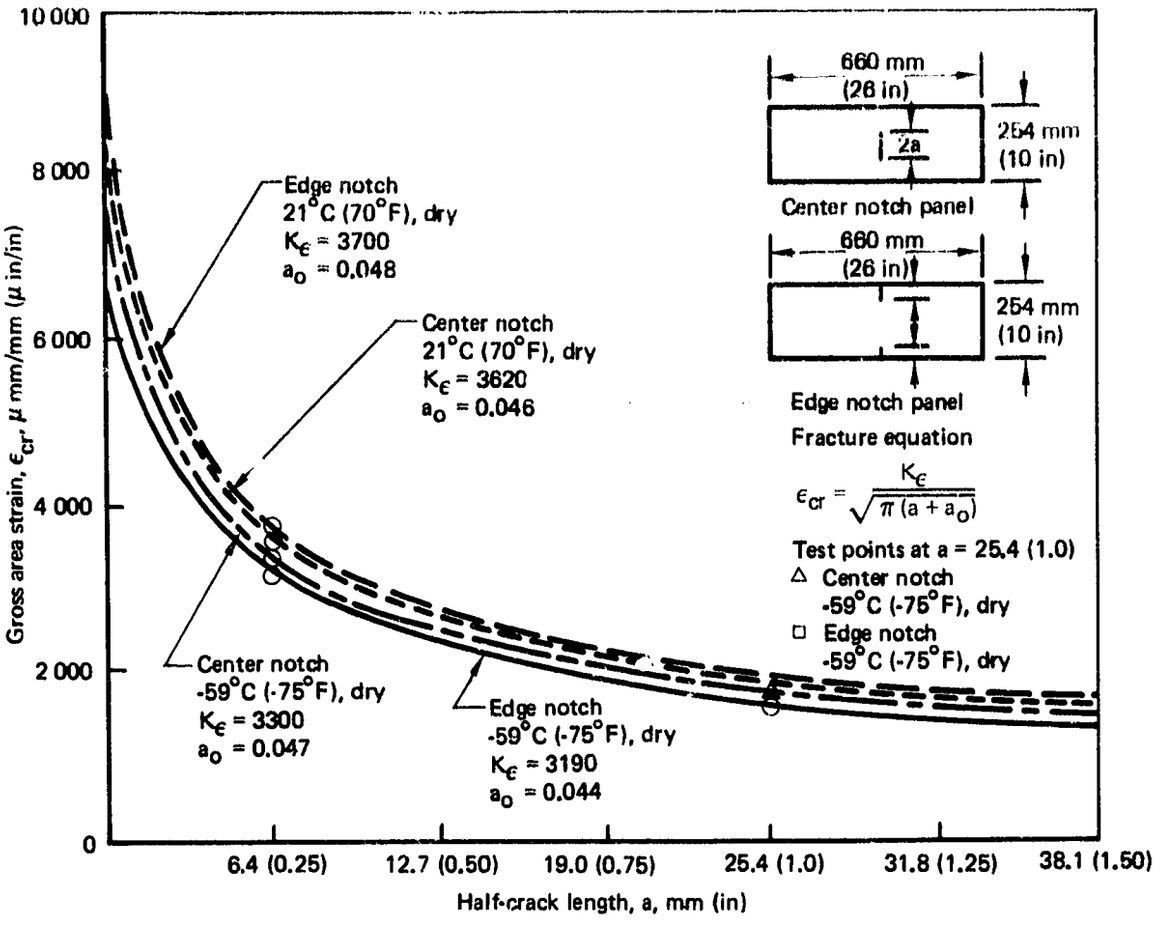

Figure 121. Tension Fracture Panels (Layup B)

After the rear spar was manufactured, specimens were tested to verify the material properties. Figure 133 shows the locations from where the specimens were taken, and Table 28 presents the test results.

4.2.6 Repair Panels

This test evaluated the strength of typical skin panel repairs. The panels were damaged, the damaged skin and stringers were removed, and the area repaired using the procedure described in Appendix A.

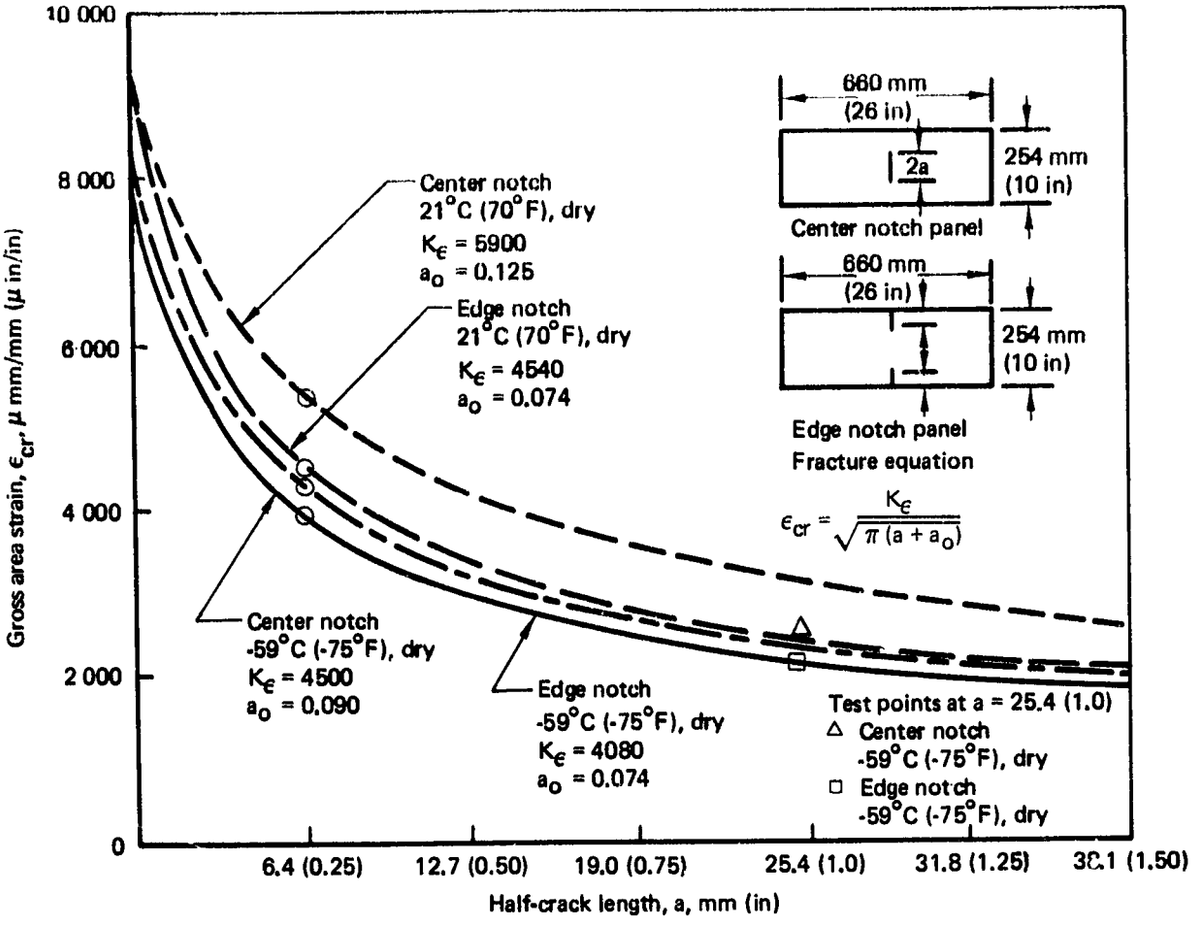

Figure 122. Tension Fracture Panels (Layup C)

The skin panel configurations were identical to panels from the skin panel test (Test 10). Compression and fatigue panels from Test 10 were used as baseline undamaged data. The compression repair panels were statically tested in the same manner as the baseline specimens. The repair fatigue panels were cyclically loaded the same as Test 10 condition A, and then statically failed in tension. (See sec. 4.2.3.1 for compression panels and 4.2.3.4 for fatigue panels.) The results are shown in Tables 29 and 30 with corresponding baseline results for comparison.

4.2.7 Lightning Protection Panel Tests

Lightning distribution studies, scale model, and flight experience show that the horizontal stabilizer and elevator are likely to be struck by lightning. The predominant lightning attachment point on the stabilizer is at the outboard tip. Therefore, an aluminum flame-spray coating covers the outboard 48 cm (18 in) of the graphite-epoxy stabilizer (figs. 20 and 21). A discussion of the lightning strike threat and requirements is presented in Section 4.1.1.4.

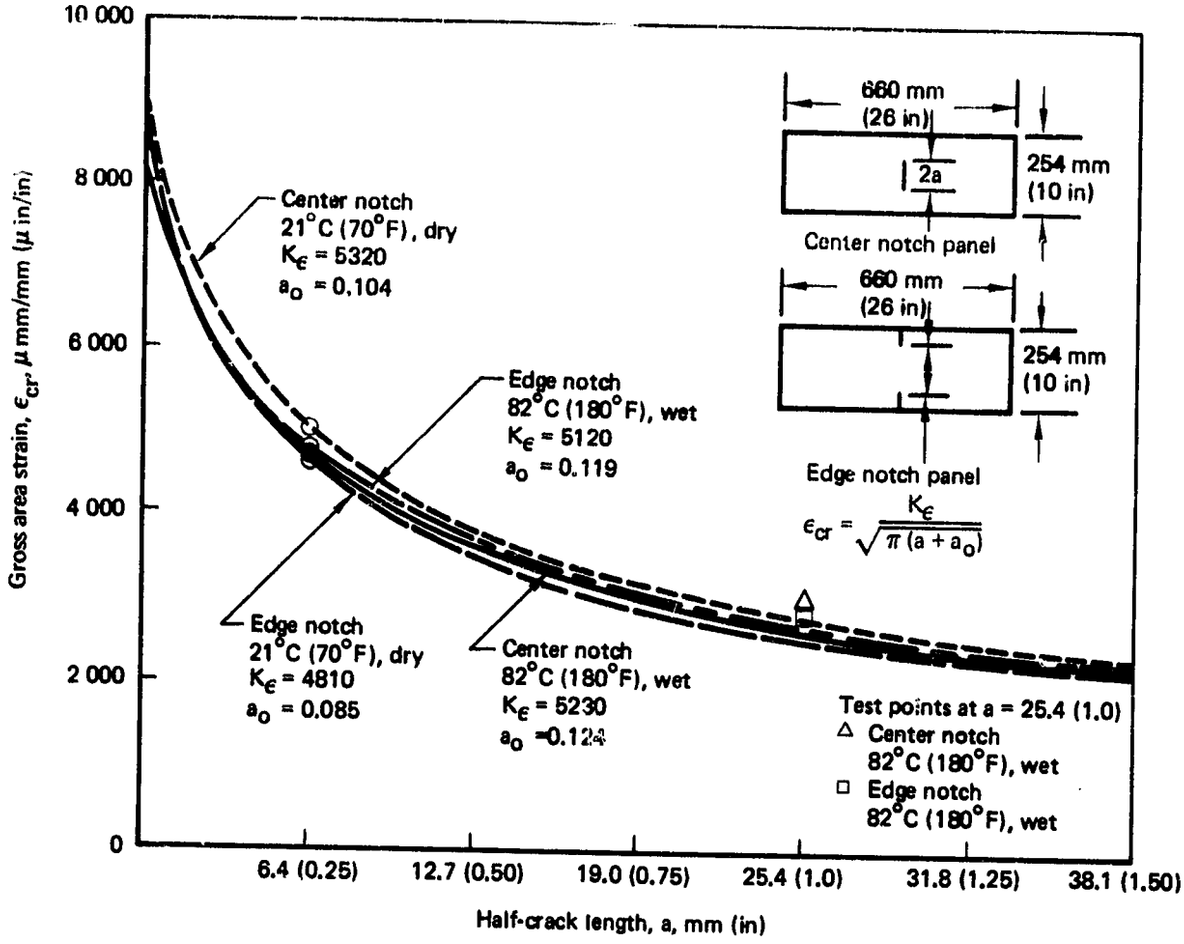

Figure 123. Compression Fracture Panels (Layup A)

Lightning protection system tests were performed on subcomponents of the stabilizer. The tests were required to:

- Validate the existing bonding requirements
- Determine lightning damage to the graphite-epoxy structure
- Determine lightning damage at the interface between the aluminum and graphite-epoxy structure
- Determine P-static current conduction through a coated fiberglass panel to the graphite-epoxy structure
- Validate the lightning protection system for the stabilizer

The lightning protection system is described in Section 3.2.9. Testing was performed in Boeing's lightning laboratory. Lightning strike waveform components as set forth in MIL-STD-1757 are described in Figure 134.

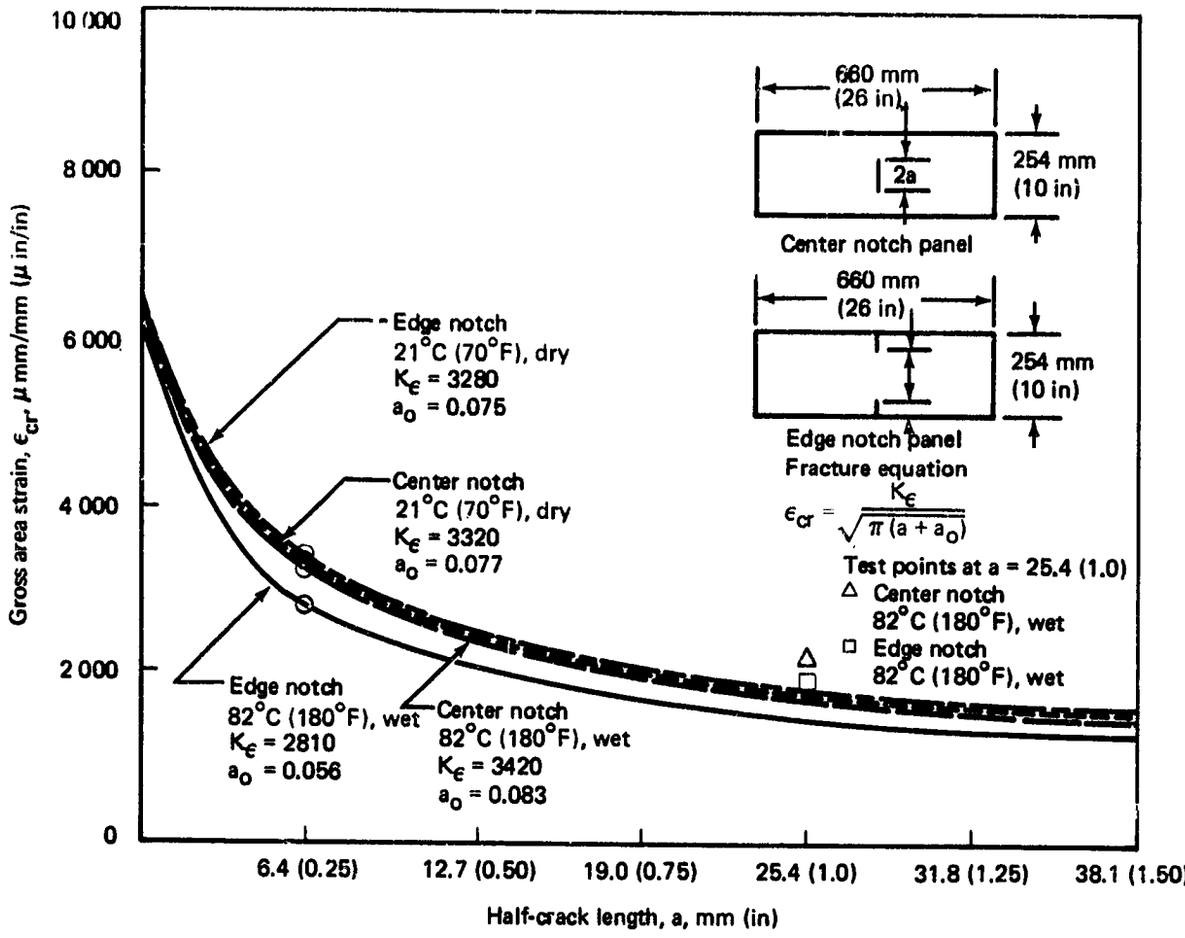

Figure 124. Compression Fracture Panels (Layup B)

Lightning test generators were electrically connected to the test article by remote switches that allowed sequencing of the discharge (fig. 135). The titanium strap length controlled the resistance of the test circuit. Circuit parameters were calculated and displayed by the computerized oscilloscope.

4.2.7.1 Tip Section

The tip section test specimen was a panel of stringer stiffened skin and included the lightning protection system proposed for the outboard stabilizer surface. An aluminum leading edge, rear-spar cap, closure rib, and an aluminum bus bar were included to reproduce the current paths of the production configuration.

The first series of tests (figs. 136 and 137) resulted in penetration of the skin and delamination of the stringers. Review of the test specimen and data showed that the peak current was 29% high, the energy of the strike (action integral) exceeded requirements by approximately 115%, and the support system for the test panel was not consistent with the flight hardware. Based on this review, additional panels were manufactured and tested.

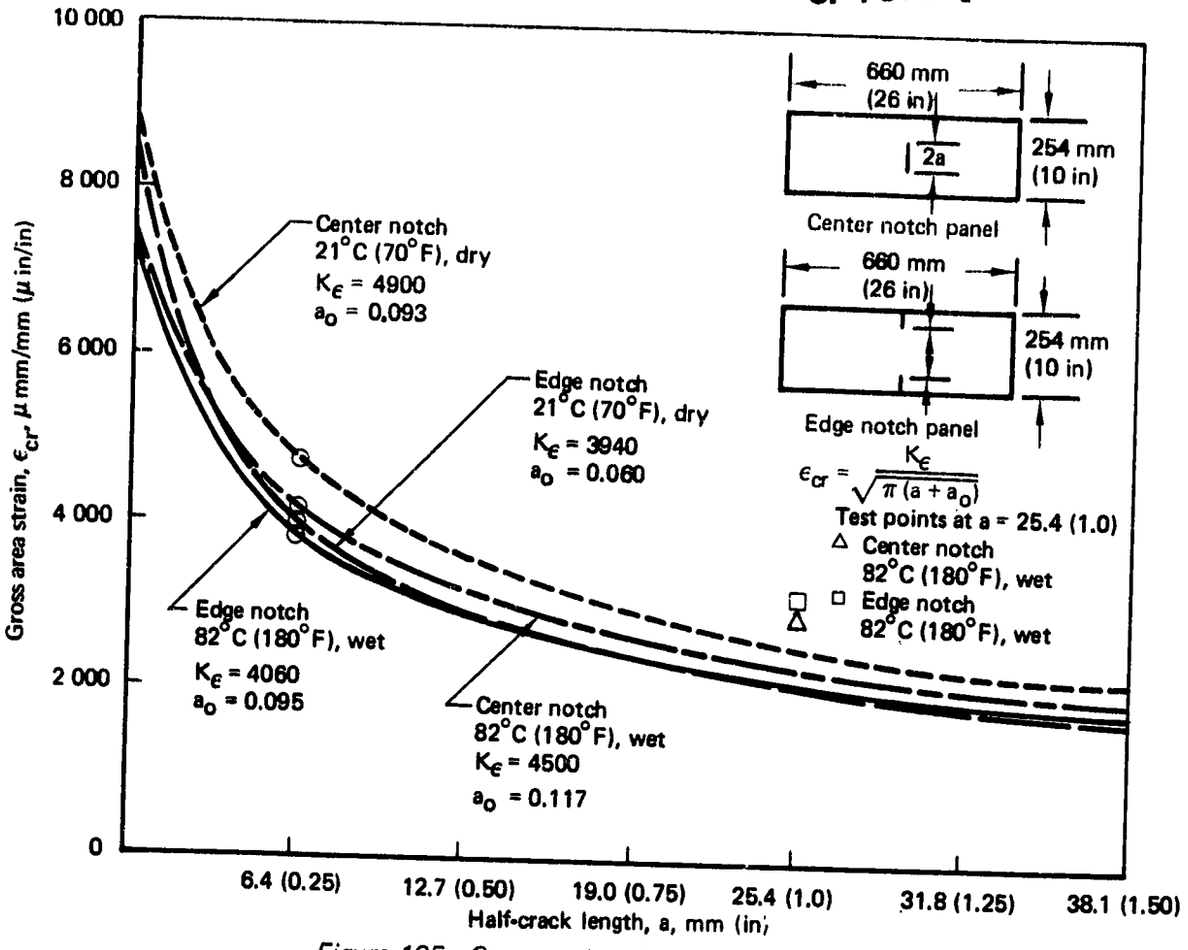

Figure 125. Compression Fracture Panels (Layup C)

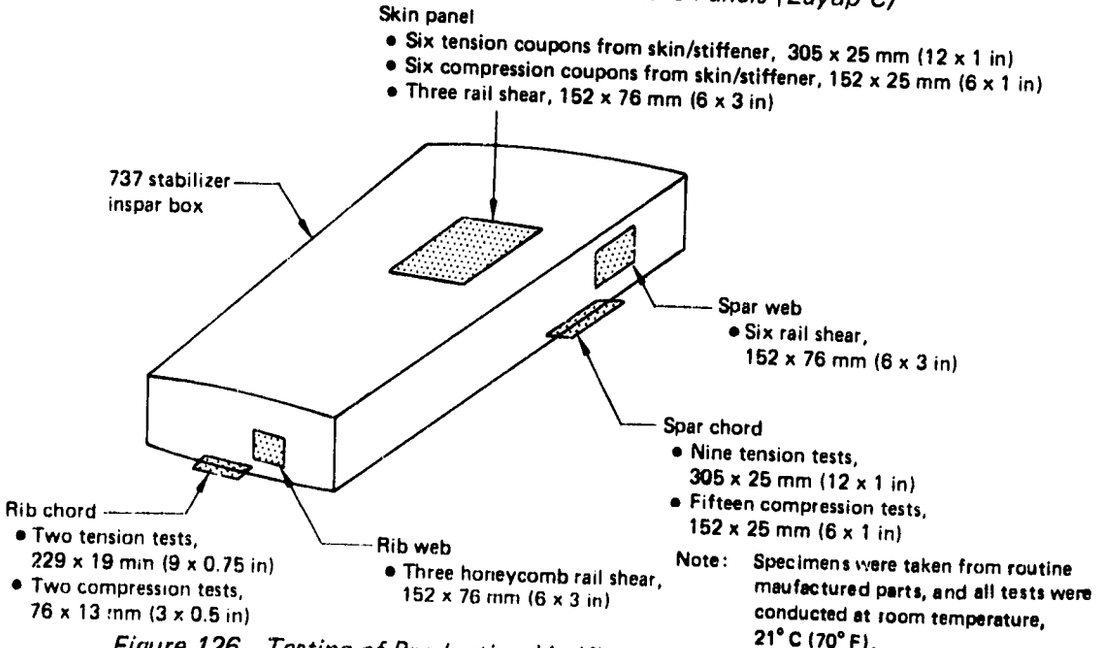

Figure 126. Testing of Production Verification Hardware (Test 25)

ORIGINAL PAGE
BLACK AND WHITE PHOTOGRAPH

Figure 127. Stabilizer Stub Box Skin

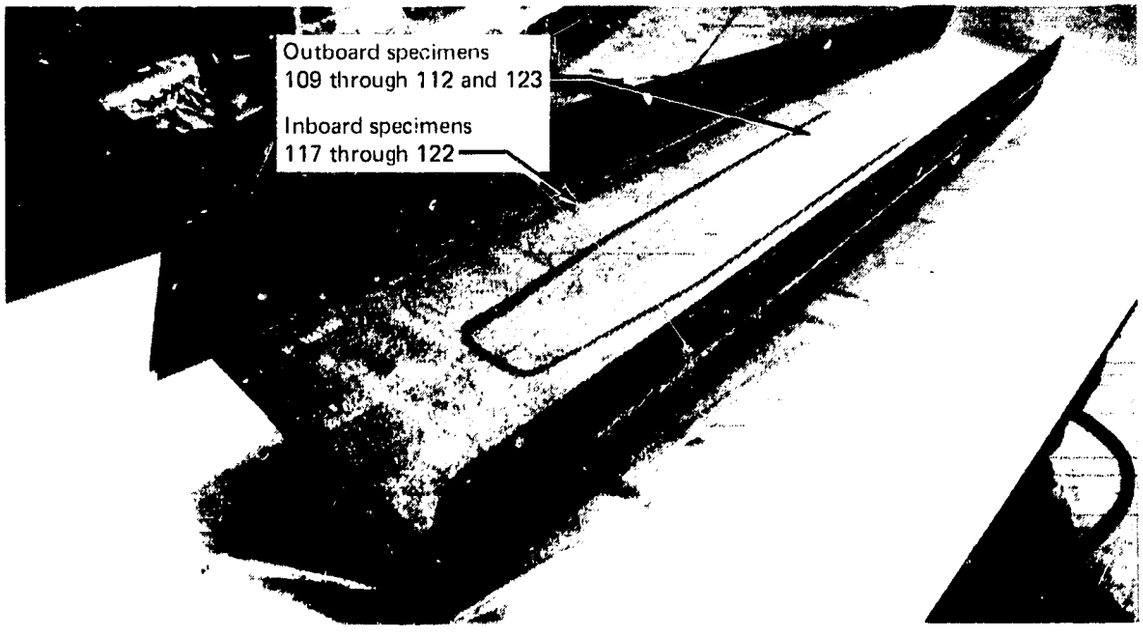

Figure 128. Stub Box Rear Spar

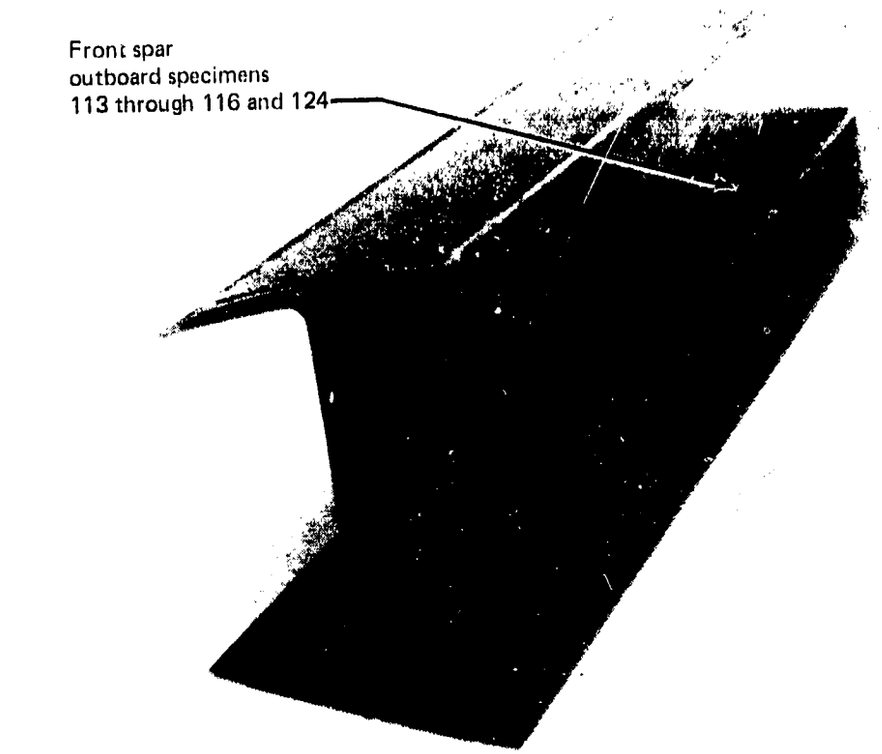

Figure 129. Front-Spar Section

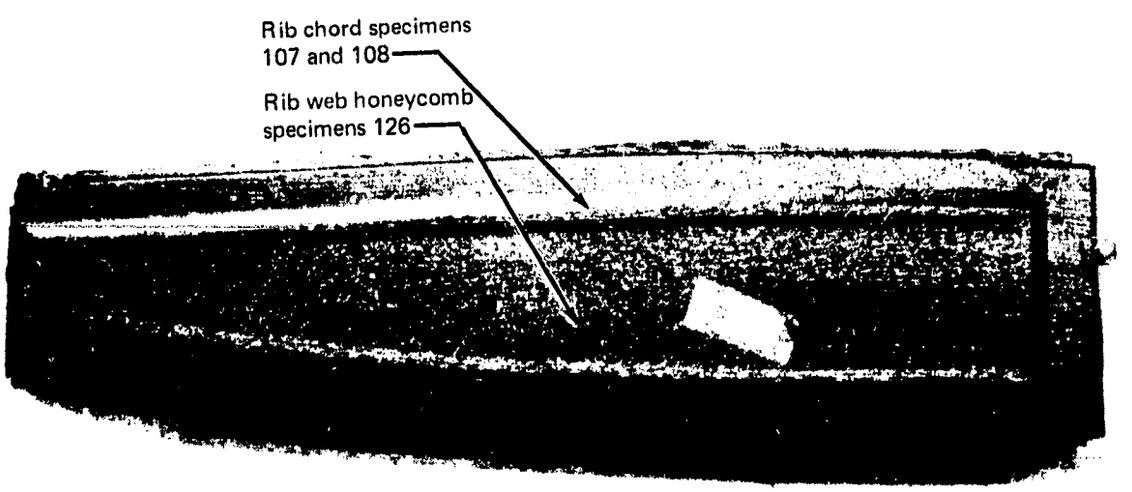

Figure 130. Typical Honeycomb Rib

Table 25. Tension and Compression Test Results (Test 25)

Specimen identification number	Test type	Specimen geometry								Area		Failure load		Failure stress		Nominal modulus		Failure strain	Specimen information	
		L		W1		W2		t												
		mm	(in)	mm	(in)	mm	(in)	mm	(in)	mm^2	(in^2)	kN	(lb)	MPa	(ksi)	MPa x 10^3	(ksi x 10^3)	mm/mm or in/in	Description	Ply layup
101-1	Tension	305	(12)	25.4	(1.00)	38.1	(1.50)	1.35	(0.053)	34.2	(0.053)	11.6	(2605)	338.9	(49.15)	36.75	5.33	0.0092	7 ply skin	2 ~ 0°/90° (F) 5 ~ ±45° (F)
101-2		305	(12)	25.4	(1.00)	38.1	(1.50)	1.35	(0.053)	34.2	(0.053)	12.0	(2700)	351	(50.9)	36.75	5.33	0.0096	7 ply skin	2 ~ 0°/90° (F) 5 ~ ±45° (F)
103-1		229	(9)	12.7	(0.50)	21.6	(0.85)	1.52	(0.6)	19.4	(0.030)	8.8	(1985)	457	(66.2)	46.0	6.67	0.0100	8 ply stringer web	4 ~ 0°/90° (F) 4 ~ ±45° (F)
103-2		229	(9)	12.7	(0.50)	21.6	(0.85)	1.52	(0.06)	19.4	(0.030)	8.2	(1835)	422	(61.2)	46.0	6.67	0.00927	8 ply stringer web	4 ~ 0°/90° (F) 4 ~ ±45° (F)
105-1		229	(9)	12.7	(0.50)	21.6	(0.85)	2.11	(0.083)	27.1	(0.042)	21.2	(4760)	781.2	(113.3)	99.98	14.5	0.0078	11 ply stringer inner chord	6 ~ 0° (tape), 3 ~ ±45° (F), 2 ~ 0°/90° (F)
105-2		229	(9)	12.7	(0.50)	21.6	(0.85)	2.11	(0.083)	27.1	(0.042)	14.3	(3205)	526.1	(76.3)	99.98	14.5	0.0053	11 ply stringer inner chord	6 ~ 0° (tape), 3 ~ ±45° (F), 2 ~ 0°/90° (F)
107-1		229	(9)	12.7	(0.50)	21.6	(0.85)	2.29	(0.090)	29.0	(0.045)	13.3	(2995)	459.2	(66.6)	46.0	6.67	0.00998	12 ply rib chord	6 ~ 0°/90° (F) 6 ~ ±45° (F)
107-2		229	(9)	12.7	(0.50)	21.6	(0.85)	2.29	(0.090)	29.0	(0.045)	12.5	(2815)	431.6	(62.6)	46.0	6.67	0.0094	12 ply rib chord	6 ~ 0°/90° (F) 6 ~ ±45° (F)
109-1		305	(12)	25.4	(1.00)	38.1	(1.50)	4.57	(0.180)	116.1	(0.18)	50.7	(11400)	436.5	(63.3)	46.9	6.80	0.0093	24 ply rear spar outboard flange	13 ~ 0°/90° (F) 11 ~ ±45° (F)
109-2		305	(12)	25.4	(1.00)	38.1	(1.50)	4.57	(0.180)	116.1	(0.18)	55.4	(12450)	477.2	(69.2)	46.9	6.80	0.0102	24 ply rear spar outboard flange	13 ~ 0°/90° (F) 11 ~ ±45° (F)
111-1		305	(12)	25.4	(1.00)	38.1	(1.50)	3.05	(0.12)	77.4	(0.12)	39.6	(8910)	512.3	(74.3)	40.0	5.80	0.0128	16 ply rear spar outboard web	6 ~ 0°/90° (F) 10 ~ ±45° (F)
113-1		305	(12)	25.4	(1.00)	38.1	(1.50)	2.80	(0.105)	67.7	(0.105)	33.1	(7440)	488.6	(70.9)	48.3	7.00	0.0101	14 ply front spar outboard flange	8 ~ 0°/90° (F) 6 ~ ±45° (F)
113-2		305	(12)	25.4	(1.00)	38.1	(1.50)	2.80	(0.105)	67.7	(0.105)	31.8	(7140)	468.9	(68.0)	48.3	7.00	0.0097	14 ply front spar outboard flange	8 ~ 0°/90° (F) 6 ~ ±45° (F)
115-1		305	(12)	25.4	(1.00)	38.1	(1.50)	1.52	(0.06)	38.7	(0.06)	17.5	(3936)	452.3	(65.6)	46.0	6.67	0.0098	8 ply outboard web	4 ~ 0°/90° (F) 4 ~ ±45° (F)
115-2		305	(12)	25.4	(1.00)	38.1	(1.50)	1.52	(0.06)	38.7	(0.06)	18.9	(4240)	487.5	(70.7)	46.0	6.67	0.0106	8 ply outboard web	4 ~ 0°/90° (F) 4 ~ ±45° (F)
117-1		305	(12)	25.4	(1.00)	38.1	(1.50)	4.57	(0.18)	116.1	(0.18)	41.0	(9210)	353.0	(51.2)	46.9	6.80	0.0075	24 ply rear spar inboard flange	13 ~ 0°/90° (F) 11 ~ ±45° (F)
117-2	Tension	305	(12)	25.4	(1.00)	38.1	(1.50)	4.57	(0.18)	116.1	(0.18)	56.7	(12750)	488.2	(70.8)	46.9	6.80	0.0104	24 ply rear spar inboard flange	13 ~ 0°/90° (F) 11 ~ ±45° (F)

- Dry environment
- Specimen geometry—Figure 131, Detail Specimen A
- Test temperature—21°C (70°F).

Table 25. Tension and Compression Test Results (Test 25)(Concluded)

Specimen identification number	Test type	Specimen geometry						Area		Failure load		Failure stress		Nominal modulus		Failure strain	Specimen information	
		L		W_{nom}		t_{nom}												
		mm	(in)	mm	(in)	mm	(in)	mm^2	(in^2)	kN	(lb)	MPa	(ksi)	MPa x 10^3	(ksi x 10^3)	mm/mm in/in	Description	Ply layup
102-1	Comp	143.8	(5.66)	25.4	(1.00)	1.35	(0.053)	34.2	(0.053)	12.75	(2866)	373.0	(54.1)	36.8	(5.33)	0.0101	7 ply skin	2 ~ 0°/90° (F) 5 ~ ±45° (F)
102-2		143.8	(5.66)	25.4	(1.00)	1.35	(0.053)	34.2	(0.053)	10.52	(2365)	308.0	(44.6)	36.8	(5.33)	0.0084	7 ply skin	2 ~ 0°/90° (F) 5 ~ ± 45° (F)
104-1		76.2	(3.00)	12.70	(0.50)	1.52	(0.06)	19.4	(0.03)	9.964	(2240)	515.0	(74.7)	46.0	(6.67)	0.0111	8 ply stringer web	4 ~ 0°/90° (F) 4 ~ ±45° (F)
104-2		76.2	(3.00)	12.70	(0.50)	1.52	(0.06)	19.4	(0.03)	9.118	(2050)	471.0	(68.3)	46.0	(6.67)	0.0102	8 ply stringer web	4 ~ 0°/90° (F) 4 ~ ±45° (F)
106-1		76.2	(3.00)	12.70	(0.50)	2.11	(0.083)	27.1	(0.042)	27.27	(6130)	1007.0	(146.0)	100.0	(14.5)	0.0101	11 ply stringer inner chord	6 ~ 0° (tape), 3 ~ ±45° (F), 2 ~ 0°/90° (F)
106-2		76.2	(3.00)	12.70	(0.50)	2.11	(0.083)	27.1	(0.042)	25.84	(5810)	953.6	(138.3)	100.0	(14.5)	0.0095	11 ply stringer inner chord	6 ~ 0° (tape), 3 ~ ±45° (F), 2 ~ 0°/90° (F)
108-1		76.2	(3.00)	12.70	(0.50)	2.29	(0.090)	29.0	(0.045)	12.41	(2790)	427.5	(62.0)	46.0	(6.67)	0.0093	12 ply rib chord	6 ~ 0°/90° (F) 6 ~ ±45° (F)
108-2		76.2	(3.00)	12.70	(0.50)	2.29	(0.090)	29.0	(0.045)	13.83	(3110)	477.0	(69.11)	46.0	(6.67)	0.0100	12 ply rib chord	6 ~ 0°/90° (F) 6 ~ ±45° (F)
110-1		153.4	(6.04)	25.4	(1.00)	4.57	(0.180)	116.1	(0.180)	53.0	(11835)	454.0	(65.80)	46.9	(6.80)	0.0097	24 ply rear spar outboard flange	13 ~ 0°/90° (F) 11 ~ ±45° (F)
110-2		153.4	(6.04)	25.4	(1.00)	4.57	(0.180)	116.1	(0.180)	50.0	(11295)	433.0	(62.80)	46.9	(6.80)	0.0092	24 ply rear spar outboard flange	13 ~ 0°/90° (F) 11 ~ ±45° (F)
112-1		148.8	(5.86)	25.4	(1.00)	3.05	(0.120)	77.4	(0.120)	36.0	(8065)	463.4	(67.21)	40.0	(5.80)	0.0116	16 ply rear spar outboard web	6 ~ 0°/90° (F) 10 ~ ±45° (F)
112-2		148.8	(5.86)	25.4	(1.00)	3.05	(0.120)	77.4	(0.120)	36.3	(8150)	468.3	(67.92)	40.0	(5.80)	0.01172	16 ply rear spar outboard web	6 ~ 0°/90° (F) 10 ~ ±45° (F)
114-1		148.8	(5.82)	25.4	(1.00)	2.67	(0.105)	67.7	(0.105)	29.4	(6605)	433.7	(62.9)	48.3	(7.00)	0.0090	14 ply front spar outboard flange	8 ~ 0°/90° (F) 6 ~ ±45° (F)
114-2		148.8	(5.82)	25.4	(1.00)	2.67	(0.105)	67.7	(0.105)	33.1	(7440)	488.9	(70.9)	48.3	(7.00)	0.0101	14 ply front spar outboard flange	8 ~ 0°/90° (F) 6 ~ ±45° (F)
116-1		144.3	(5.68)	25.4	(1.00)	1.52	(0.06)	38.61	(0.06)	16.0	(3526)	405.4	(58.8)	46.0	(6.67)	0.0088	8 ply front spar outboard web	4 ~ 0°/90° (F) 4 ~ ±45° (F)
116-2		144.3	(5.68)	25.4	(1.00)	1.52	(0.06)	38.61	(0.06)	16.5	(3701)	425.4	(61.7)	46.0	(6.67)	0.0092	8 ply front spar outboard web	4 ~ 0°/90° (F) 4 ~ ±45° (F)
118-1		153.4	(6.04)	25.4	(1.00)	4.57	(0.18)	116.08	(0.18)	45.0	(10095)	386.8	(56.1)	46.9	(6.80)	0.0082	24 ply rear spar inboard flange	13 ~ 0°/90° (F) 11 ~ ±45° (F)
118-2	Comp	153.4	(6.04)	25.4	(1.00)	4.57	(0.18)	116.08	(0.18)	53.0	(11820)	453.0	(65.7)	46.9	(6.80)	0.0097	24 ply rear spar inboard flange	13 ~ 0°/90° (F) 11 ~ ±45° (F)

- Dry environment
- Specimen geometry—Figure 131, Detail Specimen B
- Test temperature—21°C (70°F).

Table 26. Compression Test Results (Test 25)

Specimen identification number	Detail	Test type	Area		Failure load							Specimen information	
			mm^2	(in^2)	kN	(lb)	MPa	(ksi)	MPa x 10^3	(ksi x 10^3)	mm/mm in/in	Description	Ply layup
119-1	C	Compression	530.3	(0.640)	246.6	55 450	597	(86.6)	73.6	(10.68)	0.0081	Rear spar inboard lower chord	22 (0^o/90^oF), 30 ($\pm45^o$F) 8 (145 tape), 28 (190 tape)
121-1	D	Compression	561.4	(0.650)	266.0	59 800	634	(92.0)	66.3	(9.62)	0.0095	Rear spar inboard lower angle	22 (0^oF), 8 (145 tape) 30 ($\pm45^o$F) 28 (190 tape) Cap { 13 (0^oF) 11($\pm45^o$)
121-2	D	Compression	561.4	(0.650)	235.0	52 800	560	(81.2)	66.3	(9.62)	0.0084	Rear spar inboard lower angle	22 (0^oF) 8 (145 tape) 30 ($\pm45^o$F) 28 (190 tape) Cap { 13 (0^oF) 11($\pm45^o$)
122-1	D	Compression	561.4	(0.650)	260.7	58 600	622	(90.2)	66.3	(9.62)	0.0094	Rear spar inboard upper angle	22 (0^oF) 8 (145 tape) 30 ($\pm45^o$F) 28 (190 tape) Cap { 13 (0^oF) 11($\pm45^o$)
122-2		Compression	561.4	(0.650)	256.2	57 600	611	(88.6)	66.3	(9.62)	0.0092	Rear spar inboard upper angle	22 (0^oF) 8 (145 tape) 30 ($\pm45^o$F) 28 (190 tape) Cap { 13 (0^oF) 11($\pm45^o$)

- Environment–dry
- Specimen geometry– Figure 131, Detail Specimen C, D
- Test temperature–21°C (70°F)

Table 27. Rail Shear Results (Test 25)

Specimen identification number	Test type	Specimen geometry				Shear area		Failure load		Failure stress		Nominal shear modulus		Failure strain	Specimen information	
		$L_{effective}$		Thickness												
		mm	(in)	mm	(in)	mm^2	(in^2)	kN	(lb)	MPa	(ksi)	MPa x 10^3	(ksi)	mm/mm (in/in)	Description	Ply layup
123-1	Rail shear	126.9	(5.00)	3.05	(0.120)	387	(0.600)	84.7	(19 050)	219.3	(31.8)	21.0	(3.05)	0.0104	16 ply rear spar web	6 (0^o/90^o) 10 ($\pm45^o$)
123-2				3.05	(0.120)	387	(0.600)	83.2	(18 700)	215.	(31.2)	21.0	(3.05)	0.0102	16 ply rear spar web	6 (0^o/90^o) 10 ($\pm45^o$)
123-3				3.05	(0.120)	387	(0.600)	80.3	(18 050)	208.	(30.1)	21.0	(3.05)	0.0100	16 ply rear spar web	6 (0^o/90^o) 10 ($\pm45^o$)
124-1				1.52	(0.060)	192.9	(0.300)	58.0	(13 000)	299.	(43.3)	17.9	(2.6)	0.0167	8 ply front spar web	4 (0^o/90^o) 4 ($\pm45^o$)
124-2				1.52	(0.060)	192.9	(0.300)	53.4	(12 000)	276.	(40.0)	17.9	(2.6)	0.0154	8 ply front spar web	4 (0^o/90^o) 4 ($\pm45^o$)
124-3				1.52	(0.060)	192.9	(0.300)	53.6	(12 050)	277.	(40.2)	17.9	(2.6)	0.0155	8 ply front spar web	4 (0^o/90^o) 4 ($\pm45^o$)
125-1				1.35	(0.053)	171.3	(0.265)	44.2	(9 940)	259.	(37.5)	22.8	(3.3)	0.0114	7 ply skin	2 (0^o/90^o) 5 ($\pm45^o$)
125-2				1.35	(0.053)	171.3	(0.265)	36.9	(8 300)	216.	(31.3)	22.8	(3.3)	0.0095	7 ply skin	2 (0^o/90^o) 5 ($\pm45^o$)
125-3				1.35	(0.053)	171.3	(0.265)	35.6	(8 000)	208.	(30.2)	22.8	(3.3)	0.0091	7 ply skin	2 (0^o/90^o) 5 ($\pm45^o$)
126-1				1.142	(0.045)	144.9	(0.225)	24.9	(5 600)	172.	(24.9)	17.9	(2.6)	0.0096	Honeycomb rib web	3 (0^o/90^o) 3 ($\pm45^o$ 0.250" honeycomb
126-2				1.142	(0.045)	144.9	(0.225)	24.3	(5 470)	168.	(24.3)	17.9	(2.6)	0.0094	Honeycomb rib web	3 (0^o/90^o) 3 ($\pm45^o$) 0.250" honeycomb
126-3	Rail shear	126.9	(5.00)	1.142	(0.045)	144.9	(0.225)	24.4	(5 480)	168.	(24.4)	17.9	(2.6)	0.0094	Honeycomb rib web	3 (0^o/90^o) 3 ($\pm45^o$) 0.250" honeycomb

- Environment–dry
- Specimen geometry– Figure 131, Detail Specimen E
- Test Temperature–21°C (70°F)

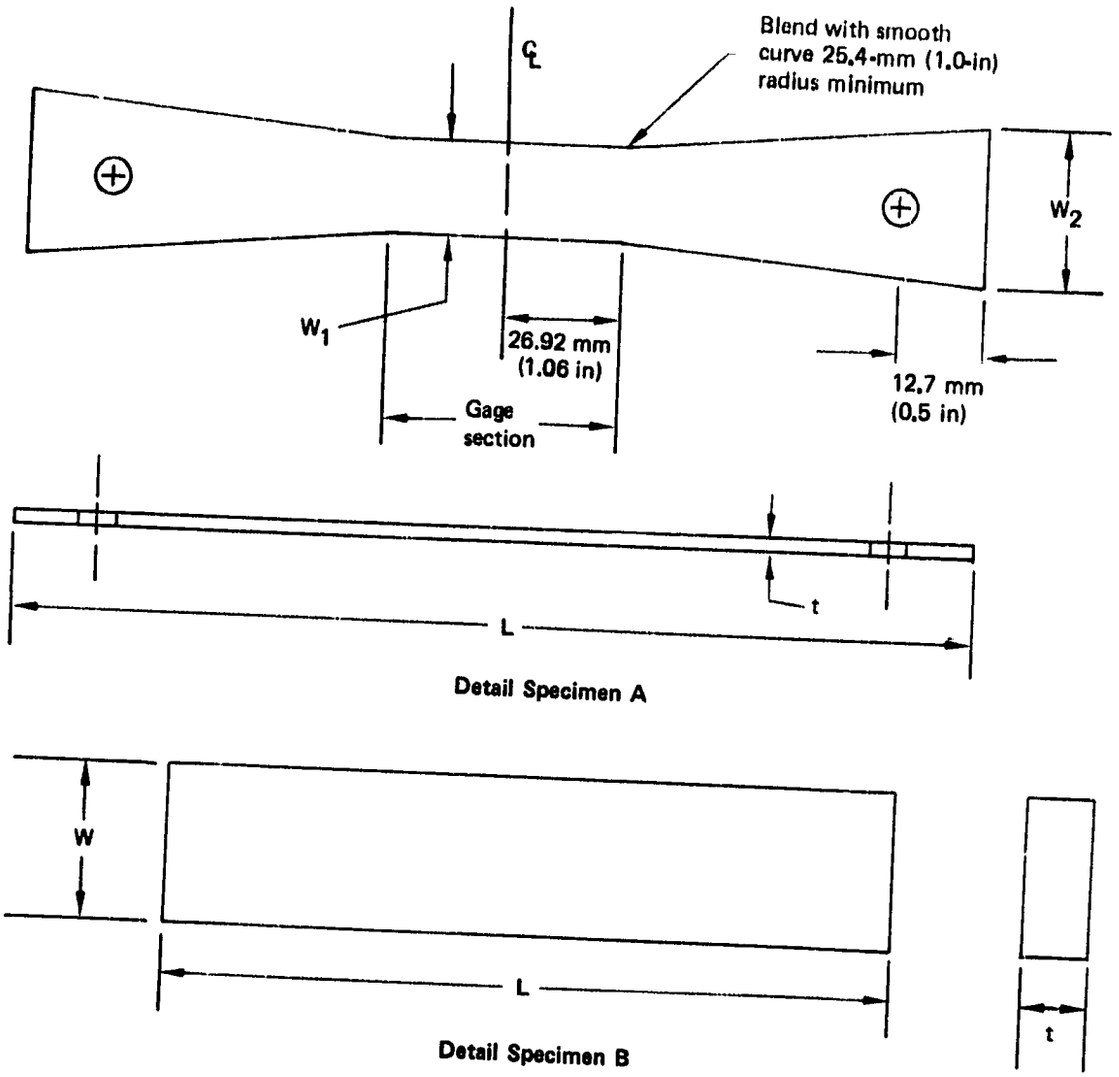

Figure 131. Detail Specimen

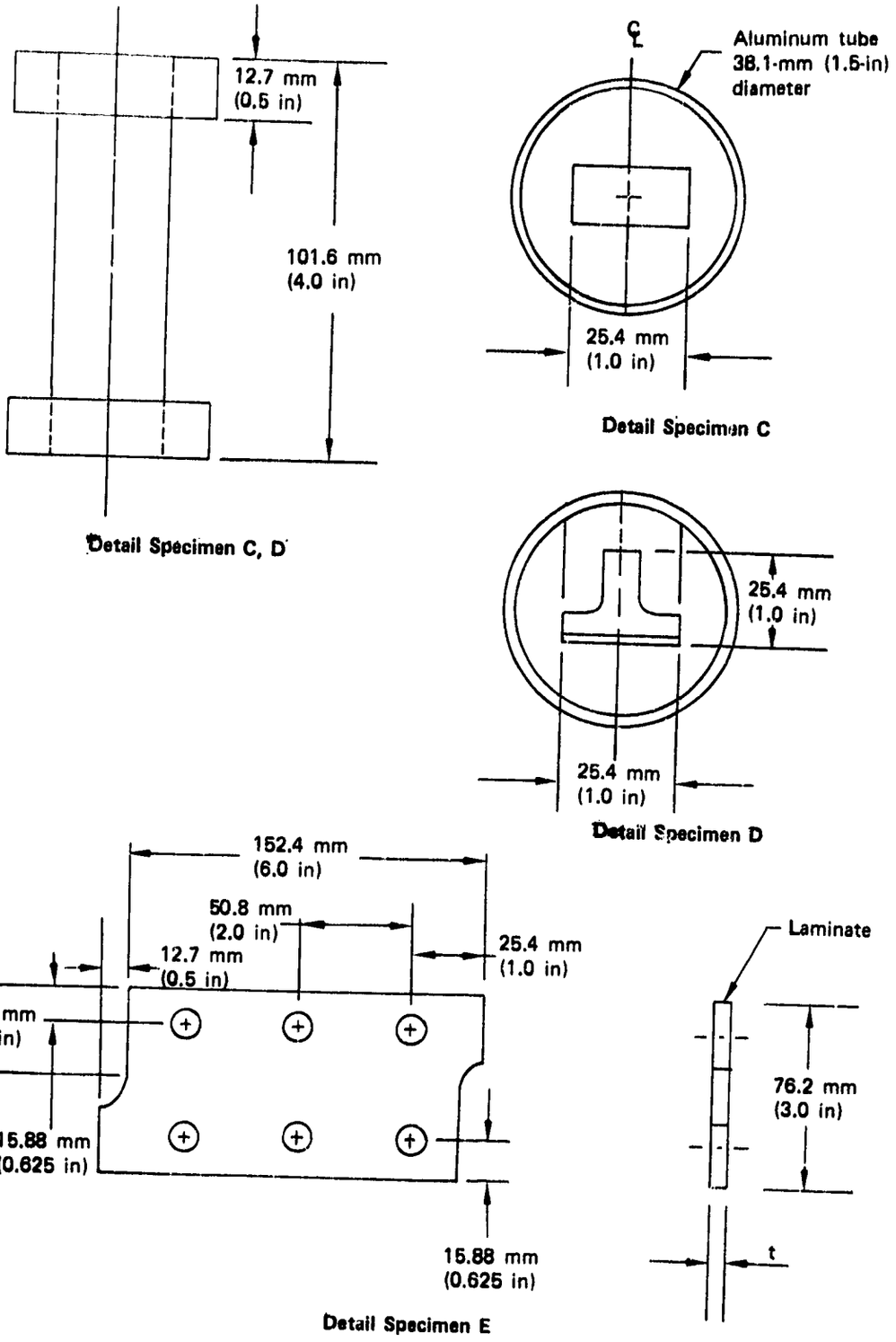

Figure 131. Detail Specimen (Concluded)

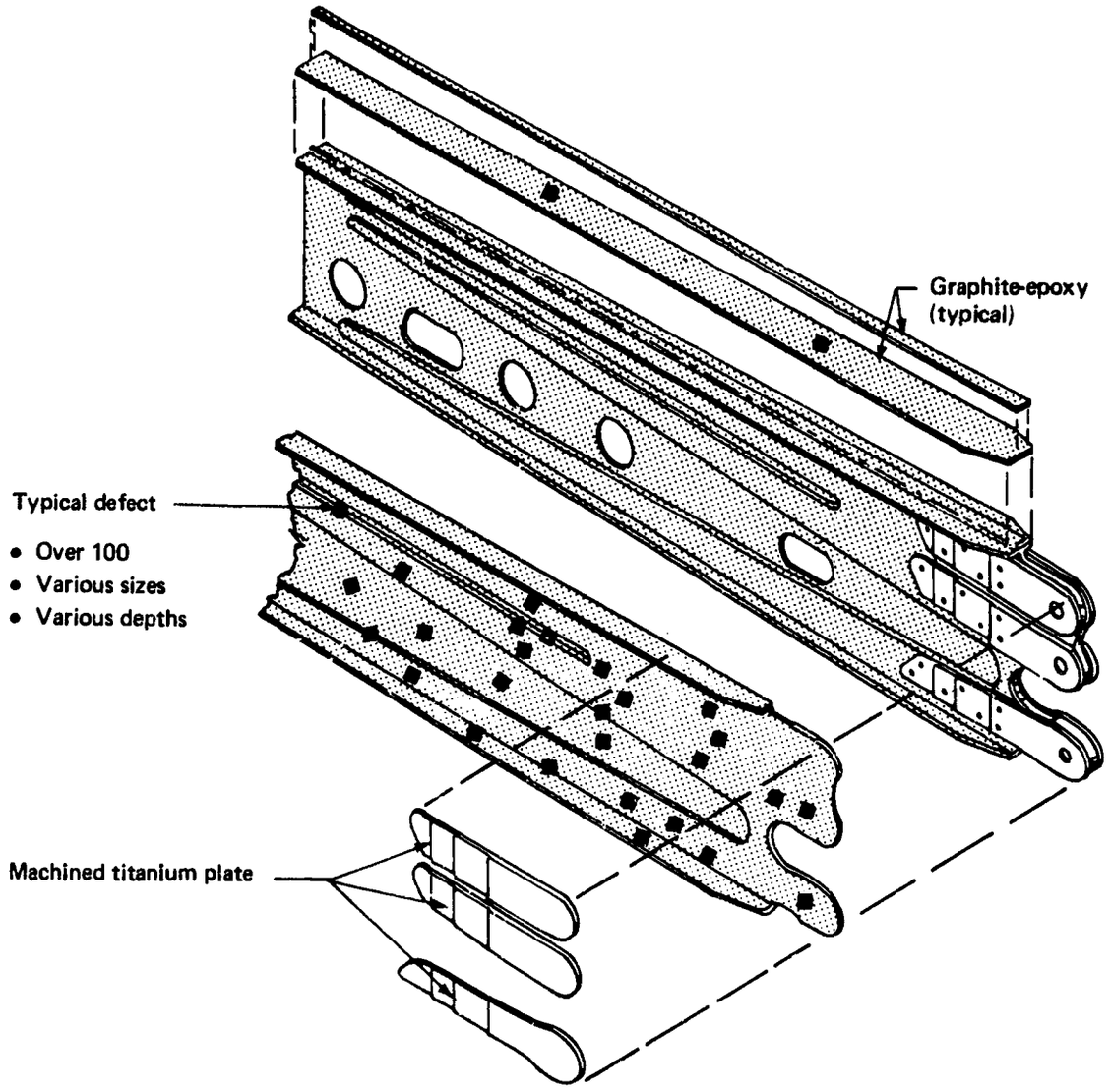

Figure 132. Spar Lug Defect Standards

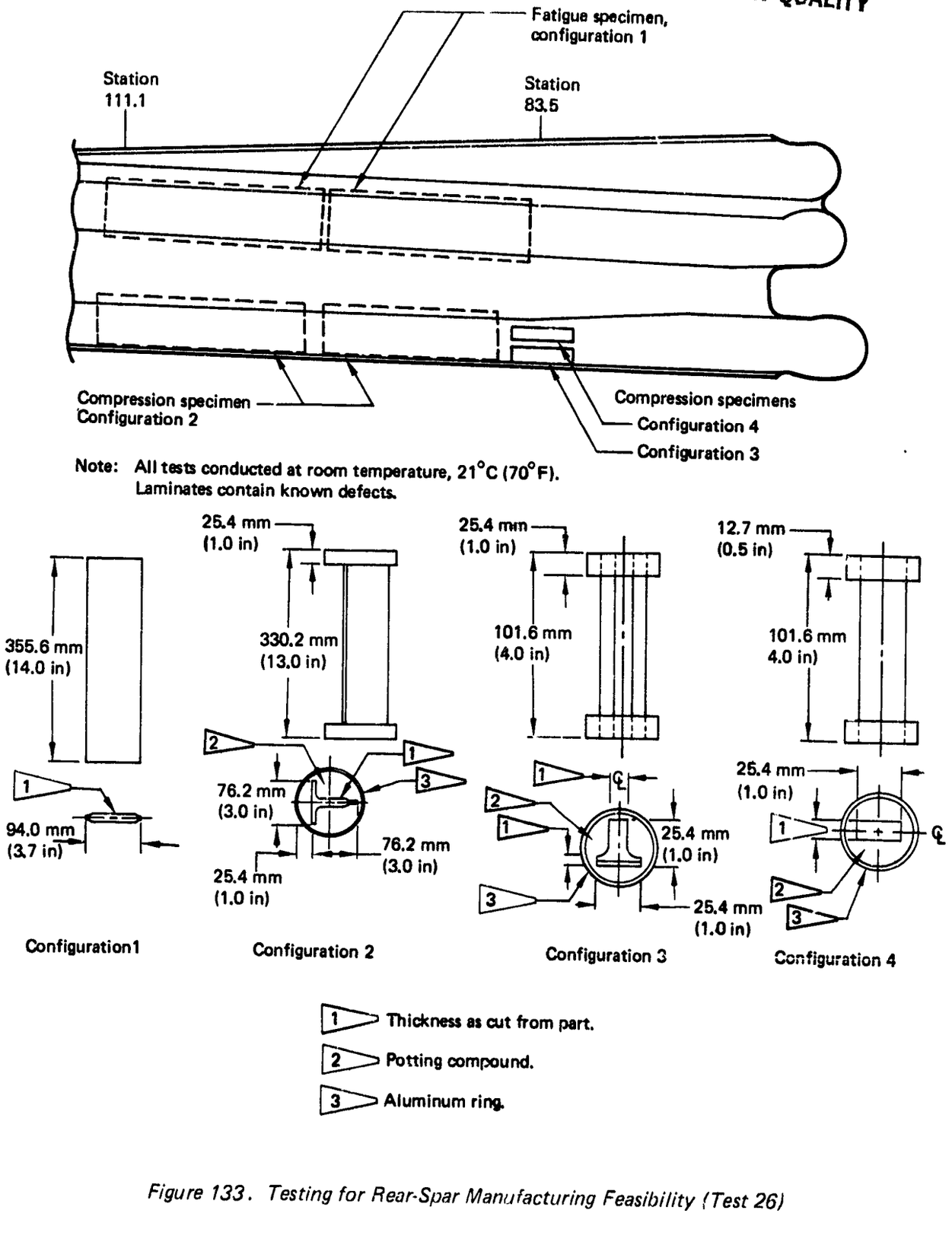

Figure 133. Testing for Rear-Spar Manufacturing Feasibility (Test 26)

Table 28. Test Results for Rear-Spar Manufacturing Feasibility (Test 26)

Configuration	Failure load, N	(lb)	
1	303 600	(68 250)	1
1	338 100	(76 000)	1
2	711 700	(160 000)	
2	638 300	(143 500)	
3	240 200	(54 000)	
4	213 300	(47 950)	

1 Fatigued, residual strength.

Table 29. Repaired Compression Panels—Test Results

Panel configuration	Temperature, °C	(°F)	Environmental condition	Failure load, N	(lb)	Baseline (undamaged), failure load N	(lb)
1-1	82	(180)	Wet	127 000	(28 560)	–	–
1-2	21	(70)	Dry	128 100	(28 800)	147 000	(33 000)
2-1	21	(70)	Wet	195 500	(43 950)	190 000	(42 700)
2-2	21	(70)		182 600	(41 050)	190 000	(42 700)
2-3	-59	(-75)		197 500	(44 400)	–	–
2-4	-59	(-75)		188 800	(42 450)	–	–
2-5	82	(180)		177 000	(39 800)	185 000	(41 350)
2-6	82	(180)	Wet	169 000	(38 000)	185 000	(41 350)
2-7	21	(70)	Dry	224 600	(50 500)	174 000	(39 000)
2-8	21	(70)	Dry	193 700	(43 550)	174 000	(39 000)

Table 30. Repaired Fatigue Panels—Test Results

Panel configuration	During fatigue cycling: Temperature, °C	(°F)	Environmental condition	During static test: Temperature, °C	(°F)	Environmental condition	Failure load, N	(lb)	Baseline (undamaged), failure load N	(lb)
3-1	-59	(-75)	Wet	21	(70)	Wet	207 700	(46 700)	231 700	(52 100)
3-2	21	(70)		21	(70)		240 650	(54 100)	231 700	(52 100)
3-3	-59	(-75)		-59	(-75)		215 700	(48 500)	–	–
3-4	-59	(-75)		-59	(-75)		187 700	(42 200)	–	–
3-5	-59	(-75)		82	(180)		235 800	(53 000)	–	–
3-6	-59	(-75)	Wet	82	(180)	Wet	222 400	(50 000)	–	–
3-7	21	(70)	Dry	21	(70)	Dry	242 900	(54 600)	222 200	(49 950)
3-8	-59	(-75)	Dry	-59	(-75)	Dry	199 700	(44 900)	–	–
4-1	-59	(-75)	Wet	-59	(-75)	Wet	202 400	(45 500)	–	–
4-2	21	(70)	Dry	21	(70)	Dry	218 000	(49 000)	276 200	(62 100)

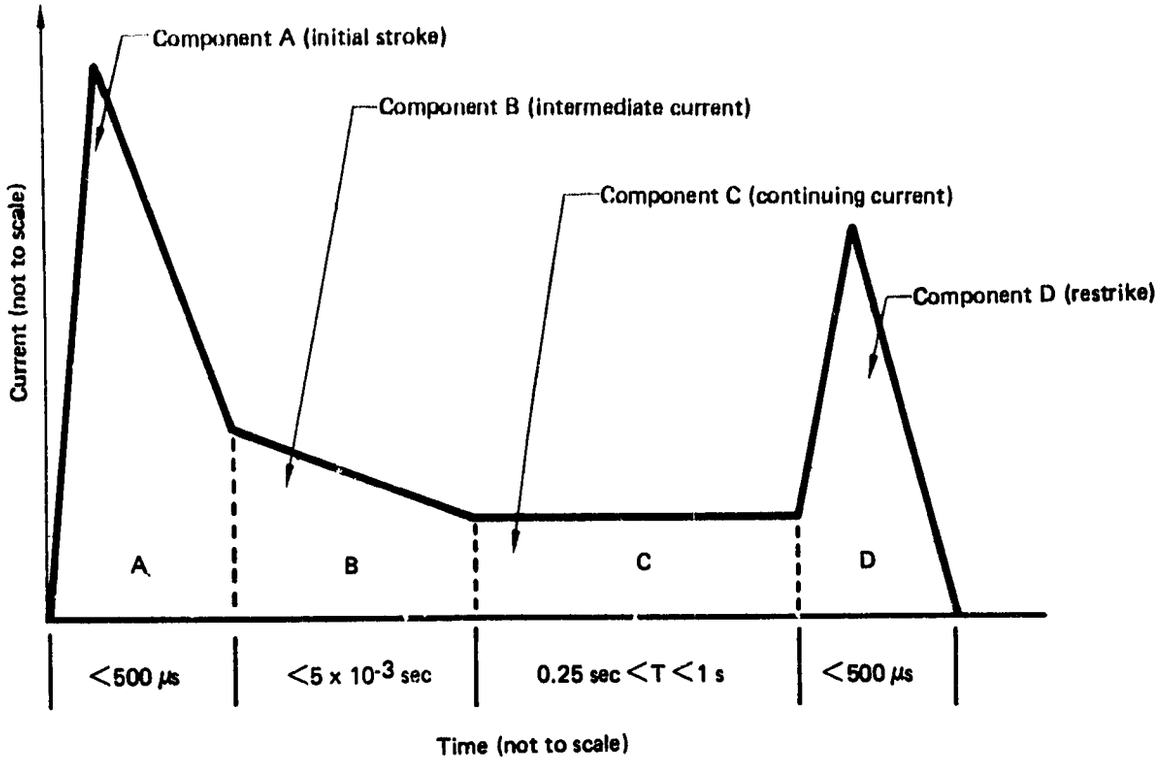

Test waveform	Parameter	Recommended test value ▷
Component A	I_{peak}(ampere)	200 000
	A (kiloampere^2-sec)	2 000
Component B	I_{avg}(ampere)	2 000
	Q(coulombs)	10
Component C	I_{avg}(ampere)	500
	Q(coulombs)	200
Component D	I_{peak}(ampere)	100 000
	A (kiloampere^2-sec)	250

▷ MIL-STD-1757

Figure 134. Lightning Discharge Current Waveform Components

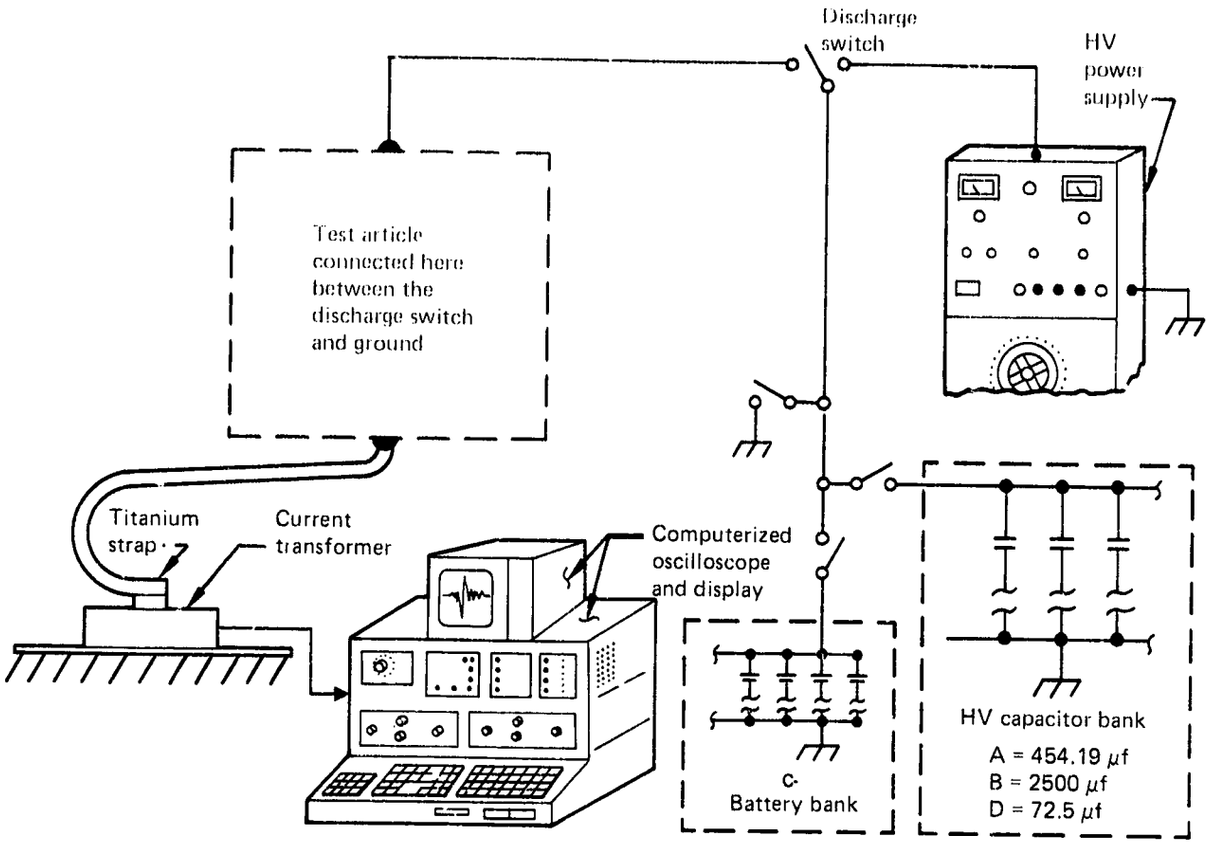

Figure 135. Electrical and Signal Connections for Lightning Discharge Testing

The first series of tests on the new panels included a rib positioned on the internal surface to provide support for the ends of the stringers. In addition, the entire support structure for the specimen was revised to simulate actual conditions. These strikes penetrated the skin, but the stringers were not delaminated.

For the second series of tests on the second new panel, the rib supporting the stringers was removed. The strike did not penetrate the skin, but the stringers did delaminate. Based on these results, a rib was incorporated into the design.

4.2.7.2 Spar/Rib Intersection

The trailing-edge rib-to-spar test specimen was assembled to produce an aluminum-to-graphite-epoxy interface that represented the structure on the stabilizer. Material finishes, fasteners, and corrosion protection were included in this interface representation.

This test specimen was subjected to a reduced Zone 3 lightning discharge because there is more than one trailing-edge rib-to-spar joint to carry the lightning current. Figure 138 shows the lightning entrance and exit points for this jointed test specimen.

Figure 136. Lightning Strike Test, Outer Surface

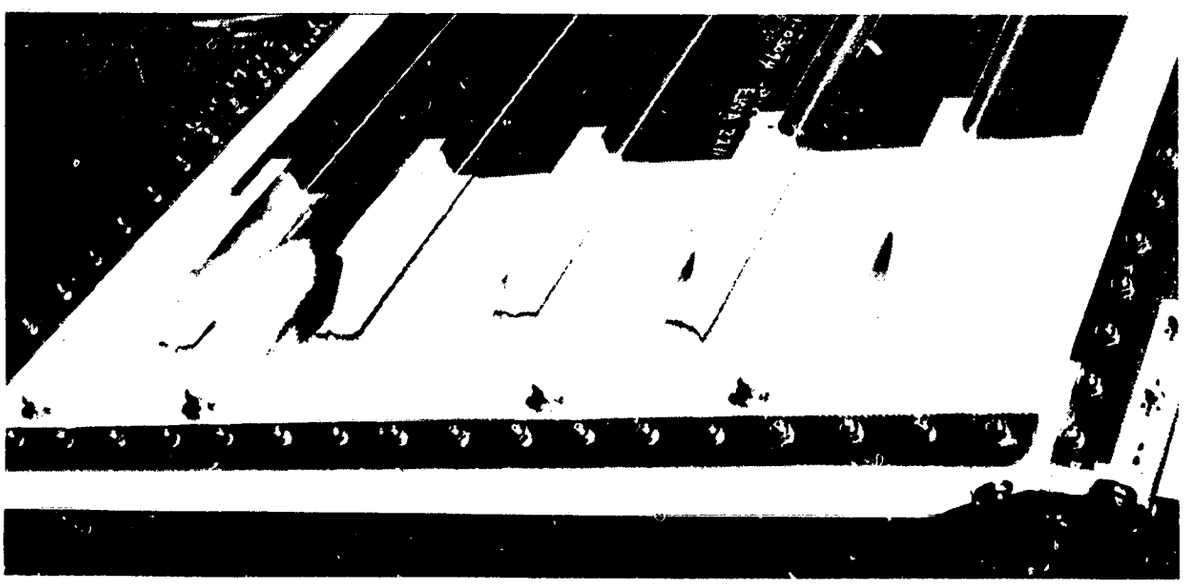

Figure 137. Lightning Strike Test, Inner Surface

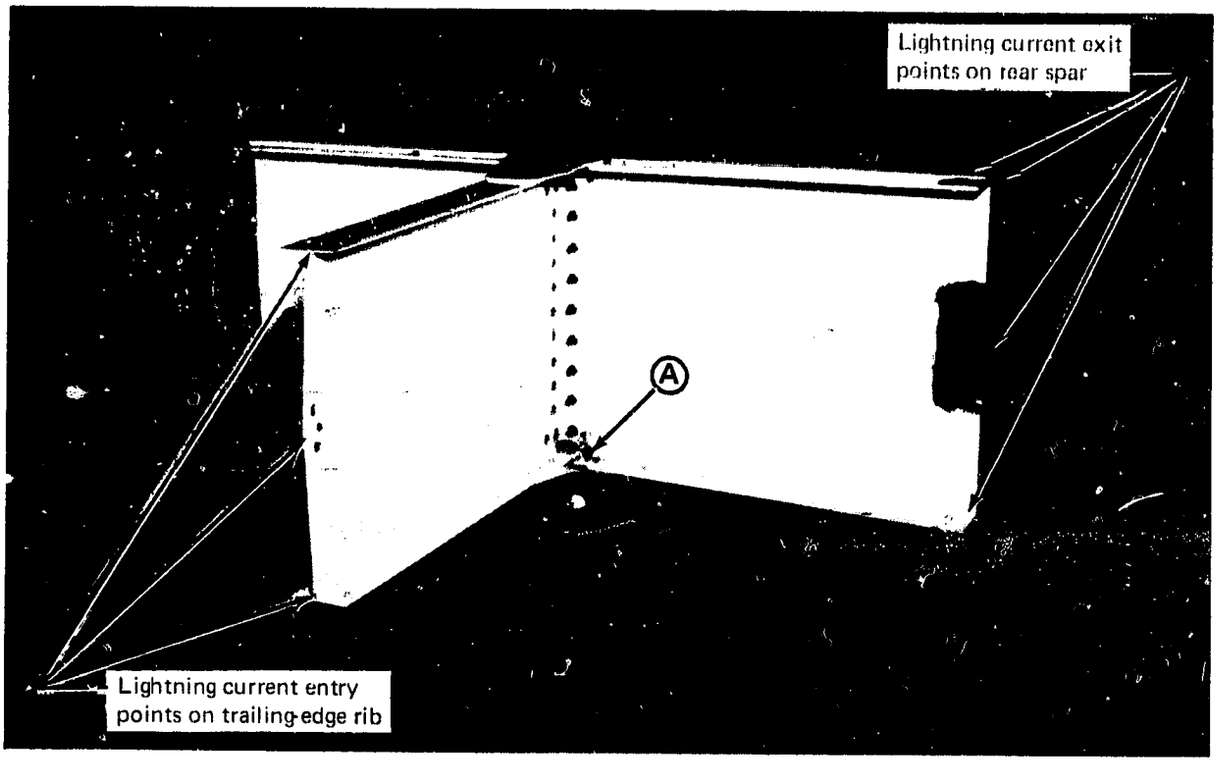

- Visual damage resulting from a Zone 3 lightning discharge was noted at location A.

Figure 138. Trailing-Edge Rib-to-Spar Jointed Test Specimen

Figure 139 is a closeup of location A in the joint, showing the damage caused by the discharge current flowing through the specimen aluminum to the graphite interface.

As seen in Figures 138 and 139, the damage to the structure is minimal. Arcing occurred at two fasteners where there is an aluminum-to-graphite-epoxy interface. This arcing left burn marks in the paint and outer surface of the graphite-epoxy, but no structural damage was present.

4.2.7.3 Spar/Trailing-Edge Panel

This test was performed to evaluate P-static current conduction through the antistatic coating on the fiberglass and the phosphate-coated titanium fasteners that interface with the graphite-epoxy substructure. The specimen was made of a section of the rear spar bolted to a trailing-edge panel. It was hardwired to a high-voltage power supply so that P-static current conduction, arc over, and corona could be evaluated.

Figure 140 shows the P-static laboratory and test setup. During the testing, each antistatic coated strip was tested for its ability to conduct P-static currents through the respective phosphate flouride-coated fastener to the graphite-epoxy spar caps without showing detrimental effects. The test results show that the stray charges were conducted to ground.

Closeup of lightning current caused damage at location A.

Figure 139. Detail of Location A—Trailing-Edge Rib-to-Spar Jointed Test Specimens

4.2.8 Sonic Box

A graphite-epoxy box specimen was tested in a sonic environment to evaluate the sonic resistance of structure that was representative of the 737 stabilizer design configuration. Overall sound pressure levels measured on the horizontal stabilizer during maximum takeoff power were 145 dB.

The test specimen was mounted in a 50-Hz grazing incidence horn as shown in Figure 141. Sine scans were conducted to establish the first three resonant frequencies. Mode shapes and node lines were defined. The specimen then was subjected to the following overall sonic pressure levels (OASPL) during the first phase of tests:

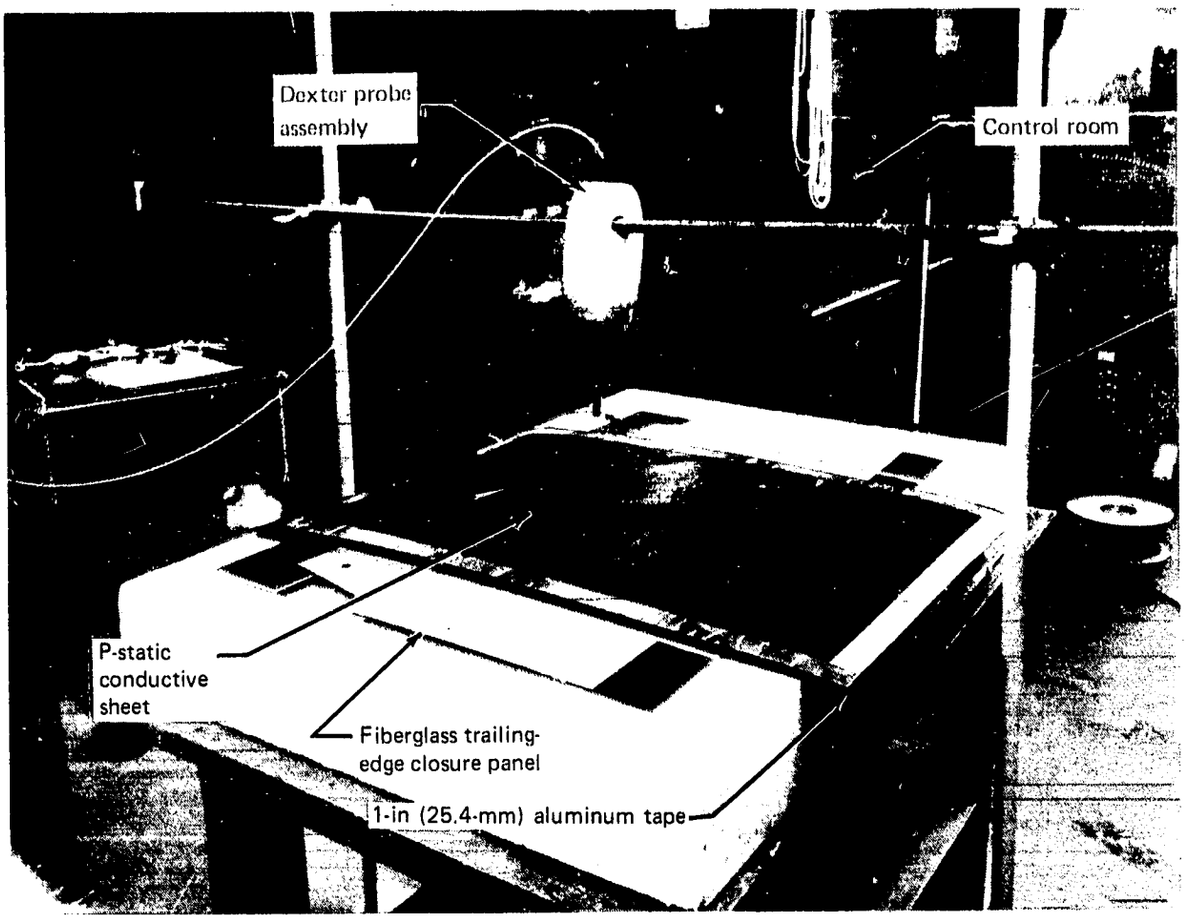

Figure 140. Fiberglass Trailing-Edge Closure Panel P-Static Laboratory Test Setup

Maximum OASPL, dB	Test time, hr
145	2
157	3
160	3
161	3

No fatigue failures occurred during the first phase of tests.

For the second phase of tests, the panel was intentionally damaged and then subjected to 161 dB (OASPL) for 3 hr. No crack propagation occurred at the intentional damage.

4.2.9 Stub Box

The stub box (fig. 142) was designed, manufactured, and tested early in the program to evaluate design concepts and details prior to fabrication of the full-scale ground specimen. It is a full-scale inboard root section of the graphite-epoxy horizontal stabilizer and consists of a structural box extending from the side-of-

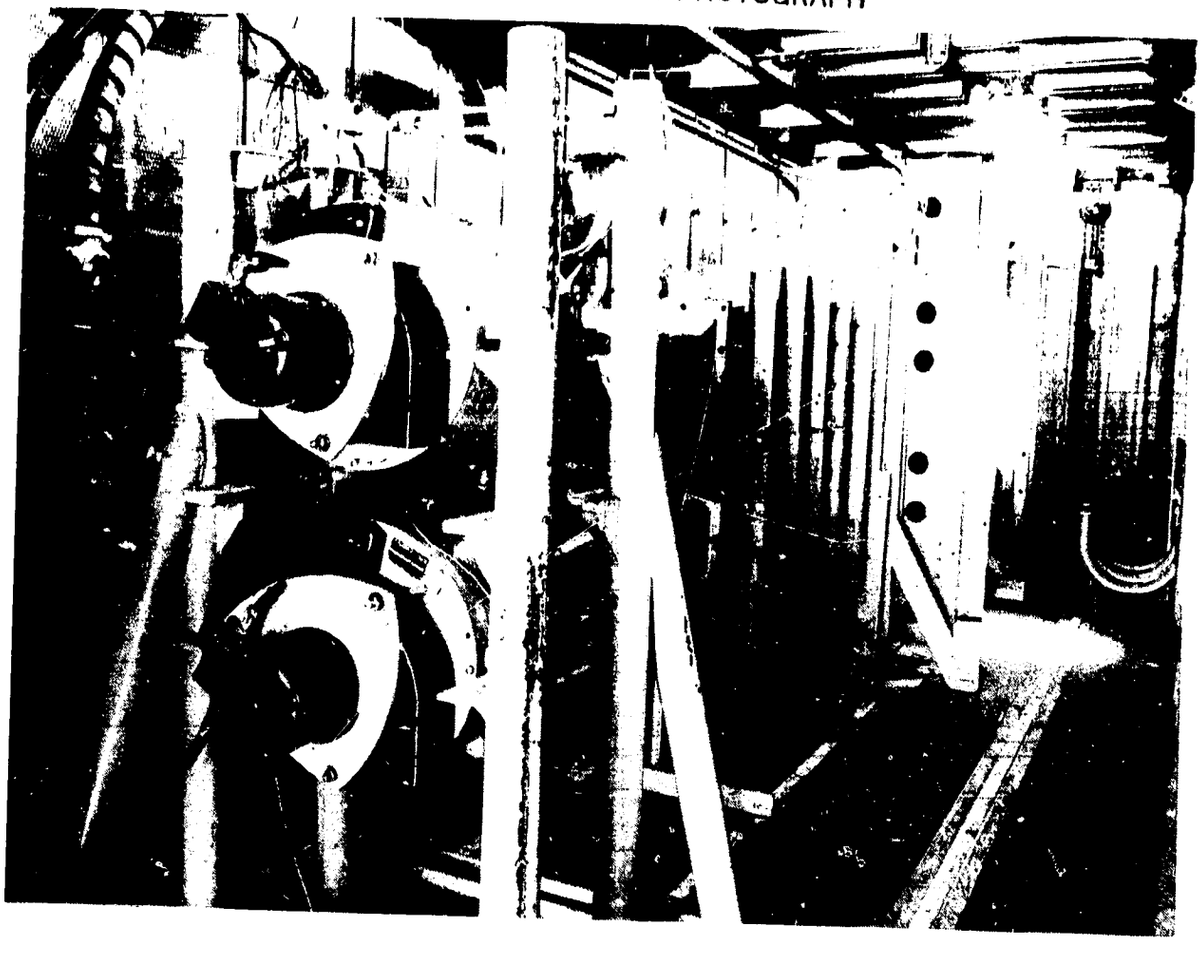

Figure 141. Sonic Box Test Setup

body fittings outboard to stabilizer station 152.45 including the trailing-edge structure and simulated leading edge. The section between stabilizer stations 138.7 and 152.45 was reinforced to provide load distribution.

4.2.9.1 Test Specimen and Setup

All details of the stub box represented production design concepts. The skin surfaces were cocured I-stiffened panels (fig. 11). The spars were composed of channels and cap members, secondarily bonded, with precured chord reinforcements at the inboard end. The front and rear spars were reinforced with titanium plates at the lugs providing strength, geometry, and envelope compatibility with the existing 737 attachment configuration (figs. 12, 13, and 14). Ribs were fabricated per production configurations. Inspar ribs were graphite face/honeycomb web (fig. 15) and the closure rib was stiffener-reinforced laminate (fig. 16).

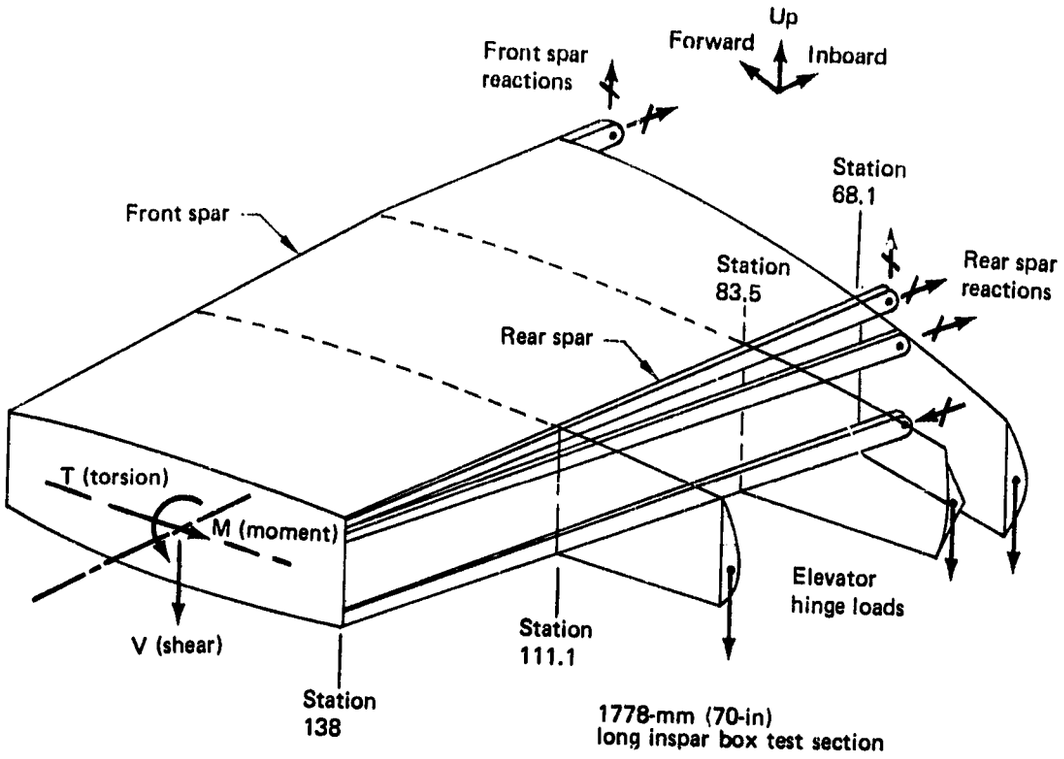

Test sequence

1. **Static test to 40% design ultimate load conditions**
2. Spectrum fatigue test (one lifetime)
3. **Static test to design ultimate load conditions**
4. Damage growth assessment (one-half lifetime spectrum loading)
5. **Fail-safe load test (three damaged areas)**
6. **Destruction test** (critical condition)

Figure 142. Design Development Test Stub Box (Test 21)

The stub box was supported at the front- and rear-spar lugs simulating the actual aircraft installation. An aluminum extension was attached to the outboard end to introduce the required shear, moment, and torsion. The test setup is shown in Figure 143. Bonded pads were attached to the upper and lower surfaces. Airload distributions to the surfaces were simulated by loading the pads through evener systems. A total of 98 rosette and 71 axial strain gages were installed to provide data regarding strain levels and distribution.

4.2.9.2 Test Results

Strain Survey—The stub box was loaded to 40% design ultimate load (DUL) for the three design load cases (LC):

- Maximum positive (up) bending (load case 4740)
- Maximum negative (down) bending (load case 4010)
- Maximum torsion (load case 3710)

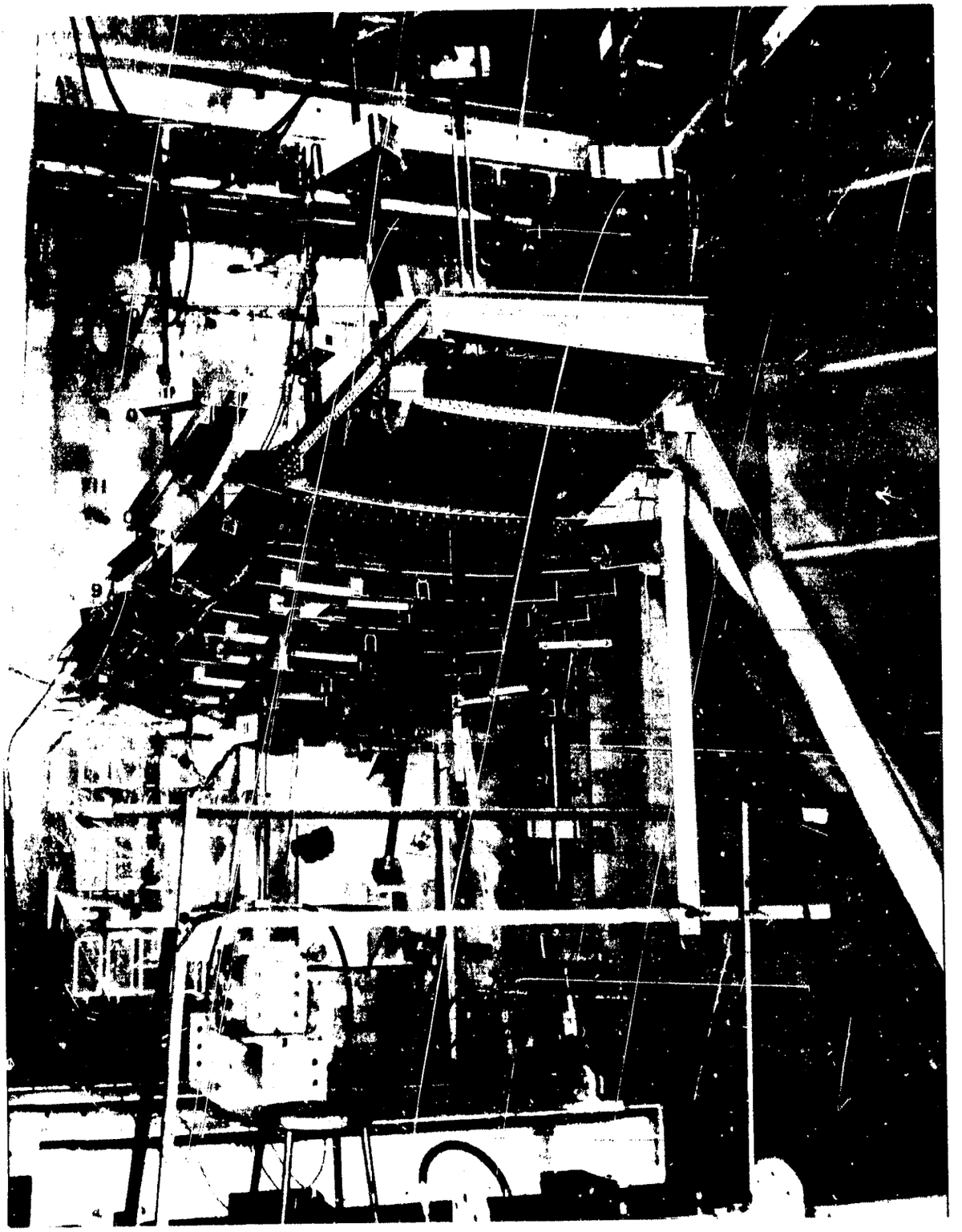

Figure 143. Stub Box Test Setup

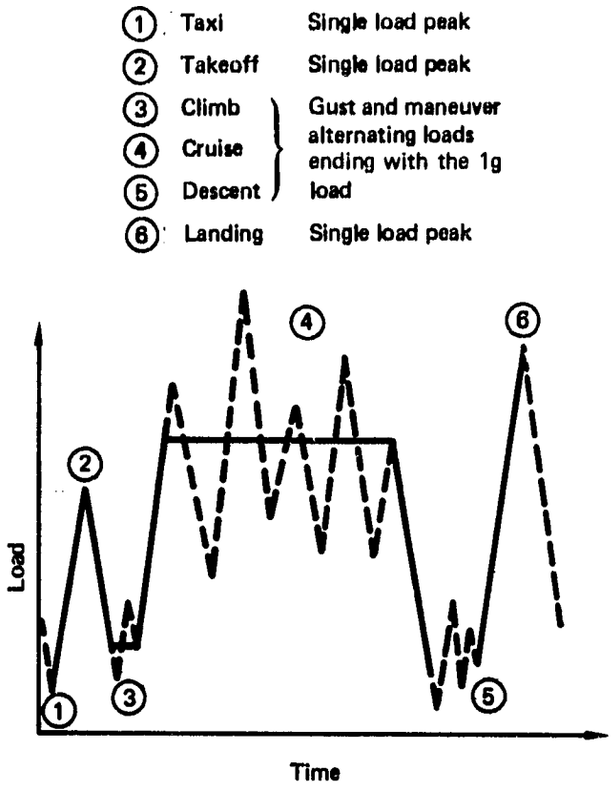

Figure 144. Test Spectrum General Loading Sequence

These load cases were applied to establish baseline distributions. The strain gage output for all three load cases was reviewed and compared with the finite element model predictions. Results showed good agreement between the calculated and measured values. In addition, five unit load cases were applied to the stub box. The deflection data taken during unit loadings were used to correlate with stiffness calculations.

Fatigue Test—Fatigue testing was performed on the stub box to indicate any fatigue critical design details. Spectrum fatigue loads representing one lifetime of service (75 000 flights) were applied.

The test load spectrum used throughout the program was developed from the original 737 fatigue analysis and 10 years of service history. The test flight phase is defined as taxi, takeoff, climb, cruise, descent, and landing. The taxi, takeoff, and landing phase alternating loads are of a relatively small magnitude; thus, these phases are represented by single excursions of the 1g load plus the secondary cycle excursion. Significant alternating loads exist during climb, cruise, and descent phases; therefore, these test phases contained an appropriate number of alternating load peaks about the 1g load levels. The load sequence has been developed to be similar to the European standard spectra TWIST and FALSTAFF (refs. 15 and 16), in which flight conditions of varying severity are applied with more and larger load peaks in severe flights than in less severe flights. The resulting general load sequence is shown in Figure 144. Truncation load levels were established according

to the standard spectrum, TWIST (ref. 15). A 10 000-flight block was established according to the TWIST spectrum, and this block was repeated eight times to accumulate 80 000 flights for one lifetime.

Many of the alternating loads contained in the test spectrum occur less than once per flight, necessitating several test flight types with different severities and frequencies. Test flight severity levels were defined in a similar manner to those defined in TWIST. Eight flight types were defined. The resulting frequency and cyclic load content of the flights is shown in Table 31. The load points for an F-type flight are shown in Figure 145. The 100% load level shown in this figure corresponds to 42% of the ultimate design bending moment at the reference station (stabilizer station 138). The 42% bending moment condition occurs once each A flight (fig. 145), which occurs once during each 10 000-flight block. The high load point (fig. 145) shown for the landing condition produces a bending moment equal to 34% of the ultimate design bending moment. This condition and level occur once every flight.

At the end of each block of 10 000 flights, nondestructive inspection (NDI) for damage was performed. Strain surveys and deflection measurements also were taken before the start of fatigue testing and after every 20 000 flights to establish comparative strain data throughout the fatigue test. No damage was detected during or after the fatigue cycling, and no changes were noted in the comparative strains or deflections.

Static Test, Design Ultimate Load Conditions—Static tests were performed by applying the three load conditions described for the strain survey (sec. 4.2.9.2). Load level and sequence were:

- Load case 3710 to 100% DUL
- Load case 4010 to 72% DUL
- Load case 4740 to 80% DUL

The box was not loaded to 100% DUL for load cases 4010 and 4740 to preclude damage to the titanium lugs. A review of the results of the strain survey resulted in a redesign and strengthening of the production rear-spar lug details. Since the stub box was scheduled for further fatigue and damage tolerance testing, reduced loads were applied to preclude failure and loss of the test specimen.

The strain gage data taken during these load applications were extrapolated to ultimate and compared with the finite element analysis results. This comparison showed:

- Good agreement between measured and calculated values
- Strain levels in the critical details compatible with the limits established as criteria for the program

Damage Tolerance Growth Assessment—Damage tolerance testing evaluated the effects of repeated loads on discrete damage. Damage was inflicted at critical locations. A description of the damage is shown on Table 32 and in Figures 146 through 148. Photos of examples of damage are shown in Figures 149 through 152.

Table 31. Flight Type Definition

Flight type / 1	Number of gust load cycles at eight amplitude levels								Number of maneuver load cycles at eight amplitude levels								Number of load points in one flight
	I	II	III	IV	V	VI	VII	VIII	I	II	III	IV	V	VI	VII	VIII	
A 1	1	1	2	2	6	14	112	766	1	3	5	2	7	3	2	3	1866
B 1		1	1	2	6	10	91	655		1	3	3	7	2	2	2	1578
C 5			1	1	2	2	39	468			2	8	7	3	1	5	1084
D 14				1	1	2	14	166				4	12	8	6	7	488
E 62					1	2	4	73					5	13	10	15	252
F 620						1	3	15						3	8	10	86
G 3100							1	6							3	8	42
H 6200								4								8	30

1 Number of flights in a 10 000-flight block.

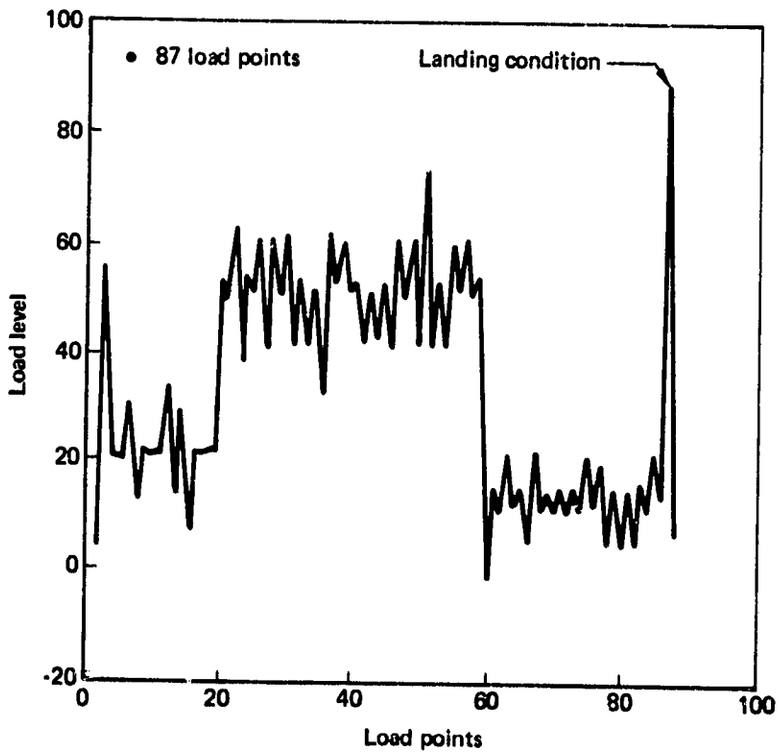

Figure 145. F-Type Flight Definition

Table 32. Stub Box Damage Location and Description

Damage identification number	Location	Description
LS-1	Lower skin at stabilizer station 77 between the rear spar and stringer 1	Cut skin 12.7mm (0.5 in) long at 45 deg to the rear spar. Simulates service damage
LS-2 and -3	Lower skin at stringer 1 and stabilizer station 111.1 rib intersection	Damaged skin in fastener countersink. Simulates delamination caused by improper fastener installation
LS-4	Lower skin to rear spar fastener at stabilizer station 80	(Same as LS-2)
LS-5	Lower skin at stringer 2 and stabilizer station 111.1 rib intersection	Impact damage. Simulates service damage 1
LS-6	Lower skin stringer 2 inner chord between stabilizer station 83.5 and 111.1	Impact damage. Simulates dropped tool during assembly 1
US-1	Upper skin (same as LS-1)	Impact damage. Simulates dropped tool or hail damage 1
US-2 and -3	Upper skin (same as LS-2 and -3)	(Same as LS-2 and -3)
US-4	Upper skin (same as LS-4)	(Same as LS-2 and -3)
RS-1	Rear spar, edge of web cutout at stabilizer station 90	Impact damage. Simulates fabrication or service damage 1
RS-2	Rear spar, edge of web cutout at stabilizer station 86	Web cut 6.4mm (0.25 in) long. Simulates fatigue or service damage
RS-3	Rear spar chord forward flange at stabilizer station 72.5	Cut from flange edge to fastener hole. Simulates fatigue or service damage
RS-4	Rear spar web at stabilizer station 96	Impact damage. Simulates fatigue or service damage 1
RS-5	Rear spar web at stabilizer station 99	Cut web 12.7mm (0.5 in) long. Simulates fatigue or service damage

1 Impact damage level. Detectable by visual inspection.

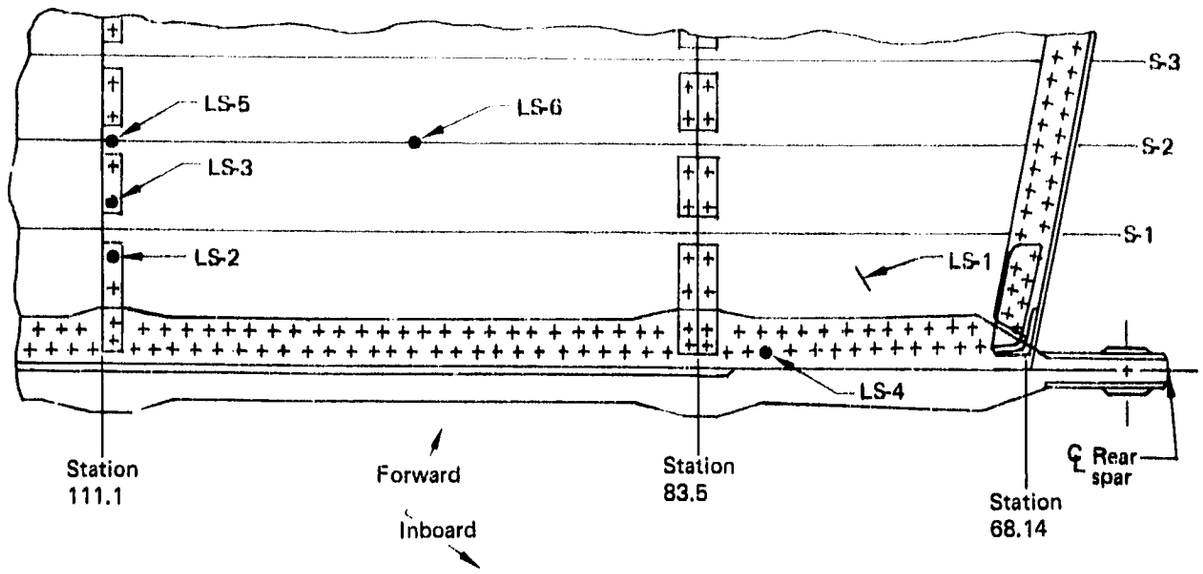

Figure 146. Lower Surface Damage Locations

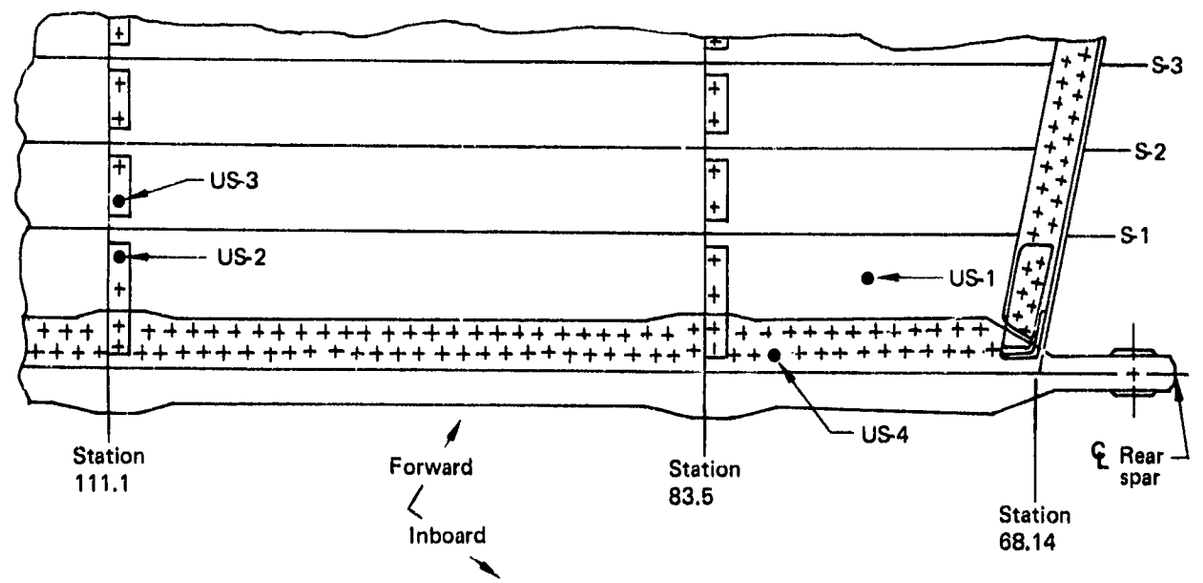

Figure 147. Upper Surface Damage Locations

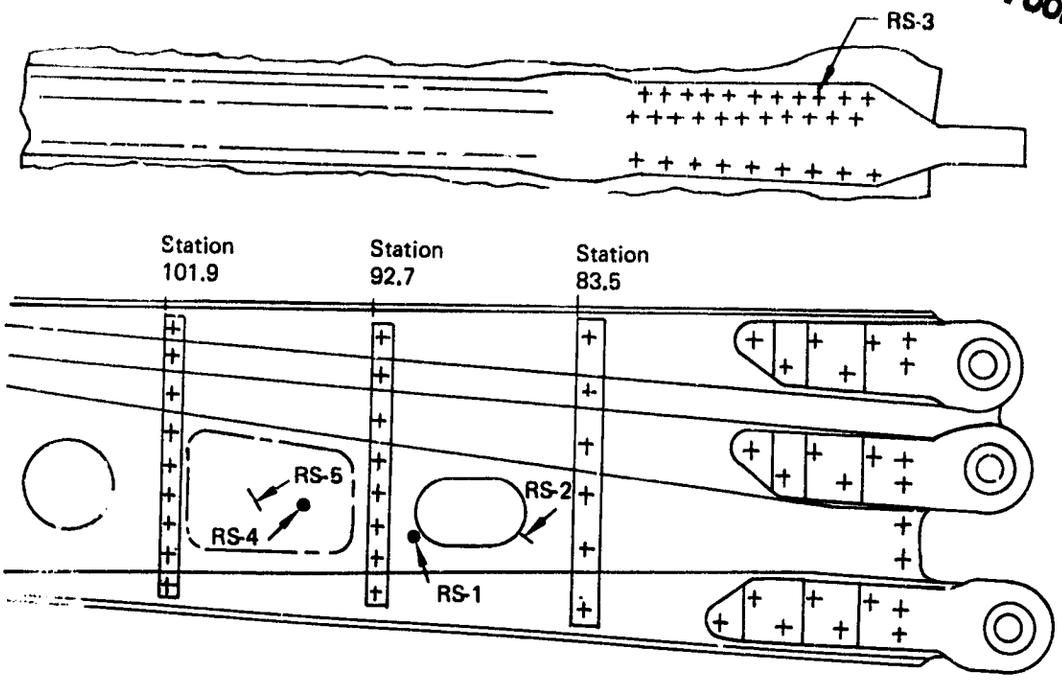

Figure 148. Rear-Spar Damage Location

Spectrum fatigue loads representing one-quarter lifetime (20 000 flights) were applied after inflicting small damage at critical locations. Inspections using Sondicator and X-ray techniques were performed after each 5000 flights. After 20 000 flights with the small damage, static loads equivalent to limit loads of load cases 4010 and 4740 were applied. The spectrum fatigue loads then were continued for 20 000 additional flights. No damage or flaw growth was detected during or after the fatigue cycling.

Damage Tolerance, Fail-Safe—Fail-safe tests demonstrated the capability of stabilizer structure to redistribute loads with a major member failed. The pins attaching the stabilizer to the aircraft center-section structure were sequentially removed to simulate lug failures. In addition, effects of the inflicted damage shown in Table 32 were included. Strain gage data were obtained for each condition for correlation with the ATLAS analysis mode. The fail-safe testing is summarized in Table 33.

X-ray inspections were performed before and after testing. Ultrasonic inspections also were performed after each load application. No increase was detected in the size of the inflicted damage after the application of these static loads.

The next test phase demonstrated that the structure can sustain damage to critical structural details and continue to carry load. Three large-area cuts were inflicted in the structure. In the first test, the front-spar upper chord and adjacent leading edge and upper skin were cut, as shown in Figures 153 through 155. Down bending

ORIGINAL PAGE
BLACK AND WHITE PHOTOGRAPH

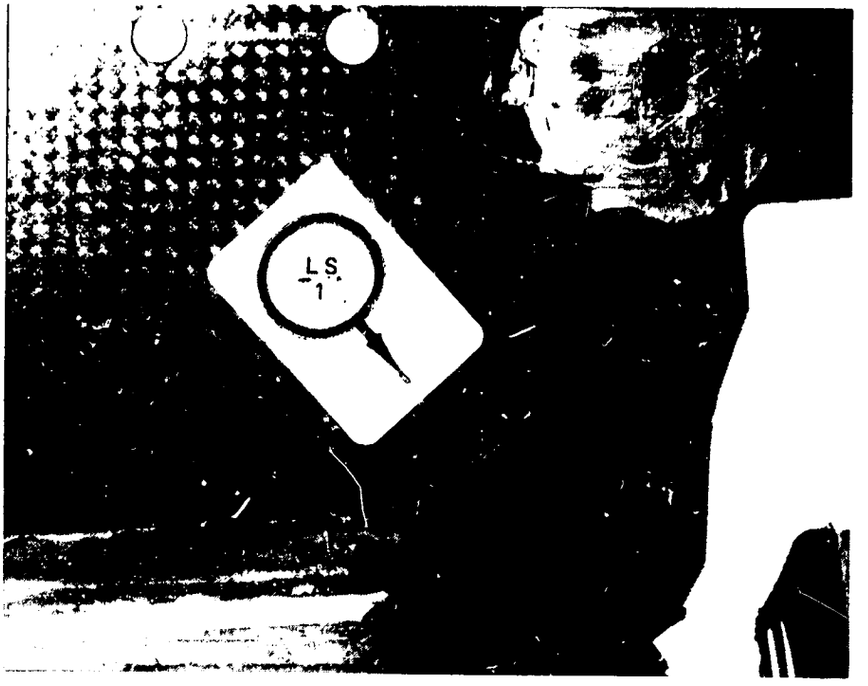

Figure 149. Lower Surface Damage (LS-1)

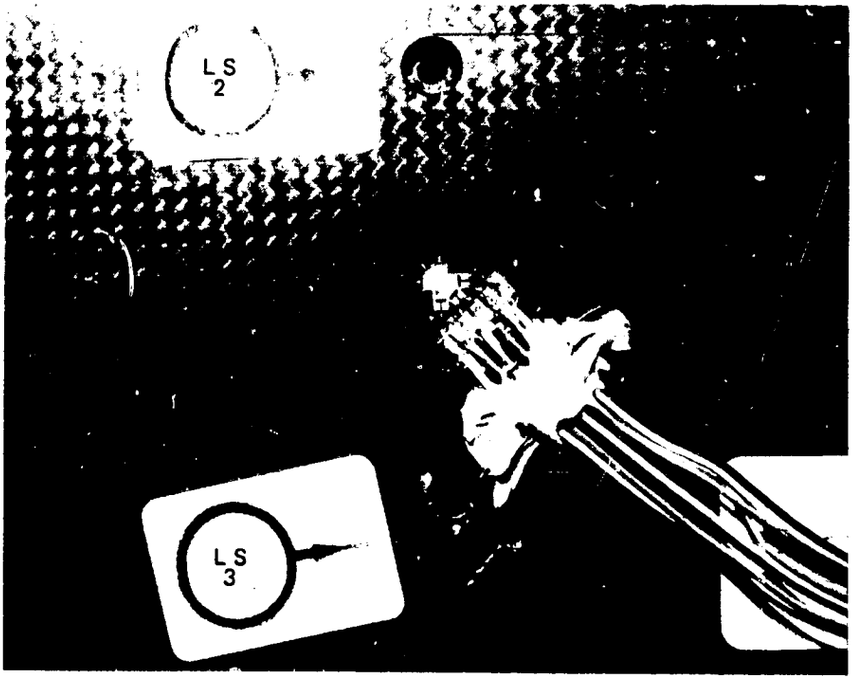

Figure 150. Lower Surface Damage (LS-2 and LS-3)

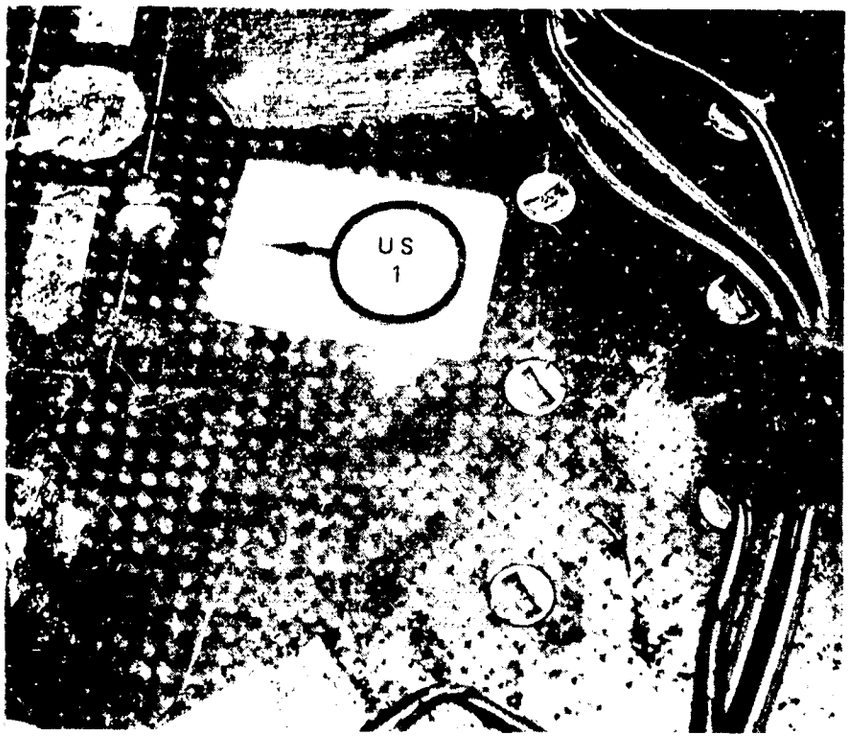

Figure 151. Upper Surface Damage (US-1)

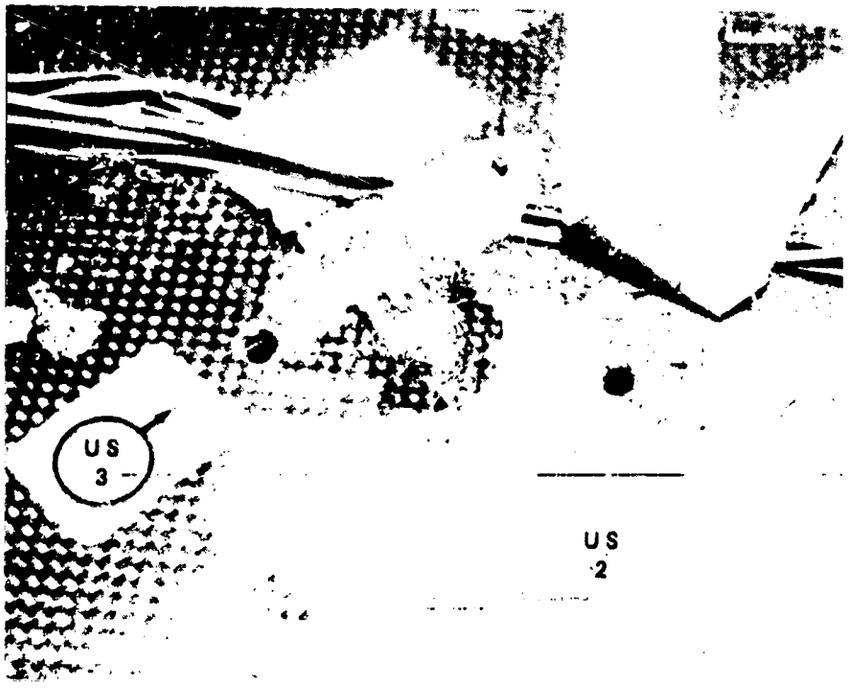

Figure 152. Upper Surface Damage (US-2 and US-3)

Table 33. Fail-Safe Test Summary

	Load case	Load level, percentage of DUL	Pin configuration
1	4010 Maximum down bending	67	All pins installed
2	4010 Maximum down bending	40	Upper rear spar pin deleted
3	4010 Maximum down bending	60	Upper front spar pin deleted
4	4740 Maximum up bending	67	All pins installed
5	4740 Maximum up bending	40	Lower front spar pin deleted
6	4740 Maximum up bending	40	Lower rear spar pin deleted

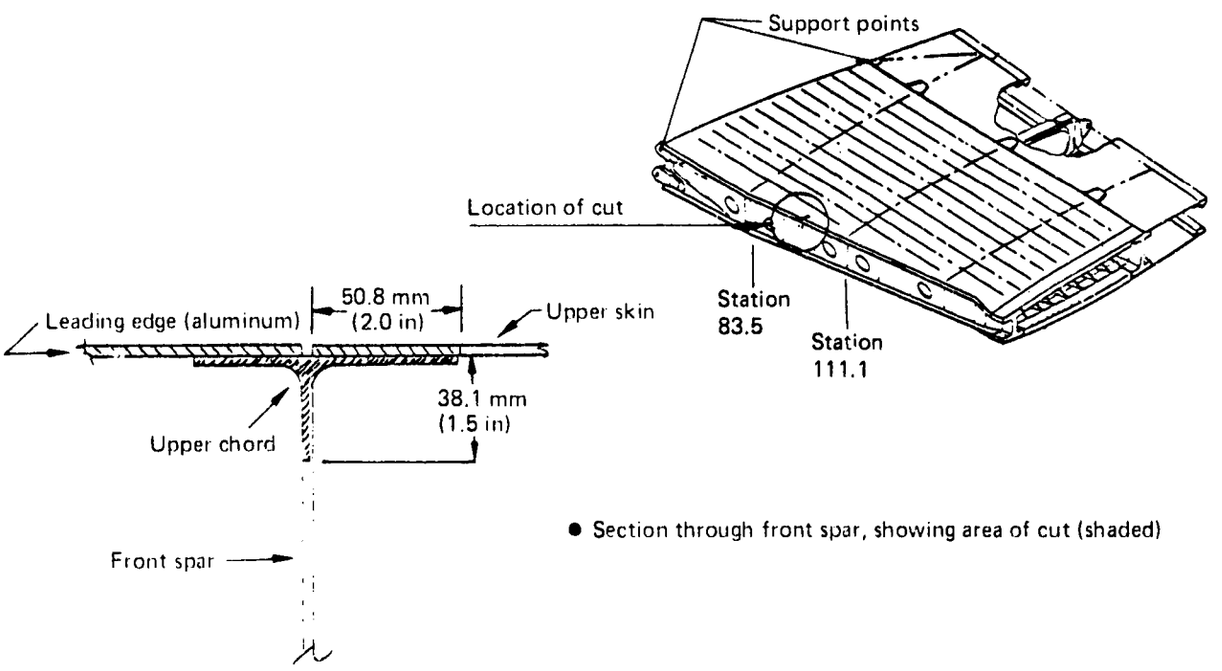

Figure 153. Stub Box Damage Tolerance Test—Front-Spar Upper Chord, Skin, and Leading Edge

• View looking aft at the front spar

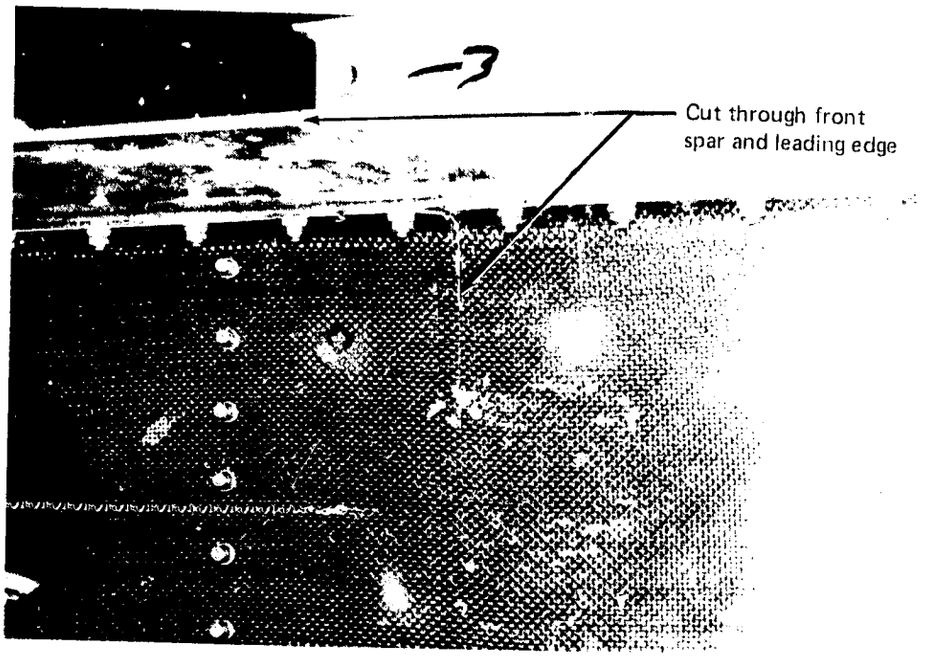

Figure 154. Stub Box Damage Tolerance Test—Cut Through Front Spar and Leading Edge

• View looking down at the upper surface

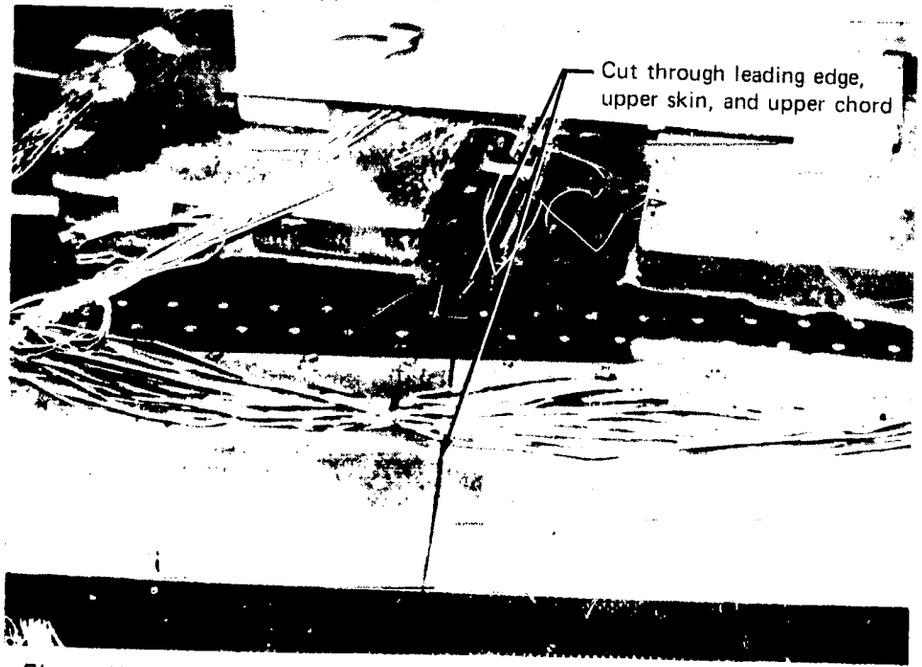

Figure 155. Stub Box Damage Tolerance Test—Cut Through Leading Edge, Upper Skin, and Upper Chord

(load case 4010) was applied to a level of 48% DUL. With this load applied, instrumentation showed a redistribution of load adjacent to the cut. Visual inspection showed cracks progressing from the ends of the cut to the upper skin and spar web. X-ray and ultrasonic inspections were performed to define the crack limits. Results of the inspection indicated that the graphite-epoxy was fractured an additional 63.5 mm (2.5 in) into both the skin panel and spar web.

Aluminum splice plates were installed over the damage to prevent further crack growth.

For the second test, the lower surface stringer 2 and the adjacent skin were cut, as shown in Figures 156 and 157. Down bending (load case 4010) again was applied. Strain gage data were recorded to determine load redistribution. Limit load (67% DUL) was applied, with no apparent crack growth. This cut was repaired, and testing continued to the third phase.

For the third damage tolerance test, cuts were made in the rear-spar lower chord. The location and size of the cuts are shown in Figures 158 and 159. The test was conducted in four steps. The stub box was loaded to 67% DUL for load case 4010 (maximum down bending) after each successive cut. The structure sustained the loadings with no apparent crack growth. The cut was repaired by adding aluminum plates, and testing continued.

For the last damage tolerance test, the aluminum repair plates were removed from the front spar. Load case 4010 was applied to determine the residual strength of the structure with the induced damage and existing crack. As load was applied, the crack progressed in the upper skin, aft and toward the rear-spar lug to the intersection of stringer 5 and the rib at stabilizer station 83.5 (fig. 160). The crack stopped at that point, and the structure sustained limit load (67% DUL) without further damage growth.

Destruction—The final test on the stub box was the application of load case 4010 to failure. The structure sustained 100% DUL without failure. Failure occurred at 114% DUL. The test is summarized as follows:

- All strains were linear to 100% DUL.
- The load system dumped at 108% DUL. Strains in the front- and rear-spar upper (tension) lugs departed from a straight line between 100% and 108%.
- The stub box was reloaded to 100% DUL. The upper rear-spar (tension lug) gages showed loss of the graphite-epoxy portion with corresponding load redistribution.
- The load system dumped again at 114% DUL.
- The stub box was reloaded to 100% DUL. The upper front-spar (tension lug) gages showed loss of the graphite-epoxy portion with additional load redistribution.

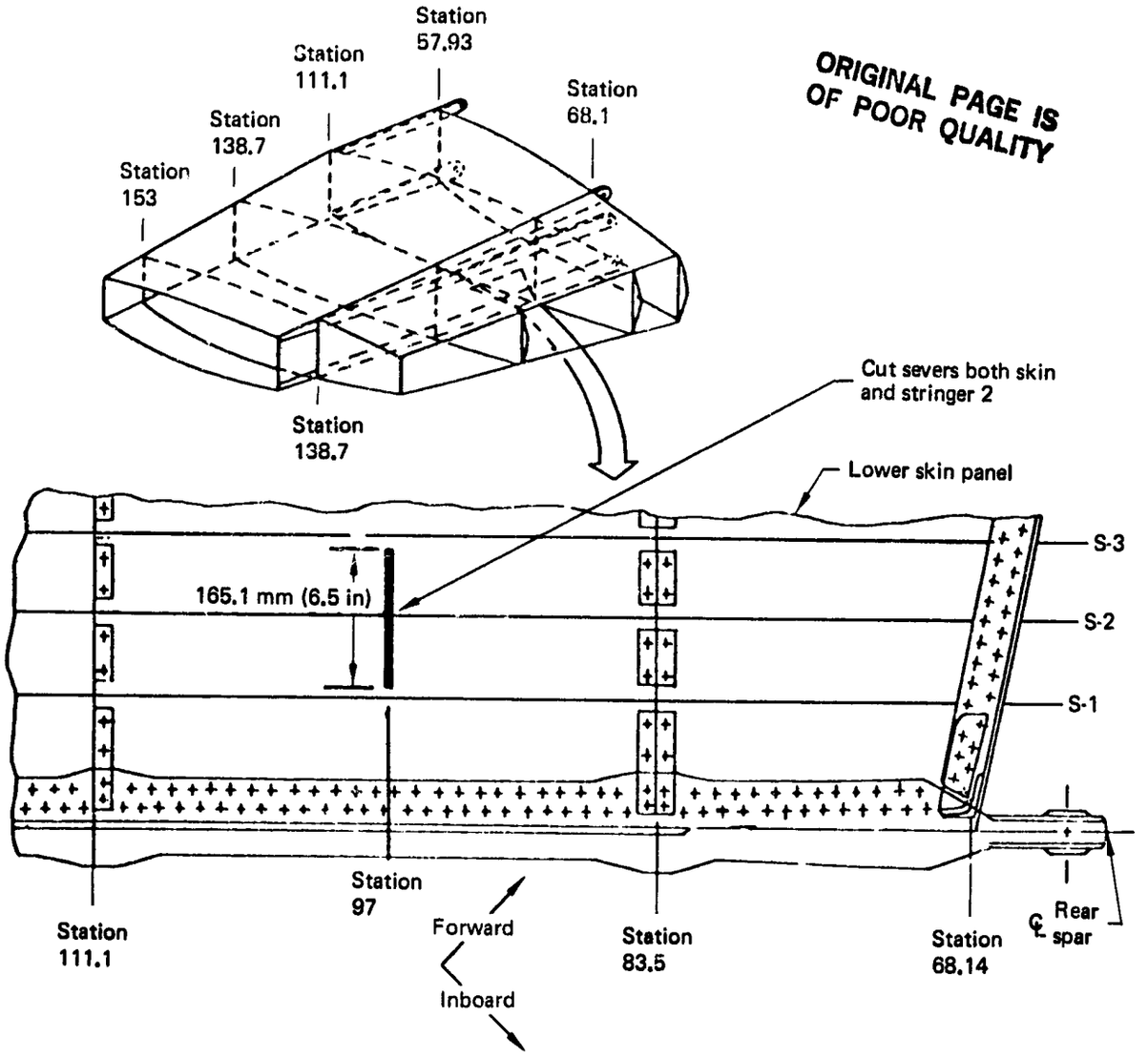

Figure 156. Stub Box Damage Tolerance Test—Lower Surface Skin and Stringer

- Failure of the (tension loaded) upper front-spar lug occurred at 114% DUL (third loading) (fig. 161). Skin damage and closure rib damage were apparent at the (compression-loaded) lower rear-spar/closure rib intersection (figs. 162 and 163).

Summary, Stub Box Test—All tests were completed successfully. The box sustained load case 4010, the critical down-bending condition, to 100% DUL without failure after completion of the full series of tests. By testing the critical structure early in the program, the following advantages were gained:

- Modifications to design (i.e., the lug change discussed in sec. 4.2.9.2, Static Test, Design Ultimate Load Conditions) were identified with minimum impact on structure and schedule

• View looking up at the lower edge

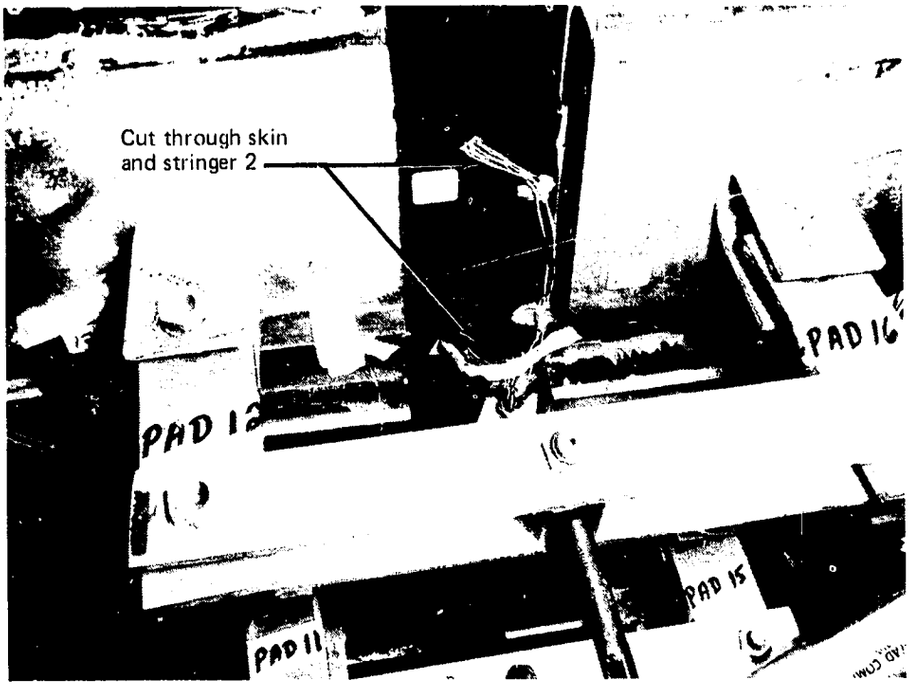

Figure 157. Stub Box Damage Tolerance Test—Cut Through Skin and Stringer

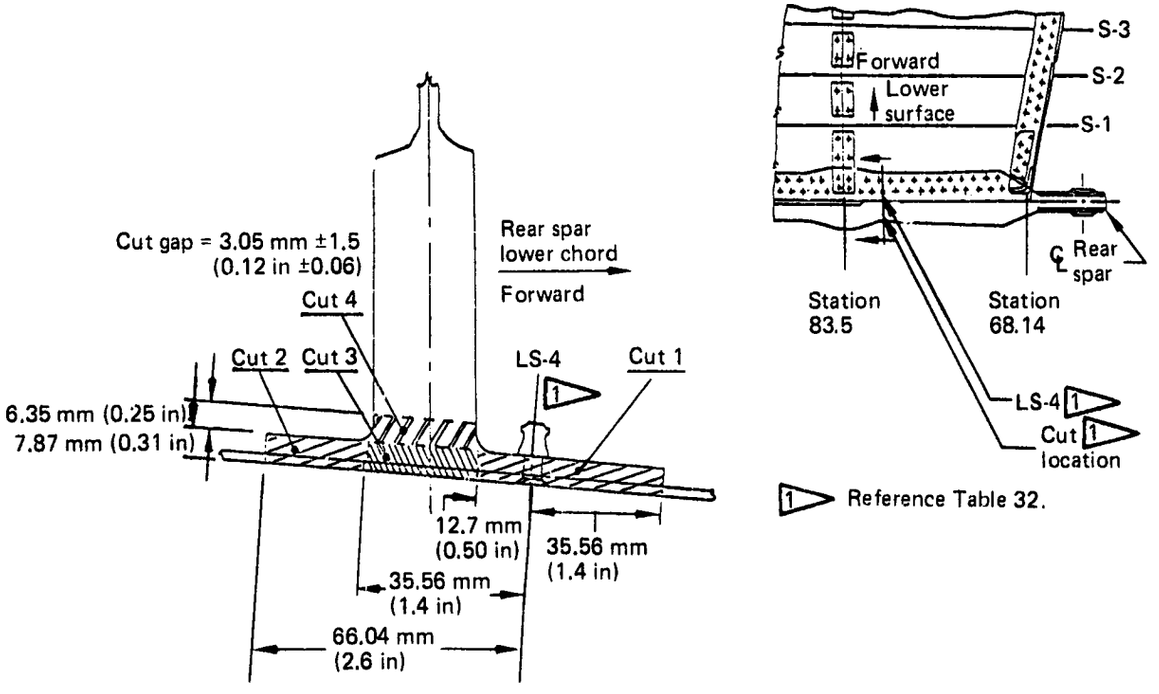

Figure 158. Stub Box Damage Tolerance Test—Rear-Spar and Lower Chord

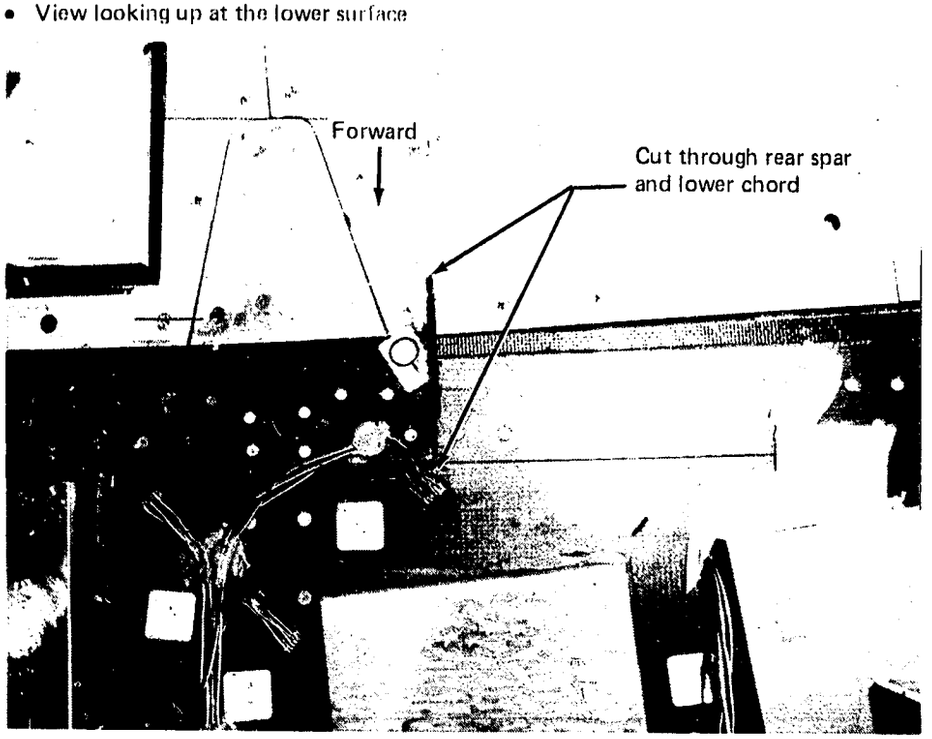

Figure 159. Stub Box Damage Tolerance Test—Cut Through Rear-Spar and Lower Chord

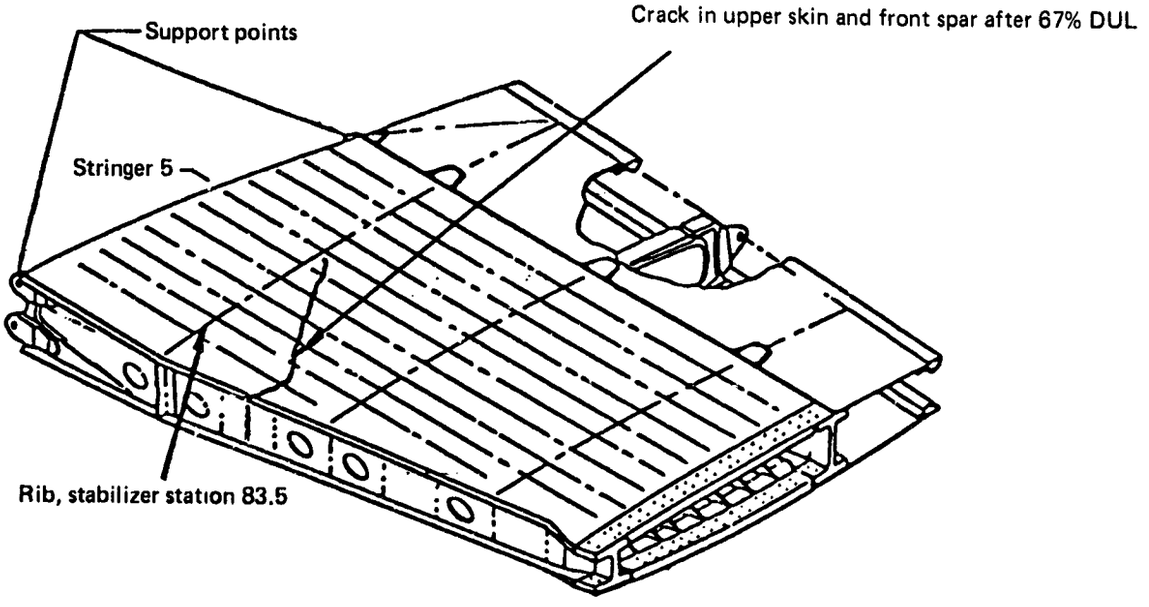

Figure 160. Stub Box Damage Tolerance Test—Upper Surface Crack

ORIGINAL PAGE
BLACK AND WHITE PHOTOGRAPH

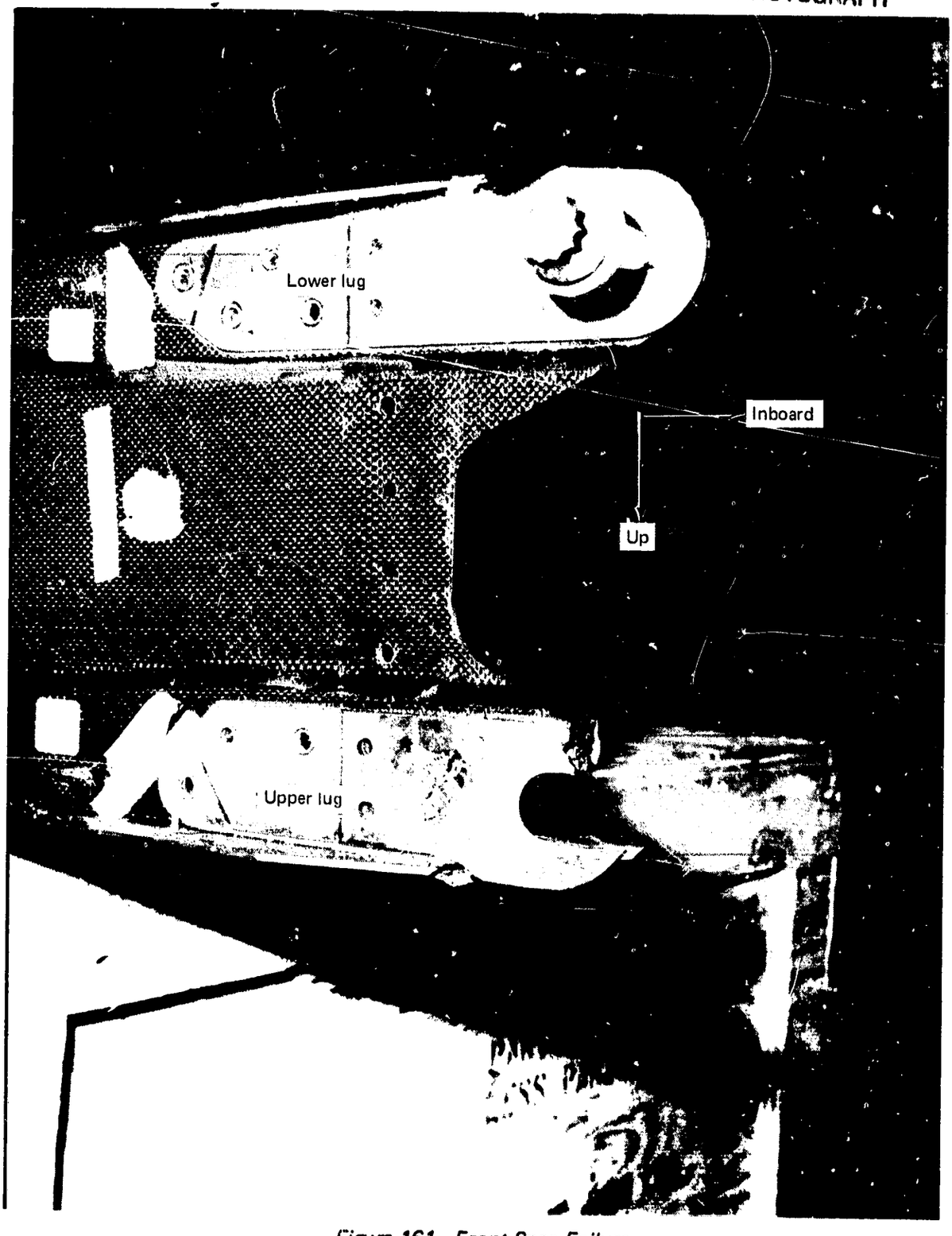

Figure 161. Front-Spar Failure

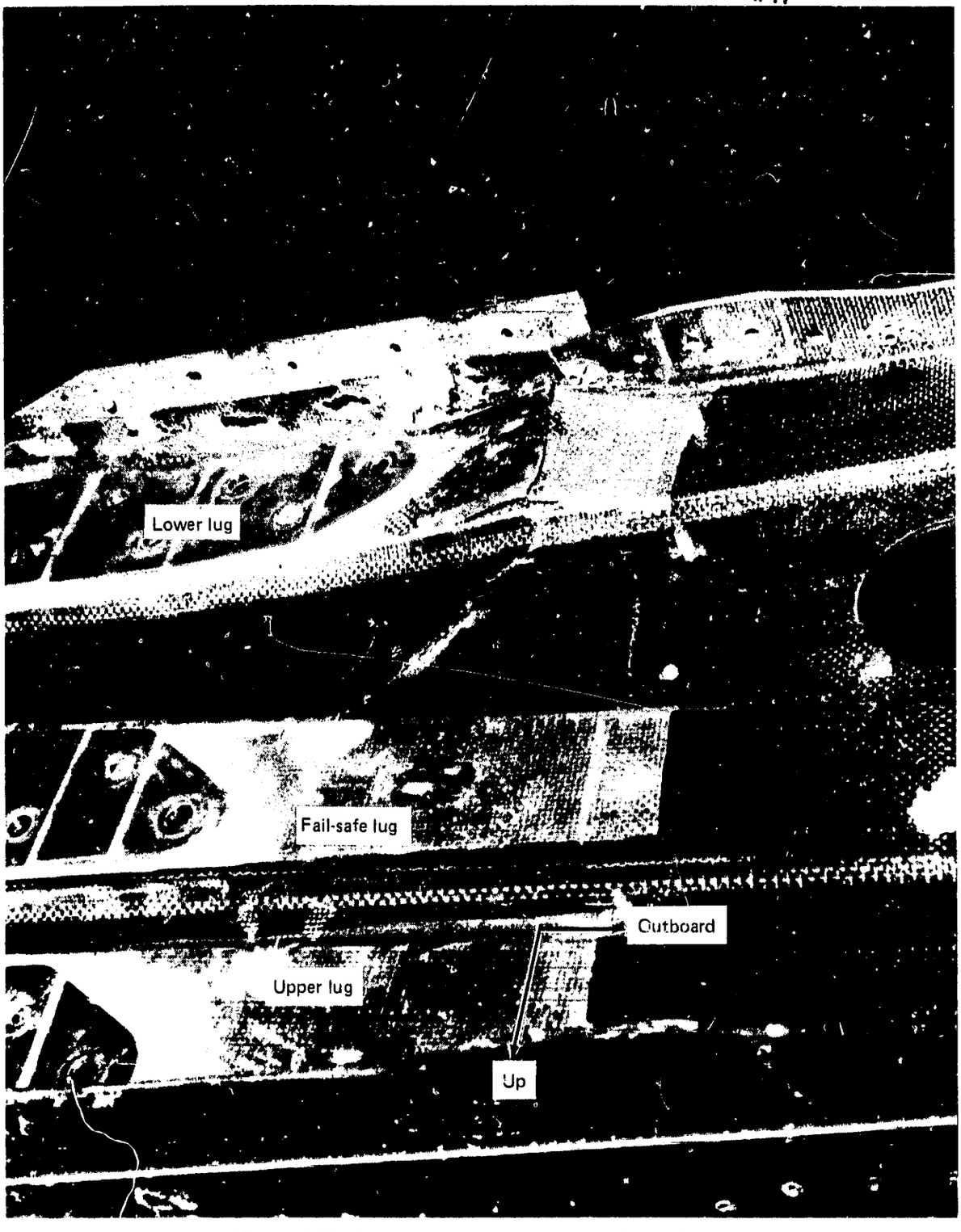

Figure 162. Rear-Spar Lower Lug and Chord Damage

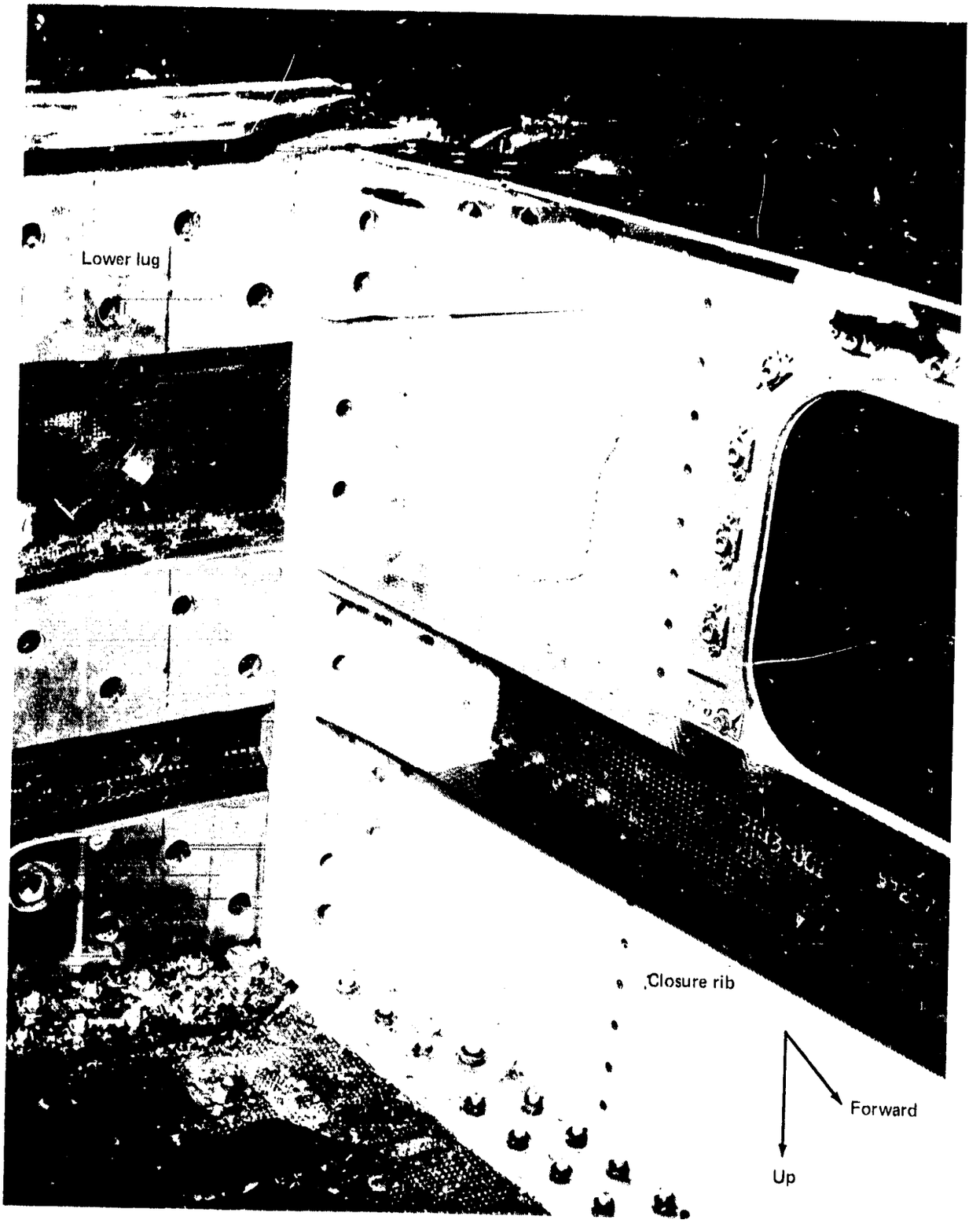

Figure 163. Closure Rib Damage

- Verification of structural load paths
- Verification of finite element model
- Data support for the no-growth damage tolerance philosophy

4.2.10 Environmental Test Panel

As part of the stabilizer certification program, an environmental test panel was tested to demonstrate:

- The effects of moisture and temperature on the strain distributions of a highly loaded structure
- The capability of the critically loaded graphite-epoxy structure to withstand limit and ultimate loads under hot-wet and cold-dry conditions
- The capability to predict the effects of moisture and temperature extremes by analysis

The test panel represented a lower surface section of the stabilizer. Loads that produced biaxial strains in critical areas were applied.

The configuration chosen for the test panel is shown in Figure 164. It was designed sufficiently large to ensure that the desired strain distributions would be obtained in the corner area formed by the closure rib and the rear spar. All spanwise applied loads are reacted by the rear spar, which was designed to 63 503 kg (140 000 lb) ultimate load (stabilizer lug design ultimate load equals 64 864 kg [140 000 lb]). Simulated elevator hinge loads are applied through three lugs on the trailing edge.

A finite element model of the panel was developed for use with the ATLAS program. The purpose was to establish a correlation between test and analysis.

The outboard and forward boundary elements have thicknesses and/or material properties designed to aid in providing comparable strains in the test panel and the full-scale article. The load case producing the strongest possible degree of biaxiality was chosen for application. Internal loads for this case were found from the full-scale ATLAS model and were factored up to obtain the 63 503-kg (140 000-lb) rear-spar lug reaction.

Figure 165 shows strain contour plots in the region of interest of the test panel and the stabilizer. The comparison showed good agreement between the stabilizer and the environmental test panel.

The test panel, assembled and ready for test, is shown in Figure 166. Testing was conducted according to the plan contained in Table 34. Cold tests were conducted at -59°C (-75°F), which was obtained by circulating liquid nitrogen through the environmental chamber. A wet condition was created by exposing the specimen to 60°C (140°F) and to 80% to 85% relative humidity until the specimen weight stabilized, as determined by a standard moisture rider. Hot-wet testing then was conducted by raising the temperature to 82°C (180°F), zeroing the gages, and applying ultimate load.

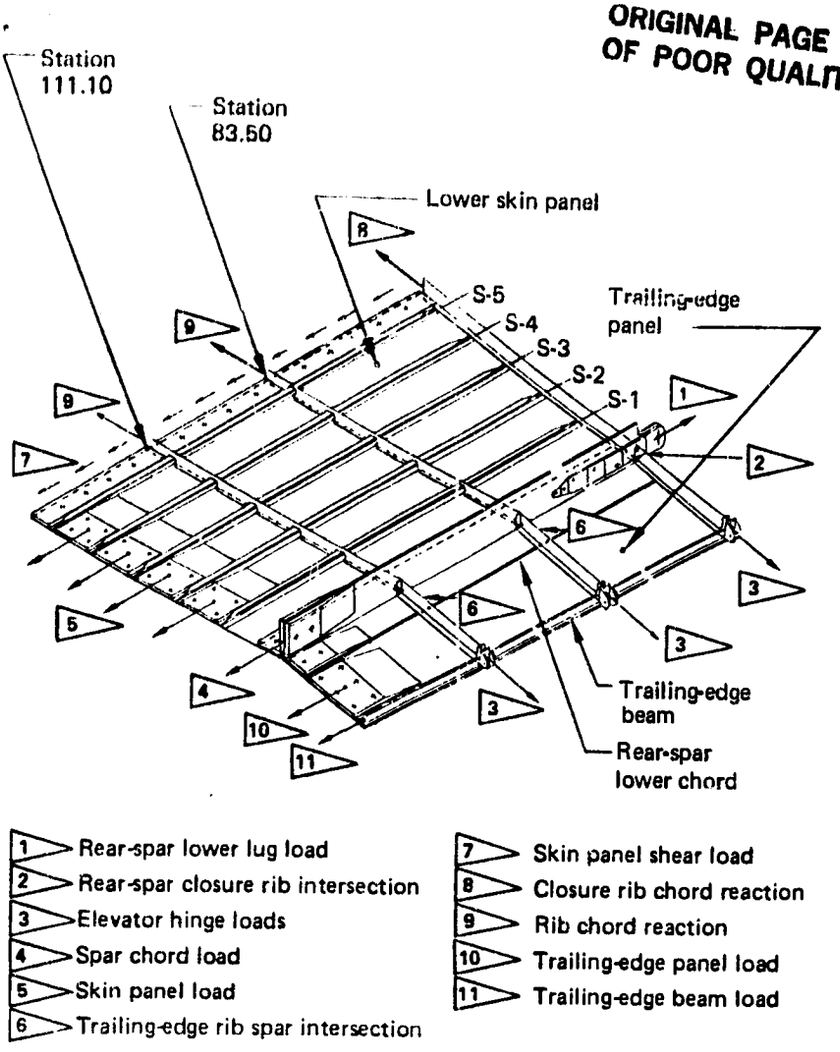

Figure 164. Environmental Test Panel

The environmental test panel was subjected to the following test conditions:

Condition	Load	Environment
1	67% DUL	21°C (70°F) ambient humidity
2	67% DUL	59°C (-75°F) ambient humidity
3	100% DUL	82°C (180°F) wet condition
4	137% DUL (failure)	82°C (180°F) wet condition (see table 34)

The test panel sustained conditions 1, 2, and 3 with no apparent damage. During condition 4, failure occurred at 137% DUL in the spar lug. This load level had been predicted by previous lug tests (sec. 4.2.3.5).

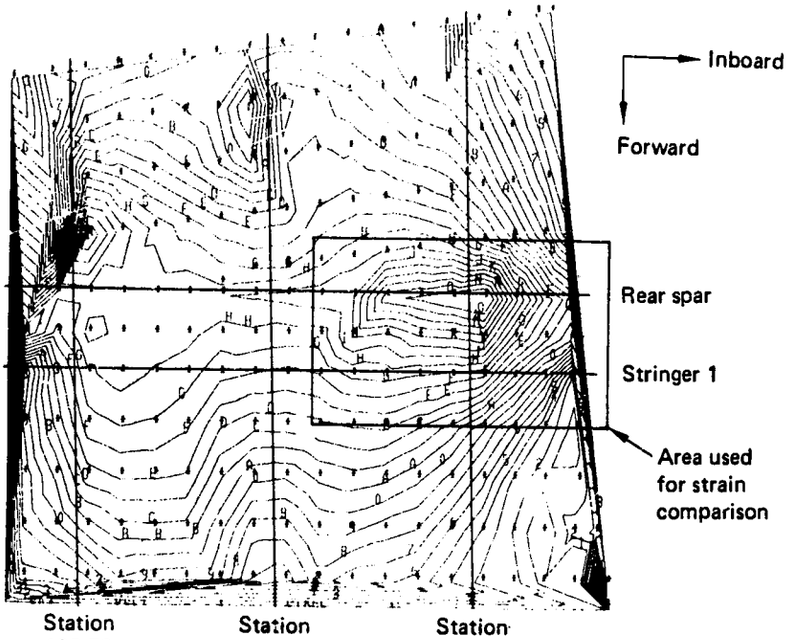

Strain contour identification

1	0.0	C	0.0012
2	0.0001	D	0.0013
3	0.0002	E	0.0014
4	0.0003	F	0.0015
5	0.0004	G	0.0016
6	0.0005	H	0.0017
7	0.0006	I	0.0018
8	0.0007	J	0.0019
9	0.0008	K	0.0020
0	0.0009	L	0.0021
A	0.0010	M	0.0022
B	0.0011	N	0.0023
		0	0.0024

(a) Environmental Test Panel--Spanwise Strain

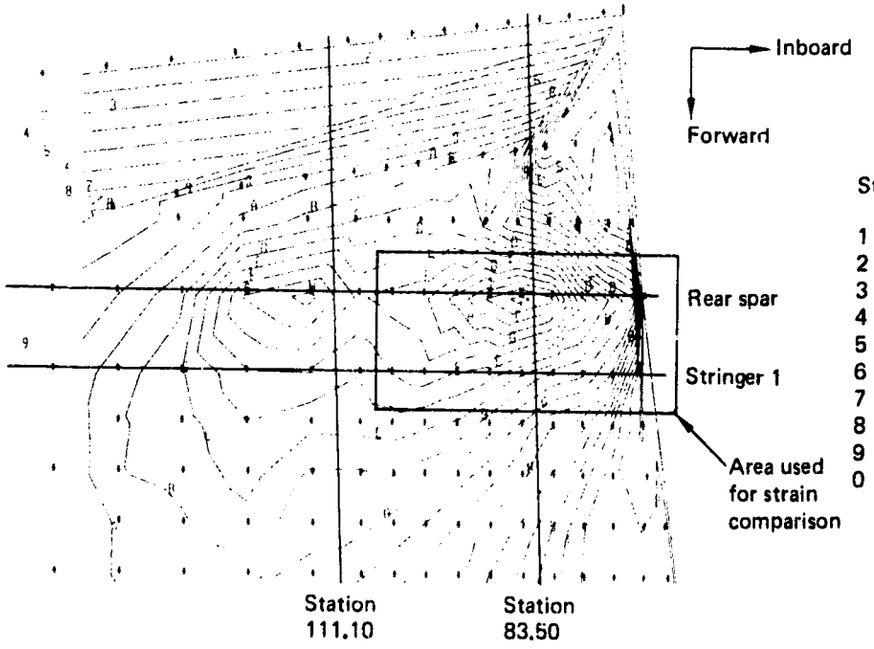

Strain contour identification

1	0.0	A	0.0014
2	0.0001	B	0.0015
3	0.0003	C	0.0016
4	0.0004	D	0.0018
5	0.0005	E	0.0019
6	0.0007	F	0.0020
7	0.0008	G	0.0022
8	0.0009	H	0.0023
9	0.0011	I	0.0024
0	0.0012	J	0.0026
		K	0.0027

(b) Stabilizer Lower Surface--Ultimate Spanwise Strain

Figure 165. Strain and Ultimate Shear Stress Contours

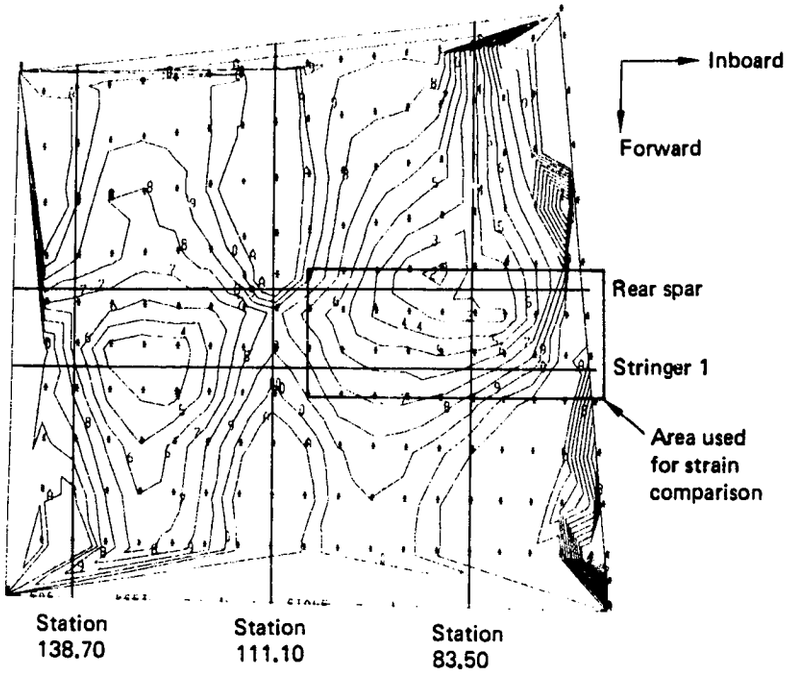

Strain contour identification

1	-0.0010
2	-0.0009
3	-0.0008
4	-0.0007
5	-0.0006
6	-0.0005
7	-0.0004
8	-0.0003
9	-0.0002
0	-0.0001
A	0

(c) Environmental Test Panel—Ultimate Chordwise Strain

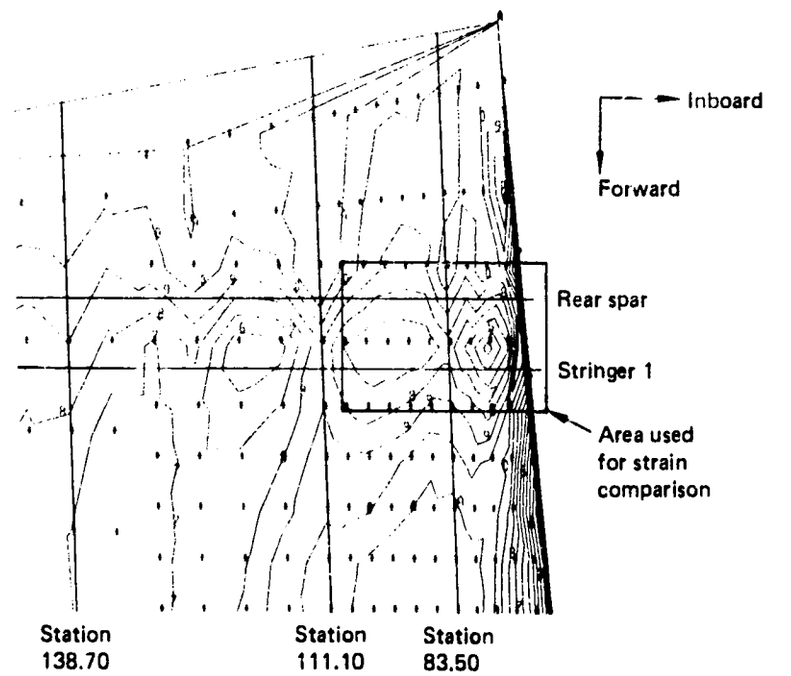

Strain contour identification

1	-0.0014
2	-0.0012
3	-0.0011
4	-0.0010
5	-0.0008
6	-0.0007
7	-0.0005
8	-0.0004
9	-0.0003
0	-0.0001
A	0

(d) Stabilizer Lower Surface—Ultimate Chordwise Strain

Figure 165. Strain and Ultimate Shear Stress Contours (Continued)

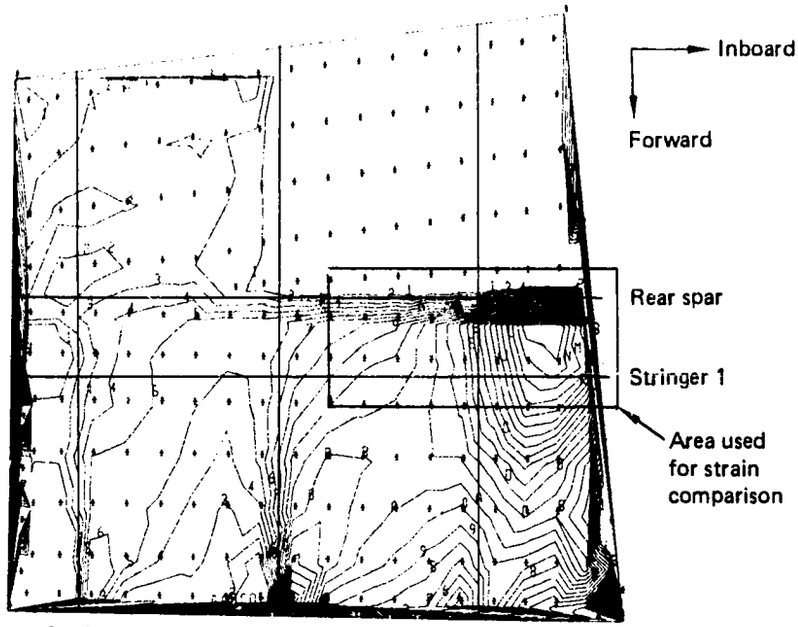

Stress contour identification

1	0	C	6000
2	500	D	6500
3	1000	E	7000
4	1500	F	7500
5	2000	G	8000
6	2500	H	8500
7	3000	I	9000
8	3500	J	9500
9	4000	K	10000
0	4500	L	10500
A	5000	M	11000
B	5500	N	11500
		O	12000

(e) Environmental Test Panel—Ultimate Shear Stress

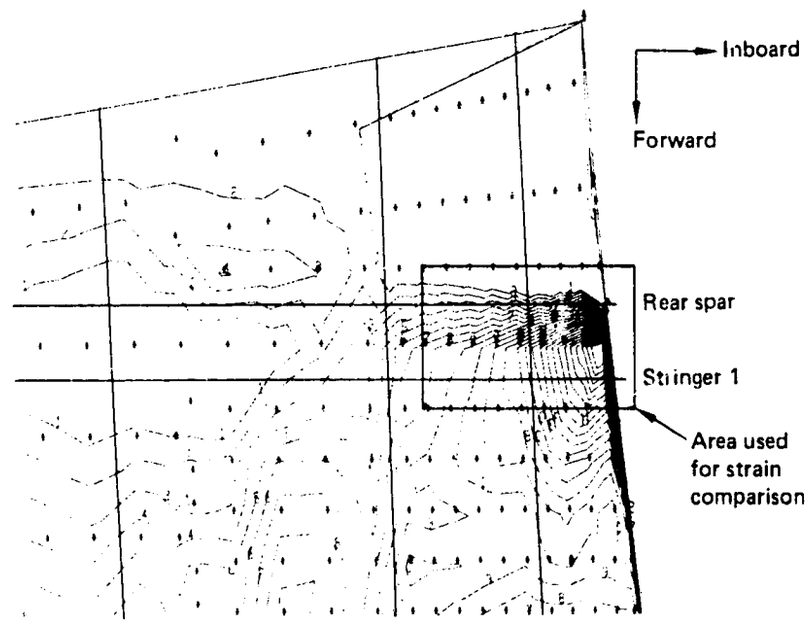

Stress contour identification

1	0	C	8200
2	700	D	8800
3	1400	E	9500
4	2000	F	10200
5	2700	G	10400
6	3400	H	11600
7	4100	I	12200
8	4800	J	12900
9	5400	K	13600
0	6100	L	14300
A	6800	M	15000
B	7500	N	15600
		O	16300

(f) Stabilizer Lower Surface—Ultimate Shear Stress

Figure 165. Strain and Ultimate Shear Stress Contours (Concluded)

ORIGINAL PAGE
BLACK AND WHITE PHOTOGRAPH

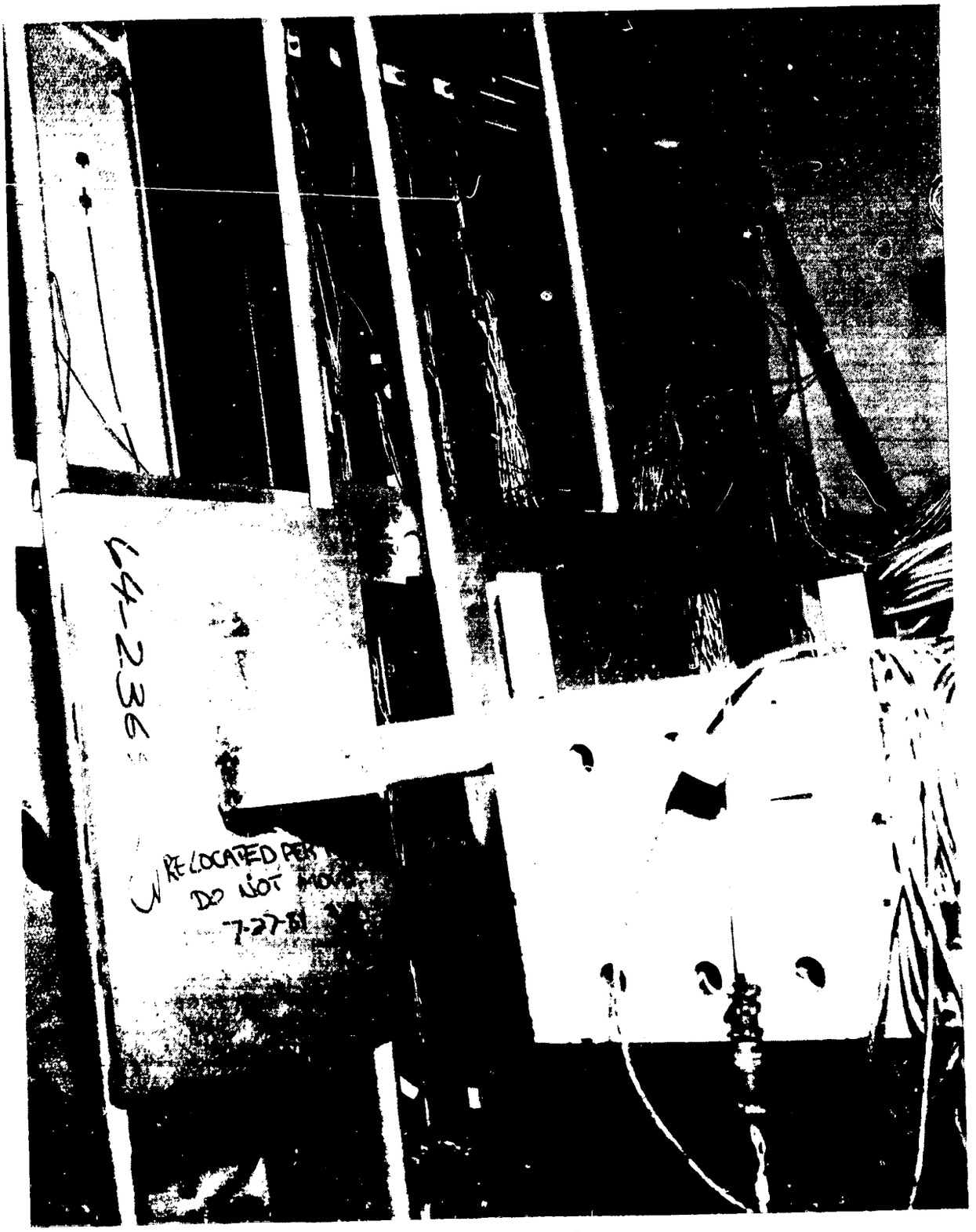

Figure 166. Test Setup

Table 34. Environmental Test Panel Test Plan

Environmental condition			Load	Data requirements
Test condition	Temperature	Humidity	[1]	
1	Ambient 21°C (70°C)	Ambient 21°C (70°F)	67% DUL	Strain and deflection data taken at zero load, 16%, 32%, 48%, 67%, 32%, 0.
2	-59°C (-75°F)	Ambient [2]	67% DUL	Strain, deflection, and thermocouple data taken at zero load, 21°C (70°F); zero load, 17.8°C (0°F); zero load, -23.8°C (-75°F); 16%, 32%, 48%, 67%, 32% and 0 while at -23.8°C (-75°F); zero load, 21°C (70°F).
3	82°C (180°F)	Wet [3]	100% DUL	Strain, deflection, and thermocouple data taken at 82°C (180°F); 16%, 32%, 48%, 67%, 80%, 100% DUL, zero load, 21°C (70°F).

[1] Refer to Figure 164. Loads given are referenced to DUL.

[2] As received after manufacturing.

[3] Wet specimens will be exposed to 60°C (140°F) ±12°C (±10°F) and 80% to 85% relative humidity until specimen weight stabilizes, as determined by a standard moisture rider.

Because of the testing sequence involved in the hot-wet condition, thermal strains associated with temperature rise from ambient to 82°C (180°F) are not part of the gage readings. However, correlation between test and analysis was obtained for the -59°C (-75°F) condition and the analysis was influenced by thermal expansion factors in the input. Consequently, the analysis was used to provide thermal contributions to strains developed during the hot-wet test.

Strain gage data, together with equivalent ATLAS values, are shown in Figure 167. The highest axial strains were observed at station 81.00 on the spar during the hot-wet test. At ultimate load, the average strain at this location was 2663 μm/m (μin/in), with a slight degree of bending. The reading at the center of the section was 2508 μm/m (μin/in) strain. The corresponding ATLAS values agreed with the test within 10%.

All the spanwise loads applied in testing this panel are reacted by the spar lug, which causes dominant axial strains along the spar. Chordwise strains are induced

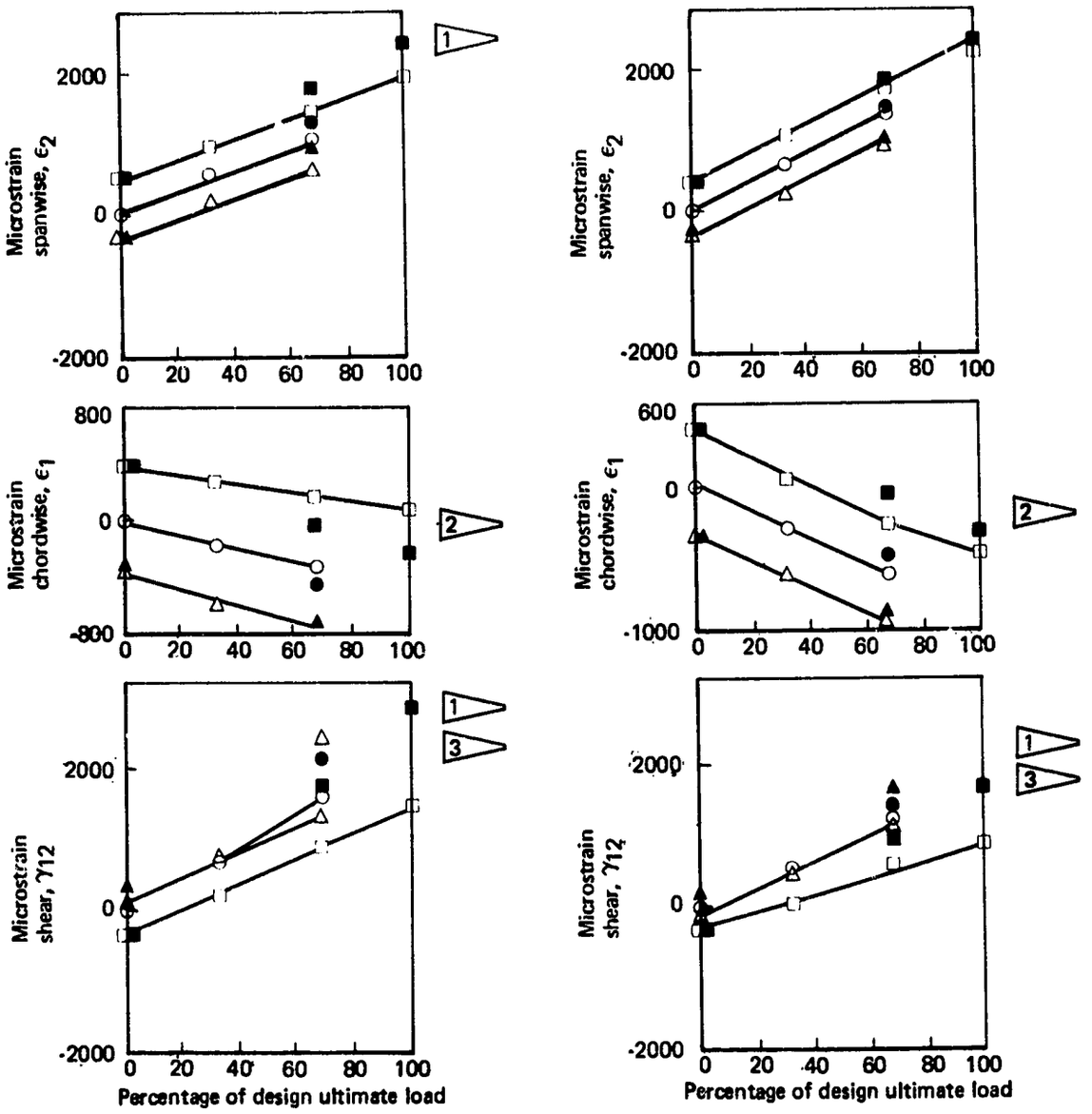

1 Back-to-back gages indicated bending. Gage output affected by long-term power application in moist environment.

2 Strain levels are too low for percentage differences to be significant.

3 Very steep spanwise strain gradient. Slight variation in gage position results in significant difference in strain measurement (see fig. 168).

4 Load case 3 (hot, wet) data contains ATLAS thremal strains.

Legend:	Test	ATLAS
Load case 1	○	●
Load case 2	△	▲
Load case 3	□	■

Figure 167. Environmental Test Panel Data

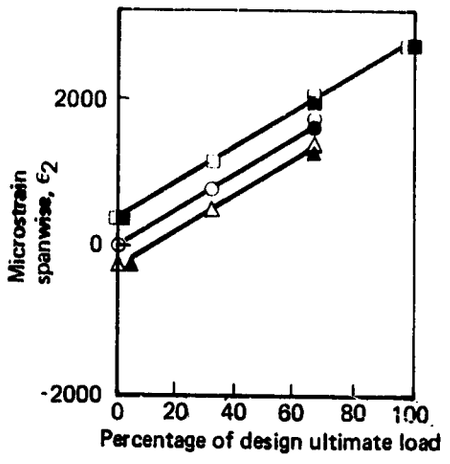

Rear spar station 81.00

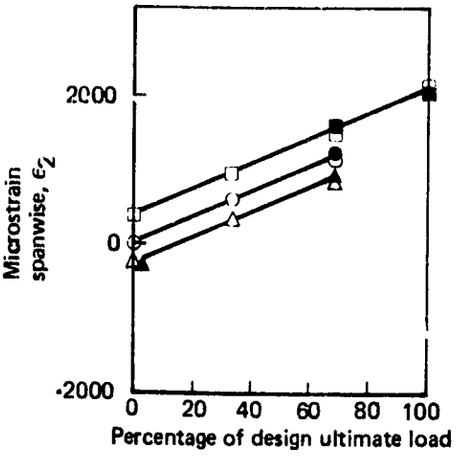

Rear spar station 108.60

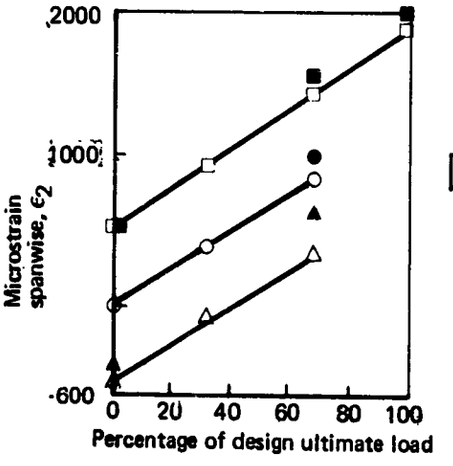

Stringer 1, station 82.4

3

Legend: Test ATLAS
Load case 1 ○ ●
Load case 2 △ ▲
4 Load case 3 □ ■

1 Back-to-back gages indicated bending. Gage output affected by long-term power application in moist environment.

2 Strain levels are too low for percentage differences to be significant.

3 Very steep spanwise strain gradient. Slight variation in gage position results in significant difference in strain measurement (see fig. 168).

4 Load case 3 (hot, wet) data contains ATLAS thermal strains.

Figure 167. Environmental Test Panel Data (Concluded)

by Poisson's effect, as seen by the decrease of strain levels with increasing loads. The same situation exists in the full-scale stabilizer with comparable test results.

In some cases, differences between test and analytical results can be explained by noting that the test gage was located in a zone of severe strain gradients. A small displacement of the gage results in large differences in strain readings. This effect is noted on appropriate data figures and is shown in Figure 168.

It was determined that strain gages should not be maintained with current applied for appreciable times in a hot-wet environment. Drift of up to 1500 μm/m (μin/in) of strain was noted in gages in this condition for longer than an hour.

4.3 WEIGHTS

4.3.1 Technical Approach

Graphite-epoxy component weights were calculated by the ply-by-ply method that was used successfully on the NASA/ACEE 727 graphite-epoxy elevator program. This method determines the areas for each ply of material within the component and summarizes them by style of fabric and/or grade of tape. Nominal drawing dimensions and nominal material areal weights were used for weight evaluations. An acutal weight program of all point design test components was instituted early in the program, and these actual weights were compared to the calculated values.

A close correlation was found between these values and a contingency addition to the calculated values to account for manufacturing and material tolerances was not required.

4.3.2 Preliminary Analysis

The inspar primary box structure of the horizontal stabilizer was selected for redesign using graphite-epoxy material. Only this structure is reported for weight comparison purposes. The existing aluminum leading edge and fiberglass-aluminum trailing-edge structures were retained, together with the tip fairing.

Design changes not considered in weight comparisons were: thermal expansion provisions, comprising a linkage system to the elevator hinge to permit usage of the existing aluminum elevator, and the change from aluminum to graphite-epoxy on the trailing-edge beams to minimize thermal expansion in the trailing-edge structure.

Initial weight evaluation of the graphite-epoxy inspar structure shown in Table 35 was developed using preliminary design information and layout drawings. Later, a complete reanalysis was performed by extrapolating the stub box design to the full-size structure using the finite element analysis data and the stub box test component drawings to represent the production structure. This resulted in a weight increase of 7.5 kg (16.6 lb).

The initial weight comparison between the graphite-epoxy structure and the existing aluminum structure showed a reduction of 29%. After incorporating the stub box design revision, a weight reduction of 27% resulted.

For production weight data analysis, see Section 3.5 of Reference 6.

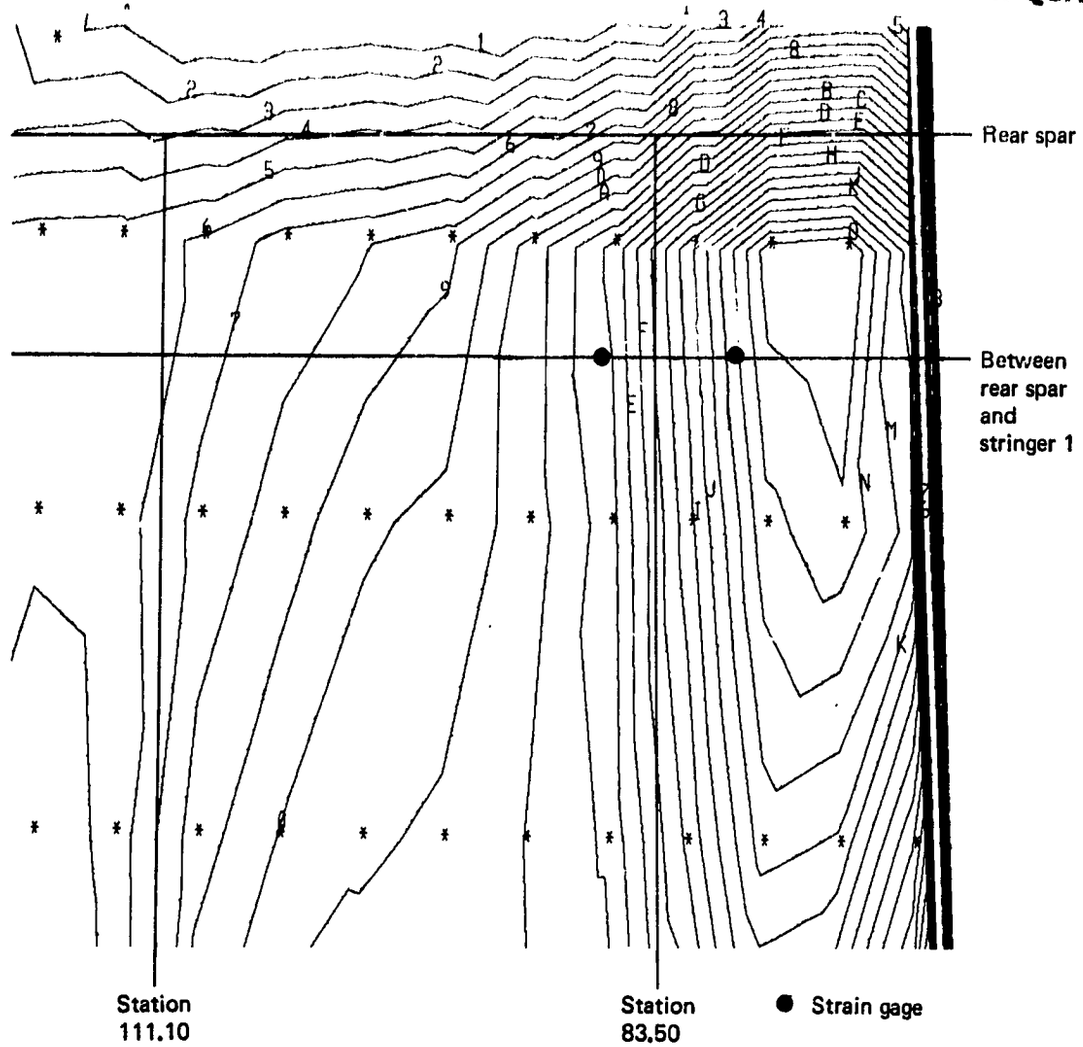

Strain contour identification

1	0	C	4000
2	333	D	4333
3	667	E	4667
4	1000	F	5000
5	1333	G	5333
6	1667	H	5667
7	2000	I	6000
8	2333	J	6333
9	2667	K	6667
0	3000	L	7000
A	3333	M	7333
B	3667	N	7667
		O	8000

Figure 168. Expanded View of Environmental Test Panel Shear Stress Contours

Table 35. Composite Stabilizer Inspar Structure Weight Comparison

Horizontal stabilizer—737	Metal design weight kg (lb)/airplane	Composite design weight kg (lb)/airplane	Weight reduction kg (lb)/airplane	Percent change
Front spar	31.3 (69.0)	20.2 (44.6)	−11.1 (−24.4)	−35.0
Rear spar	71.2 (156.9)	42.9 (94.6)	−28.3 (−62.3)	−40.0
Skins	72.3 (159.5)	71.8 (158.3)	−0.5 (−1.2)	−0.7
Ribs	60.9 (134.2)	30.3 (66.8)	−30.6 (−67.4)	−23.0
Access doors	0.7 (1.6)	0.9 (2.1)	+0.2 (+0.5)	+28.0
Total stabilizer inspar structure/ airplane	236.4 (521.2)	166.1 (366.4)	−70.3 (−154.8)	−29.0

5.0 FABRICATION DEVELOPMENT

This section presents the results of manufacturing development of tooling and fabrication processes and of quality assurance techniques and procedures. The work includes precontract, Boeing-funded, feasibility, and trade studies; ancillary test component fabrication; and manufacturing verification hardware production.

5.1 TRADE AND PRODUCIBILITY STUDIES

The following sections describe trade and producibility studies conducted prior to and during the contracted development and production of the five 737 stabilizer shipsets.

5.1.1 I-Stiffened Panel Development

A trade study was conducted to determine the producibility and cost effectiveness of the I-stiffened design for the stabilizer panels. Woven fabric and preplied unidirectional tape material forms were evaluated. Both materials were laid up on the same tooling and processed to the same Boeing specification. The woven fabric proved to be the most economical material because it required 36% less fabrication labor for debulking than the preplied material when spring-back occurred during layup. The layup sequence is shown in Figure 169, and the first test panel in Figure 170.

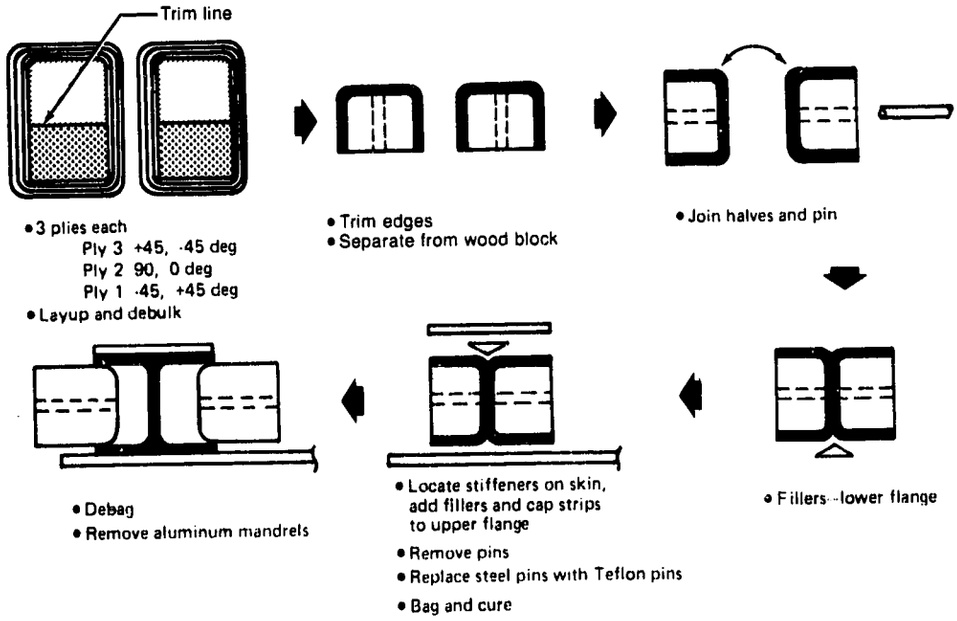

Figure 169. Layup of I-Section Stiffeners

Tooling design and manufacturing procedures were refined with the fabrication of two panels measuring 216 x 76 cm (85 x 30 in), each incorporating five I-stiffeners. To prevent stiffener misalignment, a locating (checking) template was used in conjunction with locating plates and spacers (figs. 171 and 172). These were incorporated into the design for the production tool. In practice, the locating plates and spacers are retained through the debulking and compacting cycle and then are removed for bagging and cure.

All panels fabricated during this producibility study showed some porosity on the tool surface. It was not sufficient to cause rejection, however, and the routine application of static conditioner (pin-hole filler) provided an aerodynamically acceptable finish.

5.1.2 Inspar Rib Trade Study

An inspar rib study was performed to compare the producibility of a corrugated rib with a honeycomb sandwich rib. These ribs were both fabricated on production quality tools using 3K-70-P woven fabric. One inspar rib of each type (figs. 173 and 174) was made and the fabrication labor determined. The relative cost of each design was 1.0, honeycomb; 2.1, corrugated.

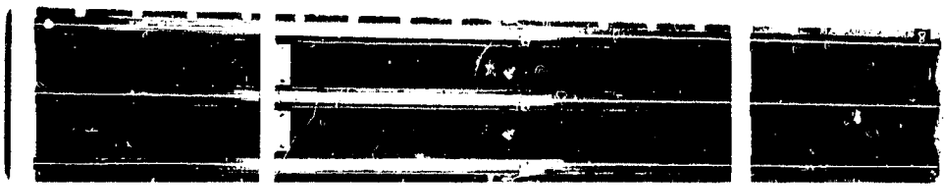

Figure 170. I-Stiffened Skin Test Panel

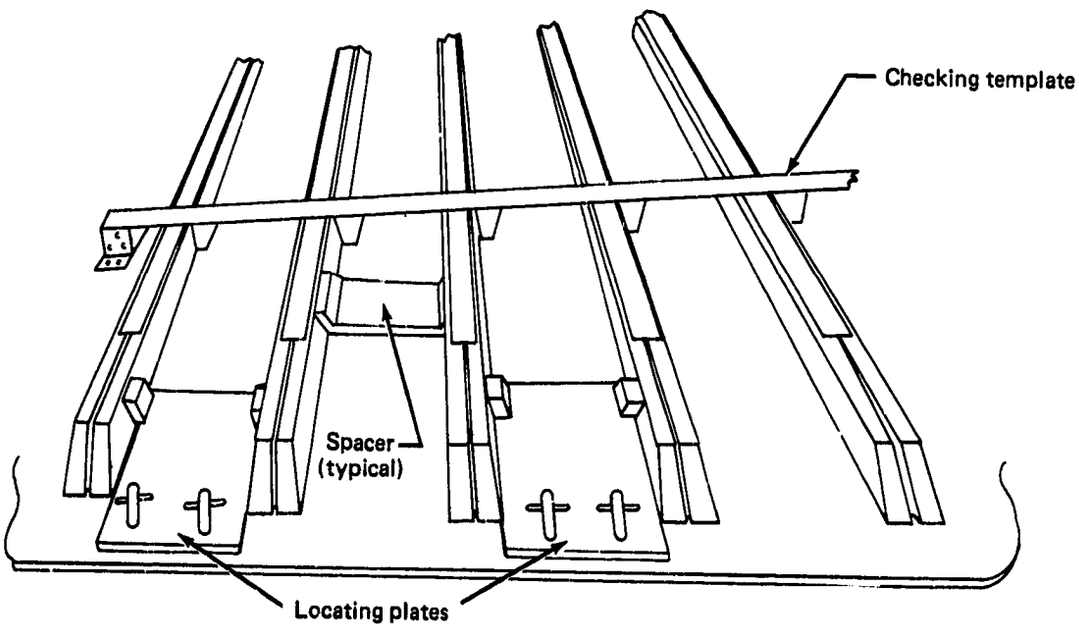

Figure 171. I-Stiffened Panel Tooling Approach

Comparing part quality, the corrugated rib showed surface porosity on the outer radii areas, a routine condition caused by fabric bridging that occurs on sinewave and corrugated designs. This study showed that the honeycomb design had definite producibility advantages over the corrugated design.

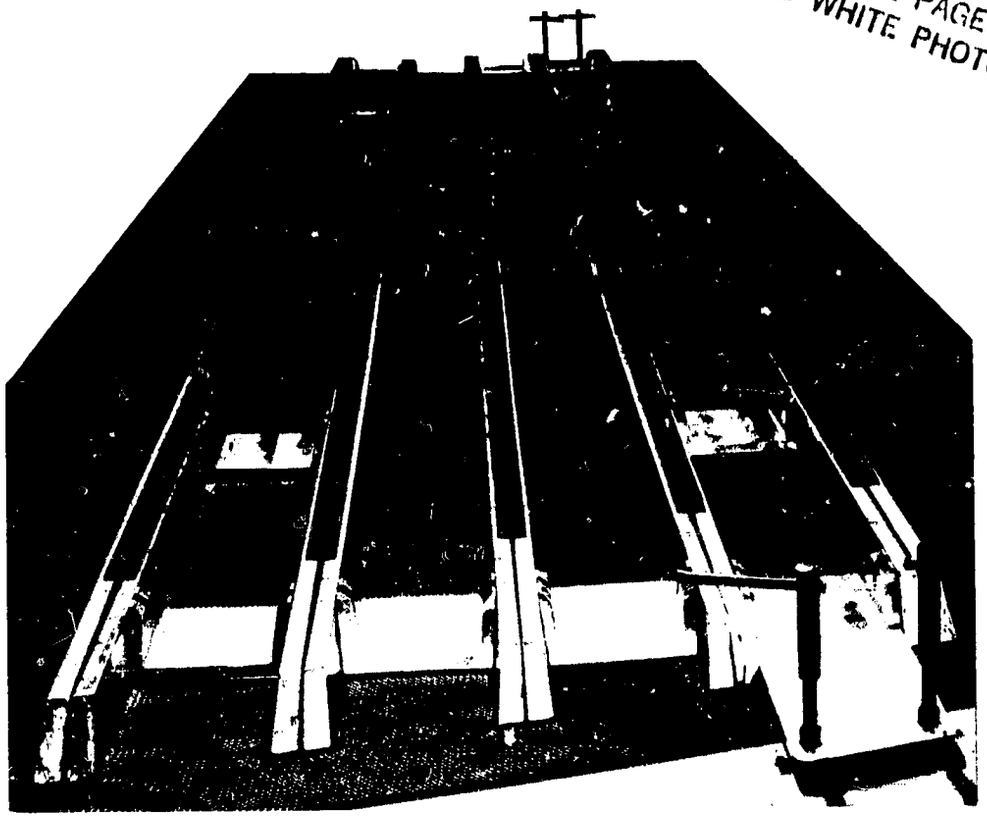

Figure 172. Tool Concept of I-Section Stiffeners

5.1.3 Spar Lug Fabrication

Three spar attach lug designs were fabricated and subjected to nondestructive testing. These designs included an all-graphite lug, graphite with bonded titanium straps, and graphite with bonded and bolted titanium straps (fig. 175). On the basis of the nondestructive inspection (NDI) test/inspection and the observed labor cost, Manufacturing recommended the lug with bonded and bolted titanium straps for production; the labor cost was one-third that of the all-graphite design, and NDI showed that bonding was significantly improved over the bonded but not bolted design.

5.1.4 Rear-Spar Lug Interface Producibility Part

Because of the complexity of the layup and assembly at the rear-spar lug interface, fabrication of a producibility test part was required to establish tooling design, layup procedures, and quality control inspection techniques. The part was a 1.8m (6 ft) section of the rear spar that included the three lugs (fig. 176). In addition, defects consisting of 2 plies of 2-mil-thick Teflon that varied in size from 0.64 cm^2 (0.25 in^2) to 5.72 x 15.24 cm (2.25 x 6.0 in) were incorporated at more than 100 locations and at different depths to allow quality control to assess NDI capabilities.

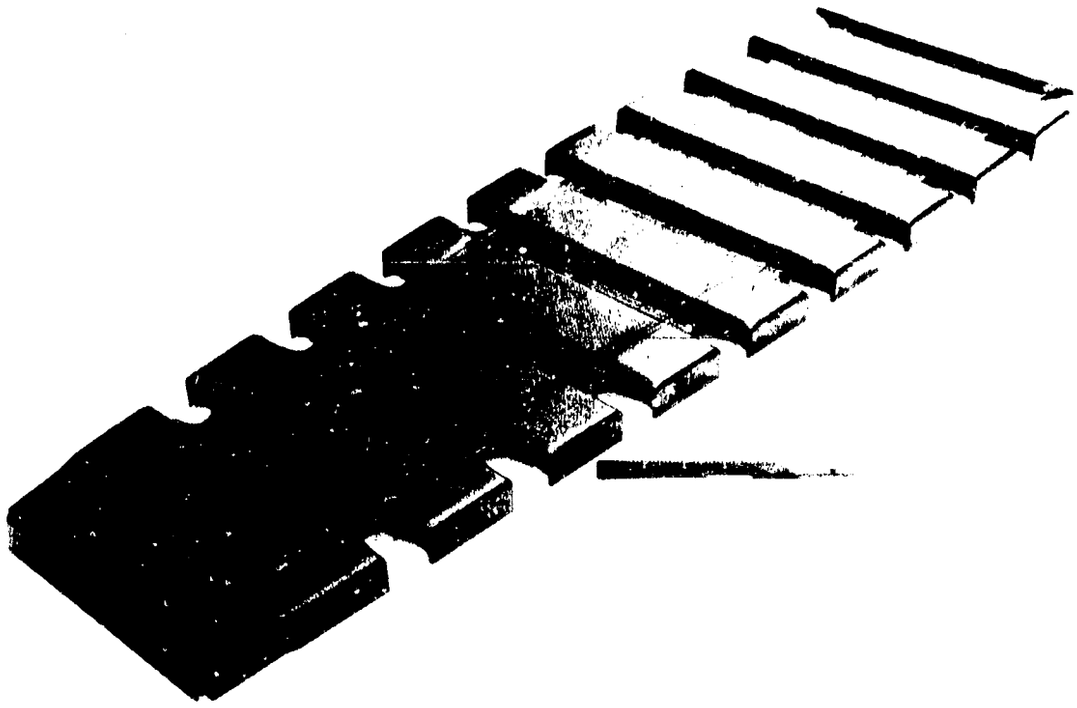

Figure 173. Corrugated Inspar Rib

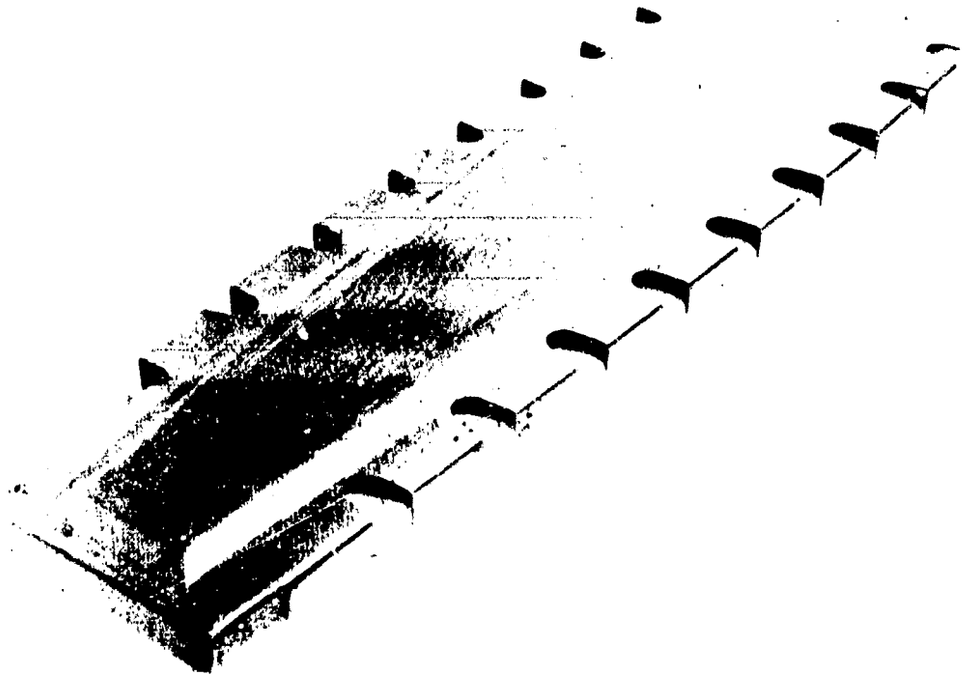

Figure 174. Honeycomb Inspar Rib

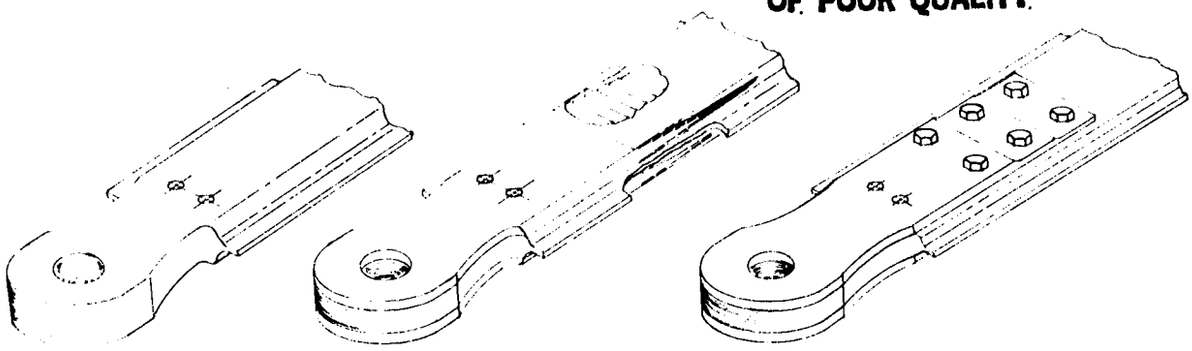

All-graphite | Bonded titanium straps | Bolted titanium straps

Figure 175. Spar Lug Concepts

5.1.4.1 Manufacturing Sequence

Fabrication of this part involved:

- Layup and cure of prebond details (figs. 177 through 180)
- Layup for the bonding operation including defect incorporation (figs. 181 through 195)
- Verifilm determination of adhesive bondline thickness and uniforming; Figures 196 through 200 illustrate the Verifilm process
- Bonding operations; Figure 201 illustrates both bonding operations and includes Verifilm determination of cap/web bondlines
- Machining of titanium straps
- Profile milling lug area (fig. 202)
- Bonding titanium straps (figs. 203 and 204)
- Drilling and fastener and bushing installation (figs. 205 through 207)

5.1.4.2 Discussion of Manufacturing Development

Verifilm, a fluorinated ethylene propylene (FEP) film used to evaluate adhesive films and to prevent adhesion during simulated cure cycles, is illustrated in Figures 196 through 199. The contrast in appearance of the two adhesives is shown in Figure 200. This test established that precured spar webs and spar caps would bond with an acceptable bondline thickness variation and an absence of porosity or voids in the adhesive film. The adhesive used to bond the producibility part and

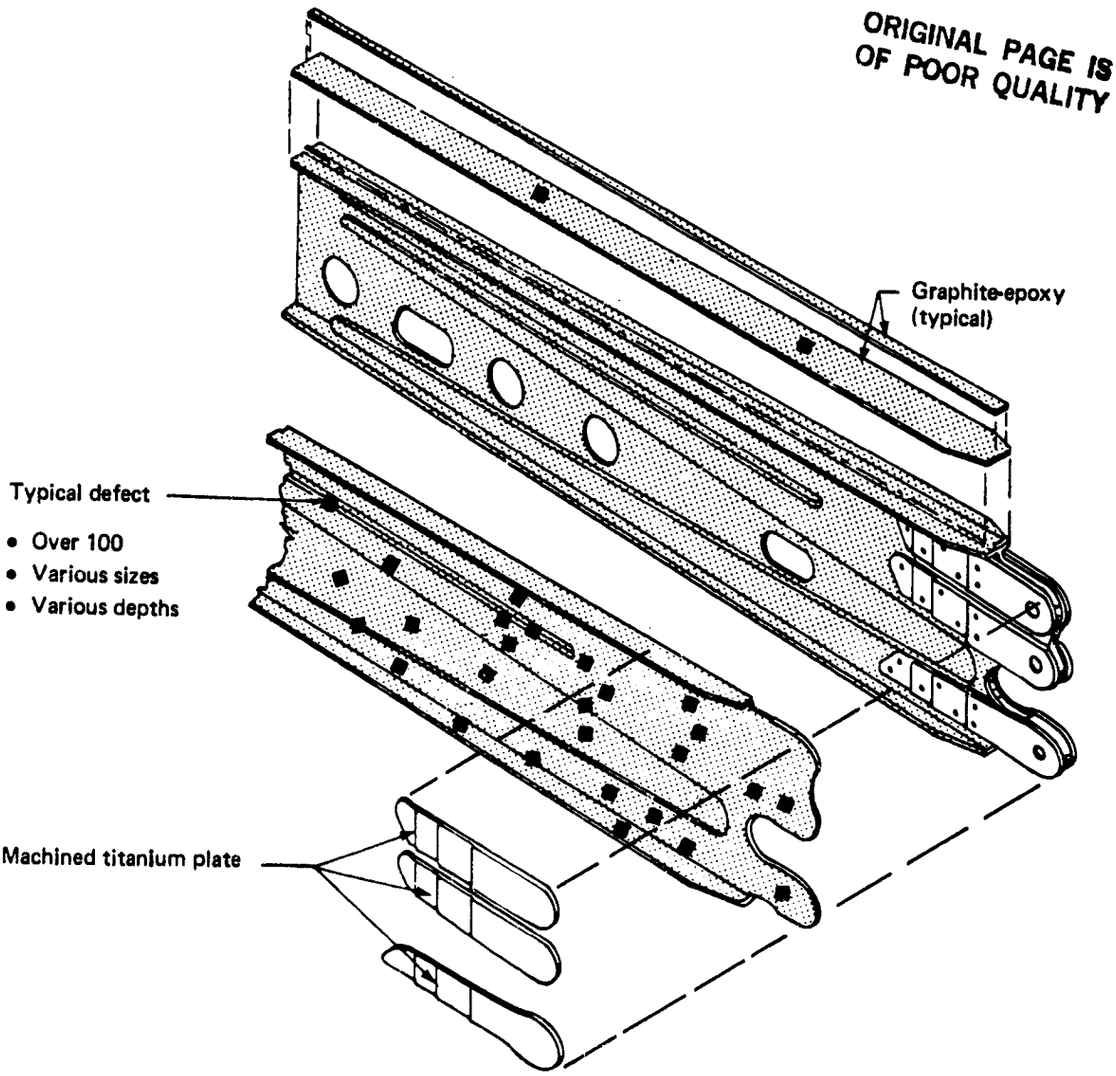

Figure 176. Spar Lug Defect Standards

subsequent production parts was American Cyanamid's FM-300, grade 05, which was later qualified as a Boeing materials standard specification supported film adhesive. Both the test and NDI inspection of the bonded part showed the absence of voids and porosity. Thickness measurements of the cured Verifilm layup varied between 0.005 cm (0.002 in) to .030 cm (0.012 in) between the webs.

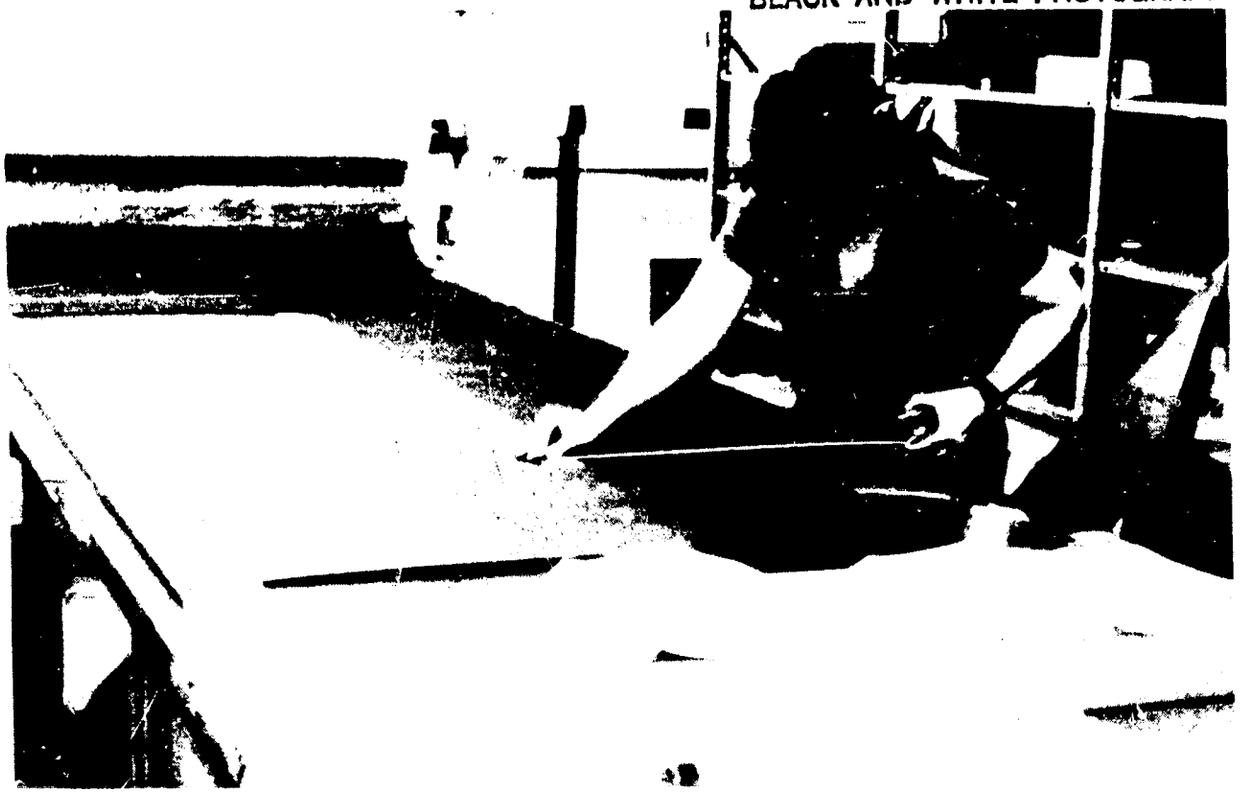

Figure 177. Cutting of Woven Graphite Fabric for Spar Lug Test Component

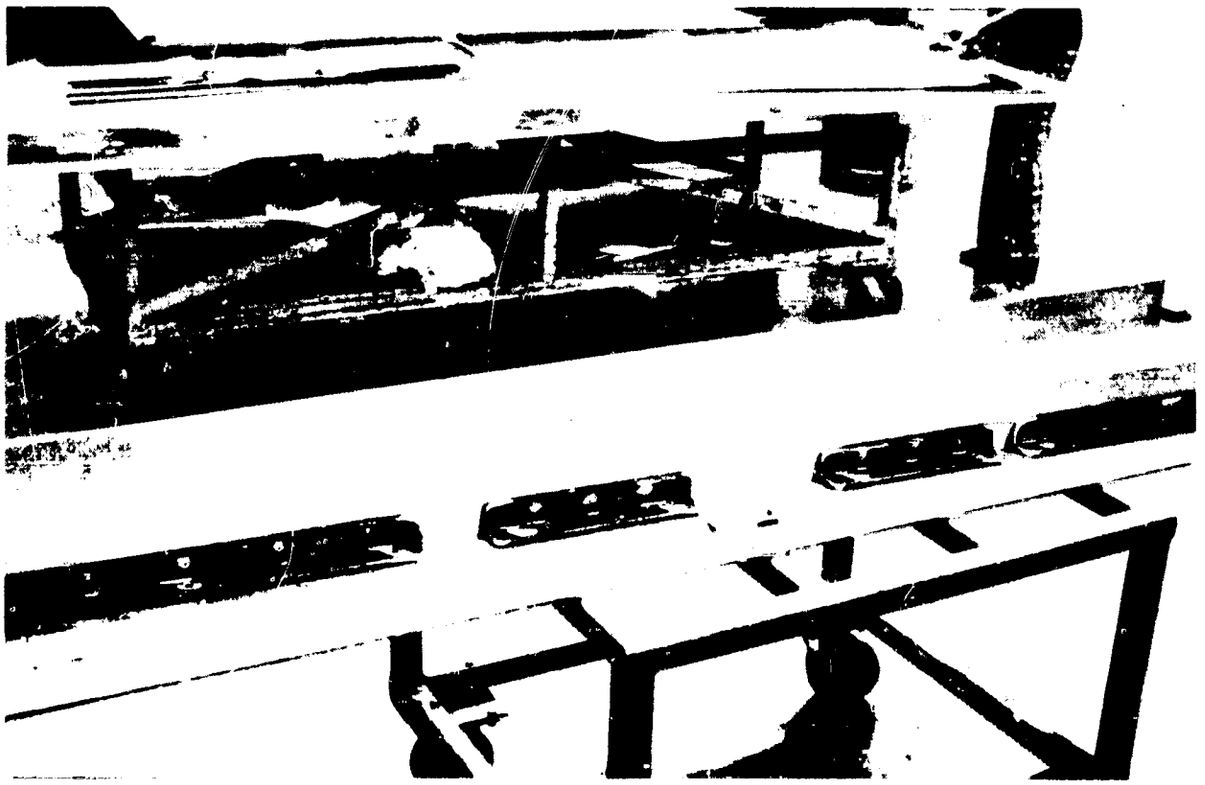

Figure 178. Layup Tool for Spar Lug Feasibility Hardware

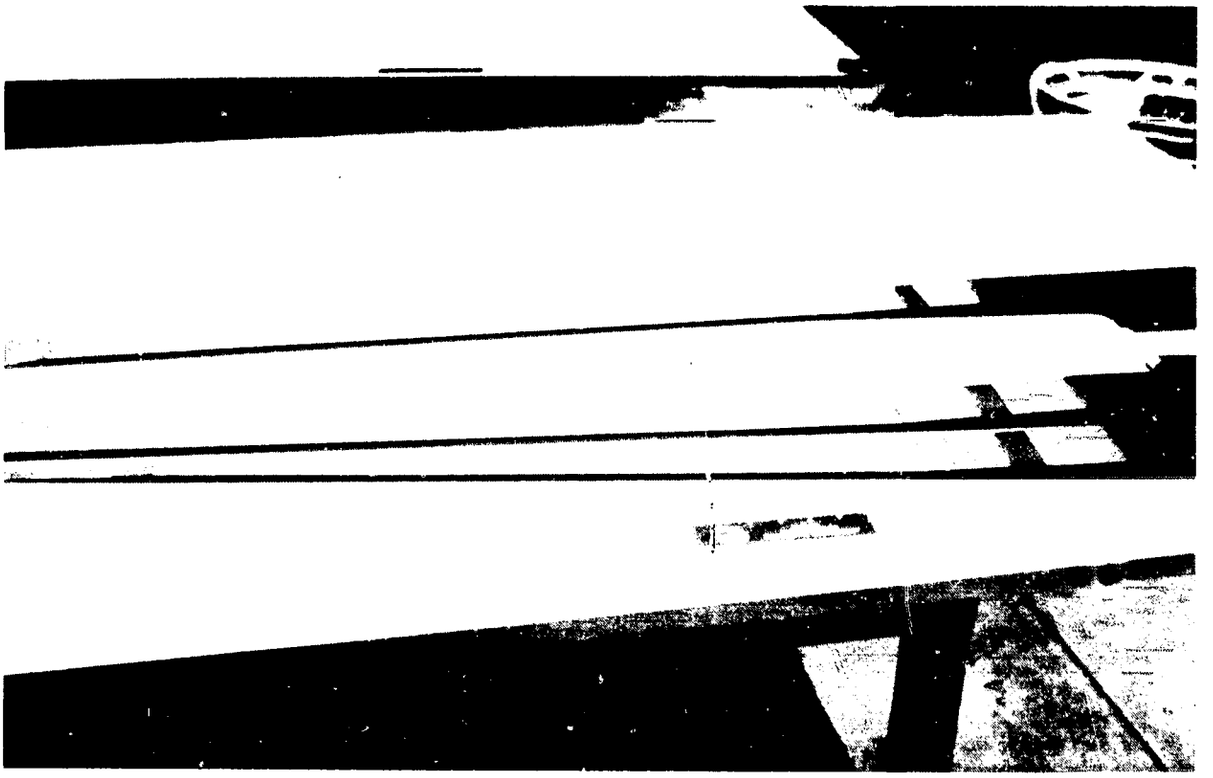

Figure 179. Precured Graphite Chords

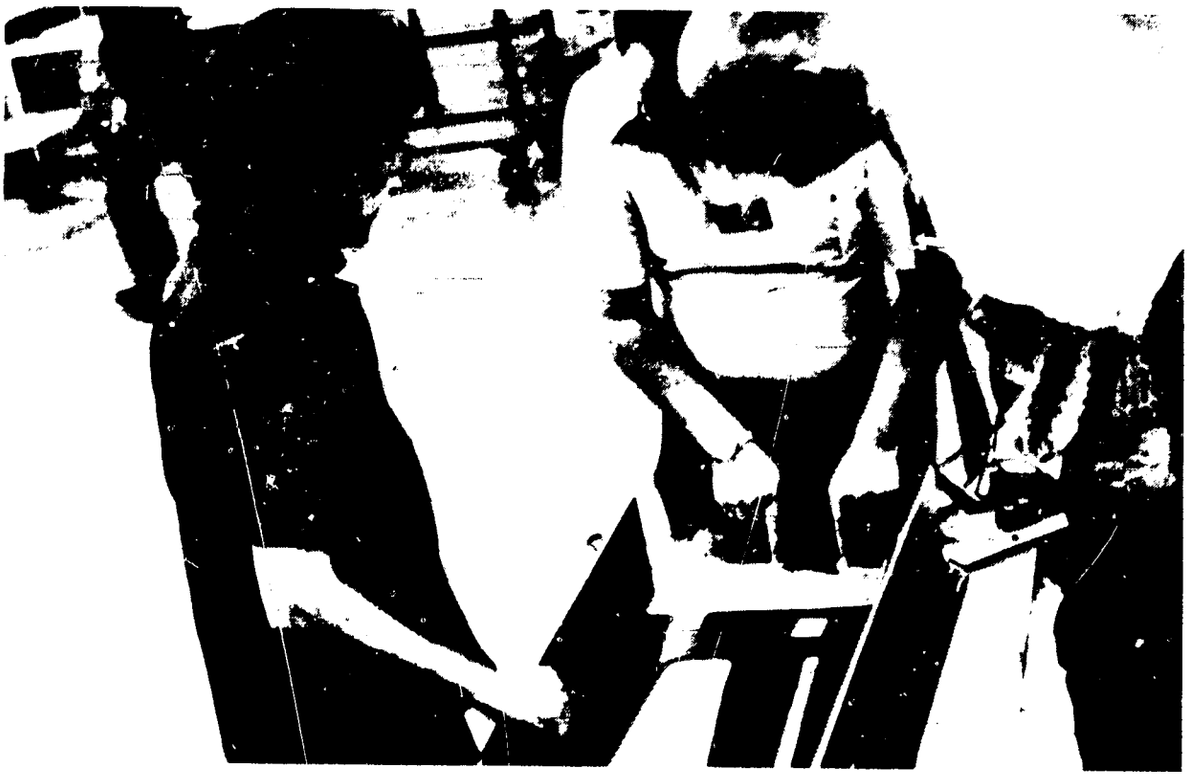

Figure 180. Checking Precured Graphite Chords Prior to Layup

ORIGINAL PAGE
BLACK AND WHITE PHOTOGRAPH

Figure 181. Layup of Preimpregnated Peel Ply on Tool

Figure 182. Layup of First Ply of Woven Graphite Prepreg

Figure 183. Layup of Woven Graphite Prepreg

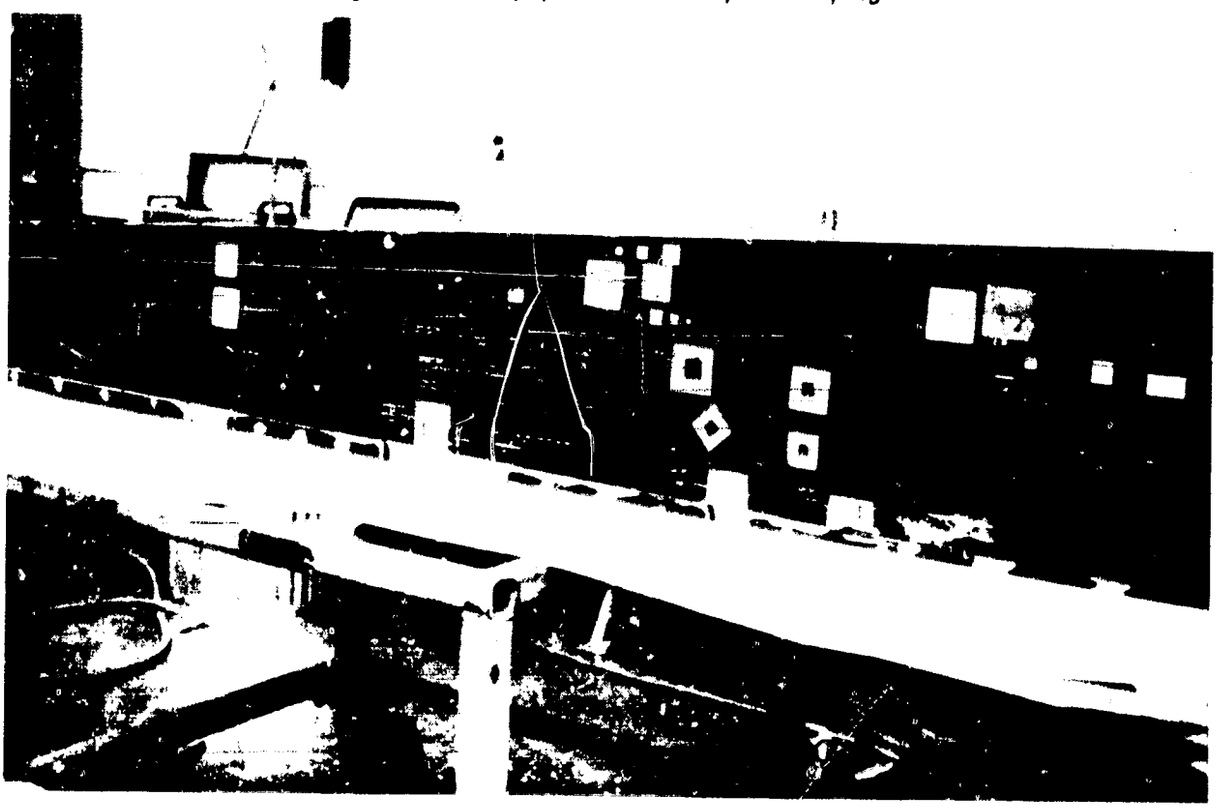

Figure 184. Locating Template for Defects and Ply Termination

Figure 185. Using Template to Locate Teflon Defects

Figure 186. Various-Sized Teflon Defects

ORIGINAL PAGE
BLACK AND WHITE PHOTOGRAPH

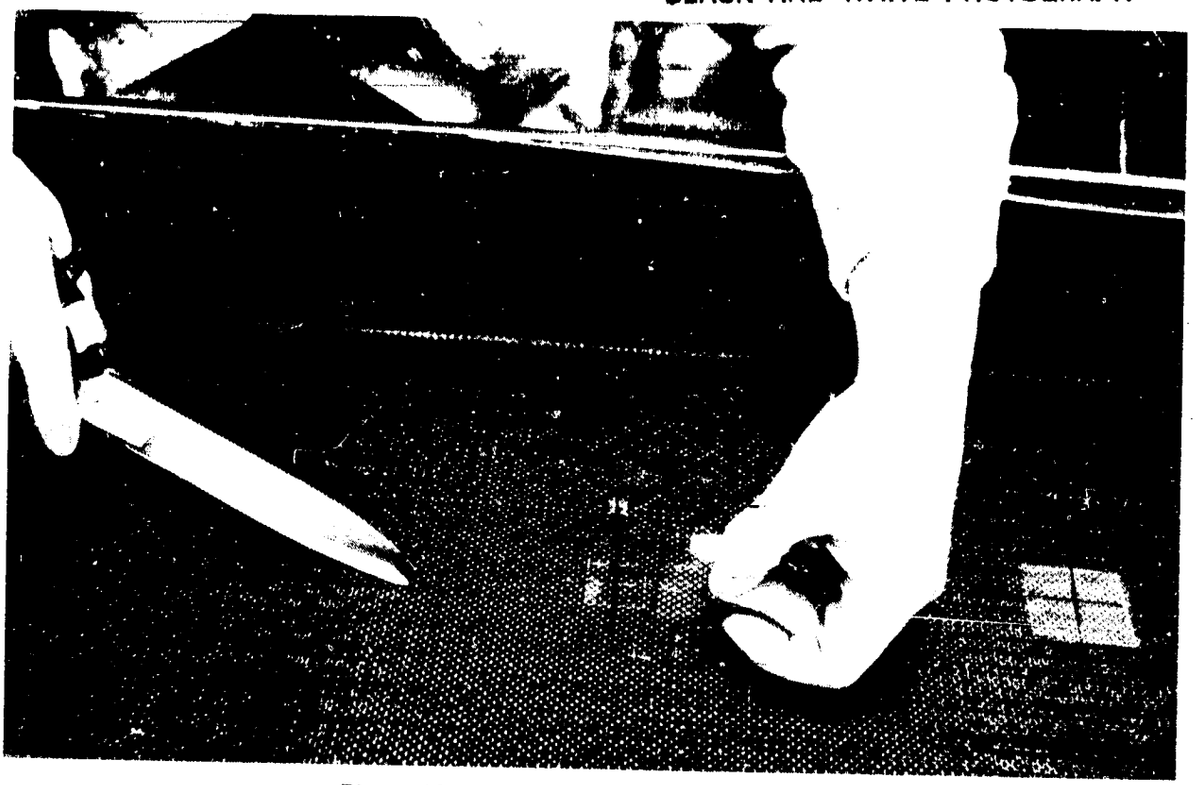

Figure 187. Placement of a Teflon Defect

Figure 188. Placing Teflon Defects on the Precured Graphite Chord

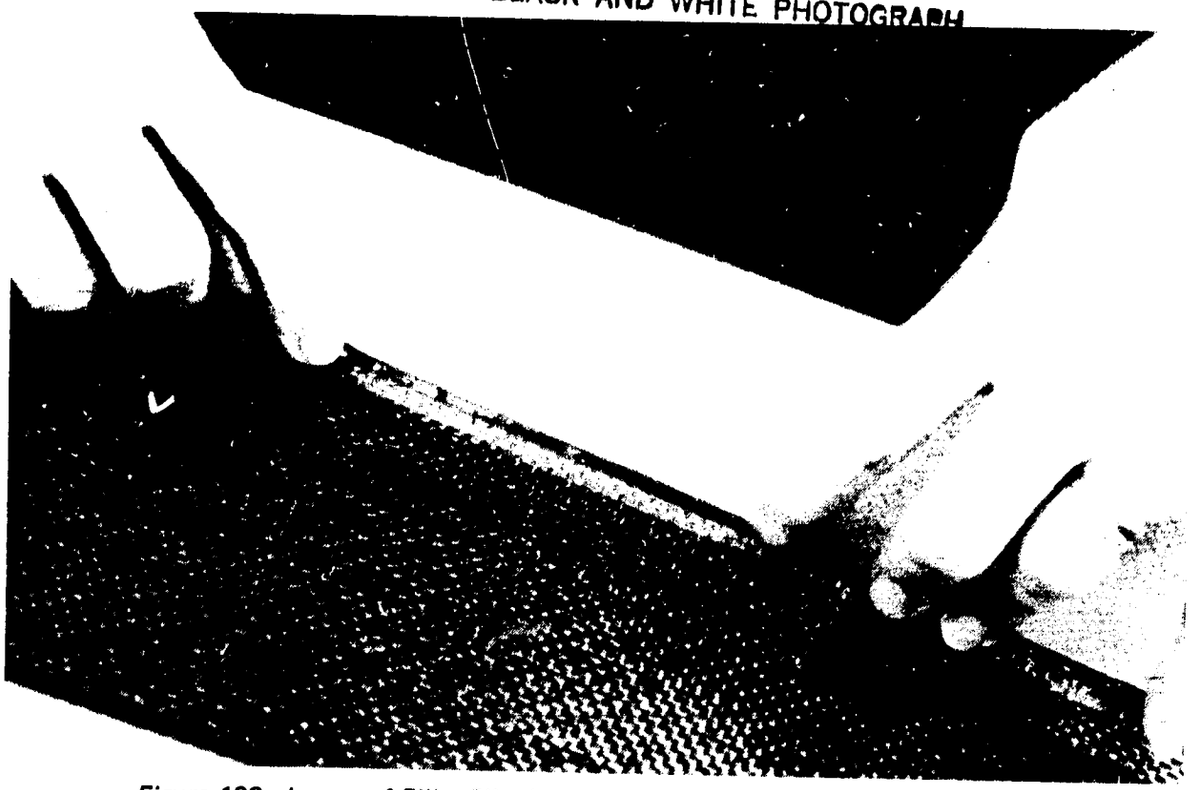

Figure 189. Layup of Filler Plies in the Transition Area of the Precured Chord

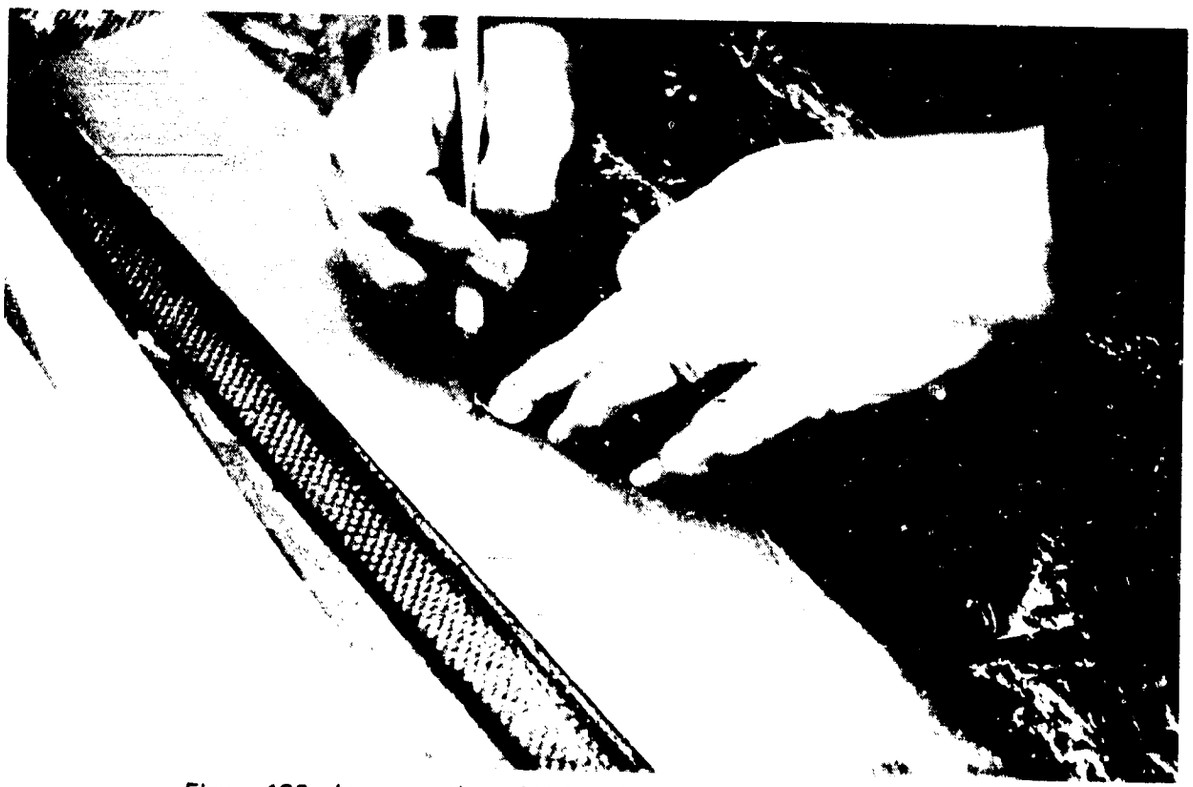

Figure 190. Incorporation of Teflon Defect into the FM-300 Adhesive

Figure 191. Adding Filler Plies to the Last Precured Chord Transition Area

Figure 192. Working Last Ply of Woven Graphite Fabric Into the Transition Areas

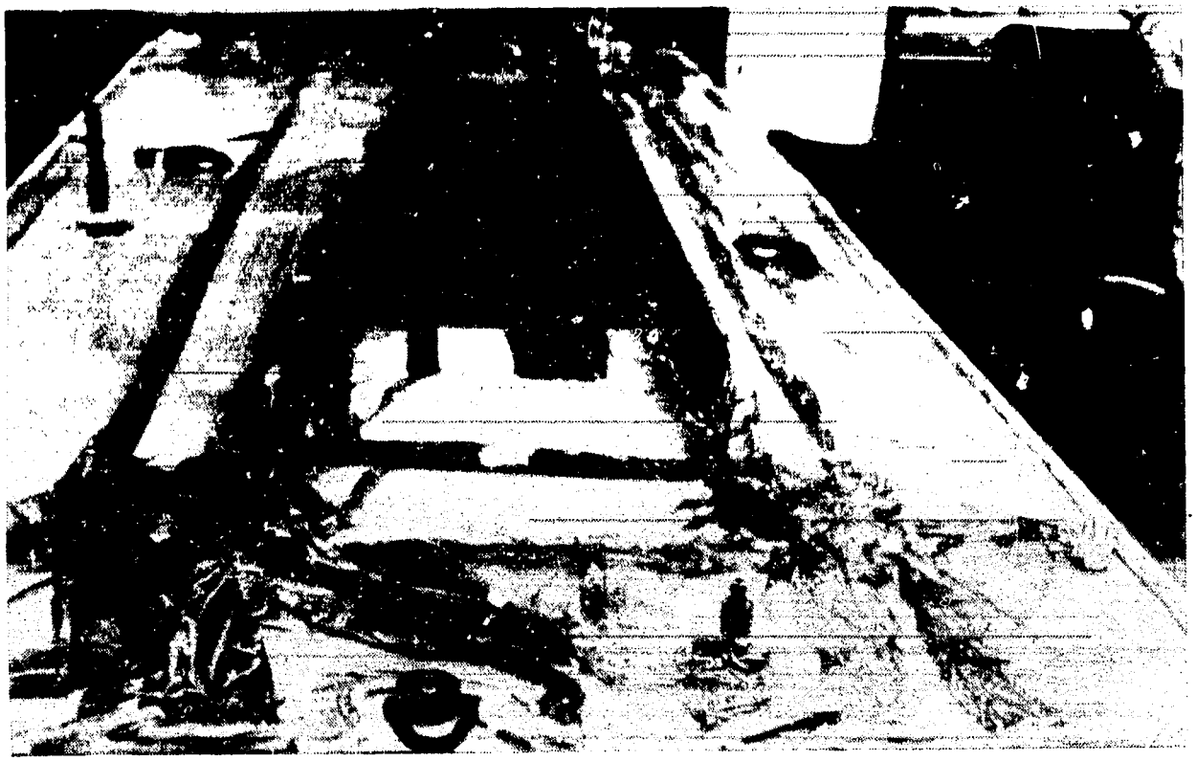

Figure 193. Spar Lug Feasibility Part Bagged and Ready for Cure

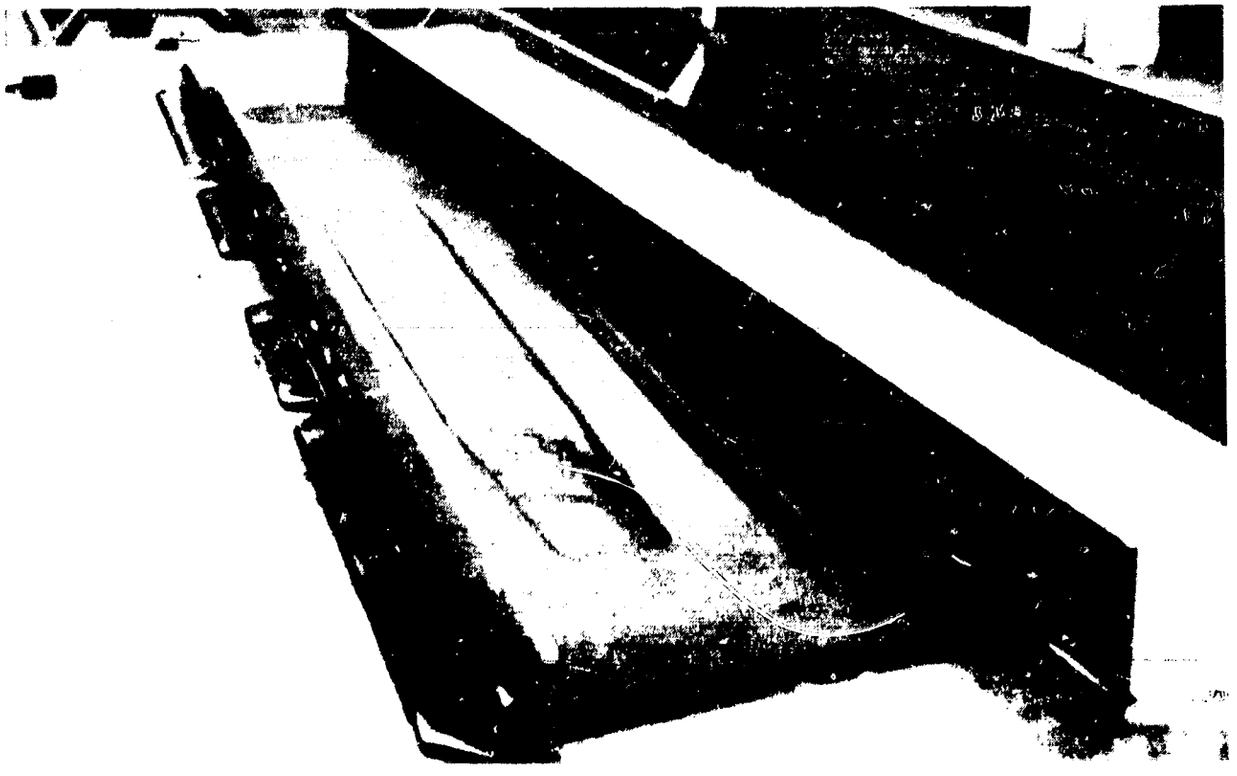

Figure 194. Completed Part in Tool

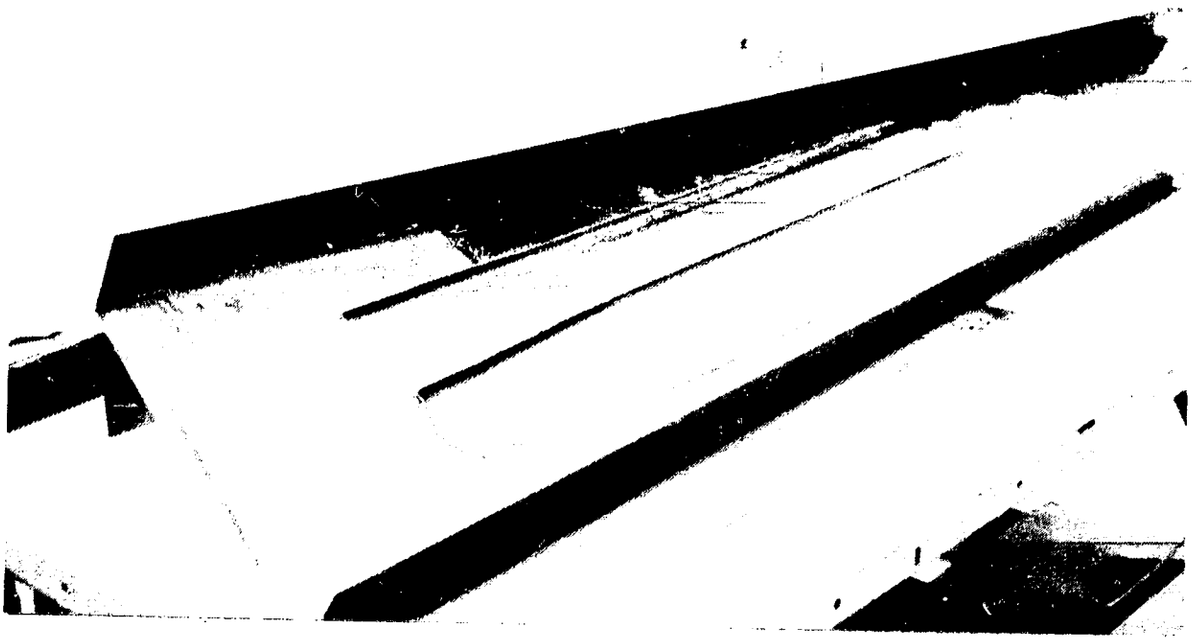

Figure 195. Completed Spar Lug Feasibility Part

Figure 196. Verifilm Positioned on Detail Part

Figure 197. Bond Surfaces Aligned

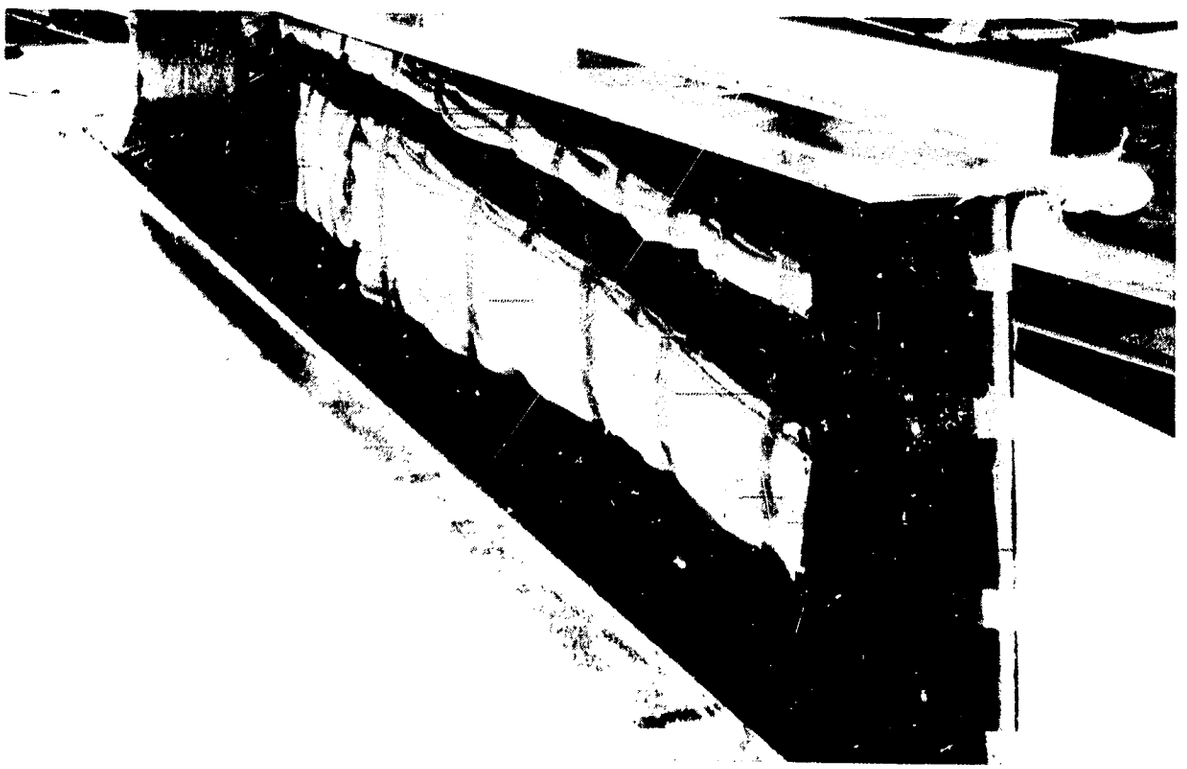

Figure 198. Bond Surfaces Together–Ready for Bagging

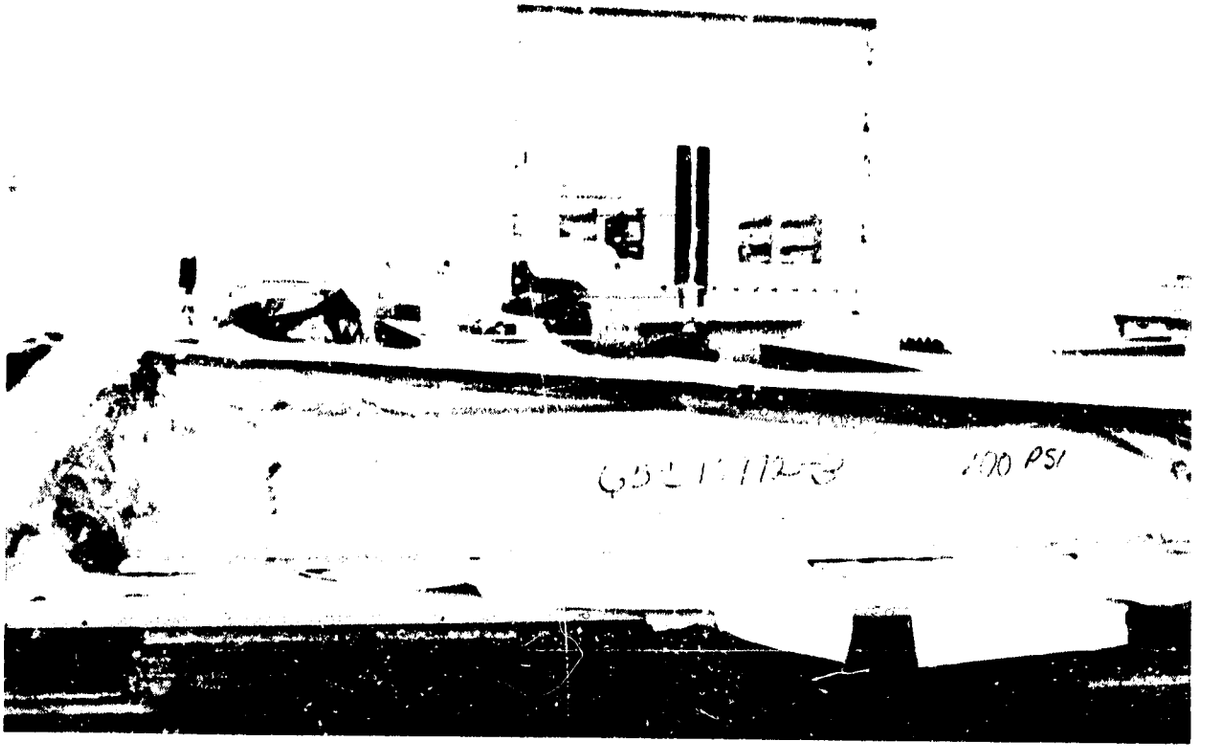

Figure 199. Part Bagged—Read, for Cure

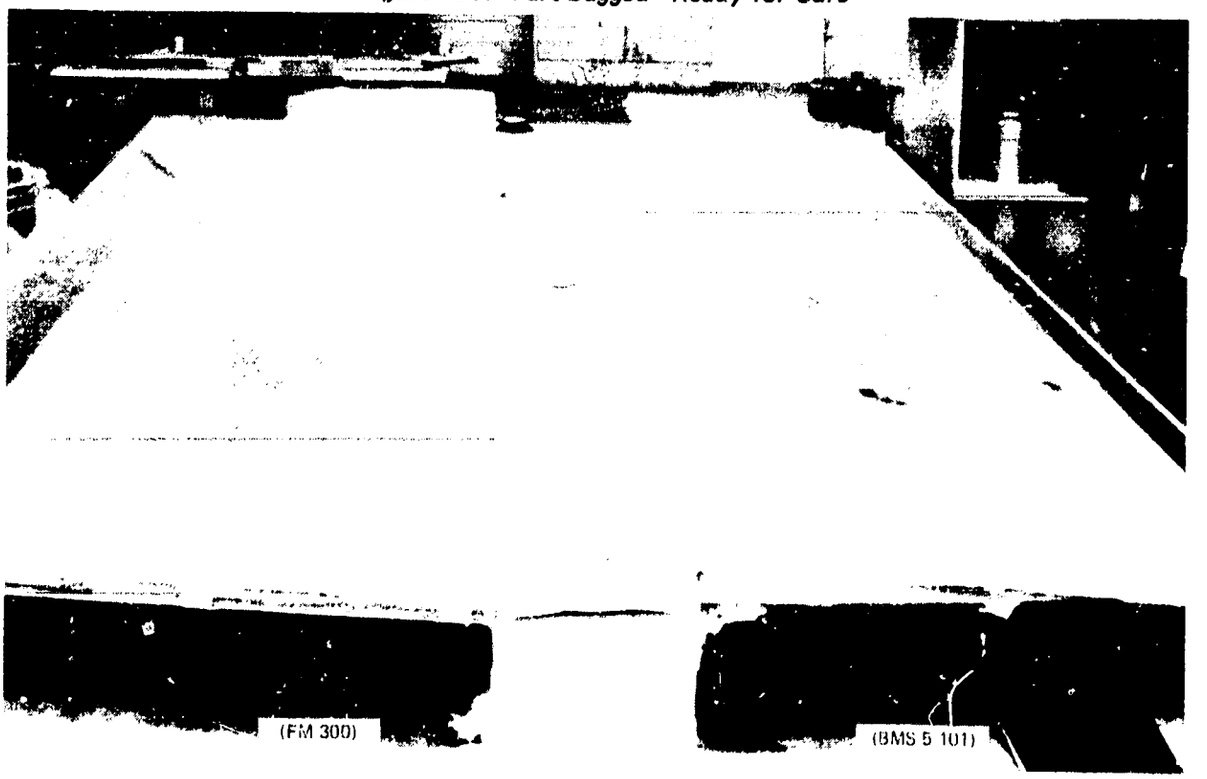

Figure 200. Results of Verifilm

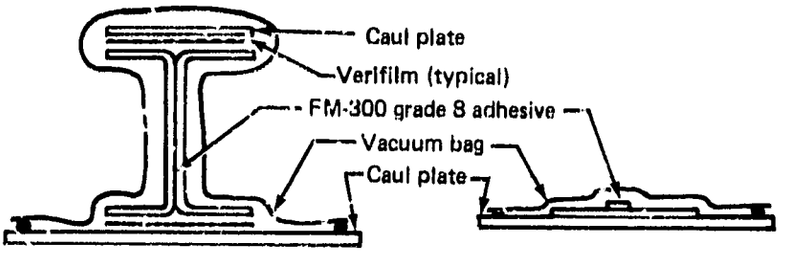

(a) Bond webs and cure filler/cap subassemblies

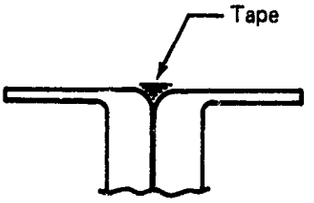

(b) Fill radii of webs with graphite-epoxy tape, upper and lower

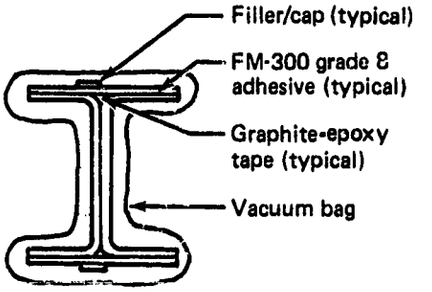

(c) Bond filler/cap to webs

Figure 201. Spar Lug Feasibility Hardware—Bonding Operation for Details and Filler/Cap

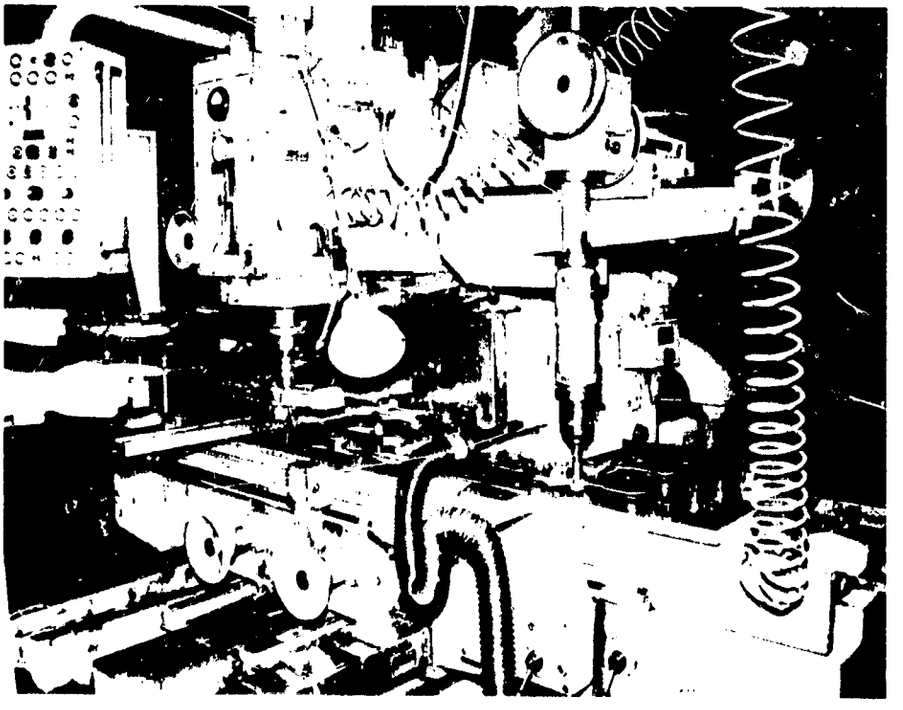

Figure 202. Spar Lug Feasibility Hardware—Machining of Graphite-Epoxy Lugs Using a Profile Mill

ORIGINAL PAGE
BLACK AND WHITE PHOTOGRAPH

Figure 203. Spar Lug Feasibility Hardware—Polysulfide Adhesive Being Applied for Bonding Titanium Strap

Figure 204. Spar Lug Feasibility Hardware—Titanium Strap Being Bonded

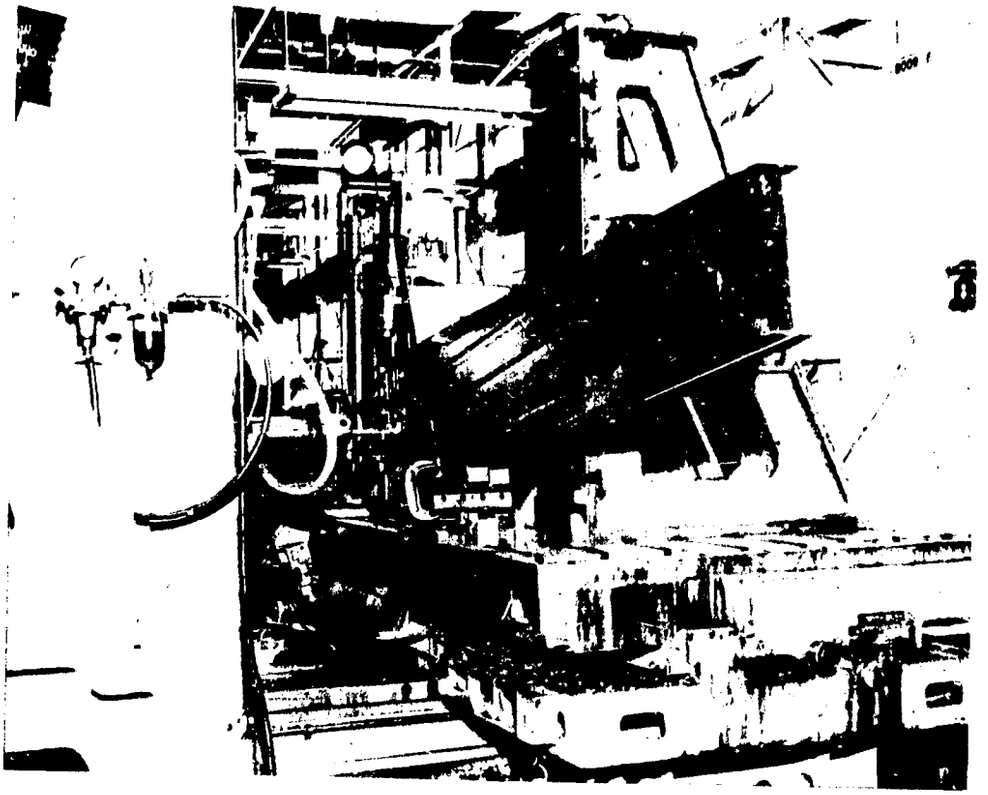

Figure 205. Spar Lug Feasibility Hardware—Bushing Hole Being Drilled

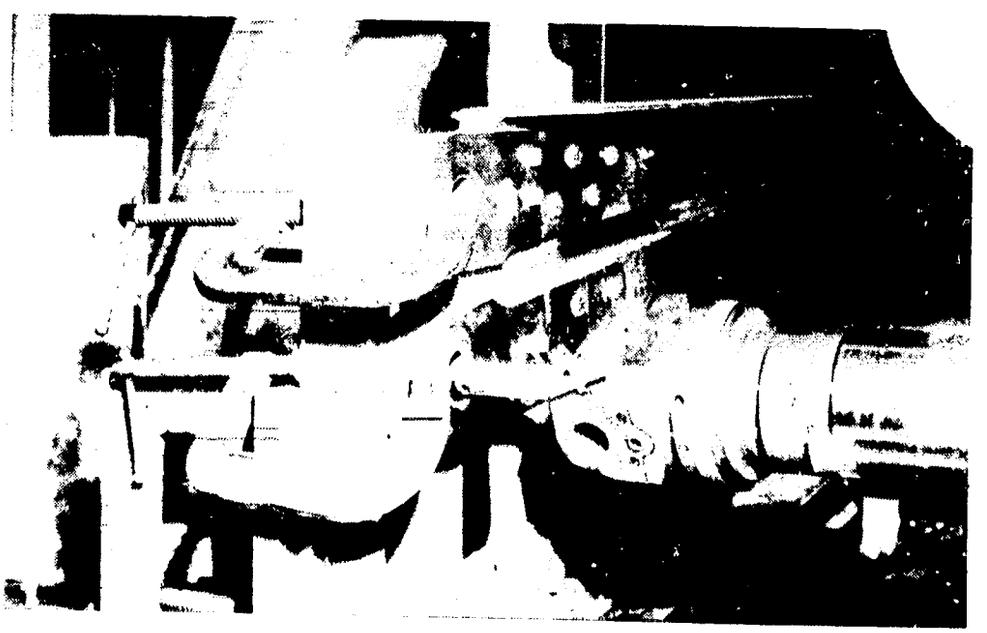

Figure 206. Spar Lug Feasibility Hardware—Bushing Hole Being Drilled

Figure 207. Spar Lug Feasibility Hardware—Finishing Cut on Bushing Hole

Machining of the graphite-epoxy lug area (fig. 202) was accomplished on a profile mill using a diamond cutter. The titanium/graphite-epoxy lug fastener holes were piloted with a carbide tip drill. The titanium lugs were then bonded to the graphite-epoxy using bolts through the pilot holes for pressure. Figures 203 and 204 illustrate the polysulfide adhesive application.

The final fastener hole size was obtained using a carbide tip drill and a carbide reamer. A boring bar and a carbide tool were used for the bushing holes (figs. 205 through 207).

5.2 ANCILLARY TEST COMPONENT FABRICATION

The ancillary test components comprise all test parts used to determine material design properties, evaluate environmental effects, and establish concept validity at the coupon, element, and subcomponent test-specimen level. The parts, all fabricated in a production environment, are listed and illustrated in sections 5.2.1 and 5.2.2.

5.2.1 Material Properties and Environmental Effects

Hardware fabricated for this portion of the ancillary test plan included laminate and honeycomb panels that provided test coupons (fig. 208) and mechanical joint test assemblies for:

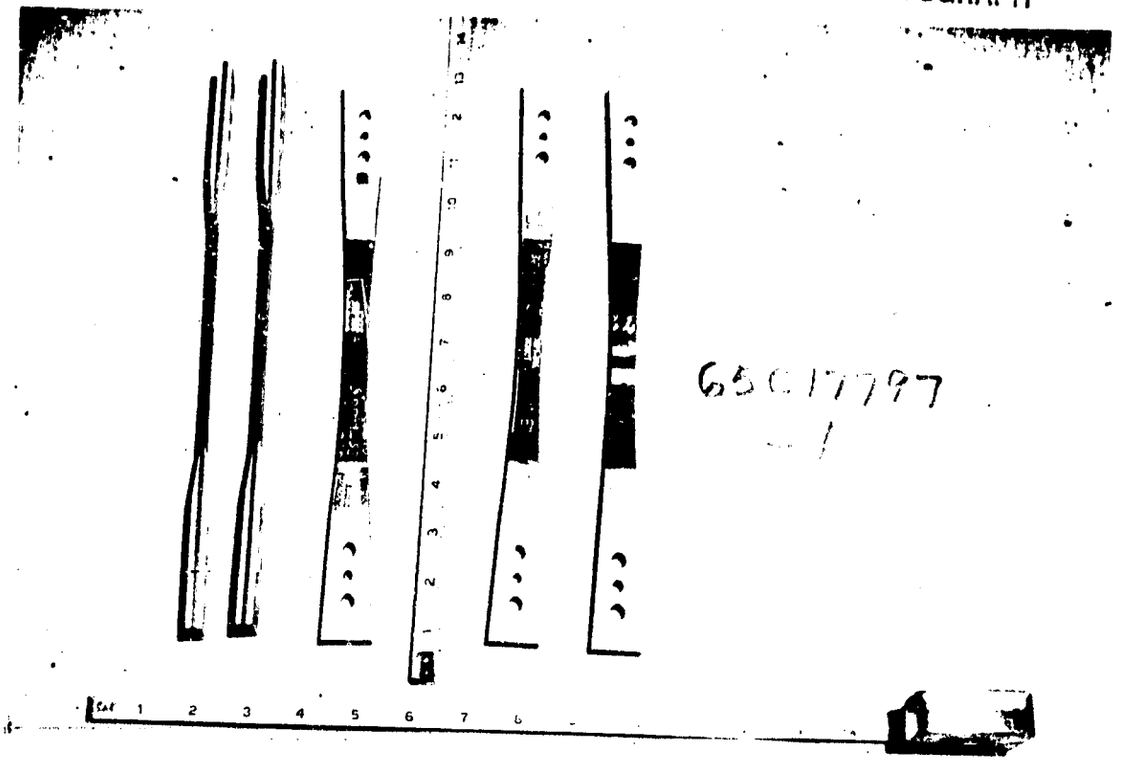

Figure 208. Ancillary Test—Typical Tensile Specimens

- Specimens for determining material properties included honeycomb panels with and without impact damage (Test 1)
- Environmental test specimens with panels, as in Test 1 (Test 4)
- Mechanical joint test with assemblies (Test 5) (figs. 209 and 210)

All of this hardware was manufactured in a production environment using materials and processes described and defined in Boeing specifications.

5.2.2 Concept Verification

This phase of ancillary test plan manufacturing was supported by Engineering, Manufacturing R&D, and Fabrication organizations and provided the following subcomponent test specimens:

Spar Chord Crippling—Figures 211 and 212 show Manufacturing-designed multiple-station end potting fixture and spar chord specimens (Test 7).

Skin-to-Rib Attachment (Also Test 24)—Figures 213 and 214 show the assembled test specimens (Test 9).

I-Stiffened Panels—Figures 169 and 215 through 220 show details of the test assembly fabrication (Test 10).

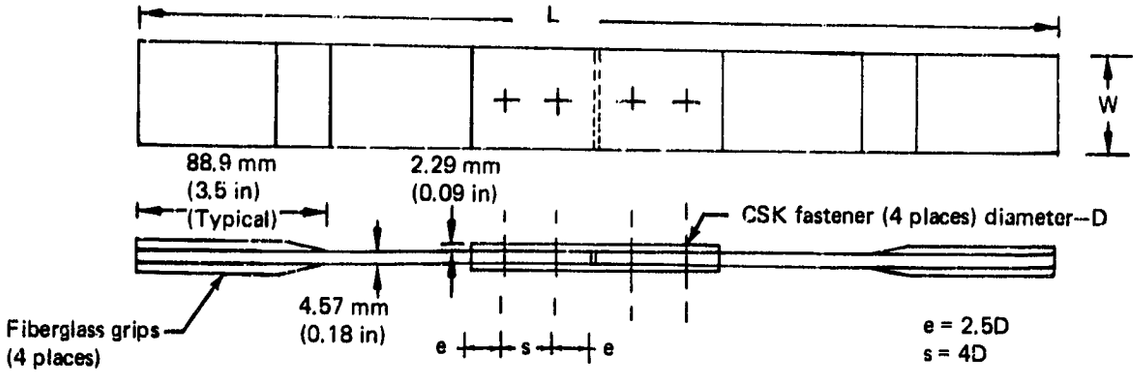

Figure 209. 50% Load Transfer Joint

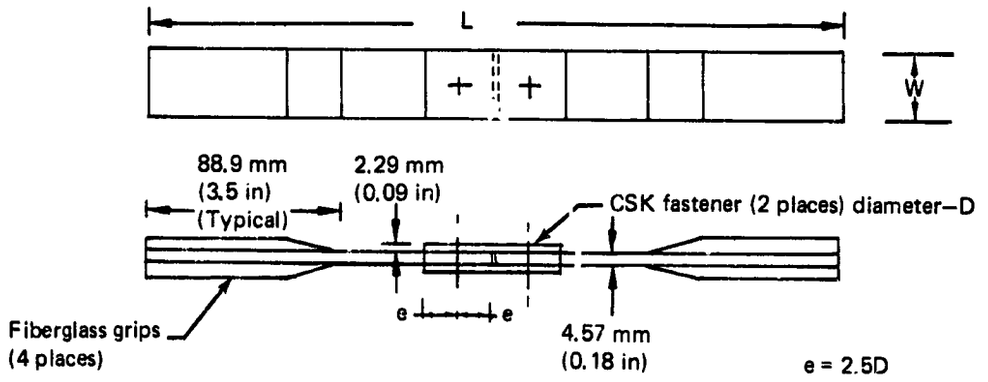

Figure 210. 100% Load Transfer Joint

Spar Lug Specimens–Test-part fabrication and completed tension and compression specimens are shown in Figures 221 through 228 (Test 12).

Sonic Test Box–Figures 229 and 230 show the test box before closure (Test 20).

Stub Box–This test part was produced as manufacturing verification hardware and is discussed in Section 5.3 and illustrated in Figures 231 through 254 (Test 21).

Front Spar Section–Production Verification–Figures 255 and 256 illustrate the precuring and two-stage bonding procedure validation (Test 25).

5.3 MANUFACTURING VERIFICATION HARDWARE

The stub box (Test 21) was used for manufacturing verification. This box is a full-scale root section of the advanced composite stabilizer and consists of the structural box from the side-of-body outboard to station 152.45. Included are the trailing-edge structure and closure rib. Problems that were encountered and resolved during fabrication of the graphite-epoxy details for the box were:

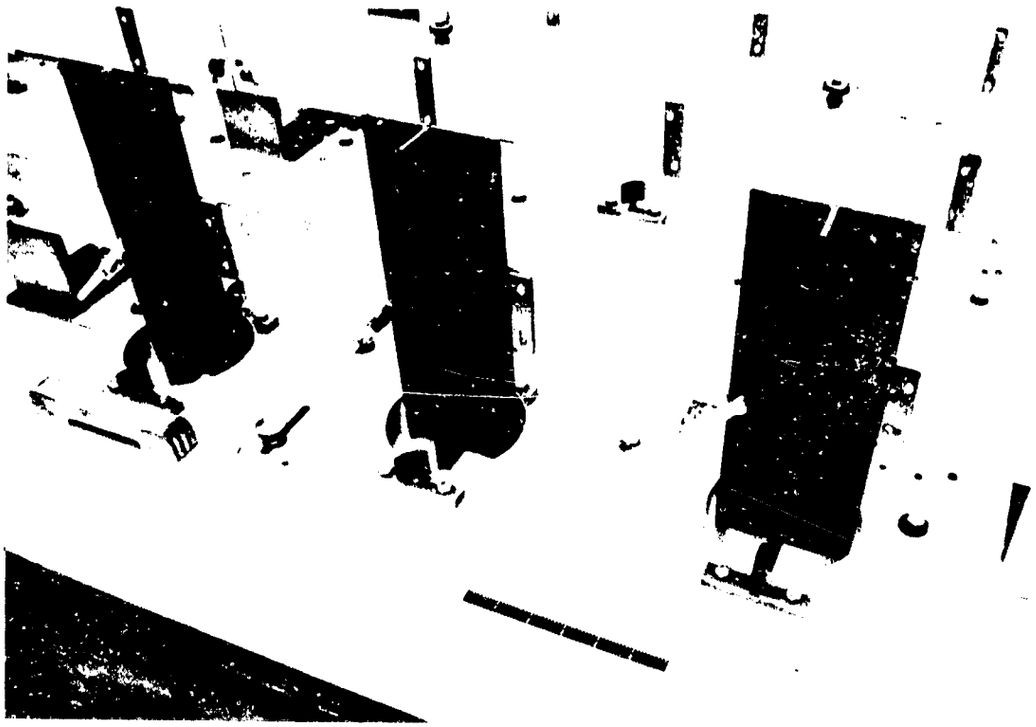

Figure 211. Spar Chord Crippling Specimen Ready for End Potting (Test 7)

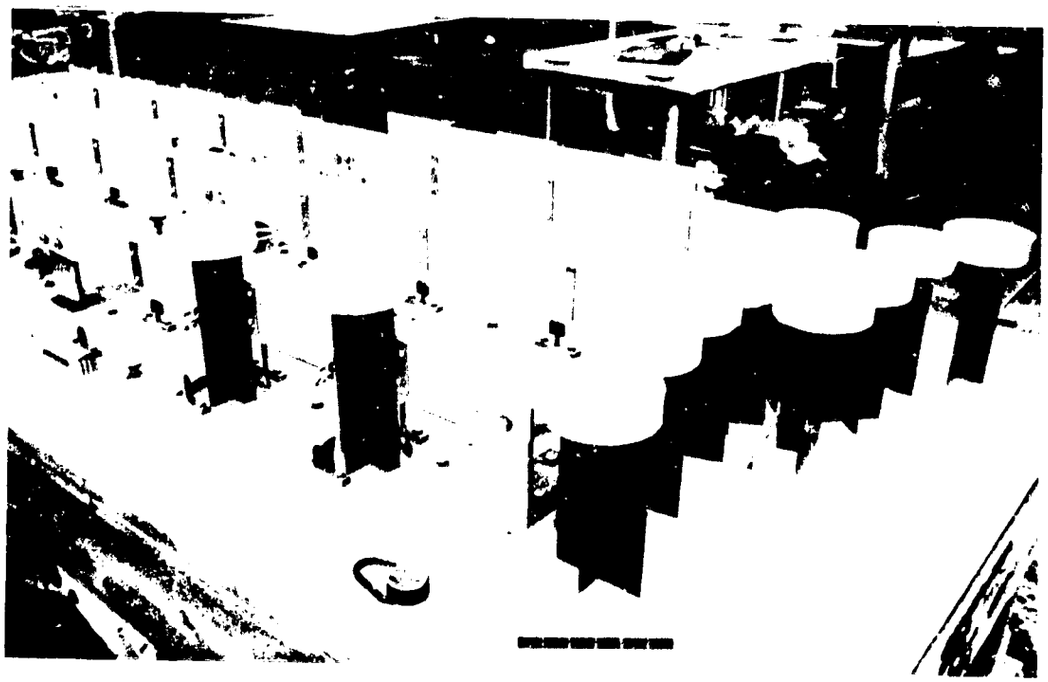

Figure 212. Spar Chord Crippling—Completed Specimens (Test 7)

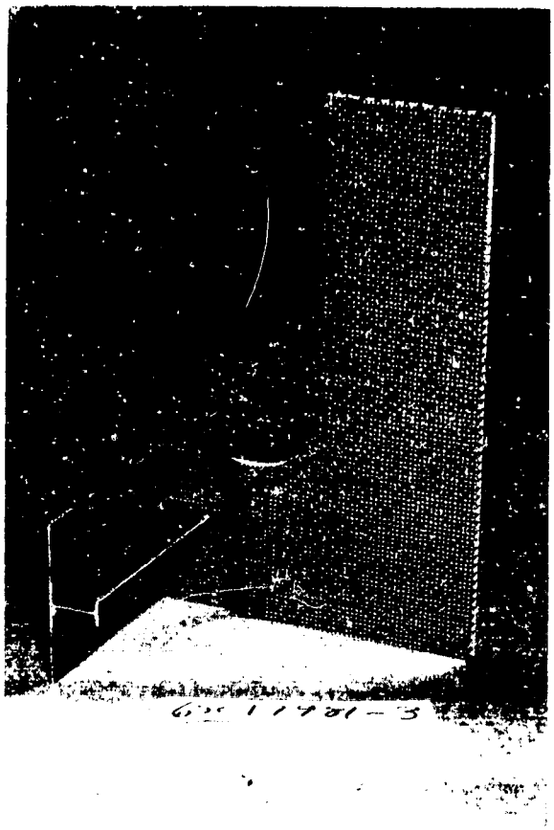

Figure 213. Panel-to-Rib Joint Test (Test 24)

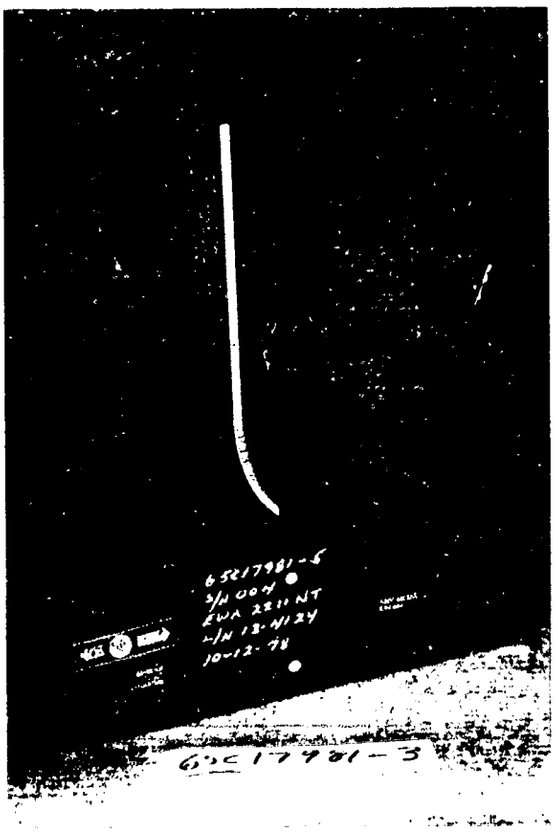

Figure 214. Panel-to-Rib Joint Test (Test 24)

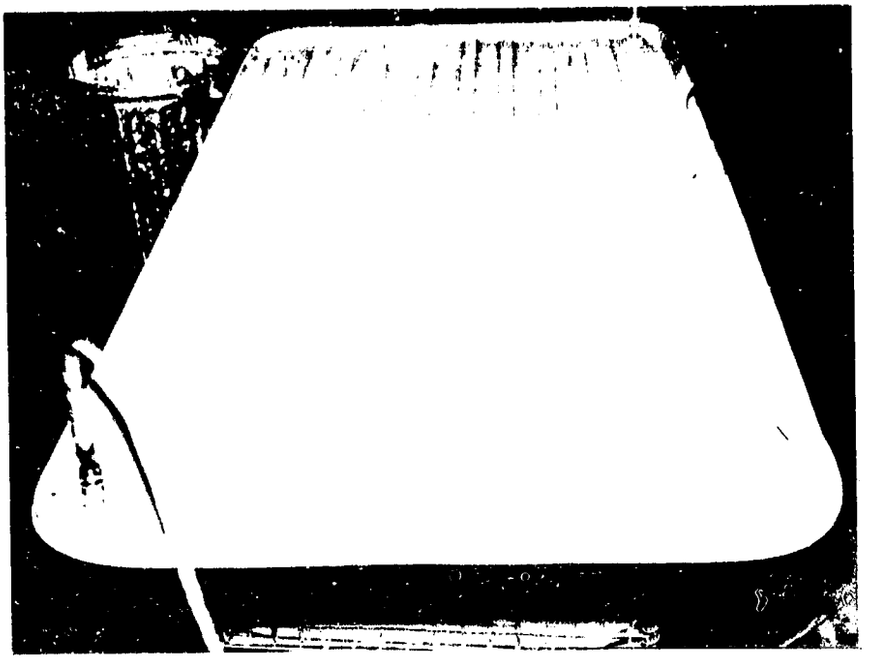

Figure 215. Temporary Bag for Compaction of Graphite-Epoxy on I-Stiffeners (Test 10)

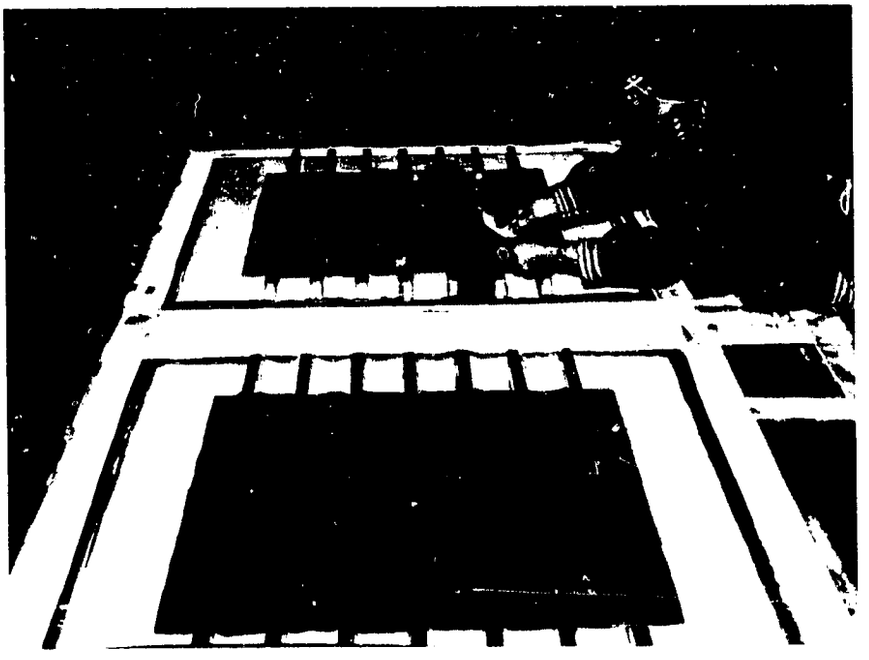

Figure 216. I-Stiffened Test Panels—Application of Peel Plies During Layup (Test 10)

Figure 217. I-Stiffened Panel Section Made for Warpage Study (Test 10)

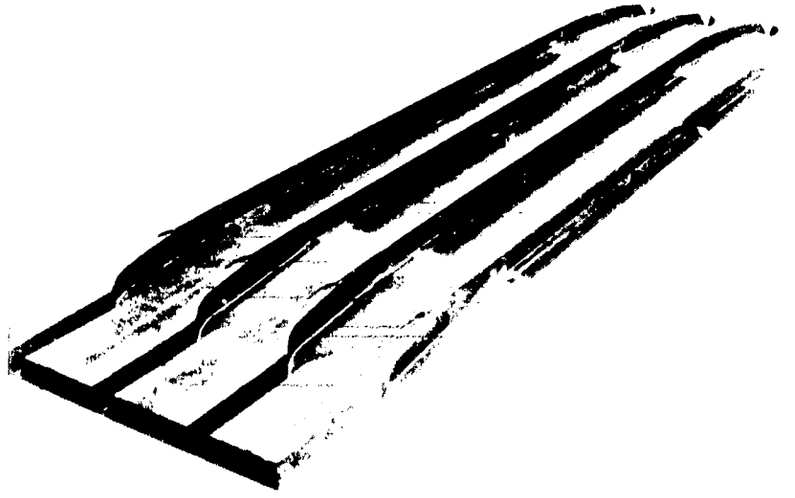

Figure 218. Fatigue Test Panel With Bonded Graphite-Epoxy Grip Tabs (Test 10)

ORIGINAL PAGE
BLACK AND WHITE PHOTOGRAPH

Figure 219. Compression Test Panel—Skin Side (Test 10)

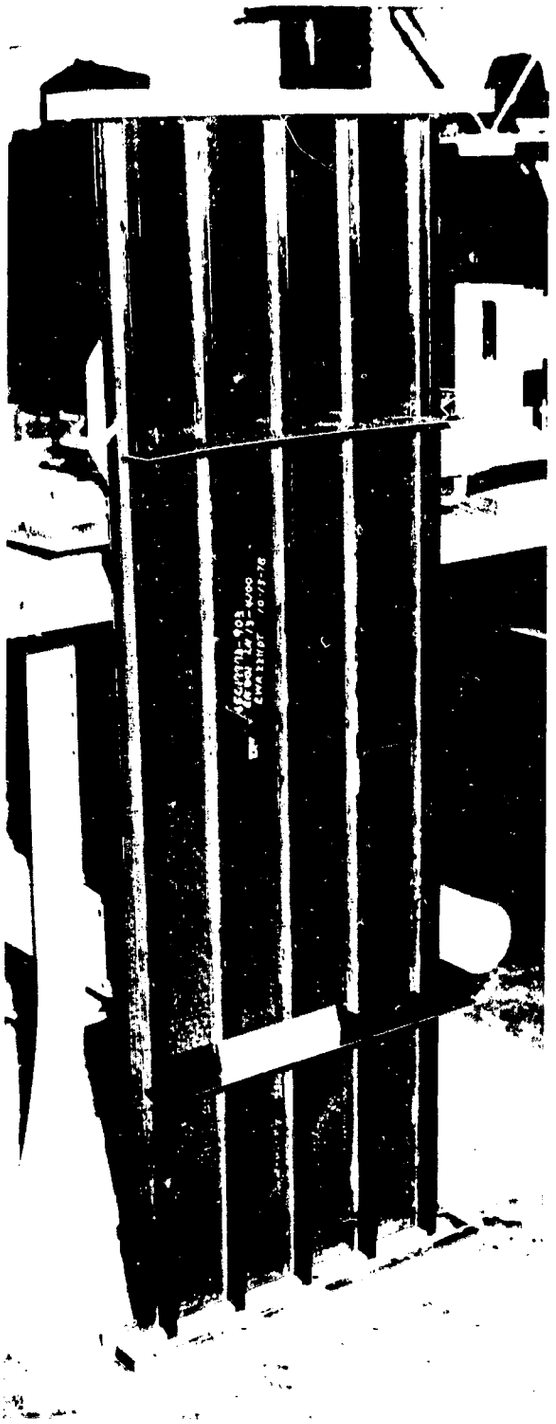

Figure 220. Compression Test Panel—Stiffened Side (Test 10)

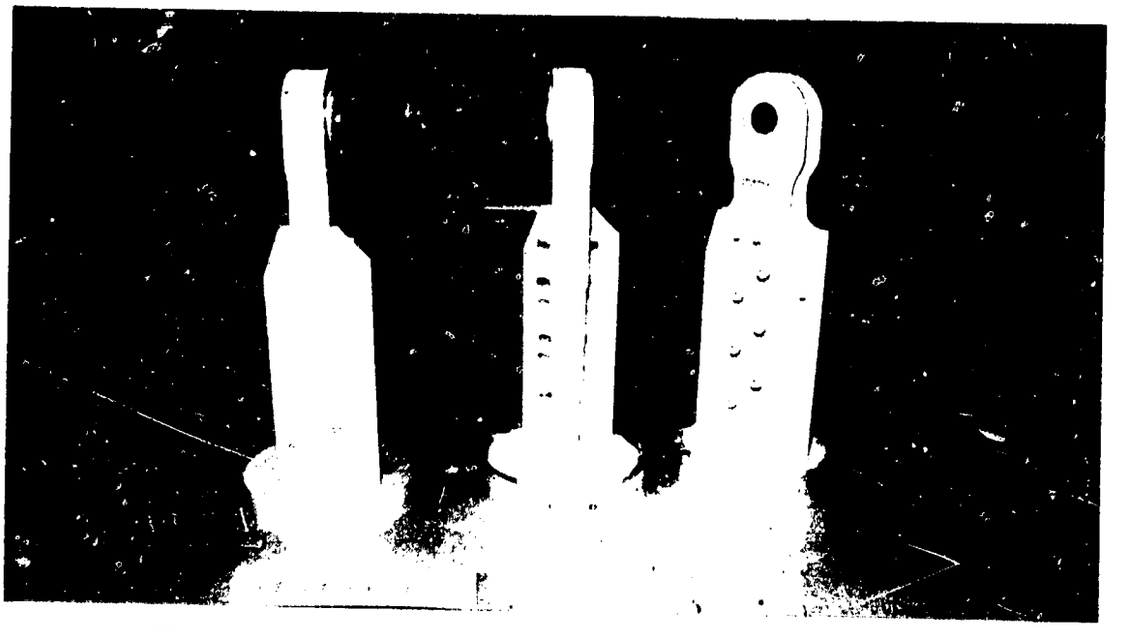

Figure 221. Spar Lug—Completed Compression Specimens (Test 12)

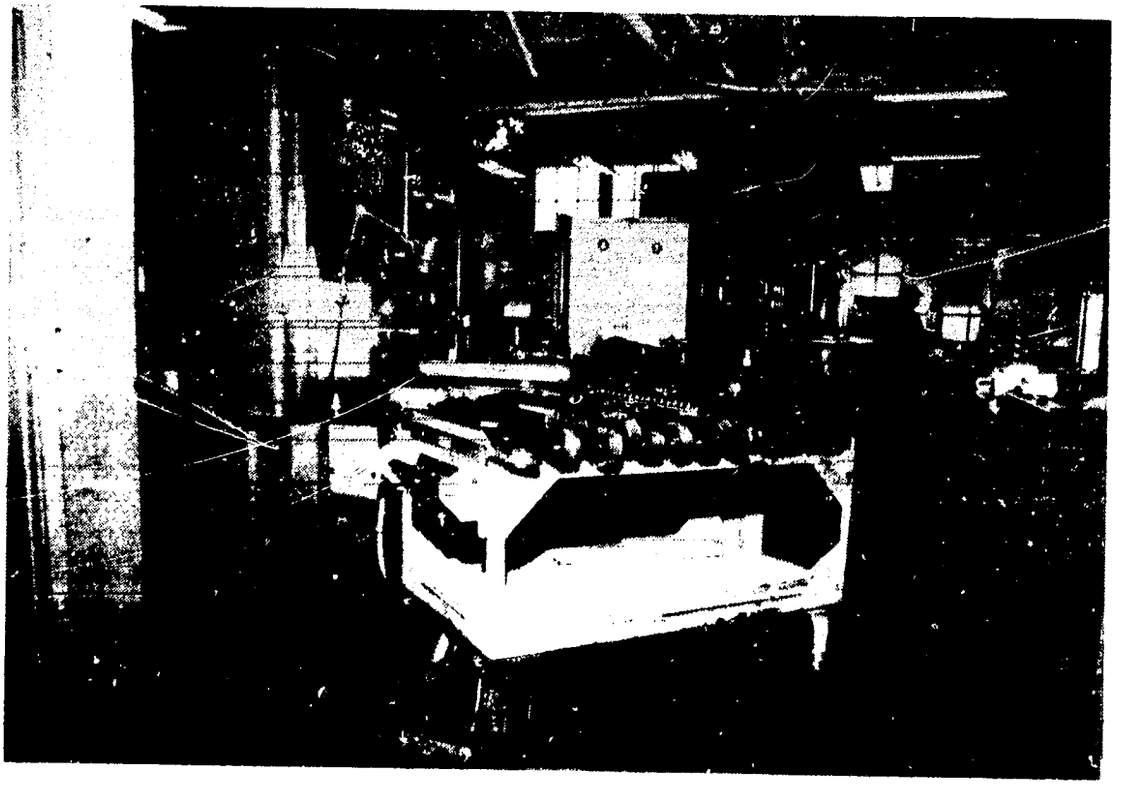

Figure 222. Spar Lug—Tension Specimens Ready for Drilling (Test 12)

Figure 223. Spar Lug—Specimens Ready for Cure (Test 12)

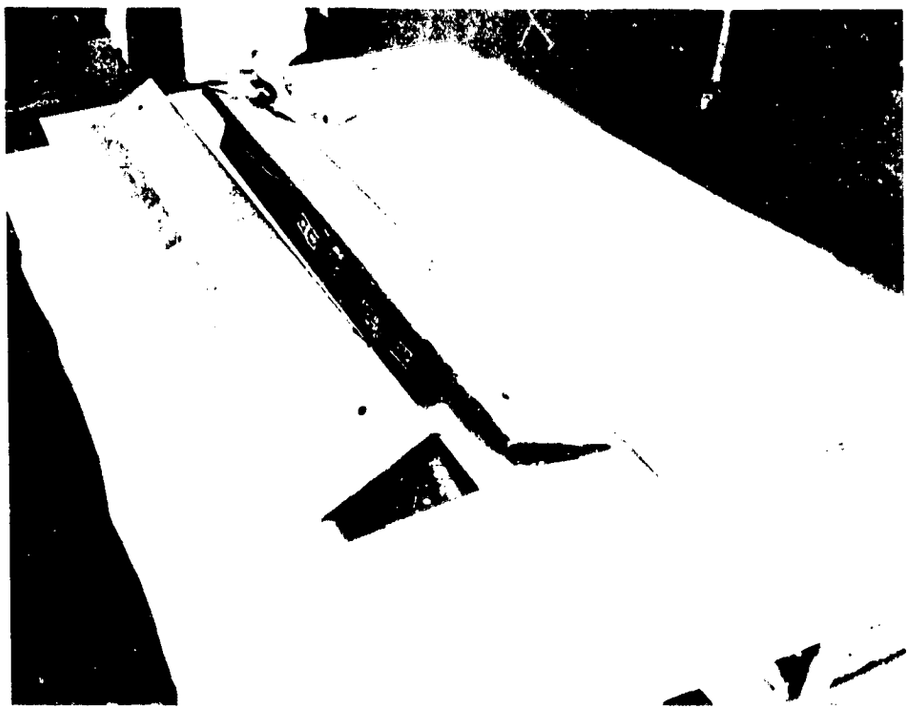

Figure 224. Spar Lug—Peel Ply Being Removed From Completed Detail Halves (Test 12)

Figure 225. Spar Lug—Completed Detail Halves Bagged and Ready for Bonding (Test 12)

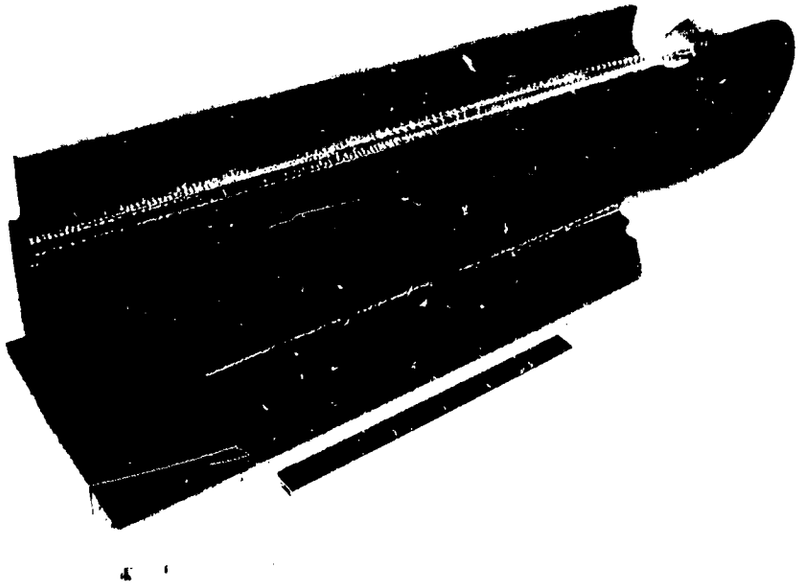

Figure 226. Spar Lug—Trimmed Compression Specimen (Test 12)

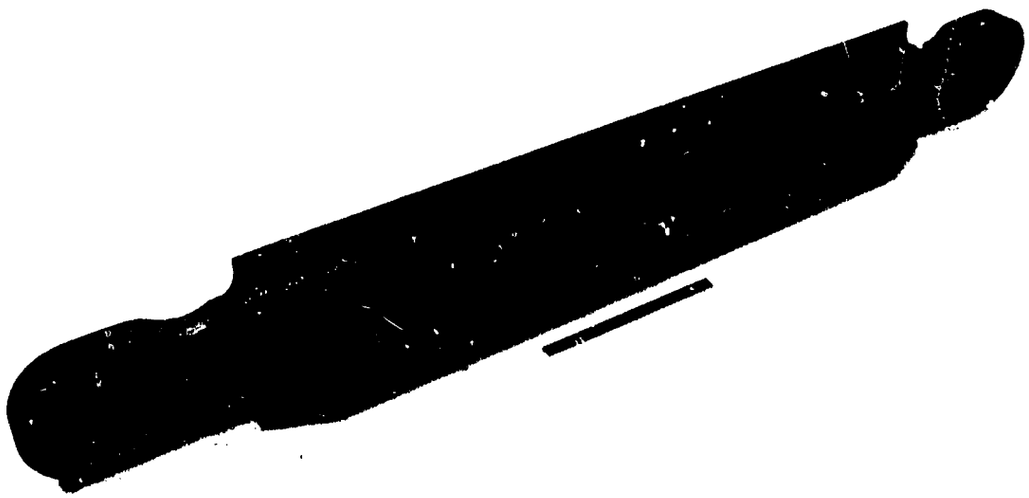

Figure 227. Spar Lug—Trimmed Tension Specimen (Test 12)

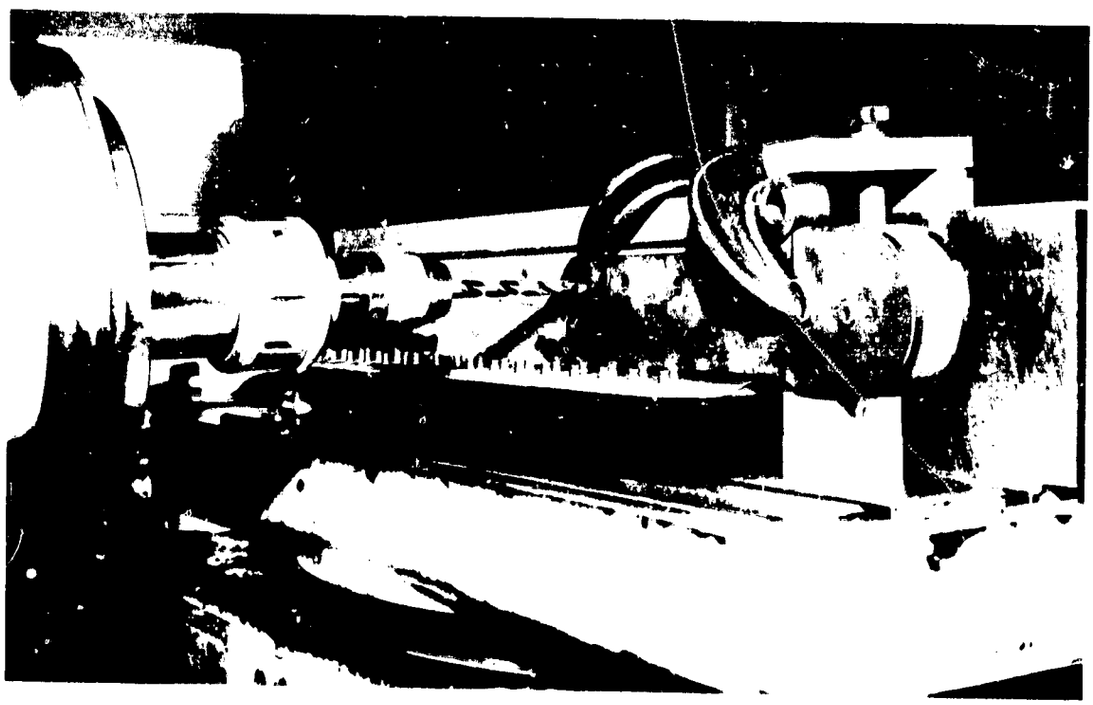

Figure 228. Spar Lug—Drilling of Fastener Holes (Test 12)

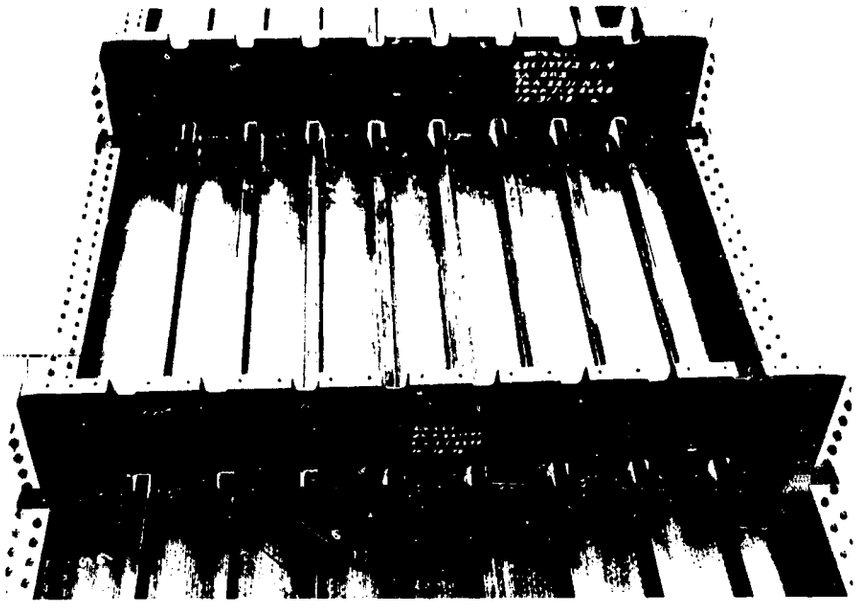

Figure 229. Sonic Test Box (Test 20)

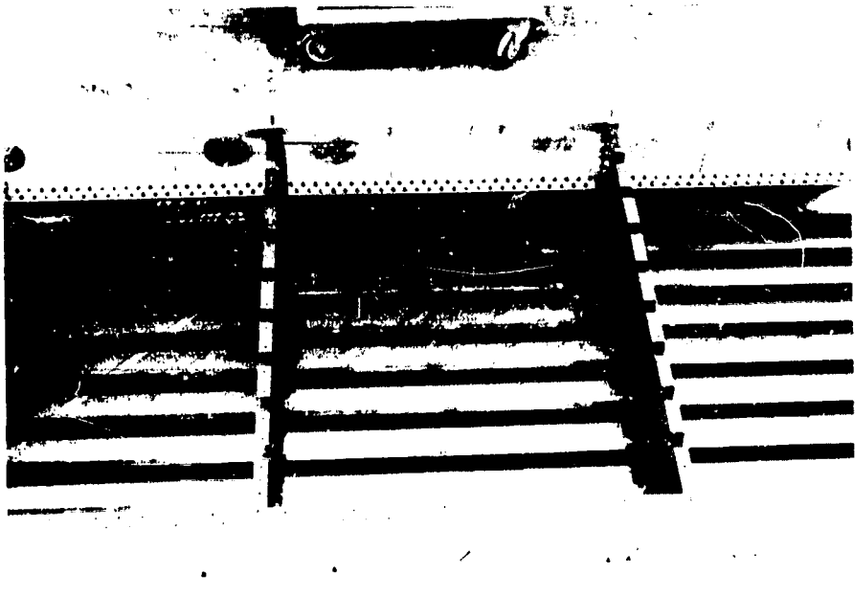

Figure 230. Sonic Test Box (Test 20)

ORIGINAL PAGE
BLACK AND WHITE PHOTOGRAPH

Figure 231. Stub Box Rear Spar—Incorporation of Precured Insert Into Layup (Test 21)

Figure 232. Stub Box Front Spar—Completed Details Being Inspected (Test 21)

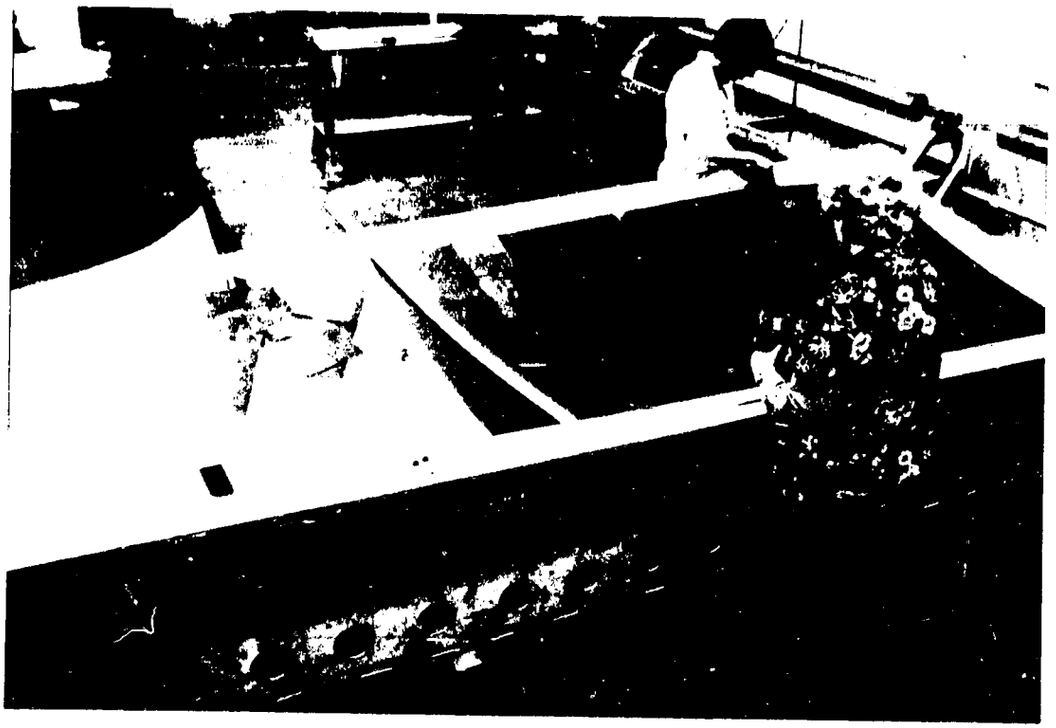

Figure 233. Stub Box I-Stiffened Skin Panel—Layup of Skin (Test 21)

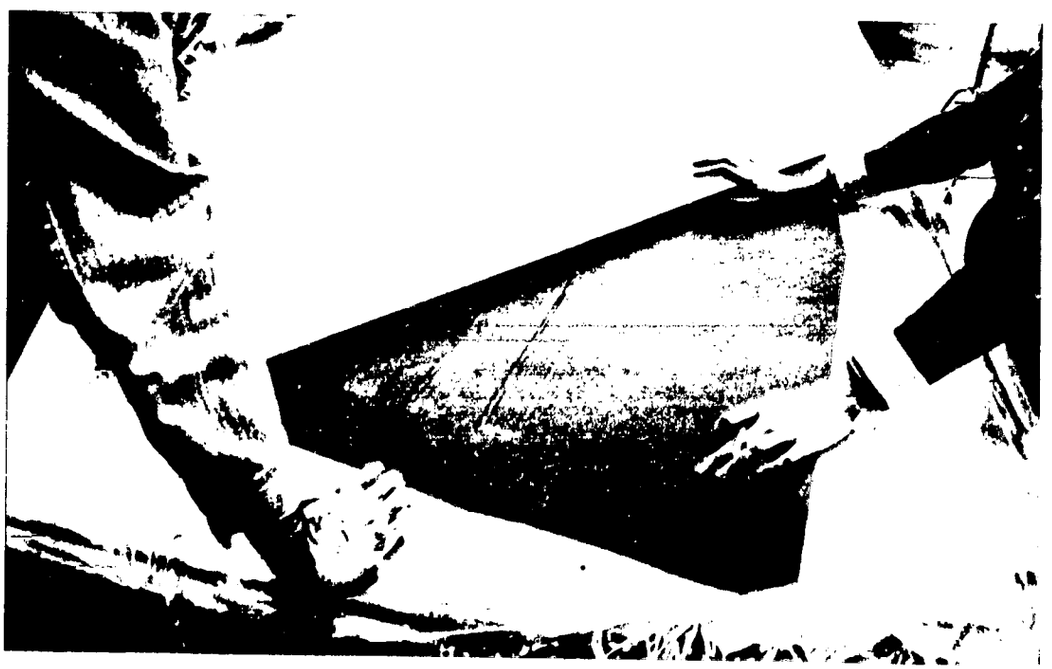

Figure 234. Stub Box I-Stiffened Skin Panel--How Locating Template Is Used (Test 21)

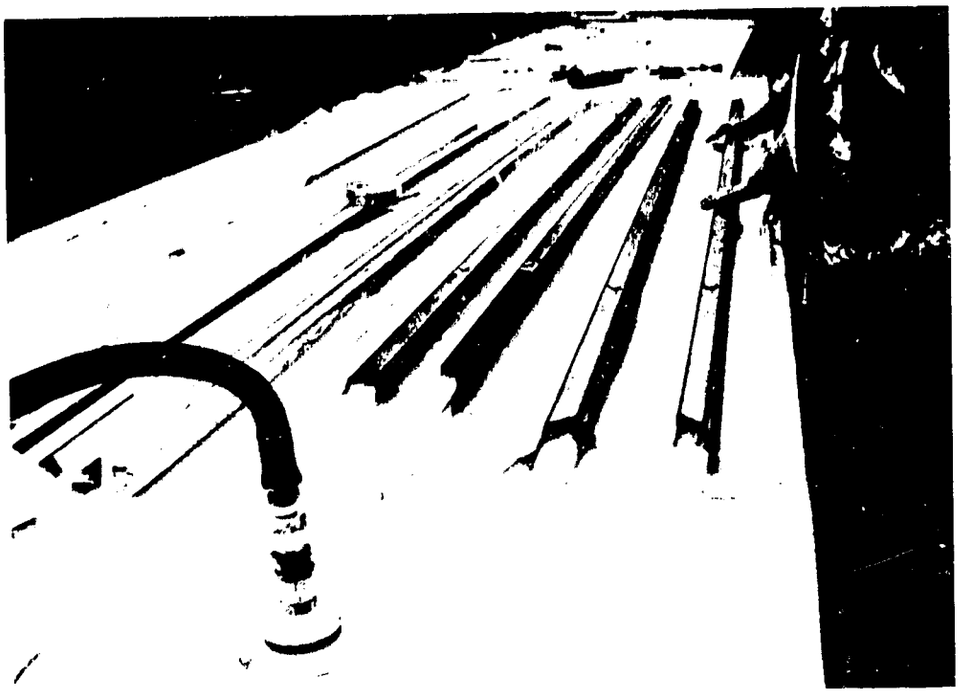

Figure 235. Stub Box I-Stiffened Skin Panel—Layup of I-Stiffeners (Test 21)

Figure 236. Stub Box I-Stiffened Skin Panel—All I-Stiffeners in Place (Test 21)

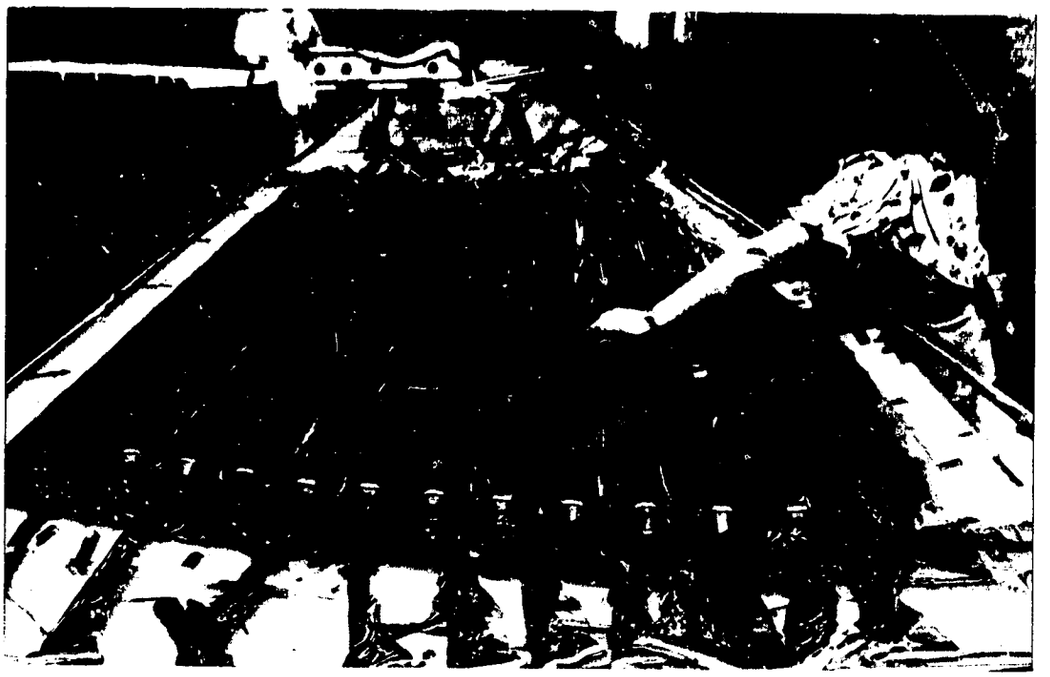

Figure 237. Stub Box I-Stiffened Skin Panel—Cured Bagged Part (Test 21)

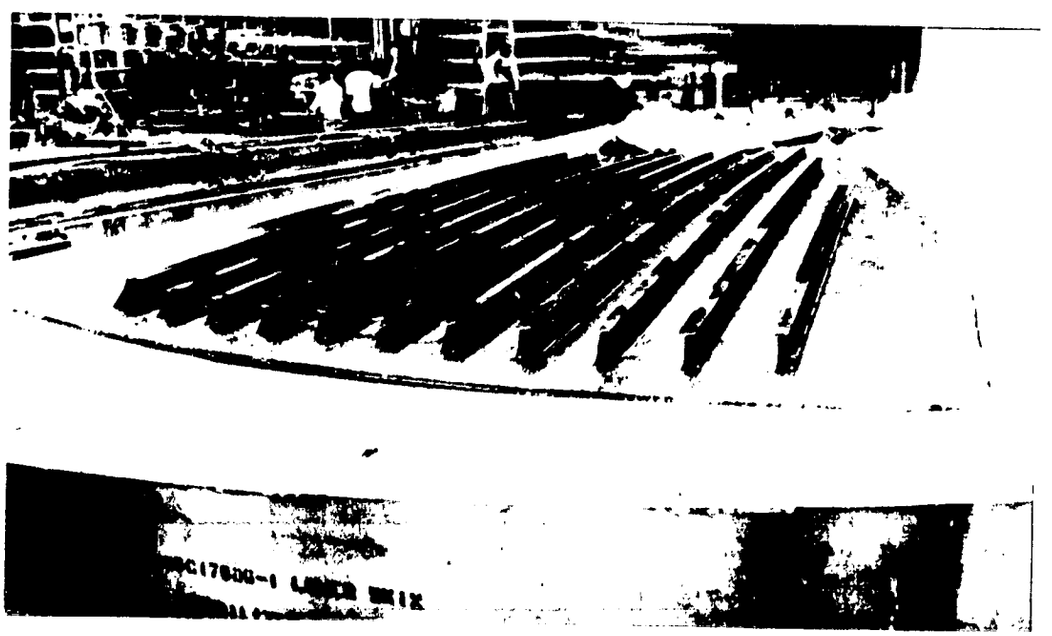

Figure 238. Stub Box I-Stiffened Skin Panel—I-Stiffened Side of Cured Panel (Test 21)

Figure 239. Stub Box I-Stiffened Skin Panel—Exterior Surface of Cured Panel (Test 21)

Figure 240. Stub Box I-Stiffened Skin Panel—Trimmed Part (Test 21)

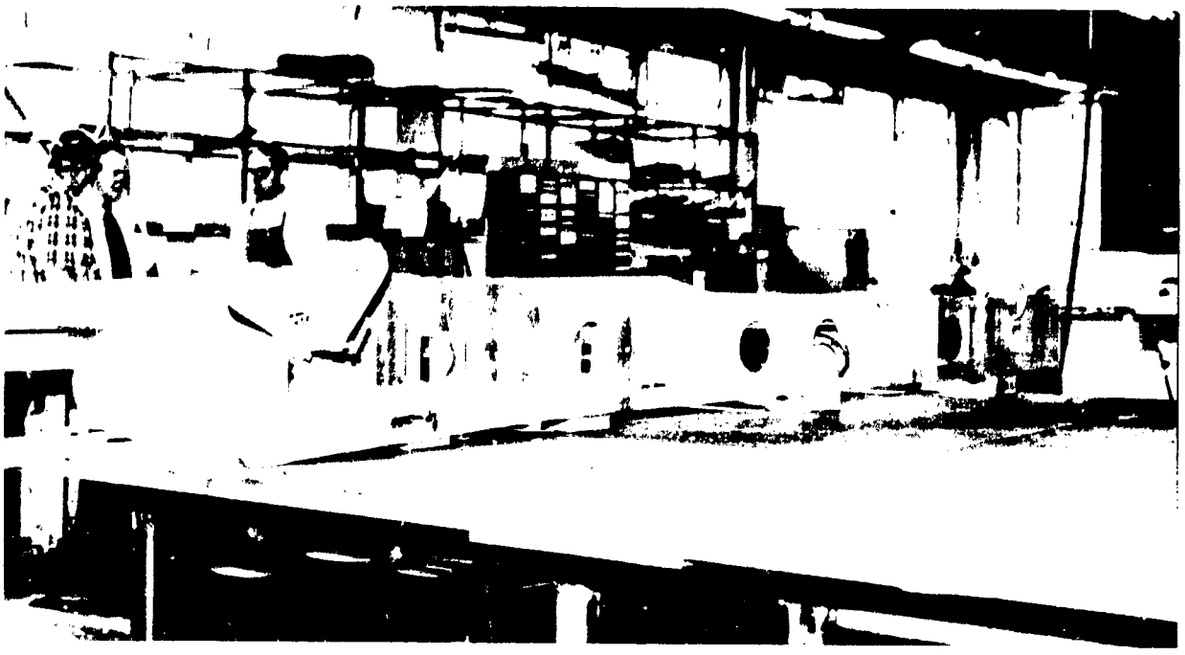

Figure 241. Stub Box—Dummy Front Spar With Aluminum Nose Ribs (Test 21)

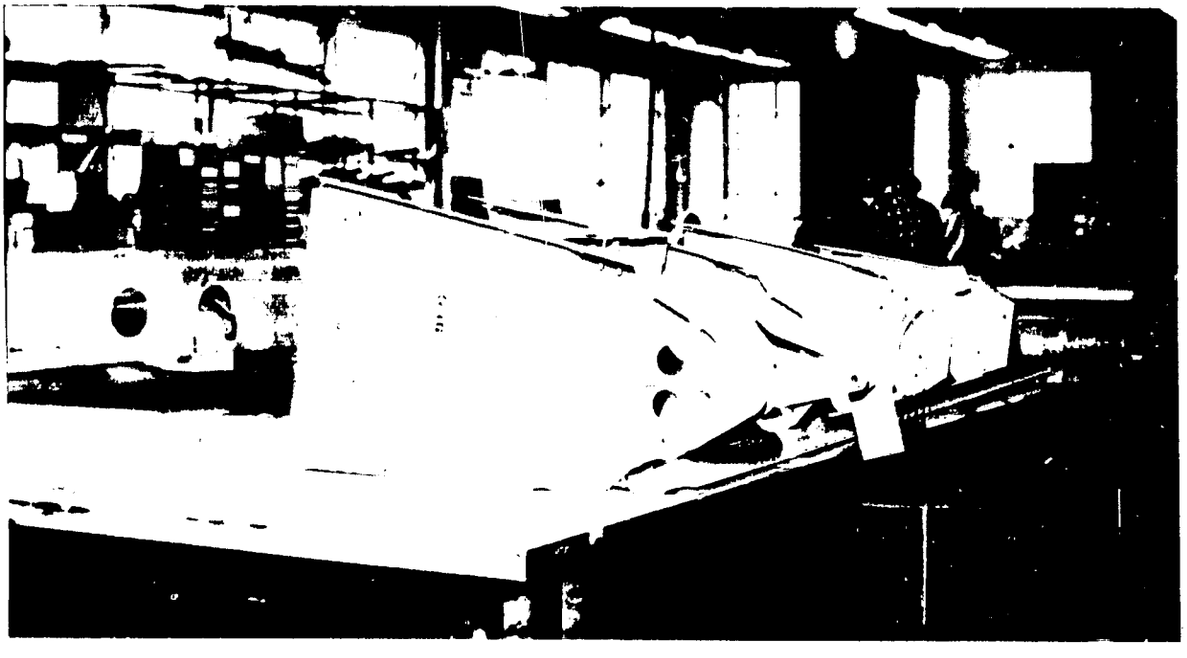

Figure 242. Stub Box—Aluminum Trailing-Edge Ribs and Fittings (Test 21)

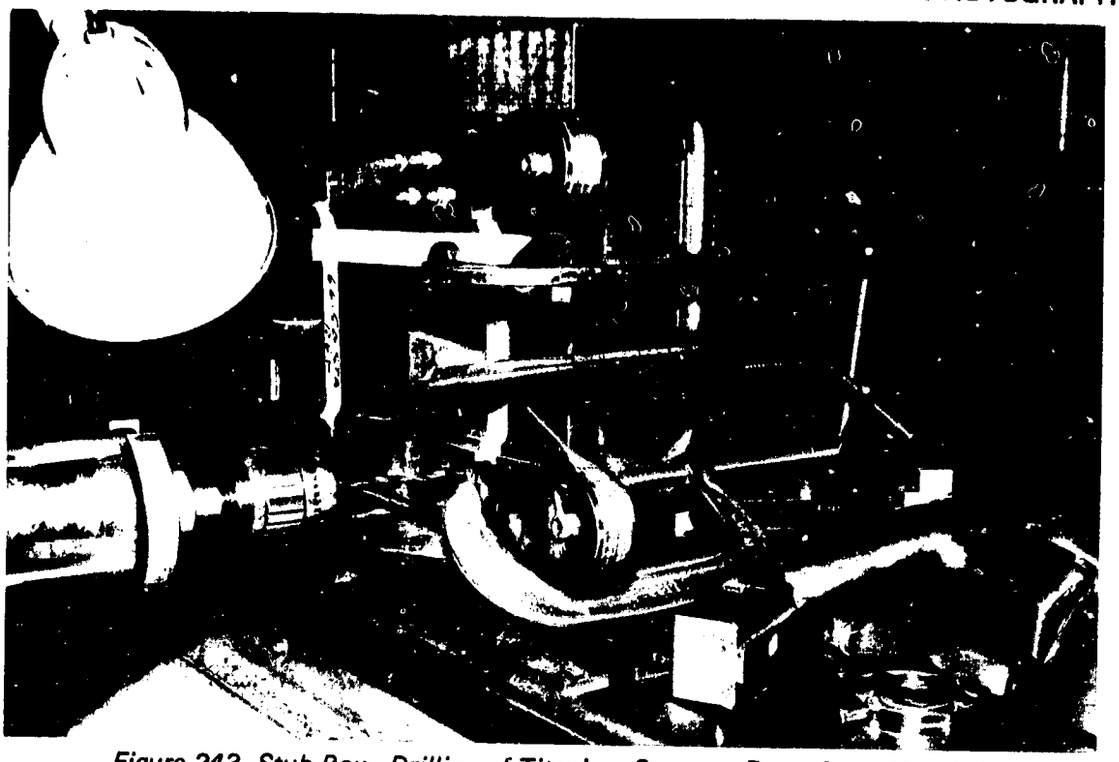

Figure 243. Stub Box—Drilling of Titanium Strap on Front Spar (Test 21)

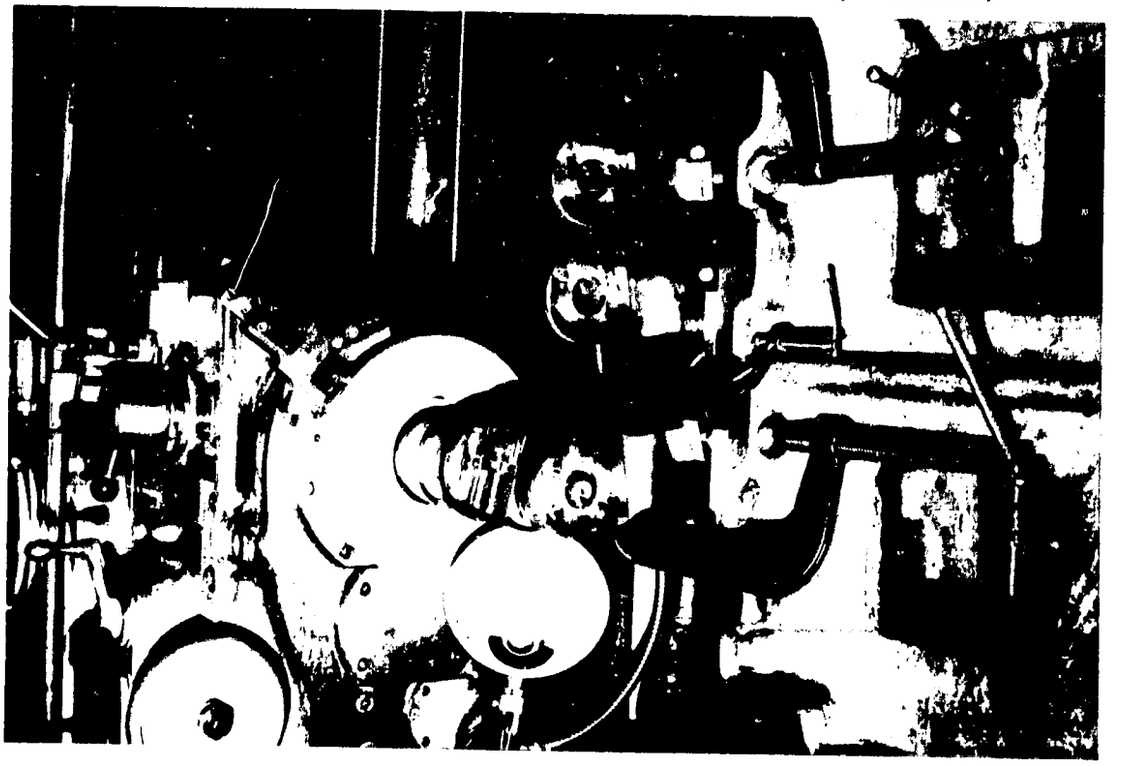

Figure 244. Stub Box—Bushing Hole Being Bored in Graphite-Titanium Stackup of Rear Spar (Test 21)

Figure 245. Stub Box—Aluminum Trailing-Edge Ribs (Test 21)

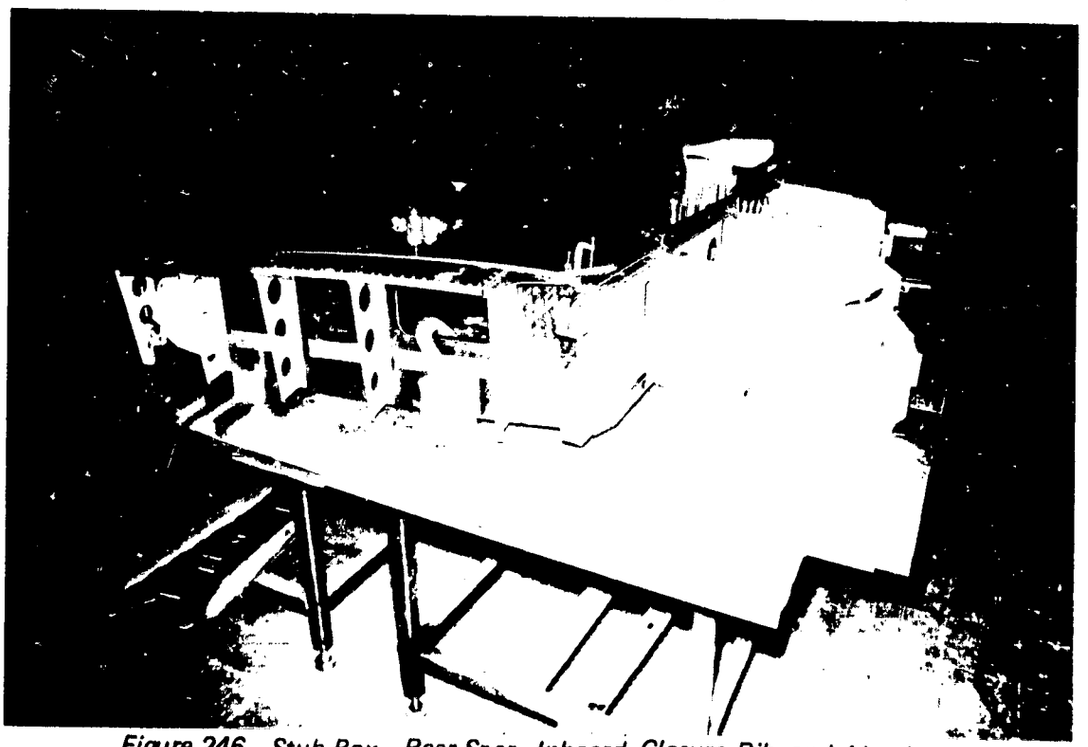

Figure 246. Stub Box—Rear Spar, Inboard Closure Rib, and Aluminum Trailing-Edge Ribs (Test 21)

Figure 247. Stub Box—Front Spar, Aluminum Nose Ribs, and Lower Skin in Place (Test 21)

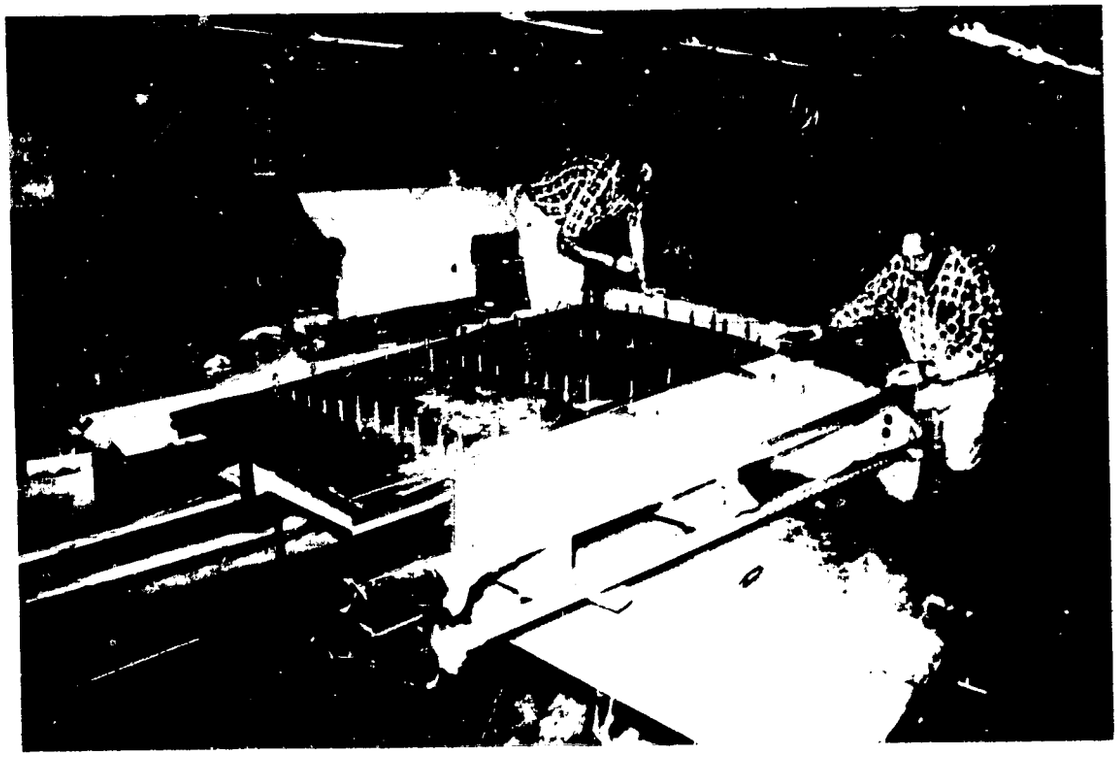

Figure 248. Stub Box—Trailing-Edge Fiberglass Closure Panel and Lower Skin in Place (Test 21)

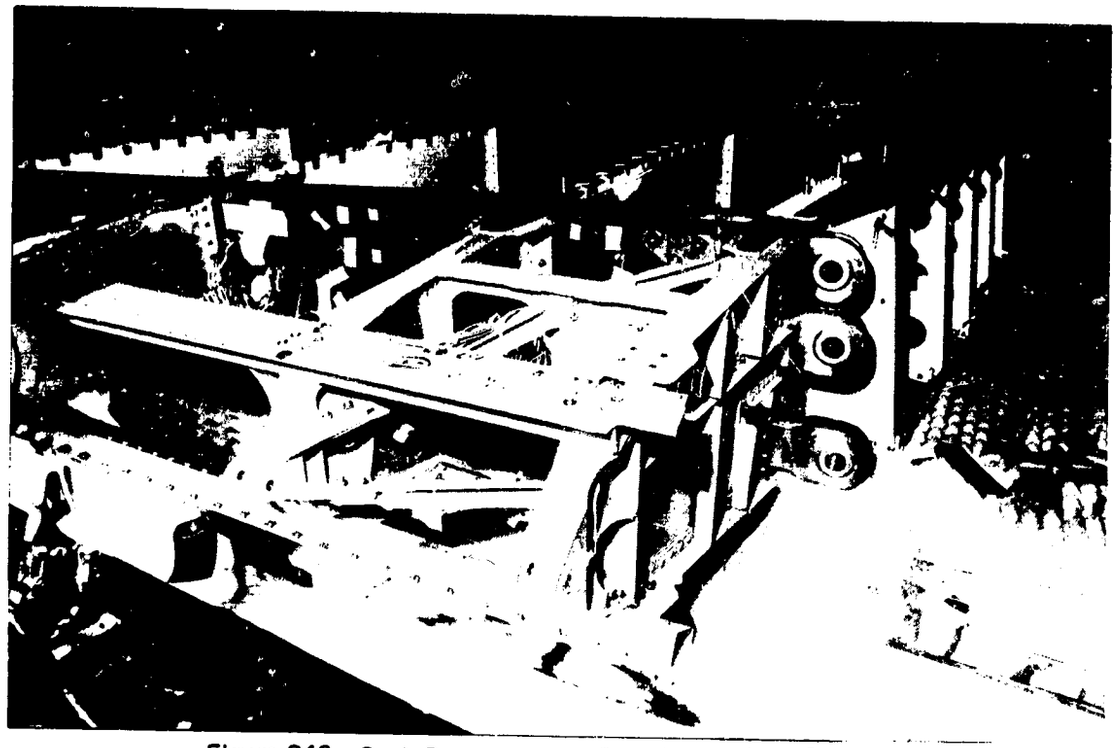

Figure 249. Stub Box—Trailing-Edge Beam, Rear Spar, and Graphite-Epoxy Ribs in Place (Test 21)

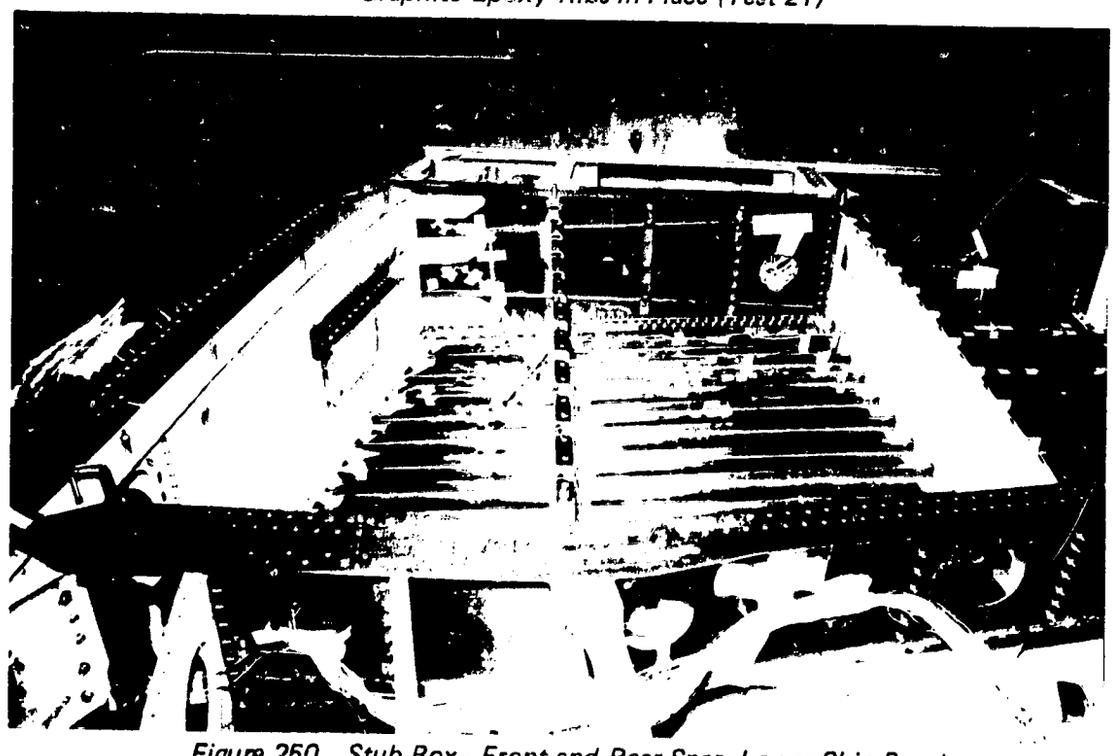

Figure 250. Stub Box—Front and Rear Spar, Lower Skin Panel, and Ribs With Instrumentation (Test 21)

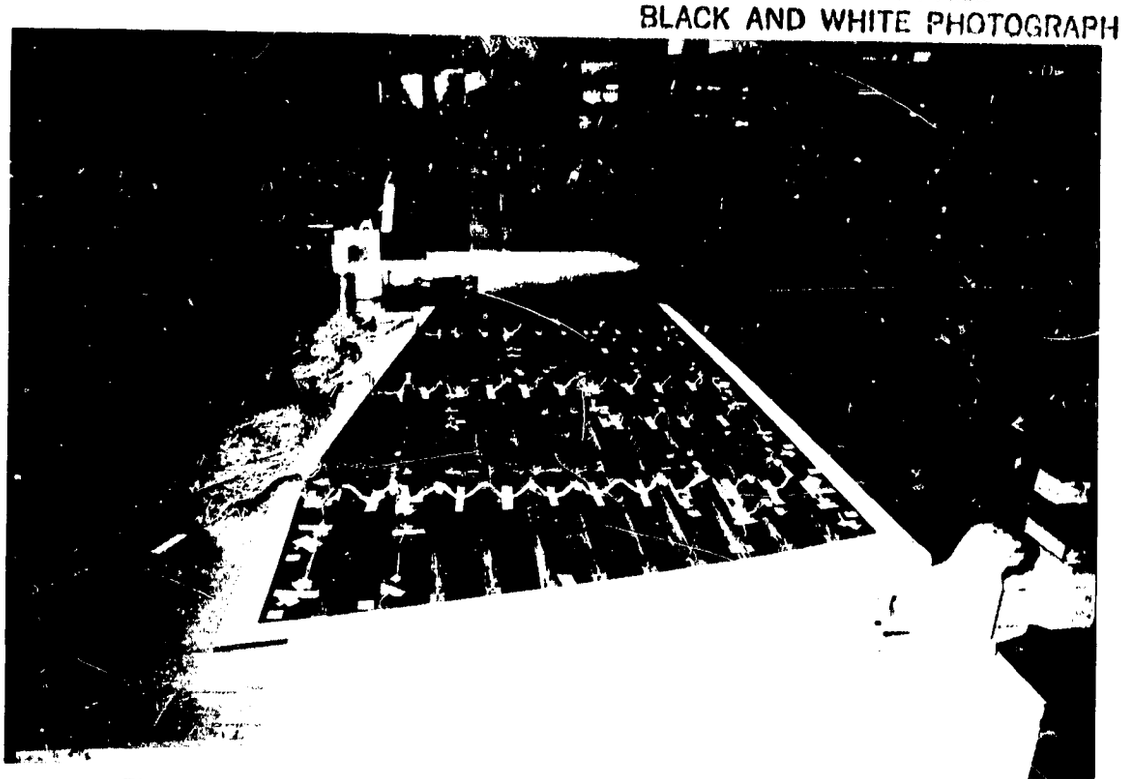

Figure 251. Stub Box —Upper Skin Panel With Instrumentation (Test 21)

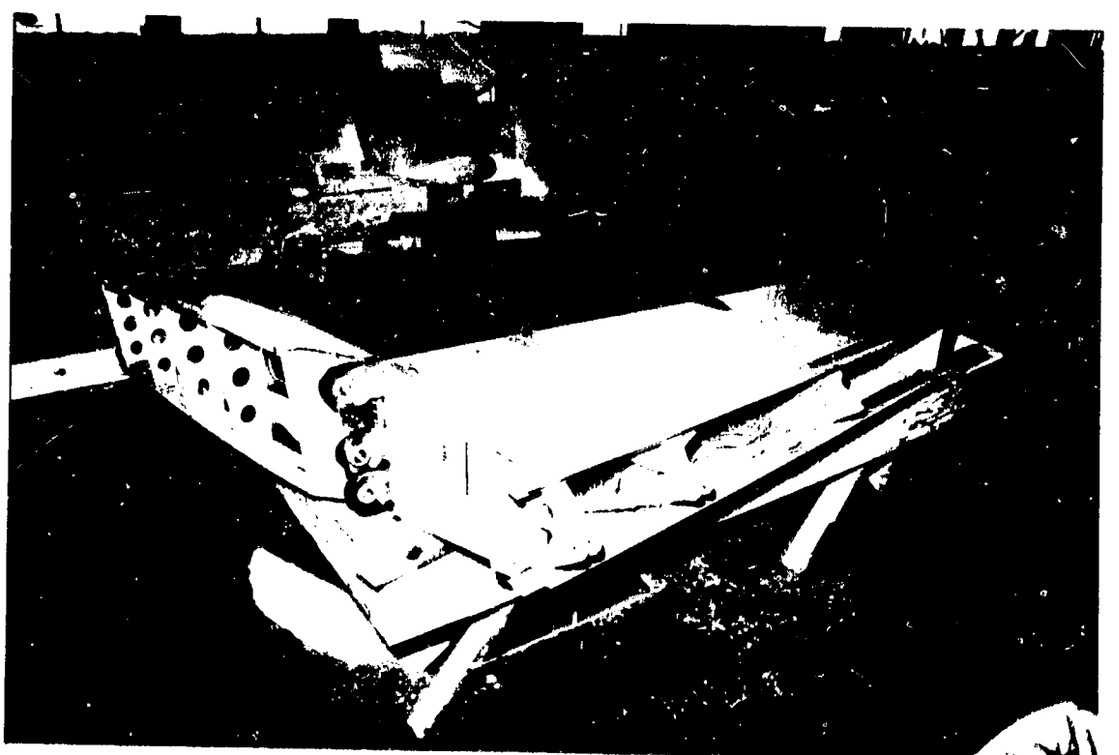

Figure 252. Stub Box—Rear View of Completed Assembly (Test 21)

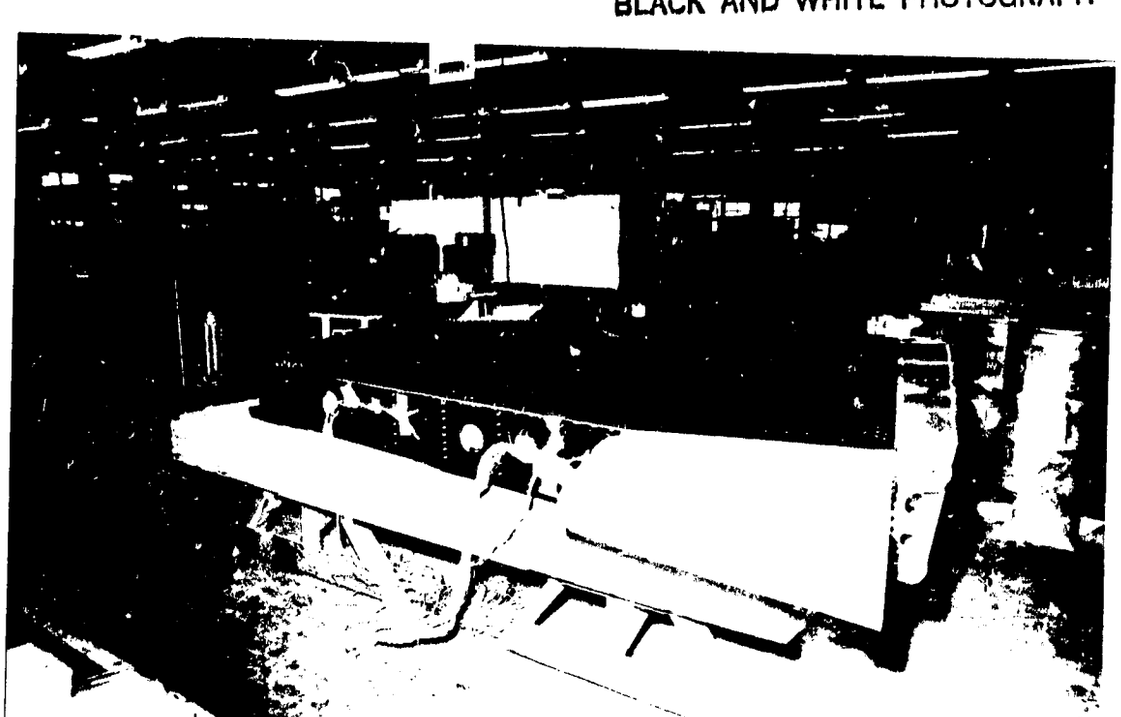

Figure 253. Stub Box—Front View of Completed Assembly (Test 21)

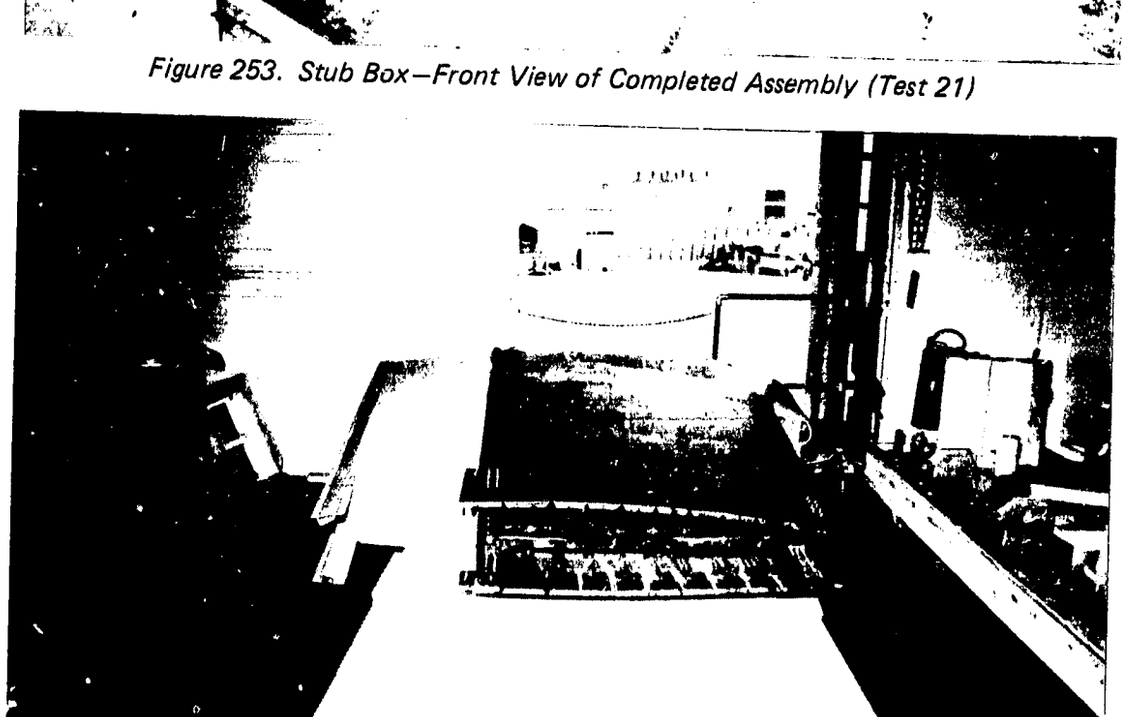

Figure 254. Stub Box—Side View of Completed Assembly (Test 21)

Figure 255. Production Verification—Front-Spar Section Prior to Trim (Test 25)

Figure 256. Production Verification—Front-Spar Section Prior to Trim (Test 25)

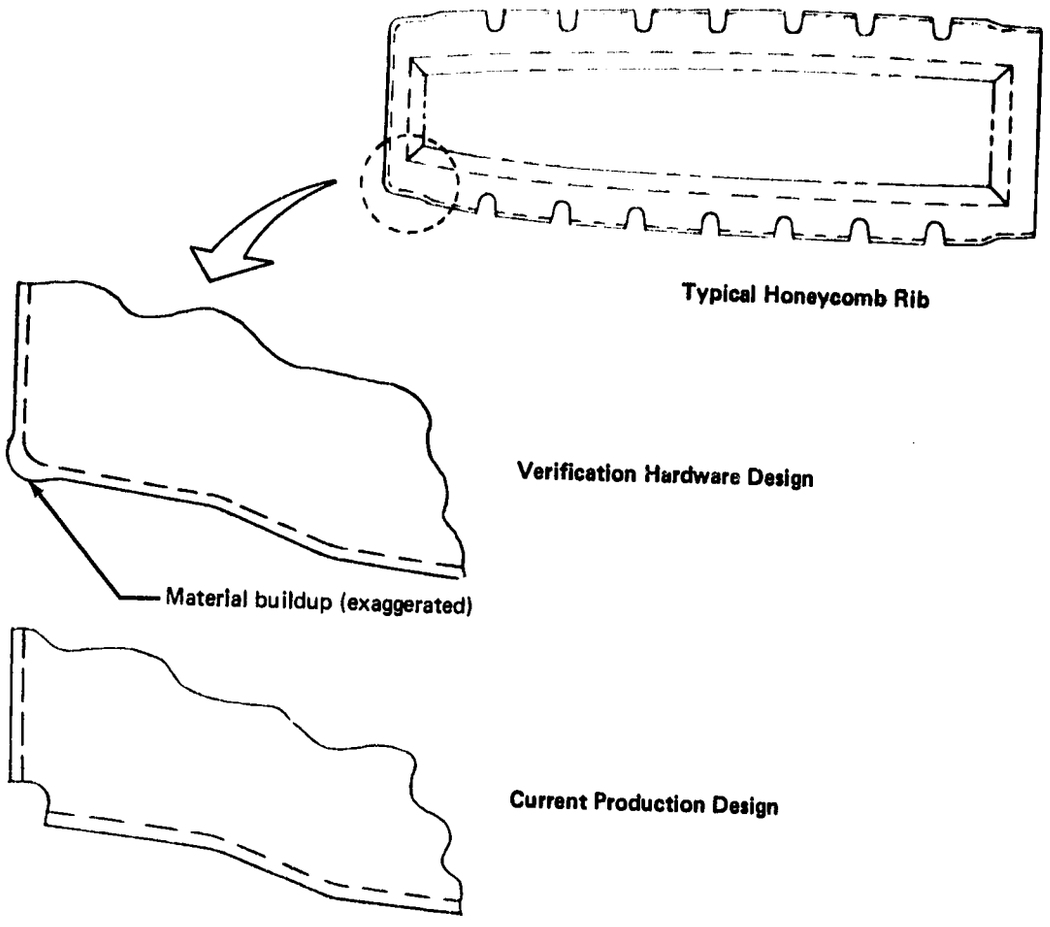

Figure 257. Honeycomb Rib Corner Details

Rear Spar Fabrication—The first chord details were scrapped because of excessive resin bleedout and bag failure during cure. Bag bridging and pleating, the causes of these discrepant conditions, were eliminated by modifying vacuum-bag installation and bag-sealant usage. These processing procedures were incorporated into a Boeing process specification.

Rib Fabrication—The first verification ribs showed excessive material buildup in the corner areas where the drawing allowed only overlap splices. Manufacturing R&D concluded that the rib design would effect some buildup in these areas in all production parts with resulting part rejection and/or expensive rework. Engineering revised and improved the rib design (fig. 257) for the production of ribs during the manufacturing phase of the program.

I-Stiffened Skin Panel Fabrication—Production of the verification I-stiffened skin panels for the Test 21 stub box showed that problems existed with excessive porosity on the panel tool surface and with panel warpage in excess of 1.40 cm (0.55 in).

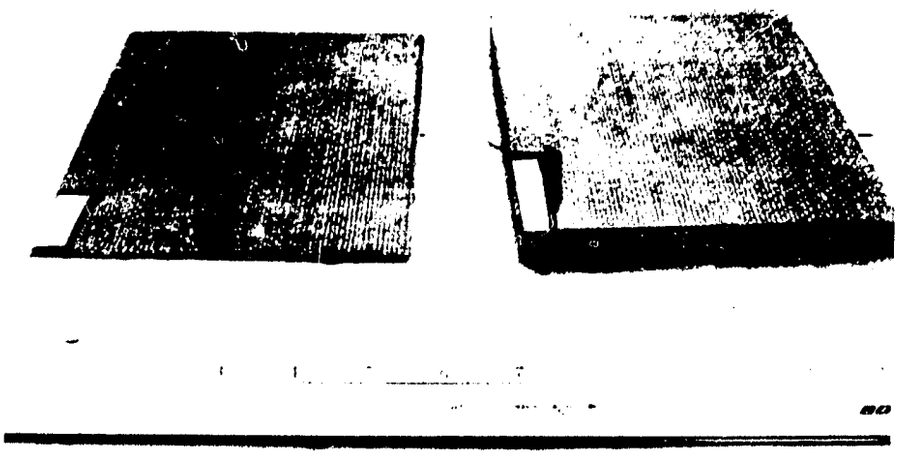

Figure 258. NDI Standards—Laminate and Honeycomb Panels

The porosity on the tool-surface side of the skin was reduced to an acceptable level by adding fiberglass yarn to provide paths for air evacuation. The Boeing process specification has been revised to require the use of fiberglass yarn in proportion to the area of the layup.

Warpage was reduced by half to 0.76 cm (0.30 in) by substituting woven graphite-epoxy fabric for the 0-deg-oriented unidirectional tape along the stringer top (fig. 169, sec. 5.1.1).

5.4 QUALITY ASSURANCE DEVELOPMENT

NDI techniques were developed and evaluated to define inspection procedures for both production and inservice use.

5.4.1 NDI Standards

Two types of standards were built and used in the evaluation: preliminary standards, which represented anticipated detail designs, and production standards, wnich exactly reproduced the production part configuration.

5.4.1.1 Preliminary Standards

The following preliminary standards were built to qualify NDI techniques for testing parts built per Boeing specifications:

Laminate Standard—0.64 x 0.64 cm (0.25 x 0.25 in) defects (figs. 258 and 259).

Honeycomb Standard—0.64 x 0.64 cm (0.25 x 0.25 in) defects (figs. 258 and 260).

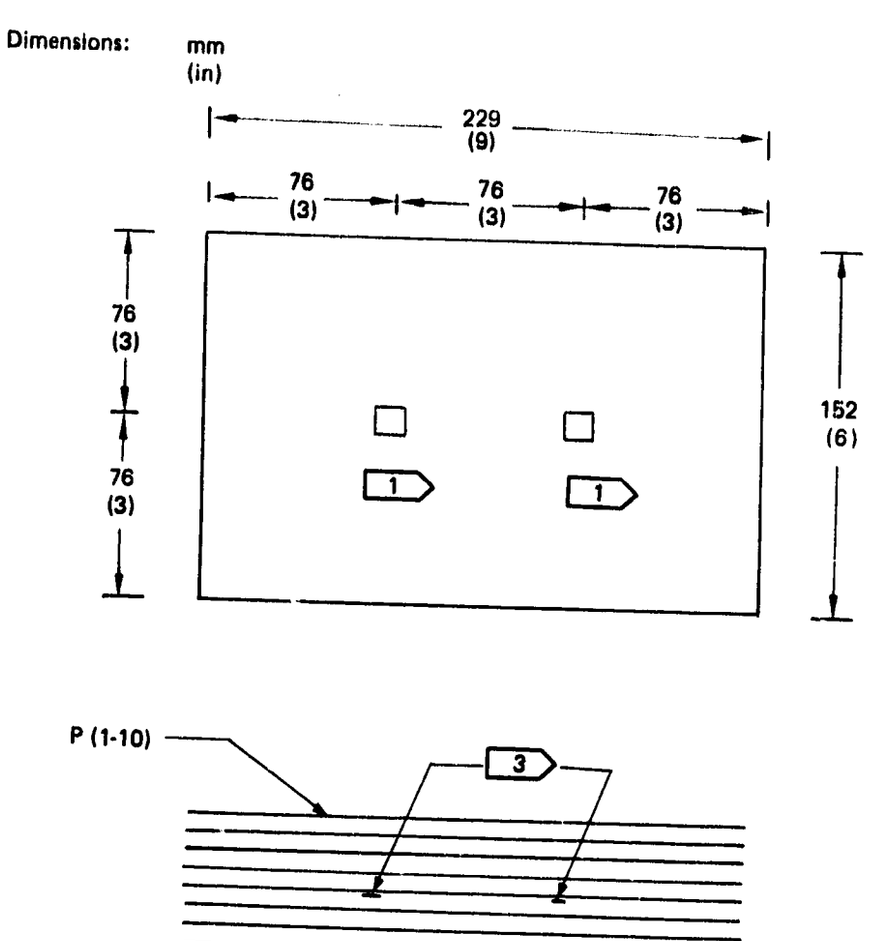

Ply No.	Orientation, deg
1	0
2	+45
3	0
4	-45
5	0
6	0
7	-45
8	0
9	+45
10	0

1 0.63-cm (0.25-in) square disbond

2 0.63-cm (0.25-in) square fabric cutout

3 0.63-cm (0.25-in) square Teflon shims—2 mil

Figure 259. NDI Reference Standard—Graphite-Epoxy Laminate

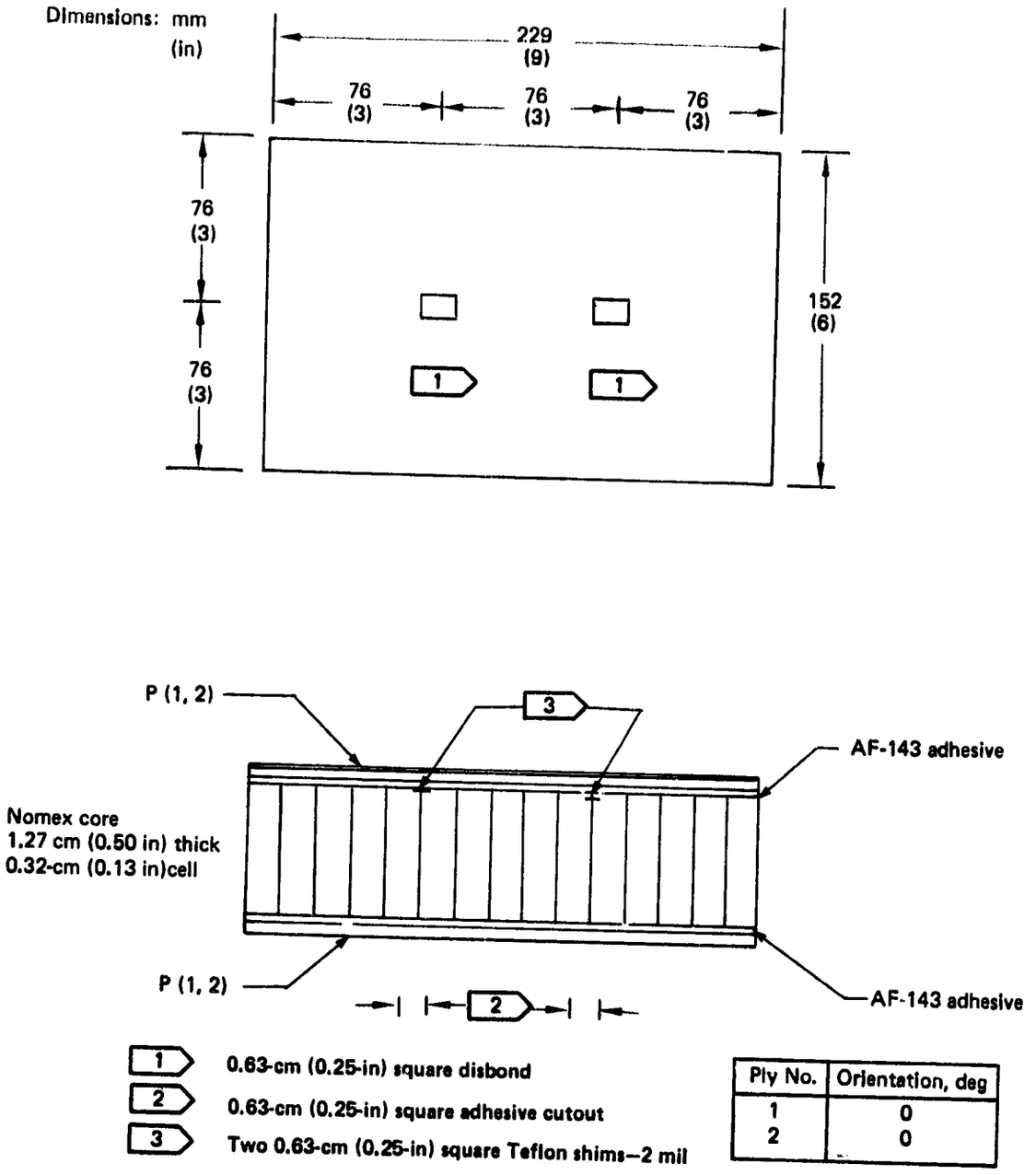

Ply No.	Orientation, deg
1	0
2	0

Figure 260. NDI Reference Standard—Graphite-Epoxy Honeycomb

Dimensions: mm
(in)

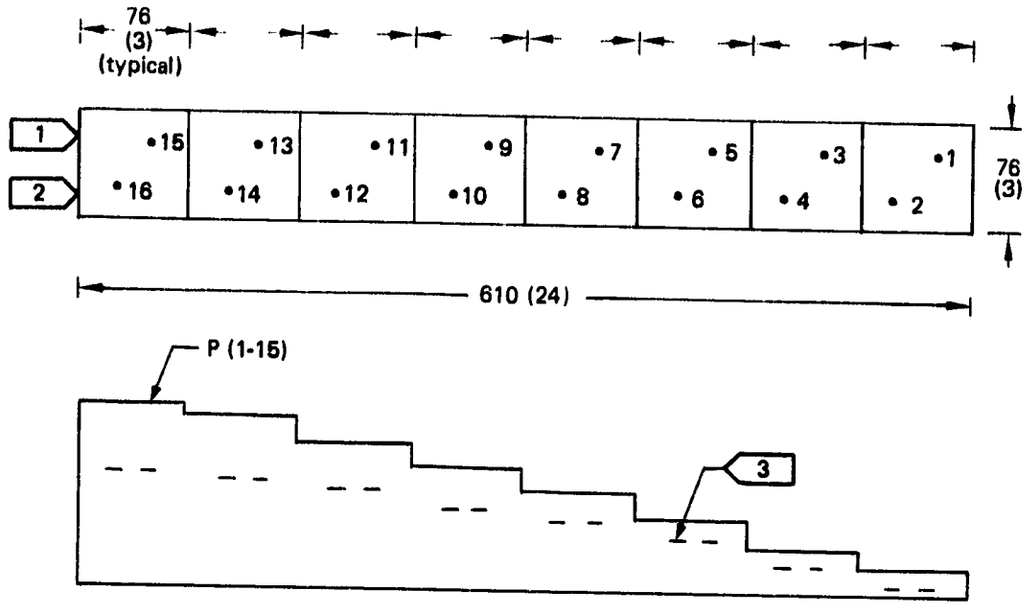

Defect 1 and 2 Between P1 and P2
Defect 3 and 4 Between P3 and P4
Defect 5 and 6 Between P4 and P5
Defect 7 and 8 Between P5 and P6
Defect 9 and 10 Between P6 and P7
Defect 11 and 12 Between P7 and P8
Defect 13 and 14 Between P8 and P9
Defect 15 and 16 Between P9 and P10

1 0.63 x 0.63-cm (0.25 x 0.25-in) defect
2 1.27 x 1.27-cm (0.5 x 0.5 in) defect
3 Two 2-mil Teflon shims of specified defect size

Ply No.	Orientation, deg	Ply No.	Orientation, deg
1	0	8	+45
2	+45	9	0
3	90	10	90
4	0	11	-45
5	-45	12	0
6	90	13	90
7	0	14	+45
		15	0

Figure 261. Laminate Step Standard

Laminate Step Standard—Eight steps of increasing thickness with 0.64 x 0.64 cm (0.25 x 0.25 in) and 1.28 x 1.28 cm (0.05 x 0.50 in) defects in each step (fig. 261).

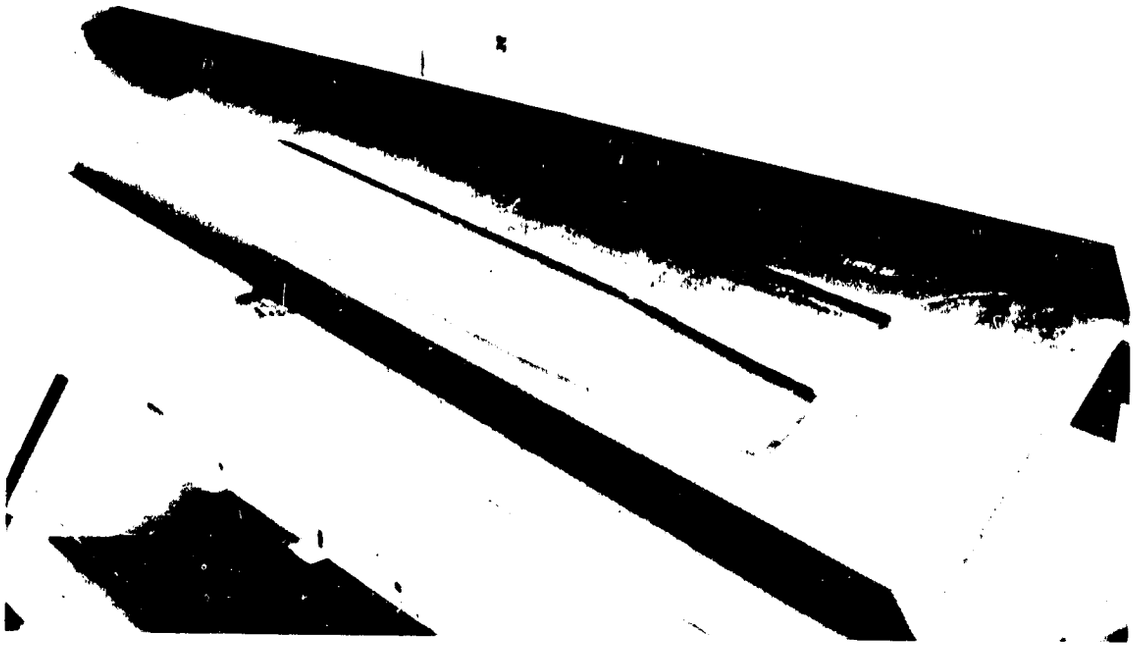

Figure 262. Rear-Spar Channel Assembly

Rear-Spar Channel Assembly—Built to full scale (fig. 262) with defects ranging from 0.64 x 0.64 cm (0.25 x 25 in) to 5.08 x 10.16 cm (2.0 x 4.0 in). Figure 263 and Table 36 illustrate configurations and details of defect incorporation.

Rear-Spar Assembly—With defects ranging from 0.64 x 0.64 cm (0.25 x 0.25 in) to 3.81 x 3.81 cm (1.5 x 1.5 in). Figure 264 shows this standard being inspected using the Fokker Bond Tester (ref. 17), and Figure 265 shows inspection using the Sondicator (ref. 17).

Honeycomb Rib—Built full scale, with defects ranging from 0.65 x 0.64 cm (0.25 x 0.25 in) to 2.54 x 2.54 cm (1.0 x 1.0 in) (fig. 266).

I-Stiffened Skin Panel—Built to scale but with defects ranging from 0.64 x 0.64 cm (0.25 x 0.25 in) to 2.54 x 2.54 cm (1.0 x 1.0 in) incorporated in both the skin and I-stiffeners (fig. 267).

5.4.1.2 Production Standards

The following were built to production prints and in accordance with Boeing standard processing:

Rear-Spar Channel Assembly—Built full scale with the same configuration and defect inclusions as the equivalent preliminary standard (figs. 262 and 263 and table 36).

Rear-Spar Assembly—Built with defects identical to the preliminary standard. Figure 265 shows this standard being inspected with the Sondicator.

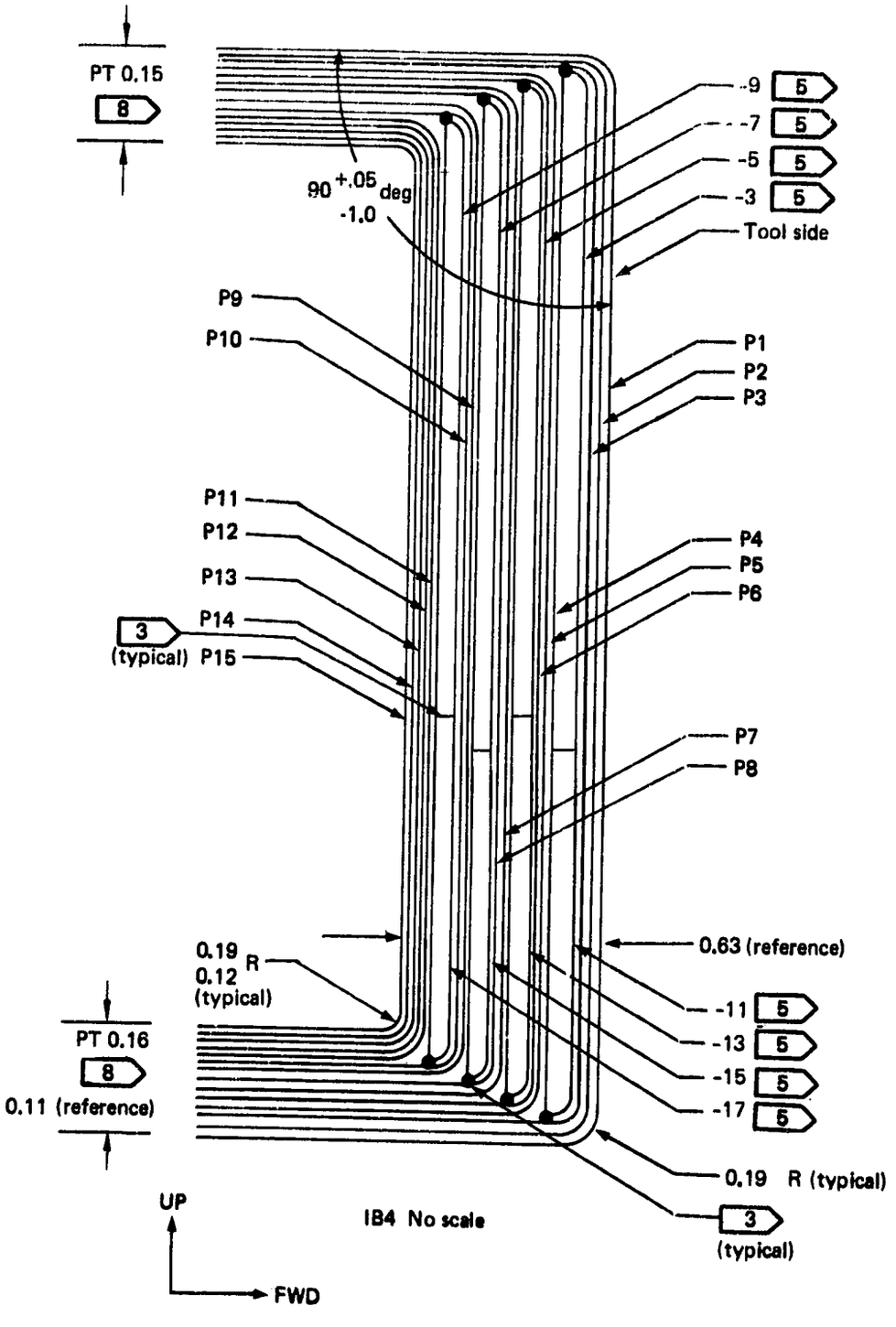

Figure 263. Rear-Spar Channel Cross-Section Detail

Table 36. Rear-Spar Channel Defects and Fabrication Details

<8> PLY TABLE

Part No.	Ply No. "P"	Material	Tape/cloth warp orientation, deg	Splice	Revision letter
-1 Assy	P1,P2,P4,P5,P7,P8 P10,P12,P14,P16-P19	<1>	+45 or -45	<4>	
	P3,P6,P9,P11,P13,P15	<1>	0	<9>	
-2 Assy	P1,P2,P4,P5,P7,P8 P10,P12,P14,P16-P19	<1>	+45 or -45	<4>	
	P3,P6,P9,P11,P13,P15	<1>	0	<9>	
-3 -4 Opp	P1,P5,P10,P14	<1>	+45 or -45	<4>	A
	P2,P3,P6,P7,P8,P9,P12,P13	<2>	0	None	A
	P4,P11	<1>	0	None	
-5 -6 Opp	P1,P5,P10,P14	<1>	+45 or -45	<4>	A
	P2,P3,P6,P7,P8,P9,P12,P13	<2>	0	None	A
	P4,P11	<1>	0	None	
-7	P2,P3,P4,P7,P8,P9 P12,P13,P14,P17,P18,P19	<1>	+45 or -45	<4>	
	P1,P5,P6,P10,P11,P15, P16,P20	<1>	0	None	
-8	P1,P3,P4,P6,P7,P9,P10,P12	<1>	+45 or -45	<4>	
	P2,P5,P8,P11	<1>	0	None	
-9	P2,P3,P4,P7,P8,P9,P12, P13,P14,P17,P18,P19	<1>	+45 or -45	<4>	
	P1,P5,P6,P10,P11,P15, P16,P20	<1>	0	None	
-10	P1,P3,P4,P6,P7,P9,P10,P12	<1>	+45 or -45	<4>	
	P2,P5,P8,P11	<1>	0	None	
-11 -12 Opp	P1,P5,P10,P14	<1>	+45 or -45	<4>	A
	P2,P3,P6,P7,P8,P9,P12,P13	<2>	0	None	A
	P4,P11	<1>	0	None	
-13 -14 Opp	P1,P5,P10,P14	<1>	+45 or -45	<4>	A
	P2,P3,P6,P7,P8,P9,P12,P13	<2>	0	None	A
	P4,P11	<1>	0	None	
-15	P2,P3,P4,P7,P8,P9, P12,P13,P14,P17,P18,P19	<1>	+45 or -45	<4>	
	P1,P5,P6,P10,P11,P15, P16,P20	<1>	0	None	
-16	P1,P3,P4,P6,P7,P9,P10,P12	<1>	+45 or -45	<4>	
	P2,P5,P8,P11	<1>	0	None	
-17	P2,P3,P4,P7,P8,P9, P12,P13,P14,P17,P18,P19	<1>	+45 or -45	<4>	
	P4,P5,P6,P10,P11,P15, P16,P20	<1>	0	None	
-18	P1,P3,P4,P6,P7,P9,P10,P12	<1>	+45 or -45	<4>	
	P2,P5,P8,P11	<1>	0	None	

<1> Epoxy impregnated graphite fabric per BMS 8-212, Type II, Class 2, Style 3K-70-P. Fabricate per BAC 5562. Peel ply required on bonding surface

<2> Epoxy impregnated graphite unidirectional tape, Type II, Class 1, Grade 145 per BMS 8-212. Fabricate per BAC 5562

<3> Graphite-epoxy fillers <2> as required

<4> Lap-splice per BAC 5562

<5> One layer of AF-143 adhesive (0.05 lb/ft^2) per BMS 5-104, to be applied to upper and lower surfaces of precured fillers during installation of wrap plies. Cocure with graphite-epoxy wrap plies per BAC 5562

<6> Tolerance on ply edge locations ±0.06

<7> Ply orientation convention:
Fabric 0 deg is parallel to the warp direction
Tape 0 deg is parallel to the fiber direction

<8> All graphite-epoxy trimmed detail parts, subassemblies and assemblies on this drawing to be weighed, and thickness measured at the locations shown. Quality control to record and submit the weights and measurements. Identity number of peel plies included in thickness measurements.

<9> No splice allowed in P3 or P6. Lap-splice <4> in P9, P11, P13, P15 is allowed in the 90 deg fibers only, at the location shown in Zones D6-2 and D6-3 (optional).

<10> Two plies of nonbondable Teflon, 2-mil thick, each. Size and location as shown. Tolerance on size ±0.05; tolerance on location ±0.12.

<11> Between -9 or -17 and P11 <10>
<12> Between P8 and -7 or -15 <10>
<13> Between P10 and -9 or -17 <10>
<14> Between P3 and -3 or -11 <10>
<15> Between P3 and P4 <10>
<16> Between -7 and P9 <10>
<17> Between P6 and P7 <10>
<18> Between P4 and P5 <10>
<19> Between -5 or -13 and P7 <10>
<20> Between -6 and P7 <10>
<21> Between P10 and P11 <10>

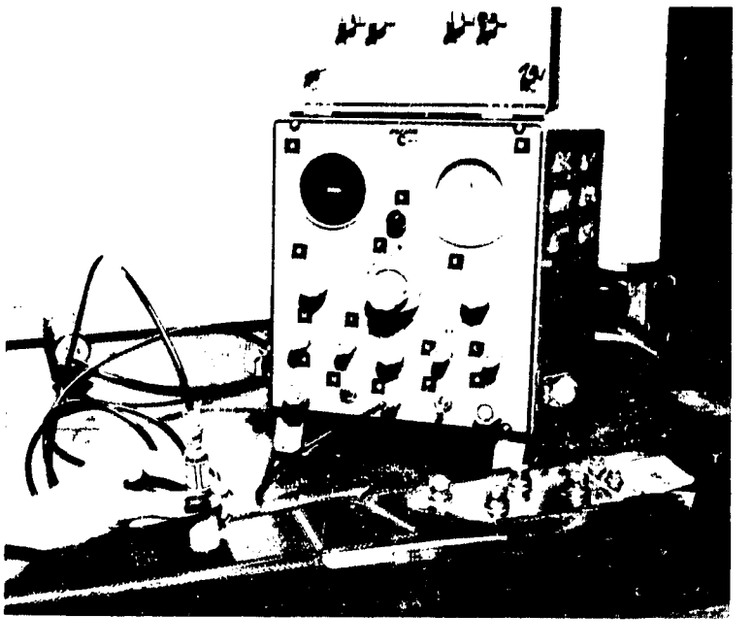

Figure 264. Fokker Bond Testing of Rear-Spar Assembly

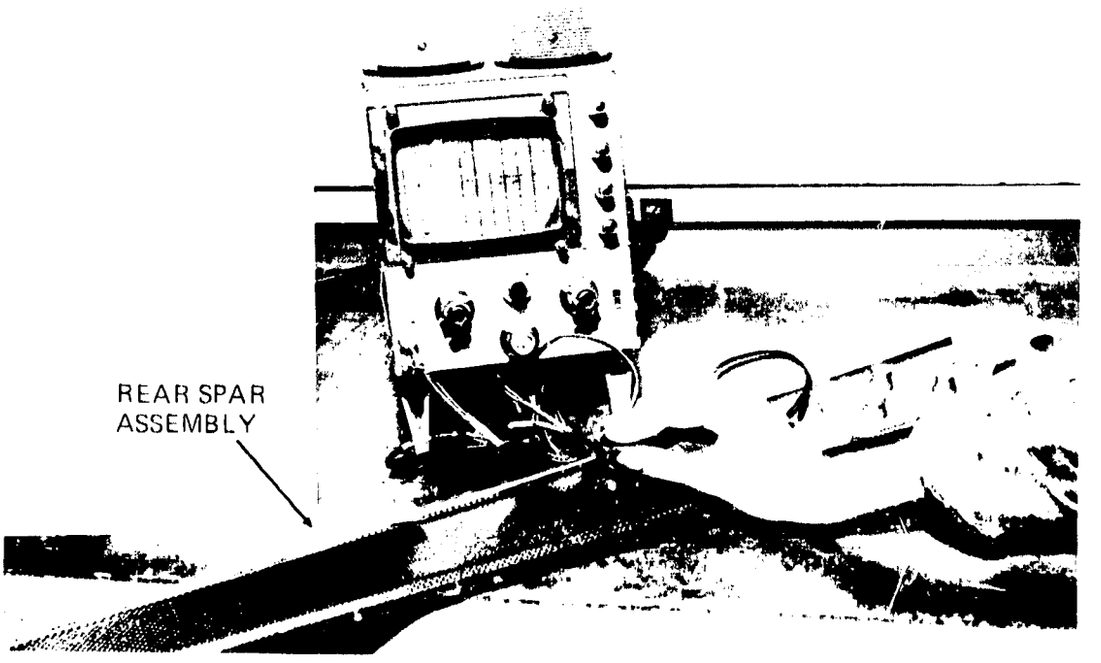

Figure 265. Sondicator Inspection of Rear-Spar Assembly

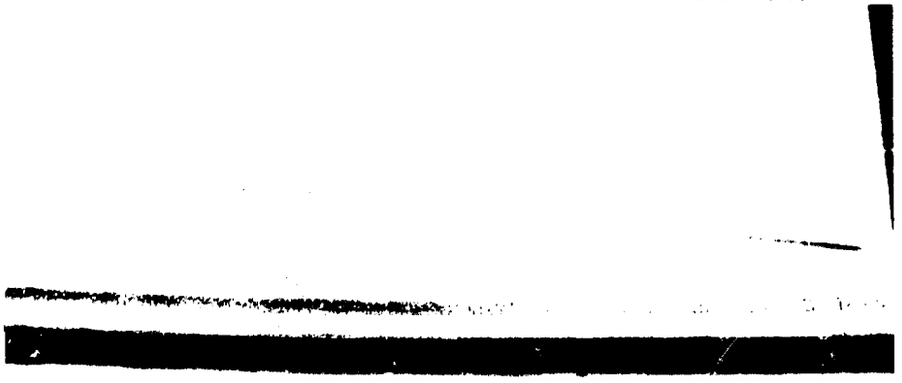

Figure 266. Honeycomb Rib

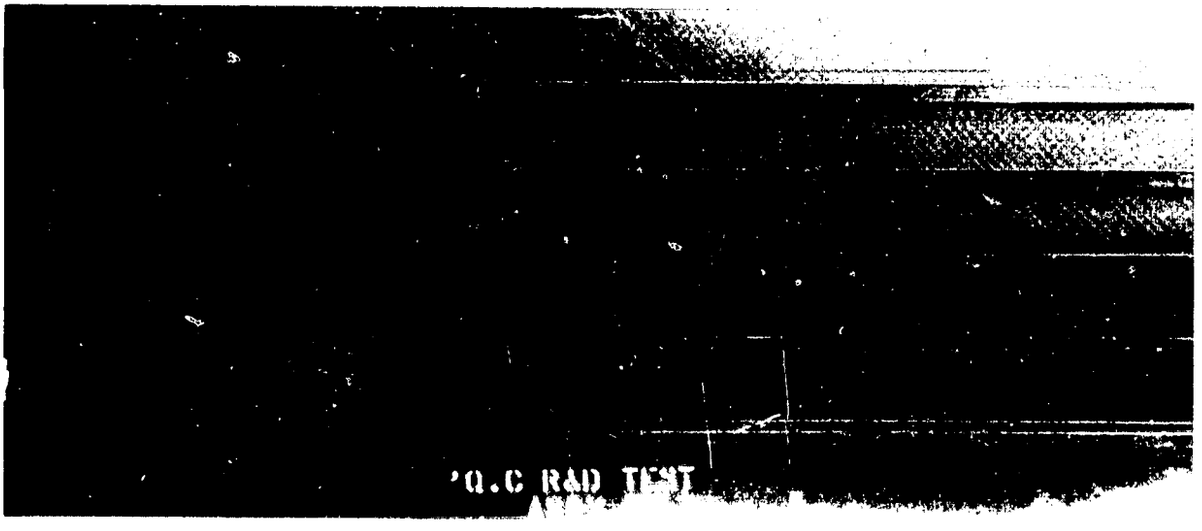

Figure 267. I-Stiffener Panel—Preliminary NDI Standard

Rear-Spar Channel No. 1—With no built-in defects but with porosity caused by blanket leaks as shown with the ultrasonic C-scan recording in Figure 268.

Rear-Spar Channel No. 2—Similar to No. 1 but without porosity as described in Figure 269.

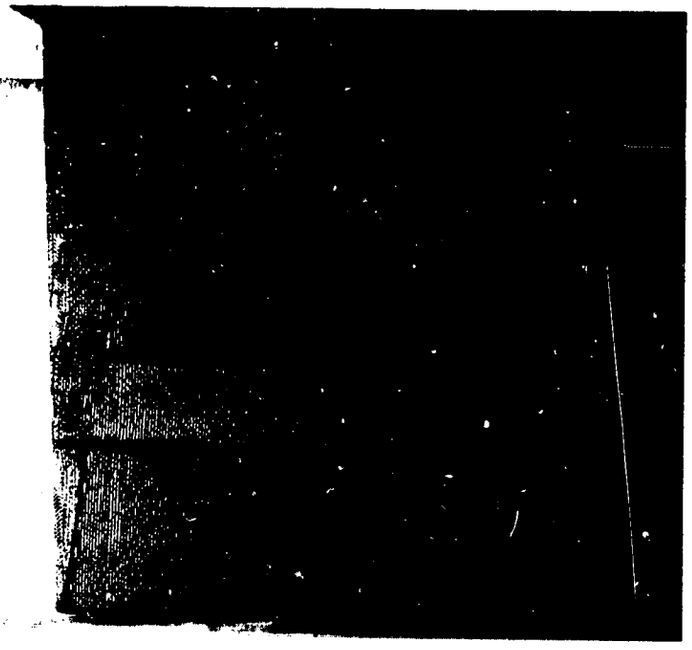

SCAN SHOWS
POROSITY

Figure 268. Rear-Spar Channel and C-Scan Recording

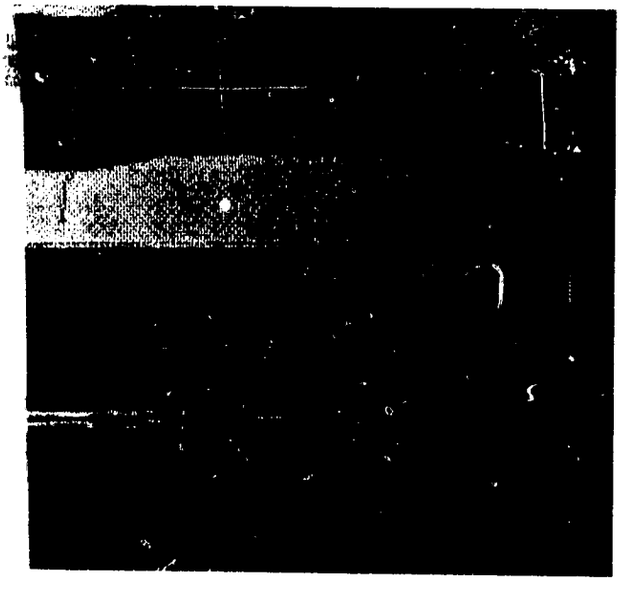

GOOD SCAN

Figure 269. Rear-Spar Channel and C-Scan Recording

Laminate Rib—Fabricated full scale with defects incorporated as described in Figure 270.

Honeycomb Rib—Fabricated full scale with defects incorporated as described in Figure 271.

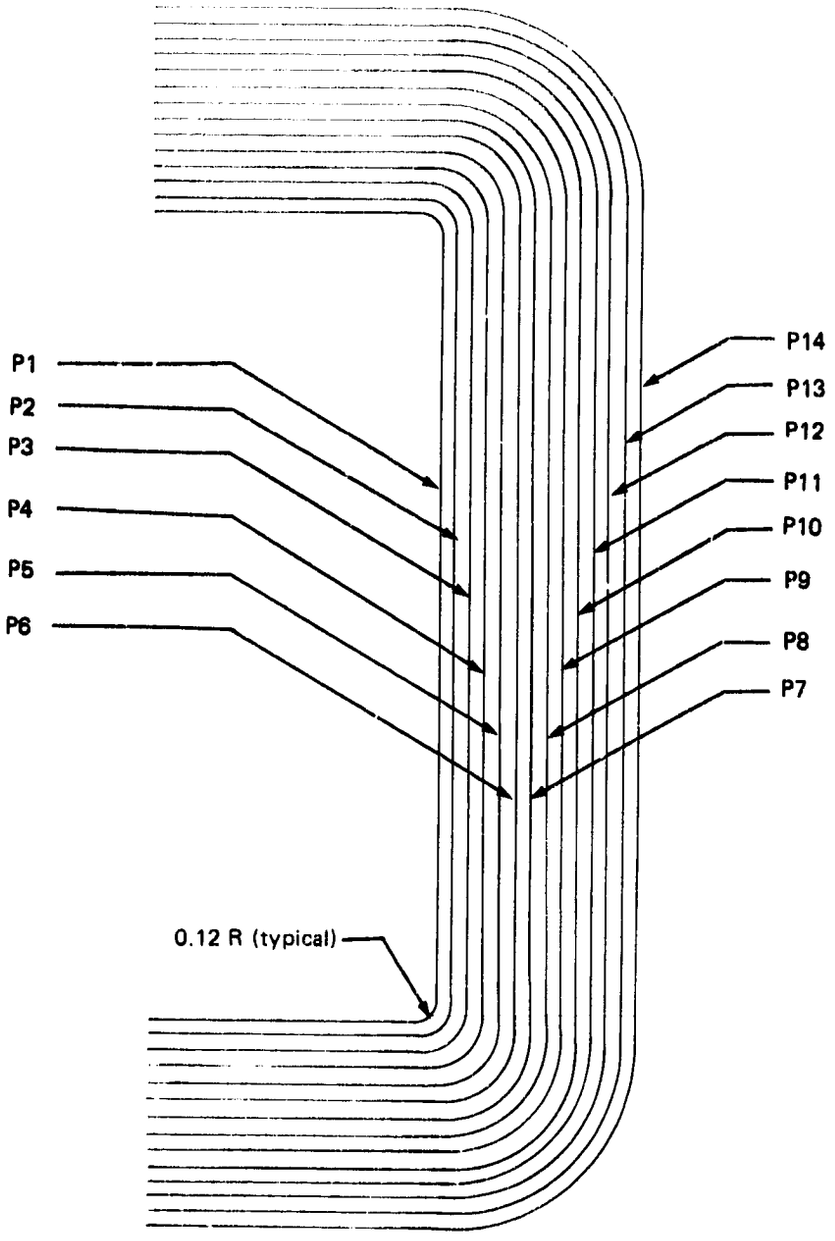

- 0.64 x 0.64-cm (0.25 x 0.25-in) and 1.28 x 1.28-cm (0.5 x 0.5-in) defects between P2 and P3; P6 and P7; P8 and P9; and P10 and P11
- 0.64 x 0.64-cm (0.25 x 0.25-in) and 1.28 x 1.28-cm (0.5 x 0.5-in) defects on both flanges

Figure 270. Laminate Rib

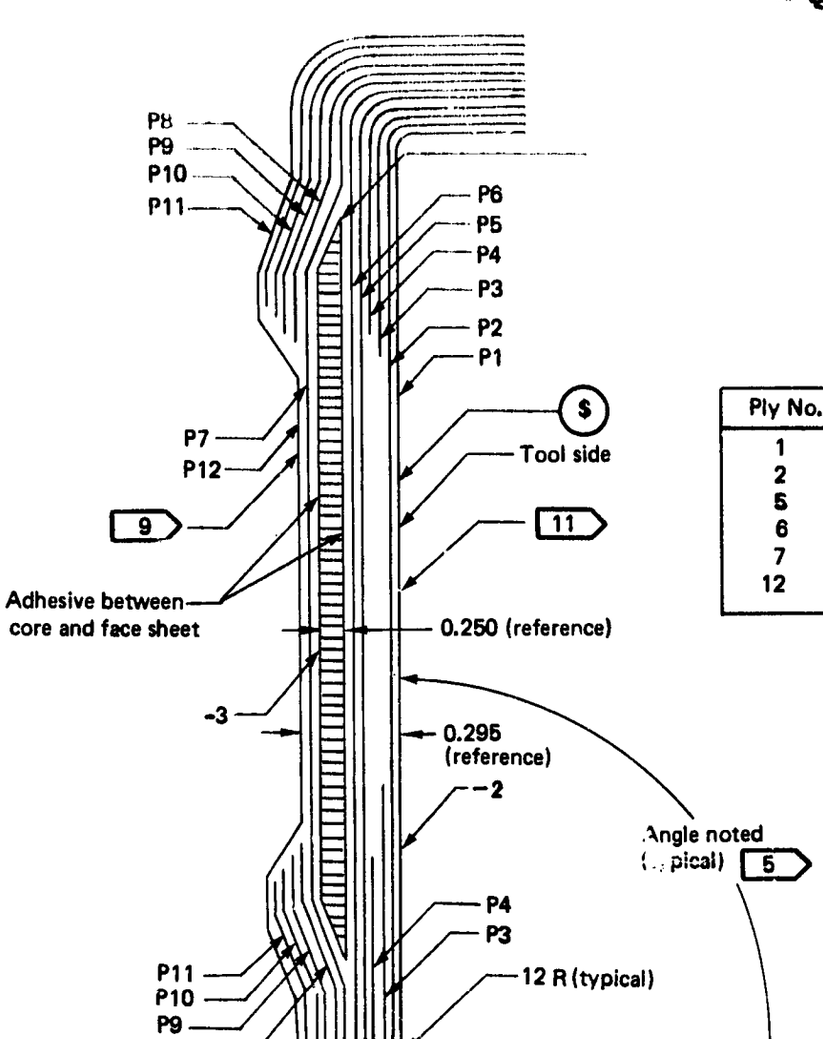

Ply No.	Orientation, deg
1	45
2	0
5	45
6	0
7	0
12	45

0.64 x 0.64-cm (0.25 x 0.25-in), 1.28 x 1.28-cm (0.5 x 0.5-in), and 2.54 x 2.54-cm (1 x 1-in) defects:

- Between P6 and honeycomb
- Between honeycomb and P7
- Between P6 and P7
- In the flanges

Figure 271. Honeycomb Rib

ORIGINAL PAGE
BLACK AND WHITE PHOTOGRAPH

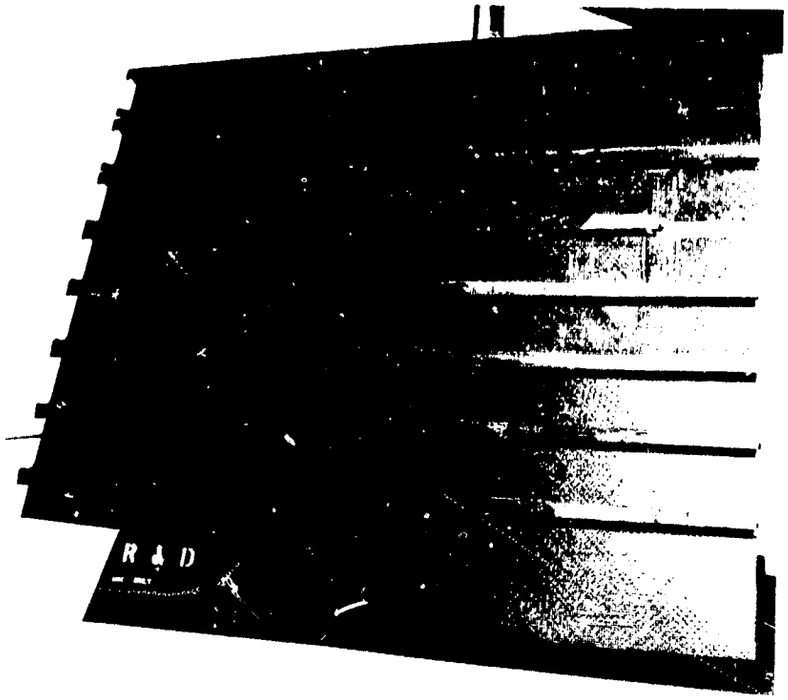

Figure 272. I-Stiffened Panel—Production NDI Standards

I-Stiffened Skin Panel—Built to full scale with 0.64 x 0.64 cm (0.25 x 0.25 in), 1.28 x 1.28 cm (0.5 x 0.5 in), and 2.54 x 2.54 cm (1.0 x 1.0 in) defects in the I-stiffener's web and cap areas as shown in Figure 272.

5.4.2 NDI Techniques

NDI techniques and equipment evaluated were:

- Low-kilovolt X-ray (15 to 40 kV)
- Sondicator, model S-1 or S-2B
- The Fokker Bond Tester, serial number 4-0028, type 0007-7217
- Through-Transmission Ultrasonic (TTU) with automated scanning and computerized C-scan recording
- TTU with manual scanning and visual signal display

5.4.3 Results and Recommendations

All defects in the NDI standards were detected by one or more of the evaluation techniques. The automated and manual TTU inspection methods provided the most sensitive defect detection to 0.64 x 0.64 cm (0.25 x 0.25 in) in most structures. The defects included voids, delaminations, porosity, and material inclusions. X-ray inspection, while not suitable for the detection of internal delamination, picked up voids in radii and delamination at machined or drilled edges when an X-ray opaque penetrant was used. Table 37 summarizes test method suitability and limitations.

Table 37. NDI Capabilities and Detection Limits

Composite Type / NDI Technique	Laminate, cm(in)	Honeycomb sandwich, cm(in)	Production Part Configuration			In service and maintenance use, cm(in)
			Flat or moderate curve, cm(in)	Radii, holes/edges, cm(in)	Flanges, cm(in)	
Through-Transmission Ultrasonic—automated [1]	To 0.64 x 0.64 (0.25 x 0.25)	To 0.64 x 0.64 (0.25 x 0.25)	To 0.64 x 0.64 (0.25 x 0.25)	Not suitable	Not suitable	Not suitable
Through-Transmission Ultrasonic—manual	To 0.64 x 0.64 (0.25 x 0.25)	To 0.64 x 0.64 (0.25 x 0.25)	To 1.27 x 1.27 (0.50 x 0.50)	Not suitable	To 1.27 x 1.27 (0.50 x 0.50)	Not suitable
Fokker Bond tester	To 0.64 x 0.64 (0.25 x 0.25)	Not suitable	To [2] 1.27 x 1.27 (0.50 x 0.50)	Not suitable	To 1.27 x 1.27 (0.50 x 0.50)	To [2] 2.54 x 2.54 (1.0 x 1.0)
Sondicator	To 0.64 x 0.64 (0.25 x 0.25)	To 0.64 x 0.64 (0.25 x 0.25)	To 1.27 x 1.27 (0.50 x 0.50)	Not suitable	To 1.27 x 1.27 (0.50 x 0.50)	To 2.54 x 2.54 (1.0 x 1.0)
[3] X-ray	Below 0.64 x 0.64 (0.25 x 0.25)	Below 0.64 x 0.64 (0.25 x 0.25)	Below 0.64 x 0.64 (0.25 x 0.25)	Below [4] 0.64 x 0.64 (0.25 x 0.25)	Below 0.64 x 0.64 (0.25 x 0.25)	Below 0.64 x 0.64 (0.25 x 0.25)

[1] C-scan capability provides printed record showing porous areas.
[2] Not suitable for honeycomb sections.
[3] Will not detect internal delamination.
[4] Requires X-ray opaque penetrant.

Figure 273 shows the automated TTU unit, and Figure 275 provides a sample C-scan recording. Semiportable TTU scanning is shown in Figure 274, while a hand-held model is used to scan a flange section in Figure 276. Figure 277 shows a portable TTU probe and its application to the inspection of I-stiffener sections. The skin-to-I-stiffener cap bond, because of accessibility, was tested using an instrument with a probe that contacts one surface only, as the Fokker Bond Tester in Figure 278.

5.4.4 Discrepancy Analysis

Production records that contained completed Manufacturing planned orders with inspection results were compiled in a central data storage area. A collation and statistical analysis of rejection tags was conducted to obtain discrepancy facts. Of the 1722 parts that were analyzed, 374 discrepancies (21.7%) were noted. Some parts had more than one discrepancy, making the actual number of tagged parts less than 21.7%.

Of the rejected parts, 49% (10.7% of the total) were structurally acceptable (use as is). Parts that required rework before use amounted to 35.0% of the total rejections (7.5% of the total). Parts that were scrapped were 16.0% of the rejections (3.5% of the total).

Discrepancies that were not related to graphite characteristics of processing or to dimensional errors and that were not manufactured to drawing requirements totaled 32% of the rejections. One of the greatest causes of graphite-related

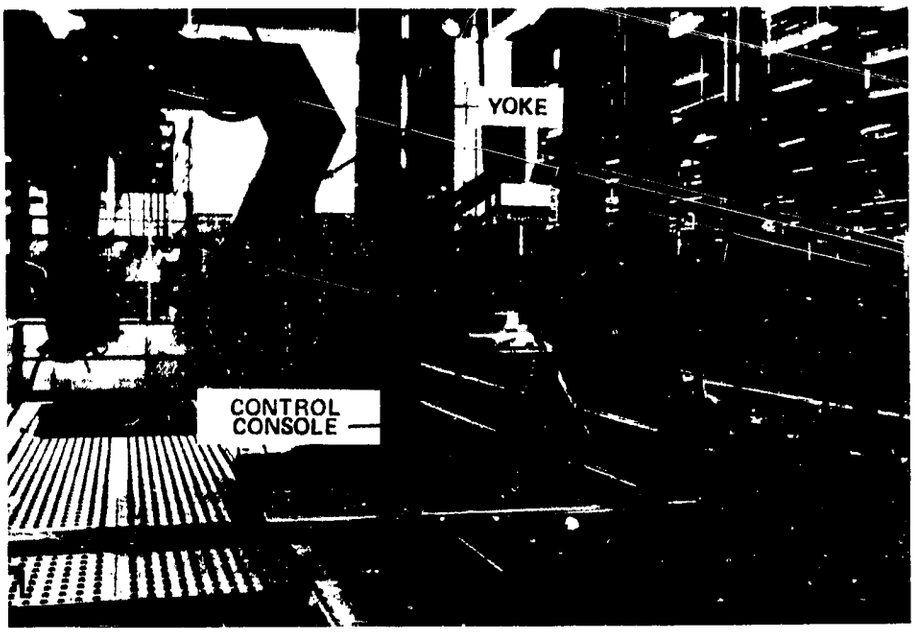

Figure 273. Automated Through-Transmission Ultrasonic

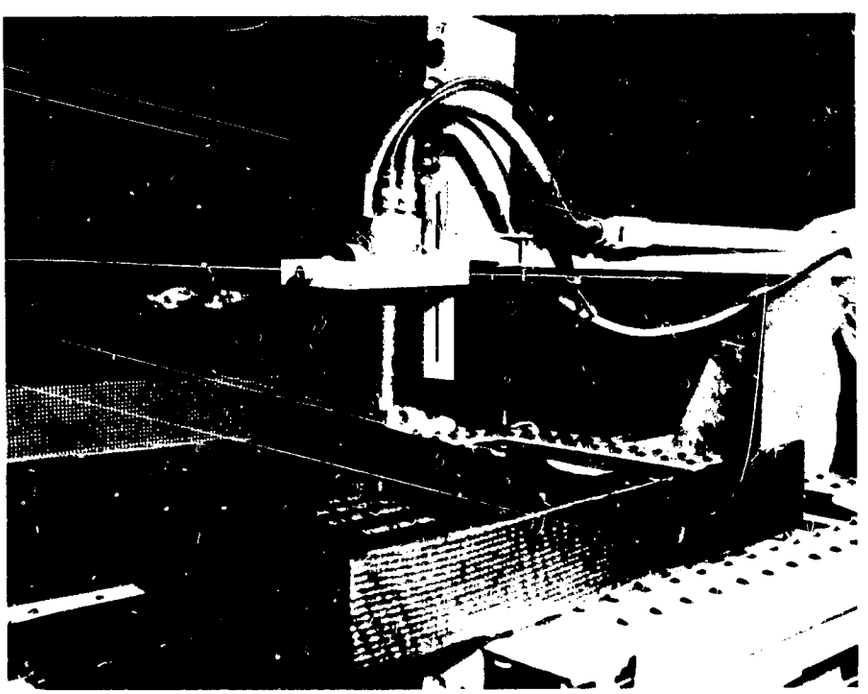

Figure 274. Through-Transmission Inspection Without C-Scan Recording Capability

PART NUMBER = 65C12721 1 SERIAL NUMBER = 1232
DATE = 2/24/78 CALIBRATION PROCEDURE = 1.2
SCANNER INDEX = 60 THOUSANDTHS SCAN PATTERN = C
X SCALE = 2 Y SCALE = 2 SCAN DIRECTION = RIGHT
PLOTTING SEQUENCE = 2,0,0,0,0,0, NUMBER OF OPERATIONAL CHANNELS = 5

SIGNAL IDENTIFICATION LEVELS

LEVEL	MAX VOLTS*100
0	1000
1	630
2	590
3	550
4	515
5	465
6	445
7	410
8	375
9	335
10	285
11	255
12	115

PLOTTED SYMBOLS

1000	.GT.	BLANK	.GE.	630
630	.GT.	*	.GE.	590
590	.GT.	1	.GE.	550
550	.GT.	2	.GE.	515
515	.GT.	3	.GE.	465
465	.GT.	4	.GE.	445
445	.GT.	5	.GE.	410
410	.GT.	6	.GE.	375
375	.GT.	7	.GE.	335
335	.GT.	8	.GE.	285
285	.GT.	9	.GE.	255
255	.GT.	10	.GE.	115
115	.GT.	11	.GE.	0

TOTAL NUMBER OF BLOCKS = 960

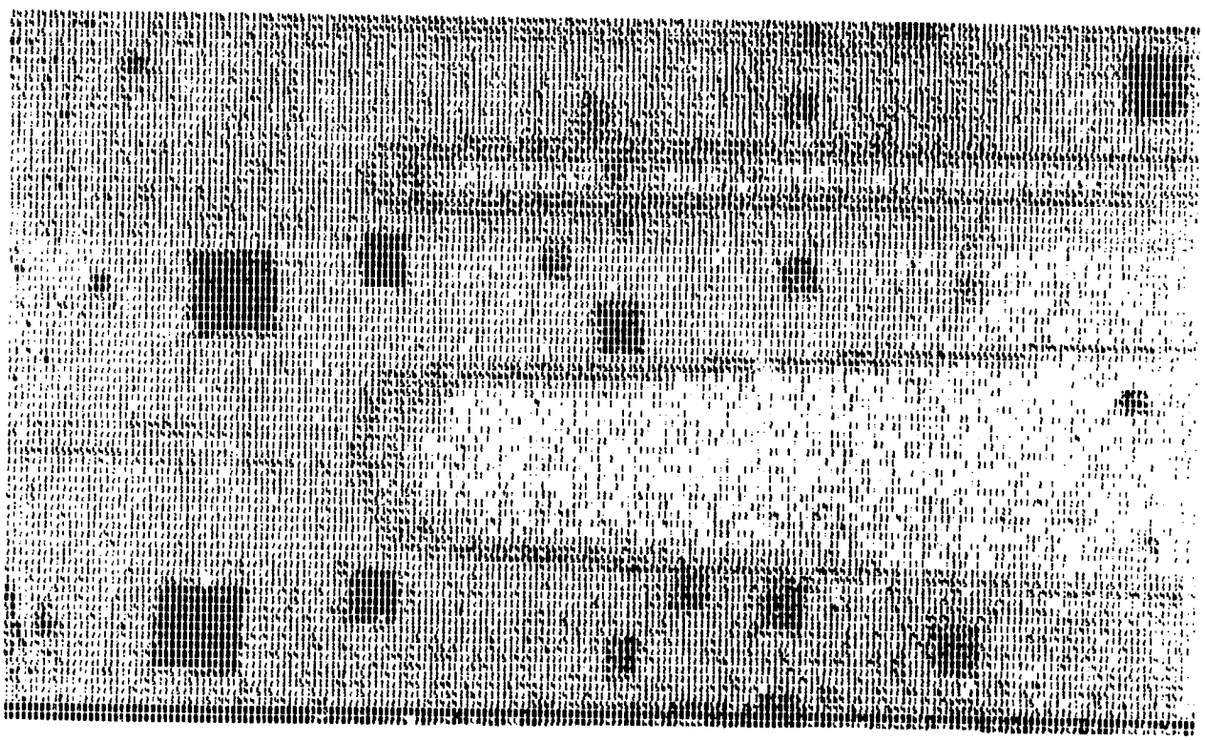

Figure 275. Computerized C-Scan Recording

rejection was resin starvation (38%). A marked improvement was shown from June 1980 to the end of the survey, however, when less than 4% of the discrepancies occurred in this category. This improvement was the result of the design change that used tape on surfaces with established visual acceptance criteria. The results of this analysis are summarized in Figure 279.

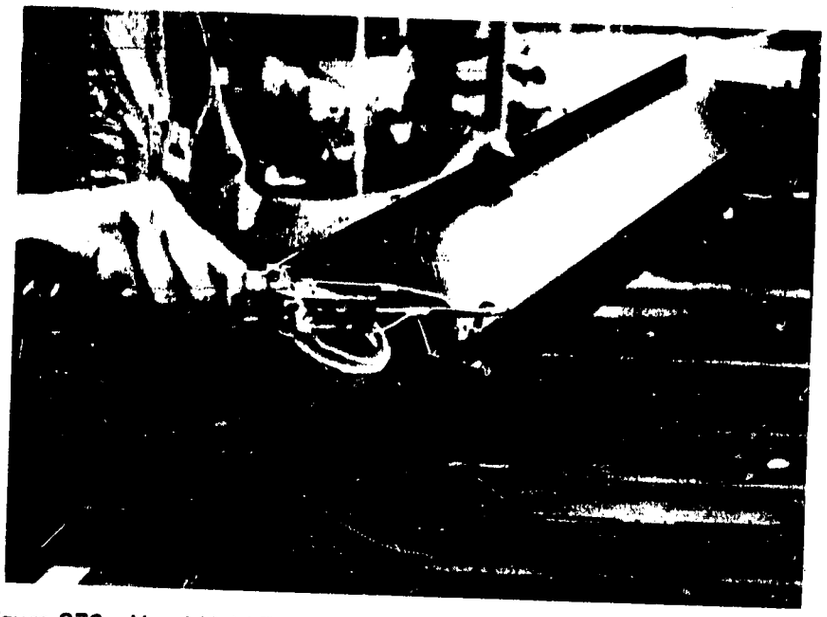

Figure 276. Hand-Held Through-Transmission Inspection of a Flange Area

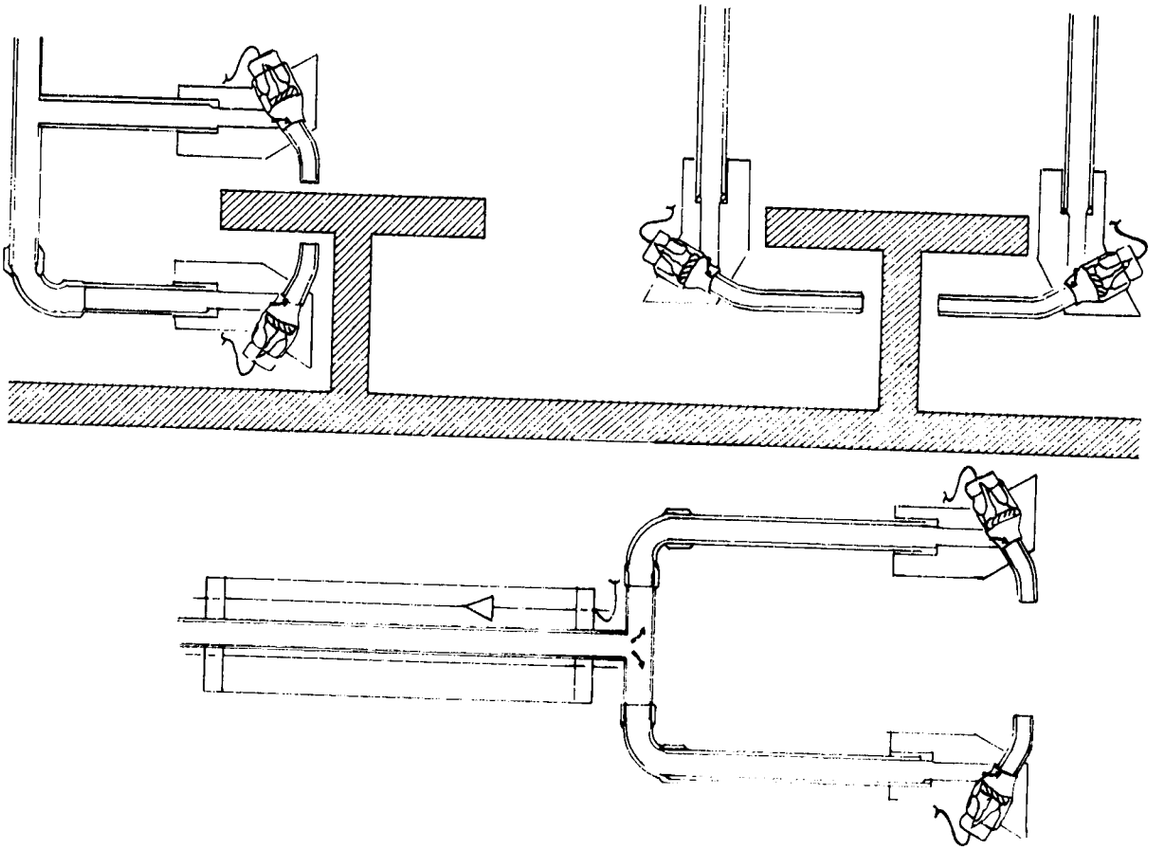

Figure 277. Portable Ultrasonic Probe

ORIGINAL PAGE
BLACK AND WHITE PHOTOGRAPH

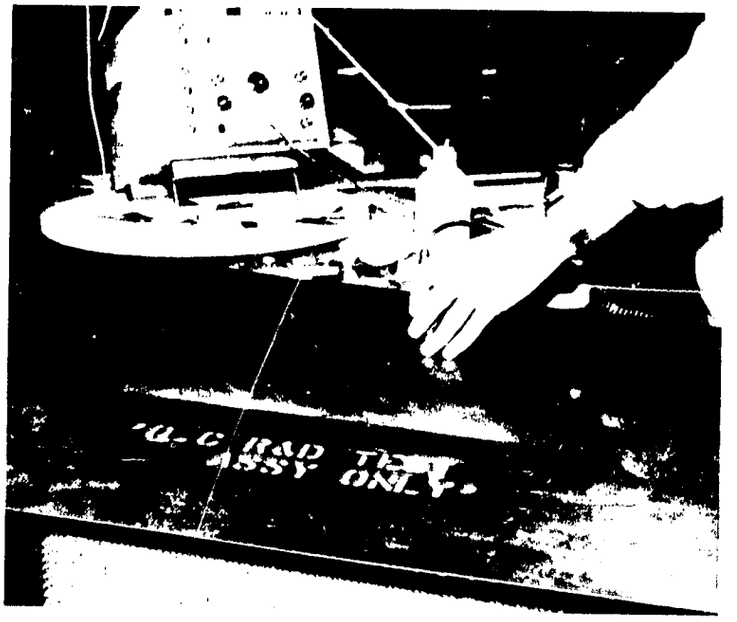

Figure 278. Fokker Bond Testing of Skin-to-Cap Bond of I-Stiffener Panel

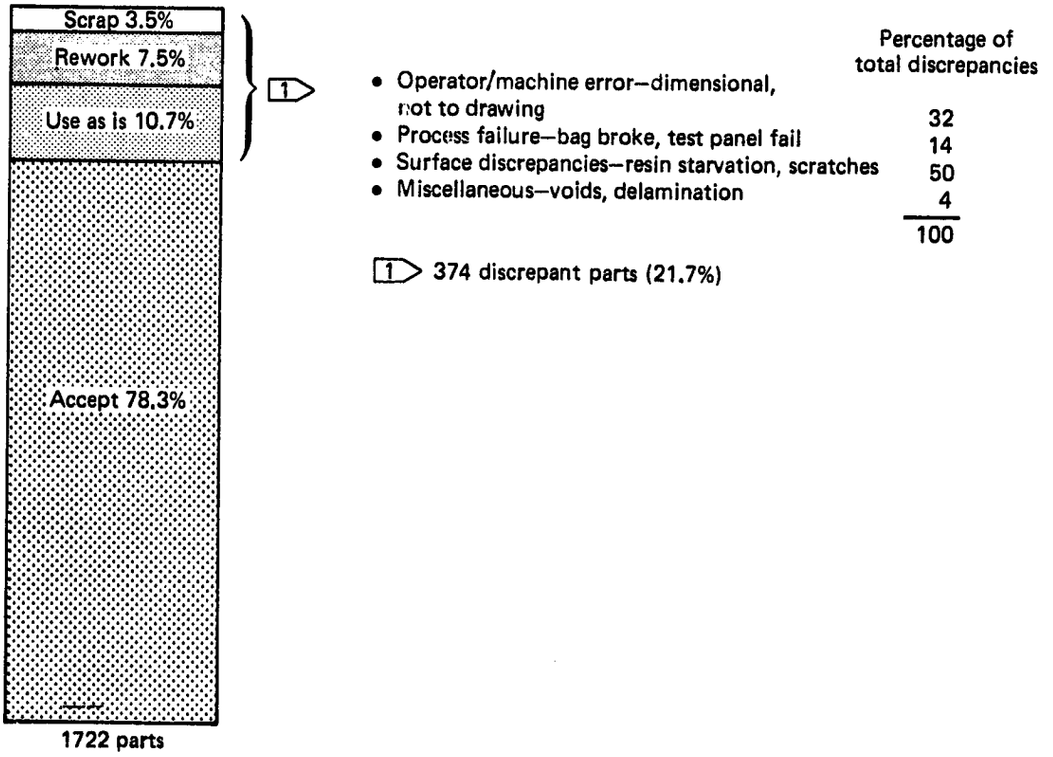

Figure 279. 737 Stabilizer Accept/Reject Evaluation

6.0 CONCLUSIONS

NASA established a program for primary composite structures under the Aircraft Energy Efficiency (ACEE) program. As part of this program, Boeing has redesigned and fabricated the horizontal stabilizer of the 737 transport using composite materials. Five shipsets were fabricated, and FAA certification has been obtained. Airline introduction will follow.

Key program results are:

- Weight reduction greater than the 20% goal has been achieved.
- Parts and assemblies were readily produced on production-type tooling.
- Quality assurance methods were demonstrated.
- Repair methods were developed and demonstrated.
- Strength and stiffness analytical methods were substantiated by comparison with test results.
- Cost data were accumulated in a semiproduction environment.
- FAA certification has been obtained.

The program has provided the necessary confidence for the company to commit use of composite structure in similar applications on new generation aircraft and has laid the groundwork for design of larger, more heavily loaded composite primary structure.

7.0 REFERENCES

1. Aniversario, R. B.; Harvey, S. T.; McCarty, J. E.; Parsons, J. T.; Peterson, D. C.; Pritchett, L. D.; Wilson, D. R.; and Wogulis, E. R.: Design, Ancillary Testing, Analysis, and Fabrication Data for the Advanced Composite Stabilizer for Boeing 737 Aircraft. Volume I—Technical Summary. NASA CR-3648, 1983.

2. Federal Aviation Regulations, Part 25, Airworthiness Standards: Transport Category Airplanes. Department of Transportation, Federal Aviation Administration, December 1978.

3. Composite Aircraft Structure, Advisory Circular 20-107. Federal Aviation Administration, July 1978.

4. Lightning Qualification Test Techniques for Aerospace Vehicles and Hardware, MIL-STD-1757, June 1980.

5. Aniversario, R. B.; Harvey, S. T.; McCarty, J. E.; Parsons, J. T.; Peterson, D. C.; Pritchett, L. D.; Wilson, D. R.; and Wogulis, E. R.: Full-Scale Testing, Production, and Cost Analysis Data for the Advanced Composite Stabilizer for Boeing 737 Aircraft. Volume I—Technical Summary. NASA CR-3649, 1983.

6. Aniversario, R. B.; Harvey, S. T.; McCarty, J. E.; Parsons, J. T.; Peterson, D. C.; Pritchett, L. D.; Wilson, D. R.; and Wogulis, E. R.: Full-Scale Testing, Production, and Cost Analysis Data for the Advanced Composite Stabilizer for Boeing 737 Aircraft. Volume II—Final Report. NASA CR-166012, December 1982.

7. Hoffman, D. J.: 737 Graphite Composite Flight Spoiler Flight Service Evaluation. NASA CR-159362, November 1980.

8. Gibbins, M. N. and Hoffman, D. J.: Environmental Exposure Effects on Composite Materials for Commercial Aircraft. NASA CR-3502, January 1982.

9. ATLAS Finite Element Structural Analysis Program, NASA CR-159043, 1979.

10. Ahlers, R. H.: Stability of Structure Following Bird Strikes, FAA-ADS-60, March 1966.

11. McNaughtan, I. I.: The Design of Leading Edge and Intake Wall Structure to Resist Bird Impact. Royal Aircraft Establishment Technical Report 72056, 1972.

12. Advanced Composites Design Guide. Air Force Materials Laboratory, Vol. I, Third Edition, January 1973.

13. Horton, W. H.; Cundari, F. L.; and Johnson, R. W.: "The Analysis of Experimental Data Obtained from Stability Studies on Elastic Column and Plate Structures." Proceedings of the Ninth Israel Annual Conference on Aviation and Astronautics, February 1967.

14. Waddoups, M. E.; Eisenmann, J. R.; and Kaminski, B. E.: "Macroscopic Fracture Mechanics of Advanced Composite Materials, Journal of Composite Materials, Vol. 5, pp. 446-454, October 1971.

15. de Jonge, J. B., et al.: "A Standardized Load Sequence for Flight Simulation Tests on Transport Aircraft Wing Structure," LBF-BERICHT FB-106, NLR TR 73029 U. Nationaal Lucht-en Ruimtevaartlaboratorium, Amsterdam, The Netherlands, March 1973.

16. Van Dijk, G. M. and de Jonge, J. B.: "Introduction to a Fighter Aircraft Loading Standard for Fatigue Evaluation," NLR MP 75017 U. Nationaal Lucht-en Ruimtevaartlaboratorium, Amsterdam, The Netherlands, May 20, 1975.

17. Horton, R. E. and McCarty, J. E.: Adhesive Bonded Aerospace Structures Standardized Repair Handbook. AFML-TR-77/AFFDL-TR-77, October 1977.

APPENDIX A

ADVANCED COMPOSITE HORIZONTAL STABILIZER

FOR BOEING 737 AIRCRAFT,

STRUCTURAL REPAIR MANUAL

TABLE OF CONTENTS

1.0 GENERAL

A. This document contains repair procedures for the graphite/epoxy horizontal stabilizer. The stabilizer structural box, consisting of ribs, skins, and spars, is fabricated of several layers of graphite tape or graphite woven fabric in an epoxy resin matrix. Solid laminates and sandwich panels stiffened with a nonmetallic (Nomex) core are used in the stabilizer. The locations of the principal components of the stabilizer are shown in Figure 1.1.

The limitations of damage that may be repaired using the techniques described in this document are shown in Figure 1.2. Repair of damage to the stabilizer structural box exceeding the criteria of Figure 1.2 or repair of damage other than to the I-section stiffened skin of the structural box (i.e., to the spars or ribs) is considered a special condition and requires coordination with Boeing engineering.

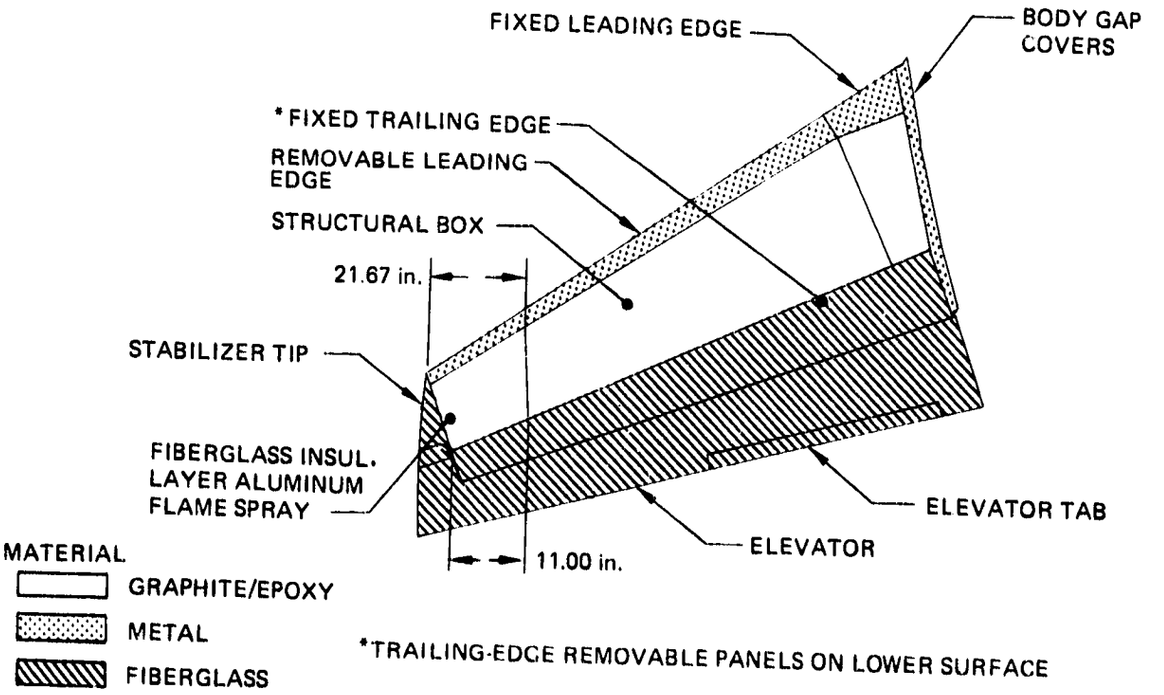

Figure 1.1--737 Graphite/Epoxy Stabilizer

CONSTRUCTION	COMPONENT	MINIMUM DISTANCE ℄ RIB FASTENERS TO EDGE OF CUTOUT	MINIMUM DISTANCE ℄ STRINGER TO EDGE OF CUTOUT	MINIMUM SPACING EDGE TO EDGE OF CUTOUTS	ALLOWABLE REPAIRS PER BAY (℄ RIB TO ℄ RIB)
Laminate graphite/epoxy	Skin	6.5 in.	1.18 in.	6 in.	[1]
	Skin and stringer	6.5 in.			Two single-stringer repairs or One double-stringer repair

NOTE: REPAIR OF DAMAGE EXCEEDING THESE LIMITATIONS REQUIRES COORDINATION WITH THE BOEING ENGINEERING DEPARTMENT.

[1] MAXIMUM OF THREE SKIN REPAIRS LOCATED ALONG THE SAME CHORDWISE STATION (±2.0 in.); OTHERWISE, SUBJECT TO SPACING LIMITATIONS ONLY.

Figure 1.2—Repair Limitations for Graphite-Reinforced Epoxy Stabilizer Components

Damage to the laminate skin may be repaired by cutting away the skin to remove the damaged area and bonding and mechanically fastening a precured graphite/epoxy patch over the damaged skin. Damage to I-section stringers may be repaired by cutting away the skin to provide access to the damaged stringers, cutting away the damaged portion of the stringer, and mechanically fastening and bonding graphite/epoxy repair channels and a precured graphite/epoxy cover over the skin cutouts.

The bonding procedure uses a 250°F-cure adhesive with pressure applied to the repair channels or patch using mechanical fasteners and/or 20 in. of mercury vacuum pressure. The necessary pressure for bonding the repair channels to the stringer is provided by fasteners only, since it is not feasible to set up a vacuum inside the stabilizer box. See Section 2.0 for repair procedures and materials.

The stabilizer is essentially divided into three zones, as shown in Figure 1.3. Zone 1 is that portion inboard of stabilizer station 138.70. In this zone, repair patches and covers will consist of 14 plies of epoxy-preimpregnated graphite fabric and will be made to conform to the existing curvature in the repair area. Zone 2 is that portion outboard of stabilizer station 138.70, excluding the aluminum flame-sprayed area, which is Zone 3. In Zones 2 and 3, the repair patches and covers will consist of nine plies of epoxy-preimpregnated graphite fabric laid up on a flat tool. In Zone 3,

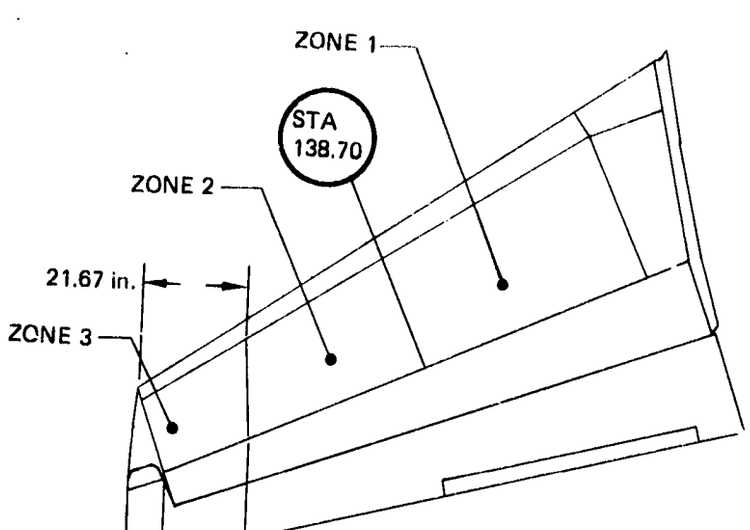

Figure 1.3–Stabilizer Repair Zones

special care should be taken to remove the aluminum flame spray from the repair area prior to the repair. A single ply of wet-layup fiberglass is applied over the patch or cover and finished per Section 3.0 herein.

To repair the metal and fiberglass components of the horizontal stabilizer, excluding the steel front- and rear-spar lug straps, use the instructions contained in D6-15565, Boeing 737 Structural Repair Manual (ref. 1). A special repair is required in the area of the lugs. Consult Boeing engineering.

B. Repaint all repairs made to the horizontal stabilizer. See Section 3.0 for refinishing procedures, materials, and limitations.

C-4

2.0 REPAIR PROCEDURES

A. Materials

Only preimpregnated graphite fabric as shown in Figure 2.1 may be used to replace damaged graphite plies. The film adhesive shown in Figure 2.1 shall be used to bond precured repair channels to damaged stringers and precured patches or covers over the damaged skin area or over the skin cutouts.

Precured patches and covers shall be fabricated using either nine plies (Zones 2 or 3) or 14 plies (Zone 1) of epoxy-preimpregnated graphite woven fabric per BMS 8-212. Figures 2.2 and 2.3 show the configurations of the precured patch and cover. The precured repair channels shall be fabricated using eight plies of epoxy-preimpregnated graphite woven fabric and six plies of unidirectional tape per BMS 8-212. Figure 2.4 shows the

MATERIAL	BOEING MATERIAL SPECIFICATION(BMS)	APPROVED SOURCE	SUPPLIER'S PRODUCT DESIGNATION
Graphite fabric preimpregnated with epoxy resin	BMS 8-212 Type IV, Class 2, Style 3K-70-PW	Celanese Corporation Narmco Materials Division 600 Victoria Street Costa Mesa, CA 92627	Rigidite 5208 Woven T-300 Style 3K-70-PW 40 percent
Graphite tape preimpregnated with epoxy resin	BMS 8-212 Type II, Class 1, Grade 190	Celanese Corporation Narmco Materials Division 600 Victoria Street Costa Mesa, CA 92627	Rigidite 5208T-300-190 35 percent
Film adhesive	BMS 5-129 Type 2, Class IIC, Grade 10 or 15	American Cyanamid Company Bloomingdale Department Havre de Grace, MD 21078	FM-123-5
Nylon peel ply	BMS 15-3 Type I, Class 3	Fiberite West Coast Corp. P.O. Box 738 Orange, CA 92699	MXM 7634/52006/60
Sealant	BMS 5-26 or BMS 5-95	Products Research and Chemical Corp. 5454 San Fernando Road Glendale, CA 91209 Essex Chemical Corp. Specialty Chemicals Division 19451 Susana Road Compton, CA 90221	
BACB30UZ6-( )		Monogram Aerospace Fasteners 3423 South Garfield Avenue Los Angeles, CA 98524	JLY12395-6-( )

Figure 2.1—Approved Materials for Use in Repairing Graphite-Reinforced Stabilizer Components

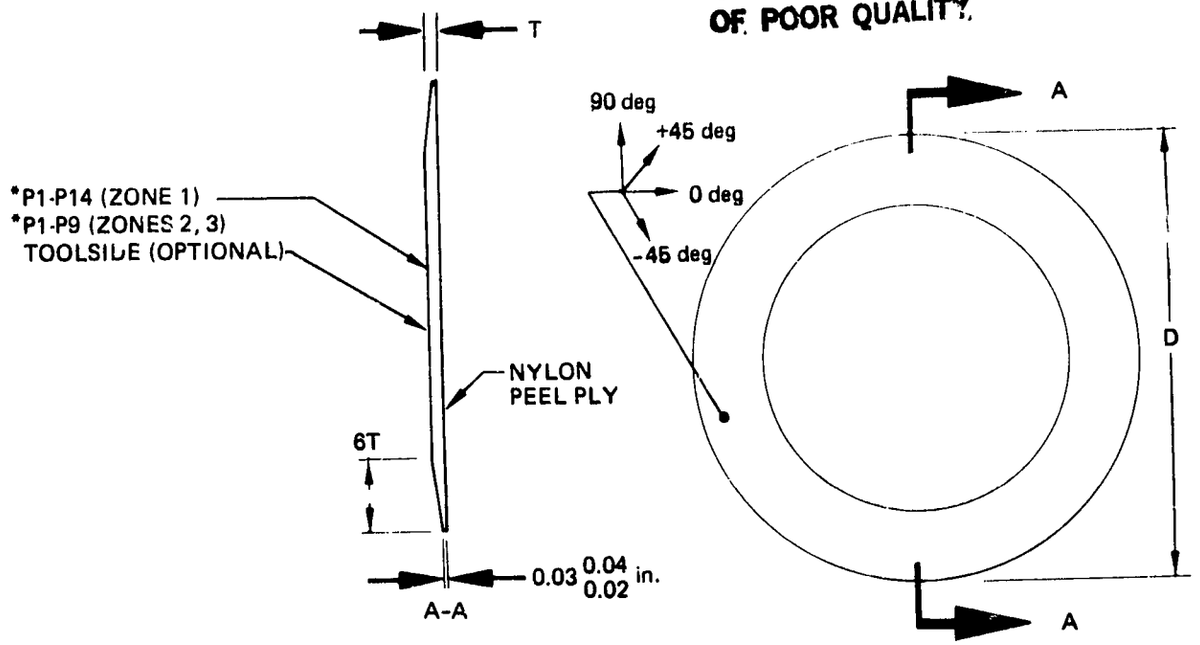

*REFER TO FIGURE 2.5 FOR MATERIAL DEFINITION AND PLY ORIENTATION
D = DIAMETER OF REPAIR CUTOUT PLUS 1.92 IN.
NOTE: TO ACCOMMODATE A REPAIR THAT REQUIRES A LONGER PATCH, THE PATCH CAN BE MADE OVAL, IN WHICH CASE THE PATCH LENGTH EQUALS THE REPAIR CUTOUT LENGTH PLUS 1.92 IN.

Figure 2.2—Precured Patch

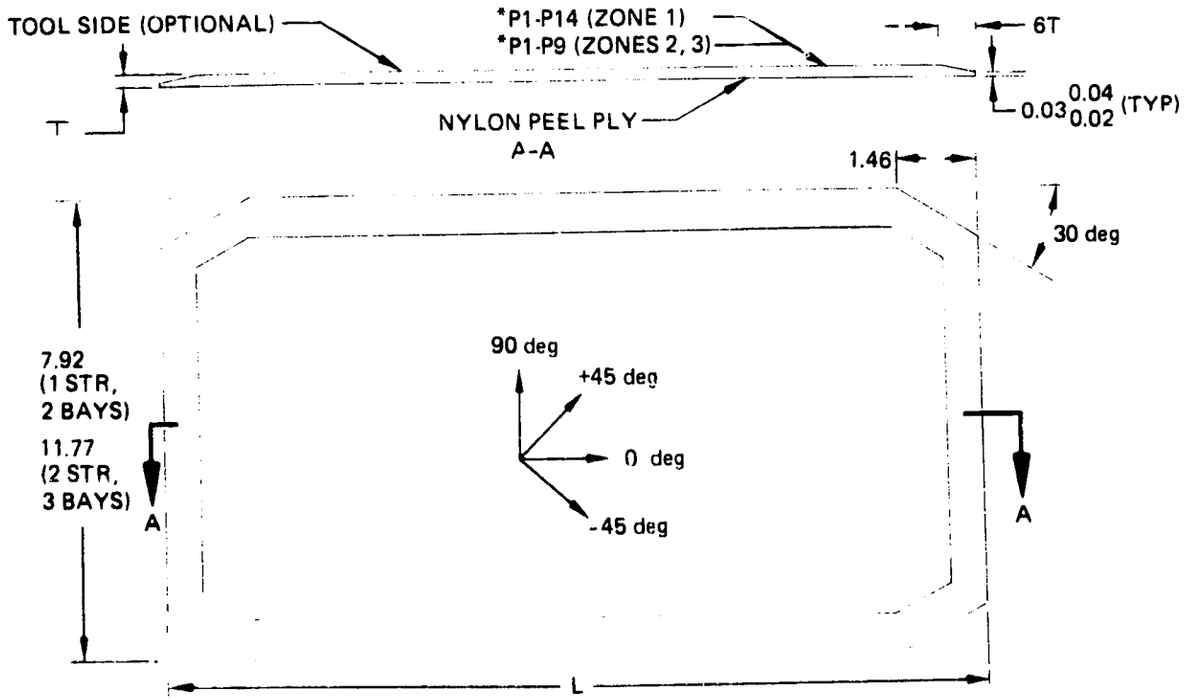

*REFER TO FIGURE 2.5 FOR MATERIAL DEFINITION AND PLY ORIENTATION
L = LENGTH OF STRINGER REPAIR CUTOUT PLUS 10.84 ±0.05 IN.
ALL DIMENSIONS IN INCHES

Figure 2.3—Precured Cover

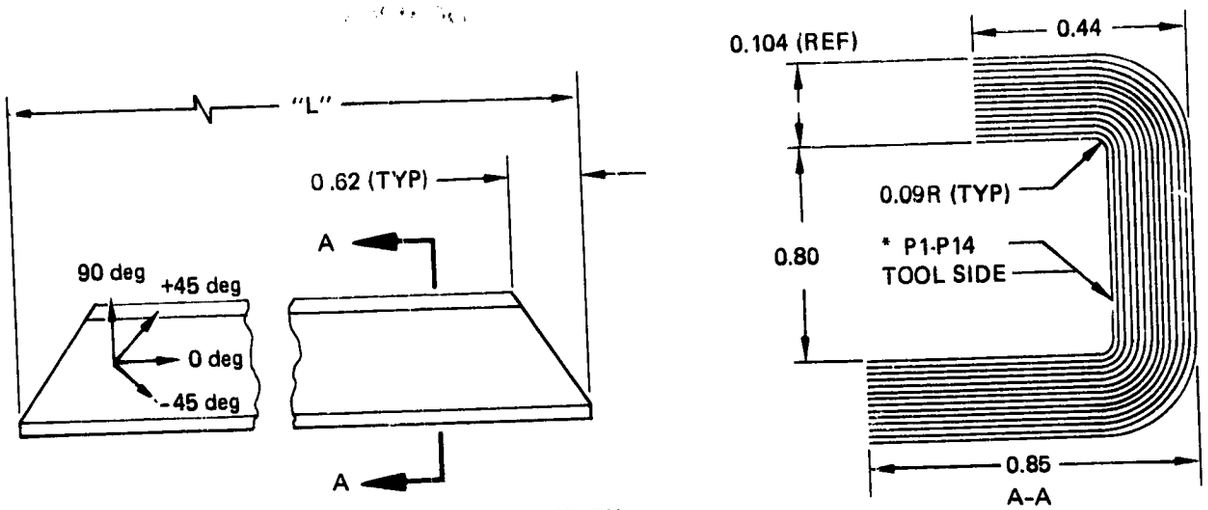

*REFER TO FIGURE 2.5 FOR MATERIAL DEFINITION AND PLY ORIENTATION
L = LENGTH OF STRINGER REPAIR CUTOUT PLUS 8.68 ±0.05 IN.
ALL DIMENSIONS IN INCHES.

Figure 2.4—Precured Repair Channel

configuration of precured repair channels. The ply table contained in Figure 2.5 shows ply layup orientation for each precured repair part. All precured layups are to be vacuum bagged and autoclave cured per Figure 2.6.

Skin and web fillers shall be fabricated using laminated phenolic sheet per MIL-P-15035 Type FBE, FBG, or FBI. Fillers shall be sized to match the thickness and length of skin and stringer web in the damaged area.

In addition, the materials shown in D6-15565 (ref. 1), including supporting equipment (except fabrics and laminating resins), may be used in the repair of graphite/epoxy components.

B. Laminate Graphite/Epoxy Stiffened Skin Panel Repair

1. Determine the extent of damage in accordance with D6-15565, Section 51-40-09 (ref. 1).

PART NAME	PLY NUMBER	MATERIAL	TAPE FIBER OR CLOTH WARP ORIENTATION	SPLICE	REV LTR
Patches and cover (inboard)	1, 3, 5, 7, 8, 10, 12, 14	1	0 deg	3	
	2, 4, 6, 9, 11, 13	1	+45 or -45 deg		
Patches and cover (outboard)	1, 3, 5, 7, 9	1	0 deg		
	2, 4, 6, 8	1	+45 or -45 deg		
Repair channels	1, 7 8, 14	1	0 deg		
	2, 6, 9, 13	1	+45 or -45 deg		
	3, 4 5, 10, 11, 12	2	0 deg		

1 EPOXY-PREIMPREGNATED GRAPHITE WOVEN FABRIC PER BMS 8-212 TYPE IV, CLASS 2, STYLE 3K-70-PW. FABRICATE PER BAC 5562 METHOD II.

2 EPOXY-PREIMPREGNATED GRAPHITE UNIDIRECTIONAL TAPE PER BMS 8-212 TYPE II, CLASS 1, GRADE 190. FABRICATE PER BAC 5562 METHOD II.

3 NO SPLICES ALLOWED

Figure 2.5—Ply Table

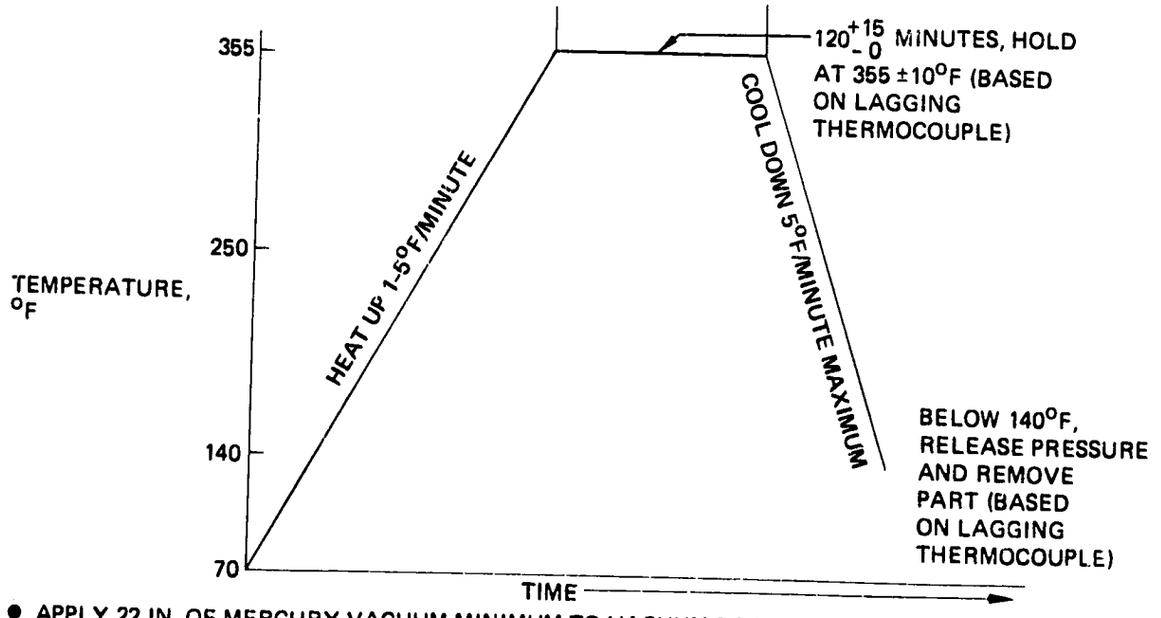

- APPLY 22 IN. OF MERCURY VACUUM MINIMUM TO VACUUM BAG
- APPLY 85^{+15}_{-0} PSIG PRESSURE TO AUTOCLAVE

NOTE: VENT VACUUM BAG TO ATMOSPHERE WHEN PRESSURE REACHES 20 PSIG.

Figure 2.6—Cure Cycle for Precured Repair Patches—Cover and Channels

a. Check for delamination around the damage. Refer to Nondestructive Test Manuals D6-7170 (ref. 2) or D6-37239, Part 1, Section 51-04-00 (ref. 3) for delamination detection equipment and calibration procedures. The instruments must be calibrated with reference standards simulating the structure to be inspected and the delamination to be detected.

b. Determine if the damage is limited to the skin panel or if it extends into the I-section stringers by visually inspecting both skin and stringer. Stringer damage can be assessed using a nondestructive inspection (NDI) reference standard simulating the original structure. In cases where a standard cannot be used, predetermined "like" areas can be used as a standard for an acceptable condition.

c. Determine the location and zone in which the damage lies in accordance with Figure 1.3. Zone 1 requires a 14-ply patch, Zone 2 requires a nine-ply patch, and Zone 3 requires a nine-ply patch and a wet layup of one ply of fiberglass. Determine if Boeing consultation is required according to the limitations set within this document. (Refer to Figure 1.2.)

2. Removal of Damage

a. Damage limited to skin panel: Cut away the damaged area to a smooth outline using a router or rotary carbide cutting disk. Proceed to step 14.

b. Damage extending into the stringer: Cut away the skin panel to provide access to the stringer using a router or rotary carbide cutting disk. The skin cutout should be centered about the centerline of the stringer to be repaired and the centerline of the damaged area, as shown in Figure 2.7. Figure 2.7 also shows the dimensions of the skin cutout for one- and two-

stringer repairs and the limitations as to the location of the skin cutout.

3. Cut away the damaged area of the stringer.

4. Lightly sand the surface of the stringer common to the precured repair channels. Use 180-grit or finer sandpaper. Avoid abrasion of graphite fibers.

5. Clean out the repair area with oil-free air. Wipe the surfaces with a clean cloth moistened with methyl ethyl ketone. Dry the repair area thoroughly.

6. Apply one layer of BMS 5-129 Type 2, Class IIC, Grade 10 or 15 to the area between the stringer and web filler and the precured channels.

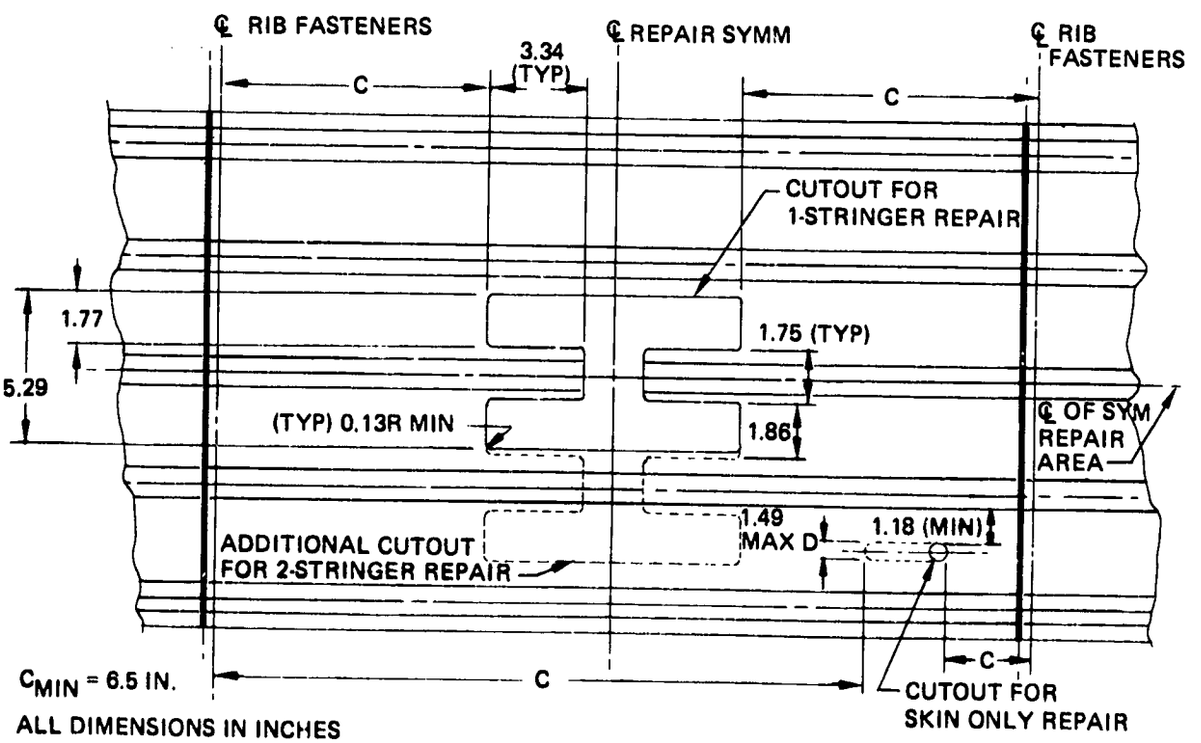

Figure 2.7—Access Hole Size and Location Limitations

7. Remove the peel ply from the bonding surface of the precured channels and install the channels and web filler per Figures 2.8, 2.9, and 2.10. Figure 2.11 shows the fastener configuration in the stringer cutout area.

8. Tape two or more thermocouples to the stringer adjacent to the repair.

9. Apply strip heat blankets to the stiffener repair area.

10. Cover the heat blankets with 3 or 4 in. of fiberglass fabric or other insulation.

11. Apply heat and maintain 225 $^{+25^{o}}_{-0^{o}}$ F for 90 $^{+15}_{-0}$ minutes. Do not heat faster than 5^{o}F per minute. Record temperature continuously.

12. After the adhesive has cured, cool slowly, remove the heat blankets, and wipe surfaces with a clean cloth moistened with methyl ethyl ketone or acetate.

13. Fill the gap between channel and stiffener with liquid shim per D6-9794, Installation of Plastic Shims and Metal Fillers (ref. 4), as shown in Figure 2.12.

14. Lightly sand the surface of the panel common to the patch or cover to remove all paint from the surface. If any portion of the repair patch or cover is in Zone 3, the aluminum flame spray also must be removed from the surface of the panel common to the patch or cover and from an area 1 in. beyond the periphery of the patch or cover. Care must be taken not to remove the underlying fiberglass layer. Use 180-grit or finer sandpaper. Avoid abrasion of graphite fibers. The skin panel patch is a bonded repair reinforced with mechanical fasteners.

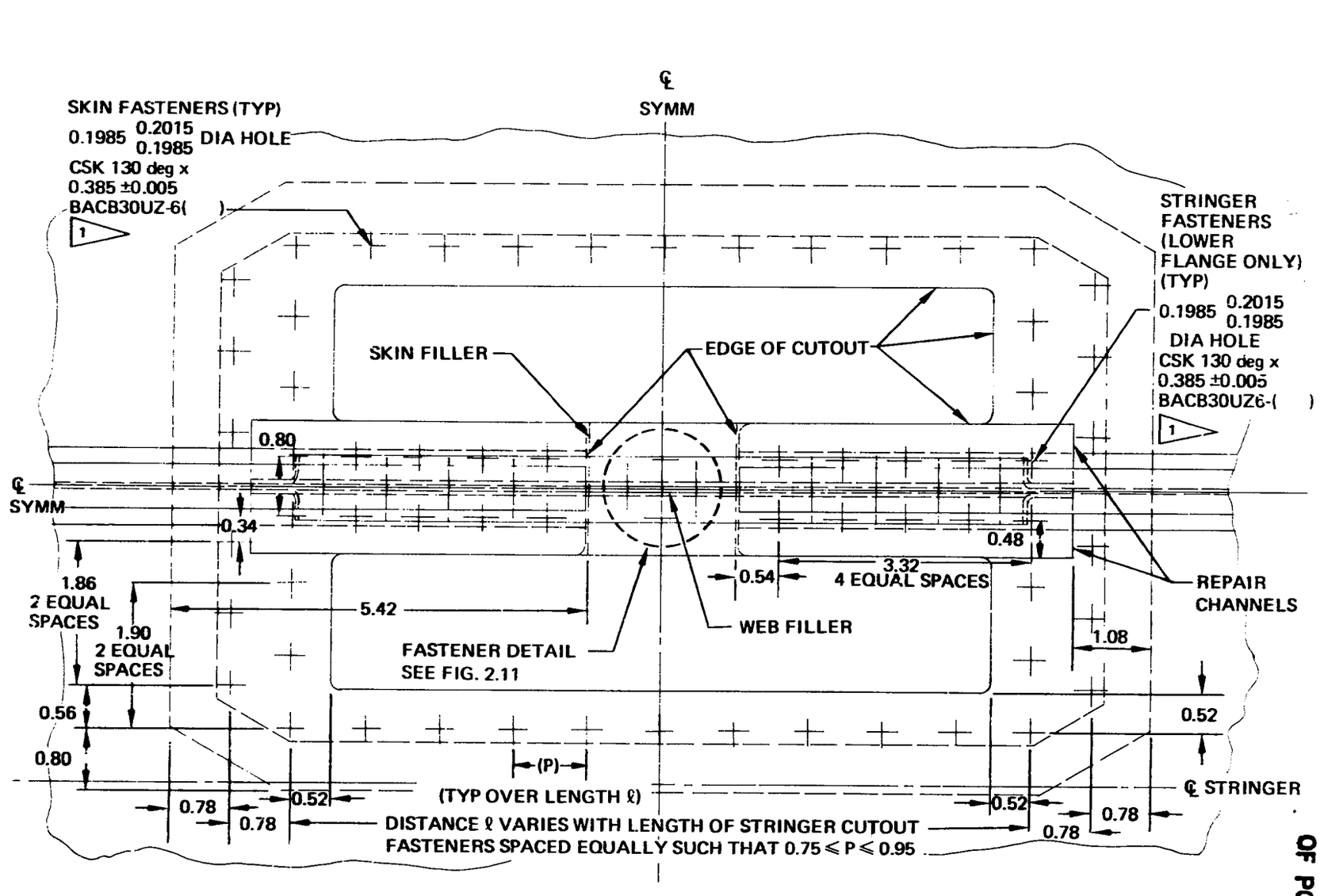

DIMENSIONS SHOWN ARE INDEPENDENT OF LENGTH OF STRINGER CUTOUT

ALL DIMENSIONS IN INCHES

1 CAUTION: GRIP LENGTHS MUST BE DETERMINED AT TIME OF INSTALLATION (PARTICULARLY IMPORTANT FOR COMPOSITE STRUCTURE)

Figure 2.8—Stringer Repair—Plan View

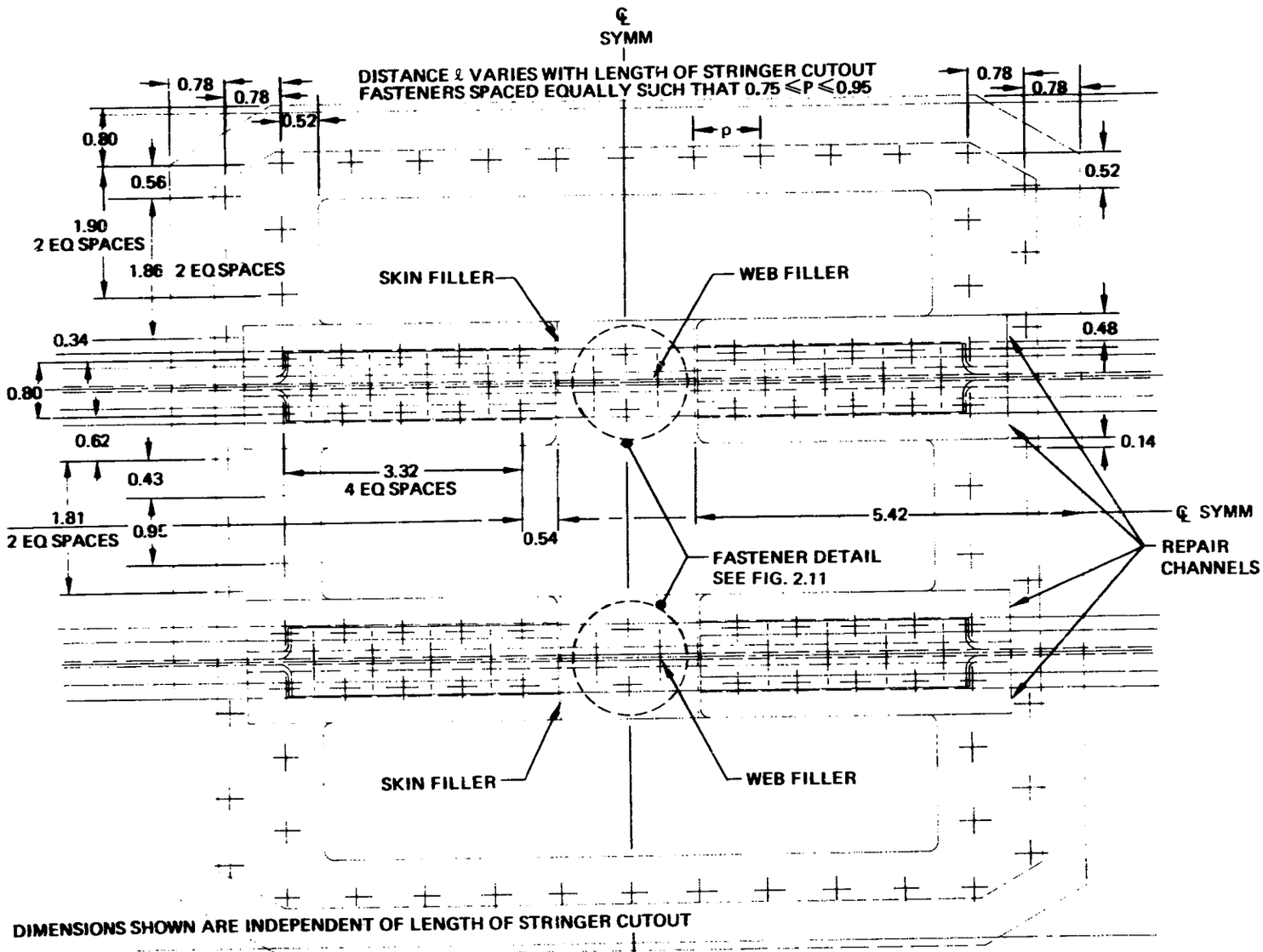

Figure 2.9—Two-Stringer Repair

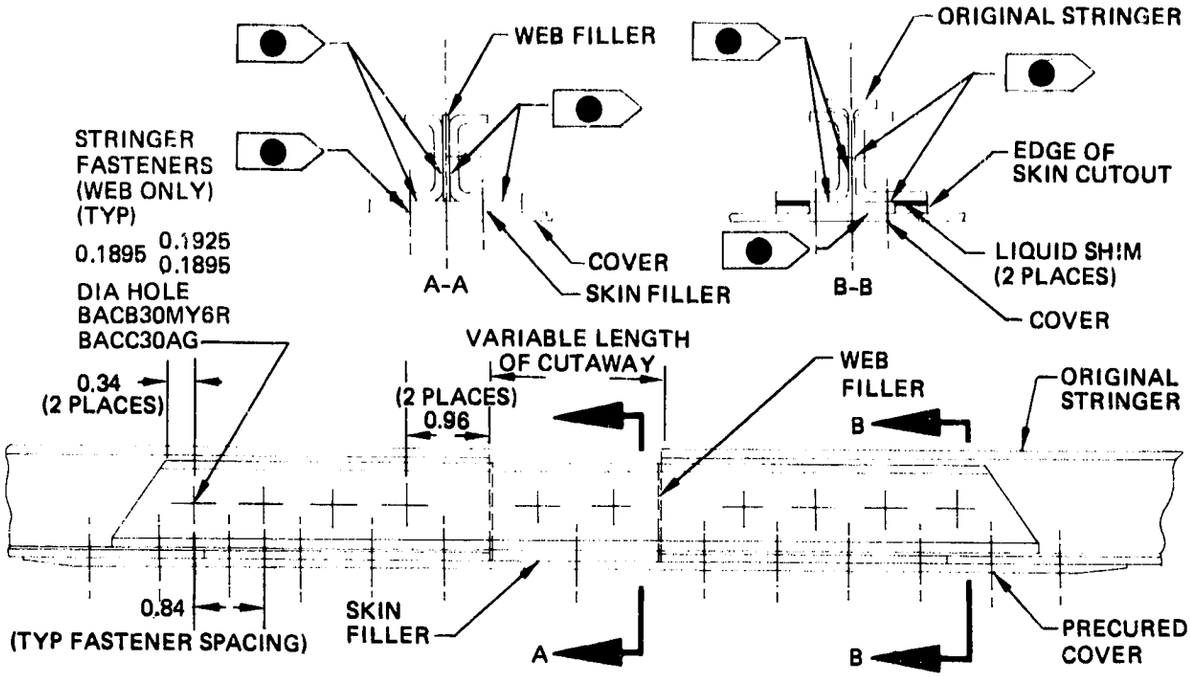

NOTE: THE NUMBER OF FASTENERS COMMON TO THE REPAIR CHANNELS AND FILLERS WILL DEPEND ON THE LENGTH OF THE DAMAGED STRINGER THAT MUST BE CUT AWAY. SEE FIGURE 2.11 FOR FASTENER DETAILS IN STRINGER CUTOUT AREA.

FILM ADHESIVE PER BMS 5-129 TYPE 2, CLASS IIC, GRADE 10 OR 15

Figure 2.10—Stringer Repair—Side View

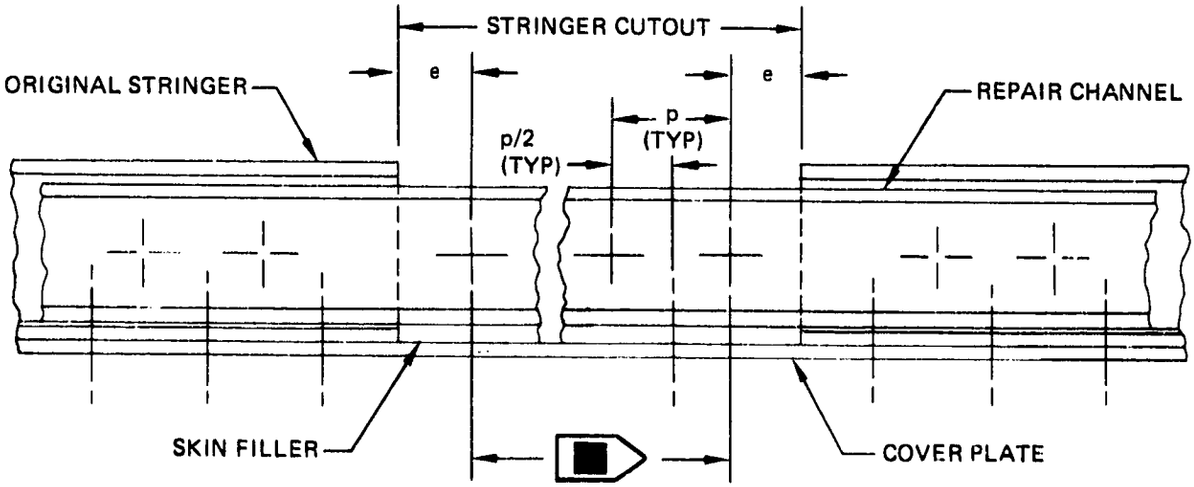

NUMBER AND SPACING OF FASTENERS IN THIS AREA VARY WITH THE LENGTH OF THE STRINGER CUTOUT. IN GENERAL, N FASTENERS IN THE WEB WILL BE SPACED EQUALLY AT A DISTANCE p APART, SUCH THAT $0.75 \leq p \leq 0.95$. DIMENSION e FOR WEB FASTENERS MUST BE IN THE RANGE $0.15 \leq e \leq 0.45$. (N - 1) FASTENERS IN THE LOWER FLANGE ARE SPACED EQUIDISTANT BETWEEN EVERY TWO WEB FASTENERS.

Figure 2.11—Fastener Configuration in Stringer Cutout Area

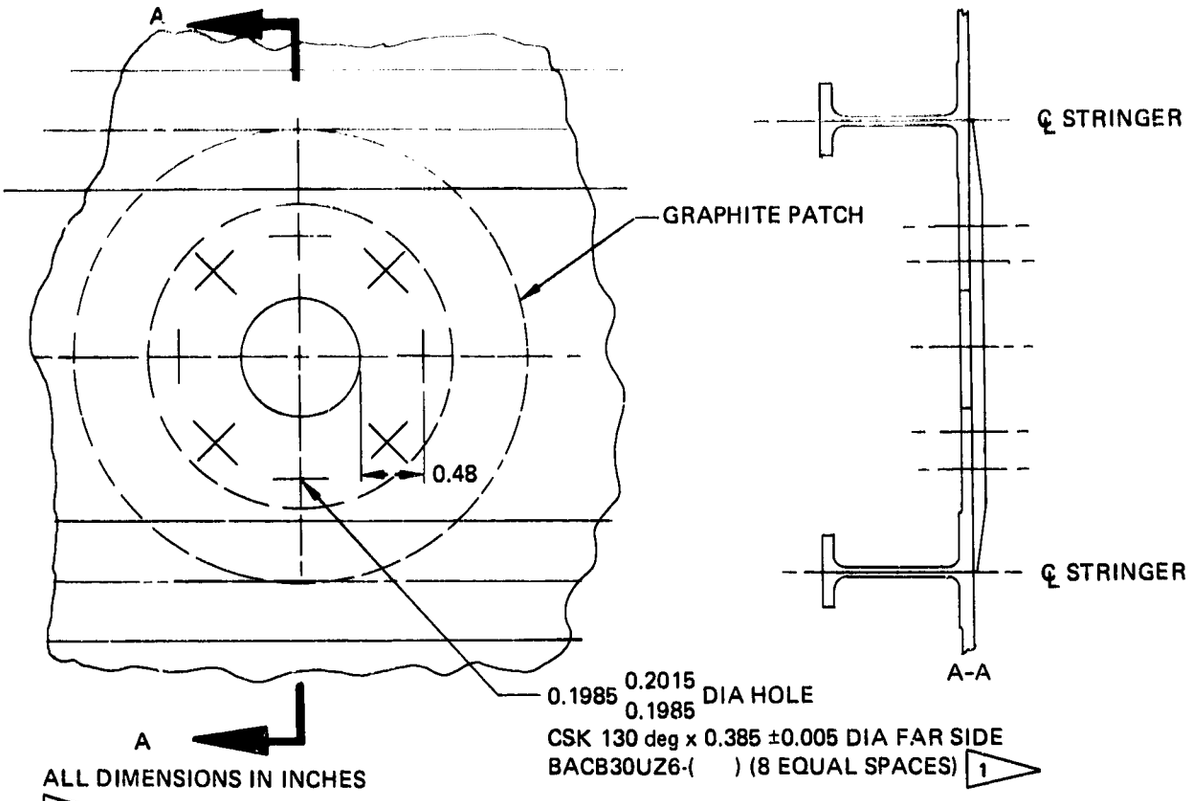

Figure 2.12–Skin Panel Repair

15. Clean out the cavity and repair area with oil-free air. Wipe the surfaces with a clean cloth moistened with methyl ethyl ketone.

16. Apply one layer of BMS 5-129 Type 2, Class IIC, Grade 10 or 15 to the area between the precured channels and the skin filler, as shown in Figure 2.10.

17. Install the skin filler.

18. Apply one layer of BMS 5-129 Type 2, Class IIC, Grade 10 or 15 to the area between the panel and cover or patch as shown in Figure 2.13.

19. Remove the peel ply from the cover or patch.

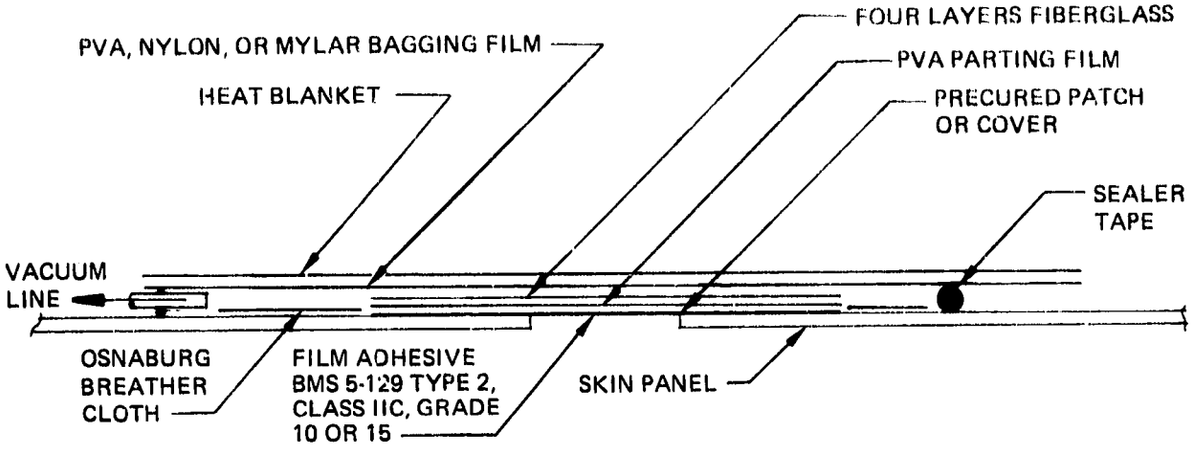

Figure 2.13—Layup Assembly for Repairing a Skin Panel Using a Precured Graphite/Epoxy Patch or Cover

20. Install the cover per Figures 2.8, 2.9, and 2.10 or patch per Figure 2.12.

21. If any portion of the repair patch or cover lies within Zone 3, a wet layup of one ply of fiberglass is to be applied. The fiberglass layer should extend 0.5 in. beyond the periphery of the patch. See D6-15565, Section 51-40-9, Paragraph 4(E) or 5(B) (ref. 1), for the wet layup procedure.

22. Directly above the patch or cover, apply a layer of PVA with four layers of fiberglass to ensure proper air removal.

23. Tape two thermocouples (minimum) to the panel adjacent to the repair patch or cover.

24. Set up a PVA, nylon, or Mylar vacuum bag as shown in Figure 2.13. Surround the patch or cover with Osnaburg breather cloth, seal the vacuum bag, and insulate the panel adjacent to the vacuum bag with 8 or 10 layers of fiberglass.

25. Apply heat blanket. The heat blanket should extend a minimum of 4 in. beyond the edge of the repair.

26. Cover the heat blanket with 3 or 4 in. of fiberglass fabric or other insulation.

27. Evacuate the vacuum bag by maintaining a minimum vacuum of 20 in. of mercury gage pressure. Check the vacuum bag for leaks that may prevent minimum vacuum pressure. Correct any leaks in the system.

28. Apply heat and maintain 225 $^{+25^{\circ}}_{-0^{\circ}}$ F for 90 $^{+15}_{-0}$ minutes. Do not heat faster than 5°F per minute. Record temperature continuously.

29. After the adhesive has cured, cool slowly and remove the vacuum bag and heat blanket.

30. Refinish surface to original condition in accordance with Section 3.0 herein.

3.0 PREPAINT CLEANING, PRETREATMENT, AND PAINTING OF SURFACES

The graphite/epoxy components of the 737 stabilizer are protected by the finishes shown in Figure 3.1. Prepaint cleaning, pretreatment, and painting of graphite/epoxy stabilizer components shall be accomplished in accordance with the sections of the 737 Maintenance Manual listed in Figure 3.2, except no chemical paint strippers may be used to remove paint.

CAUTION: CHEMICAL PAINT STRIPPERS MAY ATTACK RESIN SYSTEMS AND THEREFORE SHOULD NOT BE USED TO REMOVE PAINT.

The only acceptable method for removing paint is hand sanding using 240-grit or finer abrasive paper. In sanding, do not abrade the graphite fibers of the surface. Remove sanding dust by wiping the surface with a tack rag.

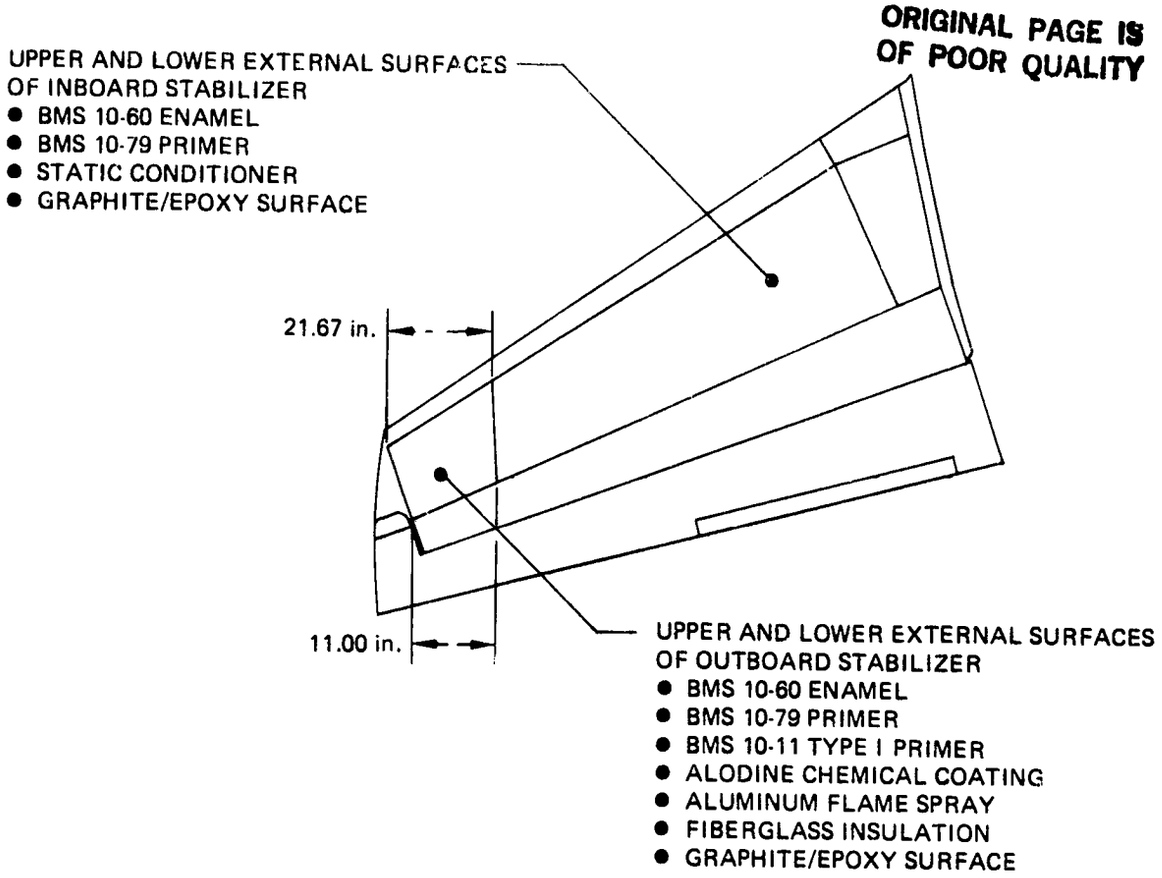

Figure 3.1—Finishes Used on Graphite/Epoxy Stabilizer Surfaces

FINISH TO BE APPLIED	BOEING 737 MAINTENANCE MANUAL SECTION TITLE (REF. 5)	SECTION NUMBER
Static conditioner (Boeing finish code F14.67)	Detailed Instructions for Prepaint Cleaning and Pretreatment of Plastic Surfaces	51-21-21
BMS 10-79 Type II primer and BMS 10-60 Type II enamel (Boeing finish code F19.41-707)	Decorative Paint System Cleaning/ Painting	51-21-171
Colored chemical coating (Boeing finish code F-17.10)	Decorative Paint System Cleaning/ Painting	51-21-171
BMS 10-11 Type I primer (Boeing finish code F-20.02)	Decorative Paint System Cleaning/ Painting	51-21-171
Aluminum Type IV flame spray	Boeing 737 Structural Repair Manual D6-15565 (ref. 1)	51-40-9 Paragraph 9

Figure 3.2--Procedures for Prepaint Cleaning, Pretreatment, and Painting Graphite/Epoxy Stabilizer Surfaces

4.0 REFERENCES

1. D6-15565, Boeing 737 Structural Repair Manual.

2. D6-7170, Nondestructive Test Manual Inspection Procedures for Boeing Jet Transports.

3. D6-37239, Nondestructive Test Manual for Boeing 737.

4. D6-9794, Installation of Plastic Shims and Metal Fillers.

5. D6-12XXX, Boeing 737 Maintenance Manual.

APPENDIX–EXAMPLES OF REPAIRS MADE TO GRAPHITE/EPOXY COMPONENTS

This appendix provides photographs of the repair procedure used to repair a laminate graphite/epoxy stiffened skin panel in which there is no access from the stiffened side of the panel, as in the stabilizer structural box.

Figure A.1 shows a repair that was made to a laminate skin panel. The precured graphite/epoxy patch is both bonded and mechanically fastened.

Figures A.2 through A.12 show some of the major steps in repairing the I-section stringers of the stiffened skin panel.

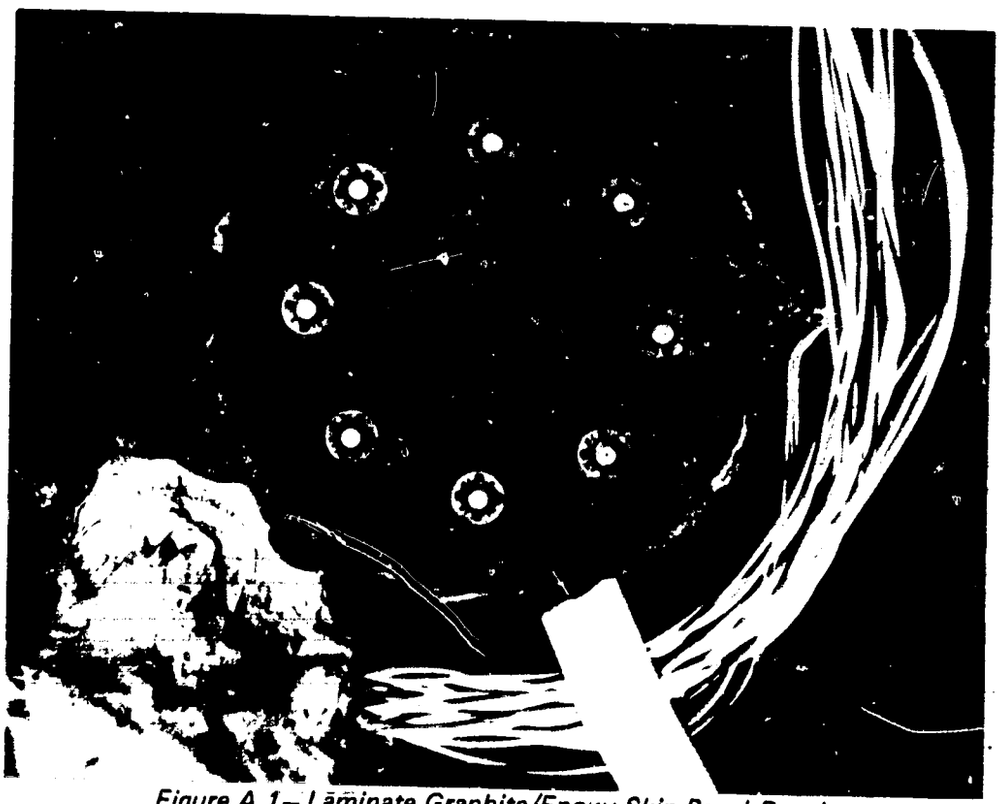

Figure A.1– Laminate Graphite/Epoxy Skin Panel Repair

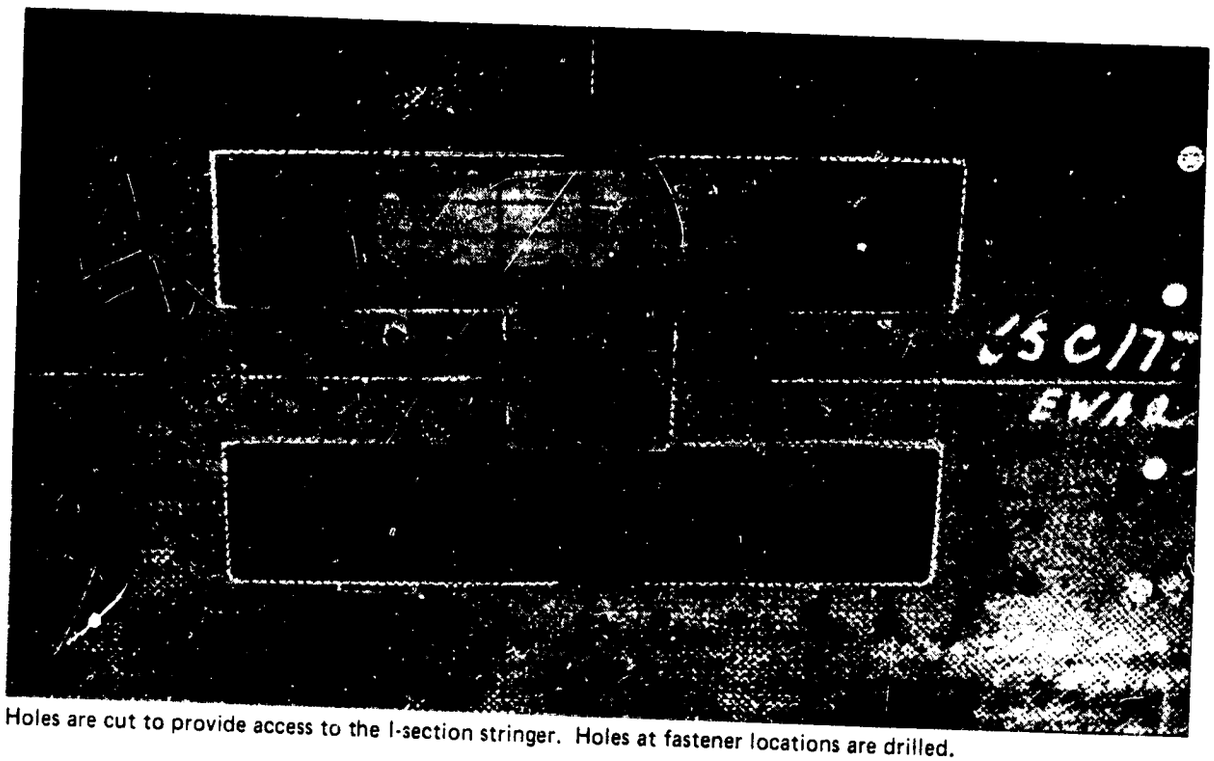

Holes are cut to provide access to the I-section stringer. Holes at fastener locations are drilled.

Figure A.2—I-Section Stringer Access Holes

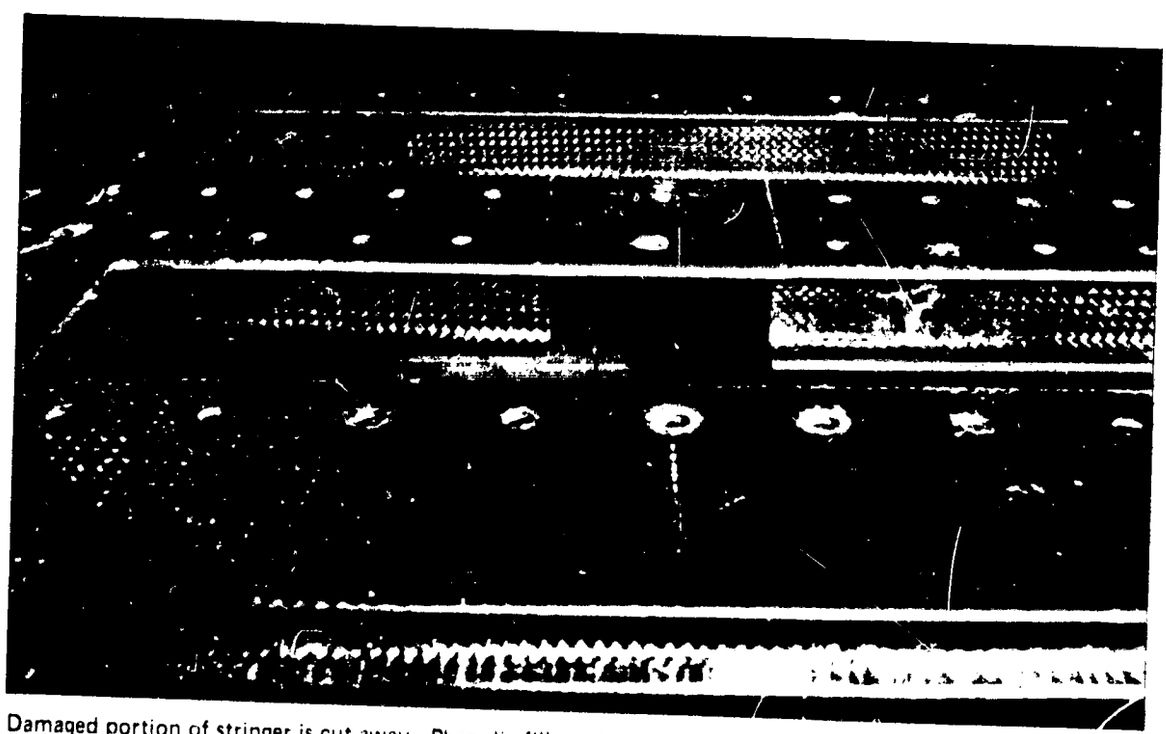

Damaged portion of stringer is cut away. Phenolic filler is in place.

Figure A.3—Access Holes With Stringer Damage Removed

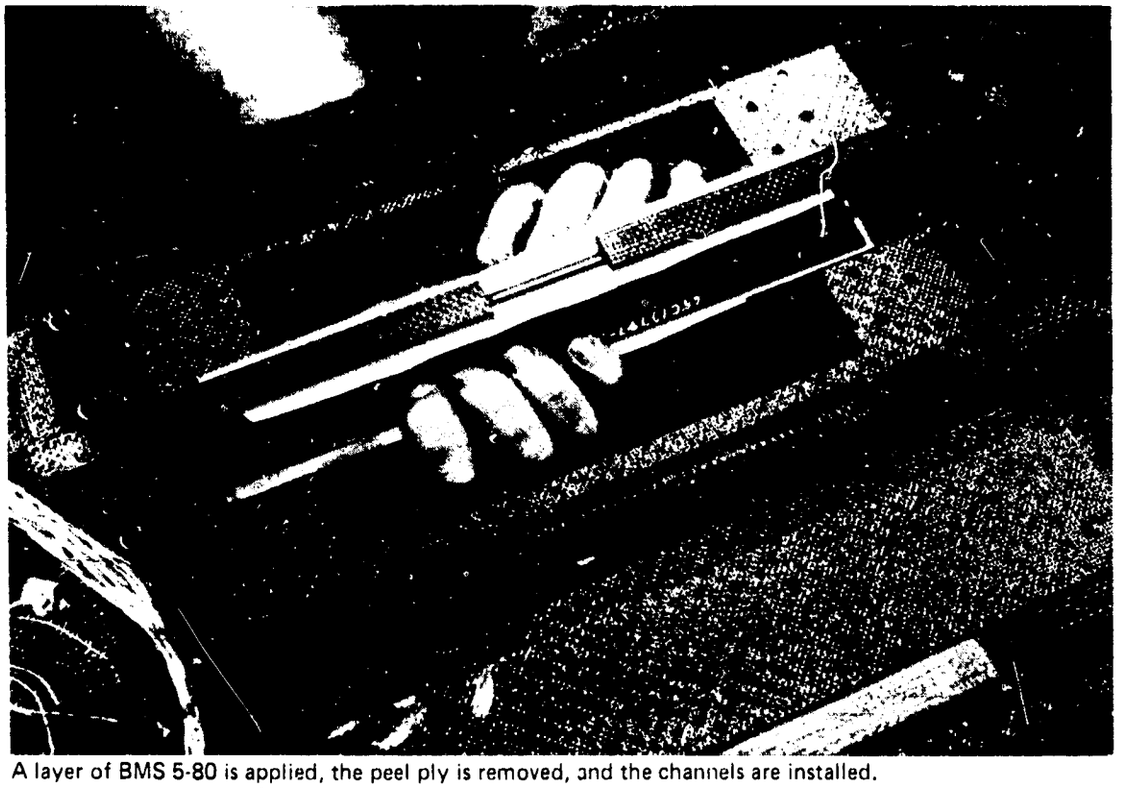

A layer of BMS 5-80 is applied, the peel ply is removed, and the channels are installed.

Figure A.4—Location of Predrilled Repair Channels

Figure A.5—Positioning of Repair Channels With Adhesive Film

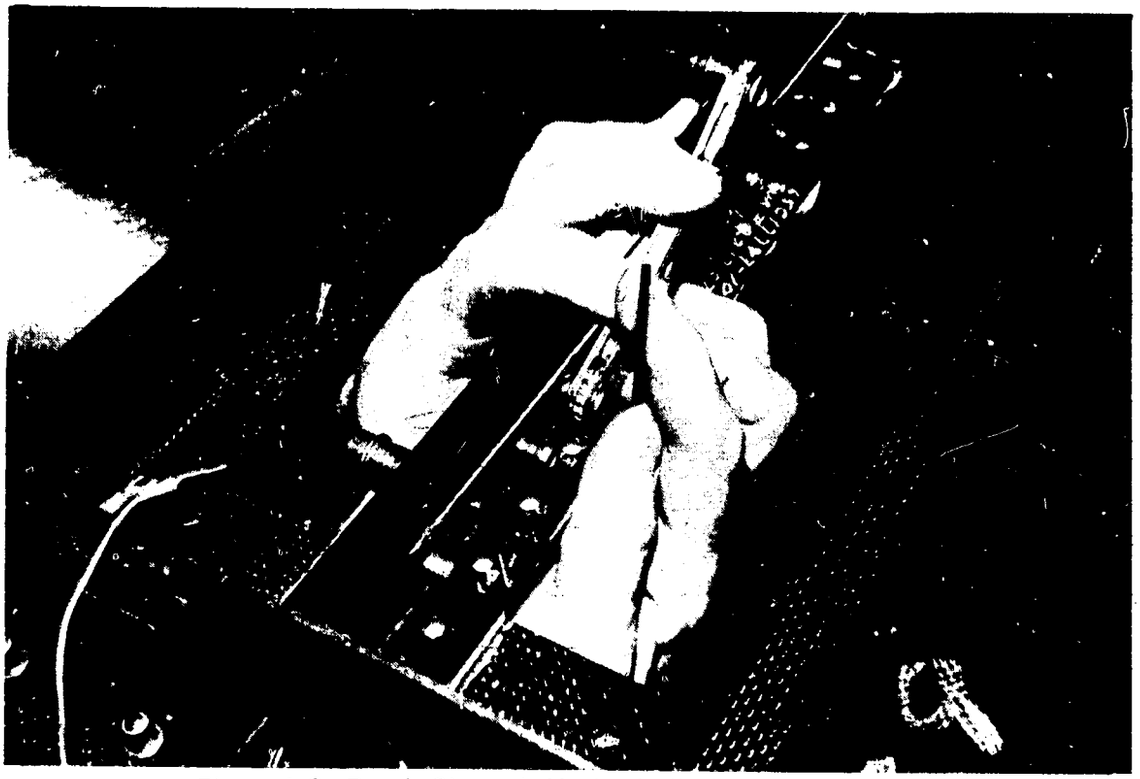

Figure A.6—Repair Channels Mechanically Fastened Into Place

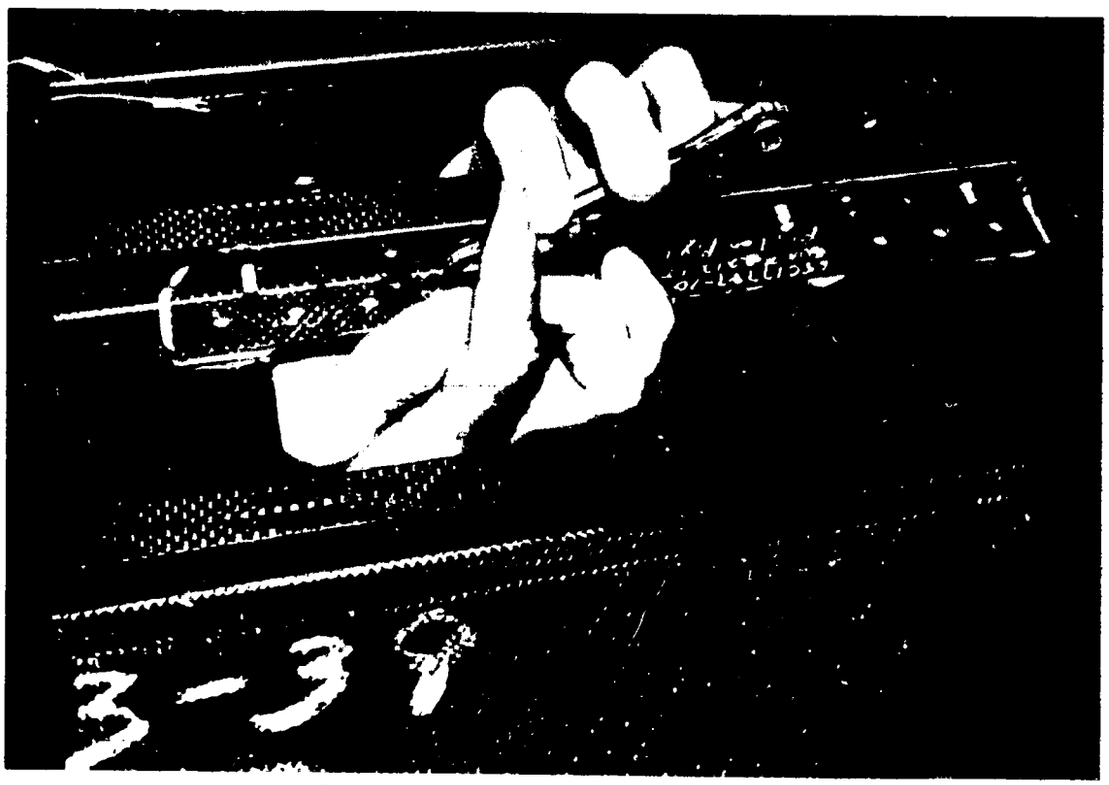

Figure A.7—Repair Channel Installation

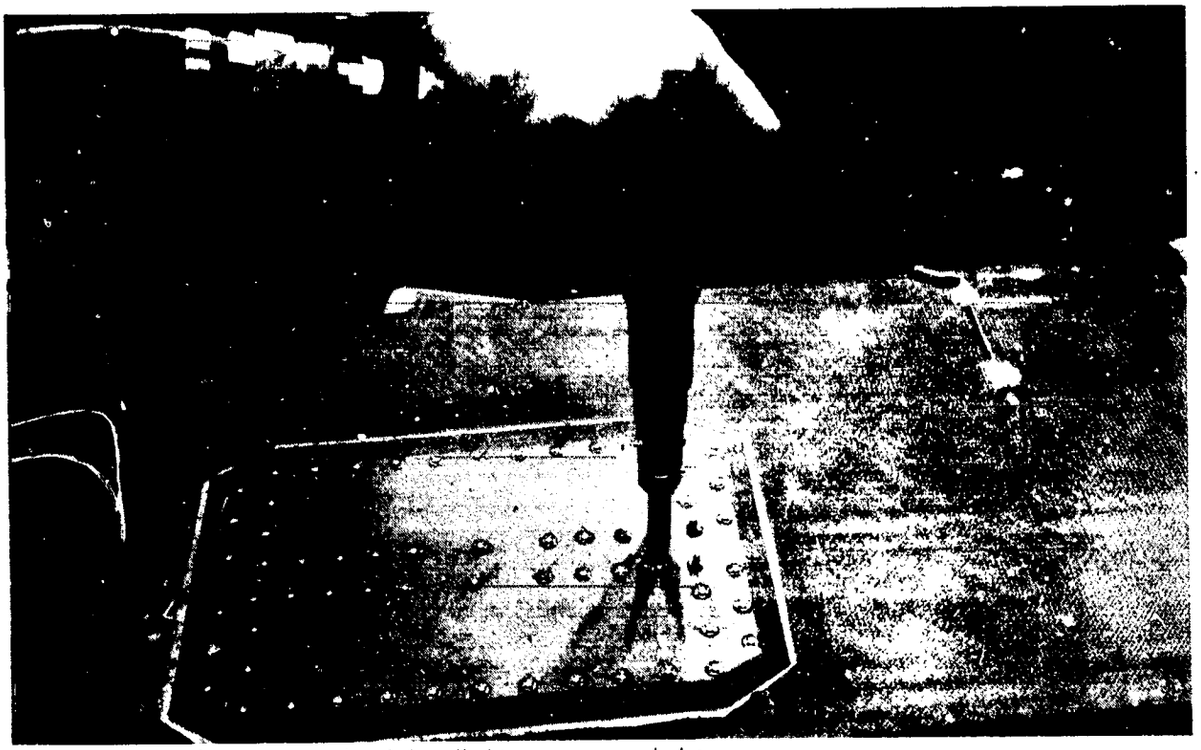

Precured graphite/epoxy cover plate is installed to cover access holes.

Figure A.8—Cover Plate Installation

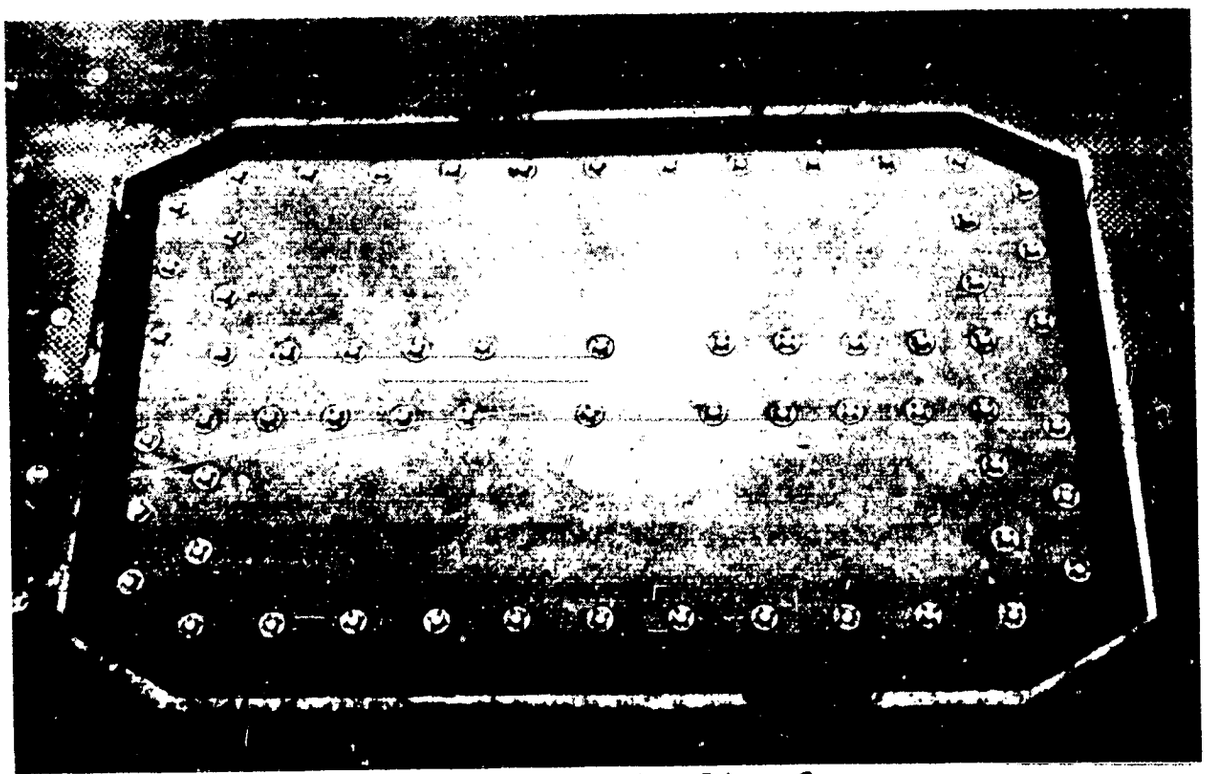

Figure A.9—Installed Cover Plate Prior to Cure

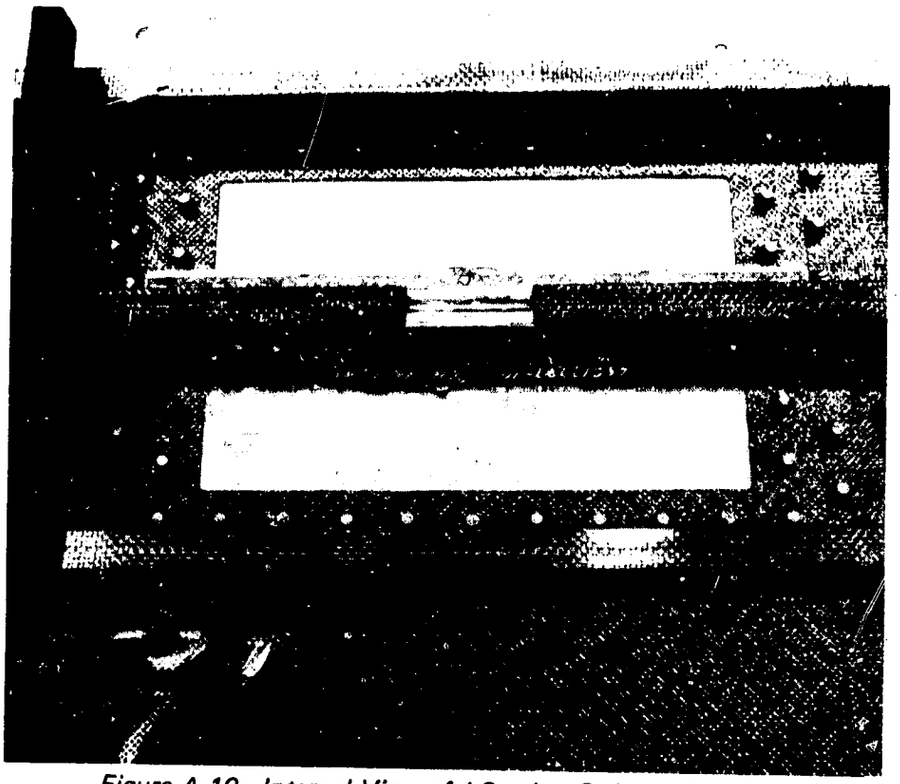

Figure A.10—Internal View of I-Section Stringer Repair

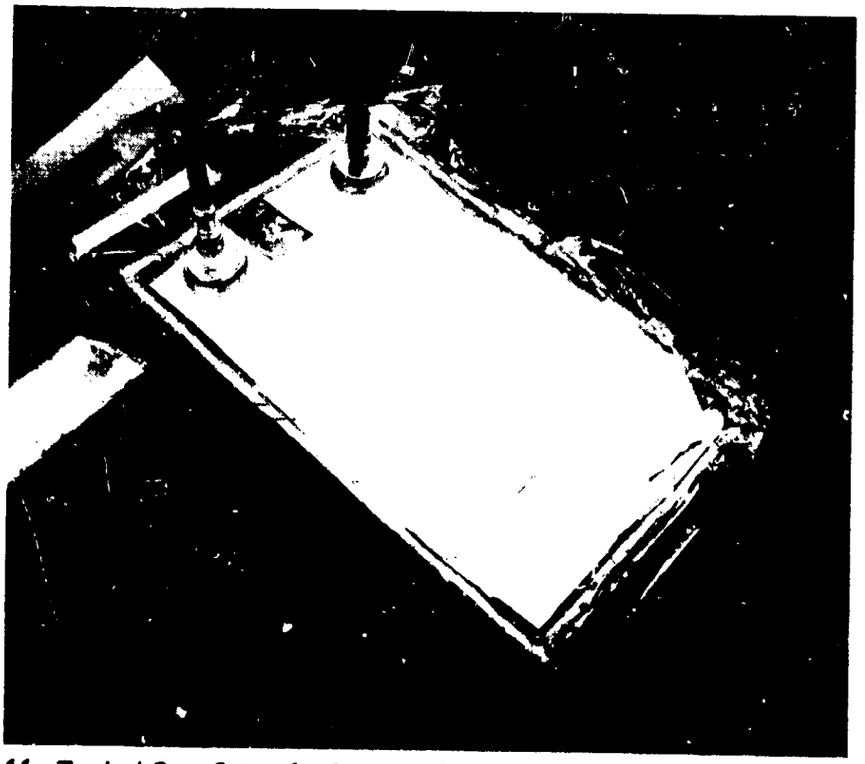

Figure A.11—Typical Cure Setup for Bonding Precured Patch to Graphite/Epoxy Skin Panel

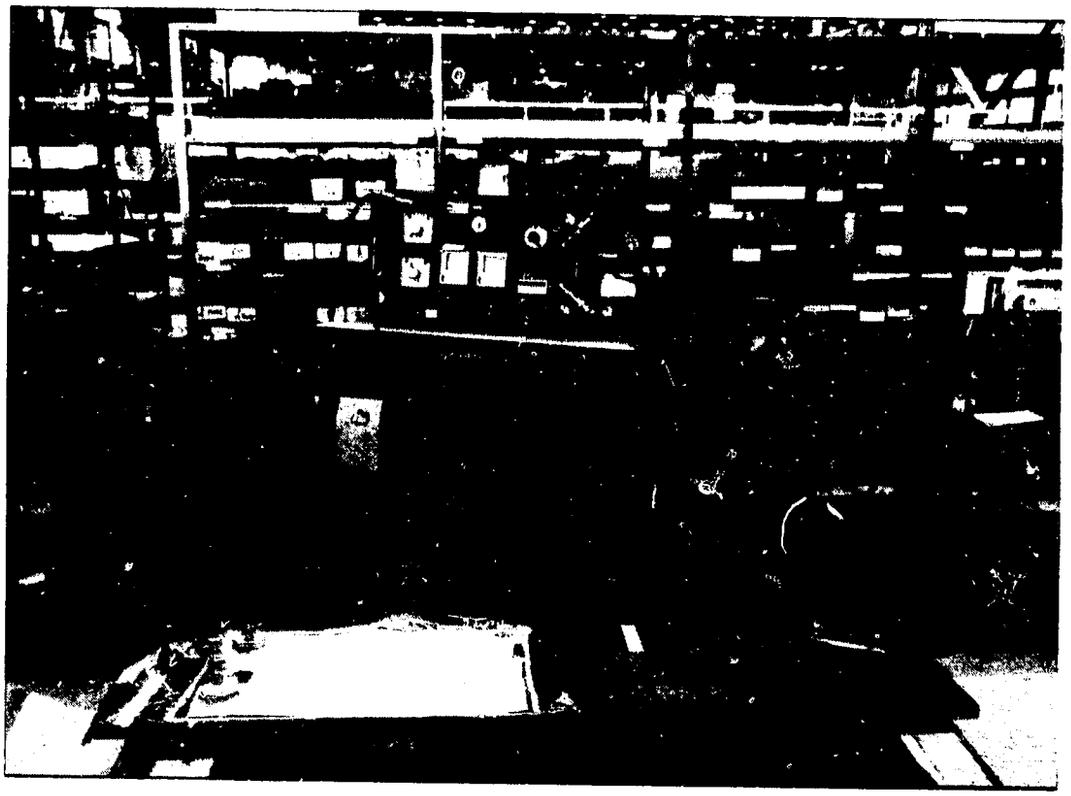

Figure A.12--Typical Cure Setup and Monitoring Device

APPENDIX B

MAINTENANCE PLANNING DATA,

AIRCRAFT STRUCTURAL INSPECTION,

COMPOSITE HORIZONTAL STABILIZER

TABLE OF CONTENTS

INTRODUCTION

This document provides general guidance in establishing individual airline maintenance programs for current production 737-200 airplanes, using a composite (graphite/epoxy) horizontal stabilizer. This document covers only the installed composite (or composite-related) parts. For the remainder of the airplane maintenance procedures, see the Boeing 737 Maintenance Planning Data Manual, D6-17594 (ref. 1). The work items in this document are recommendations and should not be considered all-inclusive or mandatory. Each airline has the final responsibility to define and establish its own maintenance program.

BOEING 737 AIRCRAFT COMPOSITE HORIZONTAL STABILIZER STRUCTURAL INSPECTION DOCUMENT

This document is composed of several sections that cover such items as stabilizer dimensions and station diagrams; general servicing requirements; related illustrations; zone diagrams; access doors and panels; scheduled maintenance checks; and structural inspection requirements.

For each type of maintenance check recommended, a basic package of specific maintenance requirements is provided. These checks contain maintenance tasks considered appropriate for maintenance planners to develop airline maintenance programs. The maintenance tasks specified in the lower check(s) must be accomplished together with those of the next higher check(s); i.e., the "C" check also requires the accomplishment of "preflight," "transit," "A," and "B" checks.

EXPLANATION OF TERMS

Check

A "check," as used in this document, means a maintenance action requiring thorough examination of an item for general condition, as applicable, with special emphasis directed to the following areas: proper attachment, safety wiring, cotter pins and fasteners, linkages, bearings, alignment, clearance tolerances, lubrication, obvious damage, cracks, blistering, delamination, fraying, excessive wear or play, corrosion, rubbing, aging, preservative coating or finish, cleanliness, and general appearance.

Corrosion Prevention

For metallic parts, Boeing Corrosion Prevention Manual D6-41910 (ref. 2) provides general information on inspection, detection, corrosion removal, and preventive maintenance measures. The 737 corrosion-prevention tasks outlined in the reference manual are to be completed when called for in Section 4-0 of this document. Also, it is imperative that aluminum parts located within 4 in. of graphite/epoxy parts be repainted locally, if paint is found to have been removed.

For graphite/epoxy parts, all external surfaces and any surfaces within 4 in. of aluminum parts are to be repainted as required when paint is found to have been removed.

On-Condition (O/C)

"On-condition" maintenance is applicable to components on which a determination of continued airworthiness may be made by visual inspection, measurements, tests, or other means, without a teardown inspection or overhaul. On-condition checks are to be performed within time limitations and intervals prescribed for each check or inspection. Performance tolerances and wear or deterioration limits shall be contained in the air carriers' maintenance manuals. The periodic scheduled O/C checks must constitute meaningful determination of suitability for continued operation for another scheduled interval. If the check discloses enough evidence about the condition and failure resistance of the item to ensure a reasonable probability of its continued airworthiness during the next check interval, the item is properly categorized as on-condition.

Wear/deterioration curves for components in the O/C category must be progressive and not of a catastrophic nature. Otherwise, the determination of suitability for continued operation during another check interval cannot be made.

MAINTENANCE MANHOUR ESTIMATES

The maintenance task requirements contained herein show estimated time standards required to perform scheduled maintenance. Estimated work times are for the performance of listed tasks and do not include removal or replacement of access doors and panels. Time standards shown in the "elapsed" columns take into consideration optimum use of manpower and equipment. These standards are based on best judgment factors, use of skilled personnel, and ready availability of required tools and equipment.

SECTION 1-0

GENERAL INFORMATION

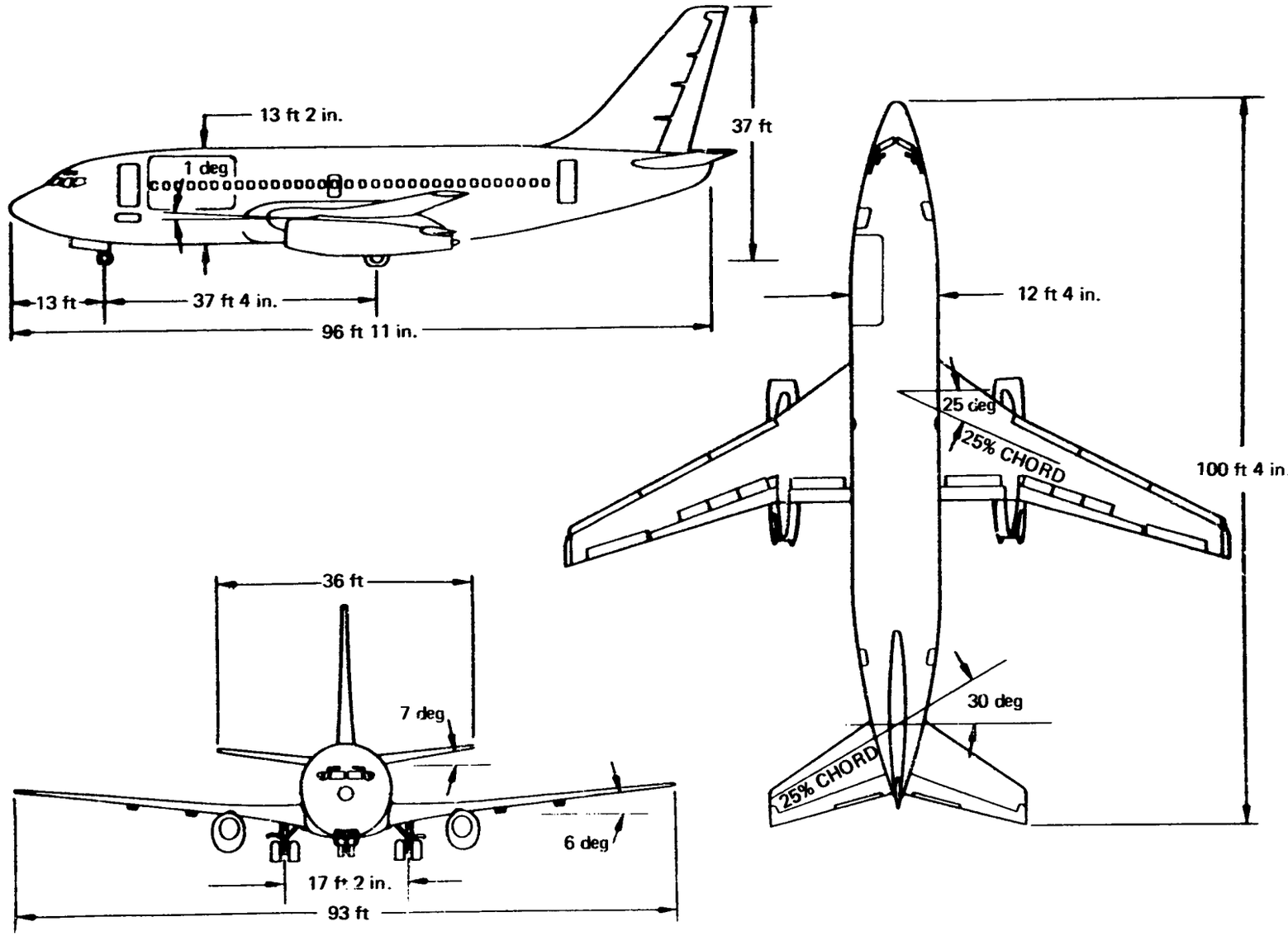

Principal Dimensions, –200 and –200C Series

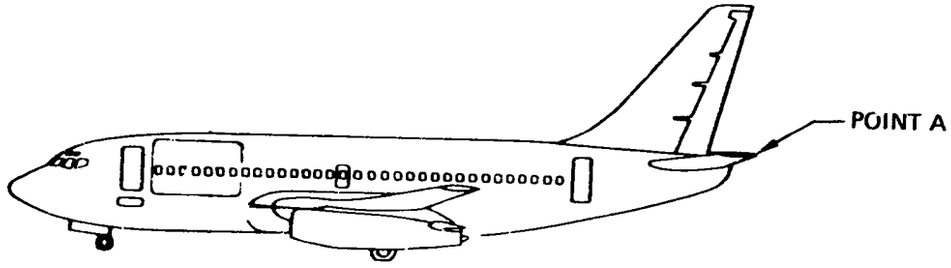

POINT	O. W. E.	MAX TAXI WEIGHT	TAIL HIGH	TAIL LOW	LEFT WING HIGH	RIGHT WING HIGH	RIGHT WING LOW	LEFT WING LOW	ON JACKS	POS* ERROR	NEG* ERROR
A	201.66	204.99	217.21	178.21	216.07	197.81	196.05	179.25	213.10	0.73	-0.73
COND	1	2	3	4	5	6	7	8	9		

*Assuming 0.20-in. error in main gear and nose gear deflections

GROUND CLEARANCE CONDITION

1. Operating weight empty 62,000 lb, cg at 24% mac
2. Maximum taxi weight 116,000 lb, cg at 5% mac
3. Weight 62,100 lb, cg at 24% mac, nose landing gear oleos deflated, nose wheel tires flat (tail high)
4. Weight 62,100 lb, cg at 33% mac, both main landing oleos deflated, all main wheel tires flat (tail low)
5. Weight 62,100 lb, cg at 24% mac, right-hand main gear and nose gear oleos deflated, right-hand main wheel and nose wheel tires flat (left wing high)
6. Weight 62,100 lb, cg at 24% mac, left-hand main gear and nose gear oleos deflated, left-hand main wheel and nose wheel tires flat (right wing high)
7. Weight 62,100 lb, cg at 33% mac, right-hand main gear oleo and tire deflated (right wing low)
8. Weight 62,100 lb, cg at 33% mac, left-hand main gear oleo and tire deflated (left wing low)
9. Airplane on jacks in level attitude for landing gear functional tests with 2-in. ground clearance on the maximum extension of the main landing gear; height above ground includes wing deflection for empty tanks

Dimensions and Areas, Ground-Clearance Data, Selected Points, Height Above Ground (Inches), 737-200, 40 x 14–20 PR Tires

ZONE DIAGRAM

General

The 737 zone diagram is composed of seven major zones covering the fuselage, wings, nacelles, and empennage. Further identification breakdown is achieved by use of areas, which denote specific compartments, equipment bays, doors, engines, etc., in conjunction with major zones.

Zone and Area Identification

The zone and area are identified by a number consisting of a first digit, indicating the zone, followed by a dash and a number of one or two digits, indicating the area. Thus, 7-9 is read zone 7, area 9, which identifies the empennage and the left side horizontal stabilizer. This document covers only items in zone 7, areas 9 and 10.

Zone Locations

Zone 1—upper half of fuselage (reference)
Zone 2—lower half of fuselage (reference)
Zone 3—left wing (reference)
Zone 4—right wing (reference)
Zone 5—left nacelle (reference)
Zone 6—right nacelle (reference)
Zone 7—empennage (see page 5)

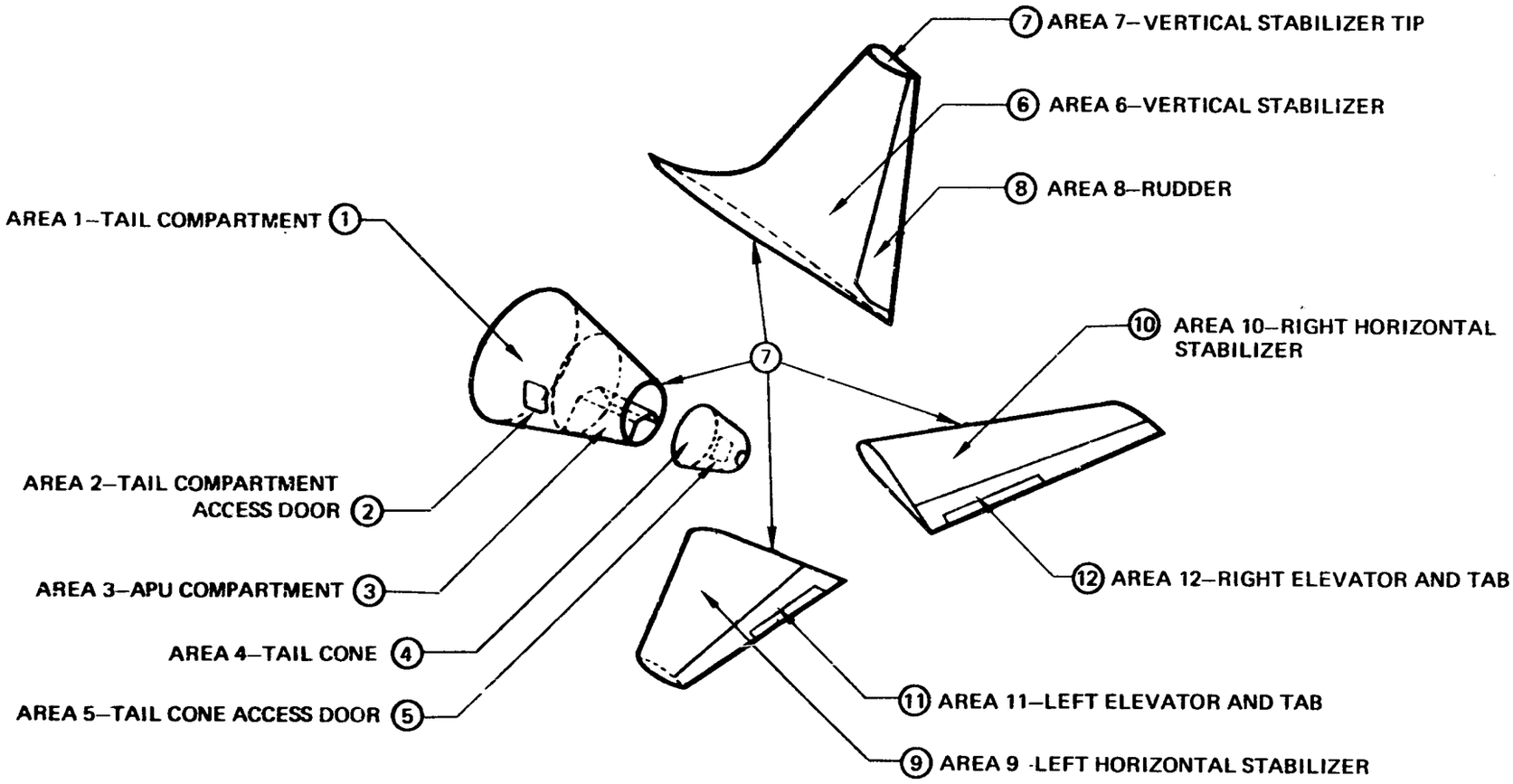

Zone 7–Empennage

ACCESS DOORS AND PANELS–EXTERIOR

General

Access doors and panels have been assigned a four-digit number, in accordance with a procedure formerly used for identification and location. However, with the introduction of the zone and area diagrams for designating the location of the aircraft components and work areas on maintenance work requirement cards, the zone and area concept also is used to designate the location of access doors and panels. This section contains identification numbers and locations for access panels for composite stabilizer inspection.

Implementation

To implement the above procedure in this document, an additional column listing the zone and area will be placed adjacent to the column listing access doors and panels. The last column lists the primary items or areas to which the panel provides maintenance access.

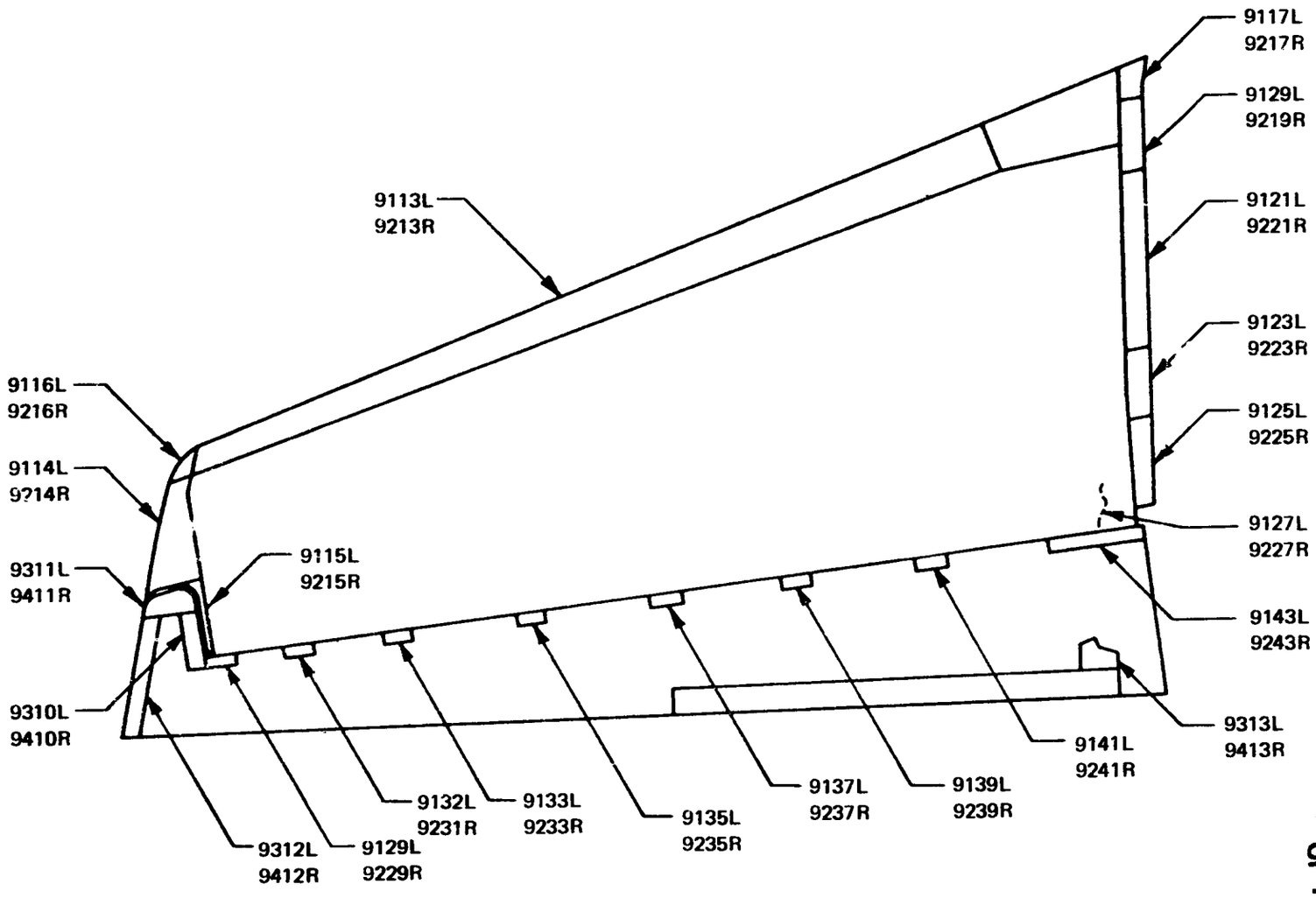

Upper Stabilizer and Elevator—Left Hand Shown, Right Hand Opposite

Access Doors and Panels

PANEL NUMBER	AIRPLANE SECTION—UPPER STABILIZER AND ELEVATOR LH AND RH	ZONE AND AREA	PROVIDES ACCESS TO:
9113L	Removable leading edge	7-9	Stabilizer internal structure
9213R	Removable leading edge	7-10	
9114L	Removable tip	7-9	
9214R	Removable tip	7-10	
9115L	Removable stabilizer tip—aft	7-9	
9215R	Removable stabilizer tip—aft	7-10	
9116L	Removable stabilizer tip—fwd	7-9	
9216R	Removable stabilizer tip—fwd	7-10	Stabilizer internal structure
9117L	Gap cover stabilizer to body	7-9	Stabilizer front and rear spar-to-center section attachment fittings
9217R		7-10	
9119L		7-9	
9219R		7-10	
9121L		7-9	
9221R		7-10	
9123L		7-9	
9223R		7-10	
9125L		7-9	
9225R	Gap cover stabilizer to body	7-10	Stabilizer front and rear spar-to-center section attachment fittings
9127L	Access panel—elevator hinge support rib	7-9	Internal structure
9227R	Access panel—elevator hinge support rib	7-10	Internal structure
9129L	Elevator nose cover	7-11	Elevator hinge fitting number 8
9229R		7-12	Elevator hinge fitting number 6
9131L		7-11	Elevator front spar—internal structure
9231R		7-12	Elevator front spar—internal structure
9133L		7-11	Elevator hinge fitting number 5
9233R		7-12	Elevator hinge fitting number 5
9135L		7-11	Elevator front spar—internal structure
9235R		7-12	Elevator front spar—internal structure

Access Doors and Panels (Concluded)

PANEL NUMBER	AIRPLANE SECTION—UPPER STABILIZER AND ELEVATOR LH AND RH	ZONE AND AREA	PROVIDES ACCESS TO:
9137L	Elevator nose cover	7-11	Elevator hinge fitting number 4
9237R	↓	7-12	Elevator hinge fitting number 4
9139L	↓	7-11	Elevator front spar—internal structure
9239R	↓	7-12	Elevator front spar—internal structure
9141L	↓	7-11	Elevator hinge fitting number 3
9241R	↓	7-12	Elevator hinge fitting number 3
9143L	↓	7-11	Elevator hinge fitting number 1 and number 2
9243R	Elevator nose cover	7-12	Elevator hinge fitting number 1 and number 2
9310L	Elevator tip panel	7-11	Internal structure —elevator station 218.34
9410R	↓	7-12	↓
9311L	↓	7-11	↓
9411R	↓	7-12	Internal structure—elevator station 218.34
9312L	↓	7-11	Internal structure—elevator station 212.15
9412R	Elevator tip panel	7-12	Internal structure—elevator station 212.15
9313L	Elevator mast fitting fairing	7-11	Elevator tab push rods
9413R	Elevator mast fitting fairing	7-12	Elevator tab push rods

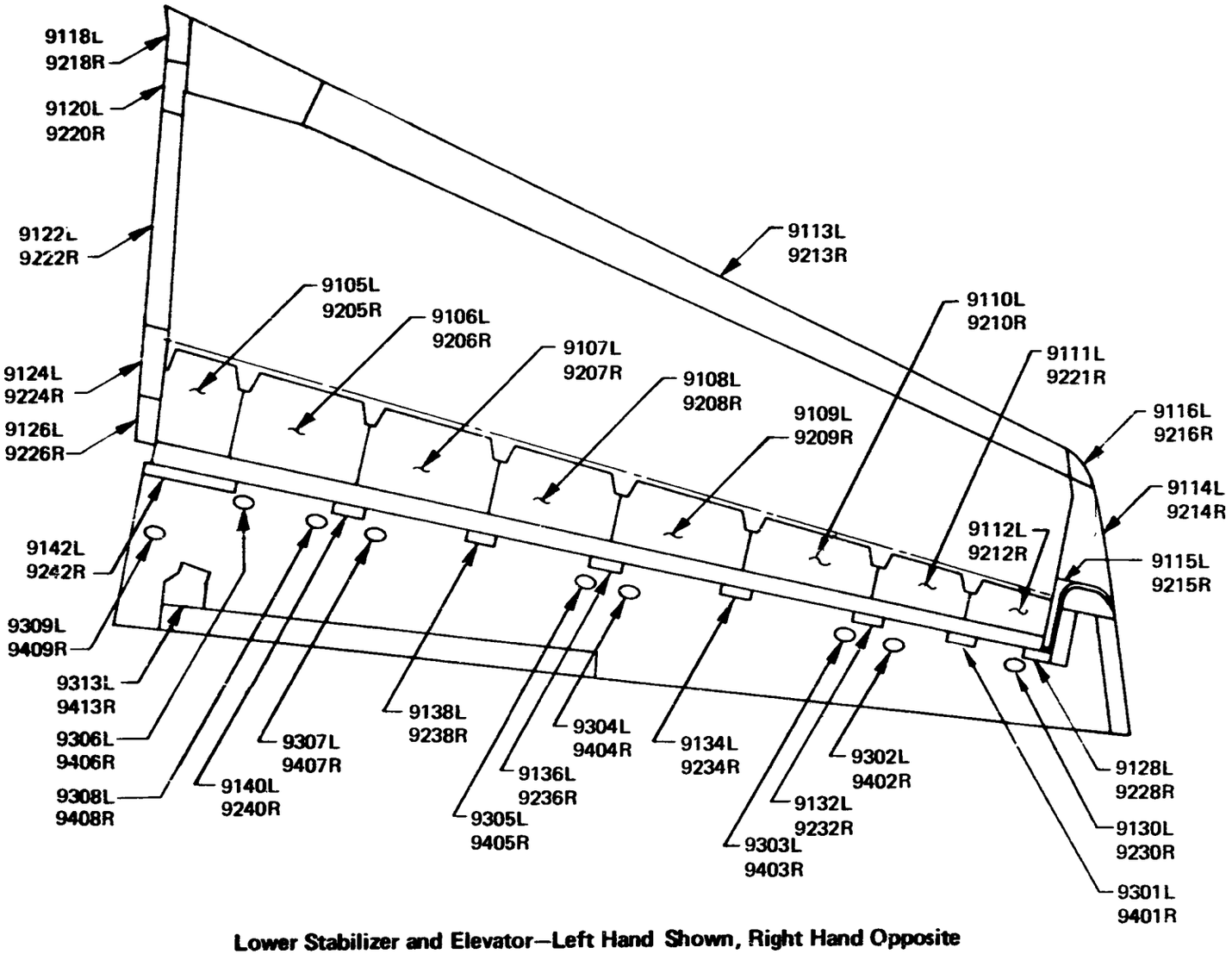

Lower Stabilizer and Elevator—Left Hand Shown, Right Hand Opposite

Access Doors and Panels

PANEL NUMBER	AIRPLANE SECTION—LOWER STABILIZER AND ELEVATOR LH AND RH	ZONE AND AREA	PROVIDES ACCESS TO:
9105L	Trailing-edge access panel	7-9	Internal structure inspar area—elevator station 24.09—39.02
9205R		7-10	Internal structure inspar area—elevator station 24.09—39.02
9106L		7-9	Stabilizer trailing-edge internal structure
9206R		7-10	
9107L		7-9	
9207R		7-10	
9108L		7-9	
9208R		7-10	
9109L		7-9	
9209R		7-10	
9110L		7-9	
9210R		7-10	
9111L		7-9	
9211R		7-10	
9112L		7-9	
9212R	Trailing-edge access panel	7-10	Stabilizer trailing-edge internal structure
9113L	Removable leading edge	7-9	Stabilizer internal structure
9213R	Removable leading edge	7-10	
9114L	Removable tip	7-9	
9214R	Removable tip	7-10	
9115L	Removable stabilizer tip—aft	7-9	
9215R	Removable stabilizer tip—aft	7-10	
9116L	Removable stabilizer tip—forward	7-9	
9216R	Removable stabilizer tip—forward	7-10	Stabilizer internal structure
9118L	Gap cover—stabilizer to body	7-9	Stabilizer front and rear spar-to-center section attachment fittings
9218R		7-10	
9120L		7-9	
9220R		7-10	

Access Door and Panels (Continued)

PANEL NUMBER	AIRPLANE SECTION—LOWER STABILIZER AND ELEVATOR LH AND RH	ZONE AND AREA	PROVIDES ACCESS TO:
9122L	Gap cover—stabilizer to body	7-9	Stabilizer front and rear spar-to-center section attachment fittings
9222R	↓	7-10	↓
9124L		7-9	
9224R		7-10	
9126L		7-9	
9226R	Gap cover—stabilizer to body	7-10	Stabilizer front and rear spar-to-center section attachment fittings
9128L	Elevator nose cover	7-11	Elevator hinge fitting number 6
9228R	↓	7-12	Elevator hinge fitting number 6
9130L		7-11	Elevator front spar—internal structure
9230R		7-12	Elevator front spar—internal structure
9132L		7-11	Elevator hinge fitting number 5
9232R		7-12	Elevator hinge fitting number 5
9134L		7-11	Elevator front spar and internal structure
9234R		7-12	Elevator front spar and internal structure
9136L		7-11	Elevator hinge fitting number 4
9236R		7-12	Elevator hinge fitting number 4
9138L		7-11	Elevator front spar and internal structure
9238R		7-12	Elevator front spar and internal structure
9140L		7-11	Elevator hinge fitting number 3
9240R		7-12	Elevator hinge fitting number 3
9142L		7-11	Elevator hinge fitting number 1 and number 2
9242R	Elevator nose cover	7-12	Elevator hinge fitting number 1 and number 2
9301L	Elevator access panel	7-11	Internal structure—elevator station 207.00
9401R	↓	7-12	Internal structure—elevator station 207.00
9302L		7-11	Internal structure—elevator station 155.75
9402R		7-12	Internal structure—elevator station 155.75

Access Doors and Panels (Concluded)

PANEL NUMBER	AIRPLANE SECTION—LOWER STABILIZER AND ELEVATOR LH AND RH	ZONE AND AREA	PROVIDES ACCESS TO:
9303L	Elevator access panel	7-11	Internal structure—elevator station 143.00
9403R		7-12	Internal structure—elevator station 143.00
9304L		7-11	Internal structure—elevator station 132.00
9404R		7-12	Internal structure—elevator station 132.00
9305L		7-11	Internal structure—elevator station 121.00
9405R		7-12	Internal structure—elevator station 121.00
9306L		7-11	Internal structure—elevator station 48.00
9406R		7-12	Internal structure—elevator station 48.00
9307L		7-11	Internal structure—elevator station 76.00
9407R		7-12	Internal structure—elevator station 76.00
9308L		7-11	Internal structure—elevator station 65.00
9408R		7-12	Internal structure—elevator station 65.00
9309L		7-11	Internal structure—elevator station 37.00
9409R	Elevator access panel	7-12	Internal structure—elevator station 37.00
9313L	Fairing mast fitting elevator inboard	7-11	Elevator tab mast fitting and pushrod
9413R	Fairing mast fitting elevator inboard	7-12	Elevator tab mast fitting and pushrod

SECTION 2-0

PREFLIGHT, TRANSIT, AND "A" CHECKS

MAINTENANCE CHECKS

The airline industry has categorized airplane "minor" maintenance tasks, using terminology such as preflight, transit, through service, overnight service, turnaround, station check, line check, and daily inspection. Boeing has elected to use the terms "preflight" and "transit" in this document to designate those minor maintenance checks performed at time intervals less than the "A" check.

Preflight Check

The preflight check, more comprehensive than the transit check, is intended for use at a route terminus and includes all inspection items in the lesser transit check. A preflight check should be performed before the first flight of the day, or when an aircraft remains on the ground for 4 hours or more.

Transit Check

The transit check requires minor maintenance and servicing and is intended to ensure continuous serviceability of a transiting aircraft. This check is planned for use at an en-route stop and is basically a walkaround inspection that requires a check of the aircraft interior and exterior for obvious damage, leaks, proper operating equipment, security of attachment, and required servicing.

"A" Check

The "A" check is considered a primary inspection and is intended to disclose the general condition of the aircraft. The "A" check is done in conjunction with the above-mentioned lesser maintenance inspections (preflight and transit checks). The "A" check may be done at specified hourly or calendar time intervals.

Definitions of terms such as check and manhour estimate criteria are provided in Section 0-4 of this manual.

The preflight, transit, and "A" checks as shown herein are recommended minimum maintenance requirements and may be augmented or revised accordingly by the operator.

Preflight/Transit Check

MODEL 737 200	TASK			REFERENCE	LOCATION		TIME	
DESCRIPTION	CHECK	LUBRICATE	OTHER		ZONE AND AREA		HOURS AND TENTHS	
							ELAPSED	MANHOURS
From ground level, visually inspect horizontal stabilizer (walkaround check)	X				7-9 7-10		0.10	0.10

"A" Check

MODEL 737-200	TASK			REFERENCE	LOCATION		TIME	
DESCRIPTION	CHECK	LUBRICATE	OTHER		ZONE AND AREA		HOURS AND TENTHS	
							ELAPSED	MANHOURS
Horizontal stabilizer Visually inspect the exterior surfaces, including skin panels, leading edge, and stabilizer tip, for loose or missing fasteners, wear, delamination, corrosion, missing paint, or obvious damage. If evidence of damage is detected, inspect using NDT inspection procedures per appendix. NDT instrumentation must be calibrated with reference standards simulating the structure to be inspected. In cases where a standard cannot be used, predetermined "like" areas may be used as a standard for an acceptable condition.	X			See Structural Repair Manual D6-46035 (ref. 3)	7-9 7-10		0.20	0.20

SECTION 3-0

"B" CHECK

"B" CHECK

The "B" check is considered to be an intermediate check and requires an examination of an aircraft to determine its general condition for ensuring sustained airworthiness. This check includes selected operational checks, filter servicing, and limited lubrication tasks and requires the opening of specific access doors and panels. The "B" check also requires accomplishment of all items contained in the "A" and preflight checks.

Refer to Section 0-4 of this document for a definition of specific terms such as check and operational check and general information concerning escalation of maintenance inspection intervals, etc. Entries that incorporate a "2" in the check column indicate that the item is to be checked at a "2B" inspection interval. Items designated "2B" are completed during every other "B" check.

The approximate number of manhours required to open and close or remove and install access doors and panels for the "B" and "2B" check are 1.5 and 2.0 manhours, respectively.

"B" Check

MODEL 737-200	TASK			REFERENCE	LOCATION		TIME	
DESCRIPTION	CHECK	LUBRICATE	OTHER		ZONE AND AREA		HOURS AND TENTHS	
							ELAPSED	MANHOURS
Horizontal stabilizer Visually inspect the exterior surface, including skin panels, leading edge, and stabilizer tip, for loose or missing fasteners, wear, delamination, corrosion, missing paint, or obvious damage. If evidence of damage is detected, inspect using NDT inspection procedures per appendix. NDT instrumentation must be calibrated with reference standards simulating the structure to be inspected. In cases where a standard cannot be used, predetermined "like" areas may be used as a standard for an acceptable condition.	X			See Structural Repair Manual D6-46035 (ref. 3)	7-9 7-10		0.20	0.20

SECTION 4-0

"C" CHECK

"C" Check

"C" CHECK

1. The "C" check (periodic) requires a greater depth of inspection throughout the airplane to ensure continued airworthiness. This task involves selected operational/functional checks and requires removal of access doors and panels to facilitate the inspection. Performance of the "C" check also requires accomplishment of all items included in the lesser checks.

2. For an explanation of terms such as check and corrosion prevention, refer to Section 0-4 of this document.

3. Zone locations shown in the following maintenance requirement sheets pinpoint specific work areas and are further identified in the master zone diagram contained in Section 1-0 of this document.

4. Entries listed under the "task" column in the following maintenance requirement sheets indicate a requirement for visual checks, operational/functional checks, lubrication, or other special maintenance such as servicing, filter replacement, or corrosion prevention.

   Some entries under the "check" column may indicate 2, 3, through 13, etc. This type of entry means that the specific maintenance requirement should be accomplished at the multiple "C" check interval indicated. Thus, a "6" in the "check" column means that the item is to be checked at each "6C" inspection interval, or every 6th "C" check.

5. The estimated work times are for performance of individual "C" check items and do not include the time required to position work stands and equipment or remove and replace access doors and panels. The estimated time standards shown in the "elapsed" columns take into consideration optimum use of manpower and equipment. These standards are based on best judgment factors, use of skilled personnel, and ready availability of tools and equipment.

   The following estimated manhours are required to open and close or remove and replace doors or access panels in the accomplishment of "C" and multiple "C" checks:

Check	Manhours
C	0.5
2C	3

"C" Check

MODEL 737-200	TASK			REFERENCE	LOCATION		TIME	
DESCRIPTION	CHECK	LUBRICATE	OTHER		ZONE AND AREA	ACCESS DOOR NUMBER	HOURS AND TENTHS ELAPSED	HOURS AND TENTHS MANHOURS
● Left-hand and right-hand horizontal stabilizer visual check	X				7-9 7-10			
Examine the following structure externally for loose or missing fasteners, wear, delamination, corrosion, missing paint, obvious damage			Corrosion prevention	1 See Section 0-4			1.5	3.0
a. Exterior surfaces including skin panels, leading edge, and stabilizer tip								
b. Sliding plate seal located in area of fuselage				See Maintenance Manual Section 55-10-0 (ref. 4)				
c. Exposed stabilizer rear spar, including hinge support ribs, trailing-edge beam								
d. The Teflon-lined bushings and hinge pins at all elevator hinge fittings								
Note: Items c and d should be performed with elevator positioned full up or down				See Section 4-0, page 5				
e. Thermal linkage fittings, struts, push rods, bell cranks								
f. Check the front and rear spar-to-center section attachment lugs; inspect steel straps; check aluminum center-section terminal lugs for evidence of corrosion	2		Corrosion prevention	1 See Section 0-4			1.0	2.0
g. Check inboard edge of rear spar web between lower- and mid-chord lugs				See Section 4-0, page 6				
Access—remove horizontal stabilizer-to-fuselage fairing								

1 For metallic parts only, see Corrosion Prevention Manual D6-41910, Sections 55-00-37 and 55-10-37 (ref. 2)

"C" Check (Concluded)

MODEL 737-200	TASK			REFERENCE	LOCATION		TIME	
DESCRIPTION	CHECK	LUBRICATE	OTHER		ZONE AND AREA	ACCESS DOOR NUMBER	HOURS AND TENTHS	
							ELAPSED	MANHOURS
• Horizontal stabilizer trailing-edge cavities—check for accumulation of dirt, lint, and debris	2						0.6	0.6

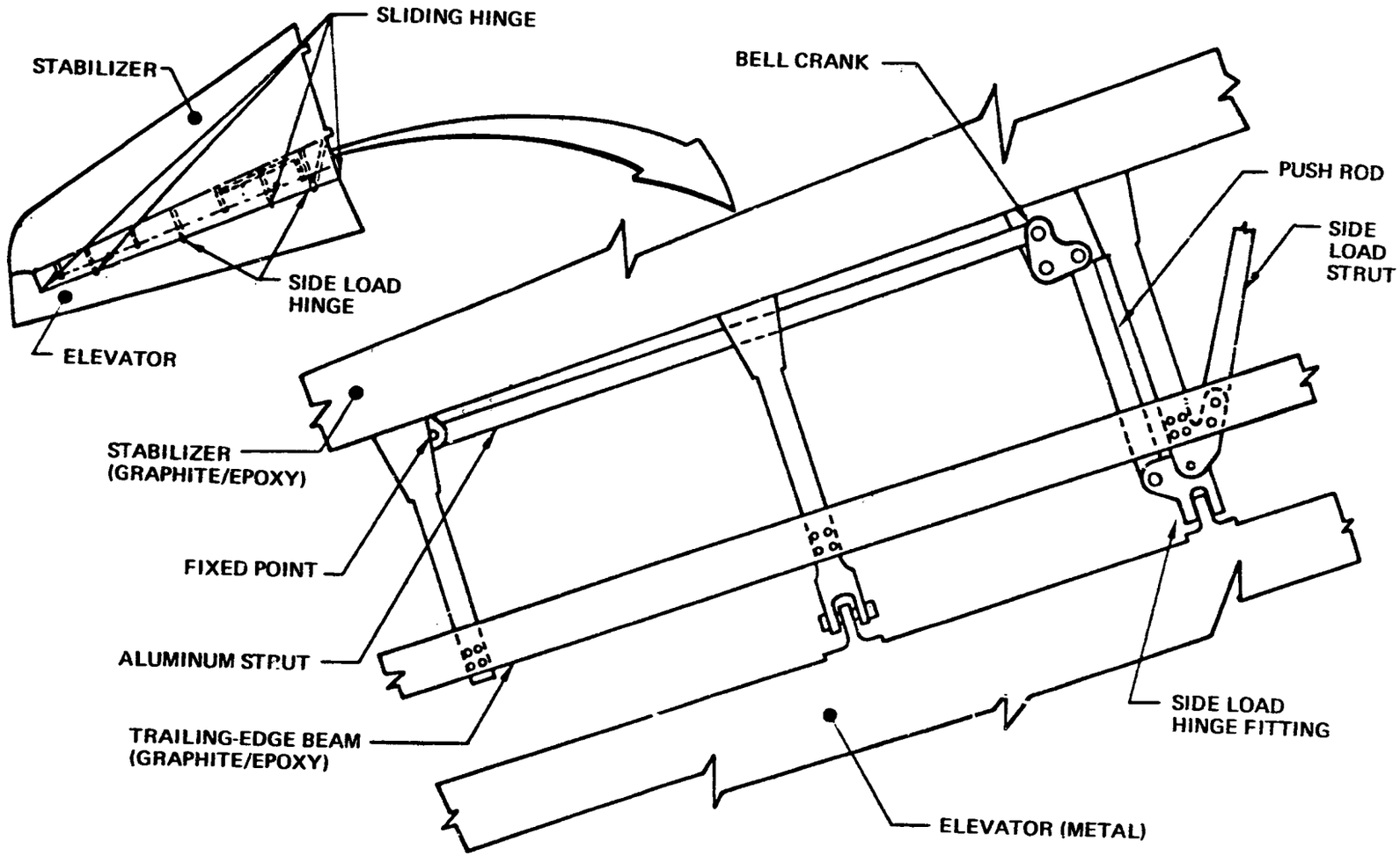

Location and Configuration of Thermal Linkage Components

ORIGINAL PAGE
BLACK AND WHITE PHOTOGRAPH

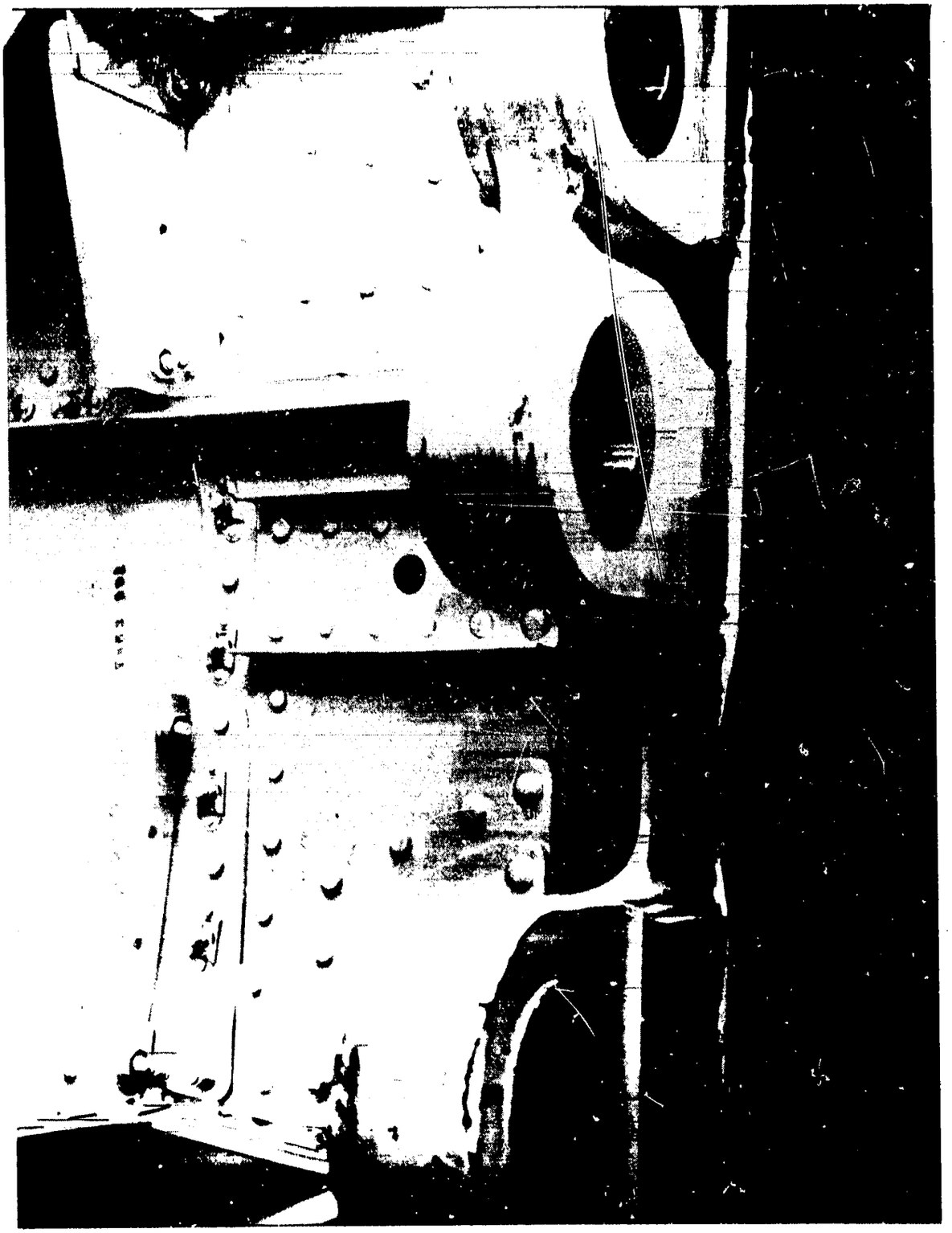

Rear Spar-to-Center Section Attachment Lugs

SECTION 5-0

STRUCTURAL INSPECTION

GENERAL

The structural inspection program described in this section is intended to serve as a guide for the development of individual airline maintenance programs. The structural items listed herein constitute minimum inspection requirements. The structural inspection requirements contained herein apply to current production airplanes or to in-service airplanes that have had all structural service bulletins accomplished as of the approximate date of this document. Operators are cautioned that time extensions for their fleet should not be based solely on time increases shown in this section, but also on the operator's experience and on service bulletin compliance status.

Each item is identified by its location and adaptability to nondestructive testing (NDT) procedures, when applicable, and shows cross reference to photographs or sketches as appropriate.

EXTERNAL INSPECTION

An external inspection implies that there is visual accessibility without detaching any parts (including access panels) from the airplane. In some instances, fairing panels may have to be removed, such as the horizontal stabilizer-to-fuselage fairing for access to the stabilizer spar-to-center section attachments.

INTERNAL INSPECTION

An internal inspection implies that there is visual accessibility only by detaching removable parts such as plates or panels or by use of NDT procedures. Such procedures are contained in the appendix of this document.

INSPECTION ITEM ELAPSED TIME AND MANHOURS

Elapsed time and manhours for each inspection item include complete access and restoration times. Therefore, inspection items completed in the same area concurrently or consecutively would allow for appropriate elapsed time and manhour reduction.

STABILIZER ACCESS

Inspection items covering external stabilizer structure include 0.5 hour for emplacement and 0.5 hour for removal of access stands. Operators who use dock facilities can reduce times for these inspection items accordingly.

STRUCTURAL PHOTOGRAPHS AND INDEX

To assist in the identification and inspection of specified structural items, a set of figures and photographs and a related index also are included in this section. Each photograph or figure is cross indexed to a specific structural inspection item or items.

DEFINITIONS

See Section 0-4 for terms and definitions.

FREQUENCY

The Boeing recommended check interval for structural inspection is 14,000 flight hours. Operators are responsible for establishing and maintaining their own inspection schedules. For two of the initial five shipsets of graphite/epoxy stabilizers, structural inspection should be performed at one-half of the recommended frequency; i.e., 7,000 flight hours.

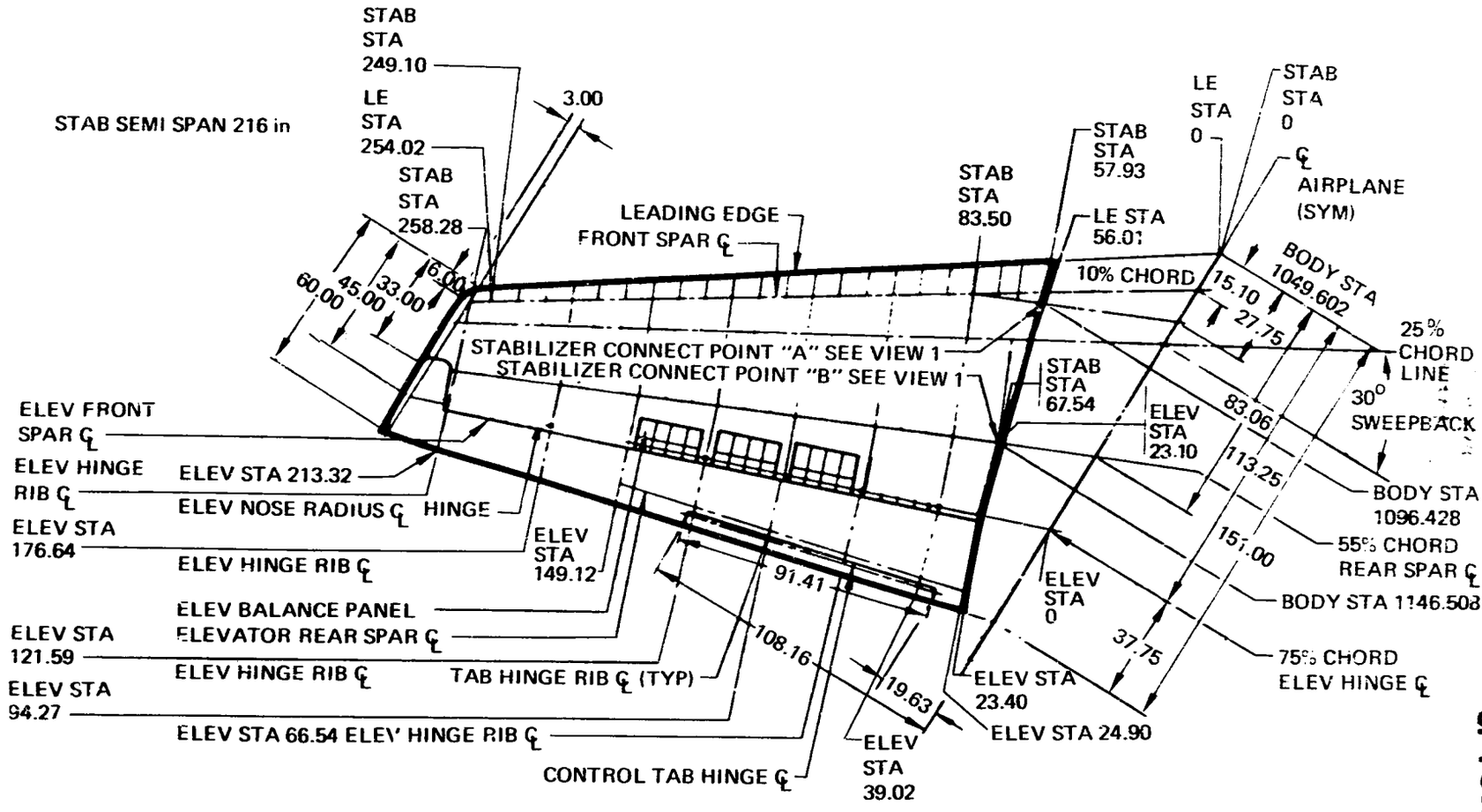

Horizontal Stabilizer and Elevator Stations

View I
Star Truss

Horizontal Stabilizer and Elevator Stations (Concluded)

Structural Inspection

Frequency: See page B-35

MODEL 737-200	ATA NO. 55	REFERENCE		LOCATION		TIME	
DESCRIPTION			ILLUS-TRATIONS	ZONE	ACCESS DOOR NUMBER	HOURS AND TENTHS	
						ELAPSED	MANHOURS
• Horizontal stabilizer center section (ref.)		Inspect per D6-17594-2, Section 6-04 (ref. 1)	P1 P2 P3 P4	7-1 7-9 7-10			
• Horizontal stabilizer skin panels				7-9 7-10		1.0	2.0
a. Visually inspect skin panels of complete external stabilizer including leading edge							
b. NDT inspect per the appendix of this document, specific areas of upper and lower skin panels as shown in illustration P5. NDT instrumentation must be calibrated with reference standards simulating the structure to be inspected. In cases where a standard cannot be used, predetermined "like" areas may be used as a standard for an acceptable condition.			P5				
Access—accessible externally							
• Horizontal stabilizer rear spar-to-center section attachment			P6	7-9 7-10	9121L through 9126L 9221R through 9226R	4.0	8.0
a. Attachment pins at upper- mid-, and lower-chord lugs (remove LH and RH pin)							
b. Pin, bushing, and fitting							
Access—remove horizontal stabilizer-to-fuselage fairing							

Structural Inspection (Continued)

Frequency: See page B-35

MODEL 737-200	ATA NO. 55	REFERENCE		LOCATION		TIME	
DESCRIPTION			ILLUS-TRATIONS	ZONE	ACCESS DOOR NUMBER	HOURS AND TENTHS	
						ELAPSED	MANHOURS
● Horizontal stabilizer front spar-to-center section attachment a. Attachment pins at upper- and lower-chord lugs (remove LH and RH pin) b. Pin, bushing, and fitting Access—remove horizontal stabilizer-to-fuselage fairing			P6	7-9 7-10	9121L through 9126L 9221R through 9226R	4.0	8.0
● Horizontal stabilizer front and rear spar-to-center section attachment fittings a. Front and rear spar attachment fittings, particularly at lugs b. Steel lug spar straps for evidence of cracks Access—remove horizontal stabilizer-to-fuselage fairing and access hole covers on inboard closure rib			P6 P7	7-9 7-10	9117L through 9126L 9217R through 9226R	4.0	8.0
● Horizontal stabilizer internal trailing-edge structure a. Hinge rib fittings, particularly in vicinity of trailing-edge beam attach bolts b. Trailing-edge beam c. Ribs and skin d. Thermal linkage installation Access—remove trailing-edge panels noted			P6	7-9 7-10	9105L through 9109L 9205R through 9209R	4.0	8.0

ORIGINAL PAGE IS OF POOR QUALITY

Structural Inspection (Concluded)

Frequency: See page B-35

MODEL 737-200	ATA NO. 55	REFERENCE		LOCATION		TIME	
DESCRIPTION			ILLUS-TRATIONS	ZONE	ACCESS DOOR NUMBER	HOURS AND TENTHS	
						ELAPSED	MANHOURS
•Horizontal stabilizer internal structure				7-9 7-10	9113L through 9126L 9213R through 9226R	8.0	16.0
a. Front spar and rear spar, including stiffeners on both; inboard and outboard closure ribs, including stiffeners and gap cover installation			P6 P7				
b. Aluminum attach fittings (5) and attach angles (2) on outboard face of inboard closure rib		1	P8				
c. Inspar rib chords and skin stiffeners							
Access—remove gap covers and access hole covers on inboard closure rib, removable leading edge, removable lower trailing-edge panels, removable tip			P9				

1 For metallic parts only, see Corrosion Prevention Manual D6-41910, Sections 55-00-37 and 55-10-37 (ref. 2).

ORIGINAL PAGE
BLACK AND WHITE PHOTOGRAPH

P1. Fuselage Skin and Stringer Splices, Crown Area, Stringers S-6 and Above, BS 1016 to 1088

ORIGINAL PAGE
BLACK AND WHITE PHOTOGRAPH

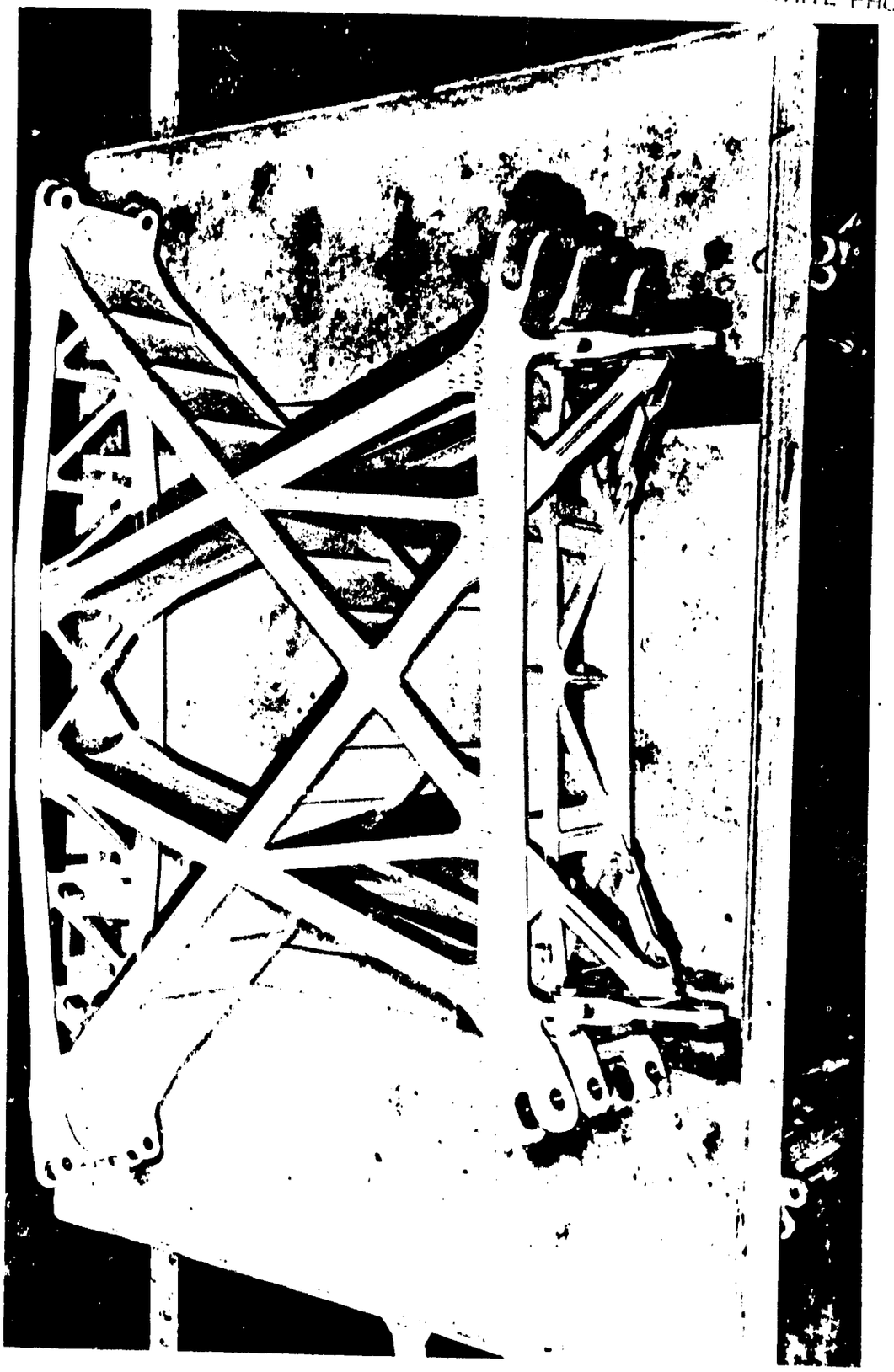

P2. Horizontal Stabilizer Center Section, Looking Forward

P3. Horizontal Stabilizer Jackscrew Fitting Attachment to Front Spar, Looking Aft

P4. Horizontal Stabilizer Center Section, Left-Hand Side View

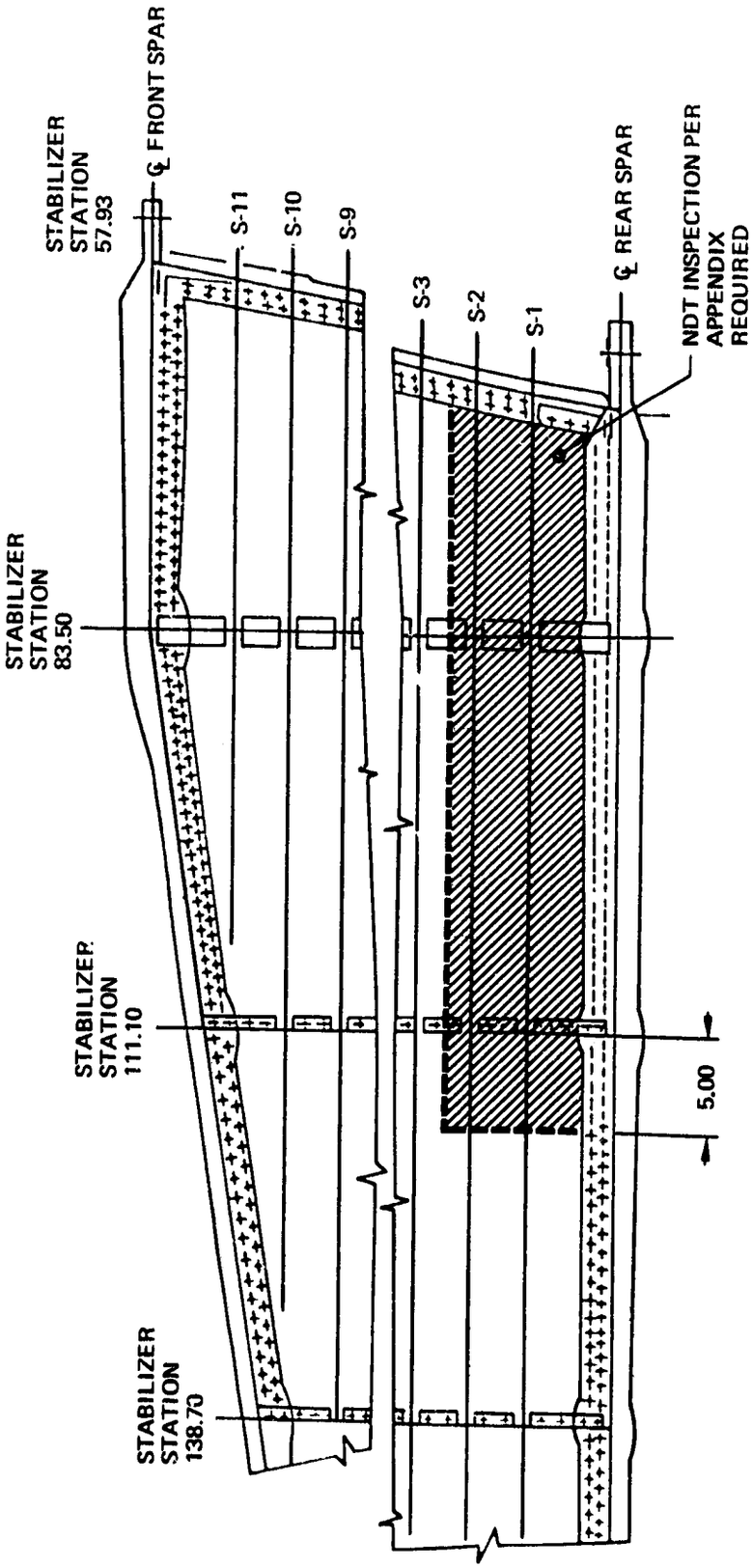

P5. Upper and Lower Skin Panel NDT Inspection Requirements

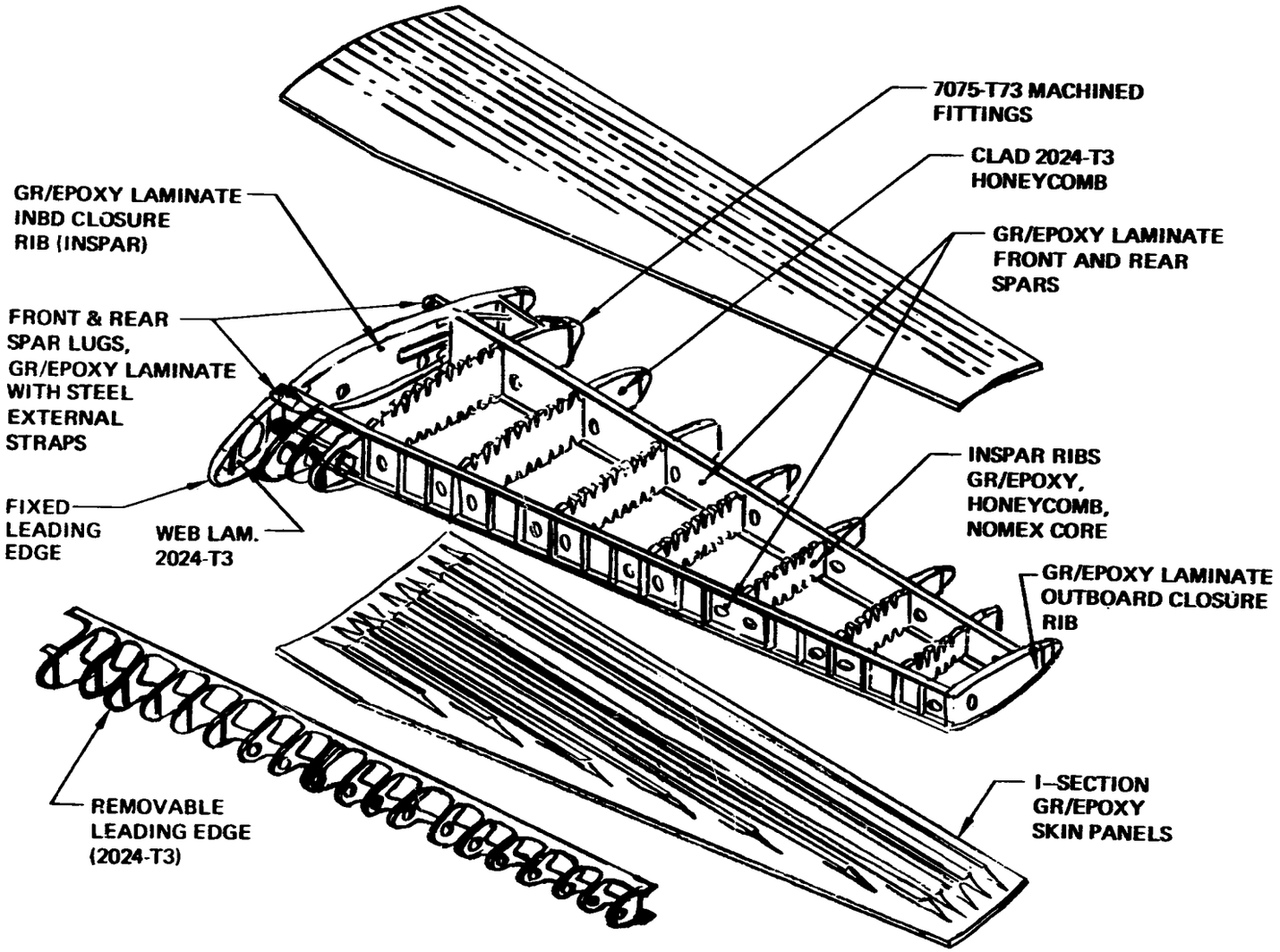

P6. Horizontal Stabilizer (Composite) Structure

ORIGINAL PAGE
BLACK AND WHITE PHOTOGRAPH

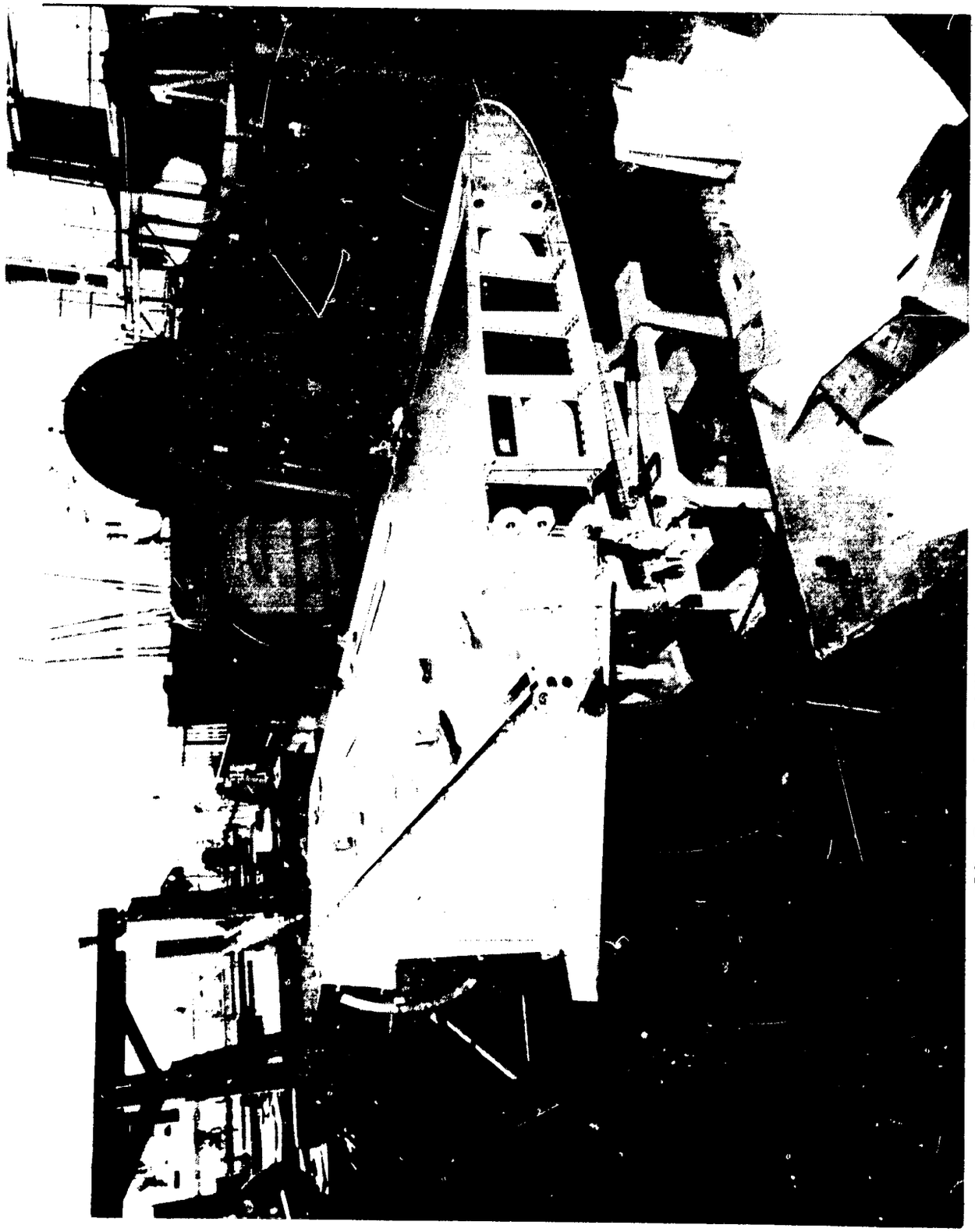

P7. Composite Stabilizer Assembly, Looking Outboard

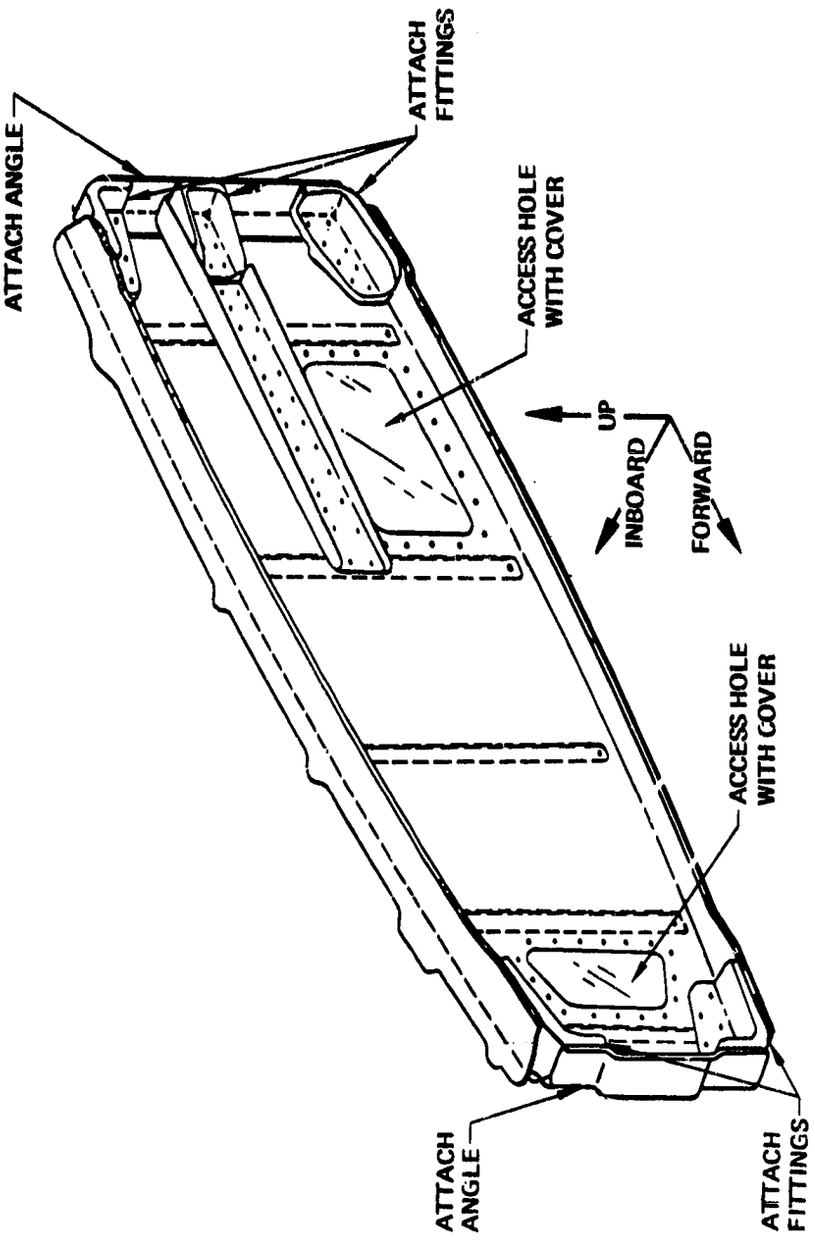

P8. Access Holes on Inboard Closure Rib

ORIGINAL PAGE
BLACK AND WHITE PHOTOGRAPH

P9. Stabilizer Inboard Closure Rib Access Holes

REFERENCES

1. D6-17594, Boeing 737 Maintenance Planning Data
2. D6-41910, Boeing Corrosion Prevention Manual
3. D6-46035, Advanced Composite Horizontal Stabilizer for Boeing 737 Aircraft/Structural Repair Manual
4. D6-12002, Boeing 737 Maintenance Manual

APPENDIX

PULSE-ECHO ULTRASONIC INSPECTION

PULSE-ECHO ULTRASONIC INSPECTION

This appendix describes the pulse-echo ultrasonic inspection method for examining the upper and lower graphite/epoxy stabilizer skin panels for delaminations or disbonds. The method, which was developed by Boeing Quality Control Research and Development, provides proven satisfactory results. It is included in this document for use as a guideline example of inspection.

PURPOSE

The purpose of the inspection is to detect delaminations or disbonds in the horizontal stabilizer graphite/epoxy composite upper and lower skin panels using pulse-echo ultrasonics.

EQUIPMENT

Any ultrasonic equipment that will satisfy the performance requirements of this procedure is suitable for this inspection. The following equipment was used to develop this procedure:

1. Ultrasonic test instrument: model NDT 131, Nortec, Inc., 421 N. Quay, Kennewick, WA 99336, (509) 735-7550.

2. Transducer: longitudinal, 10 MHz, 0.64-cm (0.25-in.) diameter, with a Lucite standoff. P/N D1R, N.D.T. Instruments, Incorporated, 15622 Graham St., Huntington Beach, CA 92649, (714) 893-2438.

   NOTE: Any substitute transducers must resolve a distinct 100% screen height reflected from the opposite surface of the skin or stringer chord flange (see Instrument Calibration section).

3. Couplant: light oil or grease.

PREPARATION FOR INSPECTION

1. Clean the inspection surface.

2. Lay out lines on the skin surface with a grease pencil to use as a guide for the scan (figs. A-1 and A-2).

INSTRUMENT CALIBRATION

1. Connect transducer and make preliminary adjustments.

   Set the reflection of the standoff at 4 on the screen (fig. A-3).

2. Place transducer on the part and adjust skin reflection to come up at 5 1/2 on the scope (fig. A-4).

   Select several locations on the part to compare with the original calibration spot to prevent calibrating over a possible defect.

3. Move transducer over the stringer chord flange. The skin reflection will drop off as you pass over the edge of the flange, and the chord reflection will come up at 6 on the scope (fig. A-5).

INSPECTION PROCEDURE

Inspect horizontal stabilizer according to Figures A-1 and A-2.

INSPECTION RESULTS

1. A discontinuity is characterized by a loss in back reflection from the skin back wall or stringer chord, whichever applies. An indication will come up between the back reflection and the standoff reflection (figs. A-6 and A-7).

2. Rejection criteria:

   a. A discontinuity that causes a complete loss of the skin reflection signal for 1.27 cm (0.5 in.) in diameter.

   b. A discontinuity that causes a complete loss of the stringer chord reflection signal for 1.27 cm (0.5 in.) in length.

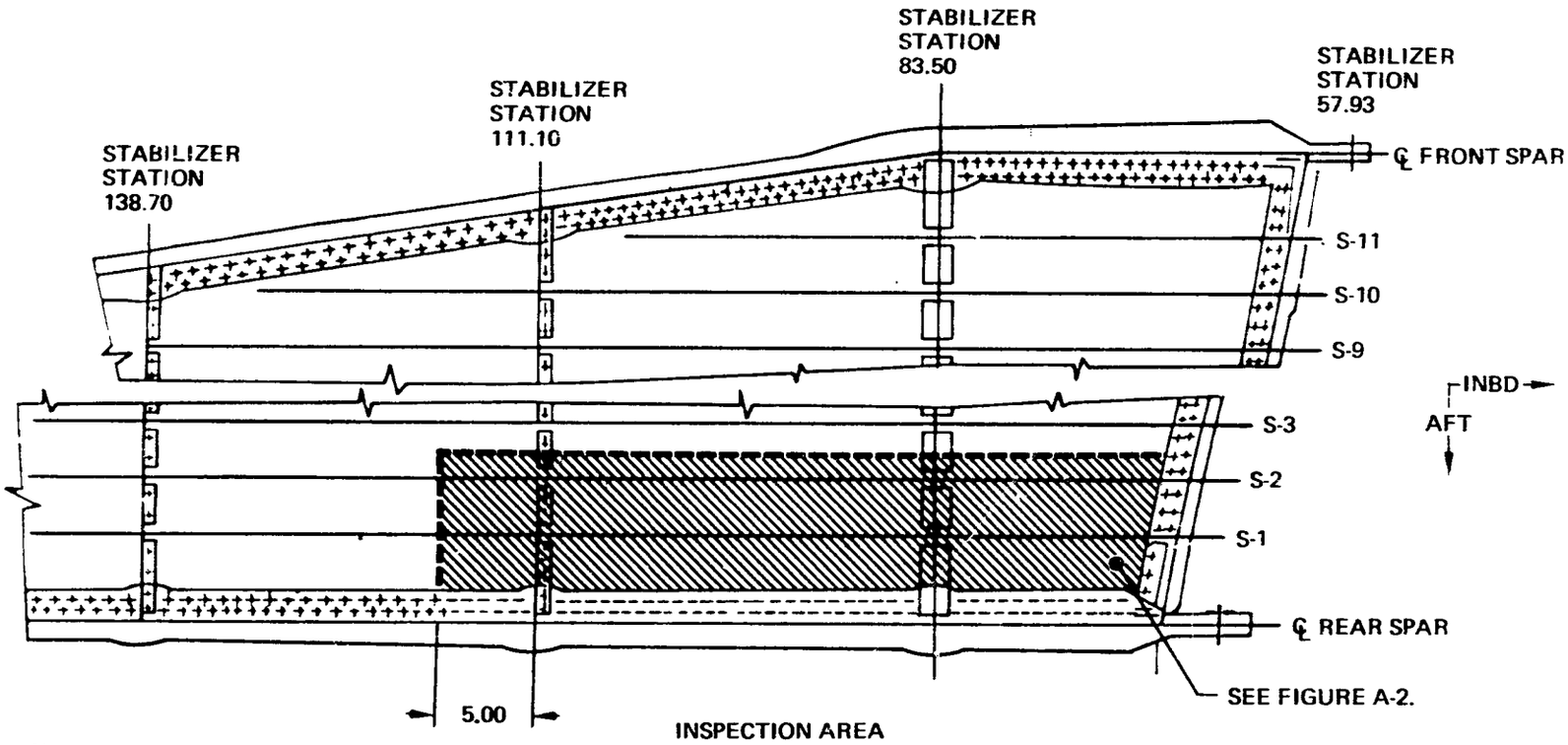

Notes:

- Top view looking down.
- See Figure A-2 for section view A-A.
- This view represents the left-hand upper skin and is typical for the left-hand lower and right-hand upper and lower skins.

Figure A-1. Upper and Lower Skin Panel NDT Inspection Requirements

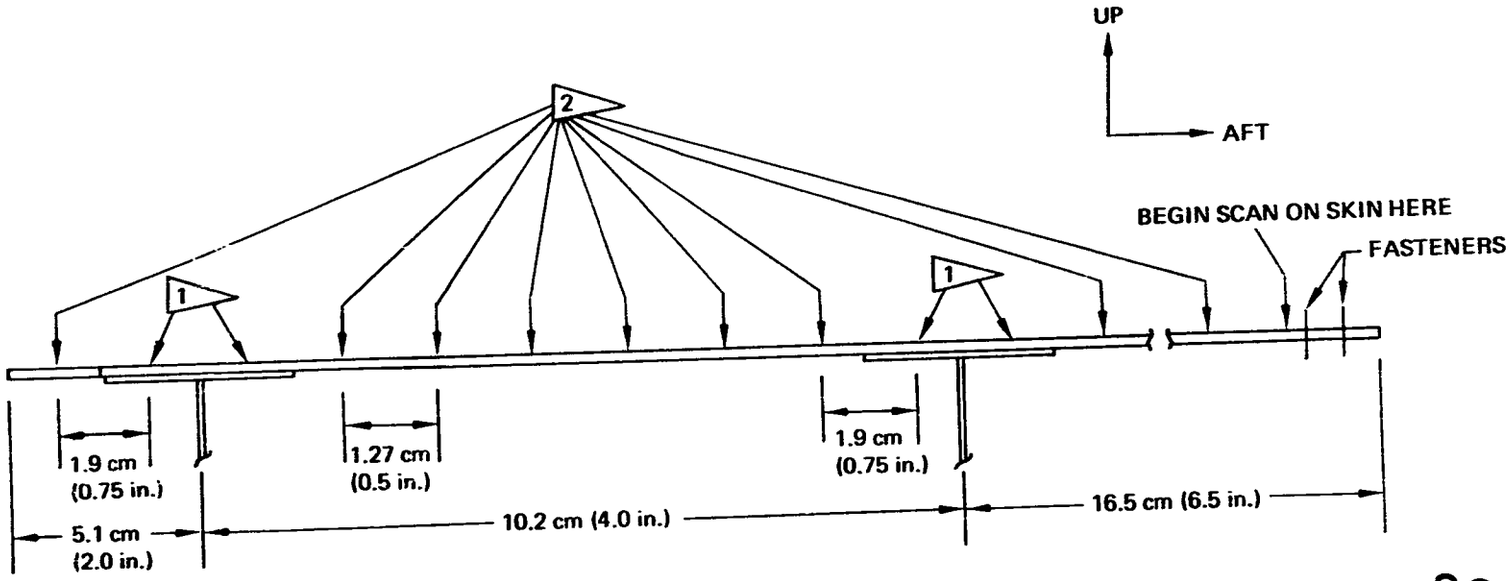

1 Place transducer on the skin over the stringer and scan for the length of the inspection area (fig. A-1).
Note: • Both the edges and the center of the chord will cause a loss of amplitude. Use a guide. (See "Preparation for Inspection," No. 2 and "Instrument Calibration," No. 3 of the text.)

2 Place transducer on the skin and scan for the length of the inspection area (fig. A-1).
Note: • The edge of the chord will cause a loss in amplitude. Use a guide. (See "Preparation for Inspection," No. 2 and "Instrument Calibration," No. 3 of the text.)
• Scan every 1.27 cm (0.5 in.)

Figure A-2. Horizontal Stabilizer Skin Panel

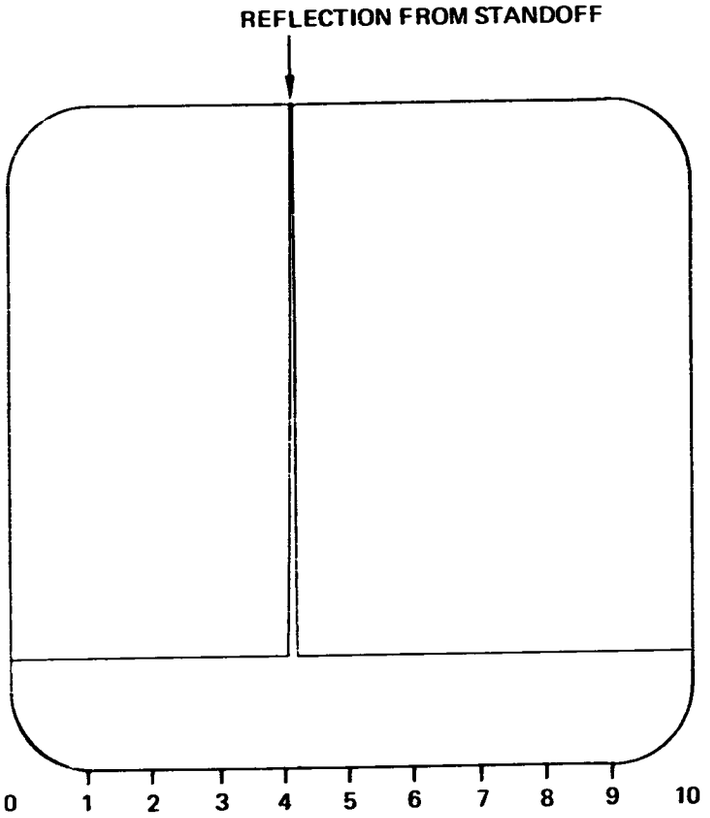

Figure A-3. Standoff Signal

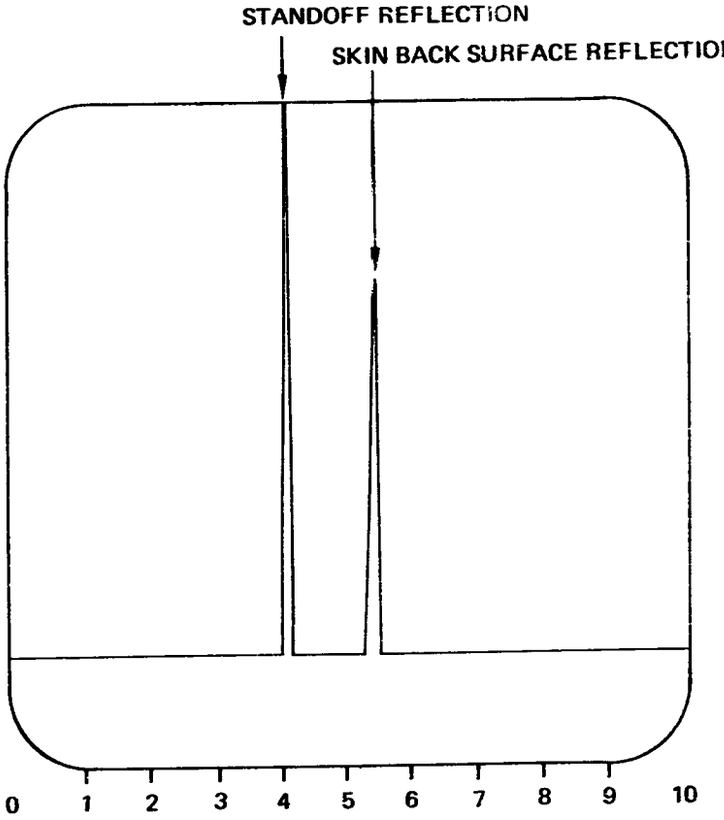

Figure A-4. Skin Back Reflection

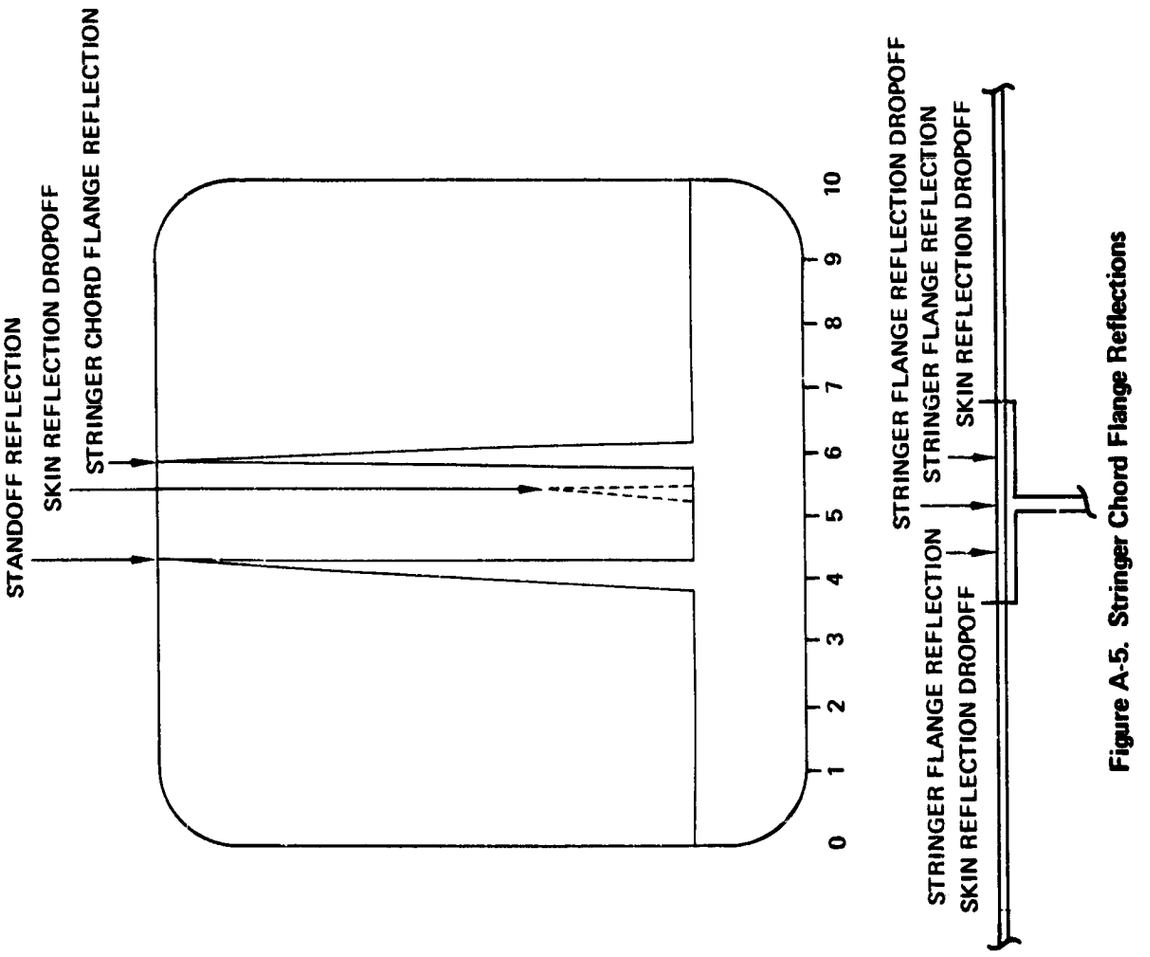

Figure A-5. Stringer Chord Flange Reflections

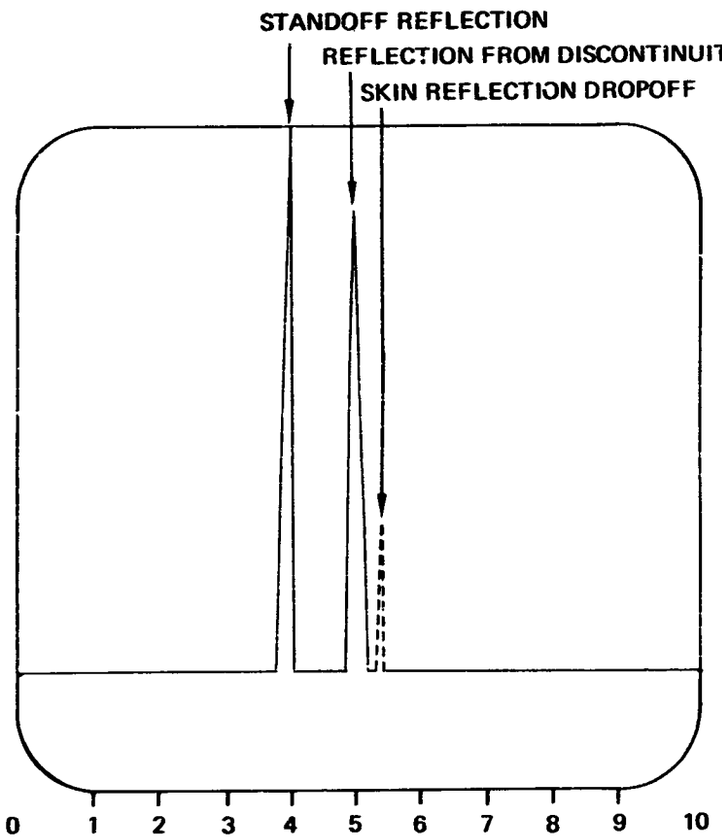

Figure A-6. Discontinuity/Skin Reflection Dropoff

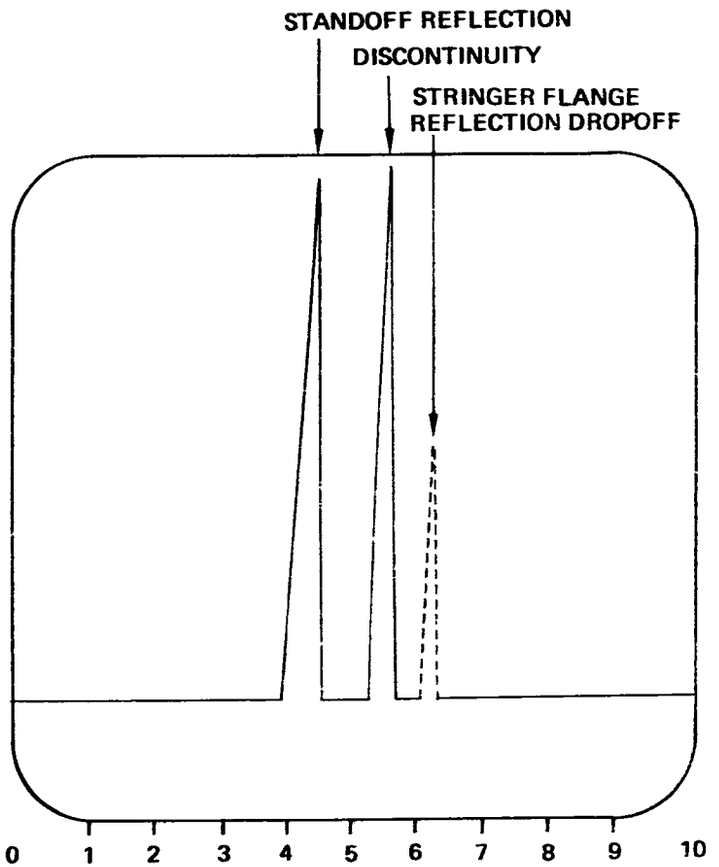

Figure A-7. Discontinuity Stringer Chord Reflection Dropoff

APPENDIX C

ANCILLARY PROGRAM TEST DATA

CONTENTS

NOTES AND ABBREVIATIONS

NOTES

[1] Material and specification

- Fabric: epoxy preimpregnated graphite fabric per BMS 8-212 Type II, Class 2, Style 3K-70-P. Fabricate per BAC 5562, nominal thickness: 0.19 mm (0.0075 in).
- Tape: epoxy preimpregnated graphite unidirectional tape per BMS 8-212 Type II, Class 1. Fabricate per BAC 5562; nominal thickness: Grade 95—0.094 mm (0.0037 in), Grade 145—0.142 mm (0.0056 in), Grade 190—0.188 mm (0.0074 in).

[2] Environmental conditioning

- Dry: normal laboratory environment
- Wet: laminate specimens conditioned according to procedure described in Section 4.1.6 of this document

[3] Maximum load during test

[4] Failure stress based on failure load, measured specimen width, and nominal ply thickness

[5] Boeing nominal extensional modulus

[6] Calculated strain based on failure load, area, and modulus

[7] Boeing nominal shear modulus

[8] Specimen supported on 38.1-mm (1.50-in) diameter ring and impacted with a 16-mm (0.625-in) diameter spherical impactor

[9] Bearing stress based on fastener nominal diameter and splice plate nominal thickness

[10] Shear strain is based on gross area, with b = 331.5 mm (13.05 in), net failure load, and shear modulus

[11] Load mode: tension

[12] Load mode: compression

[13] Fatigued one lifetime, residual tension strength

[14] Fatigued two lifetimes, residual tension strength

[15] Impact damaged, 2.82 N-m (25 lb-in)

[16] 2.82 N-m (25 lb-in) impact damage assumed

ABBREVIATIONS

mm	dimension, millimeter
µm	dimension, micrometer
in	dimension, inch
µin	dimension, microinch
N	load, newton
lb	load, pound force
MPa	stress or modulus, megapascal
lbf/in^2	stress or modulus, pound-force per square inch
RT	room temperature

STATIC TENSION--BASIC LAMINATE (TEST 31)

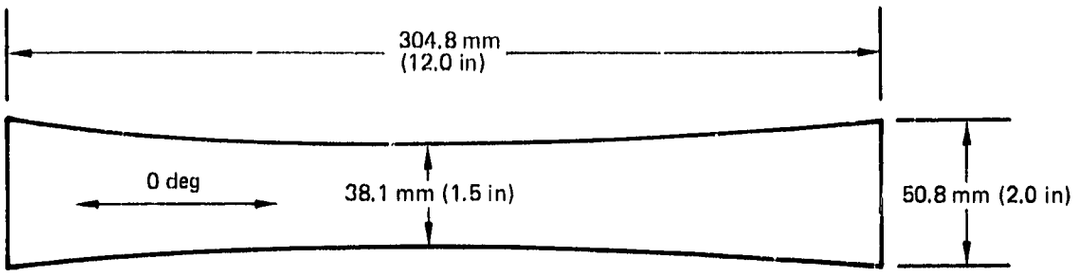

Assembly number	Ply layup [1]
-10	Fabric: 2(0, 90), 4(±45) Tape: 2(±45) Grade 95 2(0) Grade 145 2(0) Grade 190
-12	Fabric: 4(0, 90), 9(±45) Tape: 2(±45) Grade 95 2(0) Grade 190

Drawing and assembly no.	Temperature		Environment [2]	t		B		A		Failure load [3]		Stress [4]		E [5]		Strain, μm/m (μin/in) [6]
	°C	°F		mm	(in)	mm	(in)	mm^2	(in^2)	N	(lb)	MPa	(lbf/in^2)	MPa	(lbf/in^2)	
65C17980-10	21	RT	D	1.991	0.0784	38.3	1.507	76.3	0.118	48 174	10 830	628.6	91 664	6.62×10^4	9.60×10^6	9 548
	21	RT				38.2	1.505	76.3	0.118	44 616	10 030	586.1	85 006			8 855
	21	RT				38.2	1.503	76.3	0.118	43 859	9 860	576.9	83 676			8 716
	-53	-65				38.1	1.499	76.3	0.118	45 772	10 290	603.7	87 558			9 121
	-53	-65				38.0	1.496	75.5	0.117	43 148	9 700	570.2	82 704			8 615
	-53	-65				38.0	1.498	75.5	0.117	38 611	8 680	509.6	73 908			7 699
	82	180				38.0	1.497	75.5	0.117	49 064	11 030	648.0	93 980			9 790
	82	180				38.1	1.499	76.3	0.118	51 733	11 630	682.3	98 961			10 308
	82	180	D			38.2	1.503	76.3	0.118	51 844	11 610	679.3	98 527			10 263
	21	RT	W			38.0	1.496	75.5	0.117	47 863	10 760	632.5	91 741			9 556
	21	RT				38.0	1.496			48 664	10 940	643.1	93 276			9 716
	21	RT				38.0	1.496			48 397	10 880	639.6	92 764			9 663
	-53	-65				38.0	1.497			48 530	10 910	640.9	92 958			9 683
	-53	-65				38.0	1.495			45 194	10 160	597.7	86 684			9 030
	-53	-65				38.0	1.493			46 395	10 430	613.1	88 928			9 263
	82	180				38.0	1.496			50 532	11 360	667.8	96 857			10 089
	82	180				38.0	1.497			48 530	10 910	640.9	92 958			9 683
65C17980-10	82	180	W	1.991	0.0784	37.9	1.492	75.5	0.117	48 753	10 960	646.0	93 697	6.62×10^4	9.60×10^6	9 760
65C17980-12	21	RT	D	3.040	0.1197	37.8	1.490	114.9	0.178	47 196	10 610	410.2	59 489	4.81×10^4	6.98×10^6	8 533
	21	RT				37.9	1.492	115.2	0.179	47 329	10 640	410.8	59 577			8 535
	21	RT				38.0	1.495	115.5	0.179	50 309	11 310	435.9	63 201			9 055
	-53	-65				38.0	1.496	115.5	0.179	45 594	10 250	394.7	57 240			8 201
	-53	-65				37.9	1.493	115.2	0.179	43 192	9 710	374.6	54 333			7 784
	-53	-65	D			37.9	1.494	115.2	0.179	41 502	9 330	359.7	52 172			7 474
	82	180	W			38.0	1.497	115.5	0.179	50 398	11 330	435.9	63 229			9 059
	82	180	W			37.9	1.493	115.2	0.179	49 954	11 230	433.3	62 838			9 003
65C17980-12	82	180	W	3.040	0.1197	38.1	1.500	115.8	0.180	52 445	11 790	452.7	65 664	4.81×10^4	6.98×10^6	9 407

STATIC TENSION AND COMPRESSION–FRACTURE COUPON CONTROL SPECIMEN (TEST 31)

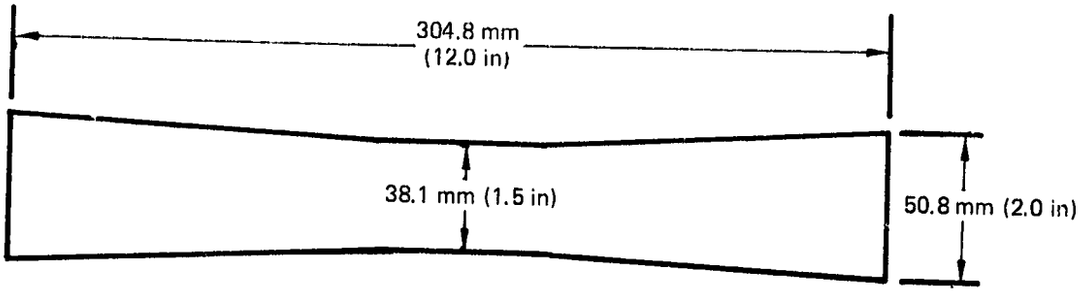

Assembly number	Ply layup [1]
-13	Fabric: 3(0, 90), 9(±45)
-14	Fabric: 2(0, 90), 5(±45) Tape: 2(0) Grade 190
-15	Fabric: 2(0, 90), 5(±45) Tape: 2(90) Grade 190

Drawing and assembly no	Temperature		Environment [2]	t		B		A		Load mode	Failure load [3]		Stress [4]		E [5]		Strain, μm/m (μin/in) [6]
	C	F		mm	(in)	mm	(in)	mm	(in)		N	(lb)	MPa	(lbf/in²)	MPa	(lbf/in²)	
65C17980-13	21	RT	D	2.29	0.0900	37.9	1.493	3.40	0.134	TENS	27 979	6290	322.8	46 811	3.59×10^4	5.2×10^6	9002
	21	RT				38.0	1.495	3.43	0.135		29 091	6540	335.2	48 606			9347
	-53	-65				37.9	1.492	3.40	0.134		27 312	6140	315.3	45 725			8793
	-53	-65				38.0	1.495	3.43	0.135	TENS	25 444	5720	293.2	42 512			8175
	21	RT				37.9	1.494	3.40	0.134	COMP	27 490	6180	316.9	45 962			8839
	21	RT	D			38.0	1.495	3.43	0.135		30 381	6830	350.0	50 762			9762
	82	180	W			38.0	1.495	3.43	0.135		26 867	6040	309.6	44 890			8633
65C17980-13	82	180	W	2.29	0.0900	38.0	1.497	3.43	0.135	COMP	25 310	5690	291.2	42 233	3.59×10^4	5.2×10^6	8122
65C17980-14	21	RT	D	1.71	0.0673	38.0	1.497	2.57	0.101	TENS	35 408	7960	544.8	79 009	5.65×10^4	8.2×10^6	9635
	21	RT				37.9	1.491	2.54	0.100		34 474	7750	532.6	77 234			9419
	-53	-65				37.9	1.493	2.54	0.100		30 470	6850	470.1	68 174			8314
	-53	-65				37.8	1.487	2.54	0.100	TENS	32 383	7280	501.6	72 745			8871
	21	RT				37.8	1.489	2.54	0.100	COMP	23 754	5340	367.5	53 288			6499
	21	RT	D			37.9	1.494	2.57	0.101		25 711	5780	396.4	57 486			7010
	82	180	W			38.1	1.501	2.57	0.101		25 488	5730	391.1	56 723			6917
65C17980-14	82	180	W			37.8	1.490	2.54	0.100	COMP	23 754	5340	367.2	53 252	5.65×10^4	8.2×10^6	6494
65C17980-15	21	RT	D			38.1	1.499	2.57	0.101	TENS	18 015	4050	276.8	40 146	3.10×10^4	4.5×10^6	8921
	21	RT				38.2	1.503	2.57	0.101		20 061	4510	307.5	44 586			9908
	-53	-65				37.9	1.493	2.57	0.101		18 282	4110	282.1	40 904			9090
	-53	-65				37.8	1.490	2.54	0.100	TENS	15 702	3530	242.7	35 202			7823
	21	RT	D			38.0	1.496	2.57	0.101	COMP	18 252	4110	281.5	40 822			9072
	82	180	W			38.0	1.498	2.57	0.101	COMP	13 345	3000	205.2	29 757			6613
65C17980-15	82	180	W	1.71	0.0673	38.1	1.500	2.57	0.101	COMP	16 681	3750	256.2	37 147	3.10×10^4	4.5×10^6	8255

STATIC TENSION WITH IMPACT (TEST 1)

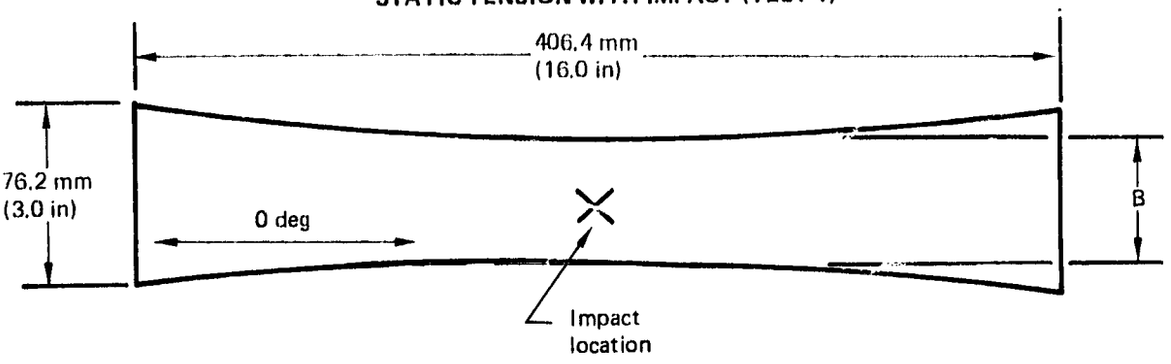

Ply code	Ply layup [1]	t mm (in)
A	Fabric: 5(0, 90), 10(±45)	2.86 (0.1125)
C	Fabric: 8(0, 90), 8(±45)	3.05 (0.12)
D	Fabric: 12(0, 90), 12(±45)	4.57 (0.18)
E	Fabric: 6(0, 90), 6(±45)	2.29 (0.09)
F	Fabric: 4(0, 90), 8(±45)	2.29 (0.09)

Drawing and assembly no.	Ply code	Temperature °C	Temperature °F	Environment [2]	Impact level [8] N·m	Impact level [8] (lb-in)	B mm	B (in)	Failure load [3] N	Failure load [3] (lb)	Stress [4] MPa	Stress [4] (lbf/in²)	E [5] MPa	E [5] (lbf/in²)	Strain, μm/m (μin/in) [6]
65C17768-5	A	21	RT	W	5.65	50	58.3	2.295	40.7	9 150	244.3	35 439	4.00×10^4	5.8×10^6	6110
↑	↑	21	RT	↑	↑	↑	58.3	2.295	40.6	9 120	243.5	35 323	↑	↑	6090
		21	RT				58.2	2.292	42.2	9 480	253.5	36 766			6340
		-53	-65				58.3	2.294	43.4	9 750	260.5	37 780			6510
		-53	-65				58.3	2.295	40.6	9 120	243.5	35 323			6090
		-53	-65				58.3	2.295	43.2	9 720	259.6	37 647			6490
		82	180				58.3	2.294	40.8	9 180	245.3	35 571			6130
↓	↓	82	180	↓	↓	↓	58.3	2.296	40.3	9 060	241.8	35 075	↓	↓	6050
65C17768-5	A	82	180	W	5.65	50	58.3	2.294	42.0	9 450	252.5	36 617	4.00×10^4	5.8×10^6	6310
65C17768-3	C	21	RT	D	2.82	25	58.4	2.298	60.3	13 560	339.0	49 173	4.76×10^4	6.9×10^6	7130
↑	↑	21	RT	↑	↑	↑	58.3	2.296	61.0	13 710	342.1	49 760	↑	↑	7210
		21	RT				58.3	2.295	64.1	14 410	360.8	52 324			7580
		-53	-65				58.3	2.296	56.2	12 630	316.1	45 841			6640
		-53	-65				58.2	2.293	59.4	13 350	334.5	48 517			7030
		-53	-65				58.3	2.295	57.9	13 020	326.0	47 277			6850
		82	180				58.2	2.292	63.8	14 340	359.5	52 138			7550
		82	180	↓			58.2	2.291	69.7	15 660	392.7	56 962			8250
		82	180	D			58.2	2.290	65.7	14 760	370.3	53 712			7780
		21	RT	W			58.2	2.292	66.7	15 000	376.0	54 538			7900
		21	RT	↑			58.3	2.297	63.0	14 160	354.2	51 371			7440
		21	RT				58.3	2.295	66.6	14 970	374.8	54 357			7880
		-53	-65				58.3	2.294	66.5	14 940	374.2	54 272			7870
		-53	-65				58.3	2.295	60.6	13 620	341.0	49 455			7170
		-53	-65				58.3	2.295	60.2	13 530	338.7	49 129			7120
		82	180				58.3	2.295	65.5	14 730	368.8	53 486			7750
↓	↓	82	180	↓	↓	↓	58.2	2.293	65.	14 700	368.3	53 423			7740
65C17768-3	↓	82	180	W	2.82	25	58.3	2.295	63.4	14 250	356.8	51 743	↓	↓	7500
65C17768-5	C	21	RT	D	5.65	50	58.2	2.292	42.6	9 570	239.9	34 795	4.76×10^4	6.9×10^6	5040

STATIC TENSION WITH IMPACT (TEST 1)(CONTINUED)

Drawing and assembly no.	Ply code	Temperature		Environment	Impact level [1]		B		Failure load [3]		Stress [4]		E [5]		Strain, μm/m (μin/in) [6]
		°C	°F	[2]	N·m	(lb·in)	mm	(in)	N	(lb)	MPa	(lbf/in²)	MPa	(lbf/in²)	
65C17768-5	C	21	RT	D	5.65	50	58.2	2.292	44.3	9 960	249.7	36 213	4.76×10^4	6.9×10^6	5250
↑	↑	21	RT	↑	↑	↑	58.3	2.296	45.1	10 140	253.7	36 803	↑	↑	5330
		-53	-65				58.3	2.294	42.4	9 540	238.9	34 656			5020
		-53	-65				58.3	2.295	38.4	8 640	216.3	31 373			4550
		-53	-65				58.3	2.294	40.7	9 150	229.2	33 239			4820
		82	180				58.3	2.295	44.6	10 030	251.1	36 420			5280
↓	↓	82	180				58.2	2.293	43.3	9 740	244.1	35 398			5130
65C17768-5	C	82	180				58.2	2.293	44.4	9 980	250.1	36 270			5250
65C17768-4	D	21	RT				58.3	2.295	90.5	20 340	339.5	49 237			7130
↑	↑	21	RT				58.3	2.295	93.4	21 000	350.5	50 835			7370
		21	RT				58.3	2.297	90.1	20 250	337.7	48 977			7100
		-53	-65				58.3	2.296	85.0	19 110	318.8	46 240			6700
		-53	-65	↓			58.3	2.294	80.7	18 150	303.1	43 955			6370
		-53	-65	D			58.3	2.295	85.4	19 200	320.5	46 478			6730
		21	RT	W			58.2	2.293	92.7	20 850	348.3	50 516			7320
		21	RT	↑			58.3	2.295	96.6	21 720	362.5	52 578			7620
		21	RT				58.3	2.297	92.6	20 820	347.2	50 356			7300
↓	↓	82	180	↓	↓	↓	58.3	2.296	96.5	21 690	361.9	52 483			7600
65C17768-4		82	180	W	5.65	50	58.3	2.294	91.9	20 670	345.1	50 058			7250
65C17768-6		21	RT	D	8.36	74	58.3	2.294	76.1	17 100	285.5	41 412			6000
↑		21	RT	↑	↑	↑	58.4	2.298	71.4	16 050	267.5	38 802			5620
		21	RT				58.3	2.294	74.5	16 740	279.5	40 541			5870
		-53	-65				58.2	2.293	68.5	15 390	257.1	37 287			5400
		-53	-65	↓			58.3	2.295	68.7	15 450	257.9	37 400			5420
		-53	-65	D			58.3	2.295	72.7	16 350	272.9	39 579			5730
		21	RT	W			58.3	2.296	75.5	16 980	283.3	41 086			5950
		21	RT	↑			58.4	2.298	72.1	16 200	270.0	39 164			5670
↓	↓	82	180	↓	↓	↓	58.3	2.296	75.3	16 920	282.3	40 941			5930
65C17768-6	D	82	180	W	8.36	74	58.3	2.294	74.7	16 800	280.5	40 686			5890
65C17768-39	E	21	RT	D	0.00	0	58.3	2.294	55.5	12 480	416.8	60 448			8760
65C17768-39	E	↑	↑	↑	↑	↑	58.2	2.293	50.7	11 400	380.9	55 241	↓	↓	8000
65C17768-39	E						58.2	2.293	50.8	11 430	381.9	55 386	4.76×10^4	6.9×10^6	8030
65C17768-40	F						58.2	2.293	45.8	10 300	344.1	49 910	4.00×10^4	5.8×10^6	8600
65C17768-40	F	↓	↓	↓	↓	↓	58.3	2.295	50.7	11 400	380.5	55 192	4.00×10^4	5.8×10^6	9510
65C17768-40	F	21	RT	D	0.00	0	58.3	2.295	51.5	11 580	386.5	56 064	4.00×10^4	5.8×10^6	9660

STATIC COMPRESSION WITH IMPACT (TEST 1)

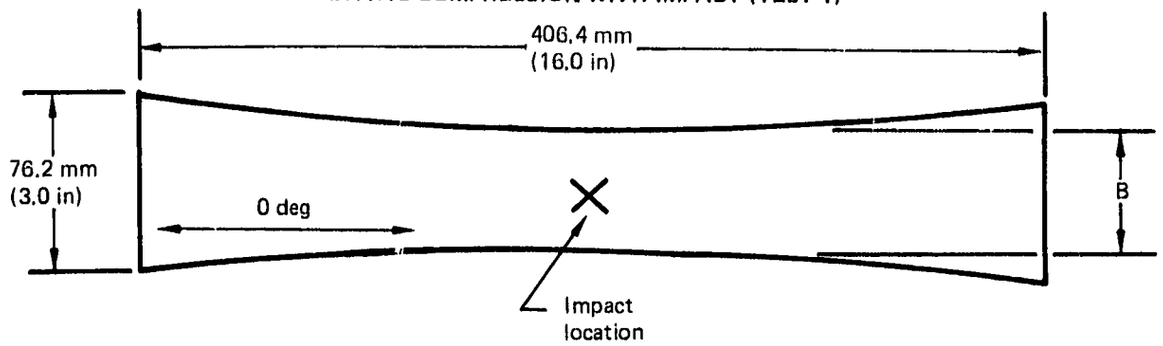

Ply code	Ply layup [1]	t mm (in)
A	Fabric: 5(0, 90), 10(±45)	2.86 (0.1125)
B	Fabric: 8(0, 90), 16(±45)	4.57 (0.18)
C	Fabric: 8(0, 90), 8(±45)	3.05 (0.12)
D	Fabric: 12(0, 90), 12(±45)	4.57 (0.18)

Drawing and assembly no.	Ply code	Temperature		Environment [2]	Impact level [8]		B		Failure load [3]		Stress [4]		E [5]		Strain, μm/m (μin/in) [6]
		°C	°F		N-m	(lb-in)	mm	(in)	N	(lb)	MPa	(lbf/in²)	MPa	(lbf/in²)	
69-69825-1	A	21	RT	D	0.00	0	58.4	2.300	58.5	13 153	350.5	50 833	4.00 x 10⁴	5.8 x 10⁶	8760
					0.00	0			50.6	11 380	303.2	43 981			7580
					0.00	0			54.4	12 223	325.7	47 239			8140
					2.82	25			34.9	7 840	208.9	30 300			5220
									35.5	7 970	212.4	30 802			5310
		21	RT						33.7	7 580	202.0	29 295			5050
		-53	-65						40.0	9 000	239.8	34 783			5990
									40.7	9 160	244.1	35 401			6100
69-69825-1							58.4	2.300	39.1	8 790	234.2	33 971			5850
65C17768-1							58.3	2.296	41.6	9 360	249.8	36 237			6250
65C17768-1							58.3	2.295	38.9	8 740	233.4	33 851			5840
65C17768-1		-53	-65				58.3	2.296	40.3	9 050	241.6	35 037			6040
69-69825-1		82	180				58.4	2.300	31.7	7 120	189.7	27 517			4740
		82	180						32.4	7 290	194.3	28 174			4860
		82	180	D					31.4	7 050	187.9	27 246			4700
		21	RT	W					33.2	7 470	199.0	28 870			4980
		21	RT						32.6	7 330	195.3	28 329			4880
		21	RT						32.4	7 280	194.0	28 135			4850
		-53	-65						39.4	8 850	235.8	34 203			5900
		-53	-65						40.7	9 150	243.8	35 362			6100
		-53	-65						39.5	8 880	236.6	34 319			5920
		82	180						31.7	7 130	190.0	27 556			4750
		82	180						31.7	7 120	189.7	27 517			4740
		82	180	W	2.82	25			30.4	6 840	182.3	26 435			4560
		21	RT	D	5.65	50			30.7	6 900	183.9	26 667			4600
									30.6	6 890	183.6	26 628			4590
69-69825-1							58.4	2.300	30.3	6 820	181.7	26 357			4540
65C17768-1		21	RT				58.2	2.293	33.8	7 590	202.9	29 423			5070
65C17768-1		-53	-65				58.2	2.291	42.3	9 520	254.7	36 937			6370
69-69825-1	A	-53	-65	D	5.65	50	58.4	2.300	34.0	7 640	203.6	29 527	4.00 x 10⁴	5.8 x 10⁶	5090

STATIC COMPRESSION WITH IMPACT (TEST 1)(CONTINUED)

Drawing and assembly no.	Ply code	Temperature		Environment [2]	Impact level [8]		B		Failure load [3]		Stress [4]		E [5]		Strain, mm/m (μin/in) [6]
		°C	°F		N·m	(lbf·in)	mm	(in)	N	(lb)	MPa	(lbf/in²)	MPa	(lbf/in²)	
69-69825-1	A	-53	-65	D	5.65	50	58.4	2.300	34.8	7 820	208.4	30 222	4.00×10^4	5.8×10^6	5210
69-69825-1	A	-53	-65		5.65	50			32.7	7 350	195.9	28 406			4900
69-69825-2	B	21	RT		0.00	0			100.4	22 580	376.0	54 541			9400
					0.00	0			100.2	22 530	375.2	54 420			9380
					0.00	0			91.3	20 520	341.7	49 565			8550
					5.65	50			56.0	12 585	209.6	30 399			5240
									54.6	12 285	204.6	29 674			5120
69-69825-2							58.4	2.300	55.0	12 370	206.0	29 879			5150
65C17768-II							58.3	2.295	57.6	12 960	216.3	31 373			5410
65C17768-II							58.2	2.293	58.3	13 110	219.0	31 763			5480
65C17768-II		21	RT				58.3	2.295	62.5	14 040	234.3	33 987			5860
69-69825-2		-53	-65				58.4	2.300	62.9	14 143	235.5	34 162			5890
69-69825-2							58.4	2.300	62.8	14 127	235.3	34 123			5880
69-69825-2							58.4	2.300	65.0	14 610	243.3	35 290			6080
65C17768-2							58.2	2.293	77.8	17 480	292.0	42 351			7300
							58.3	2.294	70.0	15 740	262.8	38 119			6570
		-53	-65				58.3	2.294	75.8	17 050	284.7	41 291			7120
		82	180				58.2	2.292	63.9	14 360	240.0	34 807			6000
		82	180				58.3	2.295	64.5	14 510	242.2	35 125			6060
65C17768-2		82	180	D			58.3	2.295	62.6	14 070	234.8	34 060			5870
65C17768-II		21	RT	W			58.3	2.296	55.6	12 500	208.5	30 246			5210
65C17768-II		21	RT				58.1	2.289	59.0	13 260	221.9	32 183			5550
65C17768-II		21	RT				58.1	2.288	58.7	13 200	221.0	32 051			5530
69-69825-2		82	180				58.4	2.300	46.6	10 477	174.5	25 307			4360
69-69825-2		82	180				58.4	2.300	46.7	10 507	175.0	25 379			4380
69-69825-2		82	180	W	5.65	50	58.4	2.300	44.7	10 040	167.2	24 251			4180
65C17768-II		21	RT	D	8.36	74	58.3	2.295	55.1	12 390	206.8	29 993			5170
65C17768-II							58.3	2.295	53.2	11 970	199.8	28 976			5000
65C17768-II							58.3	2.294	53.8	12 090	201.9	29 279			5050
69-69825-2							58.4	2.300	52.8	11 860	197.5	28 647			4940
									51.1	11 485	191.3	27 742			4780
		21	RT						51.2	11 508	191.7	27 797			4790
		-53	-65						56.9	12 797	213.1	30 911			5330
		-53	-65						58.9	13 237	220.4	31 973			5510
		-53	-65	D					57.3	12 887	214.6	31 128			5370
		82	180	W					44.7	10 060	167.5	24 300			4190
		82	180	W					42.1	9 473	157.8	22 882			3950
69-69825-2	B	82	180	W	8.36	74	58.4	2.300	42.0	9 433	157.1	22 785	4.00×10^4	5.8×10^6	3930
65C17768-1	C	21	RT	D	16	16	58.2	2.292	42.4	9 530	238.9	34 650	4.76×10^4	6.9×10^6	5020
							58.2	2.292	41.8	9 390	235.4	34 140			4950
							58.2	2.291	42.5	9 560	239.8	34 774			5040
							58.3	2.294	44.3	9 960	249.5	36 181			5240
							58.2	2.293	43.1	9 700	243.1	35 252			5110
65C17768-1		21	RT		16	16	58.3	2.296	42.4	9 540	238.7	34 625			5020
65C17768-II		53	-65		2.82	25	58.3	2.294	43.4	9 750	244.2	35 418			5130
		-53	-65				58.3	2.294	45.5	10 230	256.2	37 162			5390
		-53	-65				58.2	2.290	45.6	10 260	257.4	37 336			5410
		82	180				58.1	2.289	41.9	9 420	236.5	34 294			4970
		82	180				58.2	2.290	38.7	8 700	218.3	31 659			4590
		82	180	D			58.2	2.290	41.1	9 240	231.8	33 624			4870
		21	RT	W			58.2	2.293	40.5	9 096	227.9	33 057			4790
		21	RT	W			58.2	2.293	40.5	9 096	227.9	33 057			4790
65C17768-II	C	21	RT	W	2.82	25	58.3	2.294	46.1	10 370	259.7	37 671	4.76×10^4	6.9×10^6	5460

STATIC COMPRESSION WITH IMPACT (TEST 1)(CONTINUED)

Drawing and assembly no.	Ply code	Temperature		Environment [2]	Impact level [8]		B		Failure load [3]		Stress [4]		E [5]		Strain, μm/m (μin/in) [6]
		C	F		N-m	(lb-in)	mm	(in)	N	(lb)	MPa	(lbf/in²)	MPa	(lbf/in²)	
65C17768-II	C	82	180	W	2.82	25	58.3	2.294	34.3	7 710	193.1	28 008	4.76×10^4	6.9×10^6	4060
65C17768-II		82	180	W	2.82	25	58.3	2.295	35.1	7 890	197.5	28 649			4150
65C17768-II		82	180	W	2.82	25	58.3	2.295	37.6	8 460	211.8	30 719			4450
65C17768-1		21	RT	D	5.65	50	58.3	2.294	35.9	8 065	202.0	29 297			4250
		21	RT				58.2	2.292	41.1	9 240	231.6	33 595			4870
		21	RT				58.3	2.296	41.1	9 250	231.5	33 573			4870
		-53	-65				58.2	2.291	48.2	10 840	271.9	39 430			5710
65C17768-1		-53	-65				58.2	2.291	42.5	9 550	239.5	34 737			5030
65C17768-II		-53	-65				58.2	2.290	40.0	8 990	225.6	32 715			4740
		82	180				58.2	2.290	31.0	6 970	174.9	25 364			3680
		82	180				58.2	2.292	33.0	7 415	185.9	26 960			3910
		82	180	D			58.2	2.292	33.1	7 440	186.5	27 051			3920
		21	RT	W			58.3	2.294	34.2	7 692	192.7	27 942			4050
		21	RT				58.3	2.293	33.5	7 536	188.8	27 388			3970
		21	RT				58.3	2.293	35.9	8 060	202.0	29 292			4250
		82	180				58.2	2.292	29.5	6 630	166.2	24 106			3490
		82	180				58.2	2.293	31.8	7 140	178.9	25 949			3760
	C	82	180				58.2	2.293	31.9	7 170	179.7	26 058			3780
	D	21	RT				58.2	2.291	58.7	13 200	220.7	32 009			4640
							58.1	2.288	62.5	14 040	235.0	34 091			4940
				W	5.65	50	58.1	2.288	57.9	13 020	218.0	31 614			4580
				D	8.36	74	58.3	2.295	59.9	13 470	224.8	32 607			4730
				D			58.3	2.295	56.4	12 690	211.8	30 719			4450
				D			58.3	2.295	57.0	12 810	213.8	31 009			4490
				W			58.2	2.292	51.5	11 580	193.5	28 069			4070
				W			58.2	2.290	52.2	11 730	196.2	28 457			4120
65C17768-II	D	21	RT	W	8.36	74	58.3	2.294	49.4	11 100	185.3	26 882	4.76×10^4	6.9×10^6	3900

STATIC TENSION–DISCONTINUOUS LAMINATE (TEST 22)

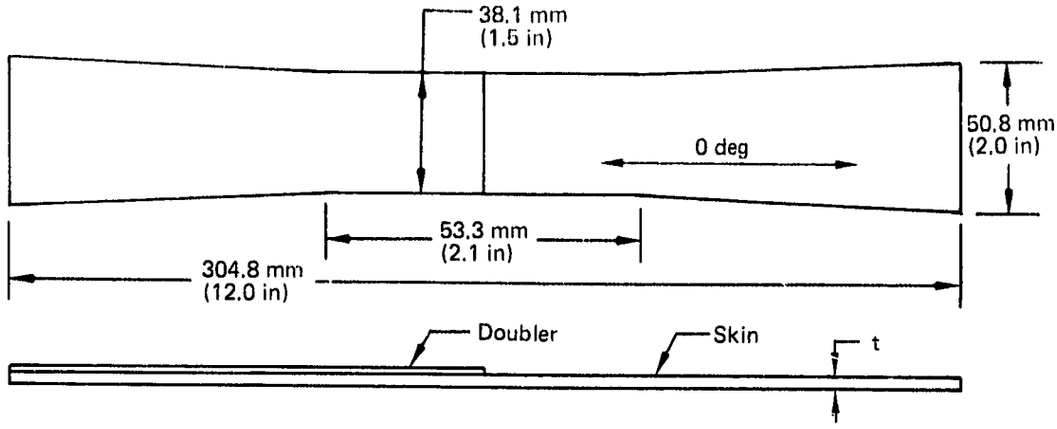

Assembly number	Skin [1]	Doubler [1]
-1	Fabric: 2(0, 90), 5(±45)	Fabric: 1(0, 90), 2(±45)
-2	Fabric: 2(0, 90), 5(±45) Tape: 2(0) Grade 145 2(0) Grade 190	Fabric: 2(0, 90), 2(±45)
-3	Fabric: 5(0, 90), 10(±45)	Fabric: 1(0, 90), 2(±45)
-5	Same as -1 skin	No doubler
-7	Same as -2 skin	No doubler
-9	Same as -3 skin	No doubler

Drawing and assembly no.	Temperature		Environment [2]	t		Minimum area		Failure load [3]		Stress [4]		E [5]		Strain, ε µm/m (µin/in) [6]
	°C	°F		mm	(in)	mm²	(in²)	N	(lb)	MPa	(lbf/in²)	MPa	(lbf/in²)	
65C17980-1	21	RT	D	1.33	0.0525	50.81	0.0788	16 192	3 640	318.5	46 193	3.76×10^4	5.45×10^6	8 476
65C17980-1	↑	↑	↑	↑	↑	↑	↑	16 192	3 640	318 5	46 193	↑	↑	8 476
65C17980-1								16 992	3 620	334.2	48 477			8 895
65C17980-5								17 837	4 010	350.9	50 888			9 337
65C17980-5								18 505	4 160	364.0	52 792			9 687
65C17980-5	21	RT						18 282	4 110	359.6	52 157			9 570
65C17980-1	-53	-65						15 369	3 455	302.3	43 845			8 045
65C17980-1								15 836	3 560	311.5	45 178			8 289
65C17980-1								14 991	3 370	294.9	42 766			7 847
65C17980 5								16 814	3 780	330.7	47 970			8 802
65C17960-5	↓	↓	↓	↓	↓	↓	↓	17 793	4 000	350.0	50 761	↓	↓	9 314
65C17980 5	-53	-65		1.33	0.0525	50.81	0.0788	16 992	3 820	334.2	48 477	3.76×10^4	5.45×10^6	8 895
65C17980-2	21	RT		1.99	0.0785	75.97	0.1178	38 877	8 740	510.7	74 068	6.25×10^4	9.60×10^6	7 715
65C17980-2	21	RT		1.99	0.0785	75.97	0.1178	40 301	9 060	529.4	76 780	6.25×10^4	9.60×10^6	7 998
65C17980-2	21	RT	D	1.99	0.0785	75.97	0.1178	41 747	9 385	548.4	79 534	6.25×10^4	9.60×10^6	8 285

STATIC TENSION–DISCONTINUOUS LAMINATE (TEST 22) (CONTINUED)

Drawing and assembly no.	Temperature		Environment [2]	t		Minimum area		Failure load [3]		Stress [4]		E [5]		Strain, ε µm/m (µin/in) [6]
	°C	°F		mm	(in)	mm²	(in²)	N	(lb)	MPa	(lbf/in²)	MPa	(lbf/in²)	
65C17980-7	21	RT	D	1.99	0.0785	75.97	0.1178	48 041	10 800	631.0	91 525	6.25×10^4	9.60×10^6	9 534
65C17980-7	21	RT						48 041	10 800	631.0	91 525			9 534
65C17980-7	21	RT						46 573	10 470	611.8	88 729			9 243
65C17980-2	-53	-65						32 828	7 380	431.2	62 542			6 515
65C17980-2								30 159	6 780	396.2	57 458			5 985
65C17980-2								33 273	7 480	437.1	63 390			6 603
65C17980-7								50 977	11 460	669.6	97 119			10 117
65C17980-7								43 103	9 690	566.2	82 119			8 554
65C17980-7	-53	-65		1.99	0.0785	75.97	0.1178	47 774	10 740	627.5	91 017	6.25×10^4	9.60×10^6	9 481
65C17980-3	21	RT		2.86	0.1125	108.90	0.1688	35 942	8 080	329.6	47 811	4.00×10^4	5.80×10^6	8 243
65C17980-3								32 739	7 360	300.3	43 550			7 509
65C17980-3								34 274	7 705	314.3	45 592			7 861
65C17980-9								40 301	9 060	369.6	53 609			9 243
65C17980-9								38 299	8 610	351.3	50 947			8 784
65C17980-9	21	RT						39 233	8 820	359.8	52 189			8 998
65C17980-3	-53	-65						30 737	6 910	281.9	40 888			7 050
65C17980-3								31 138	7 000	285.6	41 420			7 141
65C17980-3								36 209	8 140	332.1	48 166			8 304
65C17980-9								42 080	9 460	385.9	55 976			9 651
65C17980-9								40 568	9 120	372.1	53 964			9 304
65C17980-9	-53	-65	D	2.86	0.1125	108.90	0.1688	43 726	9 830	401.0	58 166	4.00×10^4	5.80×10^6	10 029

STATIC TENSION–FASTENER BEARING (TEST 1)

Assembly number	Ply layup [1]		t mm (in)
-7, -8, -9, -10	Splice	Fabric: 4(0, 90), 8(±45)	2.29 (0.09)
-42	Web	Fabric: 8(0, 90), 16(±45)	4.58 (0.18)
-11, -12	Splice	Fabric: 6(0, 90), 6(±45)	2.29 (0.09)
-13, -14	Web	Fabric: 12(0, 90), 12(±45)	4.58 (0.18)

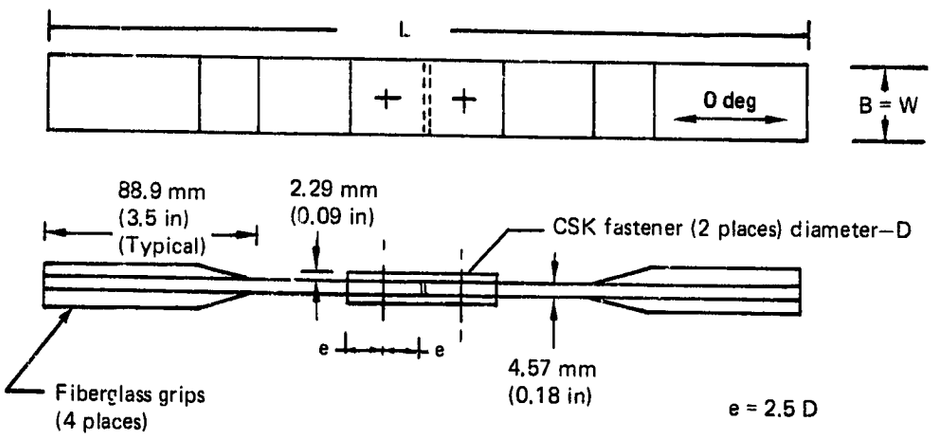

Drawing and assembly no.	L mm (in)	W mm (in)	D mm (in)	e mm (in)	W/D
65C17768-7	282.5 (11.12)	14.2 (0.56)	4.76 (0.1875)	11.9 (0.47)	3
65C17768-8	321.1 (12.64)	23.9 (0.94)	4.76 (0.1875)	11.9 (0.47)	5
65C17768-9	317.5 (12.50)	19.0 (0.75)	6.35 (0.25)	16.0 (0.63)	3
65C17768-10	368.3 (14.50)	31.8 (1.25)	6.35 (0.25)	16.0 (0.63)	5
65C17768-42	321.1 (12.64)	23.9 (0.94)	4.76 (0.1875)	11.9 (0.47)	5

STATIC TENSION--FASTENER BEARING (TEST 1)(CONTINUED)

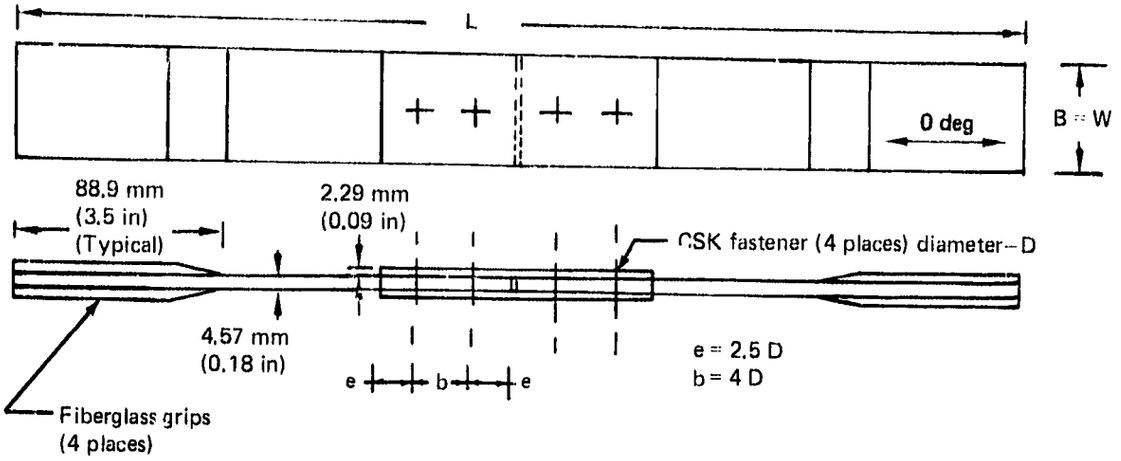

Drawing and assembly no.	L mm (in)	W mm (in)	D mm (in)	e mm (in)	W/D
65C17768-11	359.2 (14.14)	23.9 (0.94)	4.76 (0.1875)	11.9 (0.47)	5
65C17768-12	396.7 (15.62)	33.3 (1.31)	4.76 (0.1875)	11.9 (0.47)	7
65C17768-13	419.1 (16.50)	31.8 (1.25)	6.35 (0.25)	16.0 (0.63)	5
65C17768-14	469.9 (18.50)	44.4 (1.75)	6.35 (0.25)	16.0 (0.63)	7

Drawing and assembly no.	Temperature °C	Temperature °F	Environment [2]	Diameter mm	Diameter (in)	B mm	B (in)	W/D	Failure load [3] N	Failure load [3] (lb)	Stress [9] MPa	Stress [9] (lbf/in²)	E [5] MPa	E [5] (lbf/in²)
65C17768-7	21	RT	D	4.76	0.1875	14.1	0.557	3	9 452	2125	434	62 963	4.0×10^4	5.8×10^6
	21	RT				14.1	0.557		9 275	2085	426	61 778		
	21	RT				14.1	0.554		9 252	2080	425	61 630		
	-53	-65				14.1	0.555		9 897	2225	455	65 926		
	-53	-65				14.1	0.557		9 364	2105	430	62 370		
	-53	-65	D			14.1	0.557		10 120	2275	465	67 407		
	21	RT	W			14.2	0.560		10 075	2265	463	67 111		
	21	RT				14.1	0.557		10 943	2460	503	72 889		
	21	RT				14.1	0.556		10 409	2340	478	69 333		
	82	180				14.6	0.576		9 252	2080	425	61 630		
	82	180				14.8	0.584		9 719	2185	446	64 741		
65C17768-7	82	180	W			14.2	0.561	3	10 387	2335	477	69 185		
65C17768-8	21	RT	D			23.9	0.941	5	12 633	2840	580	84 148		
	21	RT				23.9	0.941		12 833	2885	589	85 481		
	21	RT				23.9	0.940		12 944	2910	594	86 222		
	-53	-65				23.9	0.940		14 012	3150	644	93 333		
	-53	-65				23.9	0.941		14 635	3290	672	97 481		
	-53	-65	D			23.9	0.940		15 102	3395	694	100 593		
	21	RT	W			23.9	0.942		13 678	3075	628	91 111		
	21	RT				23.9	0.940		13 523	3040	621	90 074		
	21	RT				23.9	0.940		13 901	3125	638	92 593		
	82	180				23.9	0.942		13 122	2950	603	87 407		
	82	180				24.0	0.944		13 250	2980	609	88 296		
65C17768-8	82	180	W	4.76	0.1875	24.0	0.945	5	12 277	2760	564	81 778	4.0×10^4	5.8×10^6

STATIC TENSION–FASTENER BEARING (TEST 1)(CONTINUED)

Drawing and assembly no.	Temperature		Environment [2]	Diameter		B		W/D	Failure load [3]		Stress [9]		E [6]	
	°C	°F		mm	(in)	mm	(in)		N	(lb)	MPa	(lbf/in2)	MPa	(lbf/in2)
65C17768-42	21	RT	D	4.76	0.1875	24.0	0.940	5	14 234	3200	664	94 815	4.0×10^4	5.8×10^6
65C17768-42	21	RT		4.76	0.1875	24.0	0.945	5	13 789	3100	633	91 852		
65C17768-42	21	RT		4.76	0.1875	23.9	0.940	5	13 945	3135	640	92 889		
65C17768-9	21	RT		6.35	0.25	19.0	0.748	3	13 689	3055	468.1	67 889		
	21	RT				19.1	0.750		13 723	3085	472.7	68 556		
	-53	-65				19.0	0.748		12 368	2785	426.7	61 889		
	-53	-65				19.0	0.748		13 945	3135	480.3	69 667		
	-53	-65	D			18.9	0.745		14 234	3200	490.3	71 111		
	21	RT	W			18.9	0.744		13 901	3125	478.8	69 444		
	21	RT				19.1	0.750		15 391	3460	530.1	76 889		
	21	RT				19.1	0.750		13 967	3140	481.1	69 778		
	82	180				19.1	0.753		15 213	3420	524.0	76 000		
	82	180				18.8	0.739		15 947	3585	549.3	79 667		
65C17768-9	82	180	W			18.7	0.738		16 058	3610	553.1	80 222		
65C17768-10	21	RT	D			19.2	0.756	3	15 213	3420	524.0	76 000		
	21	RT				31.8	1.252	5	17 926	4030	617.5	89 556		
	21	RT				31.8	1.253		19 061	4285	656.5	95 222		
	-53	-65				31.8	1.252		18 771	4220	646.6	93 778		
	-53	-65				31.8	1.252		19 639	4415	676.5	98 111		
	-53	-65				31.8	1.251		19 772	4445	681.1	98 778		
	82	180				31.8	1.251		20 351	4575	701.0	101 667		
	82	180				31.8	1.250		18 771	4220	646.6	93 778		
	82	180	D			31.8	1.251		18 771	4220	646.6	93 778		
	21	RT	W			31.8	1.252		19 394	4360	668.0	96 889		
	21	RT				31.8	1.252		18 981	4267	653.8	94 822		
	21	RT				31.8	1.252		19 065	4286	656.7	95 244		
	-53	-65				31.8	1.252		18 562	4173	639.4	92 733		
	53	-65				31.9	1.254		19 795	4450	681.8	98 889		
	-53	-65				32.1	1.263		19 661	4420	677.2	98 222		
	82	180				31.9	1.256		18 005	4250	651.2	94 444		
	82	180				32.0	1.259		17 815	4005	613.6	89 000		
65C17768-10	82	180	W	6.35	0.25	31.9	1.255		17 926	4030	617.5	89 556		
65C17768-11	21	RT	D	4.76	0.1875	23.9	0.942		16 103	3620	554.6	80 444	4.0×10^4	5.8×10^6
	21	RT				23.9	0.942		20 373	4580	467.8	67 852	4.76×10^4	6.9×10^6
	21	RT				23.9	0.941		20 951	4710	481.1	69 778		
	-53	-65				23.9	0.941		21 307	4790	489.3	70 963		
	-53	-65				23.8	0.938		19 906	4475	457.1	66 296		
	-53	-65	D			23.9	0.940		19 617	4410	450.5	65 333		
	21	RT	W			23.9	0.940		19 683	4425	452.0	65 556		
	21	RT				23.7	0.936		22 045	4956	506.2	73 422		
	21	RT				23.9	0.941		22 286	5010	511.7	74 222		
	82	180				23.9	0.940		21 262	4780	488.3	70 815		
	82	180				24.0	0.944		22 343	5023	513.1	74 416		
65C17768-11	82	180	W			24.0	0.944	5	22 032	4953	505.9	73 378		
65C17768-12	21	RT	D			33.5	1.320	7	13 692	3078	314.4	45 600		
	21	RT				33.4	1.316		28 558	6420	655.8	95 111		
	21	RT				33.4	1.314		27 490	6180	631.3	91 556		
	-53	-65				33.5	1.319		25 889	5820	594.5	86 222		
	53	-65				33.6	1.324		25 889	5820	594.5	86 222		
	-53	-65	D			33.5	1.318		24 910	5600	572.0	82 963		
	21	RT	W			33.3	1.310		25 889	5820	594.5	86 222		
65C17768-12	21	RT	W	4.76	0.1875	33.3	1.311	7	26 818	6029	615.8	89 319		
									27 935	6280	641.5	93 037	4.76×10^4	6.9×10^6

STATIC TENSION--FASTENER BEARING (TEST 1)(CONTINUED)

Drawing and assembly no	Temperature		Environment [2]	Diameter		B		W/D	Failure load [3]		Stress [4]		E [5]	
	°C	°F		mm	(in)	mm	(in)		N	(lb)	MPa	(lbf/in²)	MPa	(lbf/in²)
65C17768-12	21	RT	W	4.76	0.1875	33.5	1.310	7	26 407	5950	607.8	88 148	4.76×10^4	6.9×10^6
65C17768-12	82	180				33.5	1.319	7	27 446	6170	630.2	91 407		
65C17768-12	82	180				33.5	1.319	7	25 132	5660	577.1	83 704		
65C17768-12	82	180	W	4.76	0.1875	33.5	1.317	7	26 378	5930	605.7	87 852		
65C17768-13	21	RT	D	6.35	0.25	32.0	1.259	5	24 643	5540	424.4	61 566		
	21	RT				32.0	1.259		26 333	5920	453.6	65 778		
	21	RT				32.0	1.261		26 156	5880	450.6	65 333		
	-53	-65				32.'	1.266		24 020	5400	413.7	60 000		
	-53	-65				32 0	1.259		24 020	5400	413.7	60 000		
	-53	-65	D			32.0	1.261		23 931	5380	412.2	59 778		
	21	RT	W			32.0	1.261		27 597	6204	475.3	68 933		
	21	RT				32.0	1.259		27 001	6070	465.0	67 444		
	21	RT				32.0	1.259		28 046	6305	483.0	70 056		
	82	180				32.0	1.261		28 624	6435	493.0	71 500		
	82	180				32.0	1.259		28 268	6355	486.8	70 611		
65C17768-13	82	180	W			32.0	1.261	5	28 758	6465	495.3	71 833		
65C17768-14	21	RT	D			44.6	1.754	7	32 917	7400	566.9	82 222		
	21	RT				44.7	1.760		32 116	7220	553.1	80 222		
	21	RT				44.9	1.766		32 561	7320	560.8	81 333		
	-53	-65				44.6	1.755		29 536	6640	508.7	73 778		
	-53	-65				44.7	1.760		30 337	6820	522.5	75 778		
	-53	-65	D			44.6	1.754		29 803	6700	513.3	74 444		
	21	RT	W			44.5	1.750		33 940	7630	584.5	84 778		
	21	RT				44.4	1.749		32 361	7275	557.3	80 833		
	21	RT				44.4	1.747		33 495	7530	576.9	83 667		
	82	180				44.5	1.750		35 430	7965	610.2	88 600		
	82	180				44.4	1.749		34 807	7825	599.4	86 944		
65C17768-14	82	180	W	6.35	0.25	44.4	1.747	7	34 830	7830	599.8	87 000	4.76×10^4	6.9×10^6

MECHANICAL JOINTS (TEST 5)

Assembly number	Ply layup [1]		t mm (in)	
-1, -2, -3, -4	Splice	Fabric: 6(0, 90), 6(±45)	2.29 (0.09)	50% joint transfer
-9, -10	Web	Fabric: 12(0, 90), 12(±45)	4.58 (0.18)	
-5, -6, -7, -8	Splice	Fabric: 4(0, 90), 8(±45)	2.29 (0.09)	100% joint transfer
	Web	Fabric: 8(0, 90), 16(±45)	4.58 (0.18)	
-29	Fabric: 4(0, 90), 8(±45)		2.29 (0.09)	Basic coupons
-30, -31	Fabric: 6(0, 90), 6(±45)		2.29 (0.09)	

SPECIMEN DESCRIPTION

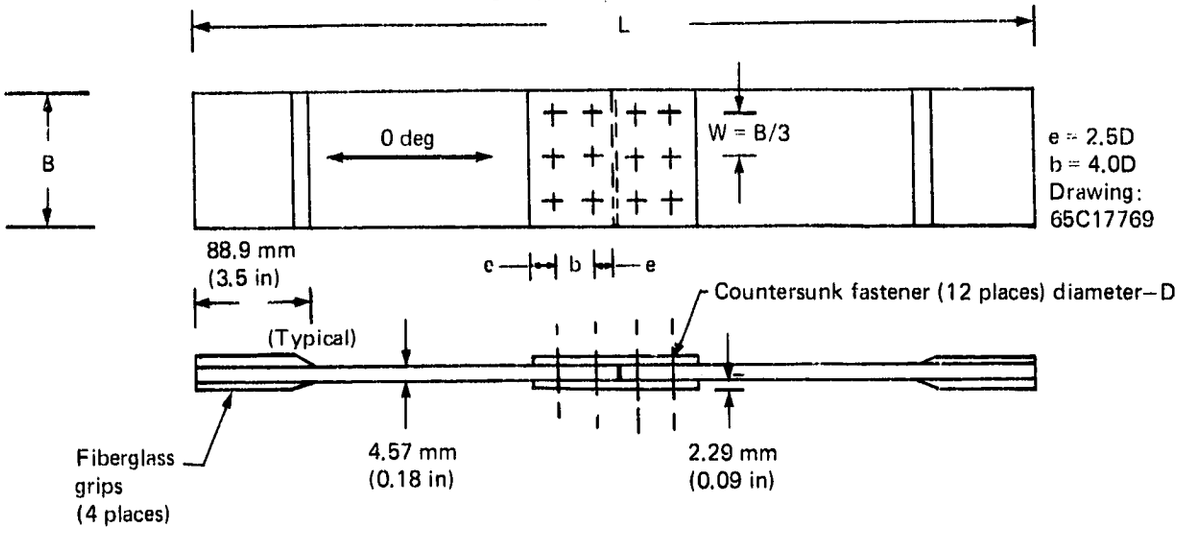

Drawing and assembly no.	L mm (in)	B mm (in)	D mm (in)	W mm (in)	e mm (in)	b mm (in)	W/D
65C17769-1	549.7 (21.64)	71.4 (2.81)	4.76 (0.1875)	23.9 (0.94)	11.9 (0.47)	19.05 (0.75)	5
65C17769-2	664.0 (26.14)	100.0 (3.94)	4.76 (0.1875)	33.3 (1.31)	11.9 (0.47)	19.05 (0.75)	7
65C17769-3	673.1 (26.5)	95.2 (3.75)	6.35 (0.25)	31.8 (1.25)	16.0 (0.63)	25.40 (1.00)	5
65C17769-4	825.5 (32.5)	133.4 (5.25)	6.35 (0.25)	44.4 (1.75)	16.0 (0.63)	25.40 (1.00)	7
65C17769-9	549.7 (21.64)	71.4 (2.81)	4.76 (0.1875)	23.9 (0.94)	11.9 (0.47)	19.05 (0.75)	5
65C17769-10	664.0 (26.14)	100.0 (3.94)	4.76 (0.1875)	33.3 (1.31)	11.9 (0.47)	19.05 (0.75)	7

MECHANICAL JOINTS (TEST 5)(CONTINUED)

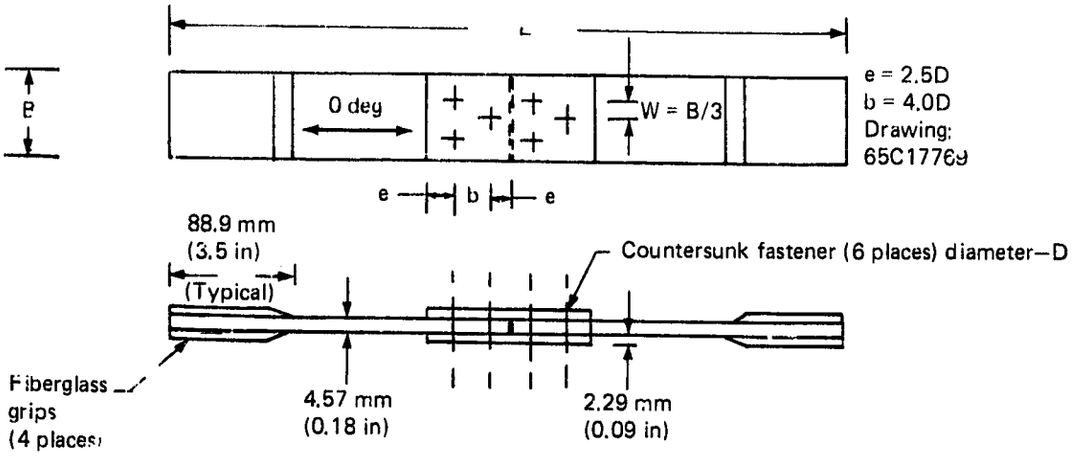

Drawing and assembly no.	L mm (in)	B mm (in)	D mm (in)	W mm (in)	e mm (in)	b mm (in)	W/D
65C17769-5	435.4 (17.14)	42.7 (1.68)	4.76 (0.1875)	14.2 (0.56)	11.9 (0.47)	19.05 (0.75)	3
65C17769-6	549.7 (21.64)	71.4 (2.81)	4.76 (0.1875)	23.9 (0.94)	11.9 (0.47)	19.05 (0.75)	5
65C17769-7	520.7 (20.50)	57.2 (2.25)	6.35 (0.25)	19.0 (0.75)	16.0 (0.63)	25.40 (1.00)	3
65C17769-8	673.1 (26.50)	95.2 (3.75)	6.35 (0.25)	31.8 (1.25)	16.0 (0.63)	25.40 (1.00)	5

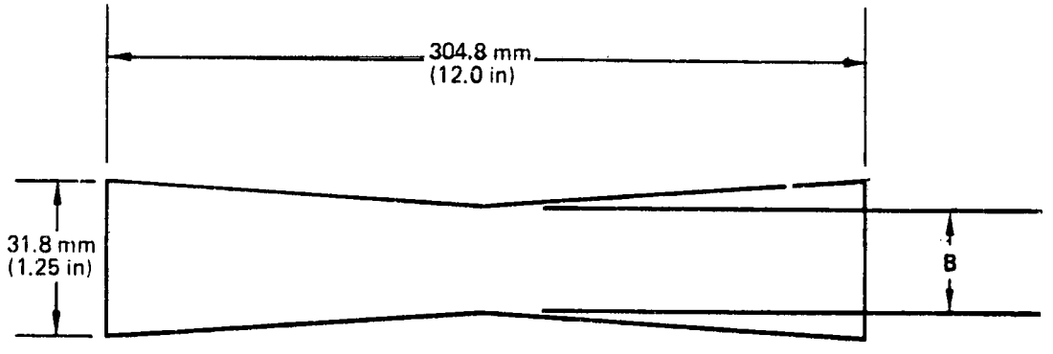

65C17769-29, -30, -31

C-5

MECHANICAL JOINTS (TEST 5)(CONTINUED)

Drawing and assembly no.	Temperature		Environment [2]	Diameter		B		W/D	Failure load [3]		Stress [9]		E [5]		Comments
	°C	°F		mm	(in)	mm	(in)		N	(lb)	MPa	(lbf/in²)	MPa	(lbf/in²)	
65C17769-1	21	RT	D	4.76	0.1875	71.3	2.809	5	67 257	15 120	514.8	74 667	4.76×10^4	6.9×10^6	[11]
			D			71.4	2.812		66 545	14 960	509.4	73 887			
			D			71.4	2.810		66 812	15 020	511.4	74 173			
			W			71.4	2.810		68 592	15 420	525.0	76 148			
			W			71.4	2.810		66 723	15 000	510.7	74 074			
65C17769-1			W			71.4	2.810	5	67 168	15 100	514.1	74 568			
65C17769-2			D			100.1	3.941	7	85 228	19 160	652.4	94 617			
			D			100.1	3.941		80 780	18 160	618.3	89 679			
			D			100.1	3.941		79 178	17 800	606.1	87 901			
			W			100.1	3.940		85 139	19 140	651.7	94 519			
			W			100.1	3.941		85 539	19 230	654.7	94 963			
65C17769-2			W	4.76	0.1875	100.1	3.940	7	83 404	18 750	638.4	92 593			
65C17769-3			D	6.35	0.2500	95.3	3.753	5	84 739	19 050	486.5	70 556			
			D			95.3	3.753		81 402	18 300	467.3	67 778			
			D			95.4	3.754		82 470	18 540	473.4	68 667			
			W			95.3	3.753		81 136	18 240	465.8	67 556			
			W			95.3	3.752		84 071	18 900	482.6	70 000			
65C17769-3			W			95.3	3.753	5	85 940	19 320	493.4	71 556			
65C17769-4			D			133.4	5.250	7	96 082	21 600	551.6	80 000			
			D			133.4	5.252		105 423	23 700	605.2	87 778			
			D			133.4	5.252		102 309	23 000	587.3	85 185			
			W			133.5	5.255		103 377	23 240	593.5	86 074			
			W			133.4	5.253		101 064	22 720	580.2	84 148			
65C17769-4			W	6.35	0.2500	133.5	5.254	7	98 395	22 120	564.9	81 926	4.76×10^4	6.9×10^6	
65C17769-5			D	4.76	0.1875	42.4	1.669	3	35 251	7 980	543.4	78 815	4.00×10^4	5.8×10^6	
			D			42.4	1.671		34 251	7 700	524.3	76 049			
			D			42.5	1.673		34 073	7 660	521.6	75 654			
			W			42.5	1.674		36 231	8 145	554.6	80 444			
			W			42.5	1.674		36 898	8 295	564.9	81 926			
65C17769-5			W			42.4	1.670	3	33 006	7 420	505.3	73 284			
65C17769-6			D			71.4	2.810	5	41 457	9 320	634.7	92 049			
			D			71.4	2.811		38 778	8 720	593.8	86 123			
			D			71.4	2.811		41 546	9 340	636.0	92 247			
			W			71.4	2.810		44 171	9 930	676.2	98 074			
			W			71.4	2.811		44 304	9 960	678.2	98 370			
65C17769-6			W	4.76	0.1875	71.4	2.811	5	44 304	9 960	678.2	98 370			
65C17769-7			D	6.35	0.2500	57.1	2.248	3	40 212	9 040	481.7	66 963			
			D			57.1	2.249		40 568	9 120	485.8	67 556			
			D			57.1	2.249		44 037	9 900	505.6	73 333			
			W			57.2	2.250		45 639	10 260	524.0	76 000			
			W			57.2	2.253		45 505	10 230	522.5	75 778			
65C17769-7			W			57.3	2.254	3	42 303	9 510	485.7	70 444			
65C17769-8			D			95.3	3.750	5	56 137	12 620	644.5	93 481			
			D			95.3	3.751		52 934	11 900	607.8	88 148			
			D			95.3	3.750		52 489	11 800	602.7	87 407			
			W			95.4	3.753		59 784	13 440	686.4	99 556			
			W			95.6	3.763		61 119	13 740	701.7	101 778			
65C17769-8			W	6.35	0.2500	95.5	3.760		55 380	12 450	635.8	92 222	4.00×10^4	5.8×10^6	[11]
65C17769-9			D	4.76	0.1875	71.4	2.810		62 987	14 160	482.1	69 926	4.76×10^4	6.9×10^6	[12]
65C17769-9						71.4	2.811		68 147	15 320	521.6	75 654			
65C17769-9						71.4	2.810	5	62 097	13 960	475.3	68 938			
65C17769-10						100.2	3.943	7	73 396	16 500	561.8	81 481			
65C17769-10	21	RT	D	4.76	0.1875	100.1	3.942	7	70 860	15 930	542.4	78 667	4.76×10^4	6.9×10^6	[12]

MECHANICAL JOINTS (TEST 5)(CONTINUED)

Drawing and assembly no.	Temperature		Environment [2]	Diameter		B		W/D	Failure load [3]		Stress [9]		E [5]		Comments
	°C	°F		mm	(in)	mm	(in)		N	(lb)	MPa	(lbf/in2)	MPa	(lbf/in2)	
65C17769-10	21	RT	D	4.76	0.1875	100.1	3.940	7	78 111	17 560	597.9	86 716	4.76×10^4	6.9×10^6	[12]
65C17769-1	↑	↑	↑	↑	↑	71.4	2.810	5	66 056	14 850	505.6	73 333	↑	↑	[13]
65C17769-1						71.4	2.810	5	64 722	14 550	495.4	71 852			↑
65C17769-1						71.4	2.810	5	65 389	14 700	500.5	72 593			
65C17769-2						100.1	3.940	7	83 671	18 810	640.4	92 88[illegible]			
65C17769-2						100.1	3.940	7	82 737	18 6[illegible]	633.3	91 852	↓	↓	
65C17769-2						100.1	3.940	7	80 869	18 180	619.0	89 778	4.76×10^4	6.9×10^6	
65C17769-5						95.3	3.750	3	36 564	8 220	559.8	81 185	4.00×10^4	5.8×10^6	
65C17769-5						95.3	3.750	3	31 333	7 044	479.7	69 570	↑	↑	
65C17769-5						95.3	3.750	3	34 162	7 680	523.0	75 852			
65C17769-6						133.4	5.250	5	40 568	9 120	621.0	90 074			
65C17769-6						133.4	5.250	5	40 701	9 150	623.1	90 370	↓	↓	↓
65C17769-6	21	RT	D	4.76	0.1875	133.4	5.250	5	40 034	9 000	612.9	88 889	4.00×10^4	5.8×10^6	[13]

Drawing and assembly number	Temperature		Environment [2]	B		Failure load [3]		Stress [4]		E [5]		Strain, μm/m (μin/in) [6]	Comments
	C	°F		mm	(in)	N	(lb)	MPa	(lbf/in2)	MPa	(lbf/in2)		
65C17769-29	21	RT	D	18.9	0.745	16 192	3640	374.3	54 288	4.00×10^4	5.8×10^6	9360	[11]
65C17769-29	↑	↑	↑	13.8	0.740	16 037	3785	391.8	56 832	4.00×10^4	5.0×10^6	9800	↑
65C17769-29				18.9	0.745	16 570	3725	383.0	55 556	4.00×10^4	5.8×10^6	9580	
65C17769-30				18.9	0.743	14 390	3235	333.6	48 377	4.76×10^4	6.9×10^6	7010	
65C17769-30				18.9	0.744	15 920	3579	368.5	53 450	↑	↑	7750	
65C17769-30				18.9	0.744	17 384	3908	402.4	58 363			8460	
65C17769-31				18.9	0.745	15 480	3480	358.3	51 971			7530	
65C17769-31	↓	↓	↓	18.9	0.744	15 235	3425	352.7	51 150	↓	↓	7410	
65C17769-31	21	RT	D	18.9	0.746	16 347	3675	377.4	54 736	4.76×10^4	6.9×10^6	7930	[11]

SKIN PANEL TO RIB ATTACHMENT (TEST 9)

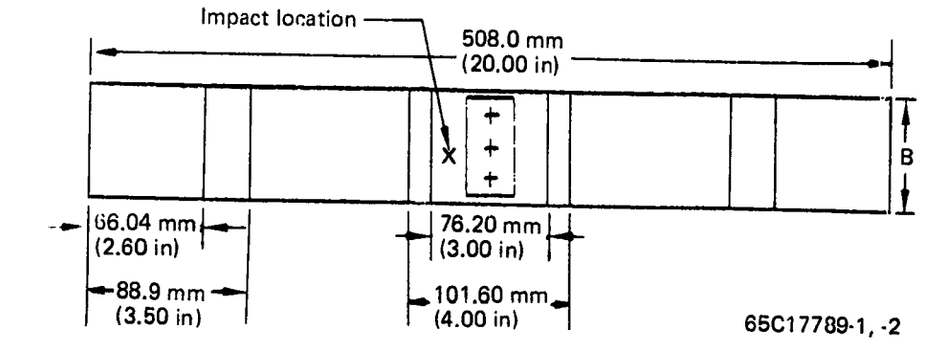

65C17789-1, -2

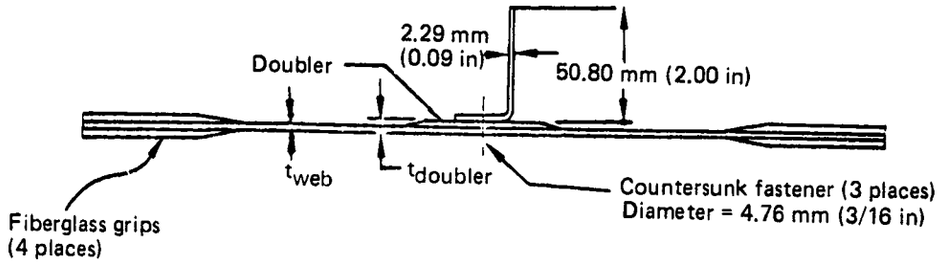

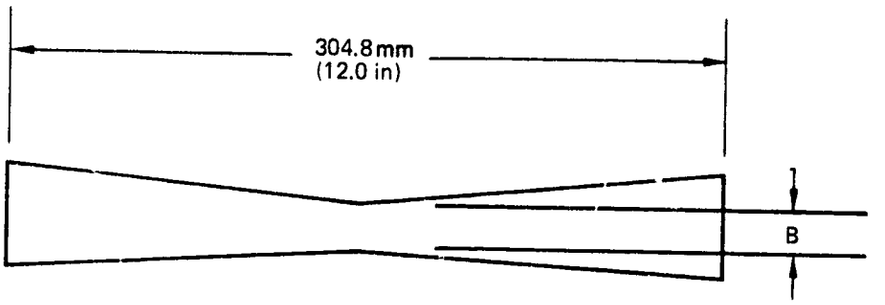

65C17789-6, 7

Item	Ply layup [1]	t mm (in)	E MPa (lbf/in^2)
Web -1, -2, -6, -7	Fabric: 5(0, 90), 2(±45)	1.9050 (0.0525)	3.75×10^4 (5.45×10^6)
Doubler -1	Fabric: 3(±45)	0.5715 (0.0225)	–
Doubler -2	Fabric: 1(0, 90), 4(±45)	0.9525 (0.0375)	–

SKIN PANEL TO RIB ATTACHMENT (TEST 9)(CONTINUED)

Drawing and assembly no.	Temperature		Environment [2]	B		Minimum area		Failure load [3]		Stress [4]		E [5]		Strain, μm/m (μin/in) [6]	Comments
	°C	°F		mm	(in)	mm²	(in²)	N	(lb)	MPa	(lbf/in²)	MPa	(lbf/in²)		
65C17786-1	21	RT	D	70.84	2.7890	95.5	0.1480	28 611	6432	299.7	43 460	3.76×10^4	5.45×10^6	7970	[11]
↑	21	RT	↑	72.52	2.8550	97.4	0.1510	29 572	6648	303.6	44 030	↑	↑	8080	↑
	21	RT		72.26	2.8450	97.4	0.1510	28 824	6480	295.9	42 910			7870	
	-53	-65		71.12	2.8000	95.5	0.1480	26 489	5955	277.4	40 240			7380	
	-53	-65	↓	72.14	2.8400	97.4	0.1510	25 132	5650	258.0	37 420			6879	
	-53	-65	D	72.39	2.8500	97.4	0.1510	26 534	5965	272.4	39 500			7250	
	21	RT	W	71.40	2.8110	96.1	0.1490	24 198	5440	251.7	36 510			6700	
	21	RT	↑	72.52	2.8550	97.4	0.1510	24 999	5620	256.6	37 220			6830	
	21	RT		72.21	2.8430	97.4	0.1510	25 221	5670	258.9	37 550			6890	
	82	180		72.52	2.8550	97.4	0.1510	26 660	5980	273.1	39 600			7270	
↓	82	180	↓	72.09	2.8380	96.8	0.1500	26 600	5845	268.7	38 970			7150	
65C17786-1	82	180	W	72.39	2.8500	97.4	0.1510	24 198	5440	248.4	36 030			6610	
65C17786-2	21	RT	D	71.65	2.8210	96.8	0.1500	26 600	5845	326.0	47 280			8680	
65C17786-2	↑	↑	↑	72.26	2.8450	97.4	0.1510	32 241	7248	331.0	48 000			8810	
65C17786-6				18.92	0.7450	25.5	0.0395	8 118	1825	318.6	46 200			8480	
65C17786-6				18.90	0.7440	25.4	0.0394	8 954	2013	352.3	51 090			9380	↓
65C17786-6				18.92	0.7450	25.5	0.0395	8 75	1968	343.5	49 820			9140	[11]
65C17786-7				18.92	0.7450	25.5	0.0395	6 824	1534	267.8	38 840			7130	[12]
65C17786-7				18.85	0.7420	25.4	0.0393	6 659	1497	262.6	38 090			6990	[12]
65C17786-7				18.87	0.7430	25.4	0.0394	4 831	1086	190.1	27 560			5060	[12]
65C17786-1				72.21	2.8430	97.4	0.1510	29 536	6640	303.2	43 970			8070	[14]
↑				70.92	2.7920	95.5	0.1480	28 691	6450	300.5	43 580			8000	[14]
	↓	↓		71.25	2.8050	96.1	0.1490	28 335	6370	294.8	42 750			7840	[14]
	21	RT		71.20	2.8030	96.1	0.1490	28 913	6500	300 8	43 620			8000	[13]
	-53	-65	↓	70.94	2.7930	95.5	0.1480	27 935	6380	292 6	42 430			7790	↑ [15]
	21	RT	D	72.21	2.8430	97 4	0.1510	30 515	6860	313.2	45 430			8340	↕
	82	180	W	72.49	2 8540	97.4	0.1510	29 492	6630	302.7	43 910	↓	↓	8060	↓
65C17786-1	21	RT	W	72 14	2 8400	97.4	0.1510	27 490	6180	282.2	40 930	3.76×10^4	5.45×10^6	7510	[13] → [15]

SPAR SHEAR WEB (TEST 11)

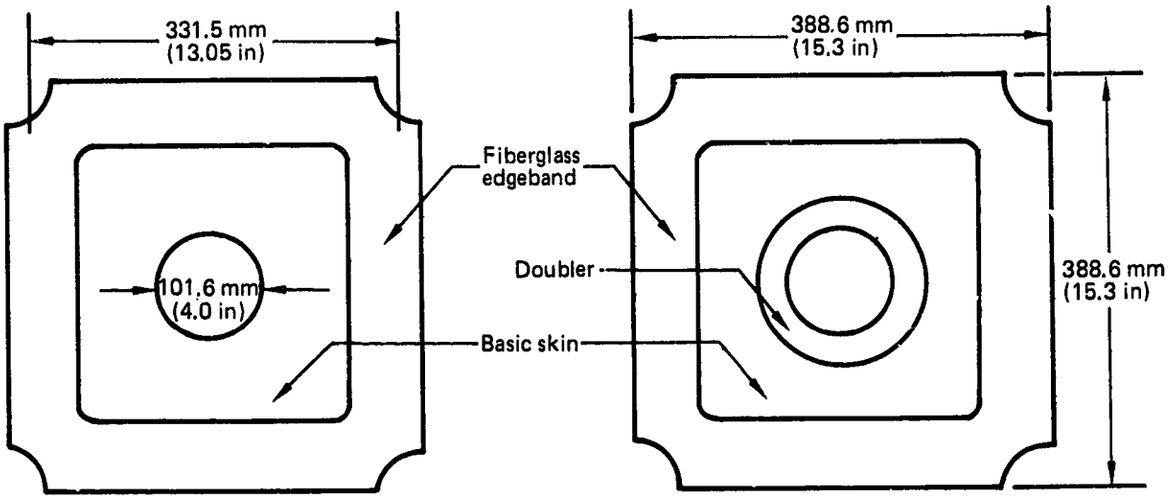

65C17789-1 configuration

65C17789-3 configuration

Assembly number	Ply layup 1	
-1	Basic skin	Fabric: 8(0, 90), 16(±45)
-3	Basic skin	Fabric: 2(0, 90), 4(±45)
	Doubler	Fabric: 14(±45)

Drawing and assembly no.	Temperature		Environment 2	Gross failure 3		Frame failure		Net failure		Shear modulus 7		γ_{max} μm/m (μin/in) 10
	°C	°F		N	(lb)	N	(lb)	N	(lb)	MPa	(lbf/in^2)	
65C17789-1	21	RT	D	219 300	49 300	15 570	3500	203 700	45 800	2.21×10^4	3.2×10^6	4308
↑	21	RT	↑	238 000	53 500	↑	↑	222 400	50 000	↑	↑	4704
↑	21	RT	↑	223 300	50 200	↑	↑	207 700	46 700	↑	↑	4393
↑	-53	-65	↑	218 600	49 150	↑	↑	203 100	45 650	↑	↑	4294
↑	-53	-65	↑	204 000	45 850	↑	↑	188 400	42 350	↑	↑	3984
↑	-53	-65	D	206 600	46 450	↑	↑	191 100	42 950	↑	↑	4040
↑	21	RT	W	223 100	50 150	↑	↑	207 500	46 650	↑	↑	4388
↑	21	RT	↑	218 000	49 000	↑	↑	202 400	45 500	↑	↑	4280
↑	21	RT	↑	234 400	52 700	↑	↑	218 900	49 200	↑	↑	4628
↑	82	180	↑	211 700	47 600	↑	↑	196 200	44 100	↑	↑	4148
↓	82	180	↓	198 400	44 600	↓	↓	182 800	41 100	↑	↑	3866
65C17789-1	82	180	W	185 000	41 600	15 570	3500	169 500	38 100	↑	↑	3584
65C17789-3	21	RT	D	86 300	19 400	13 340	3000	72 950	16 400	↑	↑	6171
65C17789-3	21	RT	D	75 170	16 900	13 340	3000	61 830	13 900	2.21×10^4	3.2×10^6	5230

SPAR SHEAR WEB (TEST 11)(CONTINUED)

Drawing and assembly no.	Temperature		Environment [2]	Gross failure [3]		Frame failure		Net failure		Shear modulus [7]		γ_{max} μm/m (μin/in) [10]
	°C	°F		N	(lb)	N	(lb)	N	(lb)	MPa	(lbf/in^2)	
65C17789-3	21	RT	D	81 850	18 400	13 340	3000	68 500	15 400	2.21×10^4	3.2×10^6	5795
↑	-53	-65	↑	78 960	17 750	↑	↑	65 610	14 750	↑	↑	5550
	-53	-65	↓	74 290	16 700			60 940	13 700			5155
	-53	-65	D	74 510	16 750			61 160	13 750			5174
	21	RT	W	76 060	17 100			62 720	14 100			5306
	21	RT	↑	78 290	17 600			64 940	14 600			5494
	21	RT		79 400	17 850			66 060	14 850			5588
	82	180		77 620	17 450			64 280	14 450			5437
↓	82	180	↓	78 290	17 600	↓	↓	64 940	14 600	↓	↓	5494
65C17789-3	82	180	W	79 180	17 800	13 340	3000	65 830	14 800	2.21×10^4	3.2×10^6	5569

SPAR CHORD CRIPPLING (TEST 7)

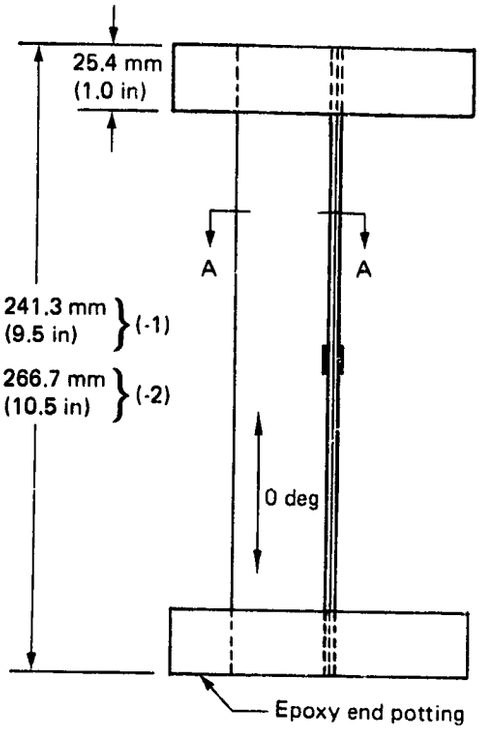

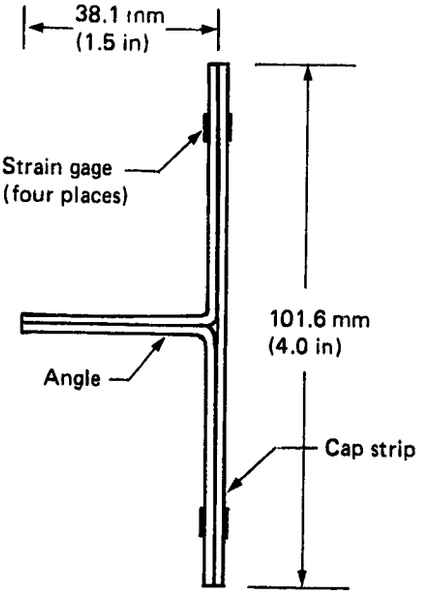

Fabric layup
(Narmco 5208
7-mil fabric)

65C17791-1, -2

Assembly number	Ply layup 1	
-1	Cap	$[(0, 90)(\pm45)(0, 90)(\pm45)(0, 90)]_S$
	Angle	$[(\pm45)(0, 90)(\pm45)]$
-2	Cap	$[(0, 90)(\pm45)(0, 90)_2(\pm45)(0, 90)]_S$
	Angle	$[(\pm45)(0, 90)(\pm45)_2(0, 90)(\pm45)]_S$

Drawing and assembly no.	Temperature		Environment 2	Area		Failure load 3		Stress 4		E 5		Strain, μm/m (μin/in) 6
	°C	°F		cm^2	(in^2)	kN	(lb)	MPa	(lbf/in^2)	MPa	(lbf/in^2)	
65C17791-1	21	RT	D	3.023	0.4686	54 940	12 350	181.7	26 355	5.01×10^4	7.26×10^6	3630
	21	RT				53 380	12 000	176.6	25 608			3530
	21	RT				52 490	11 800	173.6	25 181			3470
	-53	-65				51 150	11 500	169.2	24 251			3380
	-53	-65				48 040	10 800	158.9	23 047			3170
	-53	-65	D			46 710	10 500	154.5	22 407			3090
65C17791-1	21	RT	W	3.023	0.4686	39 590	8 900	131.0	18 993	5.01×10^4	7.26×10^6	2620

SPAR CHORD CRIPPLING (TEST 7)(CONTINUED)

Drawing and assembly no.	Temperature		Environment [2]	Area		Failure load [3]		Stress [4]		E [5]		Strain, μm/m (μin/in) [6]
	°C	°F		cm^2	(in^2)	kN	(lb)	MPa	(lbf/in^2)	MPa	(lbf/in^2)	
65C17791-1	21	RT	W	3.023	0.4686	47 600	10 700	157.4	22 834	5.01×10^4	7.26×10^6	3150
	21	RT				44 040	9 900	145.7	21 127			2910
	82	180				39 140	8 800	129.5	18 779			2590
	82	180				29 800	6 700	98.6	14 298			1970
65C17791-1	82	180	W	3.023	0.4686	35 590	8 000	117.7	17 072	5.01×10^4	7.26×10^6	2350
65C17791-2	21	RT	D	6.316	0.9790	169 900	38 200	269.0	39 109	4.66×10^4	6.76×10^6	5770
			D			169 900	38 200	269.0	39 019			5770
			D			152 600	34 300	241.6	35 036			5180
			W			142 600	32 100	226.1	32 789			4850
						149 000	33 500	235.9	34 219			5060
	21	RT				170 400	38 300	269.7	39 122			5790
	82	180				153 900	34 600	243.7	35 342			5230
	82	180				123 700	27 800	195.8	28 296			4200
65C17791-2	82	180	W	6.316	0.9790	128 600	28 900	203.5	29 520	4.66×10^4	6.76×10^6	4370

RAIL SHEAR (TEST 35)

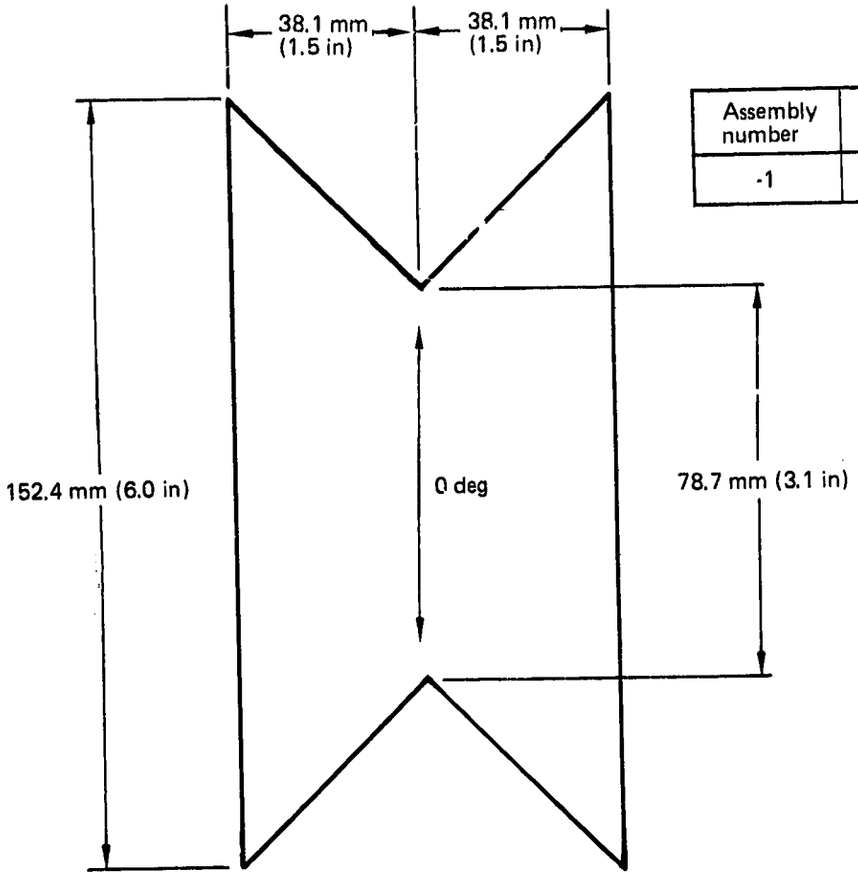

Assembly number	Ply layup 1
-1	Fabric: 5(0, 90), 7(±45)

NHS1-VNS-1

Drawing and assembly no.	Temperature		Environment 2	t		L		Failure load 3		Stress 4		G 7		Shear strain, γ μm/m (μin/in) 6
	°C	°F		mm	(in)	mm	(in)	N	(lb)	MPa	(lbf/in²)	MPa	(lbf/in²)	
NHS1-VNS-1	21	RT	D	2.29	0.09	78.7	3.1	43 059	9 680	239.2	34 695	2.03×10^4	2.95×10^6	11 760
	21	RT						41 991	9 440	233.3	33 835			11 470
	21	RT						43 948	9 880	244.2	35 412			12 000
	21	RT						44 304	9 960	246.1	35 699			12 100
	21	RT						42 970	9 660	238.7	34 624			11 740
	82	180						44 838	10 080	249.1	36 129			12 250
	82	180						45 016	10 120	250.1	36 272			12 300
	82	180						44 304	9 960	246.1	35 699			12 100
	-60	-75						43 771	9 840	243.0	35 269			11 960
	-60	-75						44 304	9 960	246.1	35 699			12 100
	-60	-75						42 970	9 660	238.7	34 624			11 740
	-60	-75						51 777	11 640	287.6	41 720			14 140
NHS1-VNS-1	-60	-75	D	2.29	0.09	78.7	3.1	45 327	10 190	251.8	36 523	2.03×10^4	2.95×10^6	12 380